PROCEEDINGS OF THE

28th International Symposium on Analytical and Environmental Problems

Szeged, Hungary

November 14-15, 2022

University of Szeged

Edited by:
Tünde Alapi
Róbert Berkecz
István Ilisz

Publisher:
University of Szeged, H-6720 Szeged, Dugonics tér 13, Hungary

ISBN 978-963-306-904-2

2022.
Szeged, Hungary

The 28th International Symposium on Analytical and Environmental Problems

Organized by:
SZAB Kémiai Szakbizottság Analitikai és Környezetvédelmi Munkabizottsága

Supporting Organizations
Institute of Pharmaceutical Analysis, University of Szeged
Department of Inorganic and Analytical Chemistry, University of Szeged

Symposium Chairman:
István Ilisz, DSc

Honorary Chairman:
Zoltán Galbács, PhD

Organizing Committee:
István Ilisz, DSc
professor of chemistry
University of Szeged, Institute of Pharmaceutical Analysis
Tünde Alapi, PhD
assistant professor
University of Szeged, Department of Inorganic and Analytical Chemistry
Róbert Berkecz, PhD
associate professor
University of Szeged, Institute of Pharmaceutical Analysis

Scientific Committee:
István Ilisz, DSc
Tünde Alapi, PhD
Róbert Berkecz, PhD
Daniela Sojic Merkulov, PhD
full professor
University of Novi Sad, Faculty of Sciences, Department of Chemistry, Biochemistry and Environmental Protection

Lecture Proceedings

CO_2 HYDROGENATION BY UTILIZING NICKEL-POOR AND ALUMINUM-RICH LAYERED DOUBLE HYDROXIDES, WITH DIFFERENT INTERLAYER ANIONS VIA REVERSE WATER GAS SHIFT ROUTE

Amin Hassani Moghaddam[1], Márton Szabados[2], Robert Mucsi, András Sápi [1,2]

[1]*Department of Applied & Environmental Chemistry, University of Szeged, H-6720 Szeged, Dóm tér 7, Hungary*
[2]*Department of Inorganic and Analytical Chemistry, University of Szeged, H-6720 Szeged, Dóm tér 7, Hungary*
e-mail: amin.hm@chem.u-szeged.hu

Abstract

The concentration of the predominant greenhouse gas, CO_2, is remarkably increasing in the atmosphere due to combustion emissions of fossil fuels. A state-of-the-art and relatively simple synthetic path of preparing $NiAl_4$-layered double hydroxides (LDHs) were developed through high-energy mixer milling pretreatment of *Al(OH)*$_3$ followed by impregnation with *Ni(II)* nitrate salt under mild circumstances (atmospheric pressure and 90°C). This method proved to be improved by the ion exchange technique, and thus various counters ($H_2PO_2^-$, HPO_3^{2-}, $H_2PO_4^-$, HPO_4^{2-}, PO_4^{3-}, $B_4O_7^{2-}$, CO_3^{2-} and HCO_3^-) anions could be intercalated. The modified LDHs proved to be active in CO_2 hydrogenation reactions at atmospheric pressure. The catalysts were characterized using XRD, TG-DTA, FT-IR and H_2-TPR. The quality of interlayer anions was found to exert a considerable influence on the topotactic transformation of LDHs, the in situ reduction of nickel, and the formation of spinel-type oxides. Furthermore, their performance in CO_2 reverse water gas shift *(RWGS)* reaction was investigated. The data analysis demonstrated that the highest catalytic performance was occurred at 550 °C pre-activation. The catalysts obtained from LDHs with tetraborate and hypophosphite interlayer anions clearly exhibits the highest CO selectivity among the studied catalysts in the range of 350–600 ℃ and the lowest CH_4 formation. Meanwhile, those generated from nitrate and carbonate counters comprising LDHs facilitated mostly and vigorously the methane formation and the intercalation of phosphate ions resulted in balanced production for both CO and CH_4. Catalysts from B_4O_7 counter containing they possessed significantly high (>70%) CO selectivity slightly dependent on the reaction temperatures, it is promising to exploit efficient RWGS reaction catalytic system.

***Keywords**: Nickel-poor layered double hydroxides, mechanochemistry, intercalation, CO_2 hydrogenation, reverse water gas shift (RWGS)*

SUPRAMOLECULAR ARCHITECTURED WATER SOLUBLE BASED ON COORDINATION COMPOUNDS WITH N-DONOR LIGANDS

Adelina-Antonia Andelescu[1], Carmen Cretu[1], Elisabeta I. Szerb[1], Anca Silvestru[2]

[1] *"Coriolan Dragulescu" Institute of Chemistry, 24 Mihai Viteazu Bvd, 300223 Timisoara, Romania*
[2] *Babes-Bolyai University, Faculty of Chemistry and Chemical Engineering, Chemistry Department, 11 Arany Janos, 400028 Cluj-Napoca, Romania*
e-mail: andelescu.ade@gmail.com

Abstract

Chromonic systems are a subclass of lyotropic liquid crystal phases, which occur from face-to-face aggregation into columns of the molecules which contain planar aromatic moieties and solubilizing hydrophilic and/or ionic groups. However, lately coordination complexes based on d-block metal centers with bulkier geometries like octahedral iridium(III) complexes have been shown to self-assemble spontaneously into ordered supramolecular organizations in water at low concentrations, like the classical chromonics. The interest in this class of materials derives from their potential applications in biosensing and imaging, thin film polarizers, micro-patterning, nano-fabrication, etc. [1]. Thus, developing such lyotropic metallomesogens based on rhodium(III) and platinumII) coordination compounds may lead to materials with potential applications in medicine as drug delivery systems [2] and/or therapeutic agents [3].

On this background, herein we report the synthesis and characterization of some new water soluble heteroleptic Rh(III) and Pt(II) complexes. The nature of the complexes was established by elemental analysis and molar conductivity and fully characterized by IR, ^{1}H-NMR and UV-Vis spectroscopy. The mesomorphic properties in water of the complexes were investigated by polarized optical microscopy (POM) using the Lawrence penetration method. The complexes show ability to self-assembly into chromonic phases in water at room temperature. The aggregation behavior in water of Rh(III) complexes will be discussed.

Acknowledgements

This work was supported by a grant of the Ministry of Research, Innovation and Digitization, CNCS/CCCDI – UEFISCDI, project number **PN-III-P1-1.1-PD-2021-0427**, within PNCDI III.

References

[1] J. E. Lydon, J. Mater. Chem. 20 (2010), 10071-10099.
[2] J. Markham, J. Liang, A. Levina, R. Mak, B. Johannessen, P. Kappen, C.J. Glover, B. Lai, S. Vogt, P.A. Lay, Eur. J. Inorg. Chem. 12 (2017) 1812–1823.
[3] (a) C.-H. Leung, H.-J. Zhong, D.S.-H. Chan, M. Dik-Lung, Coord. Chem. Rev. 257 (2013) 1764–1776; (b) M. Dik-Lung, M. Wang, Z. Mao, C. Yang, C. Ng, C. Leung, Dalton Trans. 45 **(**2016) 2762–2771; (c) M. Dik-Lung, L.-J. Liu, K.-H. Leung, Y.-T. Chen, H.-J. Zhong, D.S.-H. Chan, H.-M.D. Wang, C.-H. Leung, Angew. Chem. Int. Ed. 53 (2014) 1–6.

HOW TO ESTABLISH METABOLITE REFERENCE RANGES FOR HEALTHY ADULTS?

Boglárka Barna[1,2] Violetta Koósz[2], Ágnes Tóth[2], Gábor Endre[2], Ildikó Thibodeau[2], Csaba Varga[1]

[1]Department of Physiology, Anatomy, and Neuroscience, University of Szeged
Közép fasor 52., H-6726, Szeged, Hungary
[2]Medipredict Health Kft.
Irinyi József u. 4-20. B2 building, ground floor, H-1117, Budapest, Hungary
e-mail: boglarka.barna.md@gmail.com

The main bottleneck for the clinical implementation of metabolomics is the lack of standardized reference ranges for healthy adults. A possible solution for standardization would be the use of absolute concentration data that in theory can be directly compared between laboratories. Our study aimed to investigate the variance of absolute concentration measurements between independent laboratories and to assess whether establishing standardized metabolite reference ranges to facilitate clinical implementation of metabolomics is feasible.

We have measured 50 healthy adults' (aged 18-50) metabolomics profiles by using the Biocrates MxP500 kit measured with liquid chromatography-tandem mass spectrometry. To assess the results and to try to establish a normal range based on these measurements, we have used basic data analytical tools, a bootstrapping method, and the fitting of statistical distributions. We compared our results to Trabado et al.'s study [1] which quantified a smaller number of metabolites for 800 healthy French subjects (aged 18-86).

Our results showed that none of the measured metabolites exhibited a normal distribution and they varied in a smaller range than in the previous study. This may be explained by our smaller sample size. Alternatively, it could be explained by the younger study population which may suggest that the development of metabolite reference ranges should be stratified by age.

References

1 Séverine Trabado, Abdallah Al-Salameh, Vincent Croixmarie, Perrine Masson, Emmanuelle Corruble, Bruno Fève, Romain Colle, Laurent Ripoll, Bernard Walther, Claire Boursier-Neyret, Erwan Werner, Laurent Becquemont, Philippe Chanson, The human plasma-metabolome: Reference values in 800 French healthy volunteers; impact of cholesterol, gender and age PLoS One, 2017, 12(3) e: 0173615

BUSINESS STUDENTS' EVALUATION OF ENERGY SOURCES

László Berényi[1], Nikolett Deutsch[2]

[1] *Institute of Management Science, University of Miskolc, H-3515 Miskolc-Egyetemváros, Hungary*
[2] *Department of Strategy and Project Management, Corvinus Business School, Corvinus University of Budapest, No. 8. Fővám Square, H-1093 Budapest, Hungary*
e-mail: szvblaci@uni-miskolc.hu

Abstract
Understanding the students' opinions about energy sources allows exploring the factors of acceptance. It can contribute to supporting the changes in energy production and utilization. Focus on business students must have an emphasis since they may be the company decision-makers in the future. The study analysis the return, availability, environmentally friendly nature, knowledge requirement of the application, and future role of some renewable energy sources and nuclear power. The sample consists of 150 randomly selected students. The results show the dominance of solar energy and the marginalization of biomass energy. The students' opinions differ from the professional approach on the energy sources that raise educational challenges.

Introduction
However, it is fundamentally agreed that the depletion of fossil energy sources is inevitably approaching, the changes are slow. Finding alternative energy sources is an important but multifaceted challenge. Energy dependence is a complex social and technical challenge of the present age [1].
According to Wolsink [2], both policymakers and researchers offer renewables to solve environmental problems. It must be preferred to fossil fuels and nuclear power. The European Union and the Hungarian government highlight and force renewables [3] [4]. Figure 1 shows the trends limited to electricity production as an example that underlines the restraint in fossil sources along with a high contribution of nuclear power.

Figure 1. The proportion of energy sources in the amount of electricity produced 2006-2017 (based on https://www.ksh.hu/thm/3/indi3_1_2.html)

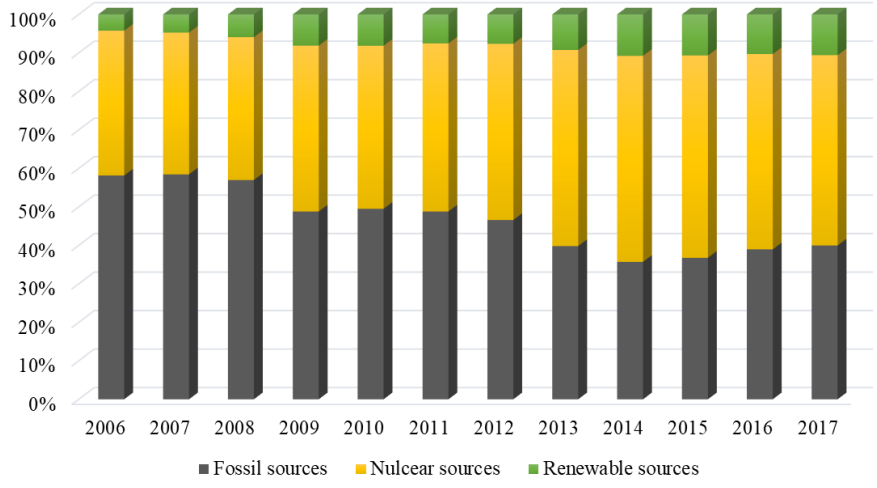

The role of the nuclear way is questionable. In some opinions, renewable and nuclear energy are two plausible alternatives to fossil sources in energy production [5]. Busu [6] formulated the idea to reduce CO_2 emissions, and one of the solutions involves increasing the use of renewables. Both methods have several advantages and challenges, including the availability or social acceptance of the technology [7]. The effectiveness of nuclear energy production is obvious, but the advantages are limited to this life cycle phase. There are several risks to consider in a life-cycle approach, especially managing nuclear waste [8] [9]. Not incidentally, the impacts of nuclear accidents [10] are horrifying.
Beyond the technical and environmental issues, there are social and managerial considerations. Among these, the acceptance of technology is emphasized in our research. Related models [11] confirm the impact of background, knowledge level, intentions, and other factors. A higher level of acceptance of technology can boost up its application.

Experimental

The direct evaluation of energy generation technologies uses a pairwise comparison with five items (this means ten pairs of statements):

- biomass energy,
- nuclear energy,
- solar energy,
- hydropower,
- wind power.

The respondents are asked to make a pairwise comparison of the items from 5 perspectives:

- Return: In your opinion, which power generation technology has the highest financial return on investment?
- Availability: In your opinion, which technology is the most accessible?
- Environmentally friendly nature: In your opinion, which technology is environmentally friendly overall?
- Knowledge: In your opinion, which energy generation technology can be utilized more simply, in general, i.e., with less specialized knowledge?
- Future: In your opinion, which power generation technology will be the most decisive in the coming decades; which one will we use more?

The preferences are presented by the frequencies of ratings and a relative weight based on the eigenvector method of Saaty [12]. The consistency of the individual evaluations is checked by the Kendall method [13]. Weight calculation is limited to the cases with a perfect consistency that means a clear preference list of the respondents. The ratio of these cases is 70% for return, 78% for availability, 78% for environmentally friendly nature, 82% for knowledge, and 72.7% for the future role. Kendall's coefficient of concordance is calculated for measuring the group level consensus for pairwise comparison (v) [14]. The value is the study is expressed in percentages of the maximum available value.
The results are based on a voluntary online survey among business students of Hungarian higher education institutions. 150 randomly selected responses of the University of Miskolc are used for the analysis. The data collection period was the fall semester of 2020. The sample's representativeness is not checked; the study can be considered a pilot, and the interpretation of the conclusions cannot be generalized.

Results and discussion

The pairwise comparison allows a comprehensive assessment of the energy sources and the technology related to them. In a hypothetical case where an energy source is preferred over all

others by each respondent, its value in Table 1 was 100%. The table shows the agreement level by comparing the number of preferences to the maximum available value. The calculations are performed for the total sample and the respondents with a clear preference order (K=1).

Table 1 %

	return		**availability**		**environmentally friendly nature**		**knowledge**		**future**	
	Total	*K=1*	Total	*K=1*	Total	*K=1*	Total	*K=1*	Total	*K=1*
hydropower	46.8	*48.6*	48.7	*48.1*	49.7	*47.9*	53.3	*53.0*	33.7	*31.9*
solar energy	76.8	*80.2*	83.3	*87.8*	79.0	*81.8*	72.0	*73.8*	77.0	*81.0*
nuclear energy	37.8	*36.2*	22.5	*19.2*	6.5	*4.1*	14.3	*11.6*	48.8	*49.3*
wind power	54.7	*55.2*	57.0	*57.5*	64.0	*65.8*	67.0	*68.7*	48.7	*47.7*
biomass energy	33.8	*29.8*	38.5	*37.4*	50.8	*50.4*	43.3	*42.9*	41.8	*40.1*
group-level consensus		*21.3*		*35.1*		*46.0*		*27.9*		*19.5*

The dominance of solar energy is remarkable. It is considered the most important energy technology in each aspect of the evaluation. According to the future role, solar energy is followed by nuclear energy; however, in other aspects, it is undervalued. Wind power has a high acknowledgment by the respondents, but the installation of the turbines is legally limited. Biomass energy has a less relevant role.

In contrast, Žnidarec et al. [15] emphasize that solar, biomass, and geothermal (not included in the survey) potential is relevant in the region, while wind and hydropower potential is marginal. The students' evaluation is not in line with the professional opinion.

It is to note that the group level consensus is reflects shared opinions, especially on the future role and the return of the investment. The highest value is found in environmentally friendly nature.

The results of weight calculations are in Table 2. The normalized eigenvectors allow a ratio-scale comparison of the results within each evaluation aspect (by rows in the table). It is to note that a comparison between these is not feasible. The scores show the relative preferences of the respondents. The dominant role of solar energy is confirmed, especially in its availability, return, and future role. Figures 2 and 3 visualize the scores.

Table 2. Normalized weights calculated with the eigenvector method

	hydropower	**solar energy**	**nuclear energy**	**wind power**	**biomass energy**
return	0.249	0.890	0.174	0.317	0.125
availability	0.169	0.949	0.057	0.234	0.109
environmentally friendly nature	0.216	0.836	0.015	0.445	0.237
knowledge	0.334	0.692	0.051	0.600	0.216
future	0.119	0.922	0.250	0.210	0.171

Solar energy has subject to general optimism. Its availability, return, and future role monopolizes the opinions, while the utilization is considered simple. Access to wind power is considered similarly easy, but its future role is lower than even nuclear energy. Biomass energy is acknowledged the third in its environmentally friendly nature, but other aspects are evaluated

low. Figure 3 skips solar energy to show the differences of the evaluations on other energy sources more spectacularly.

Figure 2. Normalized weight scores by evaluation aspects

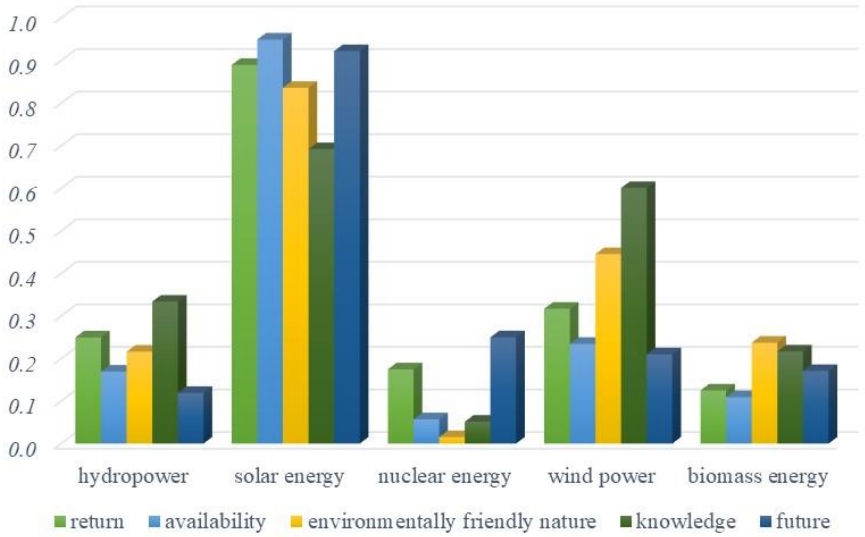

Figure 3. Normalized weight scores by energy sources, without solar energy

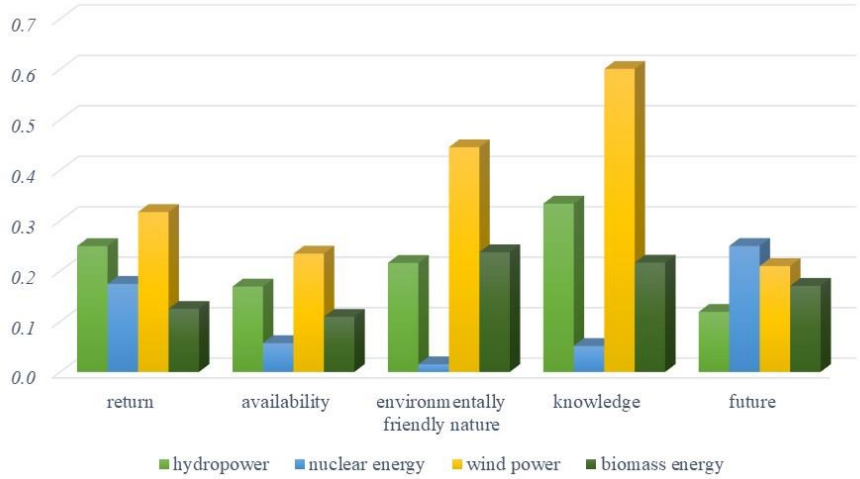

Conclusion

The results show the exceptional role of solar energy. Wind power is considered easy to apply, but its availability and future role are remarkably lower. Nuclear energy is found the least friendly to the environment and its return among the worst technologies, but there is confidence in its relevant future role compared to other energy sources.

Former results reported encouraging results on the future usage of renewable energy sources in Hungary [16] [17]. The backlog of knowledge on the topic was detectable, and it is confirmed in the present study. The students' evaluation and the professional opinions do not match.

Biomass energy must be mentioned as under-evaluated in each aspect of the analysis. Its role and opportunities are broader than imagined and expected by the business students. Since business students will become the decision-makers of companies or other institutions, the main implication of the study is giving a higher emphasis to teaching about energy issues.

Acknowledgments
The study is related to the OTKA K139225 “Management readiness level towards Strategic Technology Management Excellence” project.

References
[1] P. Högselius, A. Kaijser, Energy dependence in historical perspective: The geopolitics of smaller nations. Energy Policy 127 (2019) 438-444.
[2] M. Wolsink, Contested environmental policy infrastructure: Socio-political acceptance of renewable energy, water, and waste facilities. Environmental Impact Assessment Review 30 (2010) 302-311.
[3] 28/11/2018 – COM (2018) 773 – A Clean Planet for All: A European Strategic Long-Term Vision for a Prosperous, Modern, Competitive and Climate Neutral Economy. Available online: https://eur-lex.europa.eu/legal-content/EN/TXT/?uri=CELEX:52018DC0773 [18 02 2022].
[4] Nemzeti Energiastratégia 2030. Available online: https://2010-2014.kormany.hu/download/4/f8/70000/Nemzeti%20Energiastratégia%202030%20teljes%20változat.pdf [18 02 2022].
[5] K. Skamp, E. Boyes, M. Stanisstreet, M. Rodriguez, G. Malandrakis, R. Fortner, A. Kilinc, N. Taylor, K. Chhokar, S. Dua, Renewable and Nuclear Energy: An International Study of Students’ Beliefs about, and willingness to act, in relation to two energy production Scenarios. Research in Science Education 49 (2019) 295-329.
[6] M. Busu, The Role of Renewables in a Low-Carbon Society: Evidence from a Multivariate Panel Data Analysis at the EU Level. Sustainability 11 (2019) 5260.
[7] G. Wilkins, Technology Transfer for Renewable Energy: Overcoming Barriers in Developing Countries, Earthscan Publications, London, 2018, p. 256
[8] J.I. Dawson, R.G. Darst, Meeting the challenge of permanent nuclear waste disposal in an expanding Europe: Transparency, trust and democracy. Environmental Politics 15 (2006) 610-627.
[9] P. Hocke, O. Renn, Concerned public and the paralysis of decision-making: Nuclear waste management policy in Germany. Journal of Risk Research 12 (2009) 921-940.
[10] N. Deutsch, The changing role of nuclear power in the European Union: Reflections from official scenarios released before and after the Fukushima Daiichi accident. Theory Methodology Practice 13 (2017) 17-36.
[11] P. Isaias, T. Issa, High Level Models and Methodologies for Information Systems, Springer, Cham, p. 162.
[12] T.L. Saaty, The Analytic Hierarchy Process, McGraw Hill, New York, 1980, p. 287.
[13] J. Kindler, O. Papp, Komplex rendszerek vizsgálata: Összmérési módszerek, Műszaki Könyvkiadó, Budapest, 1978, p. 262.
[14] M.G. Kendall, Rank Correlation Methods, Griffin London, 1970, p. 272.
[15] M. Žnidarec, M. Primorac, C. Mezei, S.Zs. Kovács, Megújuló energiaforrás-potenciál és döntéstámogatás Horvátország és Magyarország határon átnyúló régiójában – egy modell-alkalmazás lehetőségei. In: D. Topić, V. Varjú, B. Horváth-Kovács (Eds.), Megújuló energia és energiahatékonysági lehetőségek rurális terekben, MTA KRTK Regionális Kutatások Intézete, Pécs, 2018, pp. 41-63.
[16] L. Berényi, N. Deutsch, Recognition of renewable energy among business students. In: T. Alapi, R. Berkecz, I. Ilisz (Eds.) Proceedings of the 26th International Symposium on Analytical and Environmental Problems, University of Szeged, Szeged, 2020, pp. 8-12.
[17] L. Berényi, Z. Birkner, N. Deutsch, A Multidimensional Evaluation of Renewable and Nuclear Energy among Higher Education Students. Sustainability 12 (2020) 1449.

DISSOLUTION OF CALCIUM(II) DODECYL SULPHATE PRECIPITATES IN THE PRESENCE OF ALCOHOLS

Csaba Bús[1], Adél Ádám[1], Szilveszter Ziegenheim[1], Pál Sipos[2], Bence Kutus[2]

[1]Department of Organic Chemistry, University of Szeged, H-6720 Szeged, Dóm tér 8, Hungary
[2]Department of Inorganic and Analytical Chemistry, University of Szeged, H-6720 Szeged, Dóm tér 7, Hungary
e-mail: bus.csaba@szte.hu

Abstract

Anionic surfactants are commonly used in chemical Enhanced Oil Recovery (cEOR) technologies, where their primary goal is to reduce the interfacial tension (IFT) between oil and water which is crucial for the overall efficiency. However, the presence of alkaline earth cations, in particular Ca^{2+} and Mg^{2+}, in brine water may cause a decrease in the surfactant concentration because of precipitation [1]. Alcohols, commonly used as co-solvents, have been reported to enhance the solubility of Ca^{2+}-surfactant salts [2]. Yet, despite the importance of this side reaction in cEOR, research focusing on the impact of alcohols on surfactant precipitation is sporadic.

In this study, we characterized the effect of alcohols on surfactant precipitation in aqueous solutions of calcium chloride and sodium dodecyl sulphate (SDS), applying spectrophotometry, tensiometry and dynamic light scattering. In the absence of metal salt, we find alcohols to increase both the size of SDS particles as well as the surface tension at the water-air interface. Upon addition of Ca^{2+} ions to aqueous samples of SDS, we observe the rapid formation of solid $CaSDS_2$. Strikingly, this precipitate can completely dissolve when alcohols are added to the system: isopropyl alcohol (20.0 V/V%), 2-butoxyethanol (10.0 V/V%) and *n*-octanol (10.0 V/V%) enhance the solubility of the precipitates up to 10.0 g/L Ca^{2+} concentration. Conversely, Methanol (MeOH) and ethanol (EtOH) do not alter the solubility significantly.

These results suggest the addition of alcohols to anionic surfactants' solutions to be a simple and effective method to suppress the interactions between the surfactant and Ca^{2+} ions.

[1] Negin, C.; Ali, S.; Xia, Q. Most Common Surfactants in Chemical Enhanced Oil Recovery, *Petroleum*, **2017**, *3*, 197–211.

[2] Miyazaki, N.; Sugai, Y.; Sasaki, K.; Okamoto, Y.; Yanagisawa, S. Screening of the Effective Additive to Inhibit Surfactin from Forming Precipitation with Divalent Cations for Surfactin Enhanced Oil Recovery. *Energies*, **2020**, *13*, No. 2430

NEW 3d METAL COORDINATION COMPLEXES WITH N- AND O- DONOR LIGANDS: SYNTHESIS, STRUCTURAL CHARACTERIZATION AND OPTICAL PROPERTIES

Ildiko Bută, Carmen Cretu, Evelyn Popa, Elisabeta I. Szerb

"Coriolan Dragulescu" Institute of Chemistry, Timisoara, Romania
e-mail: ildiko.buta@gmail.com

Abstract

Liquid crystals are anisotropic fluids, where the combination of flow and molecular ordering confers interesting optical, dielectric, and visco-elastic properties [1]. Liquid crystals have been intensively studied as functional materials in the fields of energy, water, photonics, actuation, sensing, and biotechnology [2].

Here, we present the synthesis of two isostructural Ni^{II} and Zn^{II} coordination complexes based on N^N-chelating ligands (2,2'-bipyridine and 1,10-phenanthroline) and an O-donor ligand (3,4,5-tridodecyloxybenzoate) and their structural characterization by spectroscopic and analytic methods.

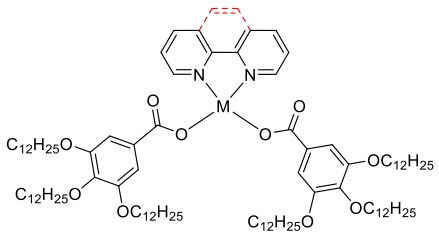

M = Zn^{II} and Ni^{II}

Figure 1. Proposed structures of Ni^{II} and Zn^{II} complexes

The complexes self-assemble into liquid crystalline supramolecular architectures, their mesomorphic properties being investigated by a combination of Polarized Optical Microscopy (POM) and Differential Scanning Calorimetry (DSC) techniques. The metallomesogens show typical columnar textures and are liquid crystalline over a wide range of temperatures. Interestingly, the mixtures obtained by simply mixing the complexes in different molar ratios show different thermal and mesomorphic behaviors comparative with their precursor complexes, depending on their composition. Preliminary results regarding the emission properties of the complexes and the new materials are presented.

References

1. M. Hird, Chem. Soc. Rev. 36 (2007) 2070.
2. J. Uchida, B. Soberats, M. Gupta,T. Kato, Adv. Matt. 34 (2022) 109063.

Acknowledgements:

We thank the Romanian Academy, Institute of Chemistry "Coriolan Dragulescu" (Project 4.1.3) for financial support. This work was supported by a grant of the Romanian Ministry of Education and Research, CNCS - UEFISCDI, project number PN-III-P4-ID-PCE-2020-1958, within PNCDI III.

INORGANIC AND PHYTOCHEMICAL CHARACTERISATION OF *Populus Nigra L.* BUDS EXTRACT

Daniela Haidu[1], Daliana Minda[2,3], Ioana Zinuca Pavel[2,3], Mariana Nela Ștefănuț[4], Corina Danciu[2,3]

[1]Romanian Academy "Coriolan Dragulescu" Institute of Chemistry, 300223 Timisoara, Romania;
[2]Department of Pharmacognosy, "Victor Babes" University of Medicine and Pharmacy 300041 Timisoara, Romania;
[3]Research Centre for Pharmaco-Toxicological Evaluation, "Victor Babes" University of Medicine and Pharmacy, 300041 Timisoara, Romania
[4]Laboratory of Electrochemical and Chemical Technologies, Department of Chemical and Electrochemical Syntheses, National Institute of Research and Development for Electrochemistry and Condensed Matter, 300569 Timisoara, Romania;
e-mail: danielahaidu1@gmail.com

Abstract

Poplar it is known to be an efficient bio accumulator of soil chemicals, allowing its use to remedy the soil of toxic elements being the subject of many studies [1]. Many parts of this tree can be used as active ingredients, but the most valuable are the buds. The aim of the study was to conduct a phytochemical characterization of *Populus nigra L*. buds extract obtained from the western areas of Romania and to determine the inorganic elements as well as the in vitro antiproliferative evaluation on the A549 human lung cancer cell line in terms of viability and cytotoxicity. Regarding the elements contained, the formulation of a phytopharmaceutical product includes several important aspects such as: the medicinal plant from which the active principles come (evaluation of the content of toxic elements, especially in the case of plants that are used for phytoremediation) and evaluation of the finished product to define active principles; ensuring that it is not contaminated with toxic metals either from the handling process or from the extractive process.

The inorganic elements concentrations were below the limit of detection for As, Co and As, whereas Cd = 0.019 µg/g, Mn = 0.59 µg/g, Cr = 0.79 µg/g, Ni = 3.28 µg/g, Cu = 6.66 µg/g, Zn = 14.84 µg/g, Fe = 39.00 µg/g and Al = 2109.87 µg/g. Pg ethanolic extract has a low contribution to trace elements in dietary intake, but the most valuable remark is regarding its safety, namely, the tested Pg extract does not produce any harmful effect of metal toxicity during therapeutic application [2].

The Pg extract was found to contain twelve different phenolic compounds consisting of dihydroxybenzoic acid, caffeic acid, chicoric acid, protocatechuic acid, apigenin-glucuronide, chrysoeriolglucuronide, 3-caffeoylquinic acid, 5-caffeoylquinic acid, tremuloidin, salicin, pinostrobin, and tremulacin. Apigenin–glucuronide was the major compound, found in an amount of 55.828 mg/g chlorogenic acid equivalent (CCE). Among all the phenolics identified, chryglucuronide and tremuloidin were also the most abundant compounds. Other results obtained for the phenols, are in line with those reported by other authors [3].

Different concentrations (10, 25, 50, 75, 100, and 150 µg/mL) of the extract were tested for the in vitro antiproliferative potential on A549 human lung cancer cell line. Poplar bud extract induced a significant decrease of tumor cell viability in a dose dependent manner with an IC50 = 72.49 µg/mL. Poplar bud extract can be regarded as a promising candidate for future studies involving lung cancer [4,5].

Acknowledgements
We acknowledge Program 4 of Institute of Chemistry „Coriolan Dragulescu“ of Romanian Academy, the Department of Pharmacognosy of “Victor Babes” University of Medicine and Pharmacy, Timisoara and the Laboratory of Electrochemical and Chemical Technologies, of National Institute of Research and Development for Electrochemistry and Condensed Matter, Timisoara, Romania.

References
[1] E. Palm, G.N. Werther, S. Mancuso, E. Azzarello, Environ. Exp. Bot. 183 (2020) 104347.
[2] K. Artwell, N. France, K. Florence, J. Environ. Public Health, 2017 (2017) ID 1476328.
[3] A.L. Santos, M.G. Soares, L.S. de Medeiros, M.J.P. Ferreira, P. Sartorelli, Phytochem. Anal. 32(6) (2021) 891.
[4] B. Kis, S. Avram Feflea, I. Z. Pavel, A. Lombrea, V. Buda, C. Dehelean, C. Soica, M. B. Yerer, F. Bojin, R. Folescu, C. Danciu, Plants. 9 (11) (2020) 1464.
[5] B. Kis, I.Z. Pavel, D. Haidu, M.N. Ștefănuț, Z. Diaconeasa, E.A. Moacă, C.A. Dehelean, S. Șipos, A. Ivan, C. Danciu. Inorganic Pharmaceutics. 13(7) (2021) 986.

THE EFFECT OF IRON DOPING TO OPTICAL PROPERTIES OF ZnO NANOPARTICLES AND ITS APPLICATION IN CO_2 HYDROGENATION

Haythem Basheer, Mohit Yadav, András Sápi

Department of Applied and Environmental Chemistry, University of Szeged, H-6720, Hungary
e-mail: haythemsuliman@gmail.com

Abstract

Global warming and pollution are a big challenge facing humanity and CO_2 emission is one of these issues. So, recycling Carbone dioxide to added value hydrocarbon is one of the solutions. In this research CO_2 has been Photocatalytic hydrogenated using ZnO doped Fe synthesized by co-precipitation method with different Iron ratios. The samples were characterized using X ray Diffractometer (XRD) and UV Visible Refractance Spectroscopy. The CO_2 photo-hydrogenation was taken place in Glass Photoreactor in batch mode using UV lamp. The XRD revealed formation of single phase of hexagonal ZnO and UV visible spectroscopy determine the maximum absorption and the band gap were calculated. Scanning Electron Microscope (SEM) and (EDS) were used to investigate the surface morphology and the composition. The Photocatalytic test results showed an enhancement in the photocatalytic activity for the doped samples with 22%, 47% conversion and 99.9% CO selectivity with small traces of CH_4 selectivity to CO for ZnO pure and iron doped ZnO respectively.

***Keywords**: Photocatalysis, Hydrogenation, Band gap, CO_2 and doping*

COMPOSITE FILM AS ANTICORROSIVE COATING OF Ti ALLOYS SURFACES

Juan Hidalgo Viteri[1], Nicoleta Cotolan[1], Galambos Ildiko[2], Graziella Liana Turdean*[1]

[1]Department of Chemical Engineering, Faculty of Chemistry and Chemical Engineering, Babeș-Bolyai University, 11 Arany János Street, 400028 Cluj-Napoca, Romania,
[2]Soós Erno Research and Development Center, University of Pannonia, 8200 Nagykanizsa, Hungary
e-mail: juansannin2595@gmail.com; graziella.turdean@ubbcluj.ro

Abstract
Causing important economic damages, the corrosion of the titanium alloys used in the different environmental or medical fields can be prevented by using a physical barrier with anti-corrosion properties. The anti-corrosive property of a film consisting of poly (methyl methacrylate) (PMMA) and ibuprofen (IBU) deposited by dip-coating on Ti alloy surface was investigated by electrochemical impedance spectroscopy method.

Introduction
The main important anticorrosive methods consist of the design of corrosion-resistant materials, the application of a film having anti-corrosion properties, the addition of corrosion inhibitors, and the use of cathodic protection. In this context, an innovative high-protective anti-corrosive strategy consists of using a composite matrix consisting of an inhibitor included in a polymeric film [1].

Experimental
Ti–6Al–4V/xIBU-PMMA (where x = 0.2, 0.4, 1 mM ibuprofen) modified surface was prepared by dip-coating method and was investigated into a 3.5% of NaCl saline solution by electrochemical impedance spectroscopy (EIS) measurements, using a PGStat 302N electrochemical workstation.

Results and discussion
In order to establish the steady-state open circuit potential (OCP) a stabilization period of 60 min was performed. The potentiodynamic polarization measurements were carried out over a potential range of ±200 mV *versus* OCP with a scan rate of 0.5 mV s^{-1}. From the obtained Tafel plots the estimation of the corrosion kinetic parameters, such as corrosion potential (E_{corr}), corrosion current density (i_{corr}), and anodic (b_a) and cathodic (b_c) Tafel slopes were performed. The EIS measurements lead to calculating the corrosion inhibition efficiency (IE%).

Conclusion
The corrosion inhibition performance of a Ti–6Al–4V/xIBU-PMMA (where x = 0.2, 0.4, 1 mM ibuprofen) interface in a 3.5% of NaCl saline solution was studied proving the inhibitory ability of ibuprofen.

Acknowledgments
Juan Hidalgo Viteri thanks for the Ph.D. fellowship offered by the Romanian Ministry of Foreign Affairs in accordance with Government Decision 477/21.04.2021.

References

[1] E. Maya-Visuet, T. Gao, M. Soucek, H. Castaneda, *Prog. Org. Coat*. 83 (2015) 36-46.

INTERACTION BETWEEN TRITON X100 AND BRIJ 58 IN THEIR BINARY MIXED MICELLES

Vesna Tepavčević, Gorana Puača, Mihalj Poša

Department of Pharmacy, Faculty of Medicine, University of Novi Sad, 21000 Novi Sad, Hajduk Veljkova 3, Serbia
e-mail: vesna.tepavcevic@mf.uns.ac.rs

Abstract
The micellization of the binary mixture of surfactants Triton X100 – Brij 58 in an aqueous solution was investigated using a spectrofluorimetric method with pyrene as a probe molecule. There are synergistic interactions between the micellar building units in the binary mixed micelles Triton X100 – Brij 58, which increase with increasing temperature. The analyzed binary mixed micelles possess molar excess entropy.

Introduction
Triton X100 is a commonly used surfactant, mainly as an additive in drug or vaccine formulation. Brij 58 is a dominantly used solubilizer and an emulsifier in the food, drug, and cosmetics industry. Their structures contain polyoxyethylene chains as hydrophilic parts of their molecules, significantly longer in Brij 58 than in Triton X100. The hydrophobic part in Triton X100 has an aromatic core and the hydrophobic part in Brij 58 has an aliphatic hydrocarbon chain. These traits lead to different behavior in terms of critical micellar concentration and affect the structure of their mixed micelle.

Experimental
Chemicals used for this study were taken from original manufacturer's packaging (Sigma Aldrich, Saint Louis, MO, USA). The critical micelle concentrations of pure surfactants and their binary mixtures in aqueous solutions were determined by the invasive spectrofluorimetric method, using pyrene as a probe molecule. Measurements were done with different molar ratios (α) of surfactants in their binary mixtures (α = 0.1, 0.2, 0.3, 0.4, 0.5, 0.6, 0.7, 0.8, 0.9), in the temperature range of T = (273.15–323.15) K, with 5 K increments. All solutions of surfactants were prepared using pyrene-saturated water. First (I_1) and third (I_3) vibration band of pyrene emission spectrum, were recorded at 373 nm (I_1) and 384 nm (I_3). Obtained fluorescence measurement results (I_1/I_3 ratio) for different work solutions' concentrations were analyzed using software Origin Lab 9 (Northampton, MA, USA). The I_1/I_3 ratio vs. total concentration of surfactants plots were analyzed using a Boltzmann fitting, where the interception of two asymptotes was considered to be the critical micellar concentration of the examined surfactant mixture, at a given temperature. The calculations of thermodynamic parameters were done according to the Regular Solution Theory (RST) [1].

Results and discussion
In the monocomponent micelles of Brij 58, the globular and the elongated conformations of surfactant molecules are randomly distributed. The substitution of Brij 58 molecules, which hydrocarbon chains are in the globular conformations, with the molecules of Triton X100, reduces hydrophobic hydration [2,3]. This results in a synergistic interaction between different micellar building units in the examined binary mixed micelles. The mean value of the interaction parameter is negative, in the examined temperature interval T = (273.15–323.15) K. Synergistic interactions are usually the result of various factors (contributions). Enthalpic

contribution most likely originates from hydrogen bonds (in the hydrophilic shell of binary mixed micelles) between the terminal OH groups in the polyoxyethylene chains of Triton X100 molecules and the ether oxygens in the polyoxyethylene chains of Brij 58 molecules. Thermodynamic stabilization of the examined binary mixed micelles increases with increasing temperature. Namely, after replacing Brij 58 molecules that have globular conformations with Triton X100 molecules, the planar aromatic rings are incorporated into micelles, which increases hydrophobic interactions of Brij 58 hydrocarbon chains (with increasing temperature, the size - intensity - hydrophobic interactions also increase [4]). As the hydrophobic segment of Triton X100 is shorter than the hydrophobic segment of Brij 58, the hydrocarbon chains of Brij 58 have a favorable packaging effect, i.e., in the inner domain of the hydrophobic nucleus of the binary mixed micelle, the number of different conformational states of the Brij 58 hydrocarbon chains increases with increasing temperature.

Conclusion

For binary mixed micelles Triton X100 - Brij 58, the RST approximation of the zero value molar excess entropy cannot be taken. In the temperature interval T = (273.15–323.15) K, with increasing temperature, the thermodynamic stabilization of the binary mixed micelle Triton X100 - Brij 58 increases in an aqueous solution concerning the hypothetical ideal state (ideal binary mixed micelle).

References

[1] J. Aguiar, P. Carpena, J.A. Molina-Bolívar, C. Carnero Ruiz, On the determination of the critical micelle concentration by the pyrene 1:3 ratio method, J. Colloid Interface Sci. 258 (1) (2003) 116–122.

[2] S. Obradović, M. Poša, The influence of the structure of selected Brij and Tween homologues on the thermodynamic stability of their binary mixed micelles, J Chem. Thermodyn. 110 (2017) 41–50.

[3] M. Poša, A. Pilipović, Activity coefficient of Triton X100 and Brij S20 in the infinitely diluted micellar pseudophase of the binary micelle Triton X100 – Brij S20 in water phase at the temperature interval T = (283.15-318.15) K, J. Chem. Eng. Data 65 (2020) 106–119.

[4] P.L. Privalov, S.J. Gill, The hydrophobic effect: a reappraisal, Pure Appl. Chem. 61 (1989) 1097–1104.

APPLICABILITY OF DIELECTRIC MEASUREMENT IN WASTEWATER SLUDGE TREATMENTS

Zoltán Jákói[1,2], Cecilia Hodúr[2], Sándor Beszédes[1]

[1]Deparment of Biosystems Engineering, University of Szeged, H-6725 Szeged, Moszvkai krt. 9
[2]Doctoral School of Environmental Science, University of Szeged, H-6720 Szeged, Aradi vértanúk tere 1.
e-mail: jakoiz@mk.u-szeged.hu

Abstract
Our research work focused on the applicability of dielectric measurement methods in wastewater-sludge treatment processes. On the one hand, we wanted to investigate how the soluble chemical oxygen demand (SCOD) - a key characteristic in sewage sludge utilization - changes due to the different sludge pre-treatment processes, and whether these changes are in connection with the dielectric behaviour of the material matrix. In addition, we also investigated whether the anaerobic digestion of sewage sludge, as a bio-energy production method can be monitored by measuring certain dielectric properties. The experimental results revealed that there is a strong correlation between the change in SCOD of different types of wastewater sludge that occurs due to the applied pre-treatment methods and the dielectric constant (at f=450 MHz frequency), and we also found connection between the nascent biogas yield and the dielectric behaviour of the fermentation medium.

Introduction
Nowadays, with the growth of population, globalization and industrialization becoming more and more pronounced, it is essential to meet the ever-increasing energy demands of different industries, sectors, and services. Fossil fuels are finite and their economically viable exploitation is becoming increasingly difficult to sustain, therefor it is necessary to exploit the potential of alternative energy sources to maintain global energy stability, and to protect the environment.
Wastewater and wastewater sludge can be considered as a type of biomass, therefore their utilization for energy purposes can be considered as CO_2-neutral [1]. However, due to the complex physicochemical structure they have, a proper pre-treatment method (such as microwave or ultrasonic treatment, chemical extraction, thermal pre-treatment) is usually needed. These pre-treatment methods often aim to directly increase the soluble organic content in wastewaters, or to enhance the disintegration degree in wastewater sludge. These processes then can contribute to the more efficient utilization of wastewater and/or sludge [2].

The dielectric behavior of various (biological) materials and systems have been investigated for decades, with the aim of using the obtained results to design and optimize several biomass pre- and post-processing devices and equipment that operate at radio and microwave frequencies. Materials, when put into an electric or electromagnetic field behave differently, based upon their dielectric properties. The absolute permittivity (ε) of a material defines how well it can respond to an electromagnetic field *E*, and to what extent this field causes an electric displacement *D* in the material:

$$D = \varepsilon E \qquad (1)$$

The applied field *E* also plays a role in the dielectric polarization (*P*), which is defined by the electric susceptibility (χ):

$$P = \varepsilon_0 \cdot \chi \cdot E \tag{2}$$

ε_0 denotes the vacuum permittivity, which is $8.85 \cdot 10^{-12}$ A·s(V·m)$^{-1}$.

As opposed to vacuum, however, the polarization in normal materials does not occur in an instant, and therefore the generalized formula as a function of time should be used:

$$P(t) = \varepsilon_0 \int_{-\infty}^{t} \chi(t - t')E(t')\, dt' \rightarrow P(\omega) = \varepsilon_0 \chi(\omega)E(\omega) \tag{3}$$

From Eq. 3 it can be seen that dielectric polarization and susceptibility depends on the applied frequency, which lead to the frequency dependence of the permittivity as well. This reflects the fact that the response the material gives to the electromagnetic field can be defined basically as a phase shift (δ). Since the magnitude and phase can be determined at the same time only with complex numbers, the absolute permittivity should be addressed as a complex function of the frequency as follows:

$$\varepsilon^*(\omega) = \left|\frac{D}{E}\right| (cos\delta - i\, sin\delta) = \varepsilon'(\omega) - i\, \varepsilon"(\omega) \tag{4}$$

The real part of the complex function, ε‘ is the dielectric constant, which indicates the electric energy storing capacity of a given material. The imaginary part, ε“ is the dielectric loss factor, which (in lossy materials) covers the dielectric loss (often called as dissipation loss, which is due to the rotation and vibration of permanent or induced dipolar molecules) and the conductivity loss (which is caused by the displacement of charged particles, like free ions).

These parameters largely depend on the physicochemical properties of a given material and can drastically change when any of these properties undergo some sort of transformation. This observation supports the idea to use dielectric measurement in wastewater and sludge treatment and utilization, since during these processes, several physical and / or chemical changes happen in the material matrix. Studies have already shown that dielectric measurements can be applied in food industry to detect enzymatic reactions [3], in foresting to determine the moisture content of wood [4], and as we have already shown in one of our previous studies, to detect organic matter removal in industrial wastewater [5].

Experimental

The changes in the extent of SCOD were investigated for three different types of sludge: meat industry-originated, dairy industry-originated and concentrated municipal sludge. These sludge samples were subjected to the same pre-treatments and the SCOD was measured from the aqueous phase after each treatment, using a standard $K_2Cr_2O_7$-based COD cuvette test. The dielectric constant of the samples was then measured at a frequency of 2450 MHz using a SPEAG DAK 3.5 dielectric sensor, attached to a Rhode&Schwarz ZVL-3 vector network analyser. For the biogas fermentation process, meat industry wastewater sludge was used, and the anaerobic digestion was carried out under mesophilic conditions (38°C). The absolute pressure values in the fermenters were recorded with automatic manometric measuring heads, and the dielectric properties of the fermentation medium were measured every second day of the experiment with the aforementioned dielectric measurement kit, in the frequency range of 300-900 MHz.

Results and discussion

In the first part of the experiments, three different types of sludge were physically pre-treated with different intensities, and after each treatment the SCOD content of the samples was

measured, as well as the dielectric constant at a fixed frequency of 2450 MHz. The change in SCOD was given as a proportion to TCOD (total chemical oxygen demand), SCOD/TCOD.

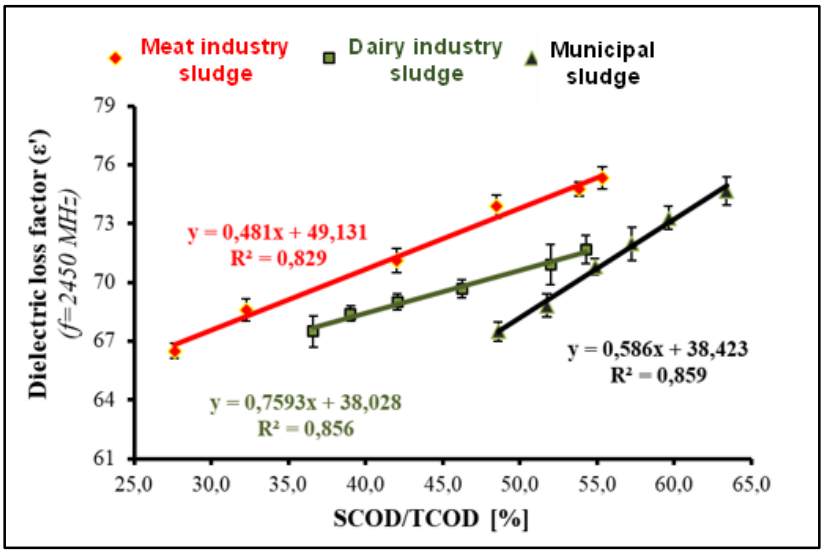

Figure 1. Correlations between SCOD/TCOD and the dielectric constant for the investigated sludge types

Based on the results, it can be concluded that the applied treatments modified the soluble COD content to different extents for different sludge types, which can be attributed to the different initial compositional proportions of the sludge samples (organic, inorganic, suspended solids, etc.) However, for all three types of sludge, there was a tendency for the SCOD values to change as a result of the treatments, with an increase in the water-soluble COD fraction, i.e. the amount of organic matter in the dissolved phase, proportional to the intensity of the treatments. The dielectric constant values determined for each sample showed a strong correlation with the water-soluble COD fraction; as the SCOD values increased, the dielectric constant values also became larger. This may be explained by the fact that the treatment, by disintegrating the sludge flocs, has resulted in the solubilization of organic molecules into the aqueous phase which are excitable at the applied microwave frequency and thus capable of absorbing more electrical energy.

In the anaerobic fermentation of meat industry sludge, the dielectric behaviour of the fermentation medium was monitored every second day of the digestion process in the frequency range of 300-900 MHz (this is the interval where the differences in the dielectric behaviour between the different materials / systems are the most observable, according to the excitation and relaxation frequencies generally typical for aqueous media). The data were analysed by comparing the maximum dielectric constant values and their corresponding frequency values for the fermentation day in the applied frequency range (Figure 2).

The results clearly show that as the anaerobic digestion process progresses, the maximum of the dielectric constant becomes lower and lower and the frequency value associated with the maximum becomes higher and higher over the frequency interval investigated. Approximating the relationship between the two variables with a second-order polynomial, the coefficient of determination is approximately 0,98, which clearly indicates a close correlation between the two values

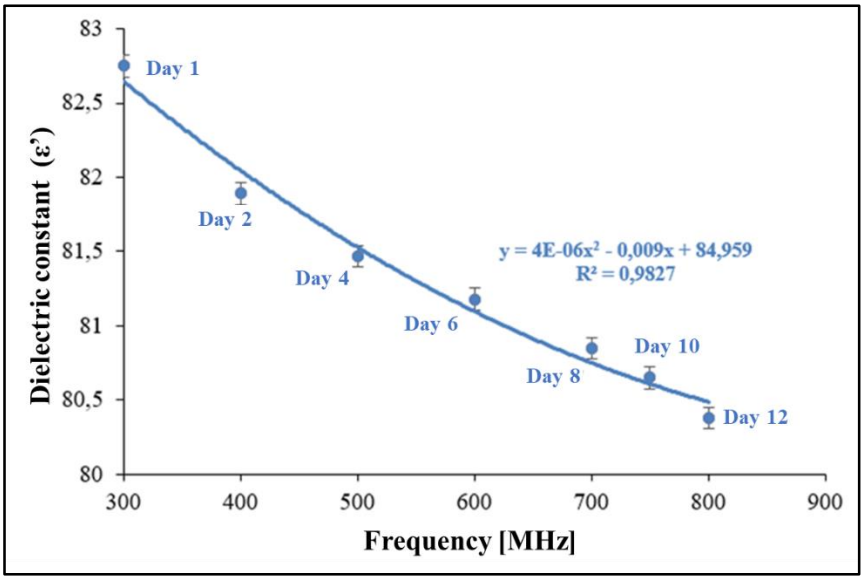

Figure 2. Frequency dependence of the maximum of the dielectric constant during anaerobic fermentation of meat industry-originated sludge

As the fermentation time progressed, the biogas yield varied according to the three distinct phases typical of anaerobic digestion (lag, log, stationery), with the stationery period occurring at the 12th day. Thus, the results support that while significant biochemical changes occur in the fermentation medium, these changes are also reflected in the dielectric behaviour, i.e. the measurement method is suitable for monitoring the different phases of anaerobic digestion.

Conclusion

Our experimental results have clearly proven that physical and chemical changes that occur in the media during wastewater and sewage sludge treatment and utilization processes can be monitored by determining the appropriate dielectric parameters – a strong correlation has been found between the change in SCOD of the pre-treated different sludge samples and the dielectric constant, as well as between the fermentation stage of the anaerobic digestion of sludge and the dielectric constant.

Acknowledgements

The research is supported by the ÚNKP-22-2-SZTE-199, UNKP-22-3-SZTE-204 and ÚNKP-22-5-SZTE-208 New National Excellence Program of the Ministry for Innovation and Technology from the source of the National Research Development and Innovation Fund, and by János Bolyai Research Scholarship of the Hungarian Academy of Sciences (BO/00161/21/4).

References

[1] Yentekakis V. I. and Goula G., *Front. Environ. Sci.*, 2017 (https://doi.org/10.3389/fenvs.2017.00007)

[2] A. Saravanan, V.C. Deivayanai, P. Senthil Kumar, Gayathri Rangasamy, R.V. Hemavathy, T. Harshana, N. Gayathri, Krishnapandi Alagumalai, *Chemosphere*, 2022 (https://doi.org/10.1016/j.chemosphere.2022.136524)

[3] Lievonen S.M.; Roos Y.H., *Innovative Food Science and Emerging Technolgoies*, 2003 (https://doi.org/10.1016/S1466-8564(03)00042-0)

[4] Salas W. A.; Ranson J. K.; Rock B. N.; Smith K.T., *Remote Sensing of Environment*, 1994 (https://doi.org/10.1016/0034-4257(94)90148-1)

[5] Z. Jákói, C. Hodúr, Zs. László, S. Beszédes, *Water Science and Technology*, 2018 (https:// doi:10.2166/wst.2018.491.)

LEVELS AND ORIGIN OF POLYCYCLIC AROMATIC HYDROCARBONS IN FLUVIAL SEDIMENT OF DRAVA RIVER

Mária Mörtl,[1] Győző Jordán,[2] András Székács [1]

[1]Agro-Environmental Research Centre, Institute of Environmental Sciences, Hungarian University of Agriculture and Life Sciences, Herman Ottó u. 15, H-1022 Budapest, Hungary
[2]Institute for Earth Sciences, ELTE Eötvös Loránd University, Pázmány Péter sétány 1/A, H-1117 Budapest, Hungary
e-mail: Mortl.Maria@uni-mate.hu

Abstract
Within the scope of an international monitoring program to assess water and sediment quality in the Danube basin, sediment samples (river bottom/bank, suspended and active floodplain/overbank) were collected in the summer of 2020 at a sampling site in the Drava river to monitor 19 polycyclic aromatic hydrocarbons (PAHs) as apparent water contaminants. Among these, 8 PAHs were specified as priority pollutants in the corresponding EU Directive on environmental quality standards (2008/105/EC). The highest levels were measured for fluoranthene (1.73 μg/g), benzo(b)fluoranthene+benzo(k)fluoranthene (0.765 μg/g) and anthracene (0.528 μg/g) sampled from the upper 5 cm layer of the bottom sediment on 5th August 2020.

Introduction
In the frame of the SIMONA project (DTP2-093-2.1) titled "Sediment-quality Information, Monitoring and Assessment System to support transnational cooperation for joint Danube Basin water management" [1], development and test of a monitoring system was carried out in test area at Drava River (Barcs, Hungary) in August 2020. Different sampling methods were compared in order to develop the harmonized sampling protocol [2] and the different sediment types were separately analyzed for different classes of pollutants (potentially toxic elements/metals, pesticides, and PAHs). The main parts of the system included a) a sediment box for collection of suspended particles, b) sensors for recording different physicochemical parameter (e.g., temperature, turbidity, dissolved oxygen level, pH), and c) passive samplers for uptake of different contaminants. Here we report the results of PAH analyses for samples taken by vacuum core-sampler (bottom sediment), spade or cake sampler (floodplain sediment) and by using a barrel for collection of water (suspended sediment). In the cases of vacuum corer and spade, sediments from two different depths were collected. Upon sample preparation and instrumental analysis, isomer ratios were calculated based on the analytical results to determine the possible origin of PAH contamination (pyrogenic or petrogenic).

Experimental
For the monitoring program, the sampling site was set up on the Drava river (Barcs, Hungary). Coordinates of the site were: WGS Lat (N) 45.95088, Long (E) 17.44650. Sampling was carried out from 5th to 8th of August in 2020.
Different sampler devices were used to collect sediment samples. Bottom sediment samples were collected by a vacuum core-sampler, and the PAH content of upper 5 cm and that of the subsequent 5 to 10 cm layer were determined. Suspended sediment samples were collected together with 30-liter batches of water into a barrel using a pump. The fine material that settled from the water collected was filtered in the laboratory. Active floodplain/overbank sediments were sampled using a spade or a cake sampler, at depths level of 0–5 cm in the topsoil (or top

layer). Another type of sample was also collected from the 40–50 cm bottom layer. The same harmonized methodology was used for the sediment sampling, performed in other test areas of the Danube river basin in the frame of SIMONA project [4-6]

Instrumental analysis was performed at the premises of Bálint Analitika Ltd. using a GC-MS method with an ion trap mass detector operating in the selective ion monitoring mode for determination of the 19 target PAH compounds. The list of these priority pollutants issued by the U.S. Environmental Protection Agency (EPA) in 1976 [3] contains 16 PAHs, which are routinely analyzed in environmental samples. Among these compounds 8 are on the list of priority compounds in the field of water policy in the European Union [7,8] as well, and 6 of them are identified as priority hazardous substances (Table 1). In addition, 3 PAH compounds (2-methyl-naphthalene, 1-methyl-naphthalene, benzo(e)pyrene) were also determined in the different sediment phases collected. Total PAH concentrations incluuded the levels of acenaphthene, acenaphthylene, benz(a)anthracene, chrysene, dibenzo(ah)anthracene, fluorene, phenanthrene and pyrene as well.

Table 1. Priority pollutant and other contaminant polyaromatic hydrocarbon (PAH) substances analysed in the present sediment monitoring study

Category	**Substance**	**Rings**	**logK_{ow} ***
Priority substances	naphthalene	2	3.28
	fluoranthene	4	4.90
Priority hazardous substances	anthracene	3	4.45
	benzo(a)pyrene	5	6.06
	benzo(b)fluoranthene	5	6.04
	benzo(k)fluoranthene	5	6.06
	benzo(g,h,i)perylene	6	6.50
	indeno(1,2,3-cd)pyrene	6	6.58
Additional measured compounds	1-methyl-naphthalene	2	3.87
	2-methyl-naphthalene	2	3.86
	benzo(e)pyrene	5	6.44

* The octanol-water partition coefficient: a measure of lipophilicity.

Results and discussion

Regarding the PAH residues, the pollution pattern and trends were in accordance with our expectations. Bottom sediment samples collected by the vacuum core-sampler had the highest PAH content, but differences between the upper 5 cm and the 5–10 cm layer were not straightforward. Typical levels were between the limit of detection (LOD=0.001 µg/g) and 0.006 µg/g. The highest levels were measured for fluoranthene (1.73 µg/g), benzo(b)fluoranthene + benzo(k)fluoranthene (0.765 µg/g) and anthracene (0.528 µg/g) sampled from the upper 5 cm on 5th August 2020 at the the Drava river. The second highest values were determined for the sample taken at the same site from the 5–10 cm layer, but containing the highest amounts of phenanthrene (1.05 µg/g), naphthalene (0.949 µg/g) and 2-methyl-naphthalene (0.719 µg/g) with significant amounts of fluorene (0.449 µg/g) and pyrene (0.355 µg/g).

The point samples collected into the barrel contained little amounts of suspended sediment. Although all target PAHs were detected, but amounts remained mostly close to the LOD. Levels in the suspended sediment phase exceeded the limit of quantitation (LOQ) for anthracene, benzo(a)pyrene, benzo(b)fluoranthene + benzo(k)fluoranthene, benzo(g,h,i)perylene, fluoranthene and indeno(1,2,3-cd)pyrene. The highest levels were determined for fluoranthene

(0.281 µg/g) and anthracene (0.292 µg/g) sampled on 5th August 2020 in Drava River. To improve the reliability of the analytical measurement, amounts of the sample could be increased by using a centrifuge additionally to remove floating material for the water phase, or applying a standardized sediment box for long-term collection, which partially separates the suspended sediment by the baffles of the box.

Sampling of floodplain sediment at two depths had the objective to identify in the analyzed samples recent contamination transported by the flood events and the pre-industrial natural background. Samples taken from the bottom layer (40–50 cm) contained only very low levels of PAHs near to the LOD. The top layer contained also low levels, and the highest concentration was measured for benzo(b)fluoranthene + benzo(k)fluoranthene (0.078 µg/g). That sample was taken by cake sampler and the corresponding value for the sample collected by spade contained only 0.060 µg/g. Some amounts of fluoranthene (0.052 µg/g) and benzo(a)pyrene (0.041 µg/g) also appeared in the same sample.

Fresh loads enter the water phase either from atmospheric depositions or from urban run-off, and different other sources appear first in the suspended sediment, as due to their hydrophobic characters their water solubility being very low. Elder contamination bound to the particulate matter are finally deposited in the bottom sediment, where slow microbial metabolism leads to the degradation of PAHs. The higher the molecular weight and the higher the octanol-water partition coefficient ($\log K_{ow}$), the slower the degradation rate. Resuspension during flood events can mobilize PAH substance, which may increase their levels in the active floodplain sediment. On the other hand, consumption and metalibolization of PAHs by aquatic species may eliminate some of the accumulated contamination from the bottom sediment.

The octanol-water partition coefficient ($\log K_{ow}$) values for the target components ranged between 3.28 and 6.58, thus, PAHs with five or more rings are proposed to be monitored in the sediment phase ($\log K_{ow} > 5$), whereas PAHs with two to four rings appear in both (water and sediment) phases ($\log K_{ow} = 3\text{-}5$). However, based on the experimental data [9], high molecular weight PAH compounds (5 or 6 rings) contributed up to 11% to the total PAH content in the non-filtered Danube river water sample. Due to the strong affinity of the target compounds to the particulate matter, filtration during sample preparation of water removes most of the hydrophobic pollutants together with the suspended sediment, which substantially influences the results of the chemical analysis. In the bottom sediment samples in our survey the four-ring PAHs dominated, whereas in suspended sediment the four- and five-ring species were equally dominant, and in flood plain sediment the most abundant group belonged to the five-ring isomers (Fig. 1.).

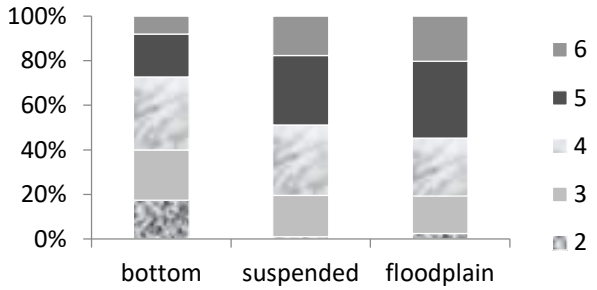

Figure 1. Composition pattern of PAH compounds measured in bottom, suspended and floodplain sediments.

The origin of the PAH contamination was determined by using the isomer ratios of different pairs. There are several molecular indices, calculated from the corresponding concentrations, that can be used for identification of the pollution source. We have used ratios for 4 isomer

pairs to identify the possible sources (see Fig. 2). Worthy of note, that zero values indicated that anthracene, fluoranthene, benz(a)anthracene or indeno(1,2,3-cd)pyrene were not detected in the corresponding sample and numberous 0.5 values for the Drava samples originate from the fact that the level of target compounds were near to limit of detection and therefore the ratio from LODs was 1:2. Nevertheless, the other values may vary as they are presented in Fig. 2.

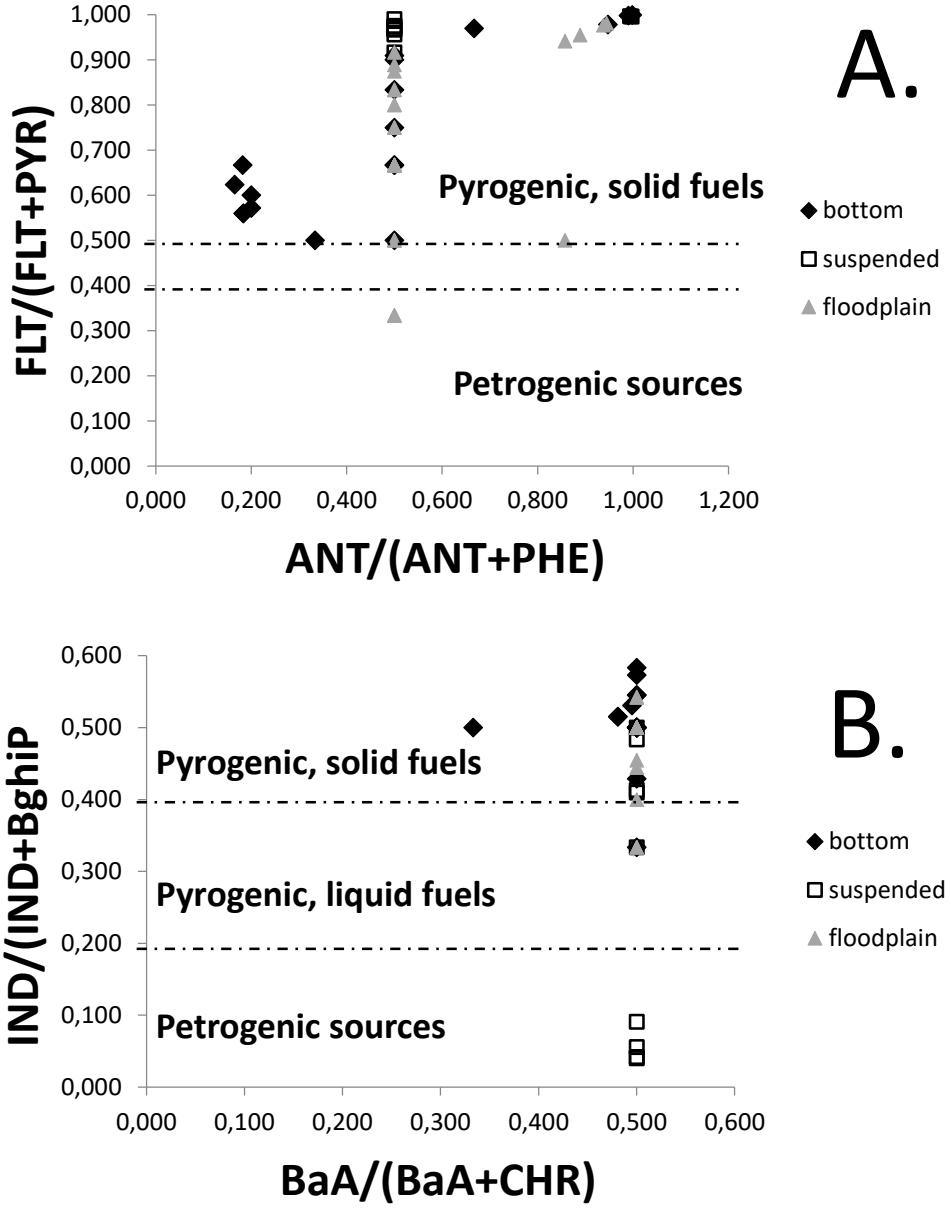

Figure 2. Cross-plot for the concentration ratios **A.** of anthracene/(anthracene + phenanthrene) (ANT/(ANT+PHE)) versus fluoranthene/(fluoranthene + pyrene) (FLT/(FLT+PYR)) and **B.** benz(a)anthracene /(benz(a)anthracene + chrysene) (BaA/(BaA+CHR)) versus indeno(1,2,3-cd)pyrene/(indeno(1,2,3-cd)pyrene + benzo(g,h,i)perylene) (IND/(IND+BghiP)) in sediments.

Typical levels were low for all types of the sediment samples taken at Drava sampling site. Ratios of anthracene/(anthracene + phenanthrene) were above 0.1 in every samples, indicating the pyrogenic origin of PAH contamination. Combustion of solid fuels as a source was confirmed by all values calculated for fluoranthene/(fluoranthene + pyrene) except three floodplain samples. Worthy of note that in these cases the concentrations of fluoranthene and pyrene were very low (LOD). Both benz(a)anthracene and chrysene levels were near to LODs,

but indeno(1,2,3-cd)pyrene/(indeno(1,2,3-cd)pyrene + benzo(g,h,i)perylene) values below 0.2 for 4 suspended sediment samples suggested petrogenic origin of PAH compounds, however indeno(1,2,3-cd)pyrene levels were around the LOD. The ratios for the remaining suspended sediment samples (0.2–0.5) indicated that combustion of liquid fuels is the main source, and also about the half of the floodplain samples belonged to this category. The calculated values for the rest of the flood plain samples were 0.5, although they contained indeno(1,2,3-cd)pyrene and benzo(g,h,i)perylene, but only near the LODs. Combustion of solid fuels was the dominant source in bottom sediment samples, except for a single case, where the ratio, calculated from the LOD for indeno(1,2,3-cd)pyrene, correlated presumably to the combustion of liquid fuels.

Conclusion

PAH contamination levels in the sediment of the Drava river are low, although all the 19 PAH components monitored in this study could be detected. The highest concentrations appeared in the bottom sediment followed by the suspended sediment, and the lowest amounts were determined in the floodplain sediment. Among the PAH compounds, the groups containing 4 or 5 rings dominated, and the larger molecules are more abundant in the floodplain sediment. Possible sources of PAH contamination are mostly related to the combustion of solid fuels.

Acknowledgements

The work was supported by the DTP2-093-2.1 SIMONA project (2018-2021). The work has been carried out as a part of a joint effort by the SIMONA Project Team [1]. Many thanks to the Bálint Analitika Ltd. (Budapest, Hungary) taking part in the method development and providing analytical data as well.

References

[1] SIMONA – Sediment-quality Information, Monitoring and Assessment System to support transnational cooperation for joint Danube Basin water management; Interreg Danube Transnational Programme: Budapest, Hungary, 2022. Available online: http://www.interreg-danube.eu/approved-projects/simona (accessed on 26 October 2022).
[2] A. Šorša, the SIMONA Project Team. 2019. Sediment quality sampling protocol for HSs. EU Interreg Danube Transnational Programme, 45 p. Available online: https://www.interreg-danube.eu/uploads/media/approved_project_output/0001/49/a478eafbee66d5b1ad8f7ad86f830e4a2b05d18b.pdf (accessed on 26 October 2022).
[3] L. Keith, Polycylic Aromatic Compounds 35(2-4) (2015) 147–160.
[4] A. Vîjdea et al., Carpathian J. Earth Environ. Sci. 17(2) (2022) 425 – 440.
[5] G. Damian et al., Carpathian J. Earth Environ. Sci. 17(2) (2022) 441 – 458.
[6] A. Šorša et al., Carpathian J. Earth Environ. Sci. 17(2) (2022) 459 – 468.
[7] Priority Substances and Certain Other Pollutants according to Annex II of Directive 2008/105/EC, OJ L 348, 24.12.2008 p. 84.
[8] Directive 2013/39/EU of the European Parliament and of the Council of 12 August 2013 amending Directives 2000/60/EC and 2008/105/EC as regards priority substances in the field of water policy. OJ. L 226. p. 1-17.
[9] A.S. Nagy, G. Simon, J. Szabó, I. Vass, Environ. Monit. Assess. 185 (2013) 4619-4631.

CHALLANGES OF VERTICALLY ALIGNED CARBON NANOTUBES PRODUCTION AND APPLICATION

Lilla Nánai, Klára Hernádi

Faculty of Materials and Chemical Engineering,
Institute of Physical Metallurgy, Metal Forming and Nanotechnology
University of Miskolc, 3515 Miskolc-Egyetemváros, C/1 108, Hungary
e-mail: nanai.lilla@student.uni-miskolc.hu

Abstract

Carbon nanotubes (CNTs) have play a dominant role in nanotechnology research for over 20 years due to their exceptional properties. Different solid catalytic substrates can be used to produce vertically aligned carbon nanotubes (VACNTs); however it is important that this structure can be achieved mainly on conductive substrates. It is important that further application of this structure is preferable on conductive substrates. The conditions under which the catalytic layer is prepared and synthesized also have major impact on the structure and properties of the resulting vertically aligned carbon nanotubes. Environmental protection and green chemistry are highly discussed topics nowadays. Therefore, the development of energy-efficient, sustainable technological solutions is also receiving increasing attention in vertically aligned carbon nanotubes research. Thus, the progress in this direction will be briefly review in this work.

Introduction

Green chemistry and sustainable techniques are focusing on the use of non-hazardous substances, plant extracts as the main precursors, and solvents that are not harmful to the environment. In the field of carbon nanotubes, the vertically aligned carbon nanotubes with their 3 dimensional structure are considered as a seperate branch, first fabricated in 1996 [1] and often referred to in the literature as CNT forests due to their distinctive structure.

The industrial application of VACNTs demands the technical development of large-scale and defect-free production techniques, where the chemical vapor technique has proven to be a promising process for large-scale and high purity production of carbon nanotubes [2]. Methods to fabricate VACNTs are still not at the desired level and further development is needed. This "imperfection" is beneficial for the development of environmentally friendly and sustainable technologies. Currently, only the chemical vapor deposition technique (CVD) and its subtypes are suitable for the production of VACNTs. There are three main directions for the development of environmentally friendly production of carbon nanotube forests. The first one is to replace the carbon sources currently used by using non-toxic, plant-derived or plastic waste, the second is to use equally precise but less energy-consuming methods for the catalyst layer deposition, and finally to improve the technical development of the synthesis method itself [3]. In the literature, there is a growing number of results where VACNTs are produced at lower temperatures of 550 °C, which initially was mainly around 800-900 °C, however, the choice of parameters used in the experiments is of course influenced by a number of factors.

Due to their remarkable physicochemical and mechanical properties VACNTs have extensive potential and application in a broad range of science and technology, emerging nano- and microelectronic devices and industry [4]. These materials can be considered as the elementary unit of molecular electrical circuits and can be used not only as a link between the active molecular elements of a device, but can also serve as a device element themselves [5]. In addition to more environmentally friendly synthesis, environmentally friendly application is

also an important goal. VACNTs have several promising applications, such as lightweight and strong composites, supercapacitors, microelectromechanical systems (MEMS), electrodes, batteries *etc.* due to their special electrical properties [3,6,7].

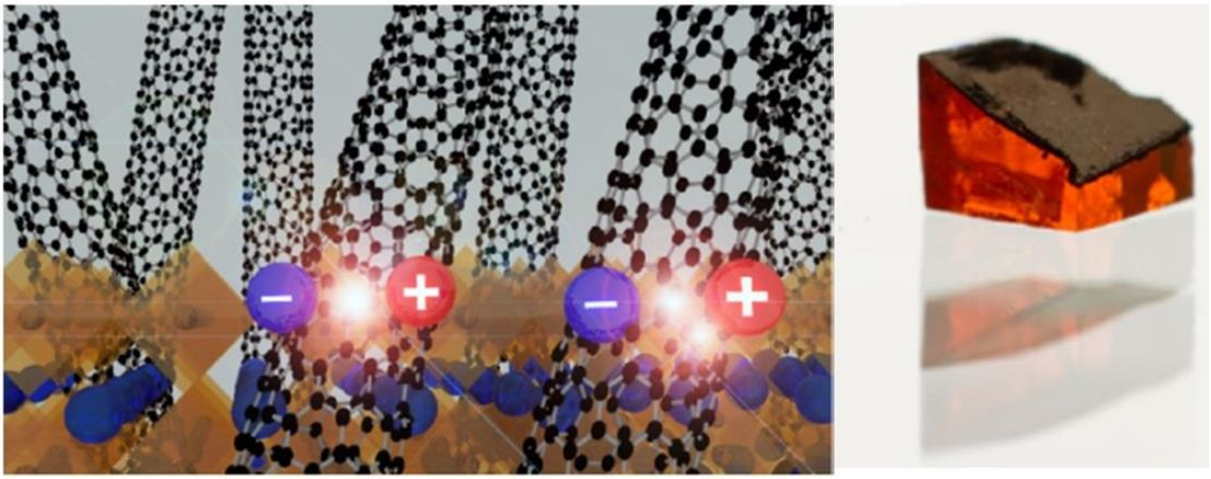

Figure 1. Single crystals of of methylammonium lead bromide ($MAPbBr_3$) grown directly on vertically alligned carbon nanotubes [7]

Experimental

During the syntheses of VACNTs, substrates are used to provide a base for growing CNT forests. On this substrate, a catalyst layer is formed by a thin layer building method, on which the growth of carbon nanotubes is achieved. Many materials can be used as substrates, depending on the purpose of use, but mainly metals (aluminium, copper, stainless steal, titanium), silicon and glass with or without transparent conductive oxide layers are used during the synthesis. Also there is a wide variaty of thin layer coating methods such as atomic layer deposition (ALD), dip coating, magnetron sputtering (MS), pulsed layer deposition (PLD), spin coating, spray coating, to build the catalyst layer on the surface of the substrate. These methods are suitable to control the parameters of catalyst layers, but there are large differences in their material, energy and cost requirements which vary significantly. Transition metals (Fe, Co, Ni, Mo *etc.*) and their alloys are mostly used as catalysts for the synthesis of CNT forests, which ensure the growth of carbon nanotubes and determine their yield and structure. During the CVD synthesis, first inert gas flows in the system, followed by hydrogen gas to create a reductive environment and then the carbon source is introduced, which decomposes into its components under the effect of both the presence of catalyst and high temperature and carbon is deposited on the catalyst particles, which initiate the growth of carbon nanotubes. Water vapor is also a common component in the synthesis process, which ensures that amorphous carbon is oxidized from the surface of the catalyst particles, thus regenerating the catalyst and improves the quality of CNTs, contributing to the height of VACNTs.

Results and discussion

In this section, the circumstances of the synthesis of VACNTs and the materials will be briefly described, as well as the efforts to make them environmentally friendly. Unfotrunately, it is a clear issue in the literature that the structure and the properties of VACNTs are affected by multiple factors during their fabrication, which is why VACNTs are underperfomed in large-scale, industrial production compared to carbon fibers and CNTs.

As it was described before in the experimental section, a thin catalyst layer is formed on the surface of the substrate, the CNT forests are grown on the surface at high temperature (600-1200 °C) *via* CVD technique.

During the synthesis inert gas is needed to provide inert environment, uniform gas flow rate in the system and to remove by-products from the system. Noble gases (Ar, He) and nitrogen gas have been used as inert gas during VACNT synthesis. The great advantage of nitrogen over noble gases is that it can be produced relatively cheaply and with simple industrial technology, yet it is chemically stable under extreme conditions of synthesis and can create a pseudo-inert environment.

The synthesis of VACNTs also requires reducing gas, in order to activate the catalyst particles on the substrate surface and to influence the catalyst particles diameter, as it is known that the catalyst distributions influence the height and structure of VACNTs. H_2 and NH_3 gases are mainly used as reducing agents, where H_2 favours uniform catalyst nanoparticles distributions and NH_3 forms mainly large clusters [8].

The range of carbon sources, which are suitable to produce carbon nanotubes, is reasonably wide. At the beginning only gaseous phase materials, mainly short-chain hydrocarbons (ethylene, methane, acetylene, natural gas, *etc.*), later organic solvents (ethanol, tholuol, acetone, cyclohexane, diethyl ether *etc.*) were used as well [9] and it was observed that small amount of oxygen-containing carbon compounds resulted low height VACNTs, on the otherhand selectivity is lower, amorphous carbon and carbon fibers were present as well. Nowadays many experiments can be found about CNTs and VACNTs where green resources such as biomass and plant extracts, CO_2 and plastic waste [10][11] [12] are used as carbon source.

Water vapor plays an important role in the synthesis of VACNT, extending the activity and lifetime of the catalyst particles by removing the amorphous carbon deposited on their surface, and improves the height, the quality and the structure of carbon nanotubes [13]. However, it is also important to consider the flow rate of water vapor, because if there is too much in the system, it will oxidize the outer walls of the carbon nanotubes as well, which will degrade the otherwise good conductive properties.

Conclusion

In summary, there is still a lot of development and work to be done before VACNTs can be manufactured industrially, but current awareness and ongoing research are working to make this process as environmentally friendly and sustainable as possible. Many researchers expect to be able to produce VACNTs and other carbon nanomaterials by using CO_2, the greenhouse gas with the highest concentration, and from the large amount of plastic waste around us in the near future. However, there are still many obstacles to overcome and resolve.

References

[1] Li, W. Z., Xie, S. S., Qian, L. X., Chang, B. H., Zou, B. S., Zhou, W. Y., Sci., vol. 274, pp. 1701–1703, **1996.**

[2] B. M. Chufa, H. C. A. Murthy, B. A. Gonfa, and T. Y. Anshebo, Green Chem. Lett. Rev., vol. 14, pp. 647–664, **2021.**

[3] E. Mostafavi, S. Iravani, R. S. Varma, M. Khatami, and F. Rahbarizadeh, Mater. Adv., vol. 3, pp. 4765–4782, **2022.**

[4] J. J. Schneider, Adv. Biosyst., vol. 1, p. 1700101, **2017.**

[5] B. J. Brownlee, J. C. Claussen, and B. D. Iverson, ACS Appl. Nano Mater., vol. 3, pp. 10166–10175, **2020.**

[6] S. M. Ubnoske, E. J. Radauscher, E. R. Meshot, B. R. Stoner, C. B. Parker, and J. T. Glass, Carbon N. Y., vol. 113, pp. 192–204, **2017.**

[7] P. Andričević, M. Kollár, X. Mettan, B. Náfrádi, A. Sienkiewicz, D. Fejes, K. Hernadi, L. Forró, and E. Horváth, J. Phys. Chem. C, vol. 121, pp. 13549–13556, **2017.**

[8] R. Pezone, S. Vollebregt, P. M. Sarro, and S. Unnikrishnan, Carbon N. Y., vol. 170, pp. 384–393, **2020.**
[9] A. Szabó, L. Nánai, Z. R. Tóth, and K. Hernadi, Solid State Sci., vol. 117, p. 106648, **2021.**
[10] N. Tripathi, V. Pavelyev, and S. S. Islam, Appl. Nanosci., vol. 7, pp. 557–566, **2017.**
[11] T. Sato, H. Sugime, and S. Noda, *Carbon N. Y.*, vol. 136, pp. 143–149, **2018.**
[12] L. Dai, O. Karakas, Y. Cheng, K. Cobb, P. Chen, and R. Ruan, Chem. Eng. J., vol. 453, p. 139725, **2023.**
[13] K. Hata, D. N. Futaba, K. Mizuno, T. Namai, M. Yumura, and S. Iijima, Scie., vol. 306, pp. 1362–1364, **2004.**

HPLC SEPARATIONS OF *N*-AZOLE COMPOUNDS IN POLAR ORGANIC AND NORMAL PHASE MODE UTILIZING AMYLOSE-BASED CHIRAL STATIONARY PHASES

Gábor Németi[a], Tam Le Minh[b], Zsolt Szakonyi[b] Antal Péter[a], István Ilisz[*a]

[a]*Institute of Pharmaceutical Analysis, University of Szeged, H-6720 Szeged, Somogyi u. 4, Hungary*
[b]*Institute of Pharmaceutical Chemistry, University of Szeged, Eötvös u. 6, H-6720 Szeged, Hungary*
e-mail: ilisz.istvan@szte.hu

The enantioseparation of potential pharmacons with *N*-azole and *N*-benzoazole functional groups attached to lactone and amide skeletons was investigated using amylose-based chiral stationary phases. The influence of acid and base additives was found to affect enantiorecognitions and retentions slightly in both normal phase (NPM) and polar organic mode (POM). The effect of mobile phase composition on the enantioseparation was investigated in both modes, and several examples for the reversal of enantiomer elution order were found. Based on the chromatographic parameters relationships were evaluated between the structure of the selector and selectand. The hysteresis effect of Phenomenex Lux Amylose-1 (amylose tris-(3,5-dimethylphenylcarbamate)) column was investigated under various conditions in POM. Importance of the column pretreatment has been proven in both NPM and POM in case of the applied lactone and amide compounds.

Acknowledgments
Supported by the ÚNKP-22-3-SZTE-156 New National Excellence Program of the Ministry for Culture and Innovation from the source of the National Research, Development and Innovation Fund. This work was also supported by National Research, Development and Innovation Office-NKFIA through projects K137607. Project no. TKP2021-EGA-32 has been implemented with the support provided by the Ministry of Innovation and Technology of Hungary from the National Research, Development and Innovation Fund, financed under the TKP2021-EGA funding scheme.

MAGNETIC NANOCOMPOSITES WITH MESOPOROUS STRUCTURES: A PROMISING ADSORBENT FOR THE REMOVAL OF ANIONIC AND CATIONIC DYES FROM AQUEOUS SOLUTIONS

Roxana Nicola[1], Simona-Gabriela Muntean[1], Maria-Andreea Nistor[1], Ana-Maria Putz[1], Cătălin Ianăşi[1], László Almásy[2], Liviu Săcărescu[3]

[1]*"Coriolan Drăgulescu" Institute of Chemistry, Romanian Academy, Bv. Mihai Viteazu, No. 24, 300223 Timisoara, Romania*
[2]*Wigner Research Centre for Physics, Institute for Solid State Physics and Optics, POB 49, Budapest 1525, Hungary*
[3]*Institute of Macromolecular Chemistry "Petru Poni", Aleea Grigore Ghica Voda, nr. 41A, 700487 Iasi, Romania*
e-mail: cc.roxana@yahoo.com

Abstract

The presence of synthetic organic dyes in water represents an environmental and ecological issues worldwide and requires feasible solutions in face of the short-term risk to human health and stability of eco-systems. Therefore, the magnetic mesoporous composites (MMC) were synthesized by surfactant template sol–gel method, using cetyl-trimethylammonium bromide (CTAB) as mesoporous structure generator and investigated for anionic and cationic dyes removal from aqueous solutions. The magnetic iron oxide nanoparticles were obtained by reverse co-precipitation, followed by mesoporous silica coating through modifed sol–gel method. The obtained materials were characterized by FT-IR spectroscopy, X-ray difraction, transmission electron microscopy, Mössbauer spectroscopy, nitrogen adsorption, small-angle X-ray scattering and magnetization measurements. The infuence of CTAB amount on the morpho-textural and structural properties of nanocomposites was studied. XRD and Mössbauer spectroscopy showed that the obtained nanocomposites were composed of pure maghemite nanoparticles, and TEM images revealed particles size around 10 nm, embedded in silica matrix. The combination of magnetic properties and high surface area values made suitable the obtained nanocomposites to be used as adsorbents. The obtained magnetic nanocomposites present high surface area values, high removal efficiency of dyes, even after four adsorbtion-desorbtion cycles, and magnetic properties, facilitating the removal of adsorbents from aqueous media.

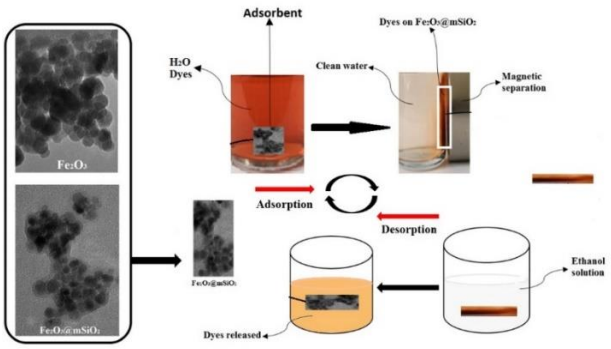

Figure 1. Illustration of the removal of dyes from aqueous media using magnetic nanocomposites with mesoporous structures

This work was supported by Program 4 of the "Coriolan Dragulescu" Institute of Chemistry, Research Projects and 4.2 and the authors thanks to Romanian Academy.

SYNTHESIS AND APPLICATION OF MAGNETIC NANOCOMPOSITES AS ADSORBENT FOR THE REMOVAL OF DYES FROM COLORED WASTEWATER

Maria Andreea Nistor[1], Simona Gabriela Muntean[1*], Robert Ianoș[2], Otilia Costișor[1]

[1]*Institute of Chemistry Timisoara of Romanian Academy, 24 Mihai Viteazul Bvd., 300223, Timisoara, Romania*
[2] *Politehnica University Timişoara, Faculty of Industrial Chemistry and Environmental Engineering, 6 Pîrvan Blv., RO-300223, Timisoara, Romania*
e-mail: *sgmuntean@acad-icht.tm.edu.ro*

Abstract

Wastewater containing dye pollutants caused by textile industry has become one of the most serious threats to ecological system [1]. Adsorption is one of the most advantageous techniques applied for the removal of non-biodegradable dyes from wastewater, due to its simplicity, efficiency and relatively low costs [2]. In recent years the application of magnetic nanocomposites as adsorbent materials has been investigated due to their unique physical and chemical properties [3,4].

In this work, new magnetite/carbon nanocomposites (MCN) were synthesized by the combustion method [5], varying the magnetite/carbon ratio in their composition. The synthesized materials were characterized by the most indicated and modern methods: X-Ray Diffraction, Fourier transform infrared spectroscopy, magnetic properties, N_2 adsorption-desorption isotherm, Thermal analysis and Scanning Electron Microscopy. The synthetized materials were applied as adsorbents for the removal of an anionic (Acid Orange 7 (AO7)) and a cationic (Rhodamine 6 G (R6G)) dyes.

The MCN materials have a specific surface between 485-1095 m^2/g and a saturation magnetization between 0.67-14.30 emu/g. With increasing carbon content, the specific surface area of the materials increased and also the dye removal efficiency, from 91.24% to 95.12% for AO7 and from 92.35% to 98.92% for R6G. Further studies were performed using sample MCN_3 containing magnetite:carbon in a ratio of 1:4.

The effect of the working conditions: solution pH (2÷12), the amount of adsorbent (0.25÷3 g/L), the initial dye concentration (10÷250 mg/L) and temperature (25°C, 40°C and 55°C), on the dyes removal efficiency was studied. Removal yields of the investigated dyes of over 92% (AO7) and 98% (R6G) were obtained working under normal conditions: solution pH and room temperature (25°C).

The absorption capacity of the MCN_3 nanocomposite was further evaluated for the simultaneous adsorption of investigated dyes from binary systems. For this purpose, the optimal working conditions established for the adsorption of dyes from single systems, were selected as initial conditions for the adsorption from the binary systems. For the simultaneous adsorption of dyes, the removal efficiency decreased (74.13% for AO7, and 77.61% for R6G), which indicated that in the bicomponent system the adsorption of dyes is competitive.

Kinetic studies indicated that the adsorption process was best described by the pseudo second order model for investigated dyes. The data obtained at equilibrium fitted best with Sips isotherm model, and the maximum adsorption capacities were determined as: 136.36 mg/g for AO7 and 266.87 for R6G. The determined values for thermodynamic parameters: Gibbs free energy (ΔG^0), enthalpy (ΔH^0), and entropy (ΔS^0) showed that the adsorption is a spontaneous and endothermic process.

The very good capacity of regeneration and reuse of the MCN_3 nanocomposite were highlighted by the yields of more than 75% obtained for the removal of the investigated dyes, even after six simultaneous adsorption-desorption cycles (Fig. 1).

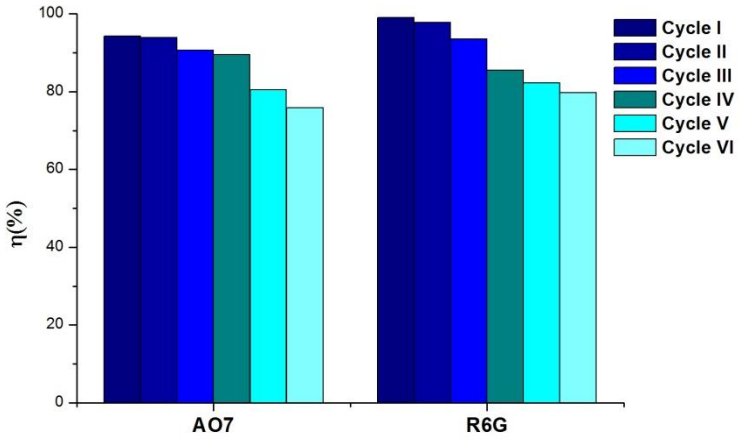

Fig.1. Reusability of MCN_3 nanocomposite in adsorption/desorption cycles

The experimental results obtained, demonstrate that the synthesized nanocomposites can be successfully used as adsorbents for the removal of the dyes from single and binary systems, even working under normal conditions (solution pH, room temperature), which is important for a possible application for the decontamination of colored industrial wastewater.

Acknowledgements
This work was supported by Program no. 2 of the "Coriolan Drăgulescu" Institute of Chemistry of Romanian, Research Project no. 2.4

References
[1] S. Jing, X. Wang, Y. Tan, Appl. Surf. Sci. 441 (2018) 654–662.
[2] S. Gao, W. Zhang, Z. An, S. Kong, D. Chen, *Adsorpt. Sci. Technol.* 37 (2019) 185-204.
[3] C. Păcurariu, G. Mihoc, A. Popa, S. Muntean, R. Ianoș, *Chem. Eng. J.* 222 (2013) 218-227.
[4] M.A. Nistor, L. Halip. S.G. Muntean, L. Kurunczi, O. Costișor, Sustain. Chem. Pharm. 29 (2022) 100778.
[5] R. Ianoș, C. Păcurariu, G. Mihoc, Ceram. Int., 40 (2014) 13649-13657.

APPLICATION OF MEMBRANE SEPARATION AND ADSORPTION FOR NUTRIENT RECOVERY FROM DAIRY WASTE WATERS

Fernanda Pantoja[1], Elias Sisay[1], Sándor Beszédes[2], Zsuzsanna László[2]

[1]*Doctoral School of Environmental Sciences, University of Szeged, H-6720 Szeged, Rerrich tér, Hungary*
[2]*Department of Process Engineering, University of Szeged, H-6725 Szeged, Moszkvai krt.9, Hungary*
e-mail: fliceth@hotmail.com

Abstract
Among the current environmental challenges facing humanity is the protection of water in quantity and quality. The objective of reduce to zero the generation of waste in productive activities by applying the concept of circular economy has led to the emergence of proposals for the production of biomaterials capable of contributing to environmental protection and that do not imply huge investments of money. As a good example of these proposals, biochar had to be mentioned which is a material with excellent adsorbent properties, with low production costs and that is made with any type of organic matter such as agricultural waste. In this work a nanoparticle-modified ultrafiltration membrane was used as a pre-treatment method prior to ammonium adsorption. As adsorbent for ammonium removal alkaline modified biochar produced from banana leaves were used. The characterization of biochar and the research about kinetics and isotherm models obtained after batch experiments. The general results obtained after the combination of membrane filtration and adsorption are promising and reflect a satisfactory ammonium removal percentage, and these results prove that biochar would be a good adsorbent for nutrient recovery from wastewaters.

Keywords: ammonium removal, water treatment, membrane filtration, biochar, adsorption.

HYDROGEN STORAGE AND MOBILITY DETERMINED FOR VARIOUS ORGANICALLY FUNCTIONALISED POROUS SILICA SYNTHETISED BY USING THE POST-GRAFTING METHOD

Giuseppe Conte[2], Ana-Maria Putz[1], Cataldo Simari[4], Carlo Poselle Bonaventura[2], Michele Porto[4], Raffaele G. Agostino[2,3] and Alfonso Policicchio[2,3]

[1]"Coriolan Drăgulescu" Institute of Chemistry, Bv. Mihai Viteazul, No.24, RO-300223, Timisoara, Romania
[2]Department of Physics, Università della Calabria, Via Ponte P. Bucci, Cubo 31C, 87036 Arcavacata di Rende (CS), Italy.
[3]CNR-Nanotec, c/o Università della Calabria, Via Ponte P. Bucci, Cubo 31C, 87036 Arcavacata di Rende (CS), Italy.
[4]Department of Chemistry and Chemical Technology, Università della Calabria, Via Ponte P. Bucci, Cubo 12C, 87036 Rende, CS, Italy
e-mail: carlo.poselle@gmail.com

Abstract

Various aspects as pore size, surface area, functionalization and pore volume of materials have to be considered when are envisaged increased hydrogen storage performances [1, 2]. Different materials were synthetized by using the post-grafting method in alkaline conditions, through a modified Stöber process. Starting the simple silica, it was used the long chain cationic surfactant, hexadecyltrimethylammonium bromide (CTAB) [3], and different organically silica precursors: tetraethyl orthosilicate and various trialkoxysilanes with different functional groups. By properly tuning surface interactions and textural characteristics, the overall efficiency of hydrogen capture processes could be improved. Hydrogen adsorption capacity was evaluated by using volumetric apparata and the performances obtained for the methyl-functionalized sample can be debited to a different sorbent-adsorbent interaction and textural properties developed. An NMR investigation aiming at clarifying the internal arrangement and diffusion properties of hydrogen molecules inside functionalized porous silica materials has been performed. The NMR spectral analysis and the T1 relaxation times [4], both carried out under different pressure loadings, indicated two different populations of hydrogen sorbate due to the molecules adsorbed in mesopores and in micropores.

References

[1] A. Policicchio, A.-M. Putz, G. Conte, S. Stelitano, C. P. Bonaventura, C. Ianăşi, L. Almásy, A. Wacha, Z. E. Horváth, R. G. Agostino, J. Porous Mater. 28 (2021) 1049.
[2] A. M. Putz, A. Policicchio, S. Stelitano, P. Sfîrloagă, C. Ianăşi, R. G. Agostino, S. Cecilia, Fullerenes Nanotub. Carbon Nanostructures 26 (2018) 810.
[3] A. Policicchio, G. Conte, S. Stelitano, C. P. Bonaventura, A.-M. Putz, C. Ianăşi, L. Almásy, Z. E. Horváth, and R. G. Agostino, Colloids Surfaces A Physicochem. Eng. Asp. 601 (2020) 125040.
[4] A. Policicchio, G. Conte, R. G. Agostino, P. Caputo, C. Oliviero Rossi, N. Godbert, I. Nicotera, C. Simari, J. CO2 Util. 55 (2022) 101809.

FUNCTIONALISED MESOPOROUS SILICA WITH GAS STORAGE PROPERTIES SYNTHESISED BY CO-CONDENSATION

Ana-Maria Putz[1], Alfonso Policicchio[2], Giuseppe Conte[2], Raffaele G. Agostino[2]

[1]" Coriolan Drăgulescu" Institute of Chemistry, Bv. Mihai Viteazul, No.24, RO-300223, Timisoara, Romania
[2]Dept. of Physics, University of Calabria, 87036 Rende, CS, Italy
e-mail: putzanamaria@yahoo.com

Abstract
In order to be tested for their gas storage properties, mesoporous silica particles were synthesized by sol-gel method, starting from tetraethyl orthosilicate silica precursor. Besides, the following precursors have been added in different molar ratios: triethoxyvinylsilan, diethoxy(methyl)vinylsilane or methyltriethoxysilane. Ammonia was used as catalyst and hexadecyltrimethyl ammonium bromide as directing agent. The aim of our study is the functionalization with different groups, with the purpose of trying to tailor their performances as gas storage materials. The molar ratio of different functionalized precursors/TEOS is varied in order to obtain different sizes for the pore diameter as for the specific surface area. The hydrogen adsorption data show that the methyl functionalized material was better from the point of view of maximum adsorption capacity for H_2, compared to the other materials. The higher adsorption capacity of the methyl-functionalized sample can be attributed to a strong sorbent-adsorbent interaction, but also to the high specific surface area and big pore volume. From the evaluated materials, only the vinyl-triethoxysilan functionalised materials have an appreciable affinity toward this gas specimen.

Acknowledgements
The authors thanks to Romanian Academy.

References
[1] A. -M. Putz, A. Policicchio, S. Stelitano, P. Sfîrloagă, C. Ianăşi, R. G. Agostino, S. Cecilia, Fullerenes Nanotub. Carbon Nanostructures 26 (2018) 810.
[2] A. Policicchio, G. Conte, S. Stelitano, C. P. Bonaventura, A.-M. Putz, C. Ianăşi, L. Almásy, Z. E. Horváth, and R. G. Agostino, Colloids Surfaces A Physicochem. Eng. Asp. 601 (2020) 125040.
[3] A. Policicchio, A.-M. Putz, G. Conte, S. Stelitano, C. P. Bonaventura, C. Ianăşi, L. Almásy, A. Wacha, Z. E. Horváth, R. G. Agostino, J. Porous Mater. 28 (2021) 1049.

BEHAVIOUR OF PtCo ALLOY NANOPARTICLES IN REVERSE WATER-GAS SHIFT REACTION

Ákos Szamosvölgyi[1]*, Fanni Czirok[1], Ádám Pitó[1], Róbert Mucsi[1], Kornélia Baán[1], András Sápi[1,2], Imre Szenti[1], János Kiss[1,4], Zsolt Fogarassy[3], Ákos Kukovecz[1], Zoltán Kónya[1,4]

[1]*University of Szeged, Interdisciplinary Excellence Centre, Department of Applied and Environmental Chemistry, H-6720, Rerrich Béla tér 1, Szeged, Hungary*
[2]*Institute of Environmental and Technological Sciences, University of Szeged, H-6720, Szeged, Hungary*
[3]*Centre for Energy Research, Institute of Technical Physics and Materials Science, H-1121, Budapest, Hungary*
[4]*MTA-SZTE Reaction Kinetics and Surface Chemistry Research Group, University of Szeged, H-6720, Szeged, Hungary*
**e-mail: szamosvolgyi@chem.u-szeged.hu*

Abstract

The effects of atropogenic CO_2 emission are among today‘s most researched topics. One of the most promising approach is to convert the CO_2 into other compounds, which could be further converted into reagents for the chemical industry. This approach should let us reach carbon neutrality. The accumulation of CO_2 in the atmosphere is due to the stability of the molecule, thus a catalyst is required to activate CO_2 and break its bonds. In this project we demonstrate the performance of PtCo alloy nanoparticle systems. PtCo nanoparticles with different Pt:Co ratios (3:1, 1:1, 1:3) were synthesized with similar size and geometry. Pure Pt nanoparticles were also synthesized and were studied as a reference material. The metal content and ratios of the alloy particles were confirmed with IPC-MS. The particles were loaded onto an inert mesoporous silica, MCF-17. The catalyts materials were characterized via TEM, XRD, BET and HAADF (S)TEM. Catalytic activity for reverse water-gas shift reaction was tested in a countinous flow reactor, where the products where separated and detected by a GC. The difference in the catalytic behaviour was further elucidated with *in situ* DRIFTS and XPS and measurements. *In situ* DIRFTS allowed us to comprehend the mechanism of the ongoing reaction by identifying the intermediates in the gas phase and adsorbed on the surface of the catalyst. XPS of the nanoparticles also provided valuable information about the composition of the nanoparticles and how the different alloys are structured, as the peak binding energies of the Pt show significants shifts depending on the coordination with Co in the crystal lattice.

ENANTIOSELECTIVE SEPARATIONS OF PROLINE ANALOGS WITH MACROCYCLIC GLYCOPEPTIDE-BASED CHIRAL STATIONARY PHASES

Dániel Tanács, Róbert Berkecz, Antal Péter, István Ilisz

Institute of Pharmaceutical Analysis, University of Szeged, H-6720 Szeged, Somogyi u. 4, Hungary
e-mail: tanacs.daniel@szte.hu

Abstract

High-performance liquid chromatography (HPLC) is a widely used technique, which can be applied to both preparative and analytical chromatography. Chiral chromatography is a specific field of chromatography. While the pharmaceutical industry pays outstanding attention to chiral compounds, it is important to realize, that they are also present as food additives, agricultural chemicals, or fragrance materials.

The chiral stationary phases (CSPs) are the backbone of direct chiral chromatography. There is a wide range of CSPs, this way a wide range of chiral analytes can be separated. These columns are also compatible with a wide range of eluents, which also helps in optimizing the separations. The development of CSPs follows the development of achiral stationary phases and nowadays there are a lot of ultrahigh-performance columns too.

These columns can be utilized in ultrahigh-performance liquid chromatography (UHPLC) instruments. UHPLCs can work at higher pressures (up to 1500 bars) compared to HPLCs, which come with several benefits. They can operate at higher flow rates, and utilize narrower capillaries, which mean they have low dead volumes, and the columns can have smaller internal volume and can be filled with smaller particles. This means we have shorter retention times and higher chromatographic performance in most cases.

Macrocyclic glycopeptides were introduced by Armstrong and co-workers as chiral selectors in 1994. The family of macrocyclic glycopeptides contains several hundreds of different structures, but only a small number of them are used as chiral selectors, such as vancomycin, teicoplanin, teicoplanin aglycon, and rifampicin. They can have multiple groups (hydroxyl, amino, carboxylic, etc.) that can interact with the sample molecules and can also contain multiple aromatic groups.

In our studies, the enantioseparation of proline analogs was investigated, and teicoplanin, teicoplanin aglycon, and vancomycin were used as selectors. The experiments were conducted on a UHPLC system.

Acknowledgments

This work was supported by the ÚNKP-22-3 New National Excellence Program of the Ministry for Innovation and Technology from the source of the National Research, Development and Innovation Fund, and the National Research, Development, and Innovation Office NKFIA through project grant K137607. Project no. TKP2021-EGA-32 has been implemented with the support provided by the Ministry of Innovation and Technology of Hungary from the National Research, Development and Innovation Fund, financed under the TKP2021-EGA funding scheme.

IL-FUNCTIONALIZED LAYERED DOUBLE HYDROXIDE: SYNTHESIS, CHARACTERISATION AND APPLICATION AS ADSORBENT MATERIALS FOR PALLADIUM RECOVER

Nick Samuel Tolea, **Lavinia Lupa, Radu Lazau, Laura Cocheci**

Faculty of Industrial Chemistry and Environmental Engineering, University Politehnica Timisoara, Blv. Vasile Parvan nr. 6, Timisoara, Romania
e-mail: nick.tolea@student.upt.ro

Abstract

Palladium (Pd) made part from the platinum group metals (PGMs), which are precious metals used in a wide range of industrial applications, being considered indispensable in cutting-edge technology. [1] While their natural resources are limited the demand for these metals increases. [2] The content of the precious metals in secondary resources was found to be much higher than their content in natural ores. To meet the continuously increasing demand for precious metals, in recent years, the recovery of PGMs from secondary resources is a potential solution.

Introduction

It is well known that the sorption processes are more appropriate for the recovery of metal ions from diluted solutions. An efficient adsorbent material must meet the following conditions: high adsorption kinetics, excellent selectivity, high adsorption capacity, thermal and chemical stability, and easy synthesis. These properties are met by layered double hydroxides (LDH). [3, 4] For more than a decade, studies have been carried out in the functionalization of different solid supports with different functional groups to increase the adsorption capacity and the selectivity of these materials. To this end, the researchers attention was focused on the use of ionic liquids (ILs) in the processes of solid supports functionalization due to the unlimited possibilities of tunability/design of new ionic liquids for specific applications and needs, insignificant volatility, high thermal stability and wide ionic and electrochemical conductivity. [5, 6] In this context, the present paper aims at the synthesis and characterization of Mg_3Al and and their functionalization with ILs (methyl trialkyl (C8-C10) ammonium chloride in order to obtain adsorbent materials with high efficiency in the removal process of PGMs from aqueous solutions.

Experimental

The studied LDHs were synthesized by the co-precipitation method at low supersaturation. The functionalization of the synthesised LDH was performed in two ways: ultrasonication and co-synthesis. The obtained adsorbent materials were subjected to structural and morphological characterization using X-ray diffraction (XRD), N_2 adsorption-desorption analysis, Fourier-transform infrared (FTIR) spectroscopy and by thermal analysis.

Results and discussion

The results of the characterization proved the fact that through ultrasonication, is assured a uniform distribution of the ILs onto the surface of the LDHs, while via co-synthesis is obtained an impregnation of the IL between the LDHs layers, which will bring a higher stability of the obtained material. Palladium adsorption studies onto the studied materials were conducted in batch mode, performing equilibrium, kinetic and thermodynamic studies. The adsorption capacity increases with the increasing contact time, increasing temperature and increasing equilibrium concentration of Pd(II).

Conclusions

The presence of ionic liquid significantly improves the efficiency of Mg_3Al in the recovery process of Pd(II) ions from aqueous solutions. The adsorption kinetics were better described by the pseudo-second-order kinetic model compared to the pseudo-first-order kinetic model. The experimental data showed a good fit with the Langmuir isotherm. The adsorption capacity increases as follows: Mg_3Al << Mg_3Al IL-US < Mg_3Al IL-COS.

By correlating the results obtained in the characterization process of adsorbent materials with the results obtained from kinetic, thermodynamic and equilibrium studies, we can conclude that in the case of the raw Mg_3Al sample, Pd recovery occurs through a physisorption mechanism, as it is adsorbed in the pores of the material. In contrast, in the case of IL (Methyltrialkylammonium chloride) functionalized samples, Pd recovery is due to a chemosorption process, indicating that the functional groups of the ionic liquid confer a beneficial influence on the adsorbent material.

Key Words: *platinum metals group; adsorption, layered double hydroxides, ionic liquids; functionalization.*

References

[1] C. Hageluken, (2006), Metall-Wirtschaft, 60 (1-2): 31–42.
[2] European Commission – (13.09.2017) Communication from the Commission to the European Parliament, the Council, the European Economic and Social Committee and the Committee of the Regions: On the 2017 list of critical raw materials for the EU, COM 490.
[3] H. Asiabi et al., (2017) Chemical Engineering Journal, 323: 212-223.
[4] A. De Martino et al., (2013) Applied Clay Science, 80-81: 154-161.
[5] M.A. Lira et al., (2016) Chemical Engineering Journal, 302: 426–436.
[6] R. Navarro et al., (2014) Separation and Purification Technology, 135: 268–277.

Acknowledgement

This work was supported by a grant of the Romanian Ministry of Education and Research, CNCS - UEFISCDI, project number PN-III-P1-1.1-TE-2019-1555, within PNCDI III.

NOVEL COPPER COMPLEXES WITH GLYOXIMES, AMINES, SCHIFF BASES, SEMI- AND THIOSEMICARBAZONES; SYNTHESIS AND PHYSICO-CHEMICAL ANALYSIS

Csaba Várhelyi jr.[1], Roland Szalay[2], György Pokol[3], János Madarász[3], Imre-Miklós Szilágyi[3], Péter Huszthy[3], Melinda Simon-Várhelyi[1], Róbert Tötös[1], Raluca-Anca Mereu[1], Alexandra Avram[1], László Korecz[5], Nóra May[4], Judith Mihály[4]

[1] Faculty of Chemistry and Chemical Engineering, "Babeş-Bolyai" University, RO-400 028 Cluj-N., Arany János str. 11, Romania
[2] Institute of Chemistry, "Eötvös Loránd" University, H-1117 Budapest, Pázmány Péter str. 1/a, Hungary
[3] Faculty of Chemical Technology and Biotechnology, Budapest University of Technology and Economics, H-1111 Budapest, Műegyetem rkp. 3, Hungary
[4] Research Centre for Natural Sciences, H-1117 Budapest, Magyar tudósok körútja 2, Hungary
e-mail: csaba.varhelyi@ubbcluj.ro

Abstract

In our research project new copper(II) complexes were synthesized with α-dioximes, amines, Schiff bases, semi- and thiosemicarbazones such as $[Cu(DioxH)_2L_2]$, ($DioxH_2$: methyl-butyl-glyoxime, ethyl-butyl-glyoxime, methyl-phenyl-glyoxime; L: diphenyl-amine, 2-methyl-imidazole, dibutyl-amine, 2-amino-4-methylpyridine, imidazole, 1-aminonaphthaline), $[Cu(octan\text{-}2\text{-}one)_2AL_2]$, (A: hydrazine, phenylhydrazine, *o*-phenylene-diamine; L: 3-amino-1*H*-1,2,4-triazole, 2-aminopyrimidine, 2-methylimidazole), $[Cu(ketone\text{-}SC)_2]$, $[Cu(ketone\text{-}TSC)_2]$, (ketone: propiophenone, butyrophenone; SC: semicarbazone; TSC: thiosemicarbazone), by the reaction of copper(II)-acetate in suitable solvent. After a short bibliographical survey, involving the classification and evolution of copper complexes with possible applications, we analyzed their physicochemical properties using FTIR, Raman, ESR, UV-VIS, powder X-ray diffraction (XRD), mass spectrometry, thermal analysis (TG, DTG, DTA) and SEM. The importance of this class of compounds lies in biochemistry as some of them are antibacterial agents and potential anti-tumour drugs.

Introduction

Copper is one of the oldest and most widely used metal. Its name originates from the Latin name of Cyprus, Cyprium. Copper is an essential element in the life of plants and animals. It is also an industrial metal bearing excellent electrical and thermal conductivity, and easy to work with it, and when is combined with other metals, its technical applications are unlimited.

Among copper coordination compounds, copper(II)-azomethines (Schiff bases, oximes, hydrazones, semi- and thiosemicarbazones, porphyrins, etc.) play very important role in many biological and biochemical processes. Schiff bases show bacteriostatic and antibacterial activities. In addition, its anti-fungal, anti-tumor and anti-cancer effects have also been reported [1]. Copper complexes formed with dioximes are also significant due to their antibacterial effect [2], and some representatives are catalysts in oxidative coupling (polymerization) reactions.

Schiff bases are privileged class of ligands in coordination chemistry, and found numerous applications in different scientific fields. Semicarbazones and thiosemicarbazones are biologically important compounds due to their potential pharmacological properties such as antibacterial, antifungal, antimalarial, anticancer, antineoplastic and antiviral activities. Medicinal chemistry shows a growing interest in the development of metal complexes as drugs

or diagnostic agents. Owing to their wide range of coordination numbers and geometries, as well as kinetic properties, metal compounds offer various mechanisms for drug action [3]. In this paper we report the synthesis and characterization of novel copper complexes with glyoximes, Schiff bases, semi- and thiosemicarbazones.

Experimental

Used materials: $Cu(OAc)_2 \cdot H_2O$, Me-Bu-Dioxh$_2$, Et-Bu-Dioxh$_2$, Me-Ph-Dioxh$_2$, diphenyl-amine, 2-methylimidazole, dibutyl-amine, 2-amino-4-methylpyridine, imidazole, 1-aminonaphthaline, 3-amino-1*H*-1,2,4-triazole, 2-aminopyrimidine, octan-2-one, hydrazine, phenylhydrazine, *o*-phenylene-diamine, propiophenone, butyrophenone, semicarbazide, thiosemicarbazide, MeOH, EtOH.

Methods:

- *Synthesis of [Cu(Dioxh)$_2$L$_2$] type complexes*

2 mmol Dioxh$_2$ (Me-Bu-Dioxh$_2$, Et-Bu-Dioxh$_2$ or Me-Ph-Dioxh$_2$) was dissolved in 20 ml EtOH or MeOH, then this solution was added to the aqueous solution of 1 mmol (0.2 g) $Cu(OAc)_2 \cdot H_2O$ dissolved in 10 ml water. Afterwards 2 mmol amine (diphenyl-amine or 2-methylimidazole or dibutyl-amine or 2-amino-4-methylpyridine or imidazole or 1-aminonaphthaline) dissolved in 5 ml EtOH or MeOH was added. The obtained solution was heated for 2–3 hours on a water bath. After cooling the crystalline complexes were filtered, washed with MeOH–water mixture (1:1). A typical reaction as an example is shown below:

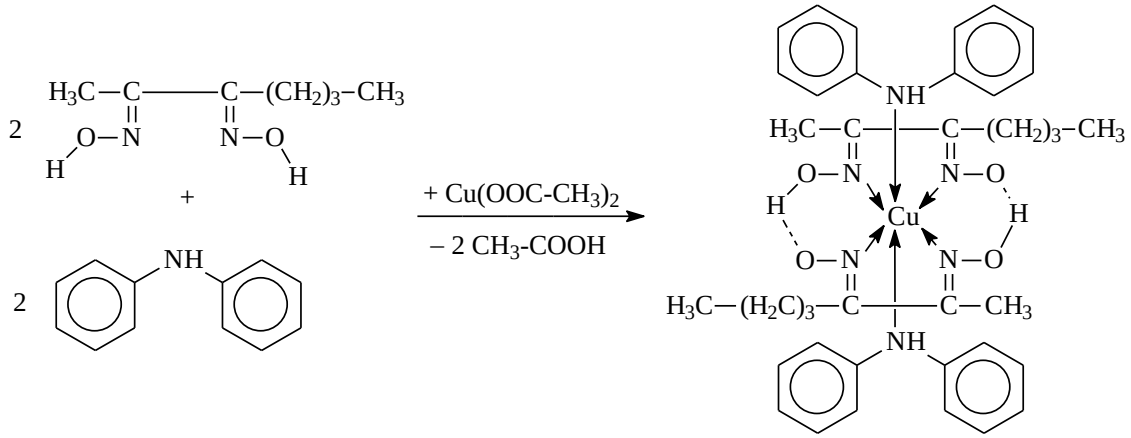

- *Synthesis of [Cu(2-octanone)$_2$AL$_2$] type complexes*

3 mmol octan-2-one (0.5 ml) and 1.5 mol diamine (hydrazine or phenylhydrazine or *o*-phenylene-diamine) were dissolved in 5 ml MeOH, then refluxed for 1–2 hours. The resulting colored solution was added to the aqueous solution of 1.5 mol (0.3 g) $Cu(OAc)_2 \cdot H_2O$ dissolved in 5 ml water. At last 3 mmol amine (3-amino-1*H*-1,2,4-triazole or 2-amino-pyrimidine or 2-methylimidazole) dissolved in 10 ml MeOH was added. The obtained mixture was refluxed in a water bath for 2–3 hours. After cooling the crystalline complexes were filtered off, washed with MeOH–water mixture (1:1), and finally dried on air. A typical reaction is the following:

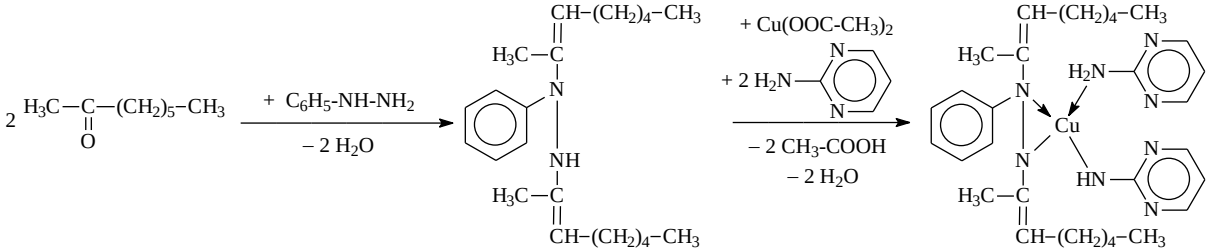

- Synthesis of [Cu(ketone-SC)$_2$], [Cu(ketone-TSC)$_2$] type complexes

1.5 mmol propiophenone or butirophenone was added to 1.5 mmol semi- or thiosemicarbazide dissolved in 5 ml water. In the case of semicarbazide 1.5 mmol CH_3COONa (0.1 g) was added to release the semicarbazide from the salt. The obtained solution was refluxed in a water bath for 1 hour, then 0.75 mmol (0.2 g) $Cu(OAc)_2 \cdot H_2O$ dissolved in 5 ml distilled water was added. The obtained mixture was refluxed in a water bath for 2–3 hours. After cooling the crystalline complexes were filtered off, washed with MeOH–water mixture (1:1), and finally dried on air. A typical reaction is displayed below:

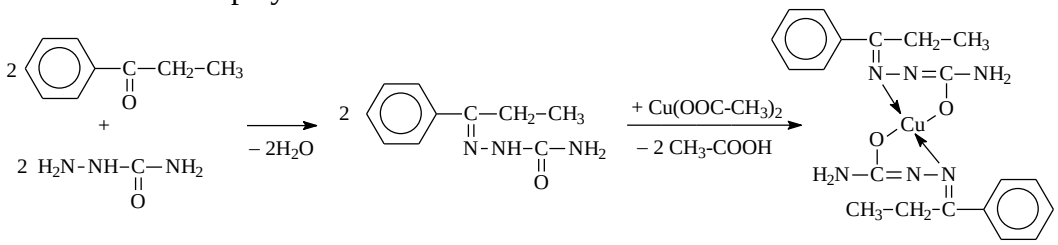

Results and discussion

Microscopic characterization and yields of the prepared complexes are presented in Table 1.

Table 1. Microscopic characterization, calculated molar masses and yields of the prepared complexes.

Nr.	Compound	Calc. mol. mass	Yield (%)	Microscopic characterization
1.	[Cu(Me-Bu-DioxH)$_2$ (diphenyl-amine)$_2$]	716.38	62	Dark brown lamellar crystals
2.	[Cu(Me-Bu-DioxH)$_2$ (2-Me-imidazole)$_2$]	542.14	17	Brown triangle-based prisms
3.	[Cu(Me-Bu-DioxH)$_2$((n-Bu)$_2$NH)$_2$]	636.42	50	Dark brown triangle-based prisms
4.	[Cu(Me-Bu-DioxH)$_2$ (2-amino-4-Me-pyridine)$_2$]	594.21	69	Dark brown triangle-based prisms (microcrystals)
5.	[Cu(Et-Bu-DioxH)$_2$(imidazole)$_2$]	542.14	56	Dark brown irregular microcrystals
6.	[Cu(Ph-Me-DioxH)$_2$ (2-amino-4-Me-pyridine)$_2$]	634.19	56	Reddish-brown triangle-based prisms
7.	[Cu(Ph-Me-DioxH)$_2$ (1-naphtylamine)$_2$]	704.28	50	Black triangle-based prisms, lamellar crystals
8.	[Cu(Ph-Me-DioxH)$_2$ (2-Me-imidazole)$_2$]	582.12	49	Dark brown triangle-based prisms (microcrystals)
9.	Cu(2-oct.)$_2$(hidrazone) (3-amino-1*H*-1,2,4-triazole)$_2$]	482.13	21	Green triangle-based prisms (microcrystals)
10.	[Cu(2-oct.)$_2$(Ph-hidrazone) (2-amino-pyrimidine)$_2$]	581.28	7	Khaki green, small triangle-based prisms (microcrystals)
11.	[Cu(2-octanone)$_2$(o-fen) (2-Me-imidazole)$_2$]	554.28	21	Dark brown triangle-based prisms (microcrystals)
12.	[Cu(propiophenone-SC)$_2$]	443.99	24	Brown, small triangle-based prisms (microcrystals)
13.	[Cu(propiophenone-TSC)$_2$]	476.11	41	Brown triangle-based prisms
14.	[Cu(butirophenone-SC)$_2$]	472.04	12	Dark gray triangle-based prisms (microcrystals)
15.	[Cu(butirophenone-TSC)$_2$]	504.17	43	Black triangle-based prisms (microcrystals)

Infrared spectroscopic study

The mid-IR spectra were recorded with a Bruker Alpha FTIR spectrometer (Platinum single reflection diamond ATR), at room temperature, in the wavenumber range of 4000–400 cm^{-1}, and the far-IR range of 500–50 cm^{-1}, respectively, on a Bio Rad – FTS 60A, PIKE Gladi ATR spectrometer, with a resolution of 4 cm^{-1}. The samples were measured in solid state (in powder form). The data of the most characteristic IR bands for the selected complexes are presented in Table 2.

Table 2. IR data of the selected complexes.

Comp. / cm^{-1}	1	5	6	7	9	10	11	12	14	15
ν_{N-H}	3191 m	3135 m	3205 w	3180 w	3318 m	3386 w	3180 w	3192 m	3169 m	3318 m
ν_{C-H}	2929 m	2930 s	2918 m	2920 w	2924 w	2924 w	2923 m	2968 w	2929 m	2963 w
$\nu_{C=C}$	-	-	1579 m	1579 w	1611 m	1655 s	1656 m	1674 vs	1676 s	1592 s
$\nu_{C=N}$	1589 s	1560 s	1545 s	1544 s	1541vs	1537 w	1565 vs	1564 vs	1568 vs	1518 vs
δ_{CH2}	1457 s	1399 s	1441 m	1440 s	1397 e	1372 vs	1441 vs	1468 vs	1456 s	1489 s
δ_{CH3}	1315 m	1327 s	1325 m	1325 m	1338 k	1347 s	1391 vs	1336 s	1344 w	1343 m
ν_{N-N}	-	-	-	-	-	-	-	1294 m	1307 m	1277 s
ν_{N-O}	1218 m	1259 w	1240 s	1242 s	-	-	-	-	-	-
ν_{N-OH}	1116 w	1185 w	1146 s	1148 s	-	-	-	-	-	-
τ_{O-H}	978 s	1085 vs	951 vs	951 vs	1066 m	1067 w	-	-	-	-
γ_{C-H}	741 vs	747 vs	694 vs	694 vs	651 m	665 m	754 vs	694 vs	767 s	697 m
ν_{Cu-N}	505 s	493 w	474 s	474 m	505 s	506 m	478 m	503 m	541 m	503 w
ν_{Cu-O}	-	-	-	-	-	-	-	460 vs	461 vs	-
ν_{Cu-S}	-	-	-	-	-	-	-	-	-	443 m
δ_{N-Cu-N}	-	-	380 s	374 s	343 w	343 w	-	-	-	-

(Abbreviations: vs = very strong, s = strong, m = medium, w = weak)

The most important bands for the characterization of complexes are $\nu_{C=N}$ (1518–1589 cm^{-1}) and ν_{Cu-N}, ν_{Cu-O}, ν_{Cu-S} (443–541 cm^{-1}). In the far IR region δ_{N-Cu-N} deformation vibrations appear (343–380 cm^{-1}) [4].

Mass spectrometry

Mass spectra of the samples were recorded using electrospray ionization (ESI). In the spectra we could detect the molecular ions and some decomposition fragments.

ESR measurements

The measurements were performed with a Bruker ELEXSYS 500 type device. By comparing the experimental and calculated spectra, and by calculating the characteristic parameters, the Cu–N couplings can be identified. In some cases, a small amount of cluster formation or two conformations can be observed.

Thermoanalytical measurements (TG-DTG-DTA)

Thermal measurements were performed with a 951 TG and 910 DSC calorimeter (TA Instruments), in Ar or N_2 at a heating rate of 10 $Kmin^{-1}$ (sample mass of 4–10 mg).

The thermal stability of complexes is limited within the temperature range of 100–130 °C. In the case of *[Cu(DioxH)$_2$L$_2$]* type complexes the first decomposition step belongs to leaving amino (L) groups, until 240 °C, then the glyoxime units leave. The end of the process is at 470 °C. Subsequently, the decomposition of the glyoxime unit is accompanied by big exothermic peaks. This behavior can be explained with the presence of oxygen in the molecule. In the case of *[Cu(octan-2-one)$_2$AL$_2$]* type complexes the first step of the decomposition

mechanism is the loss of the amino (L) groups between 50–350 °C, then the *2-octanone* units leave. Finally the diamine (A) unit is lost between 350–450 °C. The end of the process is at 500 °C. The decomposition of *[Cu(ketone-SC)$_2$]*, *[Cu(ketone-TSC)$_2$]* type complexes begins with leaving of the ketone moieties until 400 °C, then the semicarbazone or thiosemicarbazone unit leaves until 790 °C. The general mechanism for decomposition is as follows:

$$[Cu(DioxH)_2L_2] \rightarrow [Cu(DioxH)_2L] \rightarrow [Cu(DioxH)_2] \rightarrow [Cu(DioxH)] \rightarrow CuO$$

$$[Cu(octan\text{-}2\text{-}one)_2AL_2] \rightarrow [Cu(octan\text{-}2\text{-}one)_2AL] \rightarrow [Cu(octan\text{-}2\text{-}one)_2A \rightarrow$$
$$\rightarrow [Cu(octan\text{-}2\text{-}one)A] \rightarrow [CuA] \rightarrow CuO$$

$$[Cu(ketone\text{-}SC)_2],\ [Cu(ketone\text{-}TSC)_2] \rightarrow [Cu(SC)_2],\ [Cu(TSC)_2] \rightarrow CuO,\ CuS$$

UV–VIS spectroscopy

The electronic spectra were recorded with a Jasco V-670 Spectrophotometer in 10% EtOH/water solutions containing the substance in 10^{-4} mol/dm^3 concentration. Using Sörensen buffer solutions the electronic spectra were also recorded as a function of pH, and then the acidity constants were calculated, too. The obtained values were between $3.9 \cdot 10^{-12} – 6 \cdot 10^{-10}$.

Powder X-ray diffraction measurements

The crystal structure of the complexes was studied with powder XRD measurements, carried out on a PANalytical X'pert Pro MPD X-ray diffractometer. As being novel compounds their diffractograms can not be found in the Cambridge database. The majority of the complexes exhibits crystalline form, except for [Cu(octan-2-one)$_2$(*o*-fen)(2-Me-imidazole)$_2$] and [Cu(butirophenone-TSC)$_2$] which are amorphous.

SEM (scanning electron microscopy) and EDX (energy dispersive X-ray spectroscopy analysis)

The images were taken with a JEOL JSM-5500LV scanning electron microscope. For all study the beam energy was 20kV in order to obtain the excitation of all the elements and secondary electron detector (SED) were employed for measurement. The morphological study of the sample surface at five significant magnifications 10000x, 5000x, 1000x, 500x and 100x were recorded.

Conclusion

In this work new copper(II) complexes were synthesized and characterized with physico-chemical methods. Thermal decomposition mechanism was monitored with thermoanalytical measurements.

Acknowledgement

The authors wish to express their thankfulness to the "Domus Hungarica Foundation" of Hungary for the several fellowships provided to Csaba Várhelyi jr.

References

[1] X.J. Zhao, L.W. Xue, C.X. Zhang, Synthesis and Reactivity in Inorganic, Metal-Organic, and Nano-Metal Chemistry 45 (2015) 516–520.
[2] K. J. Donde, V. R. Patil, Journal of Pharmacy Research 4(1) (2011) 206–209.
[3] S. Chandra, Vandana, S. Kumar, Spectrochimica Acta Part A: Molecular and Biomolecular Spectroscopy 135 (2015) 356–363.
[4] K. Nakamoto, Infrared and Raman Spectra of Inorganic and Coordination Compounds. Part B: Applications in Coordination, Organometallic and Bioinorganic Chemistry, Wiley J., 38, NY 1997.

EFFECTS OF MILLING ENERGY ON SILICON CARBIDE PARTICLES

John Wanjala, Andras Sápi, Imre Szenti, Tamás Boldizsár, Koszma Gábor, Zita Sándor

Doctoral School of Environmental Sciences, Department of Applied and Environmental Chemistry, University of Szeged, H-6720 Szeged, Rerrich Tér 1, Hungary.
Email: namumawanjala@gmail.com

Abstract

Technical ceramics have properties that aid environmental pollution management products. Their ability to withstand high operation temperatures above 1000 ^{O}C make them suitable for applications in solar energy conversion, catalyst support, photovoltaic as well as power plant engine systems. In addition to this, ceramic materials have high resistance to thermal shock, wear and corrosive attack. As a result, ceramics are the best placed materials to use in water processing and treatment environmental technologies.

Research to improve thermo-mechanical properties of ceramics has gained momentum. Nanoparticles have been attractive in the field of material properties optimization due to their unique properties to impart '1 + 1>2' effect. Among them SiC nanoparticles are attracting global attention due to their excellent thermo-mechanical properties. However, agglomeration of SiC nanoparticles is a major setback in their ceramic applications. In this study the effects of energy on particle agglomeration in planetary milling have been investigated. SiC particles of the size range (0.2-1.8) mm were milled in a planetary mill between (100-600) rpm with varying time intervals (1-6) hours. Ball to Powder Weight Ratio and vial volume occupancy ratio were varied during sample milling. Samples were analysed using XRD, SEM-EDX and DLS.

SEM and XRD result of the fresh SiC showed that SiC particles were mostly angular shaped and of β-SiC/ 3C-SiC polytype. XRD analysis showed that crystallinity reduced from 76.65% to 20.49 % and crystallite size reduced from 52.96 nm to 5.93 nm, while the lattice strain increased from 1.7692 to 5.1493. In the sample milled at 600 rpm for 6 hours, the lattice strength dropped to 1.6902 due to highly amorphous nature (79.51%) of the sample. SEM analysis showed that milled samples were irregular and the surface morphology was rough. The Hydrodynamic diameter reduced from approximately 390 nm in samples milled at 100 rpm to 280 nm in samples milled at 600 rpm for 6 hours. The dispersity index showed that the particles were mainly polydisperse. This was attributed to the agglomeration/ aggregation of SiC particles during milling process.

Key words: *XRD, SEM-EDX, DLS, Silicon Carbide, Thermo-Mechanical Properties, Hydrodynamic Diameter and Dispersity.*

PROPERTIES OF TEM-1 β-LACTAMASE UNDER HEAVY METAL POLLUTION CONDITIONS

Zeyad H. Nafaee[1,2], Viktoria Egyed[1], Éva Hunyadi-Gulyás[3] and Béla Gyurcsik [1]

[1]*Department of Inorganic and Analytical Chemistry, University of Szeged, H-6720 Szeged, Dóm tér 7, Hungary*
[2]*University of Babylon, College of Pharmacy, Hillah 51001 Babel, Iraq.*
[3]*Laboratory of Proteomics Research, Biological Research Centre, Temesvári krt. 62, H-6726 Szeged, Hungary*
e-mail: n.zeyad@chem.u-szeged.hu

Introduction

β-Lactamases protect bacterial carboxy-transpeptidases from β-lactam antibiotics by hydrolyzing the β-lactam ring before reaching its targets [1]. Two systems of β-lactamase classification have been used; sequence information based system was introduced by Ambler [2], while the more recent activity based system was invented by Bush-Jacoby-Medeiros [3]. Accordingly, four classes are termed A, B, C, and D recognized by difference in hydrolytic activity. The active site of classes A, C, and D contains a Ser-Xaa-Xaa-Lys motif, therefore these are called serine β-lactamases. Class B is a heterogeneous group of zinc metalloenzymes, called metallo-β-lactamases [5]. The Ser-Xaa-Xaa-Lys motif employs Ser as nucleophile hydrolyzing β-lactams by forming covalent acyl-enzyme intermediate, while metallo-β-lactamases utilize Zn(II) activated water molecules as the nucleophile for hydrolysis of β-lactams [4]. As a source of development of bacterial antibiotic resistance class A TEM-1 β-lactamase is a frequent target of scientific research. Although TEM-1 β-lactamase is not a metalloenzyme, we could purify this protein by chelating to Ni(II)-loaded sepharose column[5]. This suggested that the enzyme can bind metal ions, which may influence its structure and catalytic activity. Therefore, our aim was to purify the enzyme and study the effect of metal ions, potentially present as heavy metal pollutants in the environment.

Experimental

The purity of TEM-1 β-lactamase was determined using 12-15% (w/v) sodium dodecyl sulfate polyacrylamide gel electrophoresis (SDS PAGE) with a mixture of seven unstained proteins (116, 66.2, 45, 35, 25, 18.4, and 14.4 kDa) as molecular markers (Thermo Scientific #26610), while the concentration of TEM-1 β-lactamase was determined by Cary 3500 UV–Vis double beam, multicell spectrophotometer at 25 °C controlled temperature (Agilent Technologies) in the 210–300 nm wavelength interval in a quartz cuvette (Hellma) with 1 cm path length. CD spectra were recorded at room temperature by a Jasco J-1500 CD spectrometer. The parameters were adjusted as described in the following. Wavelength range: 300 – 180 nm; path length: 0.2 mm (Hellma quartz cuvette); D.I.T.: 2 sec; bandwidth: 1.0 nm; scanning speed: 50 nm/min (continuous scanning mode). Intact protein mass measurement and top-down protein analysis was carried out on a Nanomate TriVersa (Advion) chip-based nanoelectrospray ion source coupled to a linear trap quadrupole Orbitrap Elite mass spectrometer. The protein concentration was 2.0 μM in each individual sample which contained 0, 2, 5 and 10 equivalents of $NiCl_2$. The samples were buffered at pH 7.8 with a solution containing 50 mM ammonium bicarbonate/NH_3 (aq). TEM-1 β-lactamase activity was assessed by UV absorption spectrometry via hydrolysis of series ampicillin concentrations (230 μM and 930 μM) as substrate (SERVA Electrophoresis GmbH) in 1 ml 20 mM Tris-HCl, pH 7.5.

Results and discussion

TEM-1 β-lactamase was purified by immobilized Ni(II) ion affinity chromatography, based on its metal ion binding sites without denaturation or fusing affinity tags [5]. There are several amino acids (His, Glu, Asp, Ser) in the protein behaving as potential binders to NTA-Ni(II)-resin (Fig. 1). The investigation of the Ni(II) binding of the purified enzyme by mass spectrometry, we could detect up to three bound metal ions in the presence of increasing Ni(II) excess. However, the main peak in the mass spectra of Ni(II) TEM-1 β-lactamase was assigned to the monometalated enzyme at each applied metal-to-enzyme ratio. Protein binding to two Ni(II) ions appeard at 5:1 ratio and its intensity slightly increased at 10:1 Ni(II):protein molar ratio. Traces of the protein bound to three Ni(II) were also detected. TEM-1 β-lactamase may coordinate more strongly to the first Ni(II) through H151, H156 His pair at ~3.5 Å distance. The next binding site is weaker and the third site barely binds the metal ion. Interaction of TEM-1 β-lactamase with Ni(II) was also proven by the successful purification by chelating to Ni(II)-loaded sepharose column. Only a slight change was observed in the CD spectra on increase of the Ni(II) content. TEM-1 β-lactamase most likely could bind more than one Ni(II) ion, but with low affinity and without a significant change of the secondary structure. One Ni(II) can bind to H151 and H156 or H94, and H110, or H24 and H285. Excess of Hg(II) caused a more significant change in the CD spectrum, but still not a large change in the secondary structure. Hg(II) may bind to C75 and C121, which are close to the active center of the enzyme. Sulphur donor groups of soft character from methionines (Fig. 1) close to the active centre may also support binding of Hg(II). The specific activity of the enzyme decreased by ~50% in presence of Hg(II). Future mass spectrometric measurements are planned to reveal the Hg(II) binding sites.

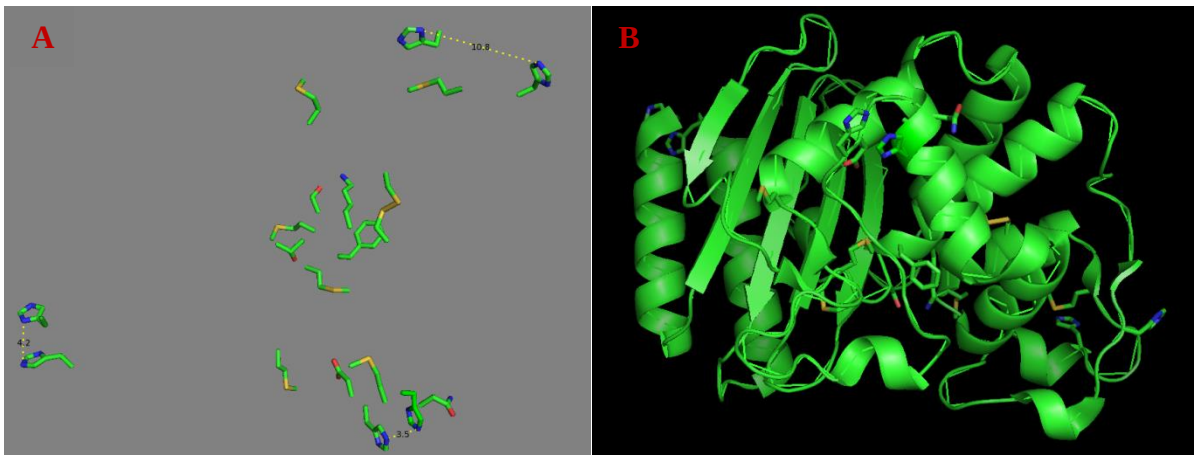

Fig. 1: Sequence and structure of the *E. coli* TEM-1 β-lactamase (PDB code: 1zg4) [6]. A: The relative positions of the side-chains of the SXXK motif and putative metal ion binding residues. B: The cartoon representation of the crystal structure of TEM-1 β-lactamase with the putative metal ion binding sites and the SXXK motif shown by sticks, 24–286 residues were detected by the X-ray diffraction method.

Conclusion

The metal binding sites of TEM-1 β-lactamase can be a good candidate to change the chemical structure of the enzyme. The CD spectra of metalized TEM-1 β-lactamase with Ni(II) and Cd(II) only slightly differed from that of the free protein suggesting that the available binding sites can coordinate to Ni(II) or Cd(II) individually without change in the secondary structure. Nevertheless, the affinity towards Ni(II) and Cd(II) significantly decreases with the binding of

the first, second and third metal ion, as confirmed by mass spectrometric measurements. Excess of Hg(II) caused a more significant change in the spectrum, but still not a large change in the secondary structure. At the same time, the presence of Hg(II) caused significant inhibition the efficiency of enzyme in hydrolysis of β-lactams by ~ 50%. This result suggests that the heavy metal ions increase the toxicity of the antibiotics against bacteria, which effect may be further enhanced by the toxic property of the metal ions themselves.

Acknowledgements
This research was supported by the Hungarian National Research, Development and Innovation Office (GINOP-2.3.2-15-2016-00038, GINOP-2.3.2-15-2016-00001, and GINOP-2.3.2-15-2016-00020, as well as 2019-2.1111-TÉT-2019-00089).

References
[1] T. Oka, K. Hashizume, and H. Fujta, The Journal of Antibiotics, 1980 (33), 11.
[2] R.P. Ambler, B Biol. Sci., 1980 (289), 1036.
[3] K. Bush, G. A Jacoby, Antimicrobial Agents and Chemotherapy, 1995 (54), 3.
[4] I. Massova, L. P. Kotra, R. Fridman, S. Mobashery, The FASEB Journal, 1998 (12), 12.
[5] Z. H. Nafaee, É. Hunyadi-Gulyás, B. Gyurcsik, Protein Express. Purif., 2023 (201), 106169.
[6] B. Stec, K.M. Holtz, C. L. Wojciechowski, E.R. Kantrowitz, Acta Crystallogr., D61 (2005).

Poster Proceedings

MACHIAVELLIANISM ATTITUDE TOWARD BUSINESS ETHICS AMONG STATE SCIENCE STUDENTS

Nur Syuhaini Abdul Wahi[1], László Berényi[2]

[1,2] *Faculty of Public Governance and International Studies, Ludovika University of Public Service, H-1083 Budapest, Üllői road 82., Hungary*
e-mail: nani_mashmallow@yahoo.com

Abstract
The study aims to explore the attitudes of state science students towards business ethics. The research used a voluntary online survey in Hungary. The results are based on the responses of 99 students from 2022. Machiavellianism is the most characteristic philosophy among state science students, similarly to business students. The analysis explored that this characteristic is not uniform; sub-groups can be defined. These clusters show different opinions about the perception of CSR. Considering Machiavellianism is a rational, opportunist philosophy, the middle way of scores is the most consistent with the idea that CSR can contribute to sustainability. Understanding the patterns allows targeted human resource management strategies to amplify environmentally conscious behavior.

Introduction
Society level and personal approaches to environmental and social problems have long been the focus of interest. Considering that decision-makers are individuals or a group of individuals, their value system is expected to be more or less reflected in organizational actions. Exploring national, local, or profession-level patterns can contribute to substantive and acceptable CSR actions. Pálvölgyi et al. [1] stated that CSR is a particular challenge in formerly socialist countries since the fulfillment of social goals was regarded for decades as solely the state's responsibility, and similarly, economic responsibilities were also limited. Although three decades have passed, traces of the previous system remain in these cultures.

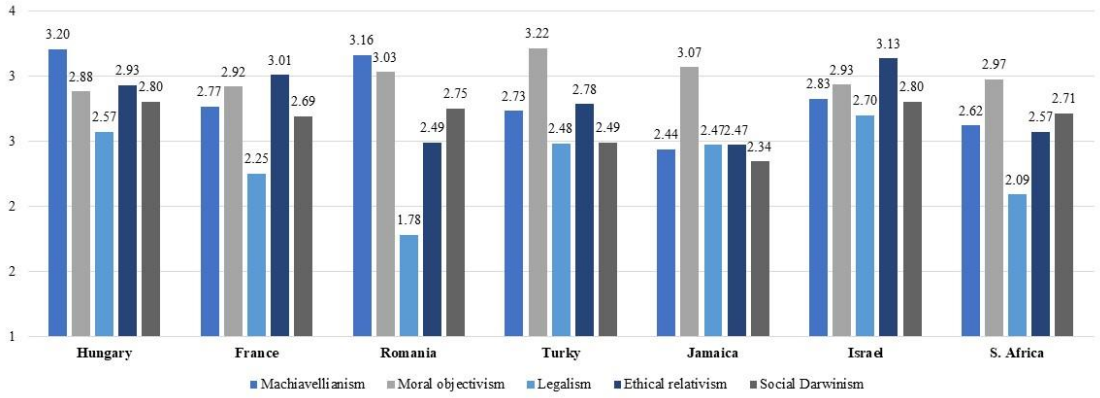

Figure 1: Business philosophy scores of selected countries [2, 3, 4]

The Attitudes Towards Business Ethics Questionnaire (ATBEQ) is an instrument oriented towards attitudes on selecting business ethics situations [5] based on the work of Stevens [6]. Clark et al. [7] present a concise summary of five business philosophies covering the ATBEQ statements: Machiavellianism, ethical relativism, legalism, social Darwinism, and moral objectivism. An extensive worldwide database is available among business students that allows an international comparison. The results pointed out that Machiavellianism is the most

prominent in the case of post-socialist countries among business students (Figure 1), and the moral objectivism score is lower in this international comparison. Hungarian data was based on the author's data collection [4].

According to Clark et al. [7], Machiavellianism covers the idea that business firms are self-contained organisms with their own 'natural laws' that can be bent but not broken. Miesing and Preble [8] highlighted that Machiavellianism is amoral since the outcome justifies the way to access it.

Machiavellianism can be considered both opportunist and realistic behavior [8]. It gives a practical approach to CSR application. According to Christie and Geis [9], in their opinion, people should believe in what they do rather than do what they believe in. Analyzing the Big Five personality trait dimensions, Czibor et al. [10] found that a high level of Machiavellianism is inversely proportional to agreeableness (friendliness) and conscientiousness. All these characteristics strengthen rationality, which is beneficial to business interests.

The study attempts to extend the investigations to public administration. Although the curriculum and teaching methods are different in the case of state science students and business students, they act as citizens and organizational decision-makers. CSR is increasingly integrated with public administration bodies, and these are supported or regulated by legal actions. The government's role in the field of social responsibility is multifaceted. Consequently, an emphasis on the field is reasoned. State science master students will play a key role in legal and administrative positions in the future on a national level. The question is whether their attitude to business ethics is similar to business students' attitude or differs from it. The study focuses on the analysis of Machiavellian characteristics.

Experimental

A voluntary online survey was used for data collection among Hungarian higher education students, including the ATBEQ questions. The research sample of this study focuses on the responses of the state science (master level) students at the Ludovika University of Public Service, Budapest. The sample consists of 99 responses, including 60 females and 39 males. Statistical analysis included analysis of variance and cluster analysis, supported by IBM SPSS software. The analysis aimed to find the most characteristic philosophy. Machiavellianism score is calculated as the mean value of 12 related statements, evaluated on a 5-point scale (1: strongly disagree; 5: strongly agree):

- The only moral of business is making money.
- A person who is doing well in business does not have to worry about moral problems.
- Business decisions involve a realistic economic attitude and not a moral philosophy.
- Moral values are irrelevant to the business world.
- "Business ethics" is a concept for public relations only.
- George X says of himself, "I work long, hard hours and do a good job, but it seems to me that other people are progressing faster. But I know my efforts will pay off in the end." Yes, George works hard, but he's not realistic.
- For every decision in business the only question I ask is, "Will it be profitable?" If yes–I will act accordingly; if not, it is irrelevant and a waste of time.
- In my grocery store every week I raise the price of a certain product and mark it "on sale." There is nothing wrong with doing this.
- A business person cannot afford to get hung up on ideals.
- If you want a specific goal, you have got to take the necessary means to achieve it.
- The business world has its own rules.

A good business person is a successful business person.

Results and discussion

The pattern of the state science students is similar to the business students' evaluation (Figure 1). Results show that Machiavellianism is the most characteristic philosophy (Table 1). However, the remarkable skewness index suggests further investigations. The distribution of the individual scores (Figure 2) confirms a mixing of samples; the state science students' Machiavellian characteristic is not uniform or follow a normal distribution.

	Mean	**Std. Deviation**	**Skewness**		**Kurtosis**	
	Statistic	Statistic	Statistic	Std. Error	Statistic	Std. Error
Machiavellianism	3.23	0.516	0.476	0.243	0.206	0.481
Moral objectivism	2.56	0.518	-0.122	0.243	-0.345	0.481
Legalism	2.87	1.157	0.181	0.243	-0.546	0.481
Ethical relativism	2.88	0.664	0.097	0.243	0.890	0.481
Social Darwinism	2.77	0.478	0.537	0.243	-0.252	0.481

Table 1: Descriptive statistics of the philosophies (n=99, measured on a 5-point scale)

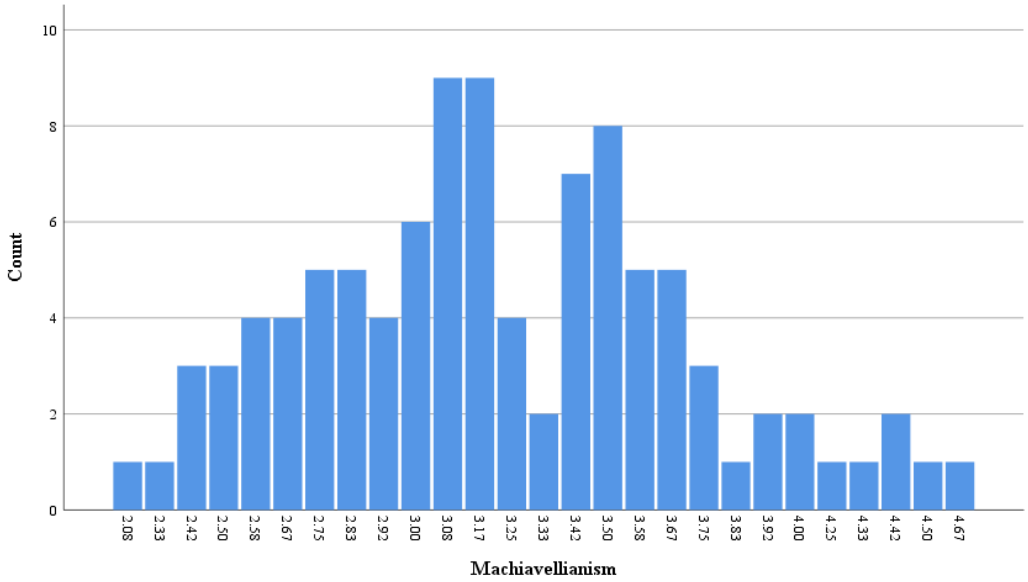

Figure 2: Distribution of Machiavellianism scores (SPSS output)

The analysis of variance confirmed only a few significant differences in the scores by gender, and any of these by other groping factors like study religiousness, CSR knowledge level, or work experience. A cluster analysis was applied to explore characteristic patterns. Hierarchical clustering by Ward-method (results the lowest variance within the groups) allowed 3 clusters (Figure 3).

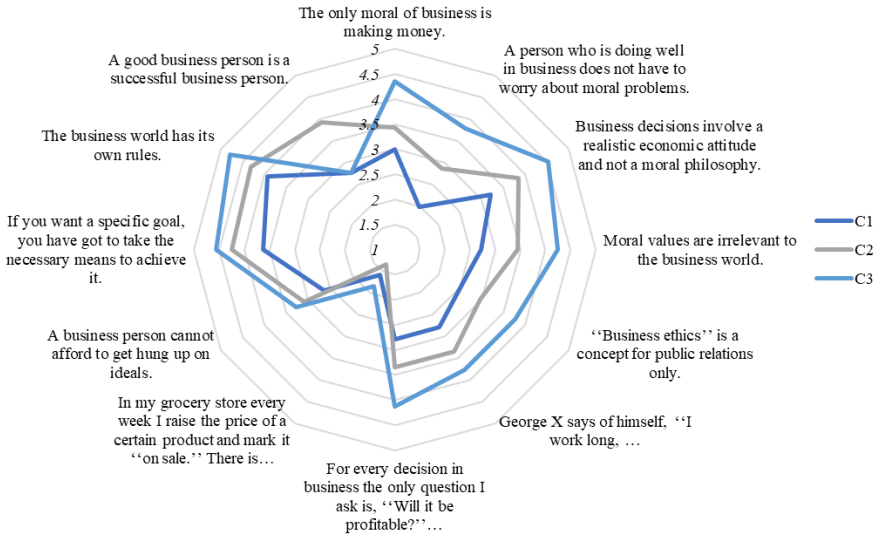

Figure 3: Survey results by clusters

Cluster 1 (n=42, Machiavellianism score=2.79) includes students with the lowest scores on most questions. Machiavellianism is the least characteristic among these students. Cluster 3 (n=25, Machiavellianism score=3.81) represents the highest scores, except for the statement that being good means being successful. Cluster 2 (n=32) presents the middle way; the Machiavellianism score is 3.35. The survey included some statements about CSR judgment (Figure 4). Clusters show significant differences in three statements:

- Another tool for companies to generate profit (F=3.724, sig.=0.028)
- CSR can only be successful in the case of large companies (F=3.909, sig.=0.023)
- CSR implementation is expensive (F=3.474, sig.=0.035)

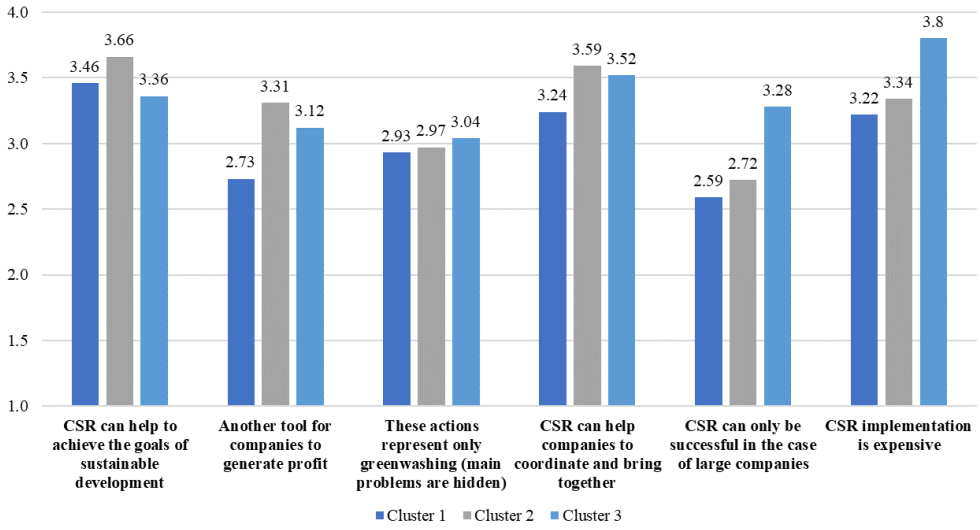

Figure 4: Evaluation of CSR by clusters

Conclusion

The attitude toward business ethics is similar among state science and business students. Survey results confirmed that Machiavellianism is the most characteristic philosophy, but the pattern is not uniform. These patterns show a correlation with opinions about social responsibility.

Cluster 1 has the lowest score in Machiavellianism but does not believe that CSR is only a tool for profit generation. They find the implementation of CSR the least expensive compared to the other clusters, as well as they found it applicable beyond large companies. Cluster 2 is represented by the medium Machiavellianism scores in most statements; they believe in the coordinative role of CSR and do not refuse it as a business interest. Considering the philosophy as a rational, opportunist approach, the middle way seems to pay off in the interest of CSR's contribution to sustainability. Cluster 3 is the most characterized by Machiavellianism, and their CSR approach is the most limited to large organizations and expensively.

The results contribute to the finding [5] that the ATBEQ instrument can be used to predict CSR perception. Since ATBEQ is dealing with the value system of the respondents, which can be considered an enabler factor, exploring the personal patterns may support effective human resource management strategies. As a result, better support of CSR efforts can be achieved by a refined division of labor meeting personal values.

Nevertheless, further investigations require the enhancement of the sample and the consideration of the other business philosophies. Moreover, correlations may be engaging with other aspects. We plan to check the relation with technology adoption propensity that can be traced back to environmental and social problem-solving.

References

[1] T. Pálvölgyi, N. Csige-Nagypál, J. Szlávik, H. Csáfor, M. Csete, Striking Oil? CSR and the EU Integration Processes: The Example of Hungary. In Barth, R., Wolff, E. (Eds.): Corporate Social Responsibility in Europe. Rhetoric and Realities, Edward Elgar, Cheltenham, UK (2009) pp. 269-288.

[2] R.L. Sims, R.L, A.E. Gegez. Attitudes towards Business Ethics: A Five Nation Comparative Study. J. Bus. Ethics 50 (2004) 253-265.

[3] D. Bageac, O. Furrer, E. Reynaud. Management Students' Attitudes Toward Business Ethics: A Comparison Between France and Romania. J. Bus. Ethics 98 (2011) 391-406.

[4] L. Berényi, N. Deutsch. Corporate Social Responsibility and Business Philosophies among Hungarian Business Students. Sustainability 13 (2021) 9914.

[5] Y. Neumann, A. Reichel. The Development of Attitudes Toward Business Ethics Questionnaire (ATBEQ): Concepts, Dimensions, and Relations to Work Values; Working Paper; Department of Industrial Engineering and Management, Ben Gurion University of the Negev, Be'er Sheva, 1987.

[6] E. Stevens. Business Ethics, Paulist Press, New York/Ramsey, 1979.

[7] D. Clark, T. Tanner, L.N. Pham, W.J. Lau, L.D. Nguyen. Attitudes toward business ethics: Empirical investigation on different moral philosophies among business students in Vietnam. Int. J. Bus. Gov. Ethics 14 (2020) 123-142.

[8] P. Miesing, J.F. Preble, A comparison of five business philosophies. J. Bus. Ethics 4 (1985) 465-476.

[9] R. Christie, F. Geis. Studies in Machiavellianism, Academic Press, New York, 1970.

[10] A. Czibor, O. Vincze, T. Bereczkei. Feelings and motives underlying Machiavellian behavioural strategies; narrative reports in a social dilemma situation. Int. J. Psychol. 49 (2014) 519-524.

DISADVANTAGES OF ELECTROCOAGULATION-FLOTATION TREATMENT OF OFFSET PRINTING EFFLUENTS

Savka Adamović[1], Vladimir Rajs[1], Dragan Adamović[1], Ivana Tomić[1], Ivan Pinćjer[1], Miroslav Dramićanin[1]

[1]Faculty of Technical Sciences, University of Novi Sad, 21000 Novi Sad, Trg Dositeja Obradovića 6, Serbia
e-mail: adamovicsavka@uns.ac.rs

Abstract
The efficiency of electrocoagulation-flotation (ECF) treatment was estimated based on the quantity of pollutants (cooper, turbidity, and organic substances) in printing effluents (waste offset printing developer and waste offset fountain solution) at selected process parameters. Four sets of aluminum or/and iron electrode combinations were applied, each with a current density of 2, 4, and 8 mA cm^{-2} and interelectrode distances of 0.5, 1.0, and 1.5 cm. In the progress of the ECF treatment, samples were taken at certain process times (1, 5, 10, 20, 40, and 60 min). Based on the obtained results, the disadvantages of ECF treatment of offset printing effluents are defined.

Introduction
The ECF treatment is an electrochemical process that includes in-situ generation of coagulants (metal hydroxides and/or polyhydroxides) by electrodissolution of a soluble sacrificial metal anode immersed in the treated wastewater, such as printing effluents [1].
ECF technique has many advantages regarding the conventional methods: easier operation, simpler equipment, a short process time, better safety, selectivity, flexibility, cost-effectiveness, lower amount of sludge [1, 2], environmental compatibility, operational and investment costs [2], and a practical method of treating various effluents and pollutants [3].

Experimental
The electrode combinations set: four iron electrodes (1), four aluminum electrodes (2), two aluminum (one was anode) and two iron electrodes (3), and two iron (one was anode) and two aluminum electrodes (4) were used. All four electrodes are the same size (10 cm x 5 cm x 0.1 cm). Each set of electrode combinations was immersed in borosilicate glass (ECF cell) with 220 mL of the printing effluent and 0.50 g of sodium chloride. The outer electrodes were connected in a bipolar mode to a digital DC power supply (DF 1730LCD). The ECF cell is set to a magnetic stirrer (IKA color squid, Germany). When the appropriate set of electrodes was selected (1, 2, 3, or 4) and adjusted the interelectrode distances (0.5, 1.0, or 1.5 cm), the suitable current density (2, 4, or 8 mA cm^{-2}) was applied. Then, ECF samples (15 cm^3) were taken at certain process times (1, 5, 10, 20, 40, and 60 min) and centrifuged for 10 min at 2000 rpm [3]. Turbidity was determined in triplicate by HI 93703 microprocessor turbiditymeter (HANNA Instruments, Portugal). The concentration levels of copper were determined in triplicate by atomic absorption spectroscopy with PerkinElmer Aanalyst 700 spectrophotometer. The UV absorbance of organic substances was detected by UV-1800 SHIMADZU spectrophotometer (at a wavelength of 326 nm and with a 1 cm quartz cell). Selected pollutants turbidity, copper, and organic substances were analysed according to the standard EPA 180.1, EPA 7000B, and AWWA–APHA–WEF method, respectively [1, 2].
The percentage of ECF removal efficiency of pollutants (cooper, turbidity, and organic substances) from investigated printing effluents was calculated as a function of process time by

the universal equation [3]: Removal efficiency = ((X_o – X_t) 100) / X_t. Where X_o – the initial values of content of copper or turbidity or organic substances in printing effluents and X_t – values of the mentioned pollutants in effluents after a particular process time (t).

Results and discussion

The results of ECF treatment show that the removal efficiencies of pollutants from the waste developer decrease in turbidity (99%) >| cooper (93%) > organic substances (53%) [3]. In the case of waste offset fountain solution, the order is cooper > turbidity > organic substances. So the removal efficiency of turbidity, copper, and organic substances from waste offset fountain solution was 90, 65, and 44%, respectively.

The electrode combinations sets with aluminum (as an anode) provide better removal efficiency of cooper and turbidity in both offset effluents. In addition, combining an iron electrode as an anode with aluminum improves the removal of organic substances.

The best current density for all pollutants in both effluents was 8 mA cm^{-2}. Interelectrode distances of cooper and turbidity in investigating printing effluents were 1 cm, while for the organic substances, it was 0.5 cm. The best process times for cooper and turbidity in waste developer was 5 minutes, while in the second effluent, the values were 20 and 60 minutes, respectively. For organic substances, the best process time was 60 minutes in both effluents.

Conclusion

The type of pollutants and offset printing effluents affect the removal order. Also, the combinations of electrodes, the current density, the interelectrode distance, and the process time determine the highest removal efficiency.

Removal efficiency increases with current densities and process time for all electrode combination sets: the higher the current density and time, the more efficient the ECF treatment for all pollutants.

Of course, ECF treatment of offset printing effluents has disadvantages. Optimization is necessary (for example, with Response Surfaces Analysis) to show the relationship between operational variables and to determine the optimum process conditions. A passivation layer on aluminum or iron electrodes was formed during the treatment, which reduces its effectiveness. Although a small amount of sludge is generated during ECF treatment, the characterization of the sludge and its safe disposal in the environment is needed. The efficiency of pollutant removal, which is lower than 90%, needs to be increased by combining the ECF treatment with other processes (for example, adsorption).

Acknowledgements

The authors acknowledge the financial support of the Ministry of Education, Science and Technological Development, Republic of Serbia through the project no. 451-03-68/2020-14/200156: “Innovative scientific and artistic research from the FTS (activity) domain”.

References

[1] M. Prica, S. Adamovic, B. Dalmacija, Lj. Rajic, J. Trickovic, S. Rapajic, M. Becelic-Tomin, Process Saf. Environ. Prot. 94 (2015) 262.

[2] S. Adamović, M. Prica, B. Dalmacija, M. Kragulj Isakovski, Đ. Kerkez, S. Rapajić, D. Adamovic, Measurement 131 (2019) 288.

[3] S. Adamović, M. Prica, B. Dalmacija, S. Rapajic, D. Novakovic, Z. Pavlovic, S. Maletic, Arab. J. Chem. 9 (2016) 152.

AMMONIUM ION REMOVAL FROM WATER BY COAGULATION USING AN ELECTROCHEMICALLY PREPARED POLYALUMINIUM CHLORIDE

Adina Pacala[1], Ciprian Radovan[2]

[1]National Research and Development Institute for Industrial Ecology ECOIND, Timisoara Subsidiary, 300431 Timisoara, Bujorilor u. 115, Romania
[2]Department of Chemistry, Faculty of Chemistry, Biology and Geography, West University of Timisoara, 300115 Timisoara, Pestalozzi u. 16A, Romania
e-mail: adina.pacala@ecoind.ro

Abstract
As part of advanced technologies, water companies tend to use the most effective coagulants, which will produce higher quality for the final treated waters and greater reliability. Alum and prehydrolyzed aluminium chloride with general formula $Al_m(OH)_nCl_{3n-m}$ (PAC) have been widely applied as coagulants in water treatment technologies. Their hydroxyl aluminium polymers were recognized as the most effective components in Al coagulants.
Using the principles of coagulant preparation and of the electrolysis process, the method of electrochemical synthesis of the Polyaluminium chloride (E-PAC) has been proposed and carried out extensively in our previous research.
In this study the coagulation properties of electrochemically obtained PAC (E-PAC) on ammonium ion removal from water was evaluated in laboratory scale and it was compared with the performance of a commercially available PAC solution and classical aluminium sulphate (alum).

Introduction

Nitrogen is an essential element for life and undergoes many chemical and biochemical processes in water. It appears mainly as ammonium, nitrite, nitrate, gaseous nitrogen and fixed in organic compounds, groups between which there are continuous transformations / transits, forming the "nitrogen cycle".
The excess leads to eutrophication, contamination of aquifers, possible damage to human health: methemoglobinemia in children, gastric cancer, etc. The presence of ammonium ion in the composition of a surface water indicates a degree of its pollution.
Ammonium sources in waters are natural and anthropogenic. These "natural" sources are often indirectly also anthropogenic. "Direct" anthropogenic sources are pointful (wastewater discharges containing ammonium) and diffuse, mainly nitrogen compounds from agriculture, chemical fertilizers, and natural fertilizers.
The removal of nitrogen compounds from drinking water is expensive and complicated. Chemical (ion exchangers) and biochemical techniques have been experimented, mixing contaminated waters with others with a lower concentration of ammonium/nitrogens[1,2] .
Here are some aspects that were the basis for choosing the ammonium ion introduced as ammonium nitrate as a pollutant in a synthetic water in order to compare the efficiency of removing this type of pollutant through the coagulation-flocculation process with aluminum sulfate (alum), polyaluminium chloride (PAC) and a new electrochemically prepared polyaluminium chloride (E-PAC).

Experimental

Coagulants and water samples

For comparison purposes, commercially available PAC (8.8 % Al_2O_3, basicity 65, density 1.22 kg/dm^3) was a a Donau Chemie product (Austria). Alum stock solution was prepared from liquid aluminium sulphate (approximately 7.5% as Al_2O_3) obtained from a local Bega water treatment plant.

The synthetic model water consisted of a stock ammonium nitrate (NN) solution prepared by adding commercial ammonium nitrate powder (NN, Merck Company, Germany) into deionized water. After that, this stock solution was stirred for 5 min., at 300 rpm.

Electrochemical preparation of E-PAC

The electrochemical reactor (ECR) for E-PAC preparation [3,4] consisted on a D.C. Power Supply (HY 3000D, China), an electrolyzer made out of organic glass (rectangular size 76 x 51 x 70mm) equipped with 6 parallel plain-plate electrodes, 3 anodes and 3 cathodes disposed in a mono-polar arrangement with 10 mm anode-cathode distance. Three sheets of Al (95 x 50 mm) were used as anodes while the cathodes were three sheets of stainless steel plates (95 x 50 mm). The system is completed by the electrolyte (200 ml aqueous solution $AlCl_3$ 0.5M) and stirring apparatus (IKA, Germany), with degree of agitation selected of 600 rpm. An ammeter and a voltmeter were used for electrical characteristics control. Electrolysis was carried out in galvanostatic conditions at optimum conditions, selected from our previous studies, respectively current density of 1.15 A dm-2, electrolysis time of 2 hours, current intensity of 1.5 A [5].

Experimental and analytical methods

Coagulation experiments were carried out at room temperature using jar test on a six-paddle gang stirrer, equipment manufactured by Velp Scientifica (Model FC6S, Italy). The 800mL working NN solution was added into the1000mL beaker. A measured amount of coagulant was added by a calibrated pipette (Multipette stream Electronic hand dispenser, Eppendorf, Germany) into the working NN solution under rapid stirring. The NN solution was stirred rapidly at 150 rpm for 2 min after coagulant dosing, followed by slow stirring at 45 rpm for 15 min, which compares to current plant conditions at the Timisoara Waterworks.

For 30 min after settling, supernatants were collected to measure residual turbidity using a Turbidimeter (HACH 2100N, USA). Total organic carbon (TOC) was analyzed after filtration through a 0.45 mm membrane and were determined using a TOC Analyzer (TOC-V CPH, SHIMADZU, Germany). pH and conductivity were determined on a laboratory multi-parameter analyser (Consort C863, Consort, Belgium). Colour in Hazen units was measuring using a photometer SQ 118 Merck (Germany). The absorbance at 254 nm (due to the Natural Organic Matter/NOM content) was measured with a Spectrofotometer UV-VIS (UV-VIZ T90+, PG Instruments Ltd, SUA), using a 1 cm path length quartz cuvette.

Results and discussion

Coagulation behaviors of E-PAC and conventional coagulants as alum and commercial product PAC were compared, using the so called „Jar test" procedure, in accordance with water treatment standards, to remove the introduced ammonium ion as ammonium nitrate from deionized water with addition of 10 mg/L of ammonium nitrate (commercial NN powder), selected for this study. The applied coagulant doses were the same 1 mg Al/L, for all three coagulants compared.

As part of the applied procedures, the level of residual turbidity, the amount of total organic carbon, the UV 254 absorbance and color were evaluated, in order to assess the efficiency of the coagulation process in all situations (E-PAC and alum as coagulants). Table 1 demonstrates the coagulation performance of all three coagulants.

Table 1. Water quality parameters of raw water and treated water with aluminium sulphate, PAC and E-PAC

PARAMETER, **UNIT**	RAW WATER	ALUMINIUM SULFATE	PAC	E - PAC
Turbidity, NTU	0.697	0.540	0.605	0.412
pH	6.51	5.05	5.25	6.13
Temperature, °C	20	20	20	20
NH_4^+, mg/L	1.67	1.57	1.5	1.23
Colour, °Hazen	12	9	10	5
UV-254, m^{-1}	0.180	0.155	0.158	0.118
Conductivity, µS/cm	25.5	29.0	24.3	29.0

Therefore, E-PAC proved to be the most efficient coagulant in terms of TOC and turbidity removal (Figure.1) on ammonium ion from synthetic water.

Figure 1. TOC results of raw water and treated water (1) with aluminium sulphate (2), PAC (3) and E-PAC (4).

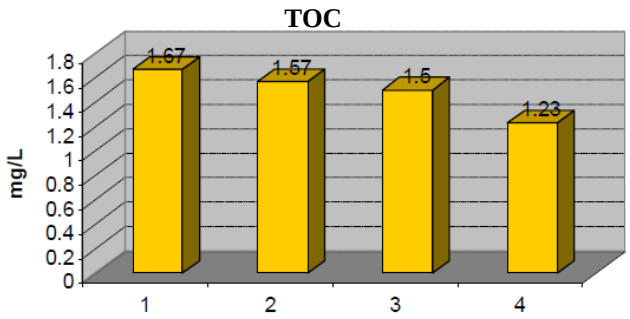

Scan Spectrum Curve for domaine 200-350 nm wavelength have been rendered with UV-254 nm absorbency, as shown in Figure 2.

Figure 2. UV absorbency spectrum curve

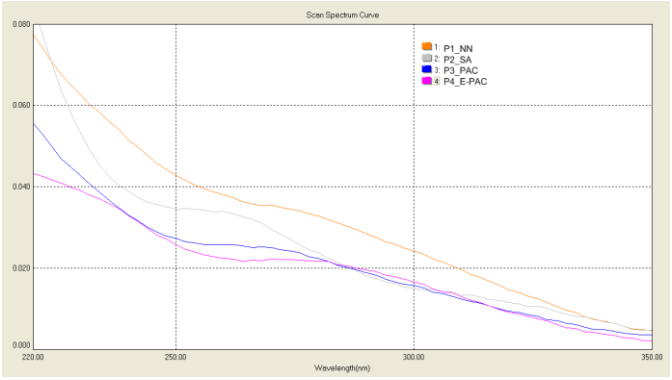

E-PAC seems to exhibit better coagulation performance than PAC and alum, especially in high coagulant dose (e.g. 10 mg Al/L). The superiority of E-PAC can be attributed to the higher Al_{13} content, than the respective values of PAC.

Conclusion

The results suggest that the electrochemically obtained E-PAC through a easily controlled electrolysis process, is a product with better properties than the commercial PAC used for comparison to remove the introduced ammonium ion as ammonium nitrate from synthetic water.

References

[1] A.I. Zouboulis, N. Tzoupanos, Desalination, 250 (2010) 339–344.
[2] C. Staaks, R. Fabris, T. Lowe, C. Chow, J. Leeuwen, M., J. Drikas, Chem. Eng., 168 (2011) 629-634.
[3] A. Pacala, I. Vlaicu, C. Radovan, Environ. Eng. and Manag. Journal, vol.8, 6 (2009) 1371-1376.
[4] A. Pacala, "Contributions to surface water treatment for drinking purpose by using electrochemically generated polyaluminium chloride, PhD Thesis, West University of Timisoara (2010).
[5] A. Pacala, C. Radovan, E-SIMI Proceedings of 25st International Symposium on "The Environment and the Industry", Bucharest, Romania, 29 September 2022, ISSN 2344-3898, DOI: http://doi.org/10.21698/simi.2022.ab02

PROTECTION AGAINST NOISE POLLUTION - A NORMATIVE FRAMEWORK OF THE REPUBLIC OF SERBIA AND HARMONIZATION WITH THE EU REGULATIONS

Aleksandra Milošević[1], Suzana Knežević[2]

[1]*University of Belgrade, Faculty of Law, King Aleksandar Boulevard No 87, Belgrade, Republic of Serbia*
[2]*Academy of Vocational Studies Šabac, Unit of Agricultural and Business Studies and Tourism, Vojvode Putnika Street No 56, Šabac, Republic of Serbia*
e-mail: alexandramilosevic77@gmail.com

Abstract

Noise and noise pollution protection are one of the current topics of environmental law. The accelerated pace of development of countries causes multiple pollution of the environment, which is reflected, among other things, in the increasing negative impact of noise on humans. The positive law of the Republic of Serbia in the area of noise protection is the Law on Environmental Noise Protection with a large number of accompanying acts that enable its application. The article consists of several thematic units, of which the first part of the paper deals with the concept of noise and its impact, the second part of the paper is dedicated to the legal regulation of the concept of noise, while third and fourth parts show the legal system of the European Union in the part that regulates noise, so that the last part of the work is dedicated to the harmonization of the Serbian legal system with the legal system of the European Union. The paper also contains the European Union recommendations, which Serbia must follow in order to harmonize the legal systems.

Introduction

Noise has been identified as one of the leading environmental problems of the modern world. Its negative impact can be considered a consequence of the accelerated pace of technical and technological development that has happened over the last fifty years. Noise and noise protection are one of current legal issues that is highlighted in the European Union legislation as a leading environmental problem both caused by industrialization and resulting from industrialization.

It has been estimated that more than 20% of the EU population have been exposed to the negative effects of noise that are harmful to human health [1]. According to the European Environment Agency, approximately 210 million people in the EU, which is more than 44% of population, are exposed to the levels of traffic noise higher than 55 dBA, and more than 50 million people are exposed to the levels of noise higher than 65 dBA during 24 hours, these being labeled as 'black' acoustic points [2].

Communal noise has a wide range of negative effects on the health of the exposed population [3]. It deteriorates the quality of life because it disturbs everyday activities, concentration, communication, sleep and rest [4]. Long-term exposure to noise can lead to a higher rate of cardiovascular disease due to permanent stimulation of the sympathetic nervous system [5]. Indirectly, noise affects various aspects of behaviour and, since it reduces productivity, it affects work results as well [6].

The concept of community noise and criteria for the demarcation of sounds

According to internationally accepted definitions, noise is every unwanted and unpleasant sound [7]. In theory, noise is defined as an appearance of unpleasant and undesirable acoustic sensations [7]. These definitions introduce the category of wanted and unwanted sound in order

to gauge harmfulness, which further means that only certain sounds are considered to be noise [9].

The previous Law on Environmental Protection from 1991 defined noise as 'an acoustic event above the prescribed level in the environment in which an individual resides', while previous Slovenian legislation (the Law from 1976) defined noise as each sound that affects psychological and physical condition of working people and citizens, in such a way that it disturbs them at work, reduces their working capacity, causes restlessness, disturbs the surroundings, disturbs people's regular rest and harms their health [10].

Today's Constitution of the Republic of Serbia [11] proclaims that every individual has a right to healthy environment and timely and complete informing on its state; that everybody, especially the Republic of Serbia and an autonomous province, is responsible for the environmental protection, and that every person is obliged to preserve and improve the environment. The Law on Environmental Protection [12] was brought in 2004 and it is a systemic, 'umbrella law' in the area of environmental protection whose aim, together with other laws, is to enable exercising a human right to life and development in a healthy environment and a balanced relationship between the economic growth and the environment in the Republic of Serbia. The first Law on Environmental Noise Protection [13] was adopted in 2009 at the proposal of the Ministry of Environment and Spatial Planning. It belongs to the so-called 'green package' – a set of 16 laws which regulate different areas of environmental protection.

Protection against noise pollution in domestic legislation

The National Assembly of the Republic of Serbia adopted the new Law on Environmental Noise Protection [14], which defines noise and expands the list of noise sources, in order to solve the existing problem in a more efficient manner. This Law is accompanied by a great number of by-laws, such as rulebooks, which make its enforcement easier and more precise.

In the Republic of Serbia, civil law regulations do not explicitly regulate the property protection in the area of environmental protection. The protection of these rights is implemented through general instruments in the area of damage compensation or through the institute of neighbourhood rights, i.e. services that regulate property relations, in which cases we talk about typical property and obligation instruments of protection [15]. The protection of the environment through criminal law is a last-resort, but at the same time very efficient and more than necessary measure. In the Serbian 2005 Criminal Law [16], there were classified, for the first time, all crimes against the environment. The Criminal Law for the environmental protection does not protect typical human rights (these being life and health) like it used to before, but it protects an individual asset – the environment, or, to be more precise, a human's right to the preserved environment. Special laws can provide administrative law, criminal law or civil law protection. The Law on Environmental Noise Protection includes violations done by a company or other legal entity, by a responsible person in the state administration body, by an authorized legal entity, and it also provides protective measures accompanied by a violation fine [13], while the Law on Environmental Protection includes economic wrongdoings and offences which are subject to sanction. The norms of environmental legislation are of special character and have advantage over general norms of the other branches of law, i.e. the rule *lex specialis, derogat legi generali* is applied [1].

Environmental noise pollution assessment and management in the EU legislation

The Article 3 of the EU Directive 2002/49/EC6 defines noise pollution as an unwanted and environmentally harmful sound in the external environment, resulting from human activity [20]. Directive 2008/99/EZ [21] on the environmental protection through criminal law prescribes the measures which member states should take in the area of criminal law, in compliance with the

attitude of the Council of Europe that criminal liability should begin to exist in cases of 'serious pollution or endangering of the environment' in order to protect the environment more efficiently.

The most important law in the area of protection against noise pollution is Directive 2002/49/EC which deals with environmental noise pollution assessment and management. This directive is of a general character as opposed to other regulations in this area. It defines environmental noise pollution as an unwanted or harmful sound in the external space, caused by human activities, including noise pollution emitted by means of transport (passenger, railway and air traffic) and noise pollution coming from industrial areas. Unlike our legislation which accepted the most general definition of noise pollution, the EU directive accepts a more specific definition which puts in the foreground a harmful impact on human health and the most significant sources of community noise.

The main goal of this directive is defining a common approach primarily aimed at avoidance, prevention or reduction of harmful effects of the exposure to environmental noise, including health disorders caused by noise pollution. The directive is applied to the noise pollution people are exposed to, particularly in urban areas, public parks or other quiet areas in agglomeration, quiet areas in nature, next to schools, hospitals and other noise-sensitive objects and areas. Based on this directive, member states are obliged to appoint competent authorities and bodies responsible for the implementation of the directive at appropriate levels, particularly in order to to carry out actions for determining the degree of exposure to noise by making 'strategic maps of noise pollution' using mutual member states methods of assessment, to collect these maps and action plans, and to provide information on the environmental noise to the public [9]. The main problem is a legislative delay of the adoption and implementation of common prescribed methods in member states, in addition to very low rates of action plans adoption [19].

The compliance of domestic normative framework with community law

The process of joining the EU is followed by changes in the legislation of a candidate state, which are conditioned by the fact that the EU has its own legal assets (*acquis communautaire*) which are different from member states legislation and international law.

The Republic of Serbia obtained its EU membership candidate status back in 2012, which came with the obligation to harmonize the domestic normative framework with the EU legislation. This obligation was established after a thorough review of Chapter 27 which deals with the environmental protection by the European Commission and which, in the form of a report, is a starting point for the analysis of the harmonization of Serbian laws with the EU laws related to the noise pollution protection.

By adopting the Law on Environmental Noise Protection, the Republic of Serbia started the process of harmonization and implementation of the EU laws in the area of protection against noise pollution which was completely unharmonized until that moment. The harmonization with international regulations and Directive 2002/49/EZ is particularly mentioned in the explanation of the draft as one of the reasons for the adoption of the new law. In addition to the law and accompanying by-laws, the area of environmental noise protection is also regulated through special laws that regulate specific forms of noise, such as the Air Traffic Law and technical regulations for motor vehicles and machines. Numerous by-laws for the implementation of Directives 89/629/EEZ, 2002/30/EZ and 2006/93/EZ have been adopted, too. According to the 2016 assessment done by the European Commission, the Republic of Serbia achieved a good level of legal regulation harmonization, but the implementation of regulations is still in the early stages [21]. The Republic of Serbia should build administrative capacities in order to make drafts of strategic maps of noise pollution and action plans [22].

In the new Law on Environmental Noise Protection, the changes to Annex II of the Directive 2002/49/ES have been taken into account [23]. In this way, an attempt was made to fully transfer European norms that refer to the mechanisms of reporting and introducing, i.e. applying the 'polluter pays' principle, which would pass the responsibility for the creation of strategic noise pollution maps to the local government and the responsibility for the creation of strategic maps of traffic noise to public companies.

The main implementation activities under institutional jurisdiction are therefore the making of strategic noise pollution maps and action plans. Strategic noise pollution maps and action plans must be complete before the EU accession date. The long-term plan of activities includes the establishing of mechanisms of reporting to the authorised EU institutions. One of the main obstacles to the implementation of the accepted EU standards are the costs of the implementation [21].A preliminary cost assessment, based on unit price and the experience of member-states and European Commission experts, can be conducted in the following way: prices of the creation of strategic noise pollution maps for settlements go between 0.25 and 1 EUR per capita. The total number of inhabitants in five big cities (Belgrade, Novi Sad, Niš, Kragujevac and Subotica) is 2.443.862. The estimated cost for the 944km of the main travel network is 600 000 EUR, whereas the estimation for the making of noise maps for airports is between 10 000 and 15 000 EUR [21].

Conclusion

A legal framework for the environmental noise protection in the Republic of Serbia is provided by the Law on Environmental Noise Protection, which was adopted for the first time within the so-called green package of laws and which is accompanied by a set of by-laws. A legislator started off from international recommendations and standards, particularly taking into consideration the relevant directives of the EU. This umbrella law thoroughly regulates the environmental protection against noise pollution, measures and conditions of environmental noise protection, environmental noise measurement; access to the information on noise pollution, monitoring and other issues of significance for the environment and human health. An important preventative role in the protection against noise pollution is played by the norms of the Criminal Law which prescribes crimes against the environment, thus protecting human right to the preserved environment, while the Law on Environmental Protection also deals with offences and wrongdoings committed by companies. The EU adopted 13 regulations of various legal force in the area of noise pollution protection, the Directive 2002/49/ES being particularly important for its general character and representing the foundation of the EU regulations in this area today. It can be concluded that a huge step was taken when the Law on Environmental Noise Protection was adopted, especially when we take into consideration the fact that this whole area of environmental protection was one of the most critical points in the process of harmonization until 2009. It will take more time to reach full state of harmonization. Amendments to the Law are planned, for the purpose of fully accepting the norms from the revised Annex II of the Directive 2002/49/EZ. As for the second phase, one of the important requirements prescribed by the EU laws that Serbia still has not met is the creation of noise pollution maps. They provide a review of an average level of noise pollution in different parts of a city, and they are important, among other things, for spatial planning, i.e. as a foundation for the creation of protection action plans. One of the greatest problems that slows down their making is a lack of financing, accompanied by the lack of experts. However, it must be pointed out that this requirement has not yet been met by some member states either, which fact was highlighted by the European Commission.

References

[1] M. Lazić, „Zaštita od buke – komunalna buka i imisija buke,“ Zbornik radova Pravnog fakulteta u Nišu, (2012).
[2] L. C. Den Boer, A. Schroten. Traffic noise reduction in Europe. Health effects, social costs and technical and policy options to reduce road and rail traffic noise. The Netherlands: CE Delft; (2007).
[3] S. A. Stansfeld, B. Berglund, C. Clark, I. Lopez-Barrio, P. Fiscer et al. Aircraft and road traffic noise and children,s cognition and health: a cross-national study. Lancet. (2005); 365:1942-9.
[4] J. Björk, J. Ardö, E. Stroh, H. Lövkvist, P. O. Ostergren, M. Albin. Road traffic noise in southern Sweden and its relation to annoyance, disturbance of daily activities and health. Scand J Work Environ Health, (2006), 32:392-401.
[5] W. Babisch. Transportation noise and cardiovascular risk: Updated Review and synthesis of epidemiological studies indicate that the evidence has increased. Noise Health, (2006), 30:1-29.
[6] Lj. Blagojević, Lj. Stošić. Environmental noise and mental disturbances in urban population. *Acta Med Median*. (2011), 50.3: 34-39.
[7] B. Berglund, T. Lindvall, D. H. Schwela, Guidelines for Community Noise, World Health Organization, Geneva, (1999), vii.
[8] M. Rogač, M. Nikić. “Uticaj buke železničkog saobraćaja na životnu sredinu“, Zbornik radova, International Quality Conference, Quality festival 2012, Kragujevac, (2012).
[9] M. Rubežić. Legal framework of protection from community noise in the Republic of Serbia and its compliance with Directive 49/2002/EC. *Glasnik Advokatske komore Vojvodine*, (2017), 89.9-12: 419-442. Available at https://scindeks-clanci.ceon.rs/data/pdf/0017-0933/2017/0017-09331712419R.pdf.
[10] B. B. Budisavljević, V. Georgijević, P. Pravica. Buka - osnovi, analiza, zaštita. Beograd: Građevinski fakultet, (1998).
[11] Ustav Republike Srbije, ("Sl. glasnik RS" br. 98/2006).
[12] Zakon o zaštiti životne sredine, ("Sl. glasnik RS" br. 135/2004, 36/2009, 36/2009, 72/2009, 43/2011 i 14/2016).
[13] Zakon o zaštiti od buke ("Sl. glasnik RS" br. 36/2009 i 88/2010).
[14] Zakon o zaštiti od buke u životnoj sredini ("Sl. glasnik RS" br. 96/2021).
[15] M. Drenovak-Ivanović, S. Đorđević, S. Važić, Pravni instrumenti ekološke zaštite – građanskopravna i krivičnopravna zaštita, OEBS / Ministarstvo poljoprivrede i zaštite životne sredine, Beograd, (2015).
[16] Krivični zakonik – KZ, (“Sl. glasnik RS“ br. 85/2005, 88/2005, 107/2005, 72/2009, 111/2009, 121/2012, 104/2013, 108/2014 i 94/2016).
[17] Directive 2002/49/EC, OJ L 189, 2002.
[18] Directive 2008/99/EC, *OJ L 328, 2008.*
[19] Commission staff working document refit evaluation of the Directive 2002/49/EC relating to the assessment and management of environmental noise, European commission, Brussels 2016.
[20] Sporazum o stabilizaciji i pridruživanju (2013). Available at https://www.mei.gov.rs/srl/srbija-i-eu/sporazum-o-stabilizaciji-i-pridruzivanju/.
[21] Post skrining dokument životna sredina i klimatske promene, Ministarstvo poljoprivrede i zaštite životne sredine, Beograd, 2016.
[22] Republika Srbija: izveštaj za 2016. godinu, Evropska komisija, Brisel, 2016.
[23] Directive 2002/49/EC, *OJ L 189, 18.7.2002, p. 12–25.*

IDENTIFICATION OF BIOACTIVE COMPOUNDS USING RP-HPLC ANALYSIS OF SOME HAWTHORN SPECIES EXTRACTS (*CRATAEGUS PINNATIFIDA BGE., C. MONOGYNA JACQ., C. CRUS-GALLI.)* AND ANTIOXIDANT ACTIVITY EVALUATION.

Areej Alsobh[1], Gyula Vatai[1], Szilvia Bánvölgyi[1]

[1]Department of Food Process Engineering, Institute of Food Science and Technology, Hungarian University of Agriculture and Life Sciences, Budapest, Hungary
e-mail: areejalsobh@gmil.com

Abstract
Hawthorn is belonging to the Rosaceae family and is one of the plants that have been used as a source of bioactive products. The goal of this work was to determine the phenolic and flavonoid contents and antioxidant activity of ethanolic extracts of some hawthorn species (Crataegus pinnatifida Bge., C. monogyna Jacq., C. crus-Galli.). The extraction was performed at 45 °C, by using ethanol 50 v/v% as a solvent (10 g of the fruit in 100 ml solvent) for 50 min. The Folin-Ciocalteu's method was used for the determination of total phenols, the aluminium chloride method was used for the determination of flavonoids, and the ferric reduction antioxidant power (FRAP) method was used to assess the antioxidant activity of extracts. The identification of phenolic compounds present in extracts was performed using RP-HPLC. A positive linear correlation between the antioxidant activity index and total phenolic content of ethanolic extracts was observed. The order of antioxidant activity in species was as follows (C. crus-Galli > C. pinnatifida Bge. > C. monogyna Jacq.) The RP-HPLC procedure showed that the most abundant compounds were chlorogenic, ferulic and ellagic acids and (+)-Catechin while gallic and caffeic acid were not detected. The extracts have significant antioxidant properties due to the existence of phenolic compounds. It is noteworthy to emphasize that for C. crus-Galli species, its extracts have not been studied or referred to, to the best of our knowledge.

Keywords:
Hawthorn, Total phenolic and flavonoid content, RP-HPLC, Antioxidant Activity

LUTEIN AND ZEAXANTHIN CONTENT IN FLOWERS OF FRENCH MARIGOLD (*TAGETES PATULA* L.) HUNGARIAN VARIETIES

Gabriella Antal[1], Erika Kurucz[1], Kitti Kovács[2], Áron Béni[2]

[1]Institute of Horticultural Science, Faculty of Agricultural and Food Sciences and Environmental Management, University of Debrecen, H-4032 Debrecen, Böszörményi u. 138., Hungary
[2]Institute of Agricultural Chemistry and Soil Science, Faculty of Agricultural and Food Sciences and Environmental Management, University of Debrecen, H-4032 Debrecen, Böszörményi u. 138., Hungary
e-mail: antal.gabriella@agr.unideb.hu

Abstract

French or dwarf marigold (*Tagetes patula* L.) is a well-known ornamental plant, but also utilized in medicine, cosmetics, agriculture and food industry due to its biologically active components (xanthophylls, carotenes, terpenes, flavonoids, benzofuran derivatives, thiophenes, etc.). Three varieties of Hungarian bred *Tagetes patula* ('Csemő', 'Robuszta kénsárga', 'Orion') were transplanted into the pot experiment (5.05.2021) in the following conditions and soil mixtures: in the greenhouse in peat-based soil; outside the greenhouse in peat-based soil, outside the greenhouse in a peat-free soil, and hydroponic system in the greenhouse (University of Debrecen, Hungary). At the beginning of June 2021, whole petals were collected from each variety and condition. The lyophilised samples were extracted by ethanol and ultrasonic assisted method. The lutein and zeaxanthin content of the extracted samples were determined by the HPLC instrument.

Tagetes patula 'Csemő' was the richest source of lutein (709.9 - 1359.5 mg/kg based on dry matter), followed by 'Robuszta kénsárga' (161.4 - 429.7 mg/kg) and 'Orion' (62.0 - 135.8 mg/kg). The highest lutein concentration was measured in the peat-free soil mixture in the field, in each variety. The concentration of lutein and zeaxanthin were depending on the conditions (greenhouse, field) and the medium (peat-based, peat-free and hydroponics), but in the field, the measured lutein and zeaxanthin content was considerably higher than in the greenhouse in the same type of soil mixture (peat-based).

Introduction

Tagetes patula L. (French or dwarf marigold) belongs to the *Asteraceae* family, is commonly known as an ornamental plant. *Tagetes* species have been distributed all over the world and can be cultivated in different soils and weather conditions with low requirements and a long flowering period. *Tagetes patula*, similar to other marigold species, has been utilized in medicine, agriculture and industry [1, 2]. Leaves and shoots of *Tagetes* sp. synthesize and accumulate different terpenes, flavonoids, benzofuran derivatives, steroids, etc., due to theirs biologically active secondary metabolites used in medicines and cosmetics industry [2, 3]. Thiophenes, which are mostly concentrated in the roots of *Tagetes patula*, are used in agriculture production, due to its repellence of insects (nematicidal), bactericide, fungicide and insecticide effects [4, 5]. Petals of *Tagetes sp.* are yellow, orange, red and a mix of these colours, contain carotenoids (especially lutein, lutein fatty acid and β-carotene), used in ophthalmology as a dietary supplement and in the food industry as a natural food colorant (E161b) [6, 7]. Xanthophyll and carotenes contents of *Tagetes* species depend on the varieties, parts of plants, climate and soil conditions etc. [2, 8, 9].

Experimental

Germination and plant experiments were conducted in Biological Research and Plant Experiment Greenhouse (Biodrome), Faculty of Agricultural and Food Sciences and Environmental Management, University of Debrecen (Hungary) and in the field outside the greenhouse, from February to August 2021. Three *Tagetes patula* Hungarian bred varieties were cultivated: 'Csemő' (TAG1), 'Robusta kénsárga' (TAG2), 'Orion' (TAG3) were derived by NARIC (National Agricultural Research and Innovation Centre, Hungary) and were bred by †Dr. Zoltán Kováts, a famous Hungarian ornamental plant breeder and colleagues [10].

Tagetes patula seeds were sown on 19th February 2021, in perlite (particle size: 2-6 mm, Magyar Perlit Kft., Hungary), in a germination chamber (humidified 4 times per day / 15 minutes, EasyGreen, USA). After 4 days, seedlings were transferred to peat-free and peat-based soil mixtures (COMPO, OBI, Hungary) into the cell seedling tray with a volume of 60 cm^3, and Grodan Rockwool cubes (25x25x40 mm, Playgrowned.com, Hungary). Terra Aquatica Tripart advanced nutrient solutions (Micro, Grow and Bloom 3-Part Flora Series, General Hydroponics Europe – GHE) were utilized with reverse osmosis water for Deep Water Culture (DWC) hydroponic production, according to the user guide of products and development phases of seedlings [11]. Three varieties of plantlets were transplanted into the pots (diameter of 14 cm, 1800 cm^3) on 5th May 2021 for pot experiments in the following conditions and soil mixtures: in the greenhouse in peat-based soil; outside the greenhouse in peat-based soil, outside the greenhouse in a peat-free soil, and hydroponic system in the greenhouse.

The first flowers appeared at the beginning of June 2021, whole petals were collected (Figure 1) and frozen in the freezer before lyophilisation. The samples were stored in the dark at room temperature before extraction and HPLC measurements.

Figure 1. Flowers of *Tagetes patula* 'Csemő' (TAG1), 'Robuszta kénsárga' (TAG2), 'Orion' (TAG3)

The lyophilised samples were grounded with a Retsch MM200 ball mill for 15 minutes. 0.1 g of the powdered samples were sonicated (NEY, Ultrasonik 3 QT HEAT, 175W) with 0.5 mL water for 15 minutes. After that 7 mL of absolute ethanol was added to the sample and sonicated at 30 minutes. Finally, the samples were filled up to 10 mL with ethanol and 0.45 µm pore size PVDF membrane filters were used for the filtration of the samples.

Extracts should be analyzed with HPLC as soon as possible, certainly within 24 hr, and must be stored at 4 ºC. The lutein and zeaxanthin content of the samples was determined with an ECOM s.r.o. ECS05 gradient analytical HPLC system. This system consisted of an ECP2000 pump, ECB2004B gradient box with a degasser, ECO2080 column oven, ECDA2800 UV/Vis PDA detector and L-3320 autosampler made by RIGOL. A 10 µL sample was injected into the HPLC and eluted with acetonitrile 63.0 %, methanol 8.60 %, water 10.4 % and ethyl-acetate (18.0 %) on a C18 HPLC column (Phenomenex, 250x4.6 mm; 3 µm) at a flow rate of 1.0 mL/min. The measurements were done at 446 nm. The applied HPLC determination method was modified version of Habib method [12]. With these parameters, the elution times were close to 7.2 (lutein), 7.6 (zeaxanthin) minutes. The chromatograms were processed with Clarity 8.7 software.

Results and discussion

Flower petal of *Tagetes patula* 'Csemő' (TAG1) was the richest source of lutein, it was between 709.9-1359.5 mg/kg (based on dry matter) depending on the conditions and medium. In the peat-based medium, the lutein content of 'Robusta kénsárga' (TAG2) was double in the field (321.6 mg/kg) than in the greenhouse (161.4 mg/kg). The highest lutein concentration of 'Orion' (TAG3) variety were measured in the peat-free soil in the field (135.8 mg/kg) and in the hydroponic systems (121.6 mg/kg) in the greenhouse. Lutein concentration of 'Orion' (TAG3) were considerably lower than other varieties (Figure 2).

Zeaxanthin content of 'Csemő' (TAG1) was also the highest among the varieties, in the field was similar (approx. 117 mg/kg) in the different soils, followed by the hydroponics and peat-based soil in the greenhouse (86.1 and 71.1 mg/kg, consequently). In the greenhouse, in case of different medium, the zeaxanthin content of 'Robusta kénsárga' (TAG2) and 'Orion' (TAG3) was almost similar (15.0-19.4 mg/kg). In the field, zeaxanthin concentration of 'Orion' (TAG3) was much lower than other varieties (Figure 2).

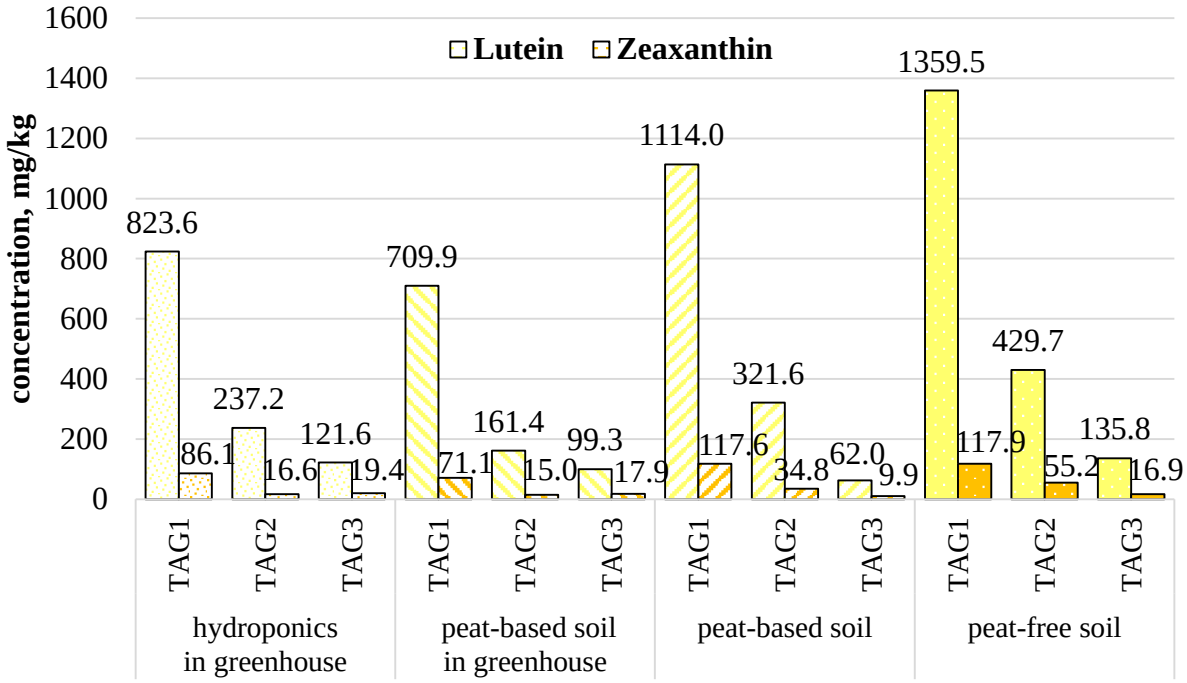

Figure 2. Lutein and zeaxanthin content (mg/kg, based on dry matter) of flowers of *Tagetes patula* Hungarian varieties in different medium and conditions (University of Debrecen, 2021)
Abbreviation: TAG1: *Tagetes patula* 'Csemő', TAG2: *Tagetes patula* 'Robuszta kénsárga', TAG3: *Tagetes patula* 'Orion'.

Based on our HPLC measurements and other authors references [2, 6, 8, 9] confirmed that the varieties, the types of the medium, the climate conditions and the fields may also affect the lutein and zeaxanthin concentration of *Tagetes patula* flowers. In our experiments, the highest lutein concentration was measured in the peat-free soil mixture in the field, in each variety. In case of peat-based soil mixtures, the measured lutein and zeaxanthin content were considerably higher in the field than in the greenhouse.

Conclusion

Tagetes patula has important chemical compounds which are considered for chemical and biological activity and they have a definite useful effect against various diseases. This

conference paper is the preliminary reports of HPLC measurements of lutein and zeaxanthin concentration from flowers of Hungarian bred *Tagetes patula* varieties. The applied HPLC method has fast, simple and cheap sample preparation.
We will continue this investigation of the *Tagetes patula* varieties because the growth of these plants at reduced use of peat and fertilizers is important for the commercial exploitation of these plant-produced compounds.

Acknowledgements
The publication is supported by the EFOP-3.6.1-16-2016-00022 project. The project is co-financed by the European Union and the European Social Fund.

References
[1] P. Vasudevan, K. Suman, S. Satyawati. Biores. Techn. 62.1-2 (1997) pp. 29-35.
[2] M. Riaz, R. Ahmad, N. U. Rahman, Z. Khan, D. Dou, G. Sechel, R. Manea. J. Ethnopharmacol. (2020) 255, 112718.
[3] P. Singh, A. Krishna, V. Kumar, S. Krishna, K. Singh, M. Gupta, S. Singh. J. Essent. Oil Res. (2016) 28:1, pp. 1-14
[4] Sz. Szarka, E. Hethelyi, É. Lemberkovics, I. N. Kuzovkina, P. Bányai, É. Szőke, Chromatographia, (2006) 63(13), S67-S73.
[5] P.C. Santos, V.H.M. Santos, G.F. Mecina, A.R. Andrade, P.A. Fegueiredo, V.M.O. Moraes, L.P. Silva, R.M.G. Silva, S. Afr. J. Bot. (2015) 100: pp. 114-121
[6] R. Piccaglia, M. Marotti, S. Grandi, Ind. Crop Prod. (1998) 8(1), pp. 45-51.
[7] P. Salachna, A. Wesołowska, E. Meller, R. Piechocki, Indust. Crops Prod. (2021) 171, 113961.
[8] J. H. Lin, D. J. Lee, J. S. Chang, J. Taiwan Inst. Chem. Engin. (2015) 49, pp. 90-94.
[9] M. Khalil, J. Raila, M. Ali, K. M. Islam, R. Schenk, J. P. Krause, F. J. Schweigert, H. Rawel, J. Funct. Foods, (2012) 4(3), pp. 602-610.
[10] M. Fári, S. Kisvarga, E. Hlaszny, A. Zsila-André, J. Koroknai, E. Kurucz, G. Antal (2019). Hung. Agr. Res. 28(2) pp. 31-37.
[11] GHE Flora Series, General Hydroponics (2021) https://www.plantplanet.de/mediafiles/Sonstiges/GHE/Terra%20Aquatica%20-%20GHE%20 -%20TriPart%20Anleitung.pdf
[12] B. Habib, World J. Pharmaceutical Res. 4 (2015) 145-156.

PHYTOREMEDIATION OF OUTDOOR AIR: A REVIEW

Katarina Antić[1], Tatjana Šolević Knudsen[1], Milena Stošić[2], Jelena Radonić[2]

[1]*Department of Chemistry, Institute of Chemistry, Technology and Metallurgy, University of Belgrade, Njegoševa 12, 11000 Belgrade, Serbia*
[2]*Department of Environmental Engineering and Occupational Safety and Health, Faculty of Technical Sciences, University of Novi Sad, Dositej Obradović Square 6, 21000 Novi Sad, Serbia*
e-mail: katarina.antic@ihtm.bg.ac.rs

Abstract
For the purpose of improving a country's economy, urbanization, industrialization, and technical advancement all had detrimental environmental effects. One of the most serious consequences of the aforementioned phenomenon is air pollution. Various air pollutants emitted by natural and anthropogenic sources have been found to have negative effects on the environment and human health after prolonged exposure. Insufficient technologies are used to reduce air pollution as a result of problems in the industry sector, including high maintenance costs, machine failure, and expensive technical equipment. Technological innovations like phytoremediation, which is sustainable and friendly to the environment, are being used to improve outdoor air quality. Cost efficiency, convenience of *in-situ* application, eco-friendly treatment, and the ability to improve the aesthetic value of the nearby environment are advantages of phytoremediation over other conventional remediation approaches. Numerous studies in the field of the outdoor air phytoremediation have found highly beneficial results, but also challenges in applying the suggested method. Plant tolerance to pollutants, environmental parameters, plant-specific features, composition of air pollutants, uncertainty in plant-microbe interactions, and plant antagonism have all emerged as a result of the use of plants in outdoor air pollution remediation. To become a complementary or alternative tool for engineering-based remediation methods, the remedy process must be optimized with supplementary treatments or the best combination junction with other methods must be found.

Key words: *air pollution, phytoremediation, sustanaible outdoor air pollution remediation technique*

Introduction
Urbanization, industrialization, and technological advancement for the purpose of expanding a nation's economy all had unfavorable environmental consequences. By 2050, 68 % of the world's population, up from more than 55 % today, is anticipated to reside in urban areas [1]. The most essential element for live organisms to survive and function, air, is excessively polluted due to the global urbanization. Although there are some natural sources of air pollution, such as volcanic eruptions, wind-blown dust, and forest fires, the majority of pollution is caused by anthropogenic sources such as industrial processes, fossil fuel combustion, waste treatment, construction, and agricultural activity. Chemical complexes used in pesticides, insecticides, fungicides, household cleaning materials, fabrics, paints, sofas, and other products, are another major cause of air pollution [2]. In addition to comprehending how air pollutants are produced, it is essential to know how they are transported and how they interact with the environment. Gaseous contaminants have the ability to travel great distances and harm species in areas further downstream. The production of secondary air contaminants during this trans-boundary transit also had an impact on the aerosol size distribution [3]. Common pollutants with anthropogenic origins include particulate matter (PM), carbon monoxide (CO), nitrogen oxides (NO_x), volatile

organic compounds (VOCs), polycyclic aromatic hydrocarbons (PAHs), potential toxic elements (PTEs), sulfur dioxide (SO_2), and secondary pollutants like ozone (O_3). However, natural air pollutants like radon and biogenic volatile organic compounds (BVOCs) are abundant [2]. People are exposed to approximately 200 different air pollutants in anthropo-ecosystems, some of which can impact citizens' life quality and well-being by increasing respiratory and cardiovascular diseases and mortality. With 400,000 cases per year in Europe, air pollution has been identified as the single greatest environmental health risk, leading to approximately 4.2 million premature deaths annually [3]. Climate change is also one of the consequences of air pollution. The combined effects of air pollution and climate change reduce future ecosystem productivity and water availability [3]. Anthropogenic emissions should be eradicated, prevented, or minimized in accordance with regulations. Following the prevention of pollutant emissions at the source, science-based methods are required to treat existing air pollutants. As a result, the development of technologies to remove/reduce air pollution has arisen as a key concern for the worldwide community.

Conventional air pollution remediation techniques

Air pollution abatement strategies must be implemented in order to reduce the air pollution. Air pollutants are controlled at the source through various policies and laws that require polluters to reduce their emissions. To reduce the impact of air pollution, emission control systems and air remediation technologies such as incineration, filtration, adsorption, photocatalysis, ozonation, ionization, electromagnetic precipitation, and wet scrubbers are used [3]. Nature-based solutions are becoming more popular means of reducing air pollution (NBS). NBS for dealing with atmospheric pollution allude to plants ability to absorb and catabolize practically any of airborne contaminants, as well as efficient pollutant deposition onto vegetation rather than artificial surfaces [1]. Furthermore, new environmentally friendly and sustainable technologies, such as phytoremediation, are being implemented. The benefits of phytoremediation over other conventional remediation technologies include cost effectiveness, ease of *in-situ* use, eco-friendly treatment, and the ability to raise the aesthetic value of the immediate environment. Additionally, phytoremediation can be used to long-term remediation of a wide spectrum of environmental contaminants.

Phytoremediation: sustanaible air pollution remediation technique

Phytoremediation is a relatively recent approach based on engineered application of plant species for the elimination of hazardous compounds through processes such as separation, accumulation, and stabilization [4,5,6,7]. The applied plant species root system and the absorption process that takes place there play a key part in the phytoremediation procedure. Polluting substances and water are separated from the treated matrix via absorption, after which the degradation process begins. Water movement through the plant is encouraged by evapotranspiration, which occurs above ground. Microbes inhabit plant roots (rhizosphere) and shoots or above-ground organs (phyllosphere) as heterotrophs. Microbes can help plants withstand abiotic and biotic challenges by absorbing nutrients and water and creating plant hormones, inhibitory allelochemicals, and siderophores [3]. Phytoremediation is a process that includes seven approaches: phytoextraction, phytovolatilization, phytodegradation, phytostabilization, rhizodegradation, rhizofiltration, and hydraulic control [3]. The surface of leaves and stems is known to adsorb considerable amounts of contaminants in the case of air pollution. Phyllosphere microbiome, which inhabit these surfaces, may therefore be of paramount relevance. Because some of the absorbed pollution makes its way into the plant, leaf endophytes are of a particular importance. By degrading, transforming, or sequestering contaminants, these phyllospheric and endophytic microbiome can detoxify a portion of

contaminants. Rainfall also results in pollutants pouring down to the soil just beneath the plant, where they come into touch with the soil, the rhizosphere, and the roots of the plant [3].

Using phytoremediation to improve outdoor air quality

An overview of phytoremediation for improving outdoor air quality is provided in **Table 2.**

Table 2. Enhancing outdoor air quality with phytoremediation

Location	Pollutants	Observations/Suggested Measures	References
Tabriz, Iran	O_3, SO_2, NO_2, CO, $PM_{2.5}$	In 2015, shrubs and trees removed 238.4 t of air contaminants, and an increase of the elimination up to 814.46 t over the next 20 years is expected if appropriate, feasible urban forest management is performed.	[8]
North Katowice, Poland	PM	Among vines, shrubs, and coniferous trees, *Parthenocissus quiquefolia* and *Betula pendula* 'Youngii' accumulated the highest amounts of PM in their wax. The accumulated PM contained carbon, oxygen, silicon, iron, and heavy metals.	[9]
Fifteen different urbanized areas in Sydney, Australia	PM	The leaf traits were not the specific factor to determine the deposition capacities of plants. Among investigated plants, *N. glabra*, *C. comosum variegatum*, *P. Xanadu*, and *S. wallisii* entrapped the most amount of PM.	[10]
Surabaya town, Indonesia	Lead (Pb)	*Wedelia trilobata* and *Syzigium olein* are grown on the main roads and exposed to heavy metals. *Wedelia trilobata*, having wider leaves, absorbed more heavy metals than *Syzigium oleina* showing a smaller leaf surface area.	[11]
Beijing Forestry University, Beijing, China	$PM_{2.5}$	Compared to broadleaved plant species, needle-leaved coniferous species accumulated higher amounts of $PM_{2.5}$. The $PM_{2.5}$ removal capacity of broadleaved species was correlated to the number of grooves and trichomes.	[12]
Hanoi, Vietnam	PM	Leaves with a lower area, hydrophilic traits, and a high abaxial stomatal density entrapped more PM; accordingly, *Muntingia calabura* showed the highest PM removal capacity among 49 screened plant species.	[13]
Birmingham New Street railway, United Kingdom	PM_1, $PM_{2.5}$, PM_{10}	*Hebe albicans Cockayne*, *Hebe x youngii Metcalf*, *Buxus sempervirens* L., and *Thymus vulgaris* L., which have small leaves, revealed the highest PM removal capacity. Leaves with adaxial surfaces showed higher PM densities compared to those with abaxial surfaces.	[14]

Kunming City, Southwest China	PM	*Platanus acerifolia* and *Magnolia grandiflora* showed the highest PM removal among deciduous and evergreen trees, respectively. PM entrap capacity depends not only on the leaf characteristics, but also on the pollution grade; *Loropetalum chinense*, *Osmanthus fragrans*, and *Cinnamomum japonicum* exhibited significant accumulation of PM in traffic and university campus areas, whereas showing moderate removal efficacy in an industrial area.	[15]
Trivandrum City, Kerala, India	Air Pollution Tolerance Indices (APTI)	Based on APTI, plants showing the highest APTI, *Agave americana*, *Anacardium occidentale*, *Cassia fistula*, *Cassia roxburghii*, *Mangifera indica*, and *Saraca asoca*, were suggested for near areas presenting heavy vehicular air pollution, and plants showing the next highest APTI for greenbelts.	[16]

Conclusion

Controlling air pollution is far more difficult than controlling soil and water pollution, and new inventive ideas and approaches are necessary to meet this requirement. Nevertheless, air quality can be enhanced by phytoremediation, which incorporates plants and their microbiomes. Because of its substantial advantages, such as being eco-friendly, cost-effective, and having publically applicable procedures, phytoremediation is an emerging prospective tool for improving *in-situ* air conditions. Phytoremediation has been shown to reduce the effects of numerous air pollutants and to cause minimum environmental disruption in treatment areas, but the removal efficacy of phytoremediation is still being studied. Because of the use of plants in outdoor air pollution remediation, the following issues have emerged: *plant tolerance to pollutants*, *environmental parameters* (wind, precipitation, temperature, pH, solar intensity, water availability), *plant-specific features* (surface roughness, thickness, ultrastructure, pubescence, wax content, leaf size, and structure), *composition of air pollutants*, *uncertainty in plant-microbe interactions*, and *plant antagonism*. These characteristics provide obstacles in phytoremediation methods and should be taken into account when developing an effective phytoremediation approach for outdoor air pollution. The techniques applicability in highly polluted air has not been clearly demonstrated. Optimizing the remedy process with supplementary treatments or finding the best combination junction with other methods is required to become a complementary or alternative tool for engineering-based remediation methods.

References

[1] Prigioniero, A., Zuzolo, D., Niinemets, Ü., Guarino, C., Nature-based solutions as tools for air phytoremediation: A review of the current knowledge and gaps, Environmental Pollution, Vol. 277, Art. No. 116817, 2021.

[2] Bandehali, S., Miri, T., Onyeaka, H., Kumar, P., Current State of Indoor Air Phytoremediation Using Potted Plants and Green Walls, Atmosphere, Vol. 12 (4), Art. No. 473, 2021.

[3] Lee, B.X.Y., Hadibarata, T., Yuniarto, A., Phytoremediation Mechanisms in Air Pollution Control: A Review, Water, Air, & Soil Pollution,Vol. 231, Art. No. 437, 2020.
[4] Vamerali, T., Bandiera, M., Mosca, G., Field crops for phytoremediation of metal-contaminated land: A review, Environmental Chemistry Letters, Vol. 8 (1), pp. 1-17, 2010.
[5] Tangahu, B.V., Abdullah, S.R.S., Basri, H., Idris, M., Anuar, N., Mukhlisin, M., A Review on Heavy Metals (As, Pb, and Hg) Uptake by Plants through Phytoremediation, International Journal of Chemical Engineering, Vol. 2011, pp. 1-31, 2011.
[6] Antonijević, M.M., Dimitrijević, M.D., Milić, S.M., Nujkić, M.M., Metal concentrations in the soils and native plants surrounding the old flotation tailings pond of the Copper Mining and Smelting Complex Bor (Serbia), Journal of Environmental Monitoring, Vol. 14, pp. 866- 877, 2012.
[7] Lee, H., Jun, Z., Zahra, Z., Phytoremediation: The Sustainable Strategy for Improving Indoor and Outdoor Air Quality, Environments, Vol. 8(11), Art. No. 118, 2021.
[8] Amini Parsa, V., Salehi, E., Yavari, A.R., van Bodegom, P.M., Analyzing Temporal Changes in Urban Forest Structure and the Effect on Air Quality Improvement., Sustainable Cities and Society (SCS), Vol. 48, Art. No.101548, 2019.
[9] Konczak, B., Cempa, M., Deska, M., Assessment of the Ability of Roadside Vegetation to Remove Particulate Matter from the Urban Air, Environmental Pollution, Vol. 268, Art. No. 115465, 2021.
[10] Paull, N.J., Krix, D., Irga, P.J., Torpy, F.R., Airborne Particulate Matter Accumulation on Common Green Wall Plants, International Journal of Phytoremediation**,** Vol. 22, pp. 594–606, 2020.
[11] Rachmadiarti, F., Purnomo, T., Azizah, D.N., Fascavitri, A., Syzigium Oleina and Wedelia Trilobata for Phytoremediation of Lead Pollution in the Atmosphere, Nature Environment and Pollution Technology**,** Vol. 18, pp. 157–162, 2019.
[12] Chen, L., Liu, C., Zhang, L., Zou, R., Zhang, Z., Variation in Tree Species Ability to Capture and Retain Airborne Fine Particulate Matter ($PM_{2.5}$), Scientific Reports, Vol. 7, pp. 1–11, 2017.
[13] Bertold, M., Joachim, M., Hoa, N.X., Cuong, N.T., van Sinh, N., Roeland, S., Particulate Matter Accumulation Capacity of Plants in Hanoi, Vietnam, Environmental Pollution, Vol. 253, pp. 1079–1088, 2019.
[14] Weerakkody, U., Dover, J.W., Mitchell, P., Reiling, K., Particulate Matter Pollution Capture by Leaves of Seventeen Living Wall Species with Special Reference to Rail-Traffic at a Metropolitan Station, Urban Forestry and Urban Greening, Vol. 27, pp. 173–186, 2017.
[15] Li, Y., Wang, S., Chen, Q., Potential of Thirteen Urban Greening Plants to Capture Particulate Matter on Leaf Surfaces across Three Levels of Ambient Atmospheric Pollution, International Journal of Environmental Research and Public Health, Vol. 16, Art. No. 402, 2019.
[16] Watson, A.S., Bai, R.S., Phytoremediation for Urban Landscaping and Air Pollution Control—A Case Study in Trivandrum City, Kerala, India, Environmental Science and Pollution Research, Vol. 28, pp. 9979–9990, 2021.

COMPARISON OF STABILITY CONSTANTS OF MACROCYCLIC COMPLEXES Cu(II) AND Co(II) DEPENDING ON THE CO-LIGANDS

Mirjana Antonijević-Nikolić[1], Slađana Tanasković[2], Branka Dražić[2]

[1]Academy of Applied Studies Šabac, Department for Medical, Business and Technological Studies, Hajduk Veljkova 10, 15000 Šabac, Serbia,
[2] Faculty of Pharmacy, Vojvode Stepe 450, 11000 Belgrade, Serbia
e-mail: mantonijevicnikolic@vmpts.edu.rs

Abstract

Stability of metal complexes may be affected by various factors like nature of central metal ion and ligand, chelating effect, etc. Some parameters like distribution coefficients, conductance, refractive index, etc. are useful for the determination of stability constants. Various modern techniques are used to determine the stability constant of simple as well as mixed ligand compounds. The stability constant is one of the crucial physicochemical parameters, necessary for the correct interpretation of the complex and determination of the metal-ligand reaction properties.

Stability constants of some binucler mixed ligand Co(II) and Cu(II) complexes with macrocycle *tpmc* = N,N',N'',N'''-tetrakis(2-pyridylmethyl)- 1,4,8,11-tetraazacyclotetradecane and different co-ligands are compared. The stoichiometric ratio of the compounds was determined spectrophotometrically at 20 ° using Job's methods of continuous variation for Cu(II) complexes and Job's method of continuous variation and Rose-Drago method for Co(II) complexes [1-4]. The values of stability constants K and Gibbs free energy ΔG were calculated and compared.

The values log*K* are in the range of 2.76 – 4.80 obtained for Cu(II) complexes with tpmc, $[Cu_2(X)tpmc](ClO_4)_3 \cdot nH_2O$ with bridging anions $X^- = F^-, Cl^-, Br^-, I^-, NO_2^-$ [5] and $[Cu_2(gly)tpmc](ClO_4)_4 \cdot 2H_2O$/ CH_3CN with glycine/alanine. For Co(II) tpmc mixed ligand complexes of formulas, $[Co_2(L)tpmc](ClO_4)_2$, L = benzoate anion, phthalate dianion, isophthalate dianion and terephthalate dianion values log*K* are in the range 5.25-5.37. It can be concluded that copper (II) complexes with halogenous and monocarboxylic ligands are less stable than cobalt(II) complexes with aromatic dicarboxylic co-ligands. Negative values for Δ*G* mean that the formation of Cu(II) and Co(II) complexes is energetically favourable and that the reactions proceed spontaneously.

References

[1] A. Özlen, Ş. Mehtap, J. Mol. Struct. 1149 (2017) 307.
[2] N. J. Rose, R. S. Drago, J. Am. Chem. Soc. 81 (1959) 6138 .
[3] L. G. Sillen and A. E. Martel (eds.), Stability Constants, The Chemical Society, London, 1971.
[4] K. Hirose, J. Inclusion Phenom. Macrocyclic Chem. 39 (2001) 193.
[5] G. Vučković, E. Asato, N. Matsumoto, S. Kida, Inorg. Chim. Acta 171 (1990) 45.

SPECIFIC PHOSPHOLIPID FATTY ACID COMPOSITION OF THE MICROBIAL BIOMASS OF CALCAREOUS CHERNOZEM AND HUMIC SANDY SOILS

Andrea Balláné Kovács, Áron Béni, János Kátai, Evelin Juhász

Institute of Agricultural Chemistry and Soil Science, Faculty of Agricultural and Food Sciences and Environmental Management, University of Debrecen, H-4032 Debrecen, Böszörményi u. 138., Hungary
e-mail: kovacsa@agr.unideb.hu

Abstract

The specific phospholipid fatty acid (PLFA) composition of the microbial biomass of calcareous chernozem and humic sandy soils was determined using a gas chromatograph with flame ionization detector (FID) and MIDI-Inc. complex data analysis software. The total PLFA extracted from the soil characterizes the microbial biomass, and the quality of PLFAs can be used to determine the presence and dynamics of specific taxon groups.

The objective of our work was to select, modify and develop the most suitable method for the parameters of our measurement system from the several sample preparation methods recommended in the literature for the measurement of soil microbial communities based on PLFA determination.

The modified sample preparation method was used to compare the phospholipid fatty acid profiles of calcareous chernozem soil (Debrecen-Látókép) and humic sandy soil (Debrecen-Pallag) from pot experiments with significantly different properties. The calcareous chernozem soil had a higher and more diverse PLFA content. The total PLFA on chernozem was 23.16 nmol/g, in sandy soil was one third lower, 7.23 nmol/g, suggesting a higher living microbial biomass in chernozem soil.

Bacterial biomass was higher than fungal biomass in both soil types. The biomass of Gram-negative bacteria slightly exceeded that of Gram-positive bacteria on chernozem and significantly exceeded that of Gram-positive bacteria on the sand. In addition, we also analysed how significantly different water supply, ideal supply and drought stress modify the PLFA composition of the microbial community of calcareous chernozem.

Our results demonstrated that drought stress reduced the total PLFA from 23.16 nmol/g to 16.49 nmol/g. Drought stress reduced the PLFA biomarker of mycorrhizal fungi by about half. The biomass of Gram-negative and Gram-positive bacteria were also reduced, but their proportions were not affected by different water supplies. The fungi/bacteria ratio decreased slightly in the drought-stressed environment. Under drought stress, the ratio of saturated to monounsaturated PLFA fatty acids, which can be sensitive to environmental stress as a stress factor, increased compared to the value in the ideal water supply model.

In conclusion, our results showed that the chernozem soil had more types and higher amount of extractable phospholipid fatty acids, which allowed to estimate a higher living microbial biomass in this soil type than in sand. The mass of living microbial biomass present in calcareous chernozem soil was significantly reduced under drought stress.

BIOLOGICAL ACTIVITY OF SILICONE-BASED MEMBRANES WITH FUNCTIONALIZED SILSESQUIOXANES. CHARACTERIZATION AND PERSPECTIVES FOR ENVIRONMENTAL APPLICATIONS

Alexandra Bargan[1], George Stiubianu[1], Mihaela Dascalu[1], Adrian Bele[1], Alina Soroceanu[1], Ana-Maria Macsim[1]

[1]Department of Inorganic Polymers, "Petru Poni" Institute of Macromolecular Chemistry, Grigore Ghica Voda Alley, 41A, 700487 Iasi, Romania,
e-mail: anistor@icmpp.ro

Abstract
A series of three silsesquioxanes (containing either the original organic function (SH) (silsesquioxane 2, SH_SS), a derivatized one (NH_3Cl) (silsesquioxane 1, A_SS) or completely chloro derivative (silsesquioxane 3, Cl_SS)) were obtained by acid hydrolysis of the three organo-trialkoxysilane (3-aminopropyltriethoxysilane, 3-mercaptopropyltrimethoxysilane and 3-cyanopropyltriethoxysilane). The biological compatibility was tested for the three composite films. The values of water vapors sorption capacities increase in the following order: P_Cl_SS < P_SH_SS<P_A_SS. Depending on the silsesquioxane type, an increasing of the dielectric constant value up to 4.5 as compared with the value for the silicone matrix was obtained. The bactericidal performance in environmental applications of the newly blends with specific microarchitecture, controlled porosity and higher hydrophobicity, is measured by its ability to maintain the balance between the biological selectivity and membranes functionalization as disinfection materials

Introduction
Three different molecular or polymeric well-determined complex structures containing silsesquioxanes moieties with different functionalities were incorporated into a polymeric matrix based on a polydimethylsiloxane of low molecular weight. After the incorporation of the silsesquioxane, the films were investigated by dynamic vapour sorption (DVS) analysis, stress–strain measurements and dielectric spectroscopy. The presence of the siloxane moiety in the material ensures good mechanical properties.

Experimental
Antibacterial and fungicidal activities of silsesquioxanes functionalized with ammonium chloride (1), mercaptopropyl (2), and chloropropyl groups (3) were evaluated by performing "in vitro" tests against pure culture of three fungi species (Aspergillus niger, Penicillium frequentans, Alternaria alternata) and against both Gram-negative (Pseudomonas aeruginosa) and Gram-positive (Bacillus polymyxa) bacteria.

Results and discussion
Three new membrane materials with three silsesquioxanes: - original organic function (SH) (silsesquioxane 2, SH_SS), - derivatized one (NH_3Cl) (silsesquioxane 1, A_SS); - completely substituted chloro derivative (silsesquioxane 3, Cl_SS). Polymeric matrix consists in low molecular weight polydimethylsiloxane. After the incorporation of the silsesquioxanes, the bactericidal performance in environmental applications of new blends with specific microarchitecture, controlled porosity, and higher hydrophobicity were measured by its ability to maintain the balance between the biological selectivity and membranes functionalization as

disinfection materials. The inhibition of the Gram-negative bacteria for the P_SH_SS was more pronounced than the inhibition for P_Cl_SS, P_A_SS and P membranes.

Conclusion

Processing of the functionalized silsesquioxanes led to new materials with high-performance characteristics designed to be used in a membrane system for wastewater treatment. Characteristics of materials generated by the structural properties of the polymeric chains and the history of the films influence the surface morphology indicating that the prepared membranes could be applied as membranes in wastewater treatment. Filtration properties of the composite silicone membranes have demonstrated the suitability of these to act as selective barriers, permitting the free transport of water vapor through the pores. Evaluation of the applicative potential of these membranes, tested in terms of antimicrobial activity, confirms their excellent performance as potential candidates in the field of wastewater treatment.

Acknowledgements

This work was supported by a grant of the Ministry of Research, Innovation and Digitization, CCCDI - UEFISCDI, project number PN-III-P2-2.1-PED-2021-3900, within PNCDI III.

References

[1] A.M.C. Dumitriu, M. Balan, A. Bargan, S. Shova, C.D. Varganici, M. Cazacu, „Synthesis of functionalized silica nanostructure: Unexpected conversion of cyanopropyl group in chloropropyl one during HCl-catalysed hydrolysis of the corresponding triethoxysilane", *Journal of Molecular Structure*, 1110, 150-155, (2016), https://doi.org/10.1016/j.molstruc.2016.01.043

[2] A.M.C. Dumitriu, M. Cazacu, A. Bargan, M. Balan, N. Vornicu, C.D. Varganici, S. Shova, „Full functionalized silica nanostructure with well-defined size and functionality: Octakis(3-mercaptopropyl)octasilsesquioxane", Journal of Organometallic Chemistry, 799-800, 195-200, (2015), https://doi.org/10.1016/j.jorganchem.2015.09.025

[3] A.M.C. Dumitriu, A. Bargan, M. Balan, C.D. Varganici, S. Shova, M. Cazacu, „Synthesis and characterization of octakis(3-chloroammoniumpropyl)octasilsesquioxane", Revue Roumaine de Chimie, 61(4-5), 385-393, (2016), http://revroum.lew.ro/wp-content/uploads/2016/04/Art_24.pdf

DIELECTRIC MONITORING OF BIOMASS HYDROLYSIS PROCESSES

Sándor Beszédes, Zoltán Jákói, Laura Haranghy, Cecilia Hodúr

Department of Biosystems Engineering, University of Szeged, Faculty of Engineering, H-6725 Szeged, Moszkvai krt. 9, Hungary
e-mail: beszedes@mk.u-szeged.hu

Abstract

Development of biomass utilization technologies is one of the main area of researches in nowadays. Many biomass utilization process use enzymatic hydrolysis step. Monitoring of the efficiency of hydrolysis plays crucial role in the determination of optimum process time and contributes to achieve lower energy demand and better economy of technologies. Therefore, development of fast, but reliable and non-destructive measurement methods has high relevance not just for the science, but also for the practice. Dielectric measurements have great potential for these purposes, but there are very few experiences related their applicability for detection of conversion efficiency of enzymatic hydrolysis and fermentation processes. Therefore, our research has focused on the investigation of the applicability of dielectric measurements at the frequency range of 200-2400 MHz for the detection of the efficiency of sludge treatment processes, and monitoring the enzymatic hydrolysis of lignocellulosic biomass. Our results have shown that the cellulose degradation during the enzymatic hydrolysis of corn cob residue, and, as well as, the increment of organic matter solubility after different sludge disintegration methods can be monitored by the measurement of dielectric constant at the frequency range of 200-1000 MHz. The correlation between the indicators of biomass hydrolysis processes and dielectric parameters enables to develop on-line and real-time monitoring methods.

Key words: dielectric constant, biomass, sludge, hydrolysis

Introduction

Dielectric properties can widely use to quantify and characterize the electric polarization when the sample is exposed to electromagnetic field. The polarization ability of the system can be measured by the complex permittivity. The real part of the complex permittivity (i.e. the dielectric constant, ε') corresponds to the ability of the medium for energy storage exposed to electromagnetic radiation; the imaginary part (dielectric loss factor, ε") relates to the energy dissipation of the medium [1].

The dielectric parameters can be determined by resonant cavity methods, using of parallel plate capacitors, free space methods, transmission line methods and coaxial techniques, respectively. Novel developed open-ended coaxial cable probes provide a low-cost and easy implementable method for the fast determination of dielectric parameters in a wide frequency range, based on the measurement of reflection coefficient by impedance analyser or vector network analyser (VNA) [2]. VNA can be used mainly for high frequency measurements (kHz-GHz ranges). In measurements with open-ended coaxial probes need a direct contact with sample surface. Errors and uncertainties of dielectric measurement process with an open-ended coaxial probe can be arisen mainly from the inhomogeneity of samples, probe-sample contact, and/or probe-sample pressure.

The dielectric parameters of the medium influence the reflection coefficient (given as Γ or S11 parameter) of an open-ended probe that is attached to sample surface. Therefore, for example, air-gap between the surface of material under test (MUT) with high roughness and the dielectric probe decreases the reliability of the measurements. Dielectric parameters can use for modelling

and optimization of microwave heat treatments, determine the moisture content of biomaterials, detect the presence of specific compounds in different multicomponent system, or monitoring of chemical and biochemical reactions, as well [3, 4].
The frequency of dielectric measurements depends on the system/material. Degradation of high voltage transformer oils can be monitored with complex dielectric permittivity measurements in frequencies between 100 MHz and 3 GHz [5]. For determination of the dielectric behaviour of biological tissues a lower frequency range (17 MHz to 2 GHz) can be applied [6]. Measurements of dielectric properties and behaviour with open-ended coaxial probes have lower accuracy if the measuring frequency is below 200 MHz and the dielectric constant and loss factor of MUT has low in magnitude. High temperature in high water contented system (suspension, solution) can led to forming of vapour bubbles on the surface of the probe that disturb the reflection of electromagnetic waves [7].
Dielectric measurements have several advantages over the conventional analytical and material testing methods, such as its non-destructive, non-invasive characteristics, no need for chemicals, and easy sample preparation [8]. Furthermore, by using reflection-based methods in vivo and in vitro measurements can be carried out in biological systems and samples, respectively. Accurate knowledge of dielectric parameters of biological tissues has great importance in medical diagnostic and electromagnetic medical (therapeutic) technologies for dosimetry calculations, as well [9].
Dielectric constant at 2450 MHz is suitable to predict the molecular weight of macromolecules produced in caprolactone polymerisation, furthermore, the dielectric parameters measured on-line show good correlation with the progress of the ring opening of caprolactone monomer [10]. At higher frequencies, the inflection point of dielectric constant and the peak value of dielectric loss correlates well with the change of dipolar relaxation time. Asymptotic value of dielectric constant indicates the end of cross-linking process [11].
In solids, water content and water activity determines mainly the dielectric behaviour. Dielectric constant increases with the increasing of water content and water activity at the microwave frequency of 915 MHz and 2450 MHz. This general tendency enables to use dielectric measurement for estimation the change of moisture content of food, for example [12].
The dielectric measurement have great potential for monitoring of chemical and biological processes, but there is a gap in the knowledge related its practical applicability. Therefore, our main aim was to investigate the applicability of dielectric constant for monitoring of the progress and efficiency of enzymatic hydrolysis of lignocellulosic biomass and preliminary hydrolysis of food industry wastewater sludge, respectively.

Experimental

For the lignocellulosic enzymatic hydrolysis tests 5 m/m% suspension (based on dry matter content) made from the grit fraction of corn cob residues (COBEX GM20) was used. This fraction has an average particle size of 780 ± 90 μm, and the cellulose/hemicellulose/lignin percentage ratio of 47.1/37.3/6.8%.
Cellic CTEC2 (Novozymes) enzyme blend was used in a dosage of 120 FPU/g_{DM} for the enzymatic hydrolysis tests carried out at the temperature of 50°C and pH of 5.2. Reducing sugars were measured by DNSA spectrophotometric method.
To increase the organic matters solubility of meat industry wastewater sludge alkaline (pH=12) and microwave pre-treatment and their combination were used. The specific energy intensity of microwave treatment (J/g) was calculated from the power of magnetron (operating at frequency of 2450 MHz), the exposure time, and the weight of the irradiated sample.
The solubility of organic matters was characterized by the ratio of soluble to total chemical oxygen demand (SCOD/TCOD). The chemical oxygen demand was measured by colorimetric

method (Hanna, COD cuvet test, after 2 hours thermodigestion at 180 °C), for separation of soluble fraction of organic matters filtration with 0.45 μm pore sized syringe filter was used after centrifugation (10 min, RCF=5500).
Dielectric constant (ε') was measured with an open-ended coaxial-line probe (SPEAG DAK 3.5), connected to a vector network analyser (ZVL-3 VNA, Rhode&Schwarz) at the frequency range of 200-2400 MHz. Immersion depth of dielectric probe was 10 mm; the temperature of the samples was controlled at 25°C during the dielectric measurements by thermostatic water bath.

Results and discussion

At the first stage of our experiments, the dielectric behaviour of meat processing sludge exposed to different pre-treatments was determined. The organic matter solubility (given as SCOD/TCOD) of the raw sludge was 0.23±0.05 and due to the microwave, alkaline and combined microwave-alkaline pre-treatment it increased to 0.34±0.08, 0.39±0.11 and 0.48±0.12, respectively. It is verified, that microwave and alkaline pre-treatments are capable to increase the organic matter solubility of sludge [13]. The dielectric behaviour of sludge has been changed after pre-treatments. Compared to the raw sludge (Control) the dielectric constant of treated sludge decreased in the frequency range of 200-1000 MHz (Figure 1).

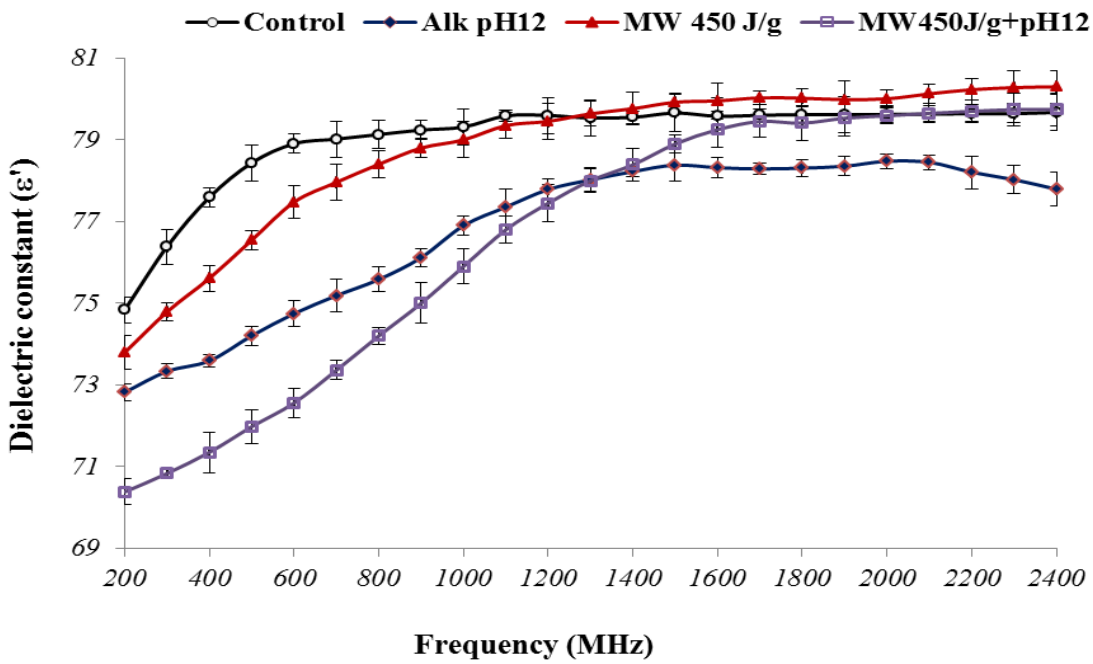

Figure 1. Dielectric constant meat industry wastewater sludge treated by alkaline (alk), microwave (MW) and with coupled method (MW+pH12) (t=25°C)

Alkaline and microwave treatment, and their combination disintegrate the sludge particles; increase the solubility of organic matter and the higher molecular weight compounds degraded partially to smaller molecules. These physicochemical changes can alter the polarisation ability of the medium which is indicated by the change of dielectric constant. At higher frequencies, there can not be found unambiguous correlation between the type and efficiency of different treatment methods and the change of dielectric constant.
During the enzymatic hydrolysis of corn-cob residue (COBEX GM) the reducing sugar yield increased to 15±1.3 mg_{RS}/g_{DM},(1.day), 53±3.6 mg_{RS}/g_{DM} (3.day), 114±7.8 mg_{RS}/g_{DM} (5.day),

and 133±6.9 mg_{RS}/g_{DM} (7.day), respectively. The frequency depending dielectric constant was also investigated for the enzymatically hydrolysed lignocellulosic biomass samples at the different hydrolysis stages. The results show that the dielectric constant decreased with the cellulose degradation in the enzymatic hydrolysis process (Figure 2).

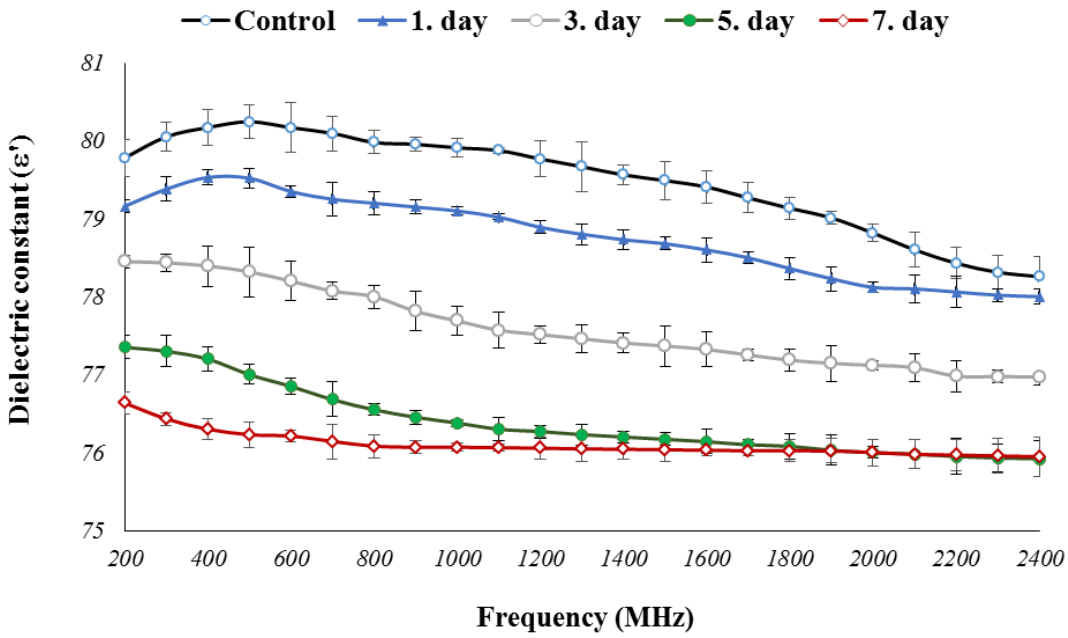

Figure 2. Dielectric constant of enzymatically hydrolysed lignocellulosic biomass (COBEX) measured at different hydrolysis time (t=25°C)

The higher difference in dielectric constant measured at different time of enzymatic hydrolysis process was found at lower frequencies (200-1000 MHz). Higher the frequency of dielectric constant lower the sensitivity of measurement for detection of cellulose degradation. At higher frequencies (1900-2400 MHz) there was any significant difference in dielectric constant of samples enzymatically hydrolysed for 5 days and 7 days (despite of the different reducing sugar yields), for example. These results verified, that the lower molecular weight compounds, produced in enzymatic cellulose degradation process, can be polarized easier in the electric field [14], therefore the dielectric constant has decreasing tendency during the hydrolysis.

Conclusion

The main aim of our research was to examine the applicability of dielectric measurements for monitoring of lignocellulosic biomass hydrolysis, and detection of the efficiency of sludge disintegration methods. For the investigation of the change of dielectric behaviour of corn cob residue contented suspension during enzymatic hydrolysis, and sludge exposed to microwave and alkaline treatments, an open-ended coaxial probe was used. Our results verified, that with the measurement of dielectric constant at frequencies of 200-1000 MHz the cellulose degradation degree and sludge disintegration efficiency can be monitored, as well. The change of dielectric behaviour has a good correlation with the standardized analytical parameters, used for the estimation of the efficiency of biomass hydrolysis.

Acknowledgements

The research is supported by the ÚNKP-22-5-SZTE-208 (Beszédes S.) and ÚNKP-22-3-SZTE-204 (Jákói Z.) New National Excellence Program of the Ministry for Innovation and

Technology from the source of the National Research Development and Innovation Fund. The authors thank the support of the János Bolyai Research Scholarship of the Hungarian Academy of Sciences (BO/00161/21/4 - Beszédes S.).

References

[1.] Vrba, J., Vrba, D. Radio. Eng. 22. 1281-1287. (2013).
[2.] Wang, J., Lim, E., Leach, M., Wang, Z., Man, K. Math. Probl. Eng. 1 1-8 (2020). https://doi.org/110.1155/2020/8942096
[3.] Jones, S., Sheng, W., Or, D. Sensors. 22. 2083 (2022) https://doi.org/10.3390/s22062083
[4.] Olkkonen, MK. Sensors. 18. 3844 (2018) https://doi.org/10.3390/s18113844
[5.] Bermudez, E.; Rico, O. Tecciencia 11. 61-67 (2016). https://doi.org/10.18180/tecciencia.2016.21.10. 10.18180/tecciencia.2016.21.10
[6.] Zajicek, R., Vrba, J., Novotny, K.. Act. Polytechn.. 46 50-54 (2006). https://doi.org/10.14311/882. https://doi.org/10.14311/882
[7.] Lau, SK:, Dag, D., Ozturk, S., Kong, F., Subbiah, J. LWT. 130. 109719 (2020). https://doi.org/10.1016/j.lwt.2020.109719
[8.] Wahab, A., Aziz, M., Rahman, A., Mohd.Sam, AR., Bhatti, A. Q., Kassim, K., You, K.Y. Const. Build. Mat. 203. 135-146. (2019) https://doi.org/10.1016/j.conbuildmat.2019.03.110
[9.] La Gioia, A., Porter, E., Merunka, I., Shahzad, A., Salahuddin, S., Jones, M., O'Halloran, M. Diagnostics. 8. 40. (2018). https://doi.org/10.3390/diagnostics8020040
[10.] Kamaruddin, M., El harfi, J., Dimitrakis, G., Nguyen, N., Kingman, S., Lester, E., Robinson, J., Irvine, D. (2011). Green Chem.. 13. 1147-1151. https://doi.org/10.1039/C1GC15102A
[11.] Yang, Y., Plovie, B., Chiesura, G., Vervust, T., Daelemans, L., Mogosanu, D., Wuytens, P., Clerck, K., Vanfleteren, J. IEEE Trans. Inst. Meas. 6004809 (2021). https://doi.org/10.1109/TIM.2021.3057291
[12.] Renshaw, R., Dimitrakis, G., Robinson, J. J. Food. Eng. 300. 110538 (2021).. https://doi.org/10.1016/j.jfoodeng.2021.110538
[13.] Dogan, I., Sanin, D. Wat. Res. 43. 2139-48 (2009). https://doi.org/10.1016/j.watres.2009.02.023
[14.] Kouzai, M., Nishikata, A., Miyaoka, S., Fukunaga, K.. (2008) 1-4. https://doi.org/10.1109/ICDL.2008.4622459

PRODUCTION CHARACTERISTICS OF CLONES OF ITALIAN RIESLING VARIETIES SK-13, SK-54 AND SK-61 ON KOBER 5BB ROOTSTOCK UNDER METEOROLOGICAL CONDITIONS IN 2021.

Blagojević Milan[1], Rašković Vera[1], Stošić Nemanja[1], Stefan Marković,[1] Vlajić Sobodan[2]

[1]Academy of Applied Studies Šabac. Unite for Agricultural Business Studies and Tourism, Republic of Serbia
[2]Institute of Field and Vegetable Crops, Novi Sad, Serbia
email: blagojevicmilan@ymail.com

Abstract

Tests were conducted in the vineyards of Erdut winery (Croatia) during 2021. Riesling Italian is a very heterogeneous variety. Clonal selection was started in 1975, and in 1991 it resulted in the discovery and recognition of three clones at the Institute of Viticulture in Sremski Karlovci. The planting density is 2.8 x 1m, the cultivation form is a one-armed guillotine with a load of 5.1 meshes/m2, where one arm with eight meshes and a condir with two meshes are left. The grape yield was determined by measuring the total amount of grapes by variety and expressed in kg/m2. The content of sugar (%) and acid (g/l) was determined using an Excel Schwolder, and by titration with NaOH with the help of bromothymol blue. Grape yield for clone SK-13 is 1.39 kg/m2, SK-54 is 1.51 kg/m2, SK-61 is 1.56 kg/m2, and the average is 1.49 kg/m2. The average sugar content in grapes for all three clones is 19.53%. The average content of acids in grapes for all three clones is 5.4g/l. The quality of the grapes, expressed through the content of sugar and acids in the grapes, shows that the achieved results are also satisfactory at the level of the Italian Riesling variety. Differences in quality favor clones SK-13 and SK-54. Given that climatic conditions significantly affect the cultivation of vines, it is necessary to continue monitoring these results over several years and different climatic conditions to ensure the results.

THE EFFECTS OF MUSHROOM POWDER ADDITION AND SALT REDUCTION ON EMULSION STABILITY, COLOR AND TEXTURE CHARACTERISTICS OF SAUSAGES

Meltem Boylu, Endrit Hasani

Department of Livestock Products and Food Preservation Technology, Institute of Food Science and Technology, Hungarian University of Agriculture and Life Sciences, Ménesi út 43-45, 1118 Budapest, Hungary
boylumeltem@gmail.com

Abstract
Mushrooms have been increasingly recognized to be a rich source of bioactive compounds and essential nutrients, including vitamins, minerals, fibres, proteins and nutraceuticals, whereas having low levels of cholesterol, calories, fat and sodium. Additionally, the production of mushrooms is sustainable compared with other protein products of both animal and plant origin, thus having less deleterious effects on the ecosystem. On the other hand, excessive consumption of sodium is a major risk factor for cardiovascular diseases, diabetes, kidney disease and also hypertension. In this research, the effects of mushroom (*Pleurotus ostreatus*) powder addition and salt reduction on some quality characteristics of sausages were investigated. Emulsion stability, color, texture profile and salt content of sausage samples were evaluated. Fresh mushrooms were dried in a tray dryer and then ground to mushroom powder using a hammer mill. Six sample groups with various levels of mushroom powder and NaCl were produced as 0MH:0% mushroom powder and 2.5% NaCl; 3MH:3% mushroom powder and 2.5% NaCl; 5MH:5% mushroom powder and 2.5% NaCl; 0ML:0% mushroom powder and 1.25% NaCl; 3ML:3% mushroom powder and 1.25% NaCl; 5ML:5% mushroom powder and 1.25% NaCl. The lowest emulsion stability values were observed in the 0ML sample group with low NaCl content and no mushroom powder ($P<0.05$). No significant difference was determined in the external surface L^*, a^*, b^* and internal surface b^*, a^* values of the samples ($p>0,05$), however internal surface L^* value of 0MH was found to be higher than the 3MH, 5MH and 5ML ($p<0,05$). 5MH and 5ML samples had the lowest values in terms of hardness, cohesiveness, gumminess, chewiness and resilience while 0MH samples had the highest. Mushroom powder addition did not cause any difference on the salt contents of the samples ($p>0,05$) and the salt content results were consistent with the NaCl added to the sausage formulations. According to these results, mushroom powder and salt improved emulsion stability. However, mushroom powder addition adversely affected the texture and caused a darker color in the inside surface of the sausages.

Keywords: mushroom, sausage, salt, *Pleurotus ostreatus*

POROUS CHALCOGENIDE BASED ON ZINC SULFIDE WITH ENHANCED ADSORPTION PROPERTIES

Adrian Ionut Cadis[1], Laura Elena Muresan[1], Lucian Ciprian Pop[2], Lucian Barbu-Tudoran[3], Gheorge Borodi[3]

[1]"Raluca Ripan" Institute for Research in Chemistry, "Babes-Bolyai" University, 30 Fantanele, 400294 Cluj-Napoca, ROMANIA
[2]Faculty of Chemistry and Chemical Engineering, "Babes-Bolyai" University, 11 Arany Janos, 400028 Cluj-Napoca, ROMANIA
[3]National Institute for Research and Development of Isotopic and Molecular Technologies, 65-103 Donath, 400293 Cluj-Napoca, ROMANIA
e-mail: adrian_cadis@yahoo.ro

Abstract
We report the preparation of porous zinc indium sulfide (ZIS) with high ability to adsorb organic dyes such as methyl orange (MO). The influence of reaction temperature and zinc concentration on the morpho-structural characteristics of ZIS were investigated.

Introduction
Purifying waste-waters of hazardous chemicals through various alternative methods, such as heterogeneous photocatalysis or adsorption, is of a real interest [1]. Chalcogenides occupy a prominent place in the study of nanomaterials with applications in photocatalysis [2].

Experimental
ZIS was synthetized using microwave (MW) and oil bath (OB) precipitation at 160^{o}C and 180^{o}C with different Zn:In ratio. The crystal phase, optical property, chemical composition and morphology of ZIS were determined by XRD, PL, UV-Vis, ICP-OES, SEM, and BET.

Results and discussion
Morphology and porosity of ZIS influences the adsorption ability. OB samples consist of globular aggregates which changes to nano-petals or hollow globules as the zinc amount increases. Rounded spongy aggregates were obtained by MW. Samples prepared with zinc excess exhibit different adsorption behavior due to complexation process in the first 5 minutes.

Conclusion
After the adsorption-desorption equilibrium, the MO adsorption vary between 35.5% - 68.6% depending on the synthesis conditions. OB samples present a higher ability for MO adsorption than MW samples due to morphology differences.

Acknowledgements
This work was supported by a grant of the Romanian National Authority for Scientific Research and Innovation, CNCS/ CCCDI-UEFISCDI, PN-III-P2-2.1-PED-202-2421.

References
[1] Y.H. Shih, C.P. Tso, L.Y. Tung, Nanotechnology 7 (2010) 16–7.
[2] Z.B. Lei, W.S. You, M.Y. Liu, G.H. Zhou, T. Takata, M. Hara, K. Domen, C. Li Chem. Commun. 17 (2003) 2142-2143.

PREPARATION AND CHARACTERIZATION OF THE INCLUSION COMPLEXES OF SALICIN WITH α- CYCLODEXTRIN AND γ-CYCLODEXTRIN

Adina Căta[1], Ioana M.C. Ienaşcu[1,2], Mariana N. Ştefănuţ[1], Daniel Ursu[1], Cristina Moşoarcă[1], Stefania Rus[1], Corina Orha[1], Anamaria Dabici[1]

[1]National Institute of Research and Development for Electrochemistry and Condensed Matter, Dr. A. P. Podeanu 144, 300569, Timişoara, Romania
[2]"Vasile Goldiş" Western University of Arad, Faculty of Pharmacy, Liviu Rebreanu 86, 310045, Arad, Romania
e-mail: adina.cata@yahoo.com

Abstract

Cyclodextrins are α-1,4-linked cyclic oligosaccharides with a three-dimensional shape like a truncated cone acting as "host" for bioactive molecules, with the complete or partial inclusion in their cavity [1]. Due to their particular structures, cyclodextrins can encapsulate guest molecules leading to the formation of inclusion complexes [2]. Cyclodextrins are used as complexing agents to improve the solubility, stability and bioavailability of the bioactive molecules [3]. In addition, many bioactive compounds such as salicin are astringent or present an unpleasant flavour and encapsulation in cyclodextrins could effectively reduce or suppress these deficiencies. Salicin is a white bitter-tasting powder and was first obtained in pure crystalline form in 1829 from willow bark and was then used for the treatment of rheumatism. Salicin is the metabolic precursor of salicylic acid and has a similar action in the human body [4].

In this paper, salicin/α-cyclodextrin and salicin/γ-cyclodextrin inclusion complexes in a molar ratio of 1:1 were prepared by wet trituration and characterized by Fourier transform infrared spectroscopy (FT-IR), Raman spectroscopy, scanning electron microscopy (SEM), X-ray diffraction (XRD), and UV-Vis-NIR spectroscopy. The obtained results were compared with those corresponding to the host components (α- and γ-cyclodextrin), the guest (salicin) and their physical mixture in order to demonstrate the formation of the inclusion complexes.

Acknowledgements

This work is part of the project PN 19 22 03 01 / 2019 "Supramolecular inclusion complexes of some natural and synthetic compounds with applications in health", carried out under NUCLEU Program funded by the Romanian Ministry of Research, Innovation and Digitization.

References

[1] V. Suvarna, B. Bore, C. Bhawar, R. Mallya. Biomed. Pharmacother. 149 (2022), 112862.
[2] A. Cid-Samamed, J. Rakmai, J.C. Mejuto, J. Simal-Gandara. Food Chem. 384 (2022), 132467.
[3] E. Pinho, M. Grootveld, G. Soares, M. Henriques. Carbohydr. Polym. 101 (2014), 121-135.
[4] J.G. Mahdi. J. Saudi Chem. Soc. 14 (2010), 317-322.

INFLUENCE OF ORAL ACIDITY AND TEMPERATURE BEHAVIOR OF VARIOUS ORTHODONTIC WIRES IN ARTIFICIAL SALIVA

COSTEA Liviu-Virgil[1], DAN Mircea Laurenţiu[1*], DIMA George-Daniel[1], POROJAN Liliana[2]

[1]Faculty of Industrial Chemistry and Environmental Engineering, "Politechnica" University Timişoara, Romania
[2]Department of Dental Prostheses Technology, University of Medicine and Pharmcy V. Babeş, Timişoara, Romania
e-mail: mircea.dan@upt.ro

Abstract
The sophisticated and highly variable, in terms of pH, electrolyte availability and temperature environment of the oral cavity can cause various biomaterials used in oral medicine to release metal ions due to corrosion phenomena. Thus, materials used in dental applications must be biocompatible and offer a solid resistance towards corrosive leakage over a wide range of pH and temperature values.

The present study aims to assess the corrosion resistance of chromium - nickel as compared to chromium - manganese commercially available orthodontic wires in artificial saliva. The two investigated wire samples have been studied by means of various electrochemical techniques like cyclic voltammetry (CV), electrochemical impedance spectroscopy (EIS), linear polarization (LV), as well as by employing chronoelectrochemical studies (chronoamperometry - CA and chronopotentiometry - CP). The afore mentioned procedures have been successfully applied in the investigation of various corrosion processes involving dental alloys. We used Fusayama artificial saliva solution as corrosive electrolyte during the electrochemical tests. While the solution pH varied in discrete steps between 3.5 and 7.5, the temperature was also modified between 27 and 47 ºC for each pH value, to most closely simulate real-life conditions of metal-electrolyte contact. Sample analysis by scanning electron microscopy (SEM) before and after each corrosion test has been performed in order to inspect potential modifications of the surface morphologies. Allergen and nickel free Cr-Mn biomaterials, exhibited good corrosion resistance, representing a good alternative to the widely used Cr-Ni alloy based orthodontic wires.

Keywords: Cr-Ni, Cr-Mn orthodontic wires; corrosion resistance; electrochemical behaviour; biomaterials.

References
[1]. Espinoza-Montero, P. J., Montero-Jiménez, M., Fernández, L., Paz, J. L., Piñeiros, J. L., Ceballos, S. M., In vitro wearing away of orthodontic brackets and wires in different conditions: A review, Heliyon, 8(9), (2022) e10560.
[2]. Katić, V., Ćurković, L., Ujević Bošnjak, M. and Špalj, S., Determination of corrosion rate of orthodontic wires based. Mat.-wiss. u. Werkstofftech., 45 (2014) 99-105.
[3]. Barcelos, A. M., Luna, A.S., de Assis Ferreira, N., Braga, A.V.C., Lago, D.C.B., Senna, L.F. Corrosion evaluation of orthodontic wires in artificial saliva solutions by using response surface methodology, Mat. Res. 16(1), (2013) 50-64.

APPLICATION OF THE LED-UV/ClO_2 METHOD FOR THE TREATMENT OF AQUEOUS SOLUTIONS OF TRIMETHOPRIM AND 5-FLUOROURACIL

Anett Covic[1], Constance Csaplár[1], Alapi Tünde[1]

Department of Inorganic and Analytical Chemistry, University of Szeged, H-6720 Szeged, Dóm tér 7, Hungary
e-mail: covicanett@chem.u-szeged.hu

In drinking water treatment, chlorination processes, based on the HOCl or ClO_2 addition, are used for disinfection. The combination of chlorination with appropriate UV radiation is an effective radical generation process. Recently, the UV/chlorine process has been investigated as an alternative to UV/H_2O_2 for water treatment [1,2]. To ensure the applicability of UV-based processes, it is essential to opt for radiation sources that are effective and affordable. With the growing availability of light-emitting diodes (LED) and their favorable features, the application of LEDs for water treatment is proposed. The use of LED lights in UV/ClO_2 processes permits the selection of wavelengths close to the absorption maximum of ClO_2 (359 nm, 1230 M^{-1} cm^{-1}), which can initiate its decomposition into reactive radicals, such as oxygen and chlorine radicals. The radical oxygen leads to hydroxyl radical (•OH) formation in aqueous media, and the UV/ClO_2 process can degrade organic compounds using reactive oxygen species (ROS) and chlorine radicals:

$$ClO_2 + hv \rightarrow ClO\bullet + O\bullet$$
$$ClO_2 + hv \rightarrow Cl\bullet + O\bullet + O\bullet$$
$$ClO\bullet + hv \rightarrow Cl\bullet + O\bullet$$

In this work LED light sources were used, which emit 367 nm UV light; the emission wavelength is close to the absorption maxima of ClO_2 [2]. Aqueous solutions of two medicinal substances trimethoprim (TRIM) and 5-fluorouracil (5-FU) were treated with the LED-UV/ClO_2 method. Trimethoprim has been used in various bacterial diseases, and many studies reported its hard biodegradability and presence in wastewater, surface water, and even in drinking water [3]. 5-FU is one of the most frequently used chemotherapeutic agents detected in hospital wastewater at a concentration of 10-100 μg L^{-1}[4].

During the experiments, the effect of light intensity, ClO_2 dosage, and pH was investigated. The biologically purified domestic wastewater was used as a matrix to test the effectiveness of the method under real conditions. The effect of HCO_3^- was also studied. After treatment, the AOX and TOC content of the samples were determined and compared to study the mineralization efficiency and the role and importance of •Cl in the transformation of target substances.

Acknowledgment
This work was sponsored by the National Research, Development, and Innovation Office-NKFI Fund OTKA, project number FK132742.

References
[1] J. D. Laat, M. Stefan. *UV/chlorine process*, in *Advanced Oxidation Processes for Water Treatment.* (2017) 383–424.
[2] D. S. Firak, L. Farkas, M. Náfrádi, and T. Alapi, *J. Environ. Chem. Eng.*, 10 (2022).
[3] Wu, Z., Fang, J., Xiang, Y., Shang, C., Li, X., Meng, F., & Yang, X., *Water Res.*, 104 (2016) 272–282.

[4] C. A. Lutterbeck, M. L. Wilde, E. Baginska, C. Leder, Ê. L. MacHado, K. Kümmerer, *Environ. Pollut.*, 208 (2016) 467–476.

DETERMINATION OF SOME ESSENTIAL MINERAL ELEMENTS FROM DIFFERENT TROPICAL FRUITS

Antoanela Cozma[1], Ariana Velciov[2], Sofia Popescu[2], Casiana Mihut[1], Anisoara Duma-Copcea[1], Maria Rada[3*]

[1]Department of Soil Sciences, University of Life Sciences "King Michael I" from Timisoara, 300645, Timisoara, Romania e-mail: antoanelacozma@yahoo.com
[2]Department of Food Science, University of Life Sciences "King Michael I" from Timisoara, 300645, Timisoara, Romania ariana.velciov@yahoo.com
*[3]*University of Medicine and Pharmacy "Victor Babes" – Faculty of Medicine, 2 Efimie Murgu Sq., 300041, Timisoara, Romania; e-mail: radamariam@gmail.com*

Abstract
The purpose of this paper is to determine the concentration of some essential macro and micro elements, from tropical fruits and the role that these minerals play in health benefits. The concentrations of Ca, Mg, Fe, Mn, Zn and Cu in bananas, grape fruits, kiwi, lemons, mandarins, oranges, pineapples and pomelo sold in Timisoara markets were determined by flame atomic absorption spectrometry method. The obtained results show that the distribution of the essential mineral elements in the analyzed fruits presents non-uniformity, depending on the fruit species and the nature of the analyzed element. The best represented among the analyzed elements are Ca and Mg (59.1-358 mg/kg Ca, respectively 92-287 mg/kg Mg). Fe, Zn, Cu and Mn were determined in much lower concentrations (1.12-3.26 mg/kg, 0.75-1.53 mg/kg, 0.45-1.21 mg/kg respectively 0.34-7.12 mg/kg), but sufficient considering the requirement of these essential microelements in the human body. However, it can be stated that the studied tropical fruits contain important amounts, especially of calcium and magnesium, but also appreciable amounts of essential microelements: Fe, Zn, Cu and Mn.

Introduction
Tropical fruits, originating from tropical and subtropical areas are particularly appreciated not only due to their organoleptic characteristics including their exclusive taste, sensory properties, and mouthfeel, but due to their particularly high nutritional values, a fact for which they are recommended for curative purposes, being considered as medicinal food [1,2]. Fruits have a significant contribution in human health and nutrition being a natural source, full of precious nutritional constituents. They contain vitamins, fatty acids, dietary fiber and essentials minerals available in various quantities and qualities. The beneficial effects of these fruits are due to the main constituents, which include the mineral substances in the form of essential macro and micro elements [5].Among the most important minerals available in fruits are calcium, potassium, iron, phosphorus, magnesium, zinc. Due to the curative effects in a range of acute and chronic diseases, the exotic fruit diet is used in modern medicine. It is recommended, prophylactic and curative, as an adjuvant, when the body accumulates significant amounts of acids; which has repercussions such as diabetes, aging, gout, and so on [1,4]. Consumption of the fruit with pulp is prescribed in the treatment and prevention of cardiovascular diseases, liver diseases, etc., that provides a high percentage of vitamins and minerals in the daily dose [5]. In South Africa, the banana is the main food, basic for about 50% of the population and the most popular fruit in industrialized countries [6]. Pineapple is a perennial herbaceous plant of the *Bromeliaceae* family with the botanical name *AnanasSativus* or *Bromelia* pineapple, originates in the tropical regions of America and the Far East [3].

The specialized literature includes numerous references regarding the beneficial effects of consuming exotic fruits obtained in tropical and subtropical areas, as well as the techniques for analyzing some mineral elements from such vegetable products.

Experimental

The paper presents data related to the distribution of some mineral elements in different imported tropical fruits, also known as exotic fruits. In order to achieve the proposed objective, exotic fruit were purchased from different local markets in Timișoara (banana fruit, grape fruits, kiwi, lemons, mandarins, oranges, pineapples and pomelo). To perform the experiment, three fruit samples were prepared for analysis, corresponding to each variety of fruit under study. The determination of the mineral elements in the analyzed fruits required two steps: mineralization, by calcination, followed by the solubilization of the inorganic matter in 0.5 M HNO_3 and the spectrophotometric determination of the absorbances of the essential elements.
The device used for this purpose was atomic absorption spectrophotometer in air flame - acetylene, brand Varian AA 240 FS, a laboratory water bath and a thermal regulation electric stove. Also, the Reagents used are Nitric acid Merck, 65% (ρ = 1.39 g/cm3) to prepare the nitric acid solution 0.5 N; standard solutions for the analyzed elements: Ca, Mg, Fe, Mn, Zn and Cu, obtained from the concentrated standard solution Merck Darmstadt - Germany, 1.000g/ml;
For each analysed element were prepared six sets of standard solutions to cover the concentration range of each element analysed; distilled water. The working parameters of the apparatus – wave length, air and acetylene pressure, burner height, etc. – were selected in accordance with the recommendations of the Varian AA 240 FS. Simultaneously with the measurement of the absorbance of analyzed samples, the absorbance of the working standards solutions were determined in the same working conditions.

Results and discussion

The experimental results obtained in the analysis of the essential mineral elements, average values, are presented in tables 1.

Table 1. The concentration (mean values) of some essential element from exotic fruits

Fruits	Bioelement, mg/kg					
	Ca	Mg	Fe	Mn	Zn	Cu
Banana	59.1	287	1.12	3.22	1.53	1.21
Grapefruit	253	94.4	1.78	0.87	1.12	0.45
Kiwi	358	128	2.92	0.58	1.14	0.68
Lemon	226	92	2.91	0.51	1.26	0.51
Mandarin	224	101	1.98	0.63	0.75	0.52
Orange	306	106	2.38	0.27	1.46	0.55
Pineapple	179	126	2.03	7.12	0.97	1.10
Pomelo	332	165	3.26	0.34	0.87	0.64

From the analysis of the experimental data obtained for the evaluation of some essential macro and micro elements: shows that the distribution of the essential mineral elements in the analyzed fruits presents non-uniformity. This depends on the fruit species and the nature of the analyzed element. The best represented elements are the macro-elements, calcium and magnesium which has the highest concentration values between 59.1-358 mg/kg Ca, respectively 92-287 mg/kg Mg. Among microelements, the best represented bioelement was iron (1.12-3.26 mg/kg Fe) followed - in slightly lower concentrations by Mn, Zn and Cu : (0.27-7.12 mg/kg Mn),

Zn (0.75-1.53 mg/kg Zn) and Cu (0.45- 1.21 mg/kg Cu). A ranking of the analyzed fruits according to their mineral intake is difficult to achieve. Calcium (Ca^{2+}), important

macroelement in formation and stability of cell walls, in maintenance of membrane structure and permeability, activates some enzymes was determined in the highest concentration, between 59.1ppm - in bananas and 358 ppm - in kiwi. Higher Ca contents were determined in kiwi, pomelo and oranges. Magnesium (Mn^{2+}), an essential macroelement, was determined in much lower concentrations than calcium, but much higher than iron, zinc, manganese and copper. Increased magnesium content is recorded in pineapples, bananas and kiwis. Iron (Fe^{3+}, Fe^{2+}), an essential microelement in plant growth and development, it was determined in the highest concentration of all the analyzed microelements from all the fruits studied, between 1.12-in bananas and- 3.26 ppm in pomelo. Zinc (Zn^{2+}), essential microelement for plants, this, participating in the formation of chlorophyll, activates some enzymes, help to maintain the health of the reproductive and immune systems. Among the analyzed fruits, the richest in Zn are: bananas– 1.53 ppm, orange – 1.46, lemon – 1.26 and kiwi – 1.14 ppm. Cooper (Cu^{+}, Cu^{2+}) is an essential microelement for plants which participates in redox processes, photosynthesis it was determined in low concentrations (between 0.45 – 1.21), but close, with the exception of pineapple, where it was detected in an amount of 1.10ppm and for banana 1.21ppm.

Conclusion

The obtained results show that the distribution of the essential mineral elements in the analyzed fruits samples presents non-uniformity, depending on the fruit species and the nature of the analyzed element. The best represented among the analyzed elements are Ca and Mg (59.1-358 mg/kg Ca, respectively 92-287 mg/kg Mg). Fe, Zn, Cu and Mn were determined in much lower concentrations (1.12-3.26 mg/kg, 0.75-1.53 mg/kg, 0.45-1.21 mg/kg respectively 0.34-7.12 mg/kg), but sufficient considering the requirement of these essential microelements in the human body. However, it can be stated that the studied tropical fruits contain important amounts, especially of calcium and magnesium, but also appreciable amounts of essential microelements: Fe, Zn, Cu and Mn. This category of fruits is important, as an additional supply of micro and macro elements, contributing at the same time to the completion of the palette of bio-elements from local fruits.

References

[1]. Sayago-Ayerdi S., García-Martínez D.L., Ramírez-Castillo A.C., Ramírez-Concepción H. R., Viuda-Martos M., Tropical fruits and their co-products as bioactive compounds and their health effects: a review, Foods 2021, 10, 1952. https://doi.org/10.3390/foods10081952
[2]. Acham I.O., Ahemen S., Ukeyima M.T., Girgih A.T., Tropical Fruits: Bioactive Properties and Health Promoting Benefits in Chronic Disease Prevention and Management, Asian Food Science Journal, 2018, 3(1):1-13
[3]. Md. Farid Hossain, Shaheen Akhtar, Mustafa Anwar (2015) - Nutritional Value and Medicinal benefits of Pineapple, International Journal of Nutrition and Food Sciences, 4(1): 84-88, Science Publishing Group
[4]. Obediah G.A., Elechi-Amadi K.N., Determination of trace mineral elements in some tropical fruits, International Journal of Science and Research, 2016, 5(4):1228-1230]
[5]. Anna Czech, Ewa Zarycka, Dmytro Yanovych, Zvenyslava Zasadna, Izabela Grzegorczyk, Sylwia Kły, Mineral content of the pulp and peel of various citrus fruit cultivars, Biological Trace Element Research, 2020, https://doi.org/10.1007/s12011-019-01727-1
[6]. http://www.nature.com/nature/journal/v488/n7410/full/nature

COLOR CHANGES DURING STORAGE OF ORGANIC AND CONVENTIONAL CARROTS

Anna Divéky-Ertsey[1], Samuel Hollinetz[1], László Csambalik[1]

[1]Department of Agroecology and Organic Farming, Institute of Rural Development and Sustainable Economy, Hungarian University of Agriculture and Life Sciences, H-1118 Budapest, Hungary
e-mail: diveky-ertsey.anna@uni-mate.hu, samuel.hollinetz@gmail.com, csambalik.laszlo.orban@uni-mate.hu

Abstract
Storage impacts the visual and nutritional characteristics of carrots (*Daucus carota* L.). The visual changes related to color parameters are interrelated to physiochemical changes, especially to those that are responsible for color, i.e. carotenoids. With a proper environment, the long-term storage of carrot is possible with the preservation of valuable nutrients.
In this study, four typical household storage environments are applied for carrot samples originating from organic and conventional production. The results indicated, that among temperature, packaging type, and cultivation type, packaging has the highest impact on the investigated color parameters of carrot homogenates, and, indirectly on carotenoids content.

Introduction
Carrot (*Daucus carota* L.) is consumed worldwide in significant amounts (Keser et al., 2020) and is a rich source of carotenoids, which is responsible for the orange color of the root. Carotenoids are highly unsaturated pigments with strong antioxidant capacity which can reduce the occurrence of cardiovascular diseases (Xia et al., 2020). Throughout storage, carrot loses the majority of its water content, thus its firmness decreases, and microorganisms appear on its surface. These processes lead to changes in surface color which can ruin the attractiveness of the product. The color change can indicate underlying disadvantageous physiochemical processes causing decreased nutritional values (Pither, 2003). Therefore, color is a significant quality indicator for fresh and processed carrots (Simon, 1985) and its observation provide useful information about the ideal storage technology for consumers.

Experimental
For the experiment, bulk and packaged carrots originating from organic and conventional production were purchased from supermarkets. All items were pre-washed. Four-four identical groups of 15 carrots were created from both organic and conventional samples in the laboratory of the Department of Agroecology and Organic Agriculture, Hungarian University of Agriculture and Life Sciences on 16 March 2022. For modeling typical household storage practices, two temperatures (4°C, 12°C) for both bulk and sealable plastic bag storage were employed. The temperature × packaging × cultivation type combinations resulted in eight distinct storage technologies (Table 1). The duration of the storage experiment was set to four weeks.

Temperature	4°C				12°C			
Storage type	Bulk		Packaged		Bulk		Packaged	
Storage type code	CB4	OB4	CP4	OP4	CB12	OB12	CP12	OP12

Table 1. Details and codes of employed storage technologies for carrot samples. C in codes refers to conventional, while O refers to organic cultivation origin.

On a weekly basis, three-three carrots were chosen from each storage groups and separated for instrumental measurements. End parts were removed, and after homogenization with a lboratory blender, homogenate color was measured in triplicate with a handheld Konica Minolta CR-410 colorimeter (Konica Minolta, Japan). CIELab values (L*, a*, b*) were retrieved, which were used for chroma (C*) and hue (h^o) values calculation.

Results and discussion

The L* value change of most carrot samples shows a somewhat similar pattern regardless of any factor (Figure 1). After a radical decrease in the first week a gradual increase is experienced. It is visible, that the cutivation system did not influence the change, while the packaging impacted the L* value changes to the highest extent. Bulk storaged carrots showed higher L* value decreases in comparison with packaged ones.

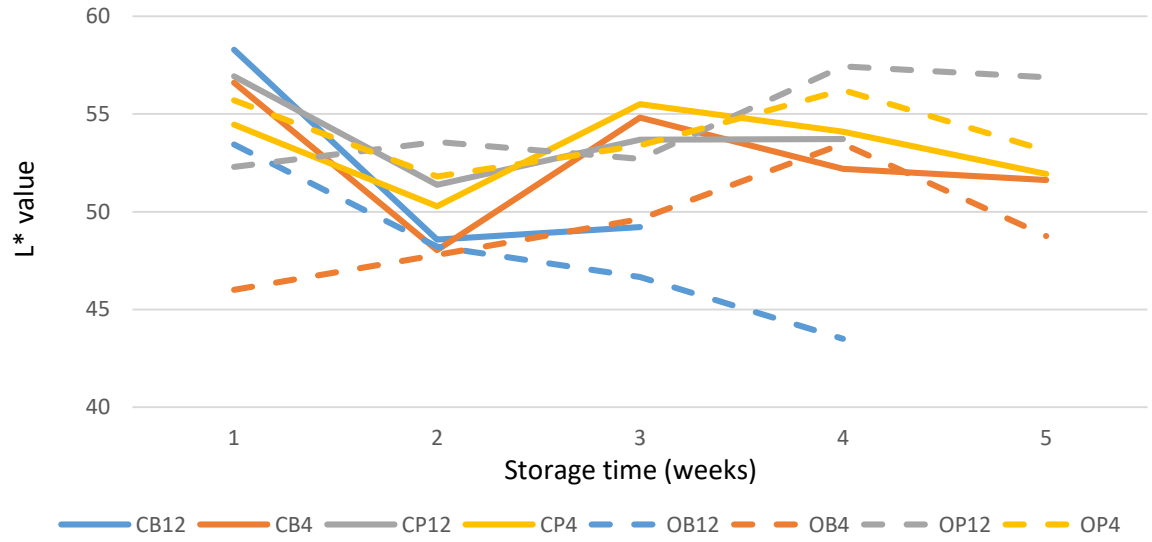

Figure 1. L* value changes of carrot samples during storage.

A slight decrease is shown by the a* values of the samples after one week storage, which is followed by a rise for the second and other weeks. Organic bulk samples show a lower a* value at the beginning of the experiment; OB12 or OB4 give the lowest values over the whole storage time in comparison with other samples. Regardless of starting values, bulk stored samples overperform those stored in plastic bags in terms of a* values throughout the storage time. With the exception of OB samples, CB, CP, and OP samples show similar trends regardless of temperature differences over storage. Organic and conventional samples do not divide.

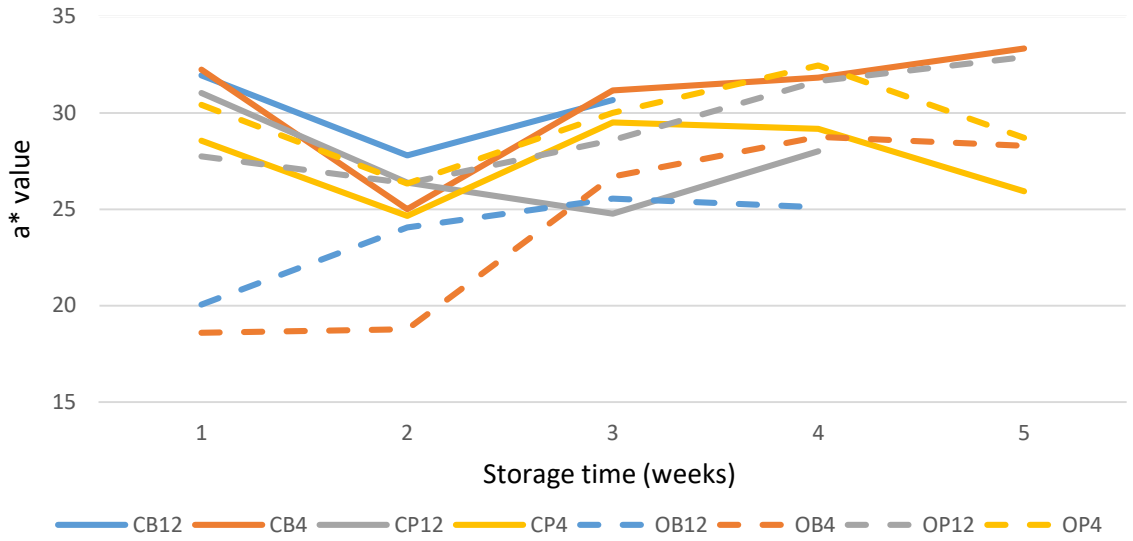

Figure 2. a* value changes of carrot samples during storage.

The Chroma value changes reflects the L* and a* value changes of carrot samples. OB samples together with CP samples show the lowest results. In case of bulk stored samples, cultivation system had an impact, possibly because of the low initial values of organic samples. Storage on higher temperatures seems to result in lower C* values regardless of cultivation type and packaging.

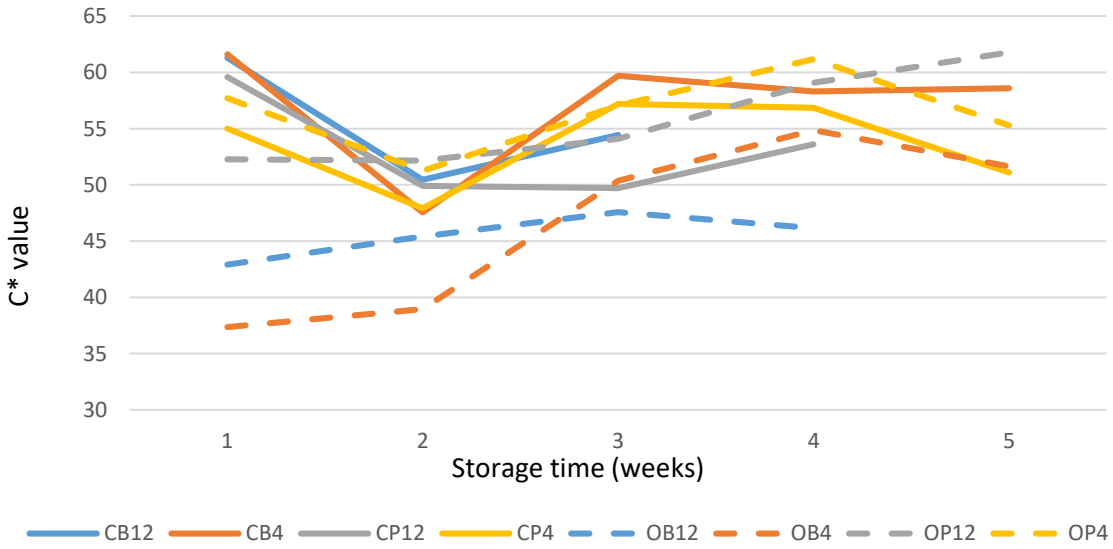

Figure 3. Chroma (C*) value changes of carrot samples during storage.

Higher initial hue values were obtained for OB samples. CB4, CB12, and OB4 samples shows the greatest decreases among storage types. In general, hue values seems to be stagnating over the storage period and no outstanding differences can be experienced. Overall, hue values are not influenced by the variations in temperature, packaging, and cultivation type.

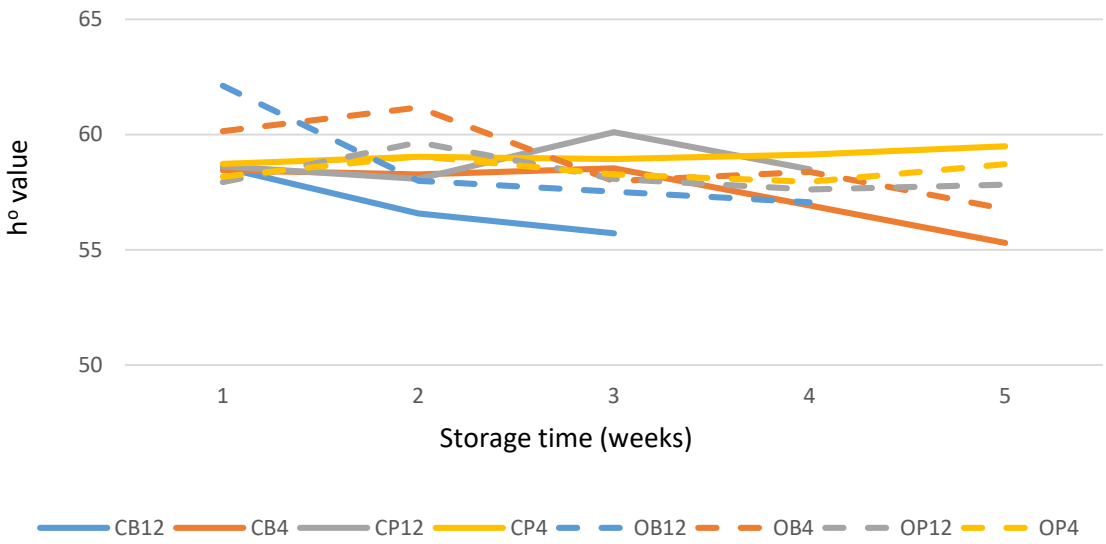

Figure 4. Hue (h°) value changes of carrot samples during storage.

Conclusion

Among the investigated temperature, packaging and cultivation parameters, packaging seems to have the highest impact on the investigated color parameters (L*, a*, C*, h°) of carrot samples. The changes in color is interrelated with certain physiochemical processes, therefore further instrumental analyses are required to explore correlations of color and phytonutrient traits.

References

[1] R.J. Pither, Enc Food Sci Nutr, 1111 (2003) 845-851.
[2] P.W. Simon, in: E. Eskin (Ed.), Evaluation of quality of fruits and vegetables, AVI Publishing Co., Westport, CT, 1985, pp. 315-328.
[3] Keser, D., Guclu, G., Kelebek, H., Keskin, M., Soysal, Y., Sekerli, Y. E., Selli, S.. Food Bioprod Proc, 119 (2020) 350–359.
[4] Xia, H., Wang, X., Su, W., Jiang, L., Lin, L., Deng, Q., Liang, D. Postharvest Biol Tech, 164 (2020) 111162.

ENHANCING AND MONITORING THE ANAEROBIC DIGESTION OF WASTEWATER SLUDGE

Viktória Csatordai[1], Zoltán Jákói[2*], Sándor Beszédes[2],Balázs Lemmer[3]

[1]Faculty of Engineering, University of Szeged, H-6725 Szeged, Moszkvai körút 9, Hungary
[2]Department of Biosystems Engineering, Faculty of Engineering, H-6725 Szeged, Moszkvai körút 9, Hungary
[3]Faculty of Engineering, University of Szeged, H-6725 Szeged, Moszkvai körút 9, Hungary
e-mail: jakoiz@mk.u-szeged.hu

Abstract

The most important key of wastewater treatment is the treatment of the wastewater sludge. Anaerobic fermentation is an effective solution for the treatment. *I*t can lower the organic content of the sludge while a renewable energy source – biogas – is produced at the same time. Our research is focused on the applicability of rheological and dielectric measurements to study if these measurements can monitor the proccess of anaerobic digestion. Moreover, microwave pre-treatment was used on the wastewater sludge to examine its effect on anaerobic digestion. Our experimental results represent that the microwave irradiation can intensify the total biogas yield by 15% during anaerobic fermentation. Furthermore, microwave irradiation was effect on viscosity, it reduced the viscosity of the fermentation media by 13%. It has been confirmed that dielectric and rheological measurements are capable of monitoring the anaerobic digestion because there is a correlation among dielectric parameters, biogas yield and absolute viscosity of the fermentation media. Changes in the dielectric parameters and absolute viscosity show similar trends, which can be explained by the connection with biogas production.

Introduction

One of the ecologically dominant problems nowadays is the large amount of waste which is a result of industrialization and growing population. Wastewaters from various origin also form a group of wastes and the proper treatment of these wastewaters plays a particularly important role in terms of the nature and the mankind as well. By subjecting the accumulated wastewaters to appropriate treatments, it is possible to reduce the use of natural energy sources, such as petroleum, coal or natural gas which are being depleted. Biologically produced alternatives - such as biofuels - offer an opportunity to solve this, as the use of biomass means significantly smaller ecological footprint. [1]

The most essential purposes of thermal treatment techniques are to reduce the moisture content of the sludge, minimize its microbial risk and improve their fermentability. As an alternative of tradicional heat transfer methods, the examination of microwave irradiation has become more and more common in recent decades, due to its fast, selective and efficient heating mechanism that can enhance several biotechnological and environmental processes. [2]

Anaerobic digestion is a promising and effective method in wastewater sludge treatment, as it can be used to remove toxic substances, reduce the volume of the sludge and produce biogas. During anaerobic digestion specific microorganisms transform the organic content of the substrate into methane (40-65%), carbon-dioxide (30-55%) and other gaseous compounds (0,3-1%). [3] The production can be divided into three different stages of microbiological activity, which are built on each other and can not be separated under natural conditions (Figure 1). [4] In the stage of hydrolysis, complex carbohydrates, lipids and proteins are transformed into sugars, fatty acids, and amino acids with their help of polymer-decomposing bacteria. In the next acidification phase the previous various compounds are used by acetogenic bacteria to

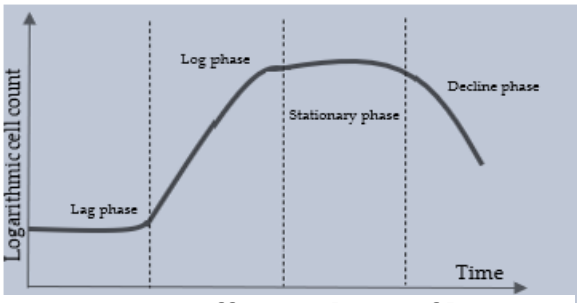

Figure 1. Different phases of biogas formation in a batch fermenter [7]

produce organic acids and alcohols, then these are almost completely modified into acetic acid. In the last stage, the so-called methanogenesis, the main component of the biogas – the methane gas – is produced by methanogenic bacteria. [5] Several key factors affect the successful completion of biogas fermentation, for example the C:N:P ratio of the substrate, the temperature, total solid concentration, pH, and the bioavailability of compounds which are involved in biochemical transformation. [6] [7].

Dielectric behaviour of normal materials largely depends on their physicochemical structure and the frequency (*f*) and strength (*E*) of the electromagnetic field they are interacting with. Given the equation

$$\frac{D}{E} = \varepsilon,$$

we can see that the absolute permittivity of a material is the ratio of the electric displacement (*D*) that was caused by the electric or electromagnetic field *E*. Polarization however does not occur instantaneously in these materials; therefore the electric displacement (*D*) can be interpreted as a phase shift. Since complex numbers allow to define magnitude and phase in the same time, the absolute permittivity of a material should be treated as a complex function of the frequency:

$$\varepsilon = f(\varepsilon_C(\omega))$$

As any complex function, complex permittivity can be separated to its real and imaginary part:

$$\varepsilon_C(\omega) = \varepsilon'(\omega) - i\varepsilon''(\omega)$$

ε' refers to the dielectric constant which indicates the electric energy storing capability of a given material, while ε'' is the dielectric loss factor. The latter contains the so-called dielectric loss (due to the rotation and vibration of permanent and induced dipolar molecules) and the effective conductive loss (due to the ionic displacement of charged particles). These dielectric properties greatly depend on the physicochemical structure of a given material, and can significantly change when this structure undergoes any form of transformation – for example, during a fermentation process. Measuring the dielectric properties of wastewater sludge is non-destructive, quick, and chemical-free method. Taking the change of dielectric properties as a basis, then changes taking place during the fermentation process can be monitored. Another potential method to analyse the efficiency of anaerobic digestion is to measure changes in dynamic viscosity. A number of biochemical reactions take place in the various phases of the anaerobic digestion, therefore changes in absolute viscosity of the fermentation media are expected to occur.

Experimental

For the anaerobic digestion experiments, we used wastewater sludge originated from a local meat processing plant as raw material in a volume of 90 cm^3 with 10 cm^3 of inoculum seed sludge added to guarantee the proper microbiological environment. Anaerobic fermentation was carried out under thermostatic conditions at a temperature of 38 °C. The samples were incubated in 250 cm^3, continuously stirred laboratory glass reactors, sealed by PTFE septum. Measurements were taken every second day. On top of the reactors WTW Oxi-Top IDS/B automatic manometric measuring heads were put, which could indicate the amount of biogas production by monitoring the absolute gas pressure during the digestion. To observe the

changes in the dielectric constant (ε') and the dielectric loss factor (ε") a DAK 3.5 (Speag, Switzerland) dielectric probe connected to a ZVL-3 (Rhode&Schwarz, Germany) VNA was used, which enables testing in the range of 200 to 2400 MHz. To derermine the absolute viscosity of the fermentation liquid, RP1 rotary viscosimeter at a speed of 200 rpm was used, which provides examination in the range of 20-13·10^6 mPas.

Microwave treatment was carried out in a Labotron 500 laboratory batch microwave equipment, which generates electromagnetic waves at the frequency of 2.45 GHz. The treatments were carried out at the power level of 250W and the radiation time of 720 seconds and 30-30 seconds on/off cycle to achieve better temperature homogenity.

Results and discussion

Firstly, we studied the applicability of viscosity measurement to both control and microwave-irradiated samples and investigated how the microwave irradiation affects the biogas production dynamics.

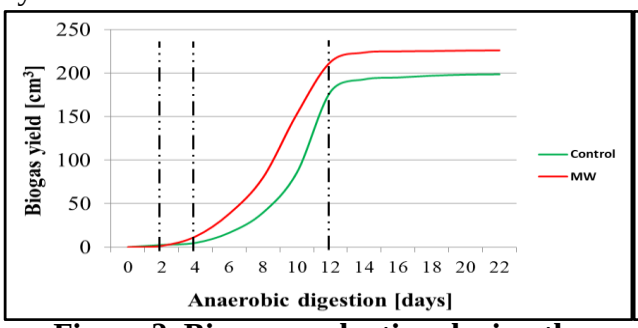

Figure 2. Biogas production during the anaerobic digestion

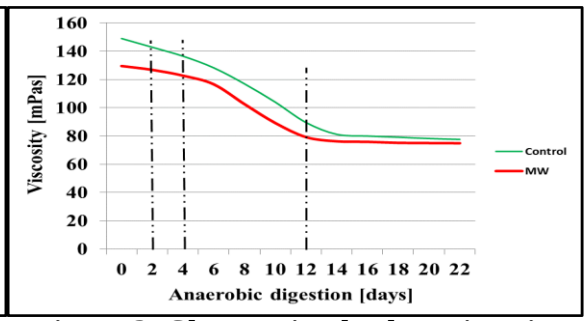

Figure 3. Changes in absolute viscosity during anaerobic digestion

Our results show (Figure 2 and 3) that the biogas production dynamic follows the stages represent in Figure 1 in terms of control and microwave irradiated samples, and at around day 12 the stationary phase sets. In case of viscosity, it declines gradually in both control and the microwave-treated samples, as the biochemical environment changed, which shares intense similarities in tendency with the curves of the biogas yield. The microwave irradiation resulted overall higher biogas yield during the whole fermentation process and the maximum achievable volume was approximately 230 cm^3 compared to the control sample, where the maximum volume was 200 cm^3. It can also been seen that microwave irradiation shortened the lag and the log phase by 1-2 days, so microorganisms could adapt to the fermentation environment more easily. When the stationary phase sets the viscosity also become nearly constant, so the changing of the biochemical environment in the different stages of the anaerobic digestion are in connection with overall viscosity of the fermentation media. In rheological properties the microwave irradiation resulted lower viscosity values during the whole fermentation by approximately 13% in average, as it was expected.

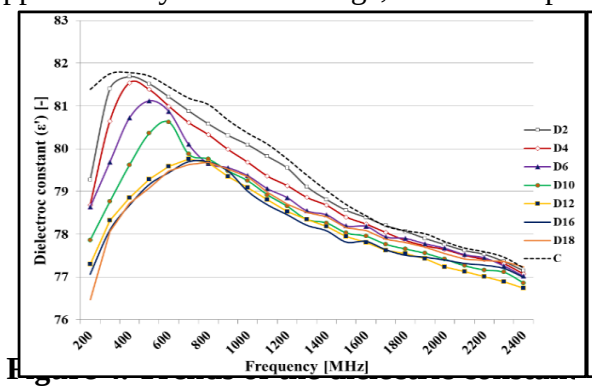

of the not-treated samples

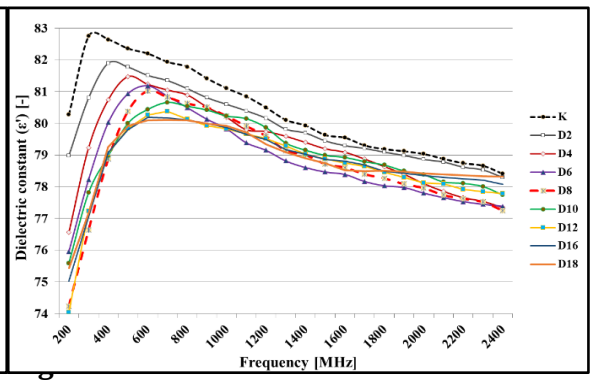

of the microwave irradiated samples

Secondly, the examination of the dielectric properties of the fermentation media during the anaerobic digestion was the focal point of our research. It can be clearly seen that the values of the dielectric constant gradually decreases in low-frequency both of control and treated samples during the whole digestion, until the 12th day of the fermentation. The frequency which correlates to the maximum ε' increases in both cases, until the 12th day of the fermentation. After that the differences of the frequency of the ε' are starting to shrink and in higher frequency ranges (1200-2400 MHz) the dielectric constant of the 12th day media becomes the lowest. Because of reaching the stationary phase the biochemical environment becomes steady-state and no significant changes occur, so the differences in the dielectric constant cease as well. In case of the microwave irradiated samples the values of the maximum dielectric constant are a bit higher, and the differences are a bit more observable in the lower frequency range (200-600 MHz). The reason is the structural changes causes by the microwave irradiation. Microwave-treated and non-treated samples show similarities, the maximum points of the dielectric constant shift towards higher frequencies during the whole fermentation, until the 12th day, when the stationary phase sets.

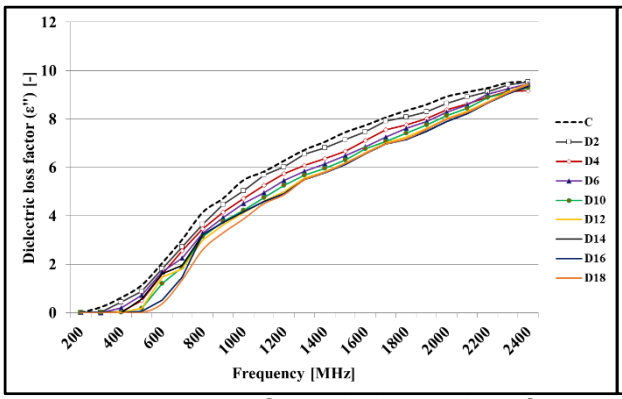

Figure 6. Trends of the dielectric loss factor of the non-treated samples

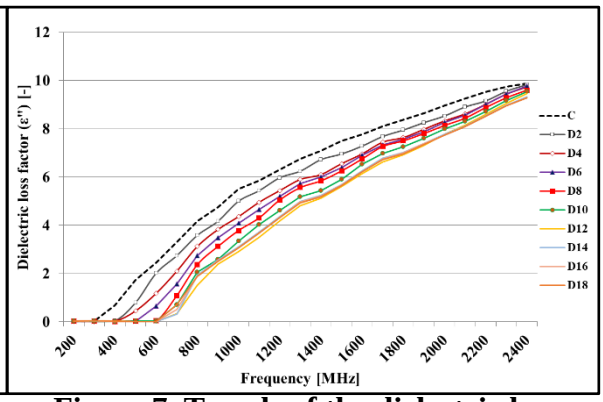

Figure 7. Trends of the dielectric loss factor of the microwave irratiated samples

Our results show that the control sample has the highest dielectric loss factor during the entire frequency range in non-treated and treated samples as well. This means that a reasonable amount of absorbed energy was turned into heat during the measurement. During the fermentation process the value of the dielectric loss factor become lower in every measurement point, until the 12th day of the fermentation, after which differences start to cease, just like in the case of the dielectric constant. Because of the biochemical changes during the fermentation, the values of the dielectric loss factor are starting to increase intensively at a well-defined frequency, but this point varies with the day of the fermentation. In case of microwave-treated samples the values of the ε'' are higher than in case of non-treated samples, especially in the lower frequency range and the differences between the fermentation days are more observable. Moreover, the values of the dielectric loss factor are starting to increase at higher frequencies compared to non-treated samples. It can be also explained with the biochemical changes during the fermentation, because larger molecules are breaking down into smaller and smaller ones.

Conclusions

In our work we studied two monitoring techniques – dielectric and rheological measurements – to discover if they are capable of identifying and tracking the various stages of the anaerobic digestion of the sludge originated from meat industry. It was verified that the biogas production follows the stages of the anaerobic digestion in each case and the standalone microwave irradiation could intensify the maximum biogas yield by 15%. Absolute viscosity measurements share strong similarities with dynamics of the biogas volume, so these

rheological measurements are able to identify and follow the different stages of the fermentation in terms of non-treated and pre-treated samples too. Because of the disintegration of the sludge, which was caused by the microwave pre-treatment the measured viscosity was lower than in case of the non-treated samples. The suitability of the measurement of the dielectric constant (ε') and dielectric loss factor (ε") for monitoring the process of the anaerobic digestion has been proven both in the case of non-treated and pre-treated samples. As the fermentation moves forward dielectric properties become lower and lower, until the 12th day of the fermentation, when the stationary phase sets. Furthermore, the frequency that is in connection with the highest dielectric constant value becomes higher as the fermentation progresses, until the 12th day of the fermentation. This means that the starting point of the stationary phase of the fermentation is determinable with this method. Based on our results the dielectric properties are due to the biochemical changes that occur in the fermentation media due to the absorbed microwave energy.

Acknowledgements

The research is supported by the ÚNKP-22-2-SZTE-199, UNKP-22-3-SZTE-204 and ÚNKP-22-5-SZTE-208 New National Excellence Program of the Ministry for Innovation and Technology from the source of the National Research Development and Innovation Fund, and by János Bolyai Research Scholarship of the Hungarian Academy of Sciences (BO/00161/21/4).

References

[1] Lachassagne, D., Soubrand, M., Casellas, M., Gonzalez-Ospina, A., & Dagot, C. (2015). *Impact of sludge stabilization processes and sludge origin (urban or hospital) on the mobility of pharmaceutical compounds following sludge landspreading in laboratory soilcolumn experiments. Environmental Science and Pollution Research, 22(21), 17135–17150.*

[2]Ngo, P. L., Udugama, I. A., Gernaey, K. V., Young, B. R., & Baroutian, S. (2021). *Mechanisms, status, and challenges of thermal hydrolysis and advanced thermal hydrolysis processes in sewage sludge treatment. Chemosphere, 281, 130890*

[3] Ding, Y.; Guo, Z.S.; Hou, X.G.; Mei, J.X.; Liang, Z.L.; Li, Z.P.; Zhang, C.P.; Jin, C. *Performance Analysis for the Anaerobic Membrane Bioreactor Combined with the Forward Osmosis Membrane Bioreactor: Process Conditions Optimization,Wastewater Treatment and Sludge Characteristics. Water 2020, 12*

[4] Refai, S., Wassmann, K., & Deppenmeier, U. *Short-term effect of acetate and ethanol on methane formation in biogas sludge. Applied Microbiology and Biotechnology, Vol. 98, pp 7271–7280 (2014)*

[5] Antoine Prandota Trzcinski, *Advanced biological, physical and chemical treatment of waste activated sludge CRC Press; 1st edition, 2018* Jákói, Z.; Hodúr, C.; Beszédes, S. *Monitoring the Process of Anaerobic Digestion of Native and Microwave Pre-Treated Sludge by Dielectric and Rheological Measurements. Water 2022, 14, 1294.*

[6] Cheng, Y.C.; Li, H. *Rheological behavior of sewage sludge with high solid content. Water Science and Technology 2015, 71, 1686-1693*

[7] Jákói, Z.; Hodúr, C.; Beszédes, S. *Monitoring the Process of Anaerobic Digestion of Native and Microwave Pre-Treated Sludge by Dielectric and Rheological Measurements. Water 2022, 14, 1294.*

FLORA, CONSERVATION VALUE AND ECOLOGICAL POTENTIAL OF THE CER BOUNDARY CHANNEL (ŠABAC, SERBIA)

Bojan Damnjanović[1], Milica Živković[2,3], Jelena Đuričić Milanković[1], Ana Vasić[1], Marijana Srećković[4], Ana Matić[1]

[1]Academy of Professional Studies Šabac, Department for Medical and Business-Technological Studies, Hajduk Veljkova 10, 15000 Šabac, Serbia
[2]University Edukons, Faculty for Environmental Protection, Vojvode Putnika 87, 21208 Sremska Kamenica, Serbia
[3]University in Novi Sad, Faculty of Sciences, Department for Biology and Ecology, Dositeja Obradovića Square 3, 21000 Novi Sad, Serbia
[4]Public Health Institute, Jovana Cvijića 1, 15000 Šabac, Serbia
e-mail: bdamnjanovic@live.com

Abstract
Channels can represent significant areas of plant diversity in urban ecosystems. The aim of this paper is to determine recent flora of aquatic macrophytes as well as determining the conservation values and ecological potential based on the macrophyte in one part of the Cer boundary channel. Field research conducted during the summer of 2020 of total lenghth of 5km upstream from the estuary. Macrophute data was collected according to the standard UKTAG LEAFPACS method. A total of 13 macrophyte species were recorded out of which three species are on the list of endangered and protected species. The ecological potential of the researched part of the channel flow was graded as good and better. Based on the results can conclude that the Cer boundary channel represents an optimal habitat for the development of aquatic vegetation and thus other hydrobionts, as well as for the development of other rare and endangered types of macrophytes. Results confirm the fact that artificial water bodies can play a significant role in biodiversity conservation in urban ecosystems.

Introduction
Artificial water bodies, such as channels, can represent significant areas of plant diversity in urban ecosystems [1]. However, data on flora, species composition, distribution and the numbers of species are rarely published for artificial and modified water bodies [1]. Aquatic macrophytes are an important indicator during monitoring of fresh water ecosystems, whereas macrophyte vegetation represent habitats for development of other groups of aquatic organisms [2, 3]. Macrophytes represent a group of water photosynthesis active organisms (plants) that can be seen with the naked eye [4].
Based on the EU Water Framework Directive (WFD) [5], as well as the national Rulebook on the parameters of ecological and chemical status of surface waters and parameters of chemical and quantitative status of underground waters [6], macrophytes represent a significant biological indicator of quality during grading of the ecological status of natural, i.e. ecological potential of artificial and significantly modified water bodies.
For the estimation of the conservation value of the ecosystem different physical or biological criteria are most often used [7]. Biological criteria are based on the presence of species categorised according to the IUCN Red list [8], or according to the national categorisation of endangered or protected species [9, 10].
Considering everything aforementioned the aim of this paper is to determine the recent flora of aquatic macrophytes in a part of the Cer boundary channel, as well as determining the conservational value and ecological potential based upon the macrophytes flora.

Experimental

The Cer boundary channel is the largest artificial water course on the territory of the town of Šabac, with a total length of 30km, and it flows into the river Sava. The research was carried out during the summer of 2020 at a part of the river flow through the town of Šabac, with a total length of 5 km upstream from the estuary (Figure 1).

Data on the macrophyte vegetation was gathered at approximately 1000 m according to the standard UKTAG LEAFPACS method [11]. The mentioned method is based on choosing a sector along the shoreline approximately of 100 m length. At every 20 m within the sector vegetation records of 1 - 9 m^2 area are taken at depths of 0.25, 0.5, 0.75 and below 0.75 m. At the middle of each sector vegetational records are taken in transect at every 0,5 m of depth increase, beginning with 1 m upto the depth at which the aquatic vegetation spreads [11]. At five sectors (K1 – K5) a total of 100 vegetation records were made based on the described methodology (Figure 1).

Vegetational data was summarized by LEAFPACS sectors, and then the species relative cover (SRC), species richness (SR). The number of protected (NP) and strictly protected (NSP) species is determined according to the Rulebook on declaration and protection strictly protected and protected wild species of plants, animals and fungi [9], after which the relative cover of protected and strictly protected species was calculated. Shannon–Weaver index of diversity (SW) was calculated in CanoDraw software ver. 4.5 [13].

Figure 1 – Researched part of Cer parameter channel on the territory of the town of Šabac with locations of LEFPACS sector (K1 – K5)

In this paper the conservatory value is shown based on the presence and relative cover of strictly protected and protected species (RCPS) [12, 9]. The calculated macrophyte indices NP and NSP give an insight into the conservation value of each LEAFPACS sector.

The ecological potential is determined based on the macrophyte indices SR and SW, according to the Rulebook on parameters of ecological and chemical status of surface waters and parameters of chemical and quantitative status of underground waters [6].

All aforementioned macrophyte indices (SR, SRC, SW, NP, NSP) are summarized at the scale of the entire researched section of the Cer boundary channel.

Results and discussion

On five LEAFPACS sectors a total of 13 macrophyte species were detected (Table 1). In most cases the channels due to their uniform morphology are distinguished by poor species richness and diversity [1] however the results of this paper confirm the opposite thesis, that artificial water bodies can represent centres of floral diversity [14]. According to the results of the study conducted on nine channels, marked as centres of diversity of aquatic macrophytes in Slovakia, the number of species were in range from 11 to 62 [1]. In this research the species with the highest relative cover were: *Lemna minor* L., *Sparganium erectum* L., *Ceratophyllum demersum* L. i *Nuphar lutea* (L.) Sm. The beforementioned species, especially *Lemna minor* and *Ceratophyllum demersum* represent very common findings in eutrophic slow waters, i.e. water ecosystems with high concentrations of nutrients in Europe [1, 15]. Such species findings were recorded in natural water bodies of similar hydromorphological characteristics on the territory of Eastern and Central Europe [15]. In numerous research it was determined that in the channels, due to the ecosystem succession and the process of terrestrification, the most dominant and frequent heliophytes are *Phragmites australis* (Cav.) Trin. Ex and *Typha latifolia* L. [1], as is the case in this research. Namely, by visual monitoring of the entire research area it was determined that the reed and cattail are the most frequent species with the highest cover between LEAFPACS sectors, as well as that those are parts of channels that dried out. On the territory of Serbia, the plant communities with domination of *Typha latifolia* and *Phragmites australis* represent a transition between aquatic and terrestrial vegetation, they are tolerant to a long period of drying, increased salinity and water pollution [16].

Among those identified, three species have conservation value. *Nuphar lutea* has the status of a strictly protected species and is also one of the species with the highest relative cover (12.15%), while *Iris pseudacorus* L. and *Potamogeton nodosus* Poiret. have the status of protected species on the territory of Serbia [9]. At least one protected or strictly protected species was recorded in each sector, which indicates the conservation importance of the investigated section. A large number of protected and endangered species have been recorded in different types of artificial water bodies on the territory of Europe, which places them in the group of ecosystems of conservation importance [1, 17]. The relative cover of protected and strictly protected species at the sector level was in range between 5.26 and 33.37%, while at the level of the entire investigated section it was 18.22%.

The number of species per sector varied between 7 – 9 which indicates a moderate ecological potential (III) of each LEAFPACS sector. SW was within the limits of 1.60 - 1.83, which indicates a good and better (II) ecological potential based on the national Rulebook [6] (Table 2). At the level of the entire investigated section, the ecological potential of the Cer boundary channel can be rated as good or better (II).

Table 1 – Relative cover of species (%) and quantitative indices of macrophyte flora at the scale of individual LEAFPACS sectors (K1-K5) and at the scale of the entire investigated section

Species	K1	K2	K3	K4	K5	Entire section
Ceratophyllum demersum L	26.31	16.67		31.91		15.9
Potamogeton nodosus Poiret. PS				6.38		1.4
Sparganium erectum L.	18.42	20.37	17.15	6.38	22.5	16.8
Nuphar lutea (L.) Sm. SPS	2.63	24.11			30	12.15
Sagitaria sagitifolia L.	10.52					1.87
Lemna minor L.	26.31		11.43	38.31	15	17.76
Iris pseudacorus L. PS	2.63	9.26	8.57	2.12		4.67
Botomus umbellatus L.	2.63		2.86	2.12	2.5	1.87
Phragmites australis (Cav.)Trin. Ex.	7.89		34.29	6.38		8.41
Hydrocharis morsus-ranae L.	2.63	16.67				4.67
Typha latifolia L.		9.27	17.15	6.38	15	9.35
Typha angustifolia L.		3.51	8.57		7.5	3.74
Glyceria maxima (Hartm.) Holmb.					7.5	1.41
SR	9	7	7	8	7	13
SW	1.83	1.83	1.74	1.60	1.75	2.26
NPS	2	2	1	2	1	3
RCPS (%)	5.26	33.37	8.57	8.5	30	18.22

PS–Protected species on the territory of Serbia [9]
SPS–Strictly protected species on the territory of Serbia [9]

Table 2 – The ecological potential of the Cer boundary channel based on the Rulebook on the parameters of the ecological and chemical status of surface waters and the parameters of the chemical and quantitative status of underground waters [6]

	K1	K2	K3	K4	K5	Entire section
SR	II	II	II	II	II	II
SW	III	III	III	III	III	II
Ecological potential	III	III	III	III	III	II

Conclusion

Based on the results it can be concluded that the Cer boundary channel represents an optimal habitat for the development of aquatic vegetation, based upon that other groups of hydrobionts as well and for the development of other rare and endangered macrophyte species. Also, results confirm the fact that artificial water bodies can have a significant role in biodiversity conservation especially in urban ecosystems. The results of this study could be used during designing and work carried out on the maintenance of the channel and flow regulation.

References

[1] Dorotovičová C., Man-made channels as a hotspot of aquatic macrophyte biodiversity in Slovakia. Limnologica 43 (2013) 277– 287.
[2] Lucena-Moya P., Duggan IC., Macrophyte architecture affects the abundance and diversity of littoral microfauna. Aquat Eco 45(2) (2011) 279-287.

[3] Baart I., Gschöpf K., Blaschkec AP., Preinera S., Heina T., Prediction of potential macrophyte development in response to restoration measures in an urban riverine wetland. Aquat Bot 93 (2010) 153-162.
[4] Chambers P.A., Lacoul P., Murphy K.J., Thomaz S.M., Global diversity of aquatic macrophytes in freshwater. Hydrobiologia 595 (2008) 9-26.
[5] European Commission. Directive 2000/60/EC of the European Parliament and the Council of 23rd October 2000 establishing a framework for community action in the field of water policy. Official Journal of the European Communities L327. 2000.
[6] Official Gazette of the Republic of Serbia, number 30/2010. Rulebook on parameters of the ecological and chemical status of surface waters and parameters of chemical and quantitative status of underground waters. Belgrade: JP "Official Gazette". 2010.
[7] Boon P., Pringle C., Assessing The Conservation Value of Fresh Waters an International Perspecitve. Cambridge University Press, Cambridge. 2009.
[8] Rosset V., Simaika PJ., Arthaud F., Bornette G., Vallod D., Samways JM., Oertli B., Comparative assesment of scoring methods to evaluate the conservation value of pond and small lake biodiversity, Aquatic Conservation: Marine and Freshwater Ecosystems, 23 (2013) 23-36.
[9] Official Gazette of the Republic of Serbia, number 5/2010 and 47/2011. Rulebook on the declaration and protection of strictly protected and protected wild species of plants, animals and mushrooms. Belgrade: JP "Official Gazette". 2011.
[10] Cvijanović D., Damnjanović B., Novković M., Živković M., Anđelković A., Vesić A., Vukov D., Radulović S., Conservation status of macrophyte vegetation in gravel pits in the floodplain of the lower course of the Drina River. Proceedings of the 47th annual conference on current topics of water use and protection, WATER 2018, June 12-14, 2018, Sokobanja, (2018) 111 – 118.
[11] Willby N., Pitt J., Phllips G., The ecological classification of UK lakes using aquatic macrophytes. Environment Agency Science Report. Project SC010080/SR. Bristol. 2009.
[12] Williams P., Biggs J., Whitfield M., Corfield A., Fox G. and Adare K., Biological techniques of still water quality assessment. Phase 2. Method development. Technical Report E56. Enviroment Agency: Bristol. 1998.
[13] ter Braak CJF., Šmilauer P., CANOCO Reference Manual and CanoDraw for Windows User's Guide: Software for Canonical Community Ordination (version 4.5). Microcomputer Power, Ithaca. 2002.
[14] Jursa M., Oťaheľová H., Distribution of aquatic macrophytes in man-modified waterbodies of the Danube River in Bratislava region (Slovakia). Ekológia, 24 (2005) 368-384.
[15] Sipos V.K., Kohler A., Köder M., Janauer G. Macrophyte vegetation of Danube channels in Kiskunság (Hungary). Arch. Hydrobiol. Suppl. 147 (1–2), Large Rivers14 (1–2), (2003) 143–166.
[16] Lakušić, D., Blaženčić, J., Ranđelović, V., Butorac, B., Vukojičić, S., Zlatković, B., Jovanović, S., Šinžar – Sekulić, J., Žukovec, D., Ćalić, I., Pavićević, D. Habitats of Serbia: Manual with descriptions and basic data. Ministry of Science and Environmental Protection, Directorate for Environmental Protection. Institute of Botany and Botanical Garden "Jevremovac", University of Belgrade. Belgrade. 2005.
[17] Oertli B., Auderset JD., Castella E., Juge R., Cambin D. and Lachavanne J-B., Does size matter? The relationship between pond area and biodiversity, Biological Conservation,104 (2002) 59-70.

HEAVY METALS IN NON-AGRICULTURAL SOILS OF THE NORTHERN SERBIA

Bojan Damnjanović[1], Ana Vasić[1], Jelena Đuričić Milanković[1], Marijana Srećković[2], Ana Matić[1]

[1]Academy of Professional Studies, Department of Medical and Business-Technological Studies, Hajduk Veljkova 10, 15000, Šabac, Serbia
[2]Public Health Institute, Jovana Cvijića 1, 15000 Šabac, Serbia
e-mail: bdamnjanovic@live.com

Abstract

Soils contamination with heavy metals is one of the biggest environmental threats and environmental problems in the world and may represent the health hazard for surrounding populations of plants, animals and humans. Anthropogenic activities are the main source of contamination such as mining and metal processing industry, transport, the use of fertilizers, sewage sludge, and many other industrial processes [1,2]. The aim of this study was to review the most common heavy metals in non-agricultular soils of the Municipalities of Northern Serbia (Province of Vojvodina). For the purposes of data analysis, publicly available databases were used [3]. The most common heavy metals whose concentrations exceed the limit values according the National Regulation [4] were cadmium (Cd), cobalt (Co), copper (Cu), nickel (Ni) and mercury (Hg). In all samples in 2021, concentration of cobalt exceeded limit value. At the Municipality of Kanjiža only concentration of cobalt exceeded limit value. Concentration of arsenic (As) exceeded limit value only in the sample from Municipality of Odžaci, and lead (Pb) only in the sample from Municipality of Sombor. Samples from the Municipality of Šid contains very high concentration of copper (179.46 mg/kg) and nickel (109.46 mg/kg) that exceed remediation values. Concentration of nickel (231.72 mg/kg) in sample from Municipality of Beočin exceeding remediation value.

References

[1] Xu, J.; Liu, C.; Hsu, P.C.; Zhao, J.; Wu, T.; Tang, J.; Liu, K.; Cui, Y. Remediation of heavy metal contaminated soil by asymmetrical alternating current electrochemistry. Nat. Commun. 10 (2019) 1–8.
[2] Zhou, H.; Zhou, X.; Zeng, M.; Liao, B.H.; Liu, L.; Yang, W.T.; Wu, Y.M.; Qiu, Q.Y.; Wang, Y.J. Effects of combined amendments on heavy metal accumulation in rice (Oryza sativa L.) planted on contaminated paddy soil. Ecotoxicol. Environ. Saf. 101 (2014), 226–232.
[3] Monitoring of non-agricultural land in AP Vojvodina JN OP 9/2021 - Studies on quality assessment and evaluation of the degree of soil endangerment http://www.ekourbapv.vojvodina.gov.rs (Accessed, 11th October 2022.)
[4] Regulation on limit values of polluting, harmful and dangerous substances in soil. Official Gazette of RS, number 30/2018. Belgrade, Serbia, 2018.

NEW LIQUID CRYSTALLINE MATERIALS BASED ON FLUORENONE AND BENZOTHIENO-THIOPHENE

Livia Deveseleanu-Corici[1], Angela Maria Spirache[1], Daniela Haidu[1], Milenca Vorga[1], Alexandru Visan[1], Xiangbing Zeng[2], Goran Ungar[3], Liliana Cseh[1]

[1]"Coriolan Dragulescu" Institute of Chemistry, Timisoara 300223, Romania
[2]Department of Materials Science and Engineering, University of Sheffield, Sheffield S1 3JD, U.K
3 State Key Laboratory for Mechanical Behaviour of Materials, Xi'an Jiaotong University, Xi'an 710049, P.R. China
e-mail: liviacorici@yahoo.com

Liquid crystals represent a fascinating state of matter which combines order and mobility at a molecular and supermolecular level with important applications in modern technology. Their mesomorphic properties depend on the molecular shape, rigidity and polarity of the molecular fragments [1-3]. Introduction of lateral dipole moments by grafting polar groups to the rigid core gives tilted phases, for example, smectic C, which are of great practical importance for switching devices [4]. A successful and widely reported rigid building block promoting the formation of SmC phase is fluorenone which has a planar and slightly bent aromatic structure [5-7]. Another interesting rigid building block for organic liquid crystals is thiophene where the polarizability of the mesogenic group is changed due to the presence of sulphur atom which changes the polarity of the local bonds.

Here we present the design, synthesis and characterization of six novel potential mesogens carrying biphenyl-benzothieno-thiophene or fluorenone rigid cores with two or more peripheral flexible alkoxy side chains of different lengths. The purity and structural characterization of the intermediates and target compounds were carried out using 1D and 2D-NMR spectroscopy and elemental analysis, while the mesomorphic properties were investigated by differential scanning calorimetry (DSC), polarizing optical microscopy (POM) and X-ray scattering (XRD). The synthetized compounds carrying biphenyl-benzothieno-thiophene rigid core were shown to support cubic phase formation depending on the length of the flexible side chains, while fluorenone-based compounds displayed smectic phase depending on the number of side chains.

Acknowledgements

We are thankful to the Ministry of Research and Innovation, CNCSIS - UEFISCDI, project numbers: PN-III-P4-ID-PCE-20160720 and PN-III-P3-3.1-PM-RO-CN-2018-0139.

References

[1] K.L. Medard, H. Hamilton, S.C. van der Moore, J. Chem. Anal. 313 (2007) 163.
[2] B.T. Metan, A. Milne, in: A.C. Thomson, P.T. Bell (Eds.), Introduction to General Chemistry, Chempublishing, Washington, 1994, pp. 547.
[1] T. Kato, N. Mizoshita, K. Kishimoto, Angew. Chem. Int. Ed. 45 (2006) 38–68.
[2] B.M. Rosen, C.J. Wilson, D.A. Wilson, M. Peterca, M.R. Imam, V. Percec, Chem. Rev. 109 (2009) 6275–6540.
[3] A. Kovářová, M. Kohout, J. Svoboda, V. Novotná, Liq. Cryst., 41 (2014) 1703-1718.
[4] J. W. Goodby, R.J. Mandle, E.J. Davis, T. Zhong, S.J. Cowling, Liq. Cryst. 42 (2015) 593–622.

[5] A.V. Ivanov, S.A. Lyakhov, M.Y. Yarkova, A.I. Galatina, A.V. Mazepa, Russ. J. Gen. Chem. 72 (2002) 1435–1438.
[6] M.D. Harjung, C.P.J. Schubert, F. Knecht, J.H. Porada, R.P. Lemieux, F.J. Giesselmann, Mater. Chem. C 5 (2017) 7452–7457.
[7] F. Lincker, A-J. Attias, F. Mathevet, B. Heinrich, B. Donnio, J-L. Fave, P. Rannou, R. Demadrille, Chem. Commun. 48 (2012) 3209–3211.

THE USING OF THE BEAR BRANCH EXTRACT AS POTENTIAL CORROSION INHIBITOR FOR COPPER IN ACID MEDIA

George-Daniel Dima, Mircea Laurențiu Dan, Liviu-Virgil Costea, Andrei Borș

University Politehnica Timisoara, Faculty of Industrial Chemistry and Environmental Engineering, Laboratory of Electrochemistry, Corrosion and Electrochemical Engineering, 6 Pârvan, 300223 Timisoara, Romania
e-mail: mircea.dan@upt.ro

Abstract
The paper investigates the corrosion inhibition property of the Bear Branch (*Heracleum sphondylium)* extract for copper in acid HNO_3 solution. Potentiodynamic polarization and chronoamperometry techniques were used in this study in order to evaluate the inhibition efficiency of the proposed corrosion inhibitor in the mentioned solution. The Tafel plot method employed to determine value of the the corrosion current i_{corr} as well as the corrosion rate. For a better simulation of the adsorption process of the extract on the metal surface, an equivalent circuit (EEC) has been modelled by using the data provided from the electrochemical impedance spectroscopy measurements. The possible interactions between the organic natural compounds molecules present in the extract of *Heracleum sphondylium*, have been evaluated by means of quantum chemical calculations and molecular modelling.

Introduction
As environmental protection laws begin to become more stringent on compounds used in corrosion protection, research has turned to finding compounds with ever lower environmental impact, low cost, and high inhibitory efficiency [1].
Lately, natural extracts have received a lot of attention for this purpose due to the complexity of the molecules of the natural compounds in their structure, the multiple bonds, the heteroatoms, or in some cases, the rings that respect the rules of aromaticity [2].
In the case of copper corrosion in nitric acid environment, previously published studies that have been carried out assessed the electrochemical behaviour of some organic compounds like Triazine derivatives [3], computational and experimental studies on heterocyclic imidazole derivatives [4], respectively theoretical and experimental studies of some amino acids such as L-methionine, L-methionine sulfoxide and L-methionine sulfone [4]. From the point of view of natural extracts used as copper corrosion inhibitors in acidic media, remarkable inhibitory efficiencies have been reported for the extract of cherokee rose (*Rosa Laevigata*) [5], an attempt to test the inhibitory effect of the Bear Branch extract in the corrosion in acid media has not been already performed.

References
[1]. G.O.H. Whillock, S.E. Worthington, Corrosion in Nitric Acid, Shreir's Corrosion, Volume 2, 2010, pp. 1250-1269.
[2]. H. Wei, B. Heidarshenas, L. Zhou, G. Hussain, Q. Li, K. Ostrikov, Mater. Today Sustain. (2020) 100044.
[3]. K. Shalabi, Ebrahim Abdel-Galil, A.H. El-Askalany, Y.M. Abdallah, J. Mol. Liq, 348 (2022) 118420.
[4]. K.F. Khaled, Corros. Sci., 52(10) (2010) 3225-3234.
[5]. Xin Zhang, Li Yang, Yu Zhang, Bochuan Tan, Xingwen Zheng, Wenpo Li, J Taiwan Inst Chem Eng, 136 (2022) 104408.

MONITORING THE ACID COAGULATION PROCESS OF MILK BY DIELECTRIC MEASUREMENT

Réka Dobozi[1], Zoltán Jákói[2], József Csanádi[1], Sándor Beszédes[2]

[1]Department of Food Engineering, Faculty of Engineering, University of Szeged, H-6724 Mars ter 7, Hungary
[2]Department of Biosystems Engineering, Faculty of Engineering, University of Szeged, H-6725 Szeged, Moszkvai krt. 9, Hungary
e-mail: dobozireka@mk.u-szeged.hu

Abstract
The application of dielectric measurement techniques is becoming increasingly widespread in several fields of science and industry, due to its simple, quick and accurate usability. The dielectric behavior of almost all materials largely depends on – among other factors – their physical structure and chemical composition, and when these properties change even to just a relatively small extent, it can be detected by monitoring appropriate dielectric parameters. In our work, we have investigated the process of acid coagulation of milk to see whether a correlation can be established between the rheological behaviour of milk and two dielectric parameters, namely the dielectric constant, and the dielectric loss factor.

Introduction
In food processing technologies, the development of rapid, sufficiently accurate and reliable controlling – monitoring methods is becoming increasingly important to ensure adequate product quality, process controllability and the stability of production capacity.
Dielectric measurements present a promising method for process monitoring and control, and have been frequently used in food industry for quite a long time now, especially for detecting moisture content [1]. Materials behave differently when put into an electric or electromagnetic field, and this behavior is mostly defined by the various physiochemical properties of the material matrix, the strength of the electromagnetic field (E), the applied frequency (ω). If an electromagnetic field with a strength of E affects a material, it will cause its charge distribution to change, and this change equals to the electric displacement D. The connection between the displacement and the applied electromagnetic field is represented by the absolute permittivity of the media as follows:

$$D = \varepsilon \cdot E \rightarrow \varepsilon = \frac{D}{E} \quad (1)$$

In practice, the permittivity is often represented by a dimensionless quantity called relative permittivity (ε_r), which is the ratio of the absolute and vacuum permittivity ($\varepsilon_{0.}$). As opposed to vacuum, the response of normal materials depends on the frequency of the electromagnetic field, i.e. the polarization of the material does not change in an instant when it is affected by an electromagnetic field, and therefore, the response can be represented by a phase shift. Complex numbers allow the specification of phase and magnitude in the same time, and for this reason, the permittivity of real materials should be treated as a complex function of frequency of the applied field:

$$\varepsilon \rightarrow \varepsilon^*(\omega) \quad (2)$$

where ε^* denotes the complex permittivity.
Since ε^* is a complex function, the real and imaginary part can be separated as follows:

$$\varepsilon^*(\omega) = \varepsilon'(\omega) - i\varepsilon''(\omega) \quad (3)$$

In Eq. 3, ε' denotes the real part of the complex permittivity function and often called the dielectric constant, ε'' is the imaginary part, and stands for the dielectric loss factor, and $i = \sqrt[2]{-1}$. In the so-called lossy materials (in which $\frac{\sigma}{i\varepsilon'} \gg 1$), the total dielectric loss usually occurs to two different mechanisms: energy dissipation due to dipole rotation, and effective conductivity loss due to ionic conductivity. These different losses are covered by the dielectric loss factor, and can be given by the following equation:

$$\varepsilon'' = \frac{\sigma}{2\pi\omega \cdot \varepsilon_0} + \varepsilon''_d \qquad (4)$$

This indicates that those materials that contain either charged particles (free ions) or dipolar molecules (or both) in high concentrations tends to "lose" their stored electrical energy, and the extent of this loss can drastically change if the chemical and / or physical structure of the material undergoes a given kind of transformation. Therefore, measuring either the storing capability (ε'), or the lossyness (ε'') of a material during a process which involves the biological, physical and / or chemical transformation of the material (such as coagulation of milk), provides the opportunity to monitor this given process via dielectric measurements.

At the normal pH of milk (6.7), the surface charge of the casein micelles is negative. During acid-type coagulation, the added inoculum bacterial culture begins to metabolize the lactose content of milk, producing nascent lactic acid. The accumulating lactic acid progressively decreases the pH of the milk, and when its value reaches the 4.5-5.0 interval, the surface charge of the casein micelles becomes neutral; this is the isoelectric point of these micelles. When they lose their surface charge, a phenomenon called destabilization begins to take place. During destabilization, the casein micelles, overcoming the potential barrier, begins to bond with each other, producing first larger and larger casein aggregates, and later these aggregates form polymer chains, and in the meantime, free Ca^{2+}-ions are released from the amino acids. The secondary molecular bonds between these chains will eventually develop the final gel form; the clot starts to solidify, and the viscosity of the now coagulated milk is significantly increased. The coagulation process involves numerous physical and chemical changes inside the bulk material, and the aim of our research was to see whether a correlation between these changes and the change in dielectric behavior can be established.

Numerous studies investigated the applicability of the measurement of dielectric properties in food-related processes in the past few years. Harindran et al. found that the proportional relationship between ε' and ε'' (denoted as tanδ, which is called the dielectric loss tangent) has a strong correlation with the change of pH in milk during coagulation [2]. Guo et al. conducted an experiment where the dielectric properties of yogurt were measured during fermentation, and found that the dielectric loss factor positively correlated with fermentation time [3].

The effect of storage time on the dielectric properties of milk and yogurt was also investigated, and results indicate that the dielectric constant of both milk and yogurt decreased with storage time, and the dielectric loss factor was found to be in connection with the changes of pH value [4]. Dihn et al. investigated the formation of yogurt by using contactless dielectric sensors, and they found that this technique is capable of monitoring both the conductivity and permittivity of the yogurt during the formation process [5].

Experimental

The acid coagulation experiment was conducted by using ESL milk in 500 ml volume, and a thermophilic yoghurt culture (FD-DVS, YC-X11, Yo-Flex, *Lactobacillus delbrueckii* subsp. *bulgaricus* and *Streptococcus thermophilus*) inoculum bacterial culture was added to the system in a concentration of 3g/100ml. The milk was kept at a constant 45 °C temperature. For the

measurement of apparent viscosity, an *A&D SV-10* vibratory viscometer was used, and the dielectric properties were measured with a *SPEAG DAK 3.5* dielectric sensor connected to a *Rhode&Schwarz ZVL-3* vector network analyzer by an open-ended 50Ω coaxial cable. The rheological and dielectric measuring took place during the process at 15, 35, 55, 75, 85, 90, 95, 100, 105, 115, and 120 minutes.

Results and discussion

Observing the results presented on Figure 1 it can be seen that as the coagulation process progressed, the maximum value of the dielectric constant gradually decreased, while the inflexion point of the curves is shifted slightly towards higher frequencies. The slope of the curves is essentially correlated with that of high water content systems, but it is noticeable that the rate of the initial rising stages decreases to a slight extent with time.

The most observable differences occurred in the low-frequency range, around 400 MHz. The rate of decrease of the dielectric constant was highest up to 95 minutes, with the differences gradually reducing in the interval thereafter.

A clear explanation to this is that the solidification of the clot, i.e. the formation of the protein-polymer network, started at about 90-95 min, as supported by the rheological data (see later).

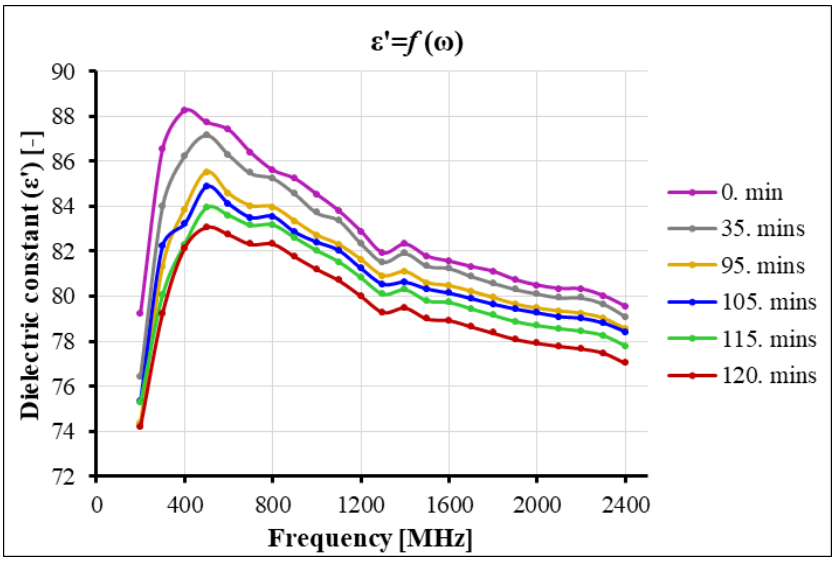

Figure 1. The change in dielectric constant in the function of frequency at different times of the coagulation process

The data obtained for the values of the dielectric loss factor indicates that as the coagulation process progressed, a decrease in the dielectric loss was present, especially in the time interval of 35-95 minutes. This strongly correlates with the tendencies experienced during the investigation of the dielectric constant, i.e. when the formation of casein aggregates begun, the dielectric behavior of the material matrix went through a significant change (Figure 2).

The sudden drop of the ε'' can be explained by the destabilization of casein micelles, which altered the average micelle concentration of the medium. High micelle concentration, especially above CMC (critical micelle concentration), has a huge impact on the conductivity of a colloid system, i.e. the conductivity above CMC increases rapidly. The destabilization of the casein micelles caused the micelle concentration to decrease, with which the conductivity of the milk also declined, and based upon Eq. 4, it caused the dielectric loss factor to decrease. Since the most observable differences were occurred in the low-frequency region, we plotted the rheological curve representing the clot formation and the relationship between the two dielectric parameters separately at 400 MHz as well (Figure 3a and 3b).

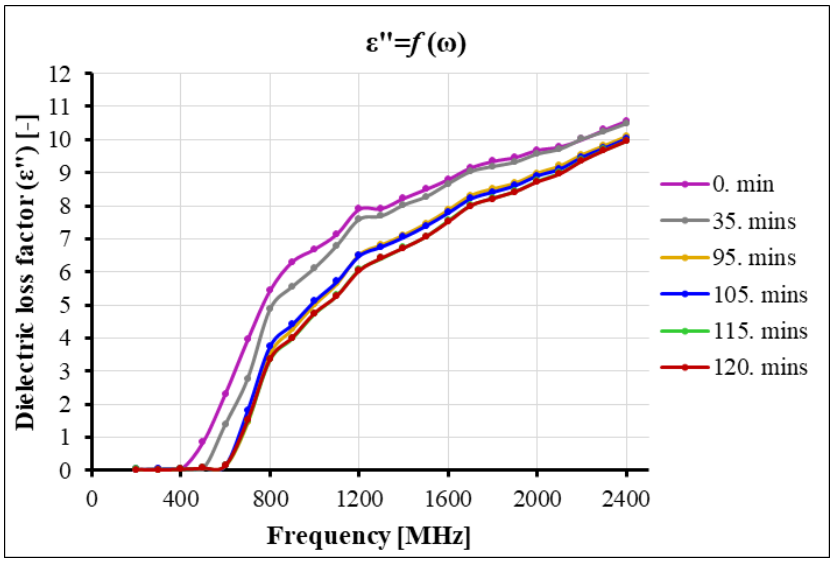

Figure 2. The change in dielectric loss factor in the function of frequency at different times of the coagulation process

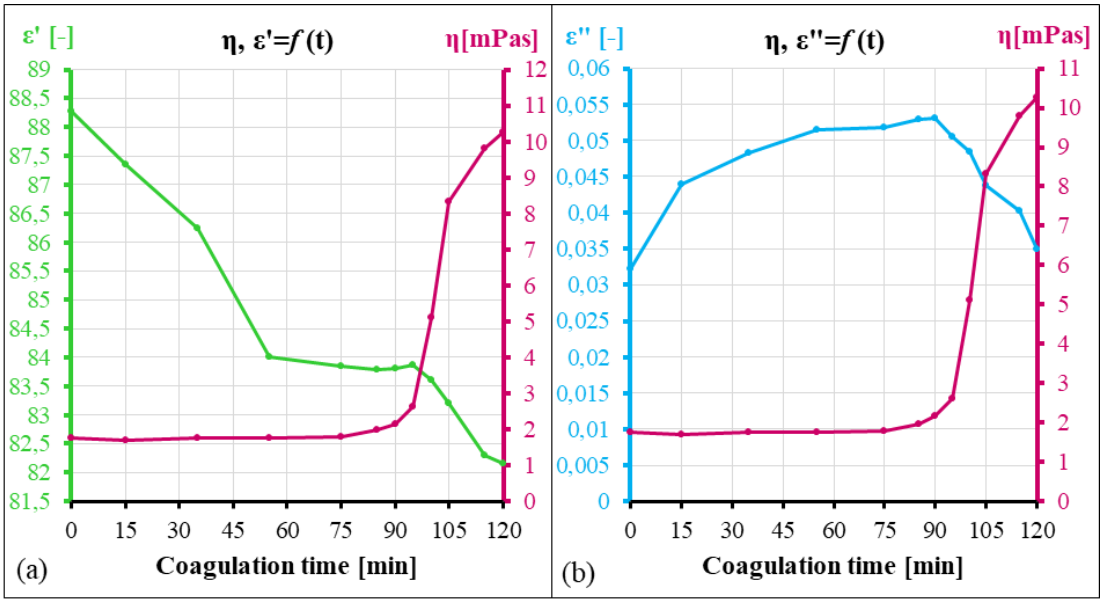

Figure 3. The apparent viscosity and dielectric constant (a), and the dielectric loss factor (b) in the function of coagulation time

From the apparent viscosity curves, it is clear to see that solid aggregates starts to form at around 90 minutes, after which the initial viscosity of around 8 mPas increases sharply to 47 mPas. During the process, the dielectric constant first decreases steeply (between 0 and 50 minutes) and then stagnates between 50 and 90 minutes. This change in the dielectric constant can be explained by the fact that the concentration of lactose, which is basically easily polarizable, gradually decreased over the 0-50 min interval due to bacterial decomposition, causing a steep decrease in the values of dielectric constant. During this period, the lactic acid, which was continuously accumulating in the system, gradually reduced the pH to the isoelectric point of the casein micelles, thus initiating the destabilisation phase (50-90 min). At this stage, the physico-chemical structure of the material matrix had not yet changed significantly, and therefore no significant change in the dielectric constants was observed. Subsequently, however, when the casein micelles, which had undergone charge loss, gradually formed the

protein-polymer network by growing into larger aggregates (i.e. the coagulum started to solidify) the dielectric constant started to decrease at a similar rate with a steep increase in apparent viscosity.

In contrast, the dielectric loss factor showed a saturation-curve-like slope over the 0-90 min interval, which could be explained, on the one hand, by the fact that the positively charged Ca^{2+} ions were being gradually released from the amino acids during the process, and especially at this frequency, this increased the conduction loss from ionic conduction, and on the other hand, by the slight increase in the free water content in the system due to the rearrangement of the casein micelles. However, at the clot solidification phase, which started around 90 min, the loss of conductivity due to micelle rearrangement was so large that it could not be compensated by free Ca^{2+} ions, so that the loss factor, similar to the dielectric constant, started to decrease sharply in the last stage of sol-gel transformation.

Conclusion

Our experimental results revealed that the process of acid coagulation of milk can be monitored by the measurement of the dielectric constant and loss factor, and that these two parameters have a strong correlation with the changes in the apparent viscosity of the milk when it undergoes the coagulation process.

Acknowledgements

The research is supported by the ÚNKP-22-2-SZTE-199, UNKP-22-3-SZTE-204 and ÚNKP-22-5-SZTE-208 New National Excellence Program of the Ministry for Innovation and Technology from the source of the National Research Development and Innovation Fund, and by János Bolyai Research Scholarship of the Hungarian Academy of Sciences (BO/00161/21/4).

References

[1] Wang, J., Fan, L., Zhou, Q., Li, J., Zhao, P., Wang, Z., Zhang, H., Yan, S., Huang, L. (2018). Determination of meat moisture content using radio-frequency dielectric measurement. IEEE Access. 6. 51384-51391. (DOI: 10.1109/ACCESS.2018.2864308)

[2] Harindran A., Madhurima V. (2020). On the efficacy of dielectric spectroscopy in the identification of onset of the various stages in lactic acid coagulation of milk. The Journal of Microwave Power and Electromagnetic Energy. 54(2). 161-181. (DOI: 10.1080/08327823.2020.1755484)

[3] Guo, C., Xin, L., Dong, Y., Zhang, X., Wang, X., Fu, H., Wang, Y. (2018). Dielectric properties of yogurt for online monitoring of fermentation process. Food and Bioprocess Technology. 11(5). 1096-1100. (DOI:10.1007/s11947-018-2072-y)

[4] Szerement, J., Szyplowska, A., Kafarski, M., Wilczek, A., Lewandowski, A., Skierucha, W. (2018). The effect of storage time on dielectric properties of pasteurized milks and yoghurt. 12th International Conference on Electromagnetic Wave Interaction with Water and Moist Substances (ISEMA). (DOI:10.1109/ISEMA.2018.8442291)

[5] Dinh, T. H. N., Martincic, E., Joubert, P.-Y., Serfaty, S. (2016). Monitoring of yogurt formation using a contactless radiofrequency dielectric sensor. 2016 IEEE SENSORS. (DOI:10.1109/ICSENS.2016.7808499)

THE MECHANISM BEHIND Pd(II) AND CARBOFURAN-INDUCED CHANGE OF GRAPHENE QUANTUM DOTS PHOTOLUMINESCENCE INTENSITY

Slađana Dorontić[1], Dušan Sredojević[1], Danica Bajuk-Bogdanović[2], Svetlana Jovanović[1]

[1]Vinča Institute of Nuclear Sciences - National Institute of the Republic of Serbia, University of Belgrade P.O. Box 522, 11001 Belgrade, Serbia
[2]Faculty of Physical Chemistry, University of Belgrade, P.O. Box 47, 11158 Belgrade, Serbia
e-mail: sladjana.dorontic@vin.bg.ac.rs

Abstract
The increasing presence of pesticides and heavy metals in the environment and their negative impact on human, animal, and plant health, demand green, low-cost, and simple methods for their monitoring. Due to photoluminescence (PL) in the visible part of the spectrum, biocompatibility, and ecological acceptability, graphene quantum dots (GQDs) are at the center of attention in the field of optical sensing. GQDs show great potential as PL sensors for Pd(II) ions and insecticide carbofuran. In this work, FTIR spectroscopy and Density Functional Theory (DFT) calculation were used to resolve the mechanism of PL change in the presence of these analytes.

Introduction
Among the many hazardous compounds present in the environment, heavy metals and pesticides are the most common pollutants. Due to high toxicity, they have harmful effects on human health, ecosystems, food, as well as drinkable water [1]. For a long time, the insecticide carbofuran (CF) was the most frequently used in crop protection against insects to improve their yield and quality [2]. The United States Environment Protection Agency (US EPA) has completely banned its application in any form [3]. Apart from agriculture, the pharmaceutical, and metal industry also contribute to global pollution. Palladium was found as an excellent catalytic agent in organic chemistry and drug production. Residues of this element in final products reach the environment causing damage [1].
One of the latest discovered members of carbon nanomaterials, graphene quantum dots (GQDs) found an important place in many scientific fields such as energy storage and conversion [4], bioimaging, photodynamic therapy, as well as antioxidative agents [5]. They are 0D nanoparticles less than 100 nm, with an sp^2 graphene core where different oxygen-contained moieties are bounded [2]. Their remarkable properties such as water solubility, biocompatibility, non-toxicity, PL in the visible part of the spectrum, as well as photostability make them a promising candidate for application in the optical detection of pesticides and heavy metals [1].
In this paper, GQDs were produced in the eco-friendly single-step top-down electrochemical oxidation of graphite electrodes. To improve their optical properties, they were gamma-irradiated at a dose of 200 kGy in the presence of 1g ethylenediamine (EDA). In earlier research, these dots were tested as PL probes for the detection of Pd(II) and CF [1, 2]. Now, we resolved the mechanism of the Pd(II) and CF-induced fluorescence change of GQDs using infrared spectroscopy with Fourier transformation (FTIR) and Density Functional Theory (DFT) calculations.

Experimental

GQDs were fabricated by the previously described method [6]. For gamma irradiation, water dispersion of GQDs in the concentration of 1 mg mL^{-1} was mixed with 1g of EDA. To remove molecular oxygen before irradiation, the mixture was bubbled with Ar. The sample was irradiated at a dose of 200 kGy. As a radioactive source, a ^{60}Co was used. Irradiated dots were labeled as γGQDs.

The morphology of γGQDs was analyzed using Quesant AFM (Agoura Hills, CA, USA). Structural characterization of γGQDs was performed at FTIR spectrometer (Thermo Nicolet iS20, Waltham, Massachusetts, MA, USA). PL spectra of γGQDs at different excitation wavelengths in the range of 300-400 nm were recorded at HORIBA Jobin Yvon's Fluoromax-4 spectrometer (Horiba, Kyoto, Japan). UV-Vis spectra were recorded using LLG-uniSPEC 2 Spectrophotometer (Lab Logistic Group, Meckenheim, Germany). For FTIR spectroscopy, $PdCl_2$ and CF solutions were mixed with GQDs and dried into powder. Powdered samples were mixed with KBr and compressed into pellets.

All DFT calculations were performed by using the Gaussian 09 suite of programs [7]. The $C_{60}O_{19}N_3H_{25}$ cluster, with 19 hexagonal C_6-rings, was employed as a model system for the DFT calculations to examine the electronic structure and adsorption properties of N-dopped GQD. The ground-state geometry optimization of bare GQD, GQD/Pd(II), and GQD···CF structures were carried out in the aqueous phase, including the SMD solvent model [8] using the B3LYP hybrid functional [9, 10] The LANL2DZ small-core ECP (effective core potential) basis set [11] was used for Pd(II) ions, in which 28 core electrons are exchanged by an effective potential, and the remaining 16 electrons occupy the valence space, while the Pople's valence double-ζ polarized 6-31G(d,p) basis set [12] was chosen for the light atoms. The frequency calculations were performed at the same level of theory to prove that the optimized structures present true minima and to estimate the Gibbs free energies of adsorption in an aqueous solution. The optimized geometries of the clusters, ESP maps, and NBO color schemes were obtained by the GaussView software [13], while the total density of state diagram (TDOS) was derived from the GaussSum program [14].

Results and discussion

Characterization of GQDs

In Fig. 1a, a 3D AFM image of γGQDs is presented and shows that dots are well-dispersed nanoparticles. Their heights vary from 0.5-5 nm which correspond to 3-5 graphene layers. In the FTIR spectrum of the sample (Fig. 1b), bands in the region 3420-3250 cm^{-1} are assigned to stretching vibration of O-H and N-H bonds in hydroxyl and amino groups, respectively.

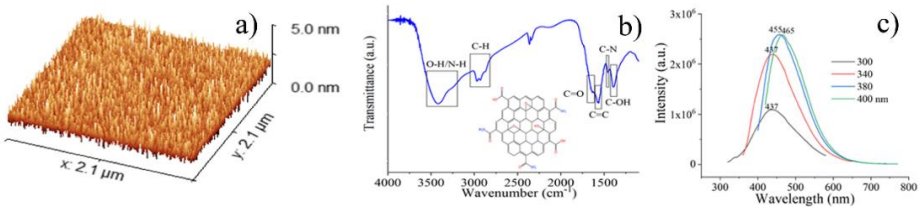

Fig. 1. a) 3D AFM image, b) FTIR spectrum with the schematic presentation of the structure, and c) PL spectra of γGQDs recorded at excitation wavelength 300-400 nm.

The weak band around 1700 cm^{-1} is attributed to stretching C=O vibrations in carboxyl moieties, while bands in region 2870-2970 confirmed the presence of C-H bonds in -CH, and -CH_2 functional groups. Band at 1570 cm^{-1}, verified the presence of graphene structure. The band detected at 1460 cm^{-1} is attributed to the C-N bending vibration of the amide functional group [2].

FTIR spectroscopy confirmed the successful incorporation of N atoms in GQDs structure in form of amide and amino functional groups. PL spectra of γGQDs (Fig. 1c) show that these dots emit light in a blue part of the spectrum, and exhibit excitation-depended PL. With the increase of the excitation wavelength, the center of the emission peak was shifted from 437 to 465 nm.

Mechanism of Pd^{2+} and CF detection

In previous investigations, we examine GQDs with amine and amide groups as PL probes for Pd(II) and CF [1, 2]. We found a linear decrease of GQDs PL intensity in the presence of Pd(II) in the concentration range 0-7.5 μmol L^{-1} with a limit of detection (LOD) of 0.66 μmol L^{-1}[1]. On the contrary, CF led to a linear enhancement of PL intensity in the range of 15-100 μmol L^{-1}, where LOD was 5.4 μmol L^{-1}[2]. The mechanism behind Pd^{2+} and CF detection was investigated using FTIR spectroscopy and DFT analysis.

In Fig. 2a FTIR spectrum of the γGQDs-Pd(II) system is presented. The band at 3420 and at 1700 are slightly reduced and moved to 3422 and 1712 cm^{-1} due to complexation between hydroxyl and carboxyl functional groups at GQDs surface and Pd(II) ions. The shift of band at 1570 attributed to stretching vibrations of C=C bonds in π-conjugated domains, to 1635 cm^{-1} indicates the transfer of GQDs π-electrons to unfilled d orbitals of Pd(II) ions [2]. In UV-Vis spectra of untreated γGQDs-200kGy (Fig. 2b, black curve) absorption bands at 200, and 250 nm are attributed to π-π* transition in sp^2 domains, and n-π* transition in C=O functional groups. After the addition of Pd(II) ions (Fig. 2b, red curve) in the system, bands at 200 and 250 nm, are becoming more pronounced and shifted to 239 and 279 nm, due to cation-π interactions and complex formation, respectively. [1].

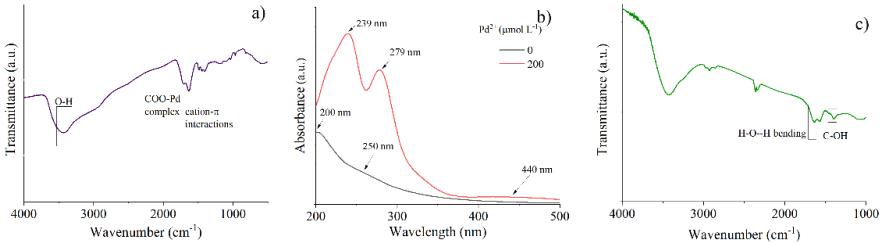

Fig. 2. a) FTIR and b) UV-Vis spectra of γGQDs in the presence of Pd(II) ions, and FTIR spectra of γGQDs in the presence of CF.

A compared with FTIR spectra of pure γGQDs (Fig. 1b) FTIR spectra of γGQDs-CF system also some changes can be noticed (Fig. 2c). Band arround 1700 cm^{-1} became more pronounced due to bending vibration of H-bonds formed between carboxyl group on GQDs surface and CF. [2].

DFT analysis

To investigate the mechanism of the Pd(II) induced fluorescence quenching of γGQDs, we employed DFT calculations to elucidate the interactions between Pd(II) ions with different parts of the GQD molecule at the atomistic level. On the other side, we estimated the energy of hydrogen bonding between carbofuran molecules with GQDs, which led to enhanced photoluminescence intensity due to the structural rigidification of GQD particles. The density of state diagram (DOS) with the spatial distribution of frontier molecular orbitals (FMOs), the optimized structure of GQD, and the electrostatic potential map of GQD molecule are presented in Fig. 3. The valence band maximum (VBM) and conduction band minimum (CBM) approximated with HOMO/LUMO orbitals of the GQD cluster are located at −5.53 and −2.98 eV, respectively (Fig. 3a). These values determine the HOMO-LUMO gap of 2.55 eV, which

is comparable with the experimentally measured absorption onset of the GQDs (~400 nm; 3 eV). The optimized structure of GQD reveals that the planarity of the molecule is perturbated owing to the hydroxy and epoxy groups on its surface, which resulted in the bent geometry (Fig. 3b). The map of electrostatic potential was calculated at the outer contour of electron density (isoval = 0.0004; mapped with ESP; Fig. 3c). It can be noticed that the H-atoms of -OH and -$CONH_2$ groups are positively charged, while the oxygen atoms of -COOH, -$CONH_2$, -OH, and epoxy groups are negative or slightly negatively charged.

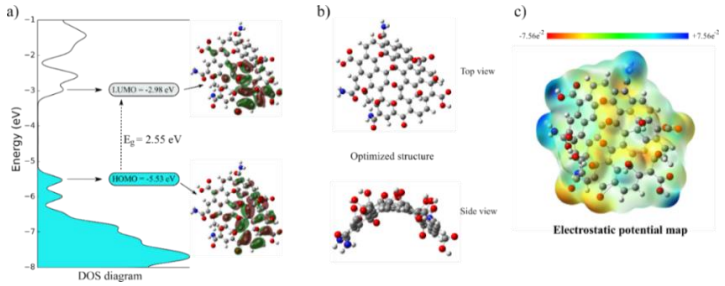

Fig. 3. a) Total density of state diagram (TDOS) of N-doped GQDs, b) the optimized structure of GQD's cluster (two views), and c) electrostatic potential map (ESP) as calculated at B3LYP/6-31G(d,p) level of theory.

To estimate the adsorption of Pd(II) ions at the GQD surface, we selected four sites of the GQDs molecule. The relative Gibbs free energy of adsorption in aqueous solution (ΔG_{sol}) was calculated as the difference between Pd/GQD adsorbed system and isolated Pd(II) ions plus free GQD molecule, based on frequency analysis upon the structure optimizations. Therefore, a negative value of ΔG_{sol} indicates that the adsorption process is energetically favorable. The strongest binding was calculated for the conformation in which the Pd(II) ion is coordinated to the deprotonated -COO^- group (ΔG_{sol} = -1.72 eV), while the weakest binding refers to the geometry where Pd(II) is located above one of the C_6-rings (ΔG_{sol} = -0.80 eV). Surprisingly, high adsorption energy was calculated for the geometry with Pd(II)-ion coordinated to the C=C double bond (Fig. 4a). The NBO charges of adsorbed Pd ions follow the order of Gibbs free energy changes: the higher positive charge on Pd indicates more negative ΔG_{sol} values and stronger adsorption (Fig. 4b).

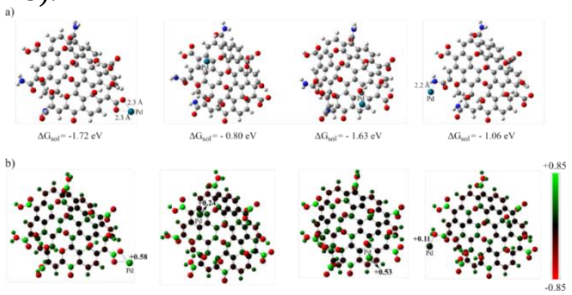

Fig. 4. a) The four optimized GQD structures in which Pd(II) ions are adsorbed to the molecule's different parts. b) The calculated NBO charges of four structures are presented in the same charge range and color scheme.

The geometry optimization of the GQD···CF system resulted in a structure with a bifurcated hydrogen-bond with respective -COO···H_2N- distances of 2.10 and 2.77 Å (Fig. 5a). The calculated ΔG_{sol} value is -0.12 eV (-2.76 kcal/mol), which is within the typical range of H-bond strengths. On the other hand, the ESC map of this adduct reveals that a highly negative region is associated with -COO···H_2N- interacting fragments of GQD and CF molecules, respectively (Fig. 5b).

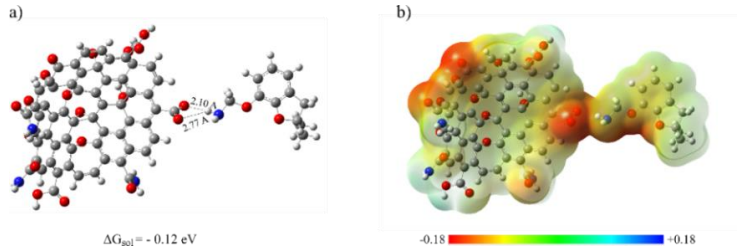

Fig. 5. a) The optimized GQD ⋯ CF structure with assigned hydrogen bonds and b) electrostatic potential map (ESC) as calculated at B3LYP/6-31G(d,p) level of theory.

Conclusion

In summary, we successfully resolved Pd(II) and CF-induced mechanism of PL change of irradiated amino/amide doped GQDs and Pd(II) using FTIR spectroscopy and DFT analysis. DFT analysis represents a promising, fast, and efficient method in the investigation of intermolecular interactions without additional consumption of chemicals.

Acknowledgements

This work was financially supported by the Ministry of Education, Science and Technological Development of the Republic of Serbia (Grant No. 451-03-9/2022-14/200017).

References

[1] S. Dorontic, A. Bonasera, M. Scopelliti, M. Mojsin, M. Stevanovic, O. Markovic, S. Jovanovic, Journal of Luminescence, 252 (2022) 119311.
[2] S. Dorontic, A. Bonasera, M. Scopelliti, O. Markovic, D. Bajuk Bogdanović, G. Ciasca, S. Romanò, I. Dimkić, M. Budimir, D. Marinković, S. Jovanovic, Nanomaterials, 12 (2022).
[3] https://archive.epa.gov/pesticides/reregistration/web/html/carbofuran_ired_fs.html.
[4] S. Dorontić, S. Jovanović, A. Bonasera, Materials, 14 (2021).
[5] S. Jovanovic, A. Bonasera, S. Dorontic, D. Zmejkoski, D. Milivojevic, T. Janakiev, B. Todorovic Markovic, Materials2022.
[6] S. Jovanović, S. Dorontić, D. Jovanović, G. Ciasca, M. Budimir, A. Bonasera, M. Scopelliti, O. Marković, B. Todorović Marković, Ceramics International, 46 (2020) 23611-23622.
[7] M.J.T. Frisch, G. W.; Schlegel, H. B.; Scuseria, G. E.; Robb, M. A.; Cheeseman, J. R.; Scalmani, G.; Barone, V.; Mennucci, B.; Petersson, G. A.; et al. Gaussian 09, Revision D.01; Gaussian, Inc.: Wallingford, CT, USA, 2009.
[8] A.V. Marenich, C.J. Cramer, D.G. Truhlar, The Journal of Physical Chemistry B, 113 (2009) 6378-6396.
[9] A.D. Becke, The Journal of Chemical Physics, 98 (1993) 5648-5652.
[10] C. Lee, W. Yang, R.G. Parr, Physical review. B, Condensed matter, 37 (1988) 785-789.
[11] P.J. Hay, W.R. Wadt, The Journal of Chemical Physics, 82 (1985) 299-310.
[12] R. Ditchfield, W.J. Hehre, J.A. Pople, Journal of Chemical Physics, 54 (1971) 724-728.
[13] A.N. Frisch, A. B.; Holder, A. J. Gauss View Molecular Visualization Program; User Manual: Pittsburg, CA, USA, 2001.
[14] N.M. O'Boyle, A.L. Tenderholt, K.M. Langner, Journal of Computational Chemistry, 29 (2008) 839-845.

REMEDIATION OF HEAVY METAL CONTAMINATED SOILS BY USING *URTICA DIOICA*

Jelena Đuričić-Milanković, Kosana Popović, Bojan Damnjanović, Jelena Jevtić, Dragana Ilić-Udovičić, Ivana Jevtić

Academy of Applied Studies Šabac, Department of Medical and Business-Technological Studies, Hajduk Veljkova 10, Šabac, Serbia
e-mail: jdjuricicmilankovic@vmpts.edu.rs

Abstract
Soil pollution with heavy metals not only degrades soil fertility, but also negatively affects the human health and well-being through the food chain. In order to protect the soil, as well as other parts of the environment, special attention should be paid to the remediation techniques of soil contaminated with heavy metals. The majority of physical and chemical remediation techniques, despite of their high efficiency, are expensive, environmentally destructive, harmful to soil fertility and therefore not well accepted by the public. Therefore, the use of environmentally friendly and cost-effective biological remediation techniques is a more acceptable approach for the remediation of contaminated soil. Phytoremediation is an eco-friendly approach that using native plants for remediation of heavy metal polluted soil in a cost-effective way. The aim of this paper is review of the most important results about of using plant stinging nettle (*Urtica dioica*) for removal of heavy metals from polluted soil.

Keywords: polluted soil, heavy metals, phytoremediation, *Urtica dioica*

Introduction
Heavy urbanization and industrialization, intensive mining and smelting activities, and the overuse of pesticides and other chemical additives in the agricultural sector have had a huge input into the degradation of vast areas by heavy metal contamination [1]. Heavy metals are the most studied among soil pollutants due to their persistence in the soil ecosystem [2]. Heavy metals are non-degradable by any biological or physical processes and remain in the soil for a long time, which poses a long-term threat to both the environment and human [3]. An excess of potentially toxic metals may be present due to natural geological sources or they may be introduced into ecosystems through anthropogenic processes [4]. They can enter into the food chain through crops and accumulate in the human body through biomagnification, thus posing a great threat to human health [5].
The possibility of remediation of the contaminated environment using different plant species attracts the attention of many scientists compared to the application of traditional expensive technologies for cleaning up contaminated sites. Methods, such as excavation, thermal treatment and chemical soil washing are typically expensive and destructive [6]. Phytoremediation, i.e. the application of plants for the restoration of a polluted environment, has been proposed as a promising green alternative to traditional physical and chemical methods [3]. Various plant species have mechanisms for the detoxification of xenobiotic compounds, with some being tolerant to high concentrations of toxic compounds and able to hyperaccumulate up to 1% of their weight [7]. Plant cultivation and harvesting are inexpensive processes compared with traditional engineering approaches involving intense soil manipulation [8].
The degree to which metals are available for plant uptake and further accumulation in the food web strongly depends on the degree of pollution and soil physico-chemical properties [9]. The

uptake of metals from soil depends on different factors such as their soluble content, soil pH, plant growth stages, types of species, etc. [10]. Modeling the translocation of metals from soil to root and root to the other parts of a plant, can be a very useful tool in heavy metal contamination and biological monitoring, in addition to the selection of tolerant or metal accumulator species [11]. The process of metal translocation in plant species is a very important factor that determines the distribution of metals in different plant tissues [12]. Several factors, including biochemical, anatomical, and physiological ones [13] determine the level of accumulation and distribution of heavy metals in the upper vegetative parts of plant.
To date, around 450 heavy metal hyperaccumulating species belonging to 45 families have been identified [14] and one such reported hyperaccumulating plant is stinging nettle (*Urtica dioica*).

Stinging nettle *(Urtica dioica)* and its potential for removing heavy metals from contaminated soil

The stinging nettle (*Urtica dioica*) belongs to the *Urticaceae* family and represents a perennial plant. The word "nettle" refers to the stinging effects of the tiny hairs on the stems and leaves, which when rubbed against the skin cause a burning sensation and temporary rash. It is widespread throughout Europe, America and Asia in different areas from temperate to tropical and it is easily adapted to many climatic conditions [15]. The main benefit of this plant species is its simplicity in terms of nutrition requirements, moreover, nettles are considered weeds due to their rapid growth and soil coverage. Stinging nettle is abundant species occuring in various types of forest, road verges and grassland sites. Stinging nettle is a plant that grows wild in the landfills and due to its ability to accumulative heavy metals in its organs, is a suitable plant species for their removal from soil [16].

In study of Bislimi et al. [11] was investigated the translocation and bioaccumulation of heavy metals such as Pb, Ni, Cd, Cu, and Fe in *Urtica dionica* and soil samples from two sites (uncontaminated and contaminated). In the contaminated site, the mean level of all the metals in soil and different parts (root, stalk, and leaf) of the plant were found to be significantly ($p<0.01$) higher than the uncontaminated site. The results revealed that *Urtica dionica* translocated high amounts of metals to its organs, especially to leaves, so that translocation factors were much higher than one (>1). On the basis of this study it can be concluded that the uptake of heavy metals from the soil to different parts of plant can be a very good biomonitoring tool for the heavy metal contamination or determination of species with high accumulation factor [11].
Shams et al. [17] examined the possibility of using the plants *Urtica dioica*, *Brassica napus* and *Zea mays* for the phytoremediation of sites contaminated with chromium and concluded that among the examined plant species, *Urtica dioica* was very effective due to its higher chromium uptake capacity (the aboveground concentrations of Cr in nettles was remarkable about 10 mg/kg). Their experiments were carried out without any chelating agents that could artificially enhance its uptake capacity. *Urtica dioica* with a mild presence of K in the chemicals produced very promising results to be considered as a unique plant for chromium remedial purposes [17].
In the study Grubor [18] specimens of *Urtica dioica* and *Sedum spectabile* collected from uncontaminated sites and transplanted in lead contaminated soil without additives (EDTA, HEDTA) to identify their natural potential for hypertolerance and hyperaccumulation of lead. This research showed that the concentrated toxic levels of lead in *Urtica dioica* and *Sedum spectabile* were about 100 or more times higher than those of non-accumulator plants, so these plants showed a natural hyper-accumulator and hyper-tolerant properties, because they have accumulated large amounts of lead without any additions - chelating compounds (EDTA,

HEDTA), to increase the uptake of lead from the soil. The results of the study by Dimitrijević et al. [19] also have shown that nettle has a tendency to accumulate lead.
According to Balabanova et al. [20] *Urtica dioica* showed potential to be used for phytoextraction for copper but not much specific potential for lead, as previously investigated by Grubor [18].
Research by Sharifi et al. [16] aimed to evaluate the absorption and accumulation of heavy metals from a simulated landfill soil using nettle. The researchers collected nettle seeds from the Tonekabon landfill, planted them in pots and after reaching the 6-leaf stage, the plants were exposed to three concentrations of four heavy metals (Pb, Cd, As and Ni) during the growing season. The results of this research showed that increases in the concentrations of the heavy metals in the soils led to their higher concentrations in all organs of the nettle plants (Pb > Ni > Cd > As), and larger quantities of the heavy metals were accumulated in the aerial parts of the plants. The results of Sharifi et al. [16] showed the ability of nettle to accumulate more heavy metals when they are present in higher concentrations in the soil.
Viktorova et al. [7] examined the plants of *Utrica dioica* which were cultivated in pots with two types of contaminated soil: first type was collected from the dumpsite of a long-term polychlorinated biphenyls (PCB) - contaminated soil in Lhenice (Czechia) and second type was obtained from mining ore at Pribram (Czechia) with excessive levels of As, Cd, Pb and Zn. The researchers in this study found a decrease in the concentration of heavy metals in soil samples for lead 4.9 ± 0.2%, for cadmium 5.3 ±0.4% and zinc 19.4 ± 0.8%, while arsenic was undetectable in nettles in this study. This investigation provided the first report that focused on remediation of PCBs with nettle. The researchers concluded that the nettle is only able to remediate less chlorinated biphenyls and determined a decrease of up to 33% for trichlorinated biphenyls (congeners 13–39), up to 12% of tetrachlorinated biphenyls (congeners 40–81) and other chlorinated biphenyls were hardly removed at all [7]. Even though their overall remediation is not very high, the remediation that they do perform is highly important.

Conclusions

Contamination of soil by various heavy metals is increasing as a result of different activities. These potentially harmful and persistent metals pose a great threat to the environment and human health. In order to protect the soil, as well as other parts of the environment, special attention should be paid to phytoremediation, as an eco-friendly approach that using native plants for remediation of heavy metal polluted soil in a cost-effective way. The stinging nettle (*Urtica dioica*) represents a perennial plant, which is widespread throughout different areas and easily adapted to many climatic conditions. The main benefit of this plant species is its simplicity in terms of nutrition requirements, moreover, nettles are considered weeds due to their rapid growth and soil coverage. *Urtica dioica* is one of the hyperaccumulating plants and its potential to remove heavy metals such as Cr, Pb, Cu, Ni, Cd and Zn from the polluted soil has been confirmed in several studies. Recent research has shown that *Urtica dioica* can be used not only for phytoremediation of heavy metals, but also for organic pollutants, which is highly important.

Reference

[1] Ali A., Guo D., Mahar A., Ping, W., Wahid F,Shen F., Li R., Zhang Z., Solid Earth Discuss. 2017, 6, 1–40.
[2] Smolders E., Oorts K., Van Sprang P., Schoeters I., Janssen C. R., McGrath S. P., Mclaughlin M. J. Environmental Toxicology And Chemistry, 2008, 28 (8), 1633-1642.
[3] Suman J., Uhlik O., Viktorova J., Macek T., Front Plant Sci., 2018, 9:1476.

[4] Ruley A.T., Sharma N.C., Sahi S.V., Singh S.R., Sajwan K.S., Environmental Pollution, 2006, 144, 1, 11-18.
[5] Rehman M. Z. U., Rizwan M., Ali S., Ok Y. S., Ishaque W., Saifullah et al. Ecotox. Environ. Safe., 2017, 143, 236–248.
[6] Wenzel WW, Lombi E, Adriano DC. In: Prasad M, Hagemeyer J (eds) Heavy metal stress in plants: from biomolecules to ecosystems, 2004, Springer Verlag, Berlin Heidelberg New York, 273–303.
[7] Viktorova J., Jandova Z., Madlenakova M., Prouzova P., Bartunek V., Vrchotova B., Lovecka P., Musilova L., Macek T., PLoS ONE, 2016, 11 (12): e0167927.
[8] Singh N., Ma L Q., International Society of Environmental Botanists, 2003, 9, 3
[9] Franz E., Romkens P., van Raamsdonk L., Van der Fels, Klerx HJ., Journal of Food Protection, 2008, 71, 12, 2504-2513.
[10] Mench M., Vangronsveld J., Didier V., Clijsters H., Environmental Pollution, 1994, 86, 3, 279-286.
[11] Bislimi K., Halili J., Sahiti H., Bici M., Mazreku I., Journal of Ecological Engineering, 2021, 22, 1, 1-7.
[12] Xiong, Z.-T., Bulletin of environmental contamination and toxicology, 1998, Springer, 60, 2, 285–291.
[13] Salt D. E., Blaylock M., Kumar N. et al., Nature Publishing Group, 1995, 13, 5, 468–474.
[14] Verbruggen N., Hermans C., Schat H., New Phytologist., 2009, 181, 4, 759–76.
[15] Virgilio N., Papazoglou EG., Jankauskiene Z., Di Lonardo S., Praczyk M., Wielgusz K., Ind. Crops Prod., 2015, 68, 42–49.
[16] Sharifi K., Rahnavard A., Saeb K., Gholamreza Fahimi F., Tavana A., Soil and Sediment Contamination: An International Journal, 2022.
[17] Shams K.M., Tichy G., Fischer A., Sager M., Peer T., Bashar A., Filip K., Plant Soil, 2010, 328, 175–189.
[18] Grubor M., Archives of Biological Sciences, 2008, 60, 2, 239–244.
[19] Dimitrijević V., Krstić N., Stanković M. , Arsić I., Nikolić R., Advanced technologies, 2016, 5, 1, 17-22.
[20] Balabanova, B., Stafilov, T., Bačeva, K., Journal of Environmental Health Science and Engineering, 2015, 13:2.

EXTRACTION OF POLYPHENOL COMPOUNDS FROM CHOKEBERRY (*ARONIA MELANOCARPA* (MICHX)) POMACE USING METHANOL AND ACETONE AT DIFFERENT CONDITIONS

Efaishe Kavela, Lilla Szalóki-Dorkó, Mónika Máté

Department of Fruit and Vegetable Processing Technology, Institute of Food Science and Technology, Hungarian University of Agriculture and Life Science, H-1118 Budapest, Villányi út 29-43, Hungary
e-mail: Kavela.Efaishe.Tweuhanga.Angaleni@phd.uni-mate.hu

Abstract
Fruits are appreciated in the food industry, due their high of bioactive compounds and sensory characteristics. Chokeberry is one of the fruits that are bioactive compounds abundant. It is used in juice production and other products, and large amount of chokeberry pomace believed to be rich in bioactive compounds is produced. Therefore, this pomace can be reused by extracting the bioactive compounds such as anthocyanins, which can be potentially used as natural food additives in the food industry. However, some compounds can be sensitive to different extraction conditions. Therefore, in this study, methanol (50%) and acetone (50%) were used as solvents for extracting antioxidants, total anthocyanins, and total phenolic compounds at room temperature and 60 °C at the duration of 30, 60 and 120 minutes. The shaker, ultrasonic sound and at room stand were used to hold the sample for 15 minutes. Room temperature extraction has been found not optimal for TPC and antioxidant at all extraction length in time, however, it is suitable for anthocyanins. Alternatively, acetone at room temperature (A20) for 120 minutes at room temperature can also be ideal. A combination of methanol at 60 °C for 60 min and holding the sample on shaker has been found appropriate for anthocyanins. The combination of extraction with acetone at 60ºC for 120 minutes and holding for 15 minutes on a shaker has been identified to be optimal TPC and antioxidant capacity extraction.

Introduction
Chokeberry (*Aronia melanocarpa* (Michx)) fruits have grown popularity in the food industry due to its abundance of phenolic compounds [1]. Aronia fruits are used in juice processing, which produces a large amount of Aronia pomace [2]. Aronia pomace has been reported rich in anthocyanins which is responsible for colours in fruits, making Aronia pomace a potential food colourant source [3]. Aronia pomace has also been reported rich in other polyphenols which can be used to preserve food [3]. However, some compounds are sensitive to different environmental conditions, and may degrade [4]. Therefore, for a significant quantity of bioactive compounds to be extracted from Aronia pomace, potential extraction methods and conditions must be considered. Solvents like methanol, acetone, ethanol, and glycerol are commonly used in polyphenol extraction from fruits [5–7]. However, there is little information on the optimal conditions and solvents for extracting polyphenols from Aronia pomace. Therefore, the aim of this study was to evaluate the efficiency of two commonly used solvents under different conditions (20°C and 60ºC) at a three different length of time (30, 60, 120 min) combined with different extraction methods (ultrasound, shaking).

Experimental

Materials and Methods

Aronia pomace were provided. Solvents were used acetone/distilled-water and methanol/distilled in 1:1 v/v and acidified with 1% formic acid.

Extraction was carried out by adding 30 mL of the solvent to ±1 g of the sample and thoroughly mixed. Some samples were extracted at room temperature (20ºC) and some at 60°C (in the water bath set at 60°C) in both methanol (50%) and acetone (50%). Both room temperature (20ºC) and 60°C samples were left to react for 20 min, 60 min and 120 minutes. After reaction time, samples were held for 15 minutes on the shaker, ultrasonic sound and on the bench (on stand) for 15 mins. This was then followed by centrifugation at 4000 rpm for 5 minutes, and the supernatant was collected and used for total anthocyanins (TA), total phenolic contents (TPC), total antioxidant capacity (FRAP) and colour parameters (L*, a*,b*).

The total anthocyanin concentration was assessed using the pH differential method[8]. The total phenolic contents were analyzed using the Folin-Ciocalteu method[9]. The antioxidant capacity was evaluated following the Ferric Reducing Ability of plasma (FRAP) assay [10].

Data analysis

The results obtained were statistically analyzed with IBM SPSS statistics software, version 27. The mean differences between factors were analyzed using the one-way analysis of variance (ANOVA) Post-hoc test (Turkey's). The significant difference between factors were determined at the interval level of $P<0.05$.

Results and discussion

The effect of time on the level of bioactive compounds

To determine the optimal extraction conditions of total anthocyanins, TPC, and antioxidants from aronia pomace, the effect of 50% methanol and 50% acetone at room temperature (20ºC) and 60ºC was evaluated at different extraction length in time (at 30, 60, and 120 minutes).

Total phenolic content: Figure 1A, indicates that the length of extraction time on samples extraction with both acetone (A20) and methanol (M20) at room temperature have no significant effects ($P<0.05$) on TPC content. However, a significant ($P>0,05$) increase of 3644 mg GA/mL (from 30 to 120 minutes) and 2945 mg GA/mL (from 30 to 120 minutes) on TPC content has been observed on samples extracted with Acetone (A60) and methanol (M60) at 60ºC, respectively. Figure 1A also indicates that acetone is more effective comparing to methanol.

Antioxidant capacity: Different extraction length in time have also been observed to have no significant effects ($P>0.05$) on the antioxidant capacity on samples extracted with both acetone (A20) and methanol (M20) at room temperature (Figure 1B). Similar to Figure 1A, a gradual increase on antioxidant capacity on samples extracted with acetone at 60ºC at 30 min, 60 min and 120 min has been observed with a significant increase ($P<0.05$) of 6013 µg AA/mL at 120 minutes from 30 minutes. Methanol extraction at 60°C has indicated no significant effects on antioxidant capacity on samples extracted at 30, 60 and 120 minutes, however the extraction of methanol at 60ºC is more effective comparing to methanol at room temperature. Studies that have looked at different durations of extraction[7] have also found similar results, where better yield of FRAP was obtained as the extraction duration increases.

Anthocyanins: In Figure 1C, 60 minutes of extraction has indicated better recovery of anthocyanins comparing to 30 and 120 minutes, on samples extracted with both acetone and ethanol. In general, anthocyanins has poor stability, factors like heat, pH and other environmental factors can affect the content of anthocyanin [11]. A significant decrease ($P<0.05$) of 243 mg/mL in anthocyanin content has been observed on sample extracted with acetone at

60ºC from 60 minutes (1032±199) to 120 minutes (789±135). This could be a degradation due to lengthy exposure of anthocyanins to high temperatures. Unlike in Figure 1A&B for TPC and FRAP; the results obtained in Figure 1C indicate extraction at room temperature for both acetone (A20) and methanol (M20) to have better recovery of anthocyanins comparing to extraction at 60º

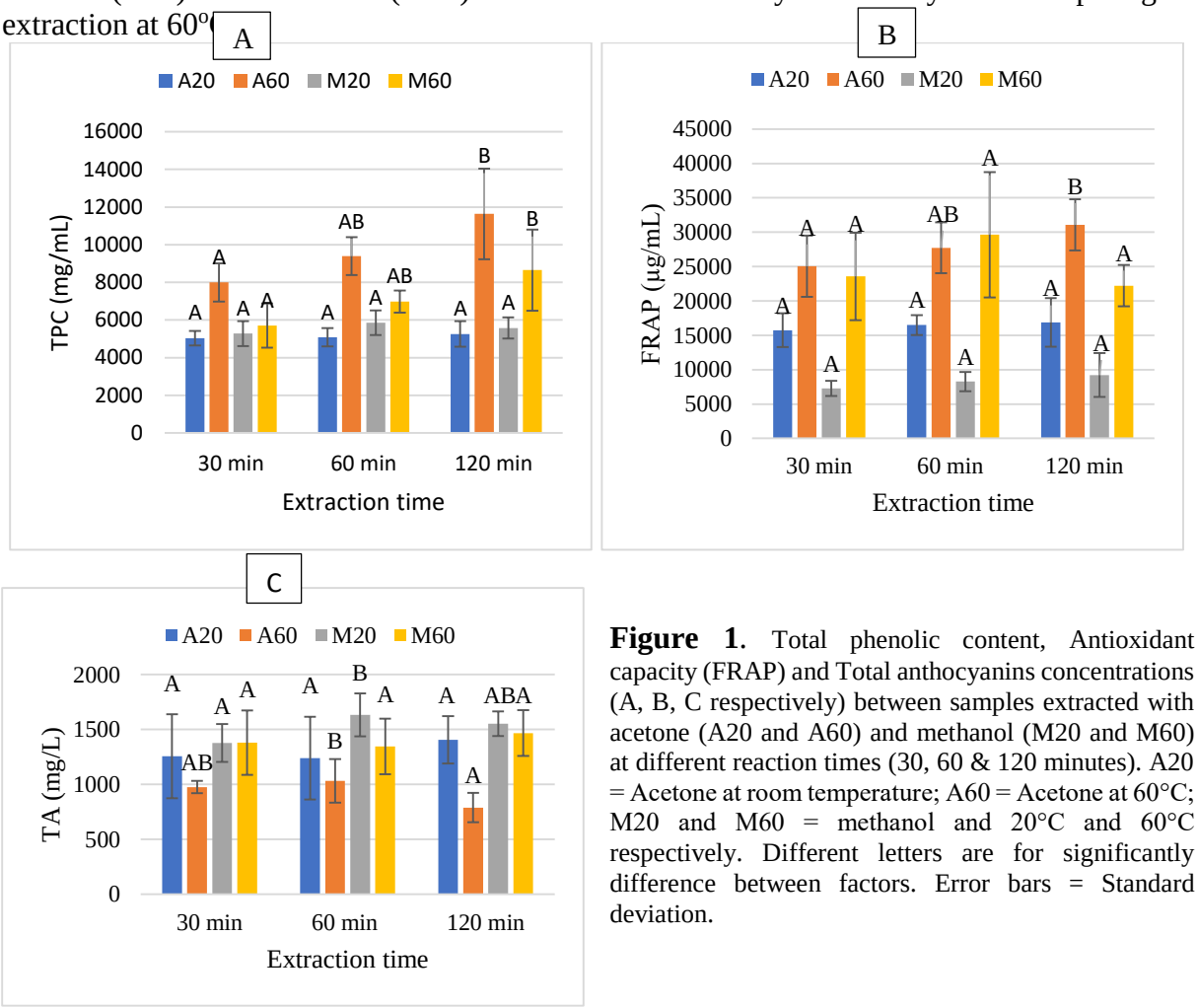

Figure 1. Total phenolic content, Antioxidant capacity (FRAP) and Total anthocyanins concentrations (A, B, C respectively) between samples extracted with acetone (A20 and A60) and methanol (M20 and M60) at different reaction times (30, 60 & 120 minutes). A20 = Acetone at room temperature; A60 = Acetone at 60°C; M20 and M60 = methanol and 20°C and 60°C respectively. Different letters are for significantly difference between factors. Error bars = Standard deviation.

The effect of a Shaker and Ultrasonic bath on the level of Anthocyanins, TPC and antioxidant

Total phenolic content: Figure 2A indicates the extraction with both acetone and methanol at 60ºC to be more effective comparing to extraction at room temperature. According to the results (Fig. 2A), the shaker has higher effects on TPC compared to room stands and ultrasonic sound for both acetone and methanol samples at 60ºC, with significantly higher recovery of 11012±263 mg/mL compared to 8113±896 mg/mL of room stands on acetone samples.

Antioxidant capacity: The results also indicate the extraction at 60ºC for both acetone (A60) and methanol (M60) to be more effective on antioxidant recovery compared to extraction at room temperature (A20 and M20) (Fig. 2B). The shaker has indicated better recovery of anthocyanins (31380±3701 µg/mL) on samples extracted with acetone, highly significant ($p<0.005$) compared to room stands (25292±2484 µg/mL). However, antioxidant capacity on samples extracted with methanol was recovered with the ultrasonic bath although not as high as antioxidants recovered with acetone on a shaker.

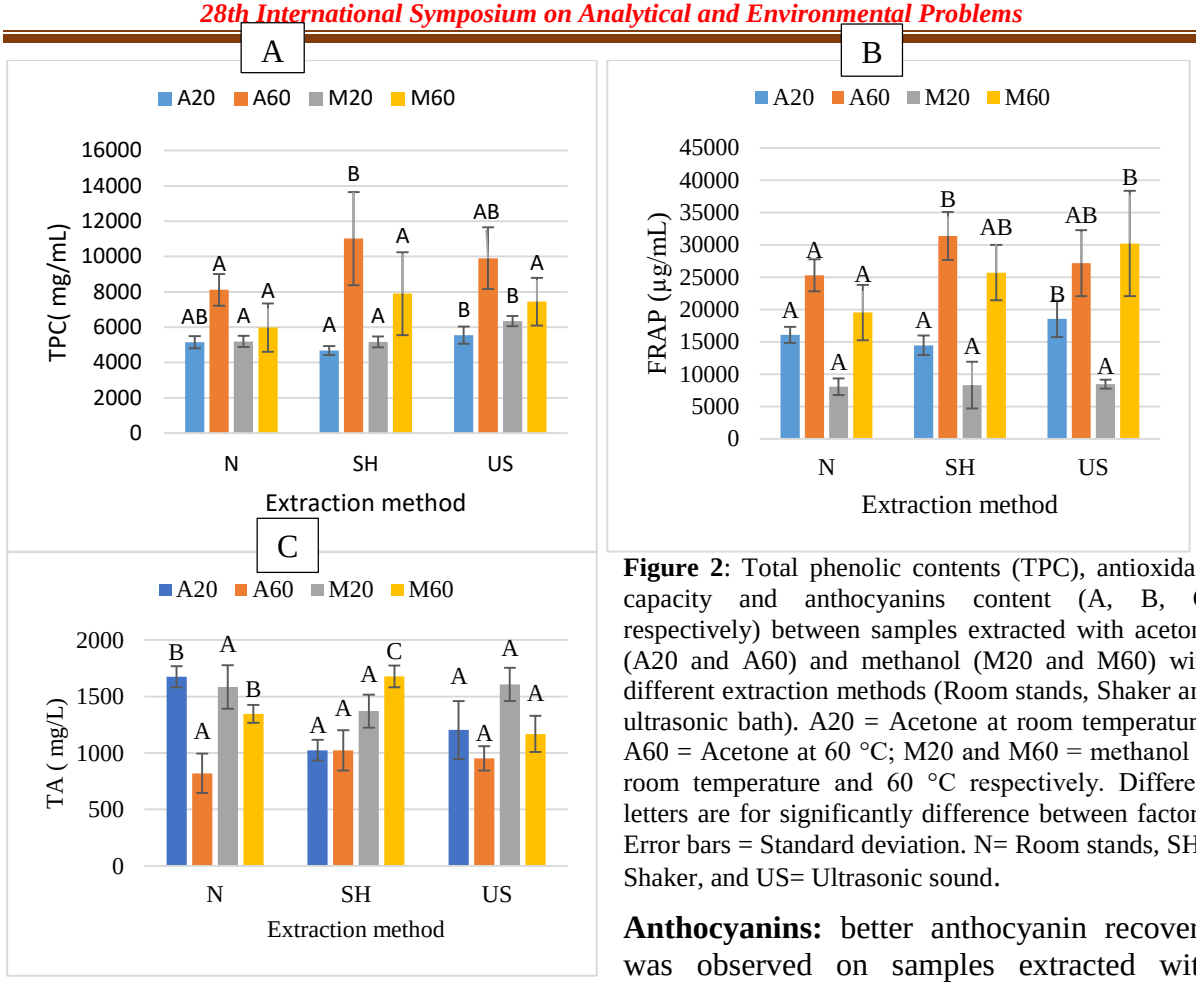

Figure 2: Total phenolic contents (TPC), antioxidant capacity and anthocyanins content (A, B, C, respectively) between samples extracted with acetone (A20 and A60) and methanol (M20 and M60) with different extraction methods (Room stands, Shaker and ultrasonic bath). A20 = Acetone at room temperature; A60 = Acetone at 60 °C; M20 and M60 = methanol at room temperature and 60 °C respectively. Different letters are for significantly difference between factors. Error bars = Standard deviation. N= Room stands, SH= Shaker, and US= Ultrasonic sound.

Anthocyanins: better anthocyanin recovery was observed on samples extracted with acetone (1674±93) and methanol (1584±193) at room temperature (A20 and M20) at room stands (N), as well samples extracted with methanol (M60) on a shaker (1678±96) and with methanol (M20) with ultrasonic bath (1607±148). Although in this case methanol at 60ºC (M60) on a shaker has yielded the highest anthocyanins, Acetone (A60) at room stand could be advisable since anthocyanin is not stable, and at room stands, there are no many factors such as heat.

Conclusion

Extraction of food components can sometimes be challenging due to the sensitivity if the compounds to be extracted. Therefore, selection of solvents and extraction conditions is very crucial for maximum concentration of polyphenols. In this study, two solvents were used at room temperature (20°C) and 60ºC at different extraction length in time and with different extraction methods. It has been concluded that room temperature extraction does not yield good results for TPC and antioxidant at all extraction length in time, however, it is suitable for anthocyanins. The optimal combination to yield high TPC and antioxidant capacity extraction would be extraction with acetone at 60ºC for 120 minutes and holding for 15 minutes on a shaker. Anthocyanins optimal conditions would be extraction with methanol at 60ºC for 60 minutes on a shaker. Alternatively, acetone at room temperature (A20) for 120 minutes at room temperature can also be ideal.

Acknowledgements

The authors acknowledge the Hungarian University of Agriculture and Life Sciences's Doctoral School of Food Science and EFOP-3.6.3-VEKOP-16-2017-00005 for supporting this study.

References

[1] Wathon, M. H., Beaumont, N., Benohoud, M., Blackburn, R. S., & Rayner, C. M. (2019). Extraction of anthocyanins from *Aronia melanocarpa* skin waste as a sustainable source of natural colorants. *Coloration Technology*, *135*(1), 5–16.

[2] Mandica-Tamara T., Landeka I., Marković, K., Zagreb, C. (2015). Phenolic Content, Antioxidant Capacity and Quality of Chokeberry (Aronia Melanocarpa) Products. *Food Technology and Biotechnology*, *53*.

[3] Babaoğlu, A. S., Unal, K., Dilek, N. M., Poçan, H. B., & Karakaya, M. (2022). Antioxidant and antimicrobial effects of blackberry, black chokeberry, blueberry, and red currant pomace extracts on beef patties subject to refrigerated storage.

[4] Bonerz, D., Würth, K., Dietrich, H., & Will, F. (2006). Analytical characterization and the impact of ageing on anthocyanin composition and degradation in juices from five sour cherry cultivars. *European Food Research and Technology*, *224*(3), 355–364.

[5] Haminiuk, C. W. I., Plata-Oviedo, M. S. V., de Mattos, G., Carpes, S. T., & Branco, I. G. (2014). Extraction and quantification of phenolic acids and flavonols from Eugenia pyriformis using different solvents. *Journal of Food Science and Technology*, *51*(10),

[6] Kowalska, G., Wyrostek, J., Kowalski, R., & Pankiewicz, U. (2021). Evaluation of glycerol usage for the extraction of anthocyanins from black chokeberry and elderberry fruits. *Journal of Applied Research on Medicinal and Aromatic Plants*, *22*,

[7] Ćujić, N., Šavikin, K., Janković, T., Pljevljakušić, D., Zdunić, G., & Ibrić, S. (2016). Optimization of polyphenols extraction from dried chokeberry using maceration as traditional technique. *Food Chemistry*, *194*, 135–142.

[8] Lee, J., Durst, R., & Wrolstad, R. (2005). *AOAC 2005.02: Total Monomeric Anthocyanin Pigment Content of Fruit Juices, Beverages, Natural Colorants, and Wines- pH Differential Method* (pp. 37–39).

[9] Singleton, V. L., & Rossi, J. A. (1965). Colorimetry of Total Phenolics with Phosphomolybdic-Phosphotungstic Acid Reagents. *American Journal of Enology and Viticulture*, *16*(3), 144.

[10] Benzie, I. F. F., & Strain, J. J. (1996). The Ferric Reducing Ability of Plasma (FRAP) as a Measure of "Antioxidant Power": The FRAP Assay. *Analytical Biochemistry*, *239*(1), 70–76.

DESIGN AND FABRICATION OF AN SURFACE ACOUSTIC WAVE SENSOR FOR GREENHOUSE GAS EMISSION MONITORING

Bucur Raul Alin, Farkas Iuliana

National Institute for Research and Development in Electrochemistry and Condensed Matter, Condensed Matter Department, No. 1 Plautius Andronescu, 300224 Timisoara, Romania.
e-mail: raul_alin_bucur@yahoo.com

Abstract

Surface acoustic wave sensors (SAW) are a type of microelectromechanical systems (MEMS) that relies on the modulation of an acoustic wave produced at the surface of piezoelectric material, correlated to a particular restrain applied onto that surface. From a technical point of view, a SAW resonator consists of a pair of micrometer comb-like metallic electrodes, aligned face to face. Also called interdigital transducers (IDT), this pair of electrodes form a resonant cavity. Using a radio frequency input signal applied to one of the electrodes, and taking into consideration the direct piezoelectric effect, this signal will generate onto the second electrode by inverse piezoelectric effect, an electric charge, that can be analyzed in terms of radio frequency output signal, relative to the input signal. The resonant frequency of the device can be tailored simply by remodeling the geometry of the interdigital pins, in terms of overall dimensions, aperture and pin spacing. The sensitivity of the SAW device is related to changes in the velocity of the surface acoustic wave traveling between IDT, as a response to a particular physical phenomenon produced on that surface. Changes in frequency, amplitude, phase, or time-delay between the input and output IDT are used to quantify the presence of the physical phenomenon. Due to their high sensitivity, tunable specificity and small size, SAW sensors can be successfully used for applications such as gas, temperature, mass, pressure, humidity or biological sensors [1, 2]. Considering the possibility of detecting small quantities of gases (ppb) and their ability to operate in "wireless" mode due to the working frequencies (MHz to GHz), the SAW based gas sensors have attracted much interest lately [3; 4].

This paper focuses on the studying of different geometrical alteration of IDT pins and wave reflectors, correlated to the frequency and output signal amplitude shift of a SAW sensor. The silver delay lines were obtained by photolithography onto a piezoelectric substrate, through the negative photo-resist method. The piezoelectric substrate was prior coated with a thick layer of silver, using thermal evaporation with Emitech K975X thermal evaporator. A thin film of UV photosensitive coating was form onto the piezoelectric substrate, using the spin coating technique. The desired IDT image was obtained by Kohler illumination, using a LEVENHUK microscope coupled to a LEVENHUK D740T 5.1M video camera. Finally, the resonant frequency shift and changes in signal level of the SAW device, in the absence and presence of the contaminant, was studied using the RIGOL DSA832 spectrum analyzer.

References

[1] Thomas, S.; Cole, M.; De Luca, A.; Torrisi, F.; Ferrari, A.C.; Udrea, F.; Gardner, J.W. Graphene-coated Rayleigh SAW Resonators for NO2 Detection. Procedia Eng. 2014, 87, 999–1002

[2] Sivaramakrishnan, S.; Rajamani, R.; Smith, C.S.; McGee, K.A.; Mann, K.R.; Yamashita, N. Carbon nanotube-coated surface acoustic wave sensor for carbon dioxide sensing. Sens. Actuators B Chem. 2008, 132,296–304

[3] P. Patial, M. Deshwal, Systematic Review on Design and Development of Efficient Semiconductor Based Surface Acoustic Wave Gas Sensor, Transactions on Electrical and Electronic Materials volume 22, pages 385–393 (2021)
[4] Jagannath Devkota , Paul R. Ohodnicki and David W. Greve, Review SAW Sensors for Chemical Vapors and Gases, Sensors 2017, 17, 801-829

COMPARISON OF ANTIOXIDANT PARAMETERS IN THREE DIFFERENT PARTS OF THE BERRIES OF SOME SEA BUCKTHORN GENOTYPES

Gitta Ficzek[1], Granit Selimaj[1,2] Sherif Mehmeti[1], Mónika Máté[2]

[1]*Hungarian University of Agriculture and Life Sciences, Institute of Horticulture, Department of Fruit Growing, Budapest*
[2]*Hungarian University of Agriculture and Life Sciences, Institute of Food Science and Technology, Department of Fruit and Vegetable Processing Technology, Budapest*
e-mail: ficzek.gitta@uni-mate.hu

Abstract

In the last few decades, the cultivation and consumption of sea buckthorn (*Hippophae rhamnoides* L.) is increasing with the extending prevalence of health-conscious nutrition. For that reason, investigation of antioxidant value and finding differences between varieties are especially current research topic.

The aim of this study was to determine the antioxidant status of the different parts of the sea buckthorn berry (skin + flesh, juice, peel) by TPC and FRAP analysis in the case of six genotypes.

Based on our results, the polyphenol content of the skin of the berries of the cultivars the 'Leikora', 'Mara' and 'Habego' was significantly higher. The highest FRAP value was for the berries of 'Mara', followed by R-01 and Askola, while the lowest value was represented by the 'Clara'. The FRAP value of the berry skin was significantly higher for the ‘Leikora’ and ‘Habego’.

Introduction

Sea buckthorn (*Hippophae rhamnoides* L.) is an important plant with a worldwide attention for the key attributes medicinal and nutritional potential [1].

The scientific evidences of the important elements and bioactive substances of the *Hippophae rhamnoides* L. is vast and continues to increase exponentially [2]. An essential source of bioactive substances such antioxidants, vitamins, fatty acids, amino acids, and minerals is found in this plant.

Human medicine comes along with health nutrition. Therefore, being rich in antioxidant properties, high vitamin C content and valuable vegetable oil content makes Sea buckthorn plant with high interest for studying [3].

Sea buckthorn is a multi-purpose plant, all parts of the berries are processed into food or dietary supplements. However, the amount of biologically active substances differs in the parts of the berry [4, 5].

In order to produce a product with an optimal composition, we need to know the valuable substances of the different parts of the berry.

The aim of this study is to determine the antioxidant content on the different parts of Sea buckthorn berries (skin + flesh, juice, skin), which was done by conducting TPC and FRAP analysis.

Experimental

Plant material

Berries of the SB cultivars (Ascola, Clara, Leikora, Mara, Habego) and one Hungarian canditate (R-01) were collected from the ecologically farmed plantation of Superberry Plus Kft. in Rákóczifalva (N. 47 °11'87", E.H. 20° 21'97). The research material were harvested manually from early August to October, when the berries began to soften and had orange colouring that is characteristic for the cultivar.

Following the fruit harvest, samples (3 kg cultivar^{-1}) were delivered to the laboratory, there the berries were separated to three part (skin with flesh, juice and skin). After than it were homogenised in a blender and stored in freezer at -28°C until analysis.

Spectrophotometric methods

1. Sample preparation for the spectrophotometric measurements. After thawing, the frozen fruit pulp was centrifuged with a Hettich EBA 21 (Hettich Instruments, Massachusetts, USA) laboratory centrifuge at 15,000 rpm for 5 minutes and polyphenol content and FRAP were determined from the diluted supernatant as needed on a Hitachi U2800A UV-VIS spectrophotometer (Chiyoda, Tokyo, Japan).

2. Total phenolic content. The total polyphenol content (TPC) was measured photometrically with Folin-Ciocalteu reagents at λ=765 nm. The calibration curve was made from gallic acid using the method of Singleton and Rossi [6]. Three parallel measurements were conducted for each sample.

3. FRAP assay. The ferric reducing antioxidant power (FRAP) assay was carried out according to [7]. The FRAP assay is based on the reduction of the Fe^{3+}-2,4,6-tripyridyl-S-triazine [3682-35-7] complex to the ferrous form (Fe^{2+}) and the intensity of the reaction is monitored by measuring the change of absorption at 593 nm. The final results were expressed as micrograms of Ascorbic Acid equivalents (AA) per liter of pulp (mM AA L^{-1}). Five parallel measurements were conducted for each sample.

Statistical analysis

For the statistical analysis of data, SPSS program was used. Statistical analysis was made by nonparametric methods, Kruskal-Wallis test and Mann-Whitney test. In that case, if on the base of a Kruskal-Wallis test based on rank numbers, there was a significant difference between samples at 95% significance level, differences between groups were examined by pair comparisons (Mann-Whitney probe).

Results and discussion

Several previous studies reported that the berries of SB varieties has a strong antioxidant effect and there is considerable variance among the cultivars [8, 9, 10]., but the antioxidant content of the different parts of the berries (skin + flesh, juice, peel) has not been investigated before. In this study, the antioxidant state of different part of berries of the investigated SB cultivars and one Hungarian candidate was characterized by total polyphenol content (TPC) and water-soluble antioxidant capacity (FRAP).

Contents of TPC in three different part of berries of sea buckthorn genotypes are displayed in Table 1. Among the investigated cultivars showed the skin +flesh part of the berries of ‘Leikora’ (1241.6 mg L^{-1}) the lowest TPC value, while the R-01 candidate had the highest polyphenol content for all three berry parts (2646.51-3063.47 mg L^{-1}).

Based on our results, the polyphenol content of the skin of the berries of the cultivars the 'Leikora', 'Mara' and 'Habego' was significantly higher, while in the case of 'Ascola', 'Clara' and R-01 there was no significant difference in the berries of the three in different parts (Fig.1).

The polyphenol content in the skin of the berry of 'Leikora' is significantly lower than the value measured in the skin of 'Mara', 'Habego' and R-01 (Table 3).

In present study, the TPC contents of the analyzed cultivars were similar or higher than the published value of 1.75 mg GAE kg^{-1} fw in berries of Indian Summer cultivar from Canada [9]. However, some Indian populations were measured extremly high TPC content (from 964 to 10.704 mg GAE 100 g^{-1}) by Korekar et al. [10].

The polyphenol content of SBT cultivars is affected by both their genetic background and by the growing and climatic conditions [11, 12, 13].

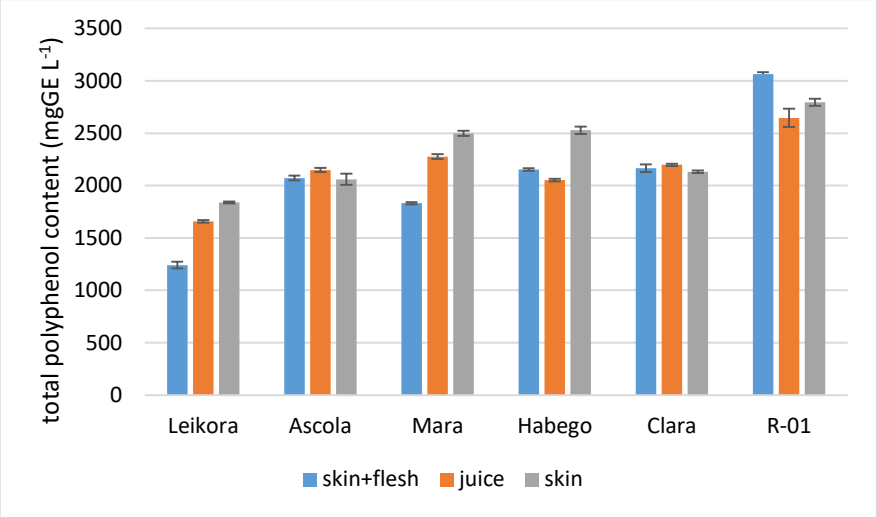

Figure 1. Total polyphenol content in three different parts of the investigated sea buckthorn genotypes (mgGE L^{-1}) (average ± standard deviation).

Based on our results, we can conclude that the berries of the investigated genotypes have a high water-soluble antioxidant capacity (6.87 – 17.7 mMAA L^{-1}). The highest FRAP value was for the berries of 'Mara', followed by R-01 and 'Askola', while the lowest value was represented by the 'Clara'. The FRAP value of the berry skin was significantly higher for the ‘Leikora’ and ‘Habego’ (Fig. 2), while in the case of the other examined cultivars there was no significant difference in the 3 different parts of the berry (Table 1).
The berry skin of 'Clara' had a statistically verifiable higher FRAP value compared to the other tested genotypes, while the FRAP value of the berry peel of 'Leikora' was significantly lower than the value measured in the berry skin of 'Mara' and R-01.

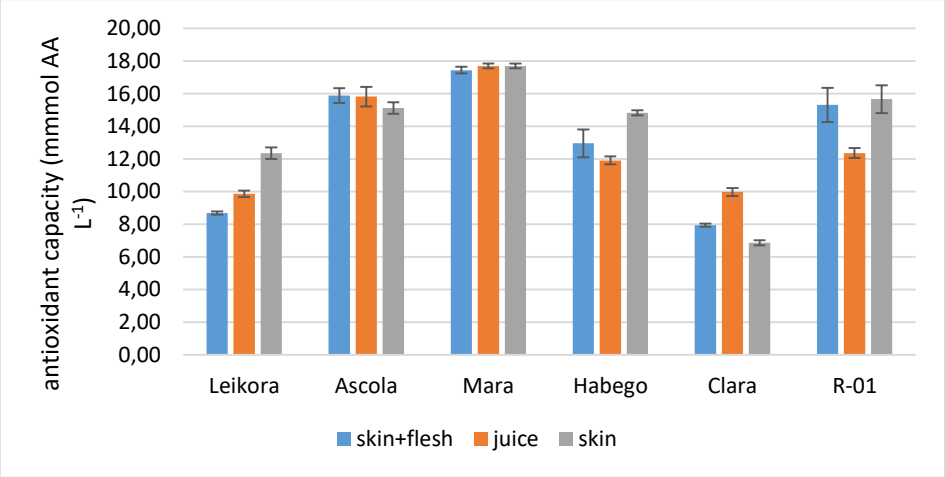

Figure 2. Antioxidant capacity (FRAP) in three different parts of the investigated sea buckthorn genotypes (mM AA L^{-1}) (average± standard deviation)

Table 1

	TPC					FRAP				
	Ascola	**Mara**	**Habego**	**Clara**	**R-01**	**Ascola**	**Mara**	**Habego**	**Clara**	**R-01**
	skin+flesh					**skin+flesh**				
Leikora	ns	ns	*	*	*	*	*	ns	ns	*
Ascola		ns	ns	ns	ns		ns	ns	*	ns
Mara			ns	ns	*			*	*	ns
Habego				ns	ns				*	ns
Clara					ns					*
	juice					**juice**				
Leikora	ns	*	ns	*	*	*	*	ns	ns	*
Ascola		ns	ns	ns	*		ns	ns	*	ns
Mara			*	ns	ns			*	*	ns
Habego				ns	*				ns	ns
Clara					ns					*
	skin					**skin**				
Leikora	ns	*	*	ns	*	ns	*	ns	ns	*
Ascola		ns	ns	ns	*		*	ns	*	ns
Mara			ns	ns	ns			*	*	ns
Habego				ns	ns				*	ns
Clara					*					*

Conclusion

Based on our results, we determined that the investigated sea buckthorn varieties are suitable for the production of products or dietary supplements containing biologically valuable active substances with functional properties. ‘Askola’ and ‘Mara’ varieties are mainly recommended for the production of juice. The peel, in the case of most varieties, has a higher active ingredient content. The peel (e.g. dried) can be used as an additional active ingredient in foods, especially the ‘Mara’, ‘Habego’ varieties and the R-1 variety candidate.

References

[1] K.L. Medard, H. Hamilton, S.C. van der Moore, J. Chem. Anal. 313 (2007) 163.
[2] B.T. Metan, A. Milne, in: A.C. Thomson, P.T. Bell (Eds.), Introduction to General Chemistry, Chempublishing, Washington, 1994, pp. 547.
[1] D. Roman, N.N. Condurache, I. Aprodu, E. Enachi, V. Barbu, G.E. Bahrim, G. Râpeanu. Insights of sea buckthorn extract's encapsulation by coacervation technique. Inventions, 6 (2021) (3) 59.
[2] C. Papuc, C. Diaconescu, V. Nicorescu, C. Criveanu. Antioxidant activity of polyphenols from Sea buckthorn fruits (*Hippophae rhamnoides*). Revista de chimie Bucharest-original edition, 59 (2008) (4) 392.
[3] F. Kreps, B. Tobolková, Z. Ciesarová, M. Potočňáková, L. Janotková, S. Schubertova, M. Jablonský. Total Content of Polyphenols, Flavonoids, Rutin, and Antioxidant Activity of Sea Buckthorn Juice. BioResources, 16 (2021) (3).
[4] L. Nilova, S. Malyutenkova. The possibility of using powdered sea-buckthorn in the development of bakery products with antioxidant properties. Agronomy Research, 16 (2018) (S2), 1444 1456
[5] D. Segliņa, I. Krasnova, A. Grygier, E. Radziejewska-Kubzdela, M. Rudzińska, P. Górnaś. Unique bioactive molecule composition of sea buckthorn (*Hippophae rhamnoides* L.) oils obtained from the peel, pulp, and seeds via physical "solvent-free" approaches. Journal of the American Oil Chemists' Society, 98 (2021) (10) 1009-1020.
[6] V.L. Singleton, JA. Rossi. Colorimetry of total phenolics with phosphomolybdic phosphotungstic acid "reagents". Amer. J. Enol. Vitic. 16 (1965) 1.
[7] I.I.F. Benzie, J.J. Strain. The Ferric Reducing Ability of Plasma (FRAP) as a measure of "antioxidant power". The FRAP assay. Annal. Biochem. 239 (1996) 70–76. https://doi.org/10.1006/abio.1996.0292.
[8] X. Gao, M. Ohlander, N. Jeppsson, L. Björk, V. Trajkovski. Changes in antioxidant effects and their relationship to phytonutrients in fruits of sea buckthorn (*Hippophae rhamnoides* L.) during maturation. Journal of agricultural and food chemistry, 48 (2000) (5) 1485-1490.
[9] M. Araya-Farias, J. Makhlouf, C. Ratti. Drying of seabuckthorn (*Hippophae rhamnoides* L.) berry: Impact of dehydration methods on kinetics and quality. Drying Technology, 29 (2011) (3) 351-359.
[10] G. Korekar, P. Dolkar, H. Singh, R.B. Srivastava, T. Stobdan. Variability and the genotypic effect on antioxidant activity, total phenolics, carotenoids and ascorbic acid content in seventeen natural population of Seabuckthorn (*Hippophae rhamnoides* L.) from trans-Himalaya. LWT-Food Science and Technology, 55 (2014) (1) 157-162.
[11] G. Ficzek, G. Mátravölgyi, D. Furulyás, C. Rentsendavaa, I. Jócsák, D. Papp, M. Stéger-Máté. Analysis of bioactive compounds of three sea buckthorn cultivars (*Hippophaë rhamnoides* L.'Askola','Leikora', and 'Orangeveja') with HPLC and spectrophotometric methods. Eur. J. Hortic. Sci. 84 (2019) 31-38.
[12] I. Sytařová, J. Orsavová, L. Snopek, J. Mlček, Ł. Byczyński, L. Mišurcová. Impact of phenolic compounds and vitamins C and E on antioxidant activity of sea buckthorn (*Hippophaë rhamnoides* L.) berries and leaves of diverse ripening times. Food chemistry, 310 (2020) 125784.
[13] Y. Li, P. Li, K. Yang, Q. He, Y. Wang, Y. Sun, P. Xiao. Impact of Drying Methods on Phenolic Components and Antioxidant Activity of Sea Buckthorn (*Hippophae rhamnoides* L.) Berries from Different Varieties in China. Molecules, 26 (2021) (23) 7189.

ROLE OF THE SOLVENT IN ELECTROSPINNING PROCESS OF FIBROUS MATERIALS BASED ON POLYSULFONE

Anca Filimon[1], Diana Serbezeanu[1], Adina Maria Dobos[1], Mihaela Dorina Onofrei[1], Daniela Rusu[1], Lavinia Lupa[2]

[1] "Petru Poni" Institute of Macromolecular Chemistry, Aleea Grigore Ghica Voda 41 A, 700487 Iasi, Romania
[2] Faculty of Industrial Chemistry and Environmental Engineering, University Politehnica Timisoara, 6 Vasile Parvan Blv, 300223, Timisoara, Romania
e-mail: lavinia.lupa@upt.ro

Modern medicine is challenged with complex problems caused by pathogenic microorganisms and their resistance to conventional antibiotic treatments. From this reason, innovative and sustainable solutions were sought to deal with these serious shortcomings by employing multifunctional materials/surfaces that prevent or reduce the adhesion and colonization of bacteria. In this context, the present work promotes a promising strategic way to design and develop of fibrous micro-/nanostructures based on polysulfone with morphological and surfaces properties tailored in accordance with the purpose of their use. Thus, by combining the properties of the quaternized polysulfone (PSFQ), cellulose acetate phthalate (CAP) and polyvinylidene fluoride (PVDF) and the proper choice of solvents for the electrospinning process of composite solutions, the quality and functionality of the fibrous materials based on PSFQ for the targeted application was guaranteed. Therefore, by controlling the weight ratio of the components in the system, blends with different compositions were obtained in different solvents, i.e., N,N-dimethylformamide (DMF) and N-methyl-2-pyrrolidone (NMP) were obtained, and subsequently electrospun. The morphological changes and characteristics of the nanofibers analyzed using SEM technique highlighted the influence of the polymeric solution properties and solvents nature (Figure 1).

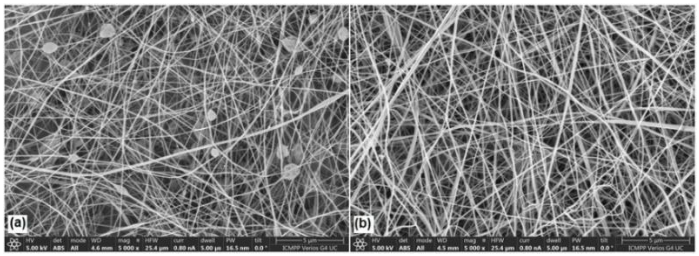

Figure 1. SEM images of PSFQ fibers obtained from solutions of 40% concentration in DMF (a) and NMP (b).

The recorded SEM images demonstrate that electrospinning of pure polymers and their blends solutions with different compositions and concentrations, enables the achievement of the fibers with different morphological characteristics and design, depending on the used solvents. Therefore, the solutions parameters associated with the polymer and solvent properties (concentrations, viscosity, boiling point of the solvents, and the surface tension) and also, the processing parameters related with the operation of the electrospinning apparatus and environmental parameters (temperature, humidity, and local atmospheric conditions) represent the key factors in electrospinning process, directly affecting the structural parameters and morphology of the electrospun fibers.

Acknowledgments
This work was supported by a grant of the Ministry of Research, Innovation and Digitization, CCCDI - UEFISCDI, project number PN-III-P2-2.1-PED-2021-2700, within PNCDI III.

ELECTROCHEMICAL DETECTION OF LEAD AT ZINC OXIDE NANOSTRUCTURE BASED MODIFIED ELECTRODE

Alexandra Belcovici[1], Carmen Ioana Fort*[1], Laura Elena Mureşan[2], Ioana Perhaiţa[2], Gheorge Borodi[3], Graziella Liana Turdean[1]

[1] Department of Chemical Engineering, Faculty of Chemistry and Chemical Engineering, Babeş-Bolyai University, 11 Arany János Street, RO-400028 Cluj-Napoca, Romania,
[2] "Raluca Ripan" Institute for Research in Chemistry, "Babes-Bolyai" University, 30 Fântânele Street, RO- 400294 Cluj-Napoca, Romania,
[3] National Institute for Research and Development of Isotopic and Molecular Technologies, 65-103 Donath, RO-400293 Cluj-Napoca, Romania
**e-mail: ioana.fort@ubbcluj.ro*

Abstract. A modified glassy carbon electrode (ZnO-Nafion/GCE) prepared by drop-casting technique, was investigated by square wave anodic stripping voltammetry (SWASV) for the detection of Pb^{2+} in synthetic and reals water samples.

Introduction. Heavy metals (HM) pollution represents one of the important dangers to the environment, and due to their toxicity, the HM detection is of great interest. Usually, the HM detection is performed by complex analytical methods such as atomic fluorescence spectroscopy, atomic absorbance spectroscopy, and inductive coupled plasma-mass spectroscopy, but, also by electrochemical methods based on the modified electrodes [1].

Experimental. The ZnO-Nafion/GC modified electrode was prepared by drop-casting method and was investigated by SWASV, using a PGStat 302N electrochemical workstation.

Results and discussion. The operational parameters (*i.e.*, HM deposition time, frequency, and pH of the buffer solution) for investigating the ZnO-NP-Nafion/GC modified electrode were optimized. The calibration curve for Pb^{2+} ions leads to obtaining the analytical parameters (*i.e.*, sensibility, linear domain, and limit of detection) which were in concordance with the literature data for other chemically modified electrodes. Moreover, the standard addition method was performed for Pb^{2+} detection in real water samples [2].

Conclusion. ZnO was used for preparing a sensitive ZnO-Nafion/GC modified electrode by a simple drop-casting method, and its investigation by SWASV led to obtaining good analytical parameters values in synthetic samples and the possibility to applying the device for detecting HM in real drilling water samples.

Acknowledgments
This work was supported by a grant of the Ministry of Research, Innovation and Digitization, CCCDI - UEFISCDI, project number PN-III-P2-2.1-PED-2021-2421, within PNCDI III.

References
[1] C.I. Fort, L.C. Cotet, A. Vulpoi, G.L. Turdean, V. Danciu, L. Baia, Popescu I. C., Sens. Actuators B:Chem. 220 (2015) 712–719.
[2] Directive 2013/35/EU, European Parliament and the Council, 2013.

A NEWLY IDENTIFIED SPECIFIC BIOLOGICAL ACTIVITY OF GLYPHOSATE – INHIBITION OF RGD-BINDING INTEGRINS

Borbála Gémes[1], Eszter Takács[1], Inna Székács[2], Enikő Farkas[2], Robert Horvath[2], Szandra Klátyik[1] András Székács[1]

[1]Agro-Environmental Research Centre, Institute of Environmental Sciences, Hungarian University of Agriculture and Life Sciences, H-1022 Budapest, Herman O. út 15, Hungary
[2]Nanobiosensorics Laboratory, Institute of Technical Physics and Materials Science, Centre for Energy Research, H-1121 Budapest, Konkoly-Thege Miklós út 29-33, Hungary
e-mail: gemes.borbala.leticia@uni-mate.hu

Abstract
In this study we investigated the inhibitory effect of the widely used broad-spectrum herbicide active ingredient glyphosate and its related analogues on αVβ3 integrin binding to the shortest oligopeptide recognizing motif of integrins, the arginine-glycine-aspartic acid (RGD) sequence. Integrin binding characteristics were assessed in a modified enzyme linked immunosorbent assay (ELISA) and by a label-free optical biosensor technique. At 22 mM, glyphosate reached full inhibition of αVβ3, and the inhibitory activity of its main metabolite, aminomethylphosphonic acid (AMPA) was also above 95%, while another environmentally relevant metabolite, sarcosine exerted only a weaker effect, approximately 35% inhibition. In turn, the half maximal inhibitory concentration (IC_{50}) of glyphosate and AMPA were reported to be 2.7±0.5 mM and 1.3±0.2 mM, respectively. The inhibitory effects of the other related compounds investigated (acetylglycine, glycine and iminodiacetic acid) at the same concentration, 22 mM were below 50%. Inhibitory effects on cell adhesion to RGD-modified surfaces by whole cells containing several types of RGD-binding integrins including αVβ3 were detected using the biosensor technique, where the integrin antagonist activity of glyphosate was also demonstrated.

Introduction
After its discovery as a potential herbicide active ingredient in 1971, glyphosate has been considered as a non-harmful compound to human health. As its popularity and usage intensity sharply increased on the market, the active ingredient and its metabolites emerged with increasing occurrence in environmental matrices as pollutants. Glyphosate residues have been detected in surface and subsurface water, soil, and also in food and biological samples. This fact paired with the contradictory toxicological classification by various international organizations (e.g., classified as probably carcinogenic to humans by the International Agency for Research on Cancer, but this statement has been refuted by the European Food Safety Authority and other risk assessment agencies) indicates uncertainties regarding the safety of this regulated product and an increasing rate of human exposure [1; 2]. Some of the revealed toxicity effects were proven to be attributable to the previously commonly used formulating agent, polyethoxylated tallowamine (POEA), yet certain effects, as the integrin antagonist activity reported in this study, clearly belong to the active ingredient itself. The basis of our modified receptor-binding enzyme-linked immunosorbent assay (ELISA) method was the connection between the arginine-glycine-aspartic acid (RGD) sequence and the αVβ3 integrin. Integrins, as cellular bidirectional signaling transmembrane receptors, have important roles in comunication between cells but are also involved in communication of the cells and their external environment [3]. Thus, integrins can bind different extracellular matrix components [4] which is provides a means for the cell to sense its surrounding medium [5]. Through specific

binding to their target ligands from the extracellular matrix integrins mediate crucial cellular physiological processes, such as cell adsorption and spreading on surfaces, migration and differentiation, and in a broader sense survival, proliferation, motility and differentiation [5, 6]. In addition, they also may contribute to pathological processes as well, as inhibitory effects on them may disturb normal cellular functions.

As RGD is the shortest recognizing motif for numerous integrins with different functions [7, 8], the inhibition of their binding can have a more extensive group of effects, including alterations in processes in several diseases comprising some types of cancer [9, 10]. Our study included characterization of cellular adhesion processes based on an Epic BenchTop (BT) optical biosensor investigation, which indicated the potential inhibitory effect of glyphosate on RGD-depended integrins [6], and compared the results with the extent of the αVβ3 integrin antagonist effect revealed in the ELISA and biosensor cell-free tests. To assess chemical moieties necessarily present in the chemical structure of the integrin antagonist, the inhibitory potential of structural derivatives of glyphosate has also been assessed within the study. All the chosen potential inhibitors are metabolites and amino acid analogs of the main target compound.

Experimental

ELISAs were carried out in high-capacity 96-well microplates (Nunc, Roskilde, Denmark, #442404) coated with 250 µg/mL PLL-g-PEG-RGD in the form of poly(L-lysine)-graft-poly(ethylene glycol) terminated with the sequence GGGGYGRGDSP (SuSos, Dübendorf, Switzerland) in 10 mM 4-(2-hydroxyethyl)-1-piperazine ethanesulfonic acid (HEPES, pH = 7.4) for 1 h and blocked after a washing step using phosphate buffer saline containing Tween with 20 mM TrisB, pH = 7.5. After washing, competition steps were performed by adding 50 µL of the inhibitor first (e.g., glyphosate in dilution series in a concentration range of 137.5 µM – 22 mM), and then 50 µL integrin (2 µg/mL) for 1 hour incubation. A subsequent washing step was followed by a 1-hour incubation of the primary antibody (mouse anti-human CD51/61, 2 µg/mL). After washing again, the second antibody labeled with a reporter enzyme horseradish peroxidase (anti-mouse IgG-HRP, 100 µL/well, 1 µg/mL) was incubated for 1 hour. After the last washing step, 100 µL/well of the substrate (hydrogen peroxide, 1.2 mM) and a chromophore (3,3′,5,5′-tetramethylbenzidine, 1.2 mM) were added together in 0.5 M citrate buffer (pH = 5.0). Incubations were performed at room temperature. The enzymatic reactions were stopped at the approppriate color intensity by adding 50 µL/well of 4 N sulfuric acid. Colorimetric signals were detected using a SpectraMax iD3 Multi-Mode Microplate Reader (Molecular Devices, San Jose, CA, USA) in endpoint mode at 450 nm.

Cell adhesion inhibition assays were performed in Epic BT instrument (Corning Incorporated, Corning, NY, USA) using 384-well Corning Epic assay microplate coated with PLL-g-PEG-RGD. The MC3T3-E1 cells were harvested and solutions containing glyphosate at varying concentrations were added to the cell suspension, resulting in a final cell density of 8000 cells/well. Then 30 µl of cell suspensions were seeded into the wells and biosensor responses were recorded for 1 h. Competitive biosensor integrin binding assays were performed in 384-well Corning Epic assay microplates coated with 250 µg/ml PLL-g-PEG-RGD. Solutions of echistatin, glyphosate, and tirofiban were added to the biosensor wells (20 µl/well). Upon stable baselines had been established for all wells, 20 µl of αVβ3 integrin solution was added to a final concentration of 4 µg/ml and biosensor responses were recorded for 1 h. Snake venom disintegrin echistatin was chosen as a positive control, while tirofiban, with no blocking effect on αVβ3 integrin, was applied as a negative control.

Comounds tested for integrin antagonist activity included, besides glyphosate, included its common or less frequent metabolites or contaminating substances. The chemical structures of

glyphosate and two of its major metabolites are depicted on Figure 1. Glyphosate was applied in the form of its zwitterionic free acid or its isoprolylammonium salt.

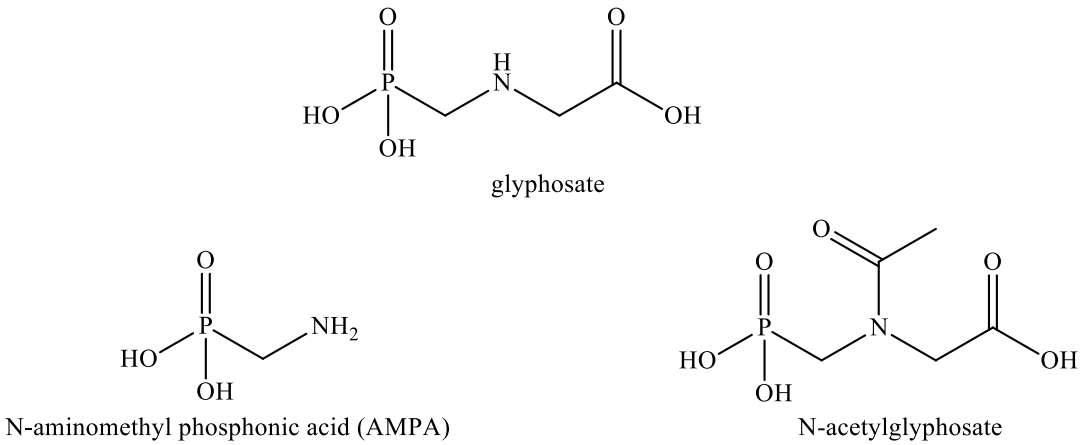

Figure 1. The chemical structure of the target compound glyphosate, and two of its metabolites, aminomethylphosphonic acid (AMPA) formed by oxidative degradation N-acetylglyphosate formed by N-acylation.

Results and discussion

ELISAs were performed to determine the inhibitory effect of glyphosate and related compounds on αVβ3 integrin binding to RGD sequence. Background levels were measured in coated and blocked wells with buffer. The main inhibitor herbicide caused total inhibition at 22 mM, but the half of that concentration (11 mM) still resulted in substantial inhibition as high as around 90% (Figure 2, left). To obtain comparable results with other compounds related to the target molecule, glyphosate, all the other compounds were investigated also up to this molar concentration, 22 mM. Surprisingly the main metabolite aminomethylphosphonic acid (AMPA) reached almost the same level of inhibition with a signal decrease above 95%, but other related compounds tested had only weaker effects with inhibition rates detected between 20% and 50%, and the activity of the weakest inhibitor, iminodiacetic acid did not reach 25%. The other important metabolite, sarcosine also caused only 35% inhibition. The potent inhibitory activity of AMPA was even more demonstrated by the half maximal inhibitory concentrations (IC_{50}s), in which AMPA showed an even slightly stronger inhibition than glyphosate: the IC_{50} values of glyphosate and AMPA were reported to be 2.7±0.5 mM and 1.3±0.2 mM, respectively.

Glyphosate is decomposed mainly by two mechanisms: a redox pathway in which aminomethylphosphonic acid (AMPA) and glyoxylic acid are formed via the C–N bond cleavage in the aminoacetic acid part of the molecule (AMPA pathway) catalyzed by the enzyme glyphosate oxidoreductase and other dehydrogenases, and a dephosphonylative pathway in which N-methylaminoacetic acid (sarcosine) and phosphate are formed via the C–P bond cleavage in the aminophosponic acid part of the molecule (sarcosine pathway) catalyzed by the enzyme C–P-lyase [1; 11]. In addition, glyphosate can also be inactivated by an N-acylation pathway in which N-acetylglyphosate is formed catalyzed by the enzyme glyphosate acetyltransferase [1; 12].

The effect of the integrin antagonist activity of glyphosate was demonstrated by determining its effect on cell adhesion of osteoblastic MC3T3-E1 cells to RGD-displaying polymer surfaces measured by label-free optical biosensing (Figure 2, right). For this purpose, the evanescent field-based surface sensitive resonant waveguide grating biosensor Epic BenchTop (Epic BT),

proven as a useful method for real-time, high-throughput, and label-free detection of cell adhesion, spreading and signaling events based on measuring of dynamic mass redistribution within a 150 nm range on the sensor surface, has been used [13-15].

The Epic cell assay was capable to assess changes in the kinetics of cell adhesion on the sensor surface. Sigmoid-shaped kinetic response is known to be typical phenomenon in receptor-mediated cell adhesion events [15-17]. In the presence of an inhibitor, cell adhesion is decreasing resulting in reduction in the maximal biosensor signal and indicating considerable effects of glyphosate on the cell adhesion process. The binding between RGD-specific integrins in the intact MC3T3-E1 cells and soluble glyphosate has been demonstrated to occur through a competition for binding to the RGD-motifs with an estimated value of the K_d of 0.352 mM and of the IC_{50} of 20.6±0.3 mM [6]. In addition, adhesion of the MC3T3-E1 cells to the RGD-modified surface was completely blocked by preincubation with 74.5 mM glyphosate. The somewhat lower integrin antagonist activity of glyphosate in the Epic BT biosensor tests than in the ELISAs can be explained by the fact that the living whole cells contain various integrins in addition to αVβ3, therefore cell adhesion facilitated by integrins other than αVβ3 can take place even when all αVβ3 integrins are fully inhibited. In competitive αVβ3 integrin binding assay in biosensor format the 11 mM glyphosate resulted in inhibition level of about 50%.

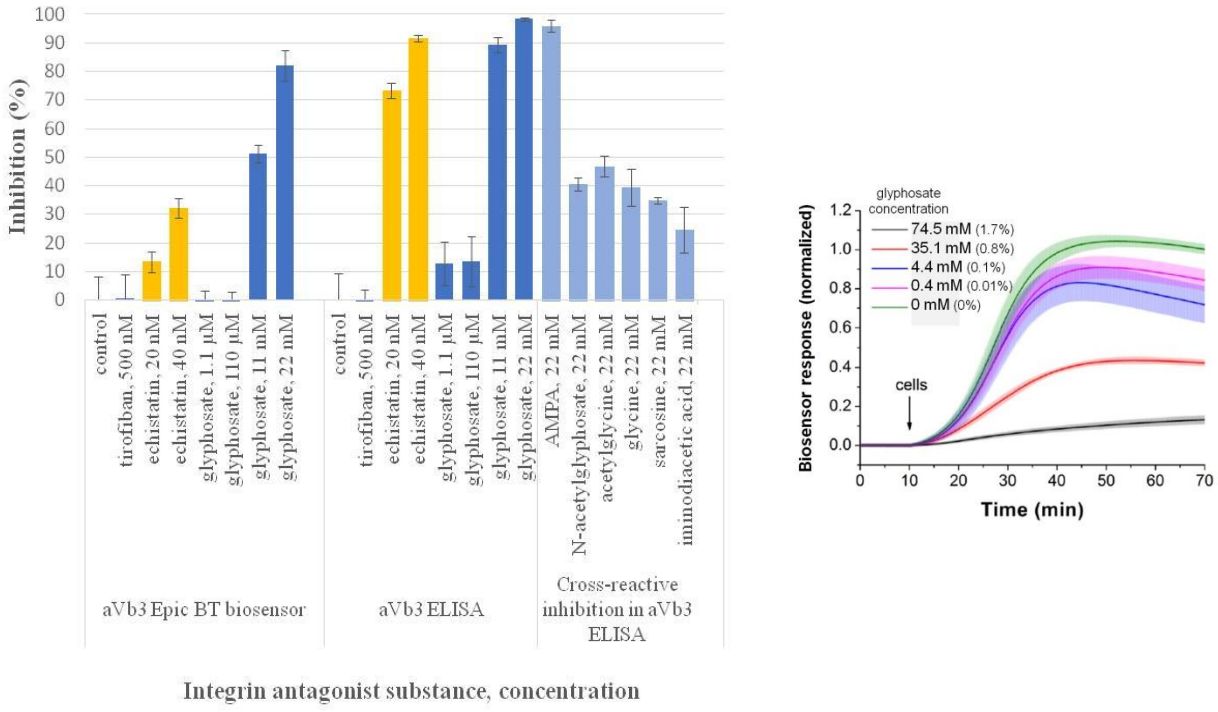

Figure 2. *Left*: Inhibitory potential of glyphosate and its structurally related analogues on αVβ3 integrin determined in a biosensor (Epic BT) and an immunoassay (ELISA) format. *Right*: Inhibition of MC3T3-E1 cell adhesion to an RGD-displaying sensor surface by glyphosate at various concentrations. A monotonous concentration-dependent inhibitory activity of glyphosate on αVβ3 integrin is observed in the concentration range of 0.4–74.5 mM (0.01–1.7%).

Conclusion

Our study has evidenced the inhibitory effect of glyphosate on αVβ3 integrin. It has also been revealed that the main metabolite AMPA, far more persistent than glyphosate itself, exerted inhibition of αVβ3 nearly as potently as glyphosate. This may emerge as a health concern not only from the aspect of environmental relevance but also when human exposure is considered.

Possible health consequences, due to the physiological processes affected by inhibition or inactivation of the functions of αVβ3 integrin may influence our approach towards safety assessment of glyphosate.

Acknowledgements
This research was funded by the Hungarian National Research, Development and Innovation Office (NKFIH) within the Cooperative Doctoral Program for Doctoral Scholarships (KDP-2020) (B.G. and A.Sz.), by the National Competitiveness and Excellence Program (project TKP2021-NVA-22, project KKP 129936) and the TKP2021-EGA-04 Program, by the Hungarian Ministry of Technology and Industry (project KEHOP-3.2.1-15-2021-00037) and by the Hungarian Academy of Sciences (Lendület (Momentum) Program) (R.H.).

References
[1] A. Székács, B. Darvas, Forty years with glyphosate; InTech: Rijeka, Croatia, 2012; pp. 247–284.
[2] A. Székács, B. Darvas, Front. Environ. Sci. 6 (2018) 78.
[3] E. M. Morse, N. N. Brahme, D. A. Calderwood, Biochemistry 53 (2014) 810–820.
[4] T. A. Haas,; E. F. Plow, Curr. Opin. Cell Biol. 6 (1994) 656–662.
[5] C. K. Miranti; J.S. Brugge, Nat. Cell Biol. 4 (2002) E83–E90.
[6] I. Szekacs, E. Farkas, B.L., Gemes, E. Takacs, A. Szekacs, A., Horvath, R., Sci.Rep. 8 (2018) 1701.
[7] M. D. Pierschbacher, E. Ruoslahti, Nature 309 (1984) 30–33.
[8] M. Barczyk, S. Carracedo, D. Gullberg, Cell Tissue Res. 339 (2010) 269–280.
[9] B. Gémes, E. Takács, I. Székács, R. Horvath, A. Székács, Int. J. Molec. Sci. 23 (2022) 12425.
[10] T. G. Kapp, F. Rechenmacher, S. Neubauer, O. V. Maltsev, E. A. Cavalcanti-Adam, R. Zarka, U. Reuning, J. Notni, H. J. Wester, C. Mas-Moruno, J. Spatz, B. Geiger, H. Kessler, Sci. Rep. 7 (2017) 39805.
[11] M. A. Wirth, L. Longwitz, M. Kanwischer, P. Gros, P. Leinweber, T. Werner, Ecotox. Environ. Saf. 225 (2021) 112768.
[12] D. L. Siehl, L. A. Castle, R. Gorton, R. J. Keenan, J. Biol. Chem. 282 (2007) 11446–11455.
[13] N. Orgovan, B. Peter, Sz. Bősze, J. J. Ramsden, B. Szabó, R. Horvath, Sci. Rep. 4 (2014) 4034.
[14] N. Orgovan, B. Kovacs, E. Farkas, B. Szabó, Na. Zaytseva, Y. Fang, R. Horvath, Appl. Phys. Lett. 104 (2014) 083506.
[15] B. Peter, E. Farkas, E. Forgacs, A. Saftics, B. Kovacs, S. Kurunczi, I. Szekacs, A. Csampai, Sz. Bosze, R. Horvath, Sci Rep 7 (2017) 42220.
[16] B. Peter, R. Ungai-Salanki, B. Szabó, A. G. Nagy, I. Szekacs, Sz. Bősze, R. Horvath, ACS Omega 3 (4) (2018) 3882–3891.
[17] M. Sztilkovics, T. Gerecsei, B. Peter, A. Saftics, S. Kuruczi, I. Szekacs, B. Szabo, R. Horvath, Sci. Rep. 10 (2020) 61.

IN VIVO AND *IN VITRO* TESTS FOR THE DETECTION OF BIOCHEMICAL AND ECOTOXICOLOGICAL EFFECTS OF THE HERBICIDE ACTIVE INGREDIENT GLYPHOSATE

Borbála Gémes[1], Szandra Klátyik[1], Marianna Oláh[1], Eszter Takács[1], Csilla Krifaton[2], András Székács[1]

[1]Agro-Environmental Research Centre, Institute of Environmental Sciences, Hungarian University of Agriculture and Life Sciences, H-1022 Budapest, Herman O. út 15, Hungary
[2]Department of Environmental Toxicology, Institute of Aquaculture and Environmental Safety, Hungarian University of Agriculture and Life Sciences, H-2100 Gödöllő, Páter K. u. 1., Hungary
e-mail: klatyik.szandra@uni-mate.hu

Abstract

Aquatic organisms are outstandingly exposed to water contaminants because of their unavoidable contact with xenobiotics, thus their exposure needs to be routinely monitored. Due to its extensive use, the herbicidal agrochemical active ingredient glyphosate realizes massive exposure, its toxic effects alone and in formulations were evaluated in different *in vivo* aquatic ecotoxicological tests on various algae species, freshwater biofilm communities, *Daphnia magna*, and *Danio rerio*, furthermore the possible cytotoxic, genotoxic, and hormone-modulating effects were evaluated *in vitro* on different cell lines and test organisms. Significant differences were detected in the individual and combined toxicity of glyphosate and its co-formulants presented in the formulations, therefore various additives cannot be classified as unequivocally inactive components. The result of the *in vivo* testing proved higher toxicity for the formulating agent and the formulation compared to the individual effect of glyphosate, and significant differences in the sensitivity of test species, and the effects on the sexual development of fish were also observed. The performed *in vitro* assays on cell lines demonstrated the potential cytotoxic and genotoxic effects of glyphosate and its formulations, and some of the effects are the result of the individual toxicity of glyphosate.

Introduction

The main part of pesticide active ingredients (e.g., glyphosate), and their formulations exert an increased load on our environment [1-3]. Plant protection products contain various additives (e.g., formulating agents) in order to enhance the effectivity and bioavailability of the formulation, and these components have long been considered as *inert* ingredients from the aspect of the required main biological effect of the formulation, although co-formulants may have a possible adverse effect on the non-target organisms [4,5]. The occurrence of the market-leading, non-selective herbicide active ingredient and desiccant glyphosate in environmental matrices (e.g. surface water) is globally observed, and these residues may exert harmful effects on non-target organisms, while the biologically active compounds can interact with the abiotic and biotic elements of the ecosystems. Our research group has been working for over a decade now on the evaluation of the ecotoxicity of glyphosate and its formulation. The main purpose of the work has been a systematic evaluation of the ecotoxicity concerns about glyphosate-based formulations carried out directly by testing of the active ingredient and the formulating agent or indirectly by comparing the biological effects of glyphosate and its formulated products. Ecotoxicological evaluation targeted on lethal or sublethal effects e.g., immobilization, algal growth inhibition, phytotoxic, cytotoxic, genotoxic, or hormonal effects tested in *in vitro* assays on cell cultures or in *in vivo* biotests on indicator organisms.

Experimental

The lethal and sublethal effects of glyphosate and its formulations were determined in different standard *in vivo* ecotoxicological standard test methods on various aquatic indicators, as the exposure of aquatic organisms to xenobiotics is unavoidable in surface waters. During our measurements the effects on the immobility of *Daphnia magna*, the growth of various algae species (unicellular floating green algae and cyanobacteria species), moreover the teratogenic effects on *Danio rerio* embryos were also evaluated based on the related OECD guidelines. Furthermore, the effects of glyphosate and its formulation (ROUNDUP CLASSIC) were assessed on the biomass and composition of algal communities in natural freshwater biofilm at the community level as well, completed with a glyphosate degradation test. Before the biofilm testing, freshwater biofilms were grown on glass substrates with the use of a special buoy developed for biofilm colonization under natural conditions in Hungarian river and standing water bodies.

The possible cytotoxic effects of glyphosate were determined *in vitro* by the evaluation of the effects on cell viability, apoptosis, cell cycle, and barrier function. Cytotoxicity of glyphosate IPA salt, its formulations, and POEA was investigated on NE-4C neuroectodermal, MC3T3-E1 preosteoblast, JEG3 placenta choriocarcinoma, and IPEC-J2 porcine intestinal columnar epithelial cell lines. Effects on viability, apoptosis, DNA-damage, caspase 3/7 activity, and cell cycle were determined by MTT (3-(4,5-dimethylthiazol-2-yl)-2,5-diphenyl tetrazolium bromide) assay, Muse Cell Analyzer flow cytometer using Muse Caspase 3/7 and Muse Cell Cycle Assay kits, while cell integrity was visualized by holographic transmission microscopy, while barrier functions of IPEC-J2 cells were determined by transepithelial electrical resistance. Furthermore, the effects of glyphosate on cell adhesion via Arg-Gly-Asp (RGD)-dependent integrins were assessed with the use of label-free optical biosensing and ELISA methods. Genotoxic effects of the components of ROUNDUP CLASSIC were determined by the sensitive Comet assay, a fluorescent method for analysis of DNA damage and DNA repair mechanisms at individual cell level on human HepG2, NE-4C, and MC3T3-E1 cell lines. Moreover, SOS-Chromotests were performed on *E. coli* PQ37 strain. The test measures the primary response of a cell to genetic damage. Briefly it detects *sos* error prone of the *sfiA* gene induced by most genotoxins and it is coupled to a gene that expresses a colorimetric endpoint. Studies also targeted on hormonal modulation and effects on sexual development by the *in vitro* determination of aromatase activity on JEG3 cell lines, while endocrine disrupting effects of the components in ROUNDUP CLASSIC were investigated also *in vivo* on *D. rerio*.

Results and discussion

Based on the results of acute immobilization tests performed on our own laboratory *D. magna* colony and on juveniles ensured by the Daphtoxkit F test kit (MicroBioTests), the order of toxicity for both tested *D. magna* strains and glyphosate-based formulations (ROUNDUP CLASSIC and MEDALLON PREMIUM) was as follows: active ingredient < formulations < formulating agents. In the algal growth inhibition tests, the order of toxicity mostly agreed with the tendency observed for *D. magna* on the basis of the calculated 72h EC_{50} values according to the result of optical density and chlorophyll-a-content measurements. The results of the algal assays indicated significant differences in the sensitivity of different algae species. The photosynthetic activity of *Pseudokirchneriella subcapitata* green algae was significantly decreased after the ROUNDUP CLASSIC exposure but only at the highest investigated concentration (18,9 mg/l POEA and 50,6 mg/l glyphosate), while photochemical efficiency of the PS II photochemical system was not affected by the exposure of glyphosate and POEA alone. During the determination of lethal and sublethal teratogenic effects of glyphosate, its formulations (ROUNDUP CLASSIC, MEDALLON PREMIUM, TOTAL, and GLYPHOS), and

formulating agents (POEA, POE alkyl phosphate ester, sodium-alkyl polyglucoside citrate, and sulfosuccinate) on *D. rerio* embryos, glyphosate was the least toxic and the formulating agent POEA showed the highest toxicity also on embryos. The highest toxicity was observed for ROUNDUP CLASSIC during the testing of the formulations. Below or near the calculated LC_{50} values, deformities, edema (pericardial), inhibition of heartbeat and circulation were the most frequently observed teratogenic malformations in every treatment. Based on the analytical determination of retinoids responsible for the differentiation, development, and embryogenesis of vertebrates, formulating agents used in glyphosate-based herbicides and the active ingredient itself has been indicated to interfere with the formation of retinoids and the retinoid acid pathway [6]. Based on the results of biofilm testing, significant differences were observed in the sensitivity of biofilms grown under different natural conditions. In glyphosate-treated biofilms (100 µg/l glyphosate a.i.), an increase of algal biomass was detected, although in some cases only after an initial decrease, while usually a decrease in the algal biomass was detected in ROUNDUP CLASSIC-exposed biofilms. Individual POEA treatment resulted in the increase of biomass values, however, in samples from Lake Velencei, but only after an initial decrease similar to the effects of glyphosate. The realignment of algal communities was detected in the treated biofilms compared to the control units, while more sensitive species were replaced by more tolerant especially filamentous green algae species, which can utilize the tested substances as a source of nutrients. At the end of the testing period, increased production of *EPS*-matrix (extracellular, mucous exopolymers) was demonstrated in the treated biofilms, especially in the presence of POEA, which can be interpreted in biofilms as an intensified stress response [7]. The result of the trait-based analysis of diatom communities' biological characteristics, significant changes were detected in the cell number ratio and ecological guild categories of the diatom communities in the treated biofilms. Based on our degradation study, the dissipation of glyphosate was highly depended on the form of glyphosate (pure active ingredient or formulated glyphosate), the presence of POEA or biofilms, and the physical/chemical characteristics of surface waters (e.g., pH, the composition of the microbial community) [7].

According to the result of cytotoxicity tests, ROUNDUP CLASSIC significantly decreased the viability of NE-4C cells, while the inhibitory effect of POEA was detected on cellular metabolism. Based on the MTT-assays performed on NE-4C and MC3T3-E1, the order of cytotoxicity was the following: glyphosate IPA salt < ROUNDUP CLASSIC < POEA. The results of the determination of the ratio of total apoptotic cells, a significantly higher level of apoptotic cells was detected for POEA compared to glyphosate IPA and ROUNDUP CLASSIC. The distribution of cells among different phases of the cell proliferation cycle is an informative indicator, whether cell division of the population has been affected upon exposure to the test substances. After 24 hrs, for all test compounds ratio of cells in the beginning DNA replicating (S) phase decreased. After the 48-hr exposition, this decrease was more outstanding, moreover ratio of cells in the growth (G_0/G_1) phase increased compared to the control [8,9]. Moreover, NE-4C cells showed a higher sensitivity for the effects of the tested compounds compared to the MC3T3-E1 cell line, and the order of the inhibitory potency was as follows: glyphosate IPA salt < < ROUNDUP CLASSIC < POEA [10]. Based on the detection of cell toxicity by label-free Epic BenchTop optical biosensor, a higher ratio of apoptotic cells was detected in cells exposed to POEA and ROUNDUP CLASSIC compared to glyphosate-treated cells at equivalent concentrations indicating higher apoptosis-inducing potential of POEA [11]. Cell morphology parameters, determined by holographic microscopy, are useful descriptors of cell viability and ongoing cell-morphological changes including the processes of cell differentiation, cell growth, and cell death. Due to the treatments, a time-dependent decrease in cell area and an increase in the maximum thickness of the NE-4C cells were demonstrated, however, the difference was statistically significant for glyphosate treatment. Average cell area showed an increase in 24

hours in the control due to cell adhesion, while it was rapidly decreasing due to extensive cell death upon the effect of POEA or ROUNDUP CLASSIC, practically equitoxic with each other at concentrations 20-fold below agricultural application [8,9]. Based on the assessment of the cytotoxic effects on human JEG3 placenta choriocarcinoma cell lines, all the tested formulating agents and formulations were comparably cytotoxic well below the agricultural dilution of 1%, while the cytotoxic effect of glyphosate was not demonstrated. During the assessment of the individual and combined effects of glyphosate and POEA on cell barrier functions, the 2-hr exposition of POEA and ROUNDUP CLASSIC increased the paracellular integrity of IPEC-J2 cells [12,13], but were toxic to various cancer cells [14]. Furthermore, the effects of glyphosate on cellular interactions via Arg-Gly-Asp (RGD)-dependent integrins were demonstrated, [15], and total inhibition of αvβ3 binding to RGD was observed for glyphosate and its primary metabolite (AMPA), and on α5β1 binding to RGD for acetylglycine [16].

Potential genotoxic effects of the investigated components were observed on the investigated cell lines based on the results of the performed Comet assays, while the results of SOS-Chromotests indicated no genotoxicity in the concentration range of 0.03–710 nM. The results of the measurements of the endocrine-disrupting effects of glyphosate IPA salt, glyphosate-based herbicides (ROUNDUP CLASSIC, ROUNDUP WEATHERMax, GLYFOS, KAPAZIN, TOTAL, MEDALLON PREMIUM), and co-formulants (POEA, POE alkyl phosphate ester, alkyl polyglucoside, quaternary ammonium compound) on JEG3 cell line demonstrated decreased aromatase activity both by the individual exposure of co-formulants (POEA and alkyl polyglucoside) and the formulations at an 800-fold lower concentration than the agricultural dilutions, while glyphosate exerted an effect only at 1/3 of the agricultural dilution demonstrating, that the endocrine-disrupting effects of the formulations primarily caused by the presence of the formulating agent [17]. During the *in vivo* assessment of the endocrine-disrupting effects of the components in ROUNDUP CLASSIC (glyphosate and POEA) *D. rerio*, hermaphroditic zebrafish were not presented in either treatment group, while the number of females was higher in glyphosate and POEA treatments after the 20-week exposition.

Besides our work on the embryotoxicity of glyphosate, its formulant and formulations on *D. rerio* [6], *in vivo* effects of these substances have been tested on an ecologically relevant earthworm species (*Lumbricus terrestris*) [18,19]. The experiments demonstrated reduced activity of earthworms upon exposure to commercial glyphosate formulations or the pure active ingredients at concentrations of 40–90 ng/g soil.

Conclusion

Co-formulants presented in the various plant protection products have long been considered as inert components, although these substances can exert biological side-effects, in given cases synergistic with those of the active ingredients of these preparations. Surfactants used in veterinary and pesticide formulations enter the environment and create potential exposure to a number of non-target organisms, therefore the toxicological and ecotoxicological evaluation of additives is essential during the environmental risk assessment of pesticide formulations applied in agricultural practice. Our results demonstrated altered toxicity of glyphosate-based formulations compared to the individual effect of glyphosate, and the identified biochemical and (eco)toxicological effects including cytotoxicity (on cell lines of epithelial, neural, and other tissues, as well as tumor cells), endocrine-disrupting effects, as well as aquatic ecotoxicity regarded to the presence of the formulating agents, although glyphosate-specific effects were identified during the measurement of RGD-specific cell adhesion.

Acknowledgements
The research was carried out within the project "Mechanism-related teratogenic hormone modulant and other toxicological effects of veterinary and agricultural surfactants" (OTKA K109865) of the Hungarian Scientific Research Fund. Special thanks are due to external collaborators Drs. Inna Székács, Enikő Farkas and Róbert Horváth at the Nanobiosensorics Laboratory, Institute of Technical Physics and Materials Science, Centre for Energy Research (Budapest, Hungary) for their contribution with biosensorics, to the late Dr. Beatrix Kotlán at the National Institute of Oncology (Budapest, Hungary) for her work on special cancer cell lines, as well as to Prof. Gilles-Eric Seralini and his research group at the University of Caen Normandy (Caen France), and to Prof. Johann M. Zaller and his research group at the University of Natural Resources and Life Sciences (Wien, Austria) for their collaboration.

References
[1] A. Székács, B. Darvas, in: M.N.A.E.-G. Hasaneen (Ed.), Herbicides – Properties, Intech, Rijeka, Croatia, 2012, pp. 247–284.
[2] A. Székács, B. Darvas, Front. Environ. Sci. 6 (2018) 78.
[3] J.E. Casida, Annu. Rev. Pharmacol. Toxicol. 57 (2017) 309–327.
[4] A. Székács, Insights Vet. Sci. 1 (2017) 024–031.
[5] R. Mesnage, C. Benbrook, M.N. Antoniou, Food Chem. Toxicol. 128 (2019) 137–145.
[6] G. Gyurcsó, M. Mörtl, E. Takács, Á. Fejes, L. Simon, B. Darvas, A. Székács, Effects of glyphosate-based herbicides and their components on the embryonal development of zebrafish (*Danio rerio*): Assessment of the role of retinoids. ISAEP, 2017, poster.
[7] Sz. Klátyik, E. Takács, M. Mörtl, A. Földi, Zs. Trábert, É. Ács, B. Darvas, A. Székács, Int. J. Envir. Anal. Chem. 97 (2017) 901–921.
[8] I. Székács, Á. Fejes, Sz. Klátyik, E. Takács, D. Patkó, J. Pomóthy, M. Mörtl, R. Horváth, E. Madarász, B. Darvas, A. Székács, Int. J. Biol. Biomol. Agric. Food Biotech. Engineer. 8 (2014) 219–224.
[9] I. Székács, R. Horvath, A. Székács, in: D.P. Nikolelis, G.-P. Nikoleli (Eds.), Biosensors for security and bioterrorism applications, Springer, Cham, Switzerland, pp. 443–468.
[10] M. Oláh, E. Farkas, I. Székács, R. Horvath, A. Székács, Tox. Rep. 9 (2022) 914–926.
[11] E. Farkas, A. Székács, B. Kovács, M. Oláh, R. Horvath, I. Székács, Hazard. Mat. 351 (2018) 80–89.
[12] E. Paszti-Gere, R.F. Barna, Cs. Kovago, I. Szauder, G. Ujhelyi, Cs. Jakab, N. Meggyesházi, A. Szekacs, Inflammation 38 (2) (2015) 775–783.
[13] E. Pászti-Gere, Á. Jerzsele, P. Balla, G. Ujhelyi, A. Székács, Reinforced epithelial barrier integrity via matriptase induction with sphingosine-1-phosphate did not result in disturbances in physiological redox status. Oxid. Med. Cell. Longev. 2016 (2016) 9674272.
[14] B. Kotlan, G. Liszkay, O. Csuka, J. Tóth, M. Oláh, M. Kasler, A. Székács, J. Immunother. Cancer 5 (2017) 82.
[15] I. Székács, E. Farkas, B.L. Gémes, E. Takács, A. Székács, R. Horvath, Sci. Rep. 8 (2018) 17401.
[16] B. Gémes, E. Takács, I. Székács, R. Horvath, A. Székács, Int. J. Mol. Sci. 23 (2022) 12425.
[17] N. Defarge, E. Takács, V.L. Lozano, R. Mesnage, J.S. de Vendômois, G.-E. Séralini, A. Székács, Int. J Environ. Res. Pub. Health 13 (2016) 264.
[18] M. Maderthaner, M. Weber, E. Takács, M. Mörtl, F. Leisch, J. Römbke, P. Querner, R. Walcher, E. Gruber, A. Székács, J. Zaller, Environ. Sci. Poll. Res, 27 (14) (2020) 17280–17289.
[19] J. Zaller, M. Weber, M. Maderthaner, E. Gruber, E. Takács, M. Mörtl, Sz. Klátyik, J. Györi, J. Römbke, F. Leisch, B. Spangl, A. Székács, Environ. Sci. Eur. 33 (2021) 51.

THE ACCIPITRIDS OF SERBIA: GLOBAL THREATS AND CONSERVATION STATUS AT EUROPEAN AND NATIONAL LEVELS

Milan Glišić, Katarina Kovanović, Nemanja Stošić, Suzana Knežević

Unite for Agricultural and Business Studies and Tourism, Academy of Applied Studies Šabac, Vojvode Putnika 56, 15000 Šabac, Serbia
e-mail: milanglisic88@gmail.com

Abstract

Twenty-six species of hawks, eagles, and vultures (family Accipitridae) are present or occasionally inhabit Serbia, although the presence of some species has not been proven with certainty. The aim of this research was to determine the threats to these species at the global level, as well as their conservation status at the European and national levels.

Globally, according to the IUCN, these birds are affected by a range of threats. Nevertheless, the most prominent threat, affecting as many as 23 of the 26 representatives of the Accipitridae family living in the territory of Serbia, is hunting. Also, renewable energy sources represent a significant cause of the population decrease of these birds, considering that 19 of them are threatened by the construction and operation of wind farms. Other threats that stand out in terms of the number of species they affect are pollution from agriculture and forestry, arable land (annual and perennial crops), tree plantations, etc.

According to the IUCN categorization at the European level, the highest number of accipitrids living in the territory of Serbia (22 out of 26) belongs to the category "least concern" (LC), while the bearded vulture (*Gypaetus barbatus*) is classified as "near threatened" (NT). Three species are considered endangered at the European level, namely the greater spotted eagle (*Aquila clanga*) and the Egyptian vulture (*Neophron percnopterus*), which are classified as "vulnerable species" (VU), while the steppe eagle (*Aquila nipalensis*) is designated as "critically endangered species" (CR) on the territory of Europe. However, there is only one unreliable finding for the steppe eagle in Serbia, so this part of Europe probably does not represent part of the natural range of this bird.

Of the 26 species of hawks, eagles, and vultures recorded in Serbia, 21 are listed in the Annex I of the Birds Directive, while only five are not on this list, namely: the northern goshawk (*Accipiter gentilis*), the Eurasian sparrowhawk (*Accipiter nisus*), the steppe eagle, the common buzzard (*Buteo buteo*), and the rough-legged buzzard (*Buteo lagopus*). Unlike the other listed species, which are not included in the Annex I because of small concern for their survival, the absence of the steppe eagle on this list can be explained by the fact that its natural range mainly covers the Asian continent, not the European continent. Regarding the Berne Convention, 25 species are included in the Annex I, while only one species is included in the Annex II, namely the steppe eagle. According to the European Birds of Conservation Concern, most bird species belong to one of the so-called SPEC categories. The European population status for eight species is currently considered secure.

The only species that is not protected by the Serbian national legislation is the steppe eagle because Serbia is generally not considered as part of its natural range. Other species are protected at the national level and listed as "strictly protected", while the only species listed as "protected" is the northern goshawk.

THE REPTILES OF SERBIA: GLOBAL THREATS AND CONSERVATION STATUS AT EUROPEAN AND NATIONAL LEVELS

Milan Glišić, Milena Kovanović, Ljiljana Tanasić, Biljana Delić Vujanović

Unite for Agricultural and Business Studies and Tourism, Academy of Applied Studies Šabac, Vojvode Putnika 56, 15000 Šabac, Serbia
e-mail: milanglisic88@gmail.com

Abstract

The reptile fauna of Serbia consists of about 26 species (including introduced ones): 4 species of turtles, 10 species of snakes, and 12 species of lizards. The aim of this research was to determine the threats to these species at the global level, as well as their conservation status at the European and national levels.

Agriculture represents the biggest threat to the reptiles of Serbia at the global level. It is estimated that 19 out of 26 species are threatened by annual and perennial crops worldwide. Also, housing and urban areas represent a significant cause of the population decrease of these animals, considering that 13 species are threatened by this factor. Other threats that stand out in terms of the number of species they influence are hunting and gathering, road and rail traffic, tourism and recreational areas, etc.

According to the IUCN categorization at the European level, the highest number of reptiles living in the territory of Serbia (20 out of 26) belongs to the category “least concern” (LC). Four species are in the category of "near threatened" taxa (NT), namely: the European pond turtle (*Emys orbicularis*), the Hermann’s tortoise (*Testudo hermanni*), the four-lined snake (*Elaphe quatuorlineata*), and the meadow lizard (*Darevskia praticola*), while the Greek tortoise (*Testudo graeca*) and the Ursini's viper (*Vipera ursinii*) are considered “vulnerable” (VU) in Europe.

Of the 26 species of reptiles recorded in Serbia, 20 are listed in the Annex II and/or IV of the Habitats Directive, while only six are not on this list, namely: the red-eared slider (*Trachemys scripta elegans*), the grass snake (*Natrix natrix*), the common European adder (*Vipera berus*), the slow worm (*Anguis fragilis*), the meadow lizard, and the viviparous lizard (*Zootoca vivipara*). Regarding the Berne Convention, 15 species are listed in the Annex I, while five are listed in the Annex III. Six species are not covered by this directive, namely: red-eared slider, the Caspian whipsnake (*Dolichophis caspius*), the sand lizard (*Lacerta agilis*), the Balkan green lizard (*Lacerta trilineata*), the European green lizard (*Lacerta viridis*) and the common wall lizard (*Podarcis muralis*). The only species not covered by either of the two directives is the red-eared turtle, which is expected considering it is a non-native species.

Only six reptile species are not protected by the Serbian national legislation, namely: the red-eared slider, the slow worm, the sand lizard, the Balkan green lizard, the European green lizard, and the common wall lizard. Two species are listed in the Annex II (protected wild species), while as many as 18 species are listed in the Annex I, which means that they are strictly protected in Serbia.

THE EFFECT OF ULTRASONIC TREATMENT AND THE ETHANOL ON THE EXTRACTION OF POLYPHENOL CONTENT OF APPLE POMACE

Faraja Gonelimali[1,2], Beatrix Szabó-Nótin[1], Mónika Máté[1]

[1]Department of Fruit and Vegetable Processing Technology, Institute of Food Science and Technology, Hungarian University of Agriculture and Life Sciences, H-1118, Budapest, Villányi street 29-43, Hungary
[2]Department of Food Science and Technology, College of Agricultural Sciences and Food Technology, University of Dar es Salaam, 16103, Dar es Salaam, Tanzania.
e-mail: fgonelimali@gmail.com

Abstract
Agro-industrial waste poses a significant effect on environmental pollution due to the challenges of waste management. Meanwhile, agro-industrial wastes are rich in bioactive compounds, particularly polyphenols that can be useful in the food, cosmetics and medicine industries. This study investigates the extraction of polyphenols from the industrial apple pomace of the variety Idared for potential use as natural food additives for the development of functional foods. Polyphenols from the dried apple pomace were extracted by the ultrasound-assisted extraction method using food-grade solvents ethanol and water. The amount of polyphenols extracted (Total phenolic content) was quantified by Folin-Ciocalteu's method. Antioxidant activity was quantified by the Ferric reducing ability of plasma (FRAP) method. Sonicating the pomace at 20 kHz for 10 and 35 minutes resulted in the extracts with extraction recovery of 27 – 33 % for all solvents. Total phenolic content (TPC) was found to be 647 – 1430 µg GAE mL^{-1} while antioxidant activity (FRAP) was found to be 436 – 842 µg AAE mL^{-1}. Results suggest that waste products (pomace) from the industrial processing of apples (variety Idared) are valuable resources for extracting useful polyphenols that can be used for functional foods development.

Keywords: Agro-industrial waste, Apple pomace, Polyphenol, TPC, Antioxidant, Functional foods

Introduction
Processing of agricultural produce results in the production of an enormous amount of waste products most of which are discarded into the environment. Apart from contributing to environmental pollution, discarding this waste into the environment results in the loss of valuable bioactive compounds that can be used in other sectors including food, cosmetics and pharmaceuticals. It has been known that there is great potential in utilizing waste from agroindustrial products for various uses such as energy production, chemicals and food additives. Recently concepts such as zero waste production in agroindustrial processing factories are being introduced where a majority of the waste products are being turned into other products [1], [2]. One of the important agroindustrial wastes that can be turned into other products is apple pomace.

Solid waste products from the industrial processing of apples to produce juice commonly referred to as apple pomace are important agroindustrial wastes that are rich in fiber, pectin and polyphenols. A small amount of this waste is being used for animal feed, energy production and as a pectin source [3], [4]. A huge amount of the pomace is still disposed into the environment despite the fact that they are rich in bioactive compounds. Research shows that

these pomaces can be used to develop natural food additives such as antioxidants, antimicrobials and food packages [5], [6]. Moreover, they are good candidates for developing functional foods such as bakery products enhanced with dietary fibers as well as health foods enriched with polyphenols for antioxidant enhancement [7], [8]. This study, therefore, focuses on investigating the potential of obtaining polyphenols from the industrial apple pomace of the Idared variety, using food-grade solvents (ethanol and water) for the development of functional foods rich in antioxidants.

Experimental

The apple pomaces were obtained from an apple juice processing company in Hungary. The pomaces were from the apples cultivated in 2020/2021 grown in Hungary and immediately frozen at -20°C after pressing to obtain the juice.

Prior to drying, the pomace were thawed overnight and drying was done using the atmospheric oven at 60°C for 3 hours followed by a vacuum drying oven at 60°, 65 mbar to reach a final moisture content of about 3 - 4%. The dried pomace was ground to make a final powder using a multi-chopper coffee grinder followed by packaging in sealed polythene bags and stored in a dry condition awaiting the extraction.

Extraction was done by ultrasound-assisted extraction method according to [9] with minor modifications. 10 g of the dried apple pomace powder was mixed with 200 mL of the solvent (Water or ethanol) in flasks. The flasks were then sonicated at 20 kHz, power 240 watts at room temperature for 10 and 35 minutes in an ultrasonic water bath. The temperature of water in a sonicating bath was maintained by periodically replacing it with cold water. The pomaces were allowed to stay in contact with the solvent overnight followed by centrifugation at 4500 RPM, followed by filtration using filter paper No. 1 under vacuum. The filtrate was then rotary evaporated to reduce the solvent to about 30% followed by further drying in the atmospheric oven at 60°C for complete drying. The obtained residues were quantified to obtain extraction recovery followed by redissolving in water to make a final concentration of 400 mg/mL.

Total phenolic content (TPC) was analyzed by means of the Folin-Ciocalteu‘s method according to [10] where Gallic acid was used for the calibration curve and the results were expressed as microgram Gallic acid equivalent per milliliter (µg GAE mL^{-1}). The antioxidant activity was quantified by the means of Ferric reducing ability of plasma (FRAP) according to [11] where Ascorbic acid was used for the preparation of the calibration curve and the results were expressed as microgram Ascorbic acid equivalent per milliliter (µg AAE mL^{-1}).

Results and discussion

Solvent type (Ethanol or water) didn’t affect the extraction recovery of the extracts from the pomace where there was no significant difference in the amount of the crude extracts obtained between the two solvents. The recovery of the extracts from the dried pomace ranged from 27% to 33% of the dried pomace for both ethanolic and aqueous extracts (Figure 1). Smaller ranges were seen from other studies where extraction recovery using methanol as extraction solvent was between 8% - 15% in different varieties of the apple pomace [12].

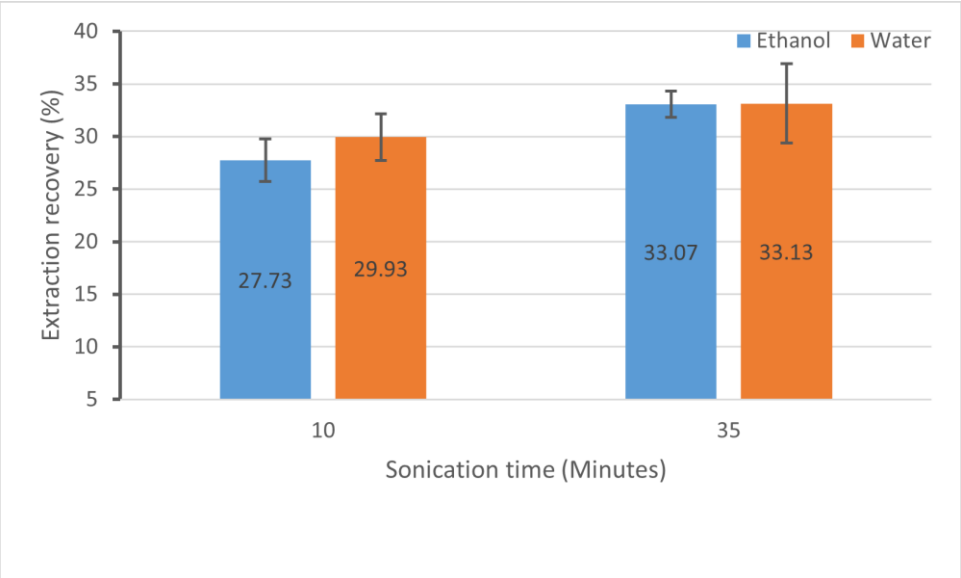

Figure 1. Influence of ethanol and water on extraction recovery of the crude extracts from apple pomace

Solvent type significantly affected the amount of polyphenol phenols extracted from the apple pomace where ethanol resulted in extracts with higher amounts of TPC compared to water. The amount of TPC was approximately 650 µg GAE mL^{-1} for aqueous extracts and 1400 µg GAE mL^{-1} for ethanolic extracts and there was no effect in the TPC when the sonication was done for both 10 and 35 minutes (Figure 2). Similar results were reported by L. Wang et al., 2018 where ethanol displayed higher TPC content compared to water. Differing observations were observed in the study of Silva et al., 2020 where there were no significant differences in TPC when ethanol and water were used as extraction solvents by ultrasound-assisted extraction.

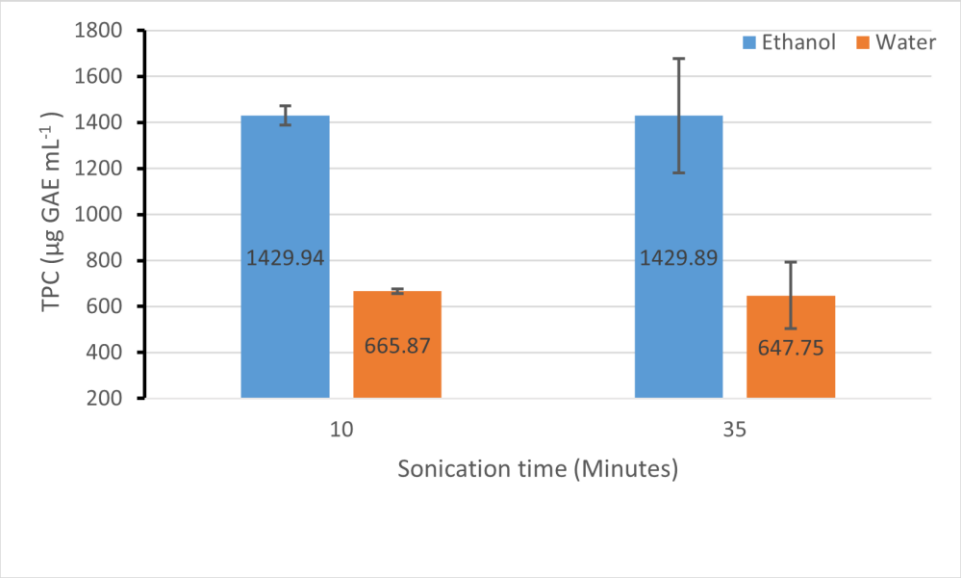

Figure 2. Effect of ethanol and water on TPC of the apple pomace extracts

There was a hugely significant difference in the antioxidant activity of the apple pomace extracts after sonicating for 10 minutes where ethanolic extracts displayed FRAP value of 842 µg AAE/ mL while aqueous extracts displayed 435µg AAE mL^{-1} . Contrarily, there was no significant difference between ethanolic and aqueous extracts when the sonication was done for

35 minutes. Opposite to our study, the study of Gharedaghi et al., 2020 found that water results in extracts with higher antioxidant capacity than ethanol when a conventional extraction method is used.

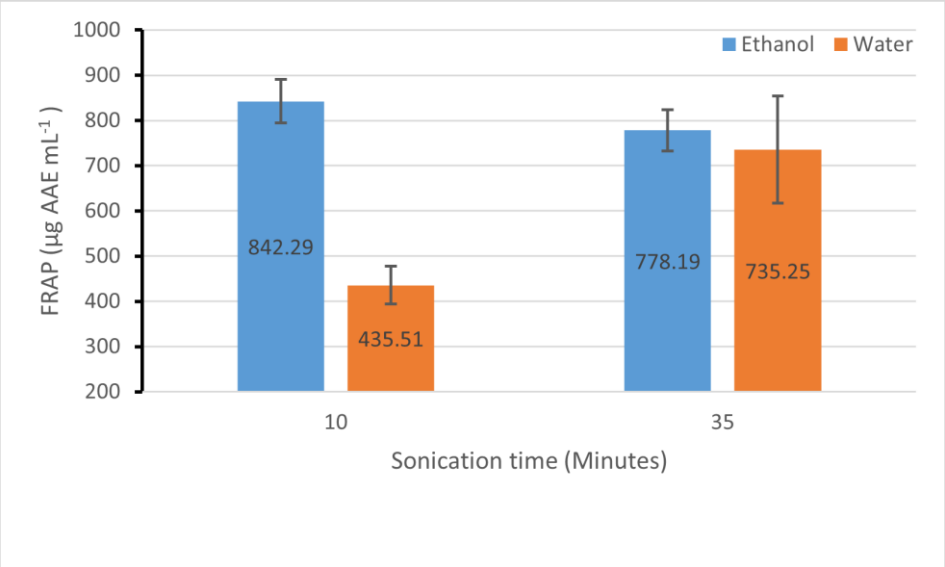

Figure 3. Effect of ethanol and water on antioxidant of the apple pomace extracts.

Conclusion

Agro-industrial wastes are known to have an enormous amount of bioactive compounds mostly, polyphenols that are known to be potentially useful in various sectors such as food and pharmaceuticals. Apple pomace from the industrial processing of the apples into juice contains a huge amount of polyphenols that can be exploited for other uses instead of disposing them into the environment. From this study, it has been seen that ethanol results in higher polyphenols and to some extent antioxidant activity than water. It is recommended that apple pomace, a cheap and reliable resource can be useful in obtaining polyphenols that can be used for the development of functional foods rich in antioxidants using food-grade solvents ethanol and water.

Acknowledgments

The authors acknowledge the support of the Doctoral School of Food Science of the Hungarian University of Agriculture and Life Sciences.

References

[1] J. L. Vukušić *et al.*, "Reshaping Apple Juice Production Into a Zero Discharge Biorefinery Process," *Waste Biomass Valorization*, vol. 12, no. 7, pp. 3617–3627, Jul. 2021, doi: 10.1007/s12649-020-01245-5.

[2] A. M. C. Heureux, T. K. Matsumoto, and L. M. Keith, "Toward a zero-waste model: Potential for microorganism growth on agricultural waste products in Hawaii," *Algal Res*, vol. 62, no. May 2021, p. 102640, Mar. 2022, doi: 10.1016/j.algal.2022.102640.

[3] A. D. Alarcon-Rojo, V. Lucero, L. Carrillo-Lopez, and H. Janacua, "Use of apple pomace in animal feed as an antioxidant of meat," *South African Journal of Animal Sciences*, vol. 49, no. 1, pp. 131–139, 2019.

[4] J. M. Costa, L. C. Ampese, H. D. D. Ziero, W. G. Sganzerla, and T. Forster-Carneiro, "Apple pomace biorefinery: Integrated approaches for the production of bioenergy, biochemicals, and

value-added products – An updated review," *J Environ Chem Eng*, vol. 10, no. 5, p. 108358, Oct. 2022, doi: 10.1016/J.JECE.2022.108358.

[5] A. Riaz *et al.*, "Preparation and characterization of chitosan-based antimicrobial active food packaging film incorporated with apple peel polyphenols," *Int J Biol Macromol*, vol. 114, pp. 547–555, 2018.

[6] T. Zhang, X. Wei, Z. Miao, H. Hassan, Y. Song, and M. Fan, "Screening for antioxidant and antibacterial activities of phenolics from Golden Delicious apple pomace," *Chem Cent J*, vol. 10, no. 1, pp. 1–9, 2016, doi: 10.1186/s13065-016-0195-7.

[7] J. Jung, G. Cavender, and Y. Zhao, "Impingement drying for preparing dried apple pomace flour and its fortification in bakery and meat products," *J Food Sci Technol*, vol. 52, no. 9, pp. 5568–5578, Sep. 2015, doi: 10.1007/s13197-014-1680-4.

[8] X. Wang, E. Kristo, and G. LaPointe, "Adding apple pomace as a functional ingredient in stirred-type yogurt and yogurt drinks," *Food Hydrocoll*, vol. 100, p. 105453, Mar. 2020, doi: 10.1016/j.foodhyd.2019.105453.

[9] M. N. Safdar, T. Kausar, S. Jabbar, A. Mumtaz, K. Ahad, and A. A. Saddozai, "Extraction and quantification of polyphenols from kinnow (Citrus reticulate L.) peel using ultrasound and maceration techniques," *J Food Drug Anal*, vol. 25, no. 3, pp. 488–500, Jul. 2017, doi: 10.1016/j.jfda.2016.07.010.

[10] V. L. Singleton and J. A. Rossi, "Colorimetry of Total Phenolics with Phosphomolybdic-Phosphotungstic Acid Reagents," *Am J Enol Vitic*, vol. 16, no. 3, pp. 144–158, Jan. 1965, [Online]. Available: http://www.ajevonline.org/content/16/3/144.abstract

[11] I. F. F. Benzie and J. J. Strain, "The Ferric Reducing Ability of Plasma (FRAP) as a Measure of 'Antioxidant Power': The FRAP Assay," *Anal Biochem*, vol. 239, no. 1, pp. 70–76, Jul. 1996, doi: 10.1006/ABIO.1996.0292.

[12] G. Ćetković, J. Čanadanović-Brunet, S. Djilas, S. Savatović, A. Mandić, and V. Tumbas, "Assessment of polyphenolic content and in vitro antiradical characteristics of apple pomace," *Food Chem*, vol. 109, no. 2, pp. 340–347, Jul. 2008, doi: 10.1016/j.foodchem.2007.12.046.

[13] L. Wang, N. Boussetta, N. Lebovka, and E. Vorobiev, "Effects of ultrasound treatment and concentration of ethanol on selectivity of phenolic extraction from apple pomace," *Int J Food Sci Technol*, vol. 53, no. 9, pp. 2104–2109, Sep. 2018, doi: 10.1111/ijfs.13835.

[14] L. C. da Silva *et al.*, "Simultaneous extraction and separation of bioactive compounds from apple pomace using pressurized liquids coupled on-line with solid-phase extraction," *Food Chem*, vol. 318, no. February, p. 126450, Jul. 2020, doi: 10.1016/j.foodchem.2020.126450.

[15] J. Gharedaghi, J. Aliakbarlu, and H. Tajik, "Antioxidant potential of apple pomace extract and its efficacy in alginate coating on chemical stability of rainbow trout fillet," *Journal of Food Measurement and Characterization*, vol. 14, no. 1, pp. 135–141, Feb. 2020, doi: 10.1007/s11694-019-00275-5.

BIODEGRADATION OF THE FUEL OXYGENATE METHYL TERT-BUTYL ETHER IN A FLUIDIZED BED BIOREACTOR

Laura Haranghy[1], Balázs Fehér[1], Katalin Perei[2], Péter Bernula[1]

[1]Department of Applied Microbiology, Bay Zoltán Nonprofit Ltd. for Applied Research, H-6726 Szeged, Derkovits fasor 2.
[2]Department of Biotechnology, University of Szeged, H-6727 Szeged, Közép fasor 52.
e-mail: haranghylaura@gmail.com

Abstract
Industrialization, increasing motorization and rapid urbanization have led to extensive soil and groundwater contamination. The main pollutants are fuel hydrocarbons and various gasoline additives. Microbial bioremediation is a cost-effective and sustainable way to promote the remediation of affected sites.
Our experiments focused on testing key parameters of a universal and promising biological treatment technology, using a lab-scale fluidized bed bioreactor and a previously isolated bacterial consortium. The aim of our work was to test our setup and provide data for the technological design and optimization of field-scale bioreactors.

Introduction
Gasoline additives such as ether oxygenates and their tertiary alcohol metabolites are common groundwater contaminants, mainly due to leaks from storage tanks. Compared to other components of gasoline, ether oxygenates, like methyl *tert*-butyl ether (MTBE), are well-soluble in groundwater and able to form an extensive contaminant plume [1].
Bioremediation is an effective and affordable way of environmental remediation. Studies have focused on the investigation of aerobic and even anaerobic biodegradation of MTBE. Many individual isolates and bacterial consortia are able to grow using ether oxygenates as a sole carbon and energy source. In some cases, natural attenuation was observed, however, with stimulation and optimized conditions enhanced biodegradation is achievable[2].
Fluidized bed bioreactor is an *ex situ* bioremediation technology that can provide the necessary nutrients and optimal growth conditions (pH, temperature, dissolved oxygen) for microbes. As a consequence of fluidization, the specific surface area is increased, enhancing bioconversion efficiency by giving an opportunity for the formation of high biomass concentration and promoting retainment. This type of reactor design is capable of treating large volumetric flow rates, as well [3].

Experimental
The total volume of our lab-scale fluidized bed bioreactor is approximately 13 L. As an affordable biomass carrier, we used sterilized, fractionated medium sand with a diameter of 1-2 mm.
In advance of the initiation, the bioreactor was sterilized with sodium-hypochlorite solution and washed several times with softened water. The volatilization of MTBE has been monitored for several days with analytical measurements (HS-GC-MS).
The reactor was inoculated with a previously grown consortium culture maintained in minimal media containing MTBE as a sole carbon source.
Influent water was delivered to the bioreactor by a peristaltic pump. To ensure the needed recirculation flow for fluidization we used a membrane pump in order to reduce shear force and

avoid the heating effect of centrifugal pumps.
We previously tested the optimal temperature for the chosen consortium at 18 °C, 20 °C, 22 °C, 23 °C 24 °C, 26 °C, 28 °C, and 30 °C, respectively. We also investigated the optimal nutrient composition for the consortium, focusing on nitrogen and phosphate supplementation, respectively.
Firstly, we were testing the effect of increasing MTBE concentration in contaminated water, while influent flow was set to a middle-low level and was unchanged during the experiment.
Our next approach was using fixed MTBE concentration in contaminated water, which was typical of an averagely polluted field. Inflow of contaminated water with unchanged MTBE concentration was raised gradually in order to find out the maximum efficiency of our experimental setup. The upper limit for MTBE concentration in effluent-treated water was 0,4 mg/l.

Results and discussion

Based on our results, the optimal temperature range for growth and efficient MTBE biodegradation is 24-27 °C. The results of preliminary experiments indicate that ten times decreased nitrogen and phosphate supplementation compared to basic minimal media was perfect for efficient workflow.
Within days after the inoculation of the bioreactor, MTBE concentration decreased by 80% compared to the starting point, thus we were able to start the continuous phase (starting the intake of contaminated water and release of treated water). MTBE concentration was monitored daily in the influent and in effluent water, respectively.
During the continuous phase, we applied necessary modifications to eliminate and prevent technical issues, for instance redesigning the aeration in order to increase its efficiency and using different types of pumps to find out, which one is the best choice.
As a result of increasing the intake gradually, we observed stable MTBE removal efficiency of 98% at a loading rate of up to 175 L/day. This achievement was much better than we expected, additionally, based on our results, there are more opportunities to improve efficiency in the near future. We are also planning to develop our bioreactor setup, making it more robust and being able to work automatically.

Conclusion

Our prototype was developed to optimize the fundamental conditions for an MTBE-degrading bacterial consortium. Our results verified that the prototype is far suitable for maintaining the optimal conditions for several microorganisms, furthermore, gives the possibility to grow a large amount of biofilm on the surface area of fluidized carrier particles in order to enhance biodegradation.
Additionally, this setup is useful for testing newly isolated microbes and microbial communities even for other types of biodegradation methods or optimizing operational parameters of a fieldscale bioreactor. The main advantage of our lab-scale bioreactor is that it gives us the possibility to model and test all of the parameters which are needed for designing and developing full-scale bioreactors, which are universally usable, efficient, and economical solutions for bioremediation of even large volumes of contaminated groundwater.

Acknowledgements
The experiment is supported by the ÚNKP-22-2-SZTE-355 (L. Haranghy) New National Excellence Program of the Ministry for Culture and Innovation from the source of the National Research, Development and Innovation fund.

References
[1] M. Hyman, in: Rojo, F. (Ed.), Aerobic Utilization of Hydrocarbons, Oils, and Lipids, Springer Cham, (2019), 389-419.
[2] B.C. Okeke, W.T. Frankenberger Jr., Microbiol. Res., (2003), 158, 99–106.
[3] B. Özkaya, A.H. Kaksonen, E. Sahinkaya, J.A. Puhakka, Water Res., (2019), 150, 452-465.

THE EFFECT OF CHILLED AND FROZEN STORAGE ON SOUS VIDE TREATED PORK CHOPS

Endrit Hasani[1,2], Meltem Boylu[1], István Dalmadi[1], György Kenesei[1]

[1]Department of Livestock Products and Food Preservation Technology, Institute of Food Science and Technology, Hungarian University of Agriculture and Life Sciences, Ménesi út 43-45, 1118 Budapest, Hungary
[2]Department of Food Technology and Biotechnology, Faculty of Agriculture and Veterinary, University of Prishtina
e-mail: endrithasani96@gmail.com

Abstract

Sous vide is a minimal processing technology used to cook meat at strictly monitored time and temperature under vacuum packaged conditions. The quality of sous vide treated meat during storage differs depending on temperature conditions. In the present study, we analysed the effect of chilled storage at 4 °C for two weeks and frozen storage at -20 °C for four weeks on weight loss, pH, hardness, lipid oxidation and color attributes (lightness, redness and yellowness) of sous vide treated pork chops. Weight loss, pH and TBARS values (lipid oxidation) of sous vide treated pork chops were increased during the chilled storage at 4 °C for 14 days. On the other hand, redness values of sous vide treated pork chops were decreased during chilled storage. Frozen storage increased weight loss, TBARS, lightness and yellowness values of cooked pork chops. In contrast, frozen storage (-20°C) had a significant effect on decreasing hardness values of sous vide treated pork chops.

STUDY OF THE METALLOGRAPHIC STRUCTURE OF TWO TITANIUM ALLOYS FOR BIOMEDICAL PROSTHESES

Héctor Guerra-Yánez[1], Santiago José Brito-García[1], Ionelia Voiculescu[2], Julia Claudia Mirza-Rosca[1]

[1]Mechanical Engineering Department, University of Las Palmas de Gran Canaria, Campus Universitario de Tafira, 35017 Las Palmas de Gran Canaria, Spain
[2]Faculty of Industrial Engineering and Robotics, Politehnica University of Bucharest, 313 Splaiul Independentei, 060042 Bucharest, Romania
e-mail: hector.guerra106@alu.ulpgc.es

Abstract

The present study has the objective of defining the metallographic structure of two titanium alloys in order to find if they can be used in medical prostheses. The composition of the alloys is: Ti4Fe (93.2% Ti, 4% Fe, 2% Al, 0,8 V) and Ti10Al (89.5% Ti, 0.5% V, 10% Al).
For the purpose of obtaining the metallographic structure, it was necessary to use an optic ZESS microscope Axio Vert A1. The materials were initially cut into samples of small volume and covered in epoxy resin in such a way as to leave a controlled surface exposed to the environment [1]. Afterwards the samples were polished and grinded with a Struers polishing machine, SiC papers and an alpha-alumina suspension of 0.1 μm [2]. When this process was finished, the samples were cleaned for preventing possible contaminations that could affect the results. The alloys were then submerged in Kroll reactive for five seconds in order to expose their metallographic structure by acid attack. Shorter immersion times were not sufficient to observe the structure satisfactorily, and longer times caused regions of the alloys to burn.

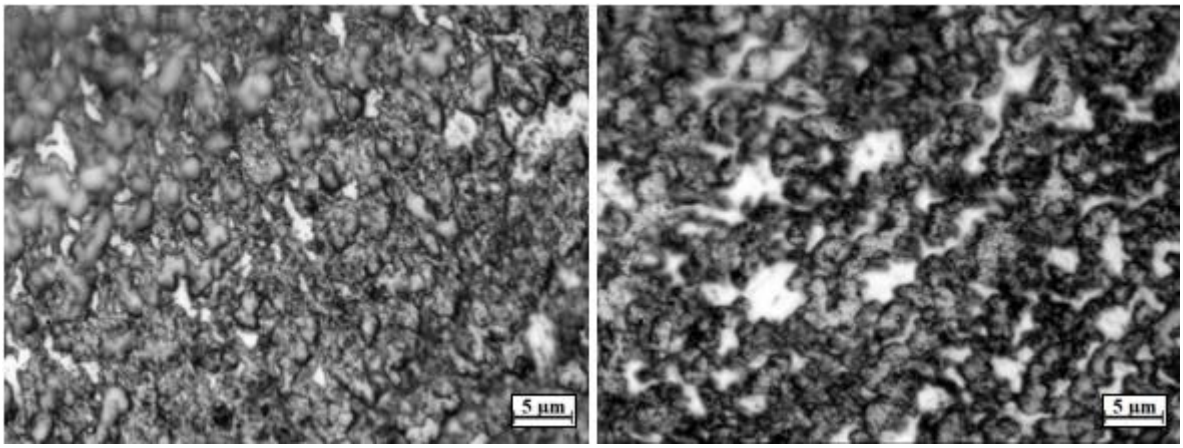

a) b)

Figure 1. Metallographic structure of alloys Ti4Fe (a) and Ti10Al (b) observed with 100x magnifications.

The presence of the allotropic forms of α-titanium and β-titanium can be seen in the two images obtained [3], although it is not possible to distinguish which of the regions corresponds to which. If one wanted to obtain this information, it would be necessary to use other tests [4,5].
It can be seen that in the Ti10Al alloy there is a greater presence of burnt regions by the acid attack of the Kroll reactive, although not enough so that the structure cannot be appreciated.

Acknowledgements

The research was sponsored by Gran Canaria Cabildo, project number CABINFR2019-07. The authors gratefully acknowledge the support received from the Romanian National Authority for Scientific Research, CNDI–UEFISCDI, through the project number PN-III-P2-2.1-PED-2019-3953, contract 514PED / 2020 „New ceramic layer composite material processed by laser techniques for corrosion and high temperature applications – LASCERHEA“, Romania.

References

[1] M. López Ríos, P.P. Socorro Perdomo, I. Voiculescu, V. Geanta, V. Crăciun, I. Boerasu, J.C. Mirza Rosca, Scientific Reports 2020 10:1 10 (2020) 1–11.

[2] P.P. Socorro-Perdomo, N.R. Florido-Suárez, I. Voiculescu, J.C. Mirza-Rosca, Metals 2021, Vol. 11, Page 928 11 (2021) 928.

[3] D.W. Hetzner, W. van Geertruyden, Mater Charact 59 (2008) 825–841.

[4] H.L. Du, P.K. Datta, D.B. Lewis, J.S. Burnell-Gray, Oxidation of Metals 45 (1996) 507–527.

[5] W. Xie, X. Wang, E. Liu, J. Wang, X. Tang, G. Li, J. Zhang, L. Yang, Y. Chai, B. Zhao, International Journal of Advanced Manufacturing Technology 119 (2022) 4745–4755.

SYNTHESIS OF RED-EMITTING FLUOROPHORES

Tamás Hlogyik[1], Erzsébet Mernyák[1]

[1]Department of Organic Chemistry, University of Szeged, H-6720 Szeged, Dóm tér 8, Hungary
e-mail: hlogyik@chem.u-szeged.hu

Abstract
Understanding the mechanism of action of biologically active compounds is of great interest in medicine, including cancer research. Chemical labeling of molecules, i.e. making them "visible" under the right conditions, is a widespread and intensively researched field of science. The fluorescent labeling of compounds offers several advantages over other methods. It might be considered as an environmentally friendly alternative to radioisotope labeling. It is highly important that fluorophores used in biomedical applications meet certain criteria, including high photostability, good cell permeability and stability under physiological conditions. However, the accessibility of the fluorophores is often limited owing to their high price and complex synthetic strategies. Here we synthesized *aza*-BODIPY fluorophores, which are red-emitting altervatives to BODIPY derivatives. The syntheses were carried out considering the principles of green chemistry. One-pot and/or microwave-assisted syntheses were performed in order to minimize the number of reaction steps and time and use of solvents.

Introduction
The labeling of biologically active compounds is necessary in biomedical applications, however it proposes several problems [1]. Radioisotope labeling in radiotherapy requires extreme caution because of its potential risks to the living organism and the environment from inappropriate dosing, and the potential for radioisotopes to be released into the atmosphere through improper handling. Activities involving radiation exposure are subject to strict safety regulations [2].
Today, intensive research is being carried out to develop techniques that could replace radioisotope tracer-based methods. One such promising technique is the use of fluorescent dyes. This imaging technique makes visible the biological processes involved in early carcinogenesis and may therefore allow the detection of small tumours at an early stage. Fluorescence imaging is based on the visualisation of fluorophores excited by light of a specific wavelength depending on the excitation spectra. The light is then re-emitted at lower energy but at longer wavelengths. The depth of penetration depends on the wavelengths tested, ranging from a few hundred micrometres to a few millimetres [3].
The extremely high cost of fluorescent dyes is encouraging researchers to develop more efficient processes for synthesizing these materials. BODIPY-based (4,4-difluoro-4-boro-3a,4a-diaza-s-indacene) compounds display a very favourable compound group for this application (Fig. 1.). In addition to their excellent suitability for fluorescent labeling of biologically active compounds due to their strong absorption in the UV range, they are characterized by narrow absorption and emission bands and high molar coefficient values. They also have the advantage of being highly photostable and insensitive to the pH of their environment, making them suitable for use under physiological conditions. As their framework can easily be modified chemically (Fig. 2.), thus their optical properties can be manipulated, and their emission can be extended to higher wavelengths [4].

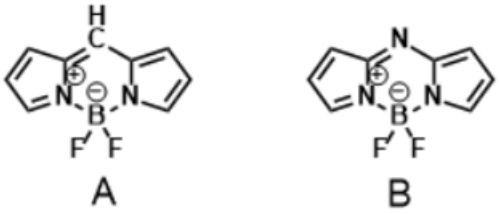

Figure 1. BODIPY (**A**) and *aza*-BODIPY (**B**) framework

The *aza*-BODIPY core (**B**), in which the carbon atom at *meso*-position is replaced by a nitrogen atom, has even more advantageous properties to those of compound **A** (Fig. 1.). A*za*-derivatives (**B**) show significant batokromic shifts. Accordingly, their emission spectra are shifted towards the red region [5]. These favourable optical properties allow their widespread biological application, especially because the radiation emitted is non-invasive, i.e. the lower energy emission does not damage cells. In addition, the light emission is also better separated from the autofluorescence of the cells (which is typically below 600 nm), which further improves the usability of the fluorophore [6].
Encouraged by the promising optical, chemical and biological properties of the *aza*-BODIPY derivatives, here we aimed to synthesize novel fluorophores based on framework **B**. Functional groups capable of later conjugation to biomolecules were introduced *via* postfunctionalization. The enhancement of water solubility was also an important aspect of our strategy. In order to consider the principles of green chemistry, one-pot and/or microwave-assisted syntheses were planned in order to minimize the number of reaction steps and time, and use of solvents.

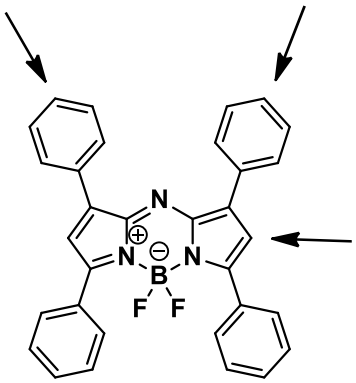

Figure 2. 1,3,5,7-tetraphenyl-*aza*-BODIPY and the possible positions for postfunctionalization

Results and discussion

The reaction sequence is depicted on Scheme 1. The base-catalyzed condensation of the benzaldehyde (**1**) and acetophenone (**2**) resulted in the corresponding chalcone (**3**). Michael addition using nitromethane as reagent was carried out on the α,β-unsaturated ketone (**3**), leading to the nitromethyl derivative (**4**) in high yield. It should be noted that the first two reaction steps were achievable in one-pot also, but the yield was slightly worse. The dipirromethene (**5**) was synthesized using NH_4OAc in EtOH solvent, under microwave irradiation. This step is the critical point of the whole reaction sequence, according to its extremely poor yield. After complexation with $BF_3.OEt_2$, the pyrrole rings were selectively formylated in a Vilsmeier-Haack reaction, leading to the monoformyl compound (**7**). The last step was the oxidation of the aldehyde, which resulted in the formation of a carboxylic acid

derivative **8**. The reaction conditions applied for the oxidation did not affect other moieties of the dye.

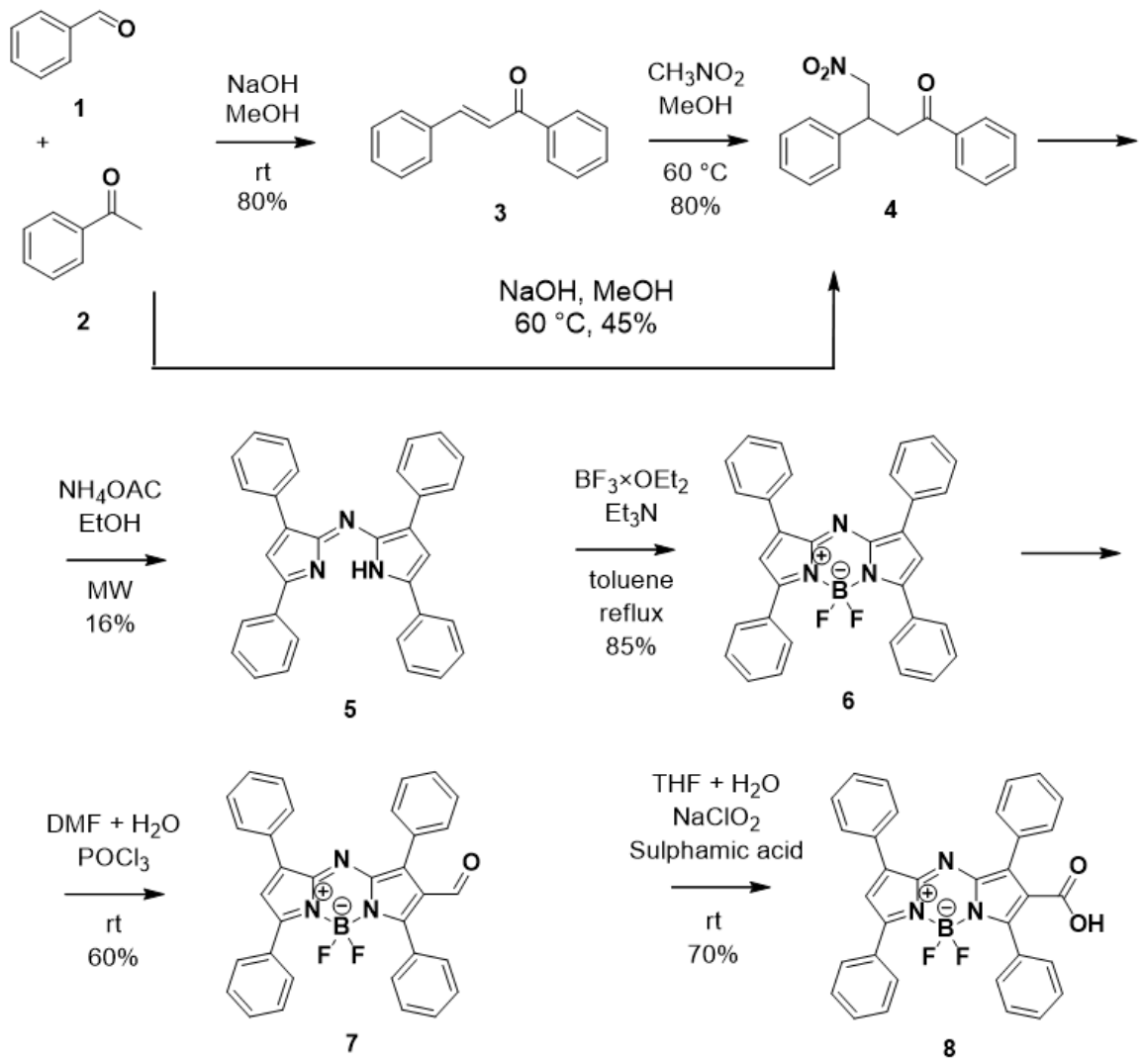

Scheme 1. Synthesis of the carboxylic acid derivative (**8**)

Conclusion

An efficient strategy was elaborated for the preparation of *aza*-BODIPY framework and the carboxylic acid derivative (**8**). The tetraphenyl derivative provides further opportunities for postfunctionalization, including enhancement of its water solubility. Our future plans involve determination of the optical properties of the newly synthesized dyes and their conjugation to certain biomolecules. The biological investigations will be carried out in cooperation.

Acknowledgements

This work was supported by National Research, Development, and Innovation Office-NKFIH through project OTKA SNN 139323.

References

[1] J. V. Jun, D. M. Chenoweth, E. J. Petersson, Org. Biomol. Chem. 18 (2020) 5747-5763.
[2] R. A. Rahman, H. E. D. M. Saleh, Principles and Applications in Nuclear Engineering: Radiation Effects, Thermal Hydraulics, Radionuclide Migration in the Environment (2018).
[3] J. Vonk, J. G. de Wit, F. J. Voskuil, M. J. H. Witjes, Oral Dis. 27 (2021) 21-26.
[4] S. Zhenxiong, H. Xu, H. Wenbo, B. Hua, P. Bo, J. Lei, F. Quli, L. Lin, H. Wei, H. Roy, Soc. Rev. 49 (2020) 7533-7567.
[5] L. Loaeza, R. Corona-Sánchez, G. Castro, M. Romero-Ávila, R. Santillan, V. Maraval, R. Chauvin, N. Farfán, Tetrahedron. 83 (2021) 131983.
[6] G. Ulrich, R. Ziessel, A. Harriman, Angew. Chem. Int. Ed. 47 (2008) 1184-1201.

EFFECT OF β-CYCLODEXTRIN COMPLEXATION ON THE ANTIBACTERIAL ACTIVITY OF SOME SALICYLANILIDE ESTERS

Ioana M. C. Ienaşcu[1,2], Adina Căta[1], Mariana N. Ştefănuţ[1], Corina Danciu[3,4], Delia Muntean[3,5,6], Raluca Pop[3]

[1]National Institute of Research and Development for Electrochemistry and Condensed Matter, 144 Dr. A. P. Podeanu, 300569 Timişoara, Romania
[2]Department of Pharmaceutical Sciences, Faculty of Pharmacy, "Vasile Goldiş" Western University of Arad, 86 Liviu Rebreanu, 310045 Arad, Romania
[3]Faculty of Pharmacy, University of Medicine and Pharmacy "Victor Babeş" Timişoara, 2 Eftimie Murgu Square, 300041 Timişoara, Romania
[4]Research Centre for Pharmaco-Toxicological Evaluation, "Victor Babeş" University of Medicine and Pharmacy, 2 Eftimie Murgu Square, 300041 Timişoara, Romania
[5]Faculty of Medicine, University of Medicine and Pharmacy "Victor Babeş" Timişoara, 2 Eftimie Murgu Square, 300041 Timişoara, Romania
[6]Multidisciplinary Research Center on Antimicrobial Resistance, "Victor Babeş" University of Medicine and Pharmacy, 2 Eftimie Murgu Square, 300041 Timişoara, Romania
e-mail: imcienascu@yahoo.com

Abstract

The aim of this research was to demonstrate the beneficial role of complexation on the efficiency of novel-designed chloro-substituted salicylanilide esters, starting from the premise that entrapping antimicrobial compounds in cyclodextrins should lead to proper control of drug release, so that the drugs could be more efficiently used. Thus, new complexes of salicylanilide ethyl esters and β-cyclodextrin, using the kneading method were obtained and tested against some Gram-positive and Gram-negative bacterial strains. For comparison, the effect of uncomplexed salicylanilide derivatives was also evaluated. Antimicrobial assays showed good activity on Gram-positive bacteria, meanwhile the Gram-negative strains proved no susceptibility on the action of tested concentrations. Among the bacterial strains, the most susceptible to the action of chloro-substituted salicylanilide derivatives proved to be *Streptococcus pyogenes* and *Streptococcus mutans*. The MBC and MIC values were equal meaning that the tested compounds action is bactericidal against the sensitive bacteria. The β-cyclodextrin complex of ethyl 2-(2-((2-chlorophenyl)carbamoyl)phenoxy)acetate preserved the same activity of the ester itself, even if the amount of the ester in the complex was 4 times smaller. This behavior can be due to the fact that complexation may disturb the cell membrane potential of bacteria and improve the membrane permeability of the drug.

Acknowledgements

This work is based on research supported by the Romanian Ministry of Research, Innovation and Digitization, project no. PN 19 22 03 01, contract no. 40N/2019 - "Supramolecular inclusion complexes of some natural and synthetic compounds with applications in health" - carried out under the NUCLEU Program.

References

[1] M. Krátký, J. Vinšová, Curr. Pharm. Des. 17 (2011) 3494.
[2] M. Krátký, J. Vinšová, E. Novotná, J. Mandíková, F. Trejtnar, J. Stolaříková, Molecules 18 (2013) 3674.

IMPACT OF WAR AND MILITARY ACTIVITIES ON BIODIVERSITY

Željko Ignjatović, Milan Glišić, Suzana Knežević, Ljiljana Tanasić

Unite for Agricultural and Business Studies and Tourism, Šabac, Academy of Applied Studies Šabac, Vojvode Putnika 56, 15000 Šabac, Serbia
e-mail: zeljkoignjatovic79@gmail.com

Abstract

Although war events cause numerous negative consequences for society and the economy, their effect on nature and biodiversity is often overlooked. The aim of this research is to present as many examples as possible of the impact of war events and military activities on biodiversity, consolidate previous conclusions on this subject, and derive basic patterns. War conflicts can be conducted in different ways, so ground, aerial, and naval war operations are distinguished. In this regard, the impacts on biodiversity can also be different depending on whether the war involves the use of infantry or artillery, aviation or navies. During all the aforementioned types of warfare, environmental damage, habitat disturbance, noise generation, contamination, and direct mortality of living beings occur. In addition to these general effects, each of the mentioned types of war conflicts can also have many specific ones. Ground war conflicts have a particularly harmful character when they involve the use of armored vehicles, which destroy vegetation and surface layer of the soil only by moving through a terrain. The specificity of the influence of military aviation is the risk of a direct collision between military aircraft and birds, which leads to their death. The most pronounced negative effect of naval military operations is the use of sonar, particularly harmful to large marine mammals, which navigate in the oceans and seas based on echolocation. The use of nuclear weapons is very harmful to biodiversity because nuclear explosions have thermal, kinetic, and radioactive effects. Thermal and kinetic effects often have an immediate impact on living beings, causing lethal or sublethal consequences. On the other hand, the radioactive effect is usually long-term and can affect future generations. The use of chemical weapons during the war primarily harms humans but can also affect other organisms. Although it can be thought that war conflicts always have negative ecological consequences, their impact can sometimes even be positive for biodiversity through the elimination of other negative anthropogenic factors.

EFFECT OF SUBCHRONIC DIBUTYL PHTHALATE TREATMENT ON ACTIVITY OF LIVER ENZYMES IN FEMALE WISTAR RATS

Ivana Ivelja, Jelena Karan, Nebojša Andrić, Jelena Marković Filipović

Department od Biology and Ecology, Faculty of Sciences, University of Novi Sad, Novi Sad, Serbia
e-mail: ivana.ivelja@dbe.uns.ac.rs

Abstract

Di-n-butyl phthalate (DBP) is an organic compound used as plasticizer, often found in numerous consumer products such as food packaging, cosmetics, adhesives and toys. Since DBP bonds non-covalently to final products, leaching and evaporation may occur. DBP released in the environment can thus be deposited or taken up by water and crops intended for livestock and human consumption. It has been shown that the main route of exposure is through oral intake. Aim of our study was to investigate wether exposure to DBP can cause liver damage by affecting the activity of aspartate transaminase (AST), alanine transaminase (ALT) and alkaline phosphatase (ALP) in female Wistar rats. Twenty-four female Wistar rats were divided into 4 groups (6 per group) and treated subchronically (3 months) with 0, 100, 500 and 5000 mg DBP/kg diet, that corresponded to 6.69, 33.73 and 344.49 mg/kg BW/day. Activities of ALT, AST and ALP in plasma were determined by Dialab Autolyser. Statistical analysis of obtained data was performed using STATISTICA® version 13.0 (StatSoft, Inc). Data from control and treated rats were compared using One-way analysis of variance (ANOVA) for multiple comparisons, followed by Tukey post-hoc tests. Statistical analysis revealed no significant difference between control and DBP-treated rats. Our results indicate that DBP subchronic treatment in applied doses does not affect activity of liver enzymes.

FOOD WASTE - WASTE OF PORK MEATS IN RESTAURANTS IN ŠABAC

Dragana Ilić Udovičić, Aleksandra Vasić, Jelena Đuričić Milanković, Jelena Jevtić Tamara Jevtić

Academy of Professional Studies Sabac, Department of Medical and Business-Technological Studies, Hajduk Veljkova 10, Šabac, Serbia
dilicudovicic@vmpts.edu.rs, aleksandra.vasic@vmpts.edu.rs, jdjuricic@yahoo.com, jevticj.vts@gmail.com, jevtic.tasa.98@gmail.com

Abstract
The hospitality industry (e.g., hotels, restaurants, fast food) are considered one of the generators of food waste. Waste is created in kitchens during food preparation and after consumption by users. Meat and meat products are an integral part of most meals in catering establishments in our country. The paper analyzes the frequency of use of pork in food preparation facilities in Šabac and the amount of waste generated on that occasion. The results showed the need to increase the yield of gastronomic products, which would lead to a reduction of unnecessary trimmings waste.

Introduction
According to the European Environment Agency, food waste generated in households, retail and wholesale, accounts for 61% of municipal waste [1]. This type of waste is a worldwide problem [2, 3] and has an impact on the environment [4, 5, 6]. Different foods have different environmental impacts. The amount of meat that is lost and wasted is not very high compared to other foods, but meat requires much more resources to produce, so wasting meat still significant impact on climate change [7].

Experimental
The research is based on the evaluation of the gastronomy offer in hotels, restaurants and fast food restaurants in the area of Šabac. The paper examines how much pork meat is present in gastronomy offer and estimation of the amount of waste generated. The catering sector is a significant producer of food waste, but there is a significant lack of reliable statistics on food waste and avoidable food waste. The research results were obtained through field research and the use of various domestic and foreign literature.

Results and discussion
The results show the dominant presence of pork dishes in the offer of restaurants, as much as 43%, in fast food restaurants 41%, and in hotels 27%. The offer includes all categories of pork. The inedible part of the meat produced in the kitchen amounted to an average of 10.8% to 35% depending on the category of pork. The results show the hotels are looking for an effective solutions for recycling and reducing food waste, while for the restaurants, food waste is seen as low priority, despite the data that show that 10 % of all the food that a restaurant buys ends up at the dumpster.

Conclusion
Increasing the yield of the gastronomic product through the implementation of the necessary training of kitchen employees could contribute to waste reduction. The obtained results indicate the need to change the way of thinking and raise awareness through education about the

importance of reducing the amount of meat waste, which requires much more resources for production and has a significant negative impact on climate change.

Keywords: food waste, pork meats, gastronomy, restaurants.

References

1. Analysis of the food waste management system in the Republic of Serbia, Beolgrade, (2019), NALED National Alliance for Local Economic Development, www.naled.rs
2. B. Okumus, B. Taheri, I. Giritlioglu, M.J. Gannon. Tackling food waste in all-inclusive resort hotels, Int. J. Hospit. Manag. (2020).
3. F. Girotto, L. Alibardi, R. Cossu, Food waste generation and industrial uses: A review, (2015), Waste Management , Vol. 45, Pages 32-41.
4. C. Martin-Rios, C. Demen-Meier, S. Gössling, C. Cornuzm, Food waste management innovations in the foodservice industry, (2018), Waste Management, Vol. 79, Pages 196-206.
5. P. Studnička, Possibilities of waste reduction in gastronomy and food industry in the context of circular economy, ICOM 2021 Zero Waste Management and Circular Economy, DOI: 10.11118/978-80-7509-820-7-0136
6. J. Markowska, E. Polak, A. Drabent, A. Tyfa, Innovative Management of Vegetable Outgrades as a Means of Food Loss and Waste Reduction. *Sustainability* 2022, *14*, 12363. https://doi.org/10.3390/su141912363.
7. FAO (2015) Food wastage footprint and climate change.

EMPLOYEE REWARD SYSTEM IN THE FUNCTION OF SUSTAINABLE DEVELOPMENT

Tamara Jevtić, Jelena Jevtić, Jelena Đuričić Milanković, Aleksandra Vasić, Dragana Ilić Udovičić

Academy of Professional Studies Šabac, Department of Medical and Business-Technological Studies, Šabac, Serbia
jevtic.tasa.98@gmail.com, jevticj.vts@gmail.com, jdjuricic@yahoo.com, aleksandravasic98@gmail.com, dilicudovicic@vmpts.edu.rs

Abstract
The development and management of human resources are important aspects of building an environmental culture in the organization. The result of adequate application of GHRM (Green Human Resource Management) is the creation of greater efficiency, lower costs and better employee engagement. The employee reward system can be a key instrument for raising environmental awareness within GHRM.

Introduction
GHRM is a concept closely related to sustainable development. Viewed from a broader perspective, this concept includes awareness of environmental issues, awareness of the importance of the social and economic well-being of employees, and thus of the organization as a whole. Sustainability ensures that the organization has long-term solutions that will improve economic well-being in the future. Employees of the organization play a key role in the sustainability process. There are great opportunities for human resource management to participate in building the organization's strategic capabilities to implement its clear orientation towards a sustainable business environment, using human resources, their knowledge and skills, attitudes and values, capacities for learning and advancement [9].
The concept of GHRM or green human resource management deals with the use of human resource management to promote sustainable development. Sustainable use of resources within companies, raising employees' awareness of environmental issues stems from unique and recognizable patterns of behavior and decisions of HR managers. Managers' green regulations can be promotional (when behavioral patterns of employees are used as an instrument to promote the concept of sustainable development) or preventive (when behavioral patterns and decisions are applied preventively to prevent negative consequences for the environment) [13, 15].
Rewards, i.e. fees and benefits are used to increase the number of employees, productivity and loyalty. They also increase employee satisfaction and motivation for work. Green reward systems should be designed to reflect management's commitment to environmental performance while reinforcing and motivating employees' pro-environmental behavior [13].
The employee reward system is a central and integrated feature of human resources management [2]. Fees (remunerations, compensations and earnings) form the basis of the reward system. They include all types of wages and rewards paid to employees for their work [4]. Compensations are intrinsic and extrinsic rewards to employees for performing work. Internal compensations reflect the psychological state of employees as a result of performing the job. Organizational development professionals are responsible for them. Extrinsic compensations include monetary and non-monetary rewards, and in larger organizations compensation managers are responsible for them [8].

However, compensation can also be seen as a direct financial cost of the organization. Labor costs can make up a significant percentage of total costs, in some countries that percentage is as much as 60% of total business costs. Precisely because of this, compensations should be viewed as investments that result in added value for the organization [17]. Total compensations are part of total rewards, they include external elements of rewards that can be quantified, which are fixed and variable parts of earnings, benefits and allowances [3].

Compensation professionals create reward programs to reward employees according to their length of service, performance levels or for the knowledge and skills they have acquired related to the work they do. Non-monetary prizes include e.g. health insurance, annual vacations or various services for employees. Most experts call these non-monetary rewards employee benefits, which represent a very important element of compensation packages [7].

The development of the compensation system begins with the analysis of the business strategy and is a very important activity of every organization. The compensation strategy and key principles of remuneration are developed taking into account the existing HRM strategy, remuneration policy and practice and the needs of the company's stakeholders [10].

Compensation objectives can be classified into three groups:

1. Efficiency - the compensation system should improve worker performance, product quality and consumer satisfaction, but at the same time should control labor costs;
2. Equality - a key assumption of the compensation system that takes into account both the performance of employees and their needs, providing a transparent compensation system for everyone;
3. Adherence to legal frameworks - it is important that the compensation system changes in accordance with the increasingly frequent changes in legal regulations [5].

The main purpose of the compensation system is to attract, retain and motivate quality workers. Organizations should pay special attention to building a compensation system for several reasons [11]. The first reason is to attract highly qualified workers who will contribute to the successful operation of the organization with their knowledge and skills. In addition to this, organizations should pay attention to keeping these workers in the organization, so that they do not look for another place to work. The goal of observing the compensation system is the motivation of workers to give their best in performing work tasks, which will ultimately lead to the achievement of the set goals of the organization. The basic role of the reward system is to align the individual interests of employees with the company's strategic goals, which is achieved through attracting, retaining, motivating and creating an organizational culture in which it will be important for employees to contribute to the success of the company in which they are employed [1].

Literature review

Based on previous research in this area, the negative effects of the environmental crisis are the consequences for man, his health and living conditions. Polluted air, polluted water, soil and food lead to the emergence of new diseases. Poverty, unequal development and distribution between the rich and the poor lead to new problems regarding human rights, the right to life, and the right to a healthy environment [12]. Under the pressure of the mentioned problems, the position was accepted that a new concept of development must be created, which would imply technological progress, but with the reduction of environmental pollution [6].

Based on the review of the literature in this area, it is concluded that the green economy creates new jobs and increases the level of social equality. Transition to a green economy also means transition to new employment policies, opening more jobs than is the case with traditional economic models. If investments are made in the green economy, agriculture, construction, forestry and transport, employment will increase in the short, medium and long term. The

concept of green economy does not replace sustainable development, but today there is more and more evidence that reaching the goals of sustainable development depends to the greatest extent on the movement in the economic sphere [16].
The relationship between man and the environment in the modern world is becoming more and more complicated. A way out is sought in the integration of economic development and environmental protection using the concept of ecologically sustainable development [14]. Sustainable development connects the economy, society and environmental protection, within which green growth strategies can be considered as an appropriate framework for practical policies.
Sustainability means ensuring a non-decreasing standard of living for future generations. It represents the transfer of natural capital to new generations in the same amount that we used. Today, damage has occurred due to global warming, and natural resources have been used up to 50%. It is believed that by 2050, the utilization of natural resources will be as much as 85%. If the demand for resources without good substitutes is a large part of the current supply, our use of natural resources is unsustainable. Environmentalists claim that natural resources and acquired capital are not good substitutes in production. The decision-makers face the demand for moderate development and preservation of the environment, with careful weighing of costs and benefits for both the economy and the environment [9].

Results and discussion

Monetary green rewards can include various bonuses and incentives, profit-sharing programs and salary increases for achieving environmental goals, while non-monetary rewards can include promotion and recognition. Based on recognition, employee awards can be for individual, team and divisional contributions to waste reduction, team awards for company-wide excellence, giving employees opportunities to attend green events, paid vacations, time off and gift certificates. Another important issue in green compensation and benefits is that these programs should be related to the acquisition of specific skills and competences (not only for performance), because they are considered important factors in long-term performance, that is, reward systems should be developed to produce desirable behaviors in environmental management. An effective green reward system should be based on:

- Rewarding the employee for achieving environmental performance and environmental knowledge and values.
- Design special monetary and non-monetary rewards for employees who achieve environmental goals.
- Design special organizational, team and individual rewards for employees.
- Design rewards for innovative employee environmental initiatives.
- Introduce new and innovative benefits for employees' environmental practices [13].

Directing the organization towards the implementation of a sustainable development strategy requires a certain process related to the role that green HR plays in that way. The basic phases of strategy implementation would be as follows:
First step: Identification and involvement of all stakeholders to whom the policies, processes and results of the HR policy apply.
Second step: Selection and prioritization of key human resource management issues relative to supporting a sustainable organization.
Third step: Review and revision of HR policies in accordance with the principles of sustainability.
Fourth step: Preparation and development of activity plans, indicators and measures of success [9].

Conclusion

The national sustainable development strategy is one of the most important elements that lead to raising environmental awareness. Sustainable development is oriented towards creating a model that eliminates or reduces impacts that pose a threat or damage to the environment and natural resources. In the long term, the effects of sustainable development would be seen through the achievement of such a scale of efficiency and technological progress, innovation of the whole society, better utilization of resources, reduction of pollution levels, prevention of future pollution and preservation of biodiversity [12]. Proactive HRM focused on sustainable development set as an imperative of modern business influences the pro-environmental thinking of employees. As found in the literature review, the compensation system has a great impact on the satisfaction of employees in the organization. This system should be aligned with numerous internal and external factors that affect modern business, and that respond to new requirements in terms of encouraging employees to change their behavior towards green champions.

References

[1] B. Bogićević-Milikić. Menadžment ljudskih resursa. Beograd: Centar za izdavačku djelatnost Ekonomskog fakulteta, 2008.

[2] D. Torrington, L. Hall L, S. Taylor S. Human Resource Management, 2005.

[3] M. Festing, A.D. Engle, P. J. Dowling, I. Sahakiants. HRM activities: pay and rewards. U C. Brewster, & W. Mayrhofer (Eds.), Handbook od Research on Comparative Human Resource Management, Cheltenham: Edward Elgar Publising Limited, (2012), pp.139-163.

[4] G. Dessler. Osnovi menadžmenta ljudskih resursa. Beograd: Data Status, 2007.

[5] G.T. Milkovich, J.M. Newman. Compensations. Boston: Irwin-McGraw-Hill, 1999.

[6] N. Berber, M. Đorđević. Menadžment troškova u funkciji zaštite životne sredine. Škola biznisa, 2, (2011), pp. 76-89.

[7] J. Martocchio. Strategic compemsation: A Human Resource Management Approach. Pearson Education International, 2017.

[8] J. Martocchio. Strategic compensation: A Human Resource Management Approach. Pearson Education International, 2009, pp. 129.

[9] J.Đorđević-Boljević, G. Dobrijević, F. Đoković. Održivost i zeleni menadžment ljudskih resursa. ECOLOGICA, Vol. 24. No 88, (2017), pp. 1-6.

[10] M. Armstrong. Armstrong's Handbook of Reward Management Practice, 3rd Edition. London: Kogan Page, (2010), pp. 392-393.

[11] M. Babić, Z. Lukić. Menadžment – teorije, funkcije, institucionalni aspekti i korporativno upravljanje. Banja Luka: Ekonomski fakultet. 2008.

[12] N. Arsić, J. Matijašević, N. Berber. Kriza životne sredine kao problematika ljudskih prava i ekološke svesti. Pravo. (2011), 23.

[13] N. Berber, M. Aleksic. Green human resource management: Organizational readiness for sustainability. In International Scientific Conference the Priority Directions of National Economy Development, Faculty of Economics, University of Niš. 2014, pp. 271-282.

[14] N. Berber. Održivi razvoj sa aspekta ekološkog menadžmenta i neoklasične ekonomije. Škola biznisa, 2, (2009), 16-22.

[15] R. Sharma, N, Gupta. Green HRM: An innovative approach to environmental sustainability. In Proceeding of the Twelfth AIMS International Conference on Management, 2015, pp. 2-5.

[16] S. Korać. Strategijski eko (green) menadžment–bezbednosna dimenzija.Zbornik radova Digitalizacija medija i ekonomija postindustrijskog doba. DOI 10.7251/BLCMES1801276K 276-292.

[17] Š. G. Šušnjar, B. Leković. Performance-based pay in human resoruces development. Strategic Management, (2009), 14(3).

INFLUENCE OF SILICON ADDITION ON THE PROPERTIES OF NEW TITANIUM ALLOYS

Cristina Jiménez-Marcos[1], Santiago José Brito García[1], Julia Claudia Mirza-Rosca[1]*, Madalina Simona Baltatu[2], Petrica Vizureanu[2]

[1]Mechanical Engineering Department, Las Palmas de Gran Canaria University, 35017 Tafira, Spain
[2]Department of Technologies and Equipments for Materials Processing, Faculty of Materials Science and Engineering, Gheorghe Asachi Technical University of Iaşi, Blvd. Mangeron, No. 51, 700050 Iasi, Romania
e-mail: julia.mirza@ulpgc.es

Abstract
The mechanical characteristics and electrochemical behavior of the new titanium alloys TiMoZr, TiMoZrSi0.5, TiMoZrSi0.75 and TiMoZrSi1 were studied to determine their microstructure, corrosion behavior and mechanical properties. Following the use of the appropriate procedures, metallographic analysis showed that both samples had biphasic and dendritic structures. According to electrochemical tests in body simulation fluid, the samples' corrosion resistance increases with decreasing silicon content since silicon-containing samples corrode more quickly. Electrochemical Impedance Spectroscopy measurements were performed at various potentials, and the acquired spectra show a two-time constant system, due to the presence of a double-layer passive film on the samples. The three-point bending test for both samples demonstrated that the values of modulus of elasticity are lower than those commercial alloys and nearly to the cortical human bone, and the microhardness test showed that the samples' surfaces had soft and hard phases.

Introduction
Nowadays, due to the increasing use of biomaterials in various fields of medicine, they must have a number of characteristics: high biocompatibility, ductility, fatigue and wear resistance, osseointegration, absence of cytotoxicity and a combination of high strength and low Young's modulus equivalent to human cortical bone ranging between 10 and 30 Gpa [1–3].
About 70-80% of implants are made of metallic biomaterials [4], with Ti and its alloys being the most widely used, as they can modify their properties by changing the composition of the alloying elements, their biocompatibility with biological materials, high corrosion resistance, high mechanical performance, low modulus and high thermal stability [3,5–7]. The Ti6Al4V alloy is the most commonly used alloy for orthopaedic applications, although vanadium is a carcinogenic and toxic material and aluminium, in large concentrations, can cause dementia or Alzheimer's [8].
Consequently, it was decided to determine the effects of four different silicon concentrations on the microstructure, corrosion behaviour, quantitative microanalysis, modulus of elasticity and hardness of the new TiMoZrSix alloy by means of metallographic, electrochemical, scanning electron microscopy, three-point bending and microhardness tests.

Experimental
The study of four new alloys with Ti, Mo, Zr, varying the composition of Si, TiMoZr, TiMoZrSi0.5, TiMoZrSi0.75, and TiMoZrSi1, has been carried out with the aim of applying different tests to find out their properties. The production of these alloys was carried out using a Voltaic Arc Remelting (VAR) furnace in which a consumable electrode was melted in a

vacuum at a controlled rate with the heat generated by an electric arc between the electrode and the ingot. As a previous step to electrochemical, metallographic and flexural tests, several processes should be performed, such as to embed into an epoxy resin cylinder the samples for cutting and their subsequent polishing in two stages: polishing with SiC abrasive papers of progressive grain size from 400 to 1200 grit and final polishing with 0.1 micrometer alpha alumina suspension. The samples are then submerged in an ultrasonic machine for 5 minutes to remove all traces of dirt, and then immersed in Kroll's reagent for 15 seconds. After chemical etching, the metallographic test was performed by taking images with the metallographic microscope, of the surface of the samples at different magnifications to characterize their microstructure. Moreover, electrochemical test consisted in inserting a specimen into an electrochemical cell together with Saturated Calomel Electrode (SCE) as reference and Pt electrode as counter electrode. Corrosion potential (E_{corr}), corrosion rate (v_{corr}) were determined, and Electrochemical Impedance Spectroscopy (EIS) and Pitting Potential were applied [9]. Three-point bending test were applied to find the value of the modulus of elasticity of each specimen. Finally, microhardness test was obtained following Vickers method by using a hardness tester and applying different loads.

Results and discussion

In the metallographic test, it can be observed that both samples had biphasic and dendritic structures, distinguishable for both magnifications. Furthermore, the size of dendrites decreased with the Si addition while the interdendritic zone increased. Moreover, in the corrosion tests, the samples were immersed in Ringer Grifols solution which simulates the physiological fluid of the human body the results obtained were processed by the EC-Lab software. From the plots of E_{corr} versus time, it has been observed that the corrosion potential tends to increase with time and thus a passive layer is formed, except for the TiMoZrSi0.75 sample, which corrodes. EIS measurements were performed on each specimen at different potentials to obtain the Bode Impedance plots, where the corrosion resistance increases the more positive the applied potential and the higher the impedance and phase angle values. After obtaining the polarization curves and performing the Tafel fit, it could be shown that the corrosion rate increases the higher the addition of silicon. In addition, no sample was corroded by the pitting technique. In the three-point bending test the value obtained for the modulus of elasticity of all samples is lower than commercial alloys. Furthermore, the graphs of Vickers hardness versus scan length for both samples show widely dispersed maxima and minima, as the surfaces of the samples show soft and hard areas and it is confirmed that the hardness increases the lower the percentage of silicon.

Conclusion

In this study, the effects of silicon content on the microstructure, microhardness, modulus of elasticity and corrosion behaviour of TiMoZrSix alloy in a simulated body fluid were investigated, and the following conclusions were drawn:

After the analysis of the results, it was confirmed, in the metallographic test, the biphasic and dendritic structure. On the other hand, in the electrochemical tests, both samples tended to passivate, apart from TiMoZrSi0.75, and it was demonstrated that the more positive the value of the applied potential, the greater the resistance to corrosion, presenting similar impedance values. The modulus of elasticity was lower than those of many commercial alloys. Finally, Vickers hardness values increases the lower the percentage of silicon and all samples presented soft and hard areas.

According to the results, the samples had good mechanical, chemical, and biological features, with the Ti20MoZrSi0.5 sample having slightly improved mechanical characteristics.

Acknowledgements
The research was sponsored by Gran Canaria Cabildo, project number CABINFR2019-07.

References
[1] D. Aggarwal, V. Kumar, S. Sharma, Drug-loaded biomaterials for orthopedic applications: A review, J. Control. Release. 344 (2022) 113-133.
[2] I. Băltatu, P. Vizureanu, F. Ciolacu, D.C. Achiţei, M.S. Băltatu, D. Vlad, In Vitro study for new Ti-Mo-Zr-Ta alloys for medical use, IOP Conf. Ser. Mater. Sci. Eng. 572 (2019) 012030.
[3] Y. Bai, Y. Deng, Y. Zheng, Y. Li, R. Zhang, Y. Lv, Q. Zhao, S. Wei, Characterization, corrosion behavior, cellular response and in vivo bone tissue compatibility of titanium–niobium alloy with low Young's modulus, Mater. Sci. Eng. C. 59 (2016) 565-576.
[4] M. Niinomi, M. Nakai, J. Hieda, Development of new metallic alloys for biomedical applications, Acta Biomater. 8 (2012) 3888-3903.
[5] J. Quinn, R. McFadden, C.W. Chan, L. Carson, Titanium for Orthopedic Applications: An Overview of Surface Modification to Improve Biocompatibility and Prevent Bacterial Biofilm Formation, iScience. 23 (2020) 101745.
[6] K. Shree Meenakshi, S. Ananda Kumar, Corrosion resistant behaviour of titanium – Molybdenum alloy in sulphuric acid environment, Mater. Today Proc. (2022).
[7] S.X. Liang, X.J. Feng, L.X. Yin, X.Y. Liu, M.Z. Ma, R.P. Liu, Development of a new β Ti alloy with low modulus and favorable plasticity for implant material, Mater. Sci. Eng. C. 61 (2016) 338-343.
[8] P.P. Socorro-Perdomo, N.R. Florido-Suárez, J.C. Mirza-Rosca, M.V. Saceleanu, EIS Characterization of Ti Alloys in Relation to Alloying Additions of Ta, Materials (Basel). 15 (2022) 476.
[9] M. López Ríos, P.P. Socorro Perdomo, I. Voiculescu, V. Geanta, V. Crăciun, I. Boerasu, J.C. Mirza Rosca, Effects of nickel content on the microstructure, microhardness and corrosion behavior of high-entropy AlCoCrFeNix alloys, Sci. Rep. 10 (2020) 1-11.

DESIGN AND OPTIMIZATION OF AN ALTERNATIVE HIGH EFFICIENCY SAMPLE INTRODUCTION SYSTEM FOR SINGLE PARTICLE ICP-MS ANALYSIS

Gyula Kajner[1,2], Ádám Bélteki[1,2], Martin Cseh[3], Balázs Vajda[3], Zsolt Geretovszky[2,3], Gábor Galbács[1,2]

[1]Department of Inorganic and Analytical Chemistry, University of Szeged, H-6720 Szeged, Dóm tér 7, Hungary
[2]Dept. of Mater. Sci., Interdiscip. Excel. Cent., Univ. of Szeged, H-6720 Szeged
[3]Dept. of Opt. and Quant. Electr. Univ. of Szeged, H-6720 Szeged, Dóm sq. 9, Hungary
e-mail: galbx@chem.u-szeged.hu

Abstract
In this study we present the development process of an alternative sample introduction system for inductively coupled plasma mass spectrometers (ICP-MS) with the aim of improving the efficiency and capabilities of single particle ICP-MS measurements. The system consists of a high efficiency pneumatic nebulizer, and a low memory effect, high transport efficiency on-axis spray chamber which are currently under manufacturing utilizing a high resolution, multijet (MJP) 3D printer. Both part underwent several fluid dynamic simulations to debunk potential design flaws and to assess their optimal operating conditions before their production.

Introduction
The relatively novel technique of single particle inductively coupled plasma mass spectrometry (spICP-MS) is a powerful tool for the characterization of nanoparticle (NP) or cell dispersions. This technique can provide information regarding elemental or isotope composition of individual particles, as well as the size distribution and particle number concentration (PNC) of their dispersions with great statistical relevance. However, the standard ICP-MS sample introduction system – which usually consists of a concentric nebulizer and a Scott-type double-path spray chamber – hardly exceeds 5% transport efficiency and shows significant memory effects which makes its sample consumption suboptimally high for efficient single particle or single cell analysis [1,2]. It has been shown that by utilizing low sample consumption, high transport efficiency nebulizers which facilitate monodisperse droplet formation, coupled with low volume spray chambers, the performance and efficiency of the spICP-MS technique can be further enhanced. The higher sensitivity, lower limit of detections, and decreased sample consumption these accessories provide, come in handy considering the ever-increasing demand for determining the above mentioned characteristics of cell or NP dispersions using lower sample volumes and concentrations [3,4].
Also, as 3D printing technologies advanced in the past years, their minimum feature size (MFS) reached the few tens of microns regime, which makes them a great tool for producing parts which require high spatial resolution and precision such as nozzles and microchannels [5].

Experimental
The connectors of the nebulizer and the spray chamber was designed to be compatible with our Agilent 7700X ICP-MS (Agilent Technologies, Santa Clara, CA, USA) instrument. The 3D models of the nebulizer and the spray chamber was made utilizing AutoCAD 2022 software (Autodesk Inc. San Rafael, CA, USA). The fluid dynamic simulations were carried out using COMSOL Multiphysics software (COMSOL Inc. Burlington, MA, USA). The production of the parts was done by utilizing ProJet MJP 3600 high precision 3D printer equipped with VisiJet M3 resin (3D Systems, Rock Hill, SC, USA).

Results and discussion

The operational principle and geometry of the nebulizer and the spray chamber was chosen to fulfil three requirements with no or relatively minor changes on the general design. (1) Their geometry (connections, size), and supplies (gas flows, liquid pumps) needed for operation should be compatible with our ICP-MS instrument. (2) Their geometry is relatively simple, does not include such small details (except the nozzle head, which inevitably on the edge of the capabilities of 3D printing) that are too challenging for the used 3D printing technique. (3) According to the literature, their efficiency is the reasonably high.

With those in mind, for the nebulizer we decided on a concentric pneumatic nebulizer. The changes we made compared for the general designs were the reduction of the inner volume and nozzle bore size as much as the design itself and the production technology allowed. As for the spray chamber, an on-axis type, low volume spray chamber with sheath gas flow was chosen, on which minor adjustments were made, decreasing its inner volume. Also, both the nebulizer and the spray chamber got equipped with connectors that are compatible with the tubing of the original nebulizer and spray chamber of the instrument. They are meant to be operated using only argon gas flows so that the plasma of the instrument remains relatively undisturbed. The application of the two chosen designs together was already reported in the literature a few times, they showed reasonably high, more than once near 100% transport efficiencies [2,6].

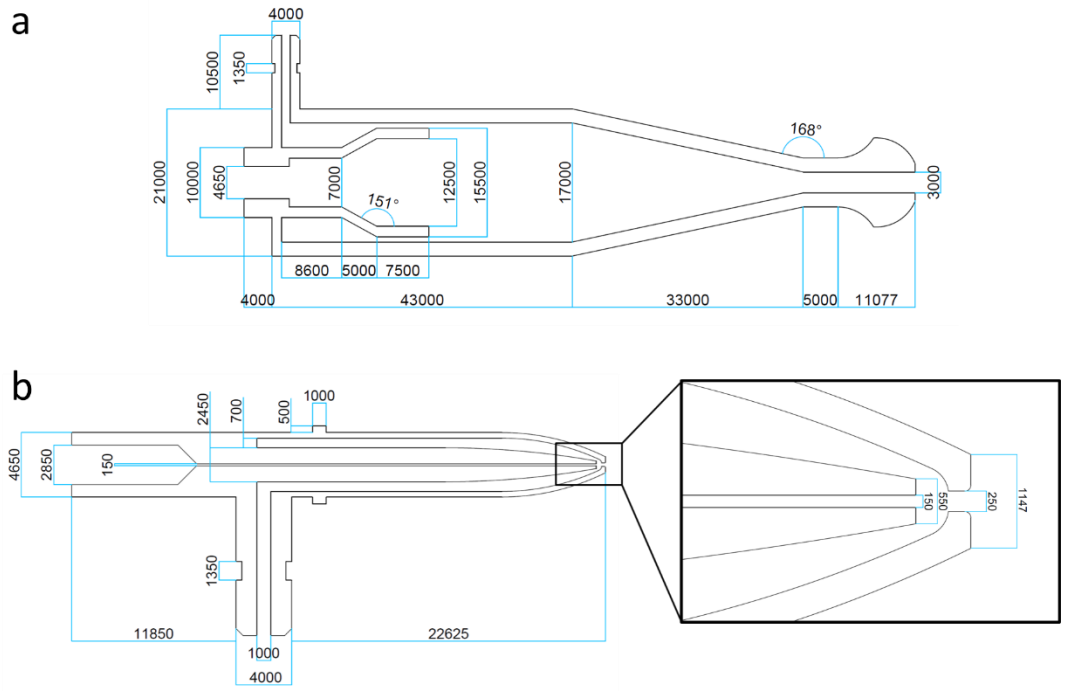

Figure 1. The final designs of the a) on-axis spray chamber b) concentric nebulizer. Values are given in µm units.

The final designs are shown on Fig. 1, the inner volume of the spray chamber accessible for the produced aerosol and the dead volume for the sample in the nebulizer are ca. 9.2 mL and 0.51 µL respectively. In the design process, several fluid dynamic simulations were carried out using COMSOL Multiphysics software. Firstly, the pressure conditions were assessed inside of the two components. In case of both designs, we concluded that they are capable enduring the inside pressure in a wide range of introduced gas flow values, thanks to the axial symmetry of the design and the good mechanical resilience of the 3D printer resin. By examining the pressure and gas flow velocity distribution inside the simulated components a few iterations per design

were made. (1) To optimize the relative velocity of the nebulizer and the sheath gas flow by adjusting the size of the constriction through which the sheath gas is introduced. (2) To ensure the optimal and reproducible nozzle position inside the chamber to reduce the chance of droplet deposition on the walls.

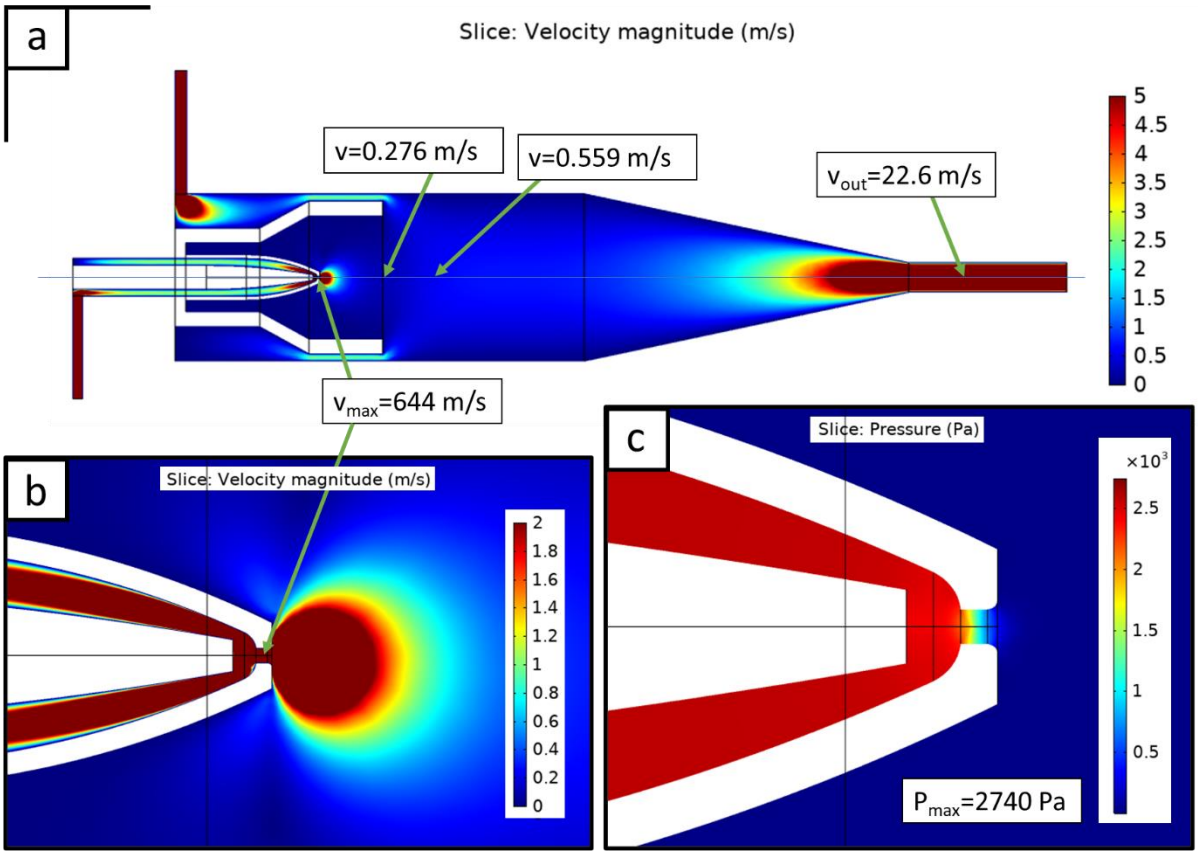

Figure 2. Simulation results showing the lateral gas velocity profiles a) on the whole model b) near the nozzle, while c) shows the lateral pressure distribution at the tip of the nozzle. All plotted in the mid-depth plane of the model.

Conclusion

An alternative, 3D printed sample introduction system containing a concentric pneumatic nebulizer, and a low volume on-axis spray chamber equipped with sheath gas flow for ICP-MS was designed to enhance single nanoparticle or cell analysis. Its geometry was based on previously published reports of high efficiency nebulizers, spray chambers and several fluid dynamic simulations which the models underwent before finalization. As the continuation of this research, we are planning to characterize the capabilities of this custom sample introduction system experimentally. Examining its transport efficiency, primary and secondary droplet size distribution, and its effect on the efficiency of spICP-MS measurements when coupled with our instrument.

Acknowledgements

The authors thankfully acknowledge the financial support of the ÚNKP-22-2-I. New National Excellence Program of The Ministry for Culture and Innovation from the source of National Research, Development and Innovation Fund.

References

[1] M. Tharaud, P. Louvat, M.F. Bennetti, Anal. Bioanal. Chem. 413 (2021) 923-933.
[2] S. Miyashita, A.S. Groombridge, S. Fujii, A. Minoda, A. Takatsu, A. Hioki, K. Chiba, K. Inagaki, J. Anal. At. Spectrom. 29 (2014) 1598-1606.
[3] M. Corte-Rodríguez, R. Álvarez-Fernández, P. García-Cancela, M. Montes-Bayón, J. Bettmer, Trends in Anal. Chem. 132 (2020) 116042.
[4] G. Galbács, A. Kéri, A. Kohut, M. Veres, Zs. Geretovszky, J. Anal. At. Spectrom. 36 (2021) 1826-1872.
[5] K. Silver, J. Potgieter, K. Arif, R. Archer, 24th Int. Conf. Mechatr. Mach. Vis. Pract. (2017) pp. 1-6.
[6] K. Inagaki, S. Fujii, A. Takatsu, K. Chiba, J. Anal. At. Spectrom. 26 (2011) 623-630.

EFFECT OF SUBHRONIC DIBUTYL PHTHALATE EXPOSURE ON THE LEVELS OF REPRODUCTIVE HORMONES IN FEMALE WISTAR RATS

Jelena Karan, Ivana Ivelja, Nebojša Andrić, Jelena Marković Filipović

Department of Biology and Ecology, Faculty of Sciences, University of Novi Sad, Trg Dositeja Obradovića 2, Serbia
e-mail: jelena.karan@dbe.uns.ac.rs

Abstract

Dibutyl phthalate (DBP), widely used as a plasticizer in different items including medical equipment, elastic plastics, cosmetic formulations and toys becomes the predominant contaminant in the environment. Phthalates are known endocrine-disrupting chemicals that can directly target the ovary, potentially causing defects in ovulation and fertility.
The aim of our study was to determine whether DBP treatment affects sex hormones levels in female rat.
Twenty-four female Wistar rats, 40 days old at the beginning of the experiment, were divided into 4 groups (6 per group) and exposed subchronically (3 months) to DBP added to the diet in concentrations: 0, 100, 500, 5000 mg DBP/kg diet, that correspond to 6.69, 33.73 and 344.49 mg/kg BW/day. At necroscopy plasma was collected in vacutainer tube for clinical biochemical tests. Biochemical analysis are performed in the Biochemical laboratory. Statistical analysis was performed using STATISTICA® version 13.0 (StatSoft, Inc). Data from control and treated rats were compared using One-way analysis of variance (ANOVA) for multiple comparisons, followed by Tukey post-hoc tests.
Statistical analysis revealed that treatment in doses of 100 and 500 mg DBP/kg diet significantly decreased estrogen levels, while in the group exposed to 5000 mg DBP/kg diet no differences in estrogen level was detected when compared with control. Results also showed a significant decrease in progesterone levels in all treated groups compared to the control group.
Taken together, our results indicated that subchronically exposure to DBP induced reduction of progesterone levels, while decreased estrogen level depends of dose. Phthalates exposure could possibly be an important environmental etiological factor of female sex hormone synthesis disorders.

THE SYNTHESIS AND NEUTRALIZATION OF HYDROXYSODALITE

Eszter Kása[1], Bence Kutus[2], Pál Sipos[2]

[1]Department of Organic Chemistry, University of Szeged, H-6720 Szeged, Dóm tér 8, Hungary
[2]Department of Inorganic and Analytical Chemistry, University of Szeged, H-6720 Szeged, Dóm tér 7, Hungary
e-mail: eszterorban94@chem.u-szeged.hu

Alumina is typically refined from bauxite ore via the Bayer process, which annually generates more than 2.7 billion tons of red mud/bauxite residue worldwide, and this quantity is still growing by 120 million tons per annum [1]. Currently, almost all bauxite residue is stored indefinitely in land-based red-mud disposal areas, bearing potential environmental risks associated primarily with its alkalinity. Therefore, the decreasing the causticity by means of neutralization is crucial for sustainable alumina production.

Sodalite (SOD, $Na_6[Al_6Si_6O_{24}]\times 2NaX$, where X can be OH^-, Cl^-, NO_3^-, $½CO_3^{2-}$, or $½SO_4^{2-}$) is the dominant phase of all by-products forming during the Bayer process, beside hematite [2]. Although sodalite can contain many different anions (depending on the medium), the isomorph containing OH^- is especially important concerning the alkalinity. Hence, this study focuses on the preparation of hydroxysodalite (HS, $Na_8Al_6Si_6O_{24}(OH)_2$) under well-controlled conditions and the neutralization of this aluminosilicate by hydrochloric acid.

Overall, we found a synthesis method that yields hydroxysodalite with unique cubic morphology. Moreover, our findings shed light on the time duration and mechanism of neutralization of this sodalite.

Acknowledgement
Eszter Kása thanks for the financial support by the National Talent Program (NTP-NFTÖ-22-B-0064) from the source of Human Resource Support Operator.

References
[1] M. Gräfe, C. Klauber, Hydrometallurgy 108 (2011) 46.
[2] J. Vogrin, T. Santini, H. Peng, J. Vaughan, Micropor. Mesopor. Mat. 299 (2020) 110086.

THE IMPORTANCE OF THE CIRCULAR ECONOMY IN THE MANAGEMENT OF PACKAGING WASTE IN SERBIA

Suzana Knežević, Jelena Ignjatović, Milan Glišić

Academy of Vocational Studies Šabac, Unit of Agricultural and Business Studies and Tourism, Vojvode Putnika 56, 15000 Šabac, Srbija
e-mail: jignjatovic985@gmail.com

Abstract
The circular economy, as the antithesis of the linear model of the economy, is considered an imperative for sustainable development and is one of the priorities of economic development in the Republic of Serbia, which will lead to a better economic perspective and sustainable economic growth. In the modern world, there is an increasing use of the circular economy, in which recycling is the leading instrument. Considering that the topic of our work is the importance of the circular economy in the management of packaging waste, it is packaging waste that can be recycled. In fact, packaging waste is any packaging or packaging material that cannot be used for its original purposes, except for residues created in the production process. Contemporary society is characterized by an increasing production of municipal waste, in which packaging waste represents a significant share. The management of packaging and packaging waste is connected with the concept of cleaner production, all with the aim of protecting the environment while respecting the principles of sustainable development. In Serbia, packaging waste is on average 14% glass, 25% plastic, 34% paper and cardboard, 5% metal, 21% wood and less than 1% of the rest. The recycling of packaging waste in accordance with the principle of producer responsibility is supported by seven operators of the packaging waste management system. Packaging waste management in Serbia is on the rise. The specific national goals for the Republic of Serbia in 2020 have been met for the reuse of waste in the value of 62.6% and for the recycling of waste in the value of 60%. Considering that the goal of our work is to point out the importance of the circular economy in the management of packaging waste in Serbia, we conclude that in the coming period we should continue the trend of waste utilization and strive to increase the number of operators.

Keywords: *circular economy, management, packaging, waste, Serbia.*

IMPACT OF AGRICULTURAL MECHANISM ON ANIMALS AND THE ENVIRONMENT

Suzana Knežević[1], Milena Milojević, Goran Stanišić

[1] *Academy of Vocational Studies Šabac, Unit of Agricultural and Business Studies and Tourism, Vojvode Putnika 56, 15000 Šabac, Srbija*
e-mail: sdknez@gmail.com

Abstract
Modern agriculture is characterized by the intensive use of agricultural mechanization. Its impact on animals can be viewed from two aspects - positive and negative. The positive aspect is reflected in better solutions for microclimatic conditions and nutrition on large farms, as well as in the use of artificial intelligence systems for performing work and detecting animals in the fields. The negative aspect is manifested by mechanical injuries, which due to the manipulation of machines and devices, in combination with noise, can lead to the death of animals. In this way, there is a disruption of biodiversity and negative consequences for the environment. Research shows that the greatest damage from agricultural mechanization is suffered by hunting game (rabbits, pheasants, mallards) and birds whose habitats are near or on parts of cultivated agricultural land. Precisely for these reasons, it is necessary to implement measures of prevention and protection of animals when using agricultural machinery.

Keywords: agricultural mechanization, prevention, impact, animals, environment

Introduction
The connection between agricultural machinery and animals is complex - "agriculture by definition involves the use of various tools (many of which must be mobile or portable) and the application of directed force" [1]. In traditional organic production, working animals provide much of the driving force, and also in the early mechanization of agriculture where animals powered machines like threshing machines. In these systems, draft animals are autonomously maintained within the agro-ecosystem and not only provide all the necessary movement power, but also supply society with fertilizers, food and draft power. The process of mechanization was very uneven around the world, shaped by social and environmental constraints [1]. Countries like Great Britain or the USA were highly mechanized in the middle of the 20th century [2], while mechanization is still very low in some countries [3]. Estimates indicate that draft animals are still used on about 50% of the global land area in the year 2000 [4]. The use of modern machines and devices in agricultural works - tillage, harvesting, mowing, application of pesticides, etc., affects hunting game (rabbits, pheasants, lanad), birds as well as grazing animals. Mostly, mechanical injuries and stress reactions occur, which can cause death. Mechanization in animal husbandry can play an important role in the prevention and control of zoonoses. Mechanized equipment kills pathogens more reliably and is more effective in blocking transmission routes. At the same time, many mechanical equipment (used in the production chains of large livestock farms) can: improve the management of the livestock industry, improve labor productivity, increase the efficiency of agriculture, improve the quality of livestock products, and reduce the burden on the environment [5].

Experimental

Modern agriculture is characterized by frequent exposure to cultivated areas, more than ten times a year. Heavy machinery is used for this, which leaves a footprint in the soil that can be compared to the footprint of a dinosaur, it happens in a few seconds, and the elimination of the consequences takes decades. Land loses its ecological, hydrological and agricultural function [6]. All this is accompanied by a negative impact on the animals that live on the cultivated land or its surroundings.

Because of the different plant species, the meadows are habitats for a large number of animals such as birds, reptiles, insects, but also various game where the young are the most endangered and are of exceptional value for biological diversity. Mowing contributes to the preservation of flora biodiversity, but reduces fauna biodiversity.

1. The impact of agricultural mechanization on wild game

Agricultural machinery causes direct and indirect damage to game. Direct damage is caused by the destruction of pheasant nests in alfalfa fields during mowing, as a result of which eggs, young and adult females are killed. Taking into account that crop mowing is done at the time of the most intensive reproduction of feathered game (late spring and early summer), damages can be significant. Rabbits suffer the most from agricultural mechanization, not only during harvest, but also during early spring pre-sowing work. In this period, the losses also have the greatest consequences for the rabbit population, because the female cubs from the spring birth are potential females that should give birth to at least one litter by the end of autumn.

Indirect damage is caused by disturbing and dispersing game, as a result of which the animals migrate to quieter parts of the hunting grounds. This can lead to an increase in the number of wild game on new terrains in a shorter period of time, and this results in increased damage from wild game to forest and agricultural crops. In addition, after cutting and harvesting crops, significant areas are left completely bare, leaving animals without food and shelter. An additional problem is the burning of stubble and corn fields, when game is directly threatened by fire and smoke, and indirectly due to the complete mineralization of organic matter and the destruction of natural food [7].

There are a large number of modern mowers (Figure 1) and harvesters on agricultural land, which are so massive and fast that game in front of them has little chance of survival. A special problem arises when a large number of harvesters work on large areas and game is found in the environment. Then there is increased suffering because the game cannot avoid the danger. Some modern combine harvesters and tractors have built-in safety systems, which are activated when a fawn or other game is found in front of the sharp scythe in wheat and grass [8].

Figure 1. Mowing with modern mechanization of a large work scope [8]

Experts recommend that when mowing the meadow, move from the middle to the outer parts. By mowing directed towards the center of the meadow, game is forced into a trap where it is very likely to die (Figure 2). For those who have meadows on a particularly long area, especially

along the road, it is advised to mow from one side to the other, so that the game has the possibility of sheltering on the neighboring plot, but not on the road. Large areas should be divided into several smaller ones where mowing from the center outwards is also applied.

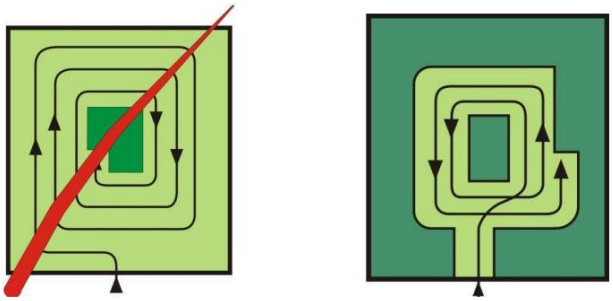

(a) (b)

Figure 2. An example of incorrect (a) and correct (b) mowing of a meadow [8]

Cultivation of monocultures on large areas, with the use of heavy and fast mechanization, as well as the application of artificial fertilizers and plant protection agents, have brought certain species of game as well as some protected species of animals in nature to the brink of survival. A special problem is the use of pesticides. Harms to wildlife from pesticides can occur directly by ingestion of contaminated food or water, by inhalation and/or through the skin [8].

2. The impact of agricultural mechanization on domestic animals

In modern conditions of agricultural production, efficient and economical harvesting and preparation of fodder crops for livestock feeding is unthinkable without the use of suitable highly productive machines, which differ in construction, capacity and quality of work. For corn ensiling on family and commercial farms, self-propelled harvesters of domestic and foreign manufacturers are used [9].

In this way, larger and better quantities of food for animals are provided, which is one of the indirect positive effects of agricultural mechanization on domestic animals.

The robotic husband is becoming more and more common on Serbian family farms and solves the problem of finding workers to work on the farm. The milking robot enables a reduction of the total working time on the farm by 30-40% because milking is performed without human intervention, except for occasional supervision, which causes less disturbance to the animals.

The robot gives freedom, so the cows can be organized in triple or quadruple milking. It is a relief for the cows because they do not have to carry 15-20 liters of milk in their udders, but are allowed to enter the robot for 6-8 hours. There is no dry milk, so the robot stops milking when the milk flow stops, which is very good for the health of the udder. This can be adjusted by the stage of lactation, or by milk production, or by both criteria.

In the beginning, it is best that the cows come to be milked as often as possible. The economic profitability is that it should be 10 liters per husband. Before milking, the cow's udder is washed with lukewarm water, the camera, the milking kit are also washed, and disinfection is carried out so that everything is sterile for the next milking. It is necessary that the number of milkers corresponds to the cow, which stays in the robot for about 6 minutes, with everything going in and out, and the milking itself lasts about 3.5 - 4 minutes per milker.

In the robotic system, it is also an advantage to balance nutrition, literally to the gram, in order to know with certainty that the cow has eaten exactly what it needs. Based on certain indicators in the milk, it is possible to regulate what the cow needs to eat. There is a certain difference,

because not all cows consume the same amount of food, and this certainly affects the quality of the milk [10].

3. The impact of agricultural mechanization on birds

During soil cultivation, as a result of the action of agricultural mechanization, a large number of birds and young birds are killed, most often by destroying their nests on the ground or in low vegetation, on or near cultivated areas. Nests suffer the most from mowers and harvesters, and many of these birds can be used as protection (biological control) of organic orchards and vineyards.

Results and discussion

The paper covers only the segment of negative impacts of agricultural mechanization on animals - hunting game and ground-nesting birds.

One of the ways to prevent the suffering of wild game from agricultural machinery is the use of modern equipped mowers with built-in infrared game detectors that react to their heat and automatically stop the operation of the machine. Microwave sensors are also used, which send microwave rays towards the ground, and they are reflected from objects with a high water content (an animal's body contains 80-90 percent water).

In developed countries, there is also the practice of using drones with infrared cameras that detect the presence of any living creature in the field and thus warn the farmer to react [11].

The use of mechanical scarecrows made of chains hanging from a steel structure placed in front of the rotary mower is also effective. In the Republic of Serbia, according to the Law on Game and Hunting, Article 22, it is stated that it is forbidden to harvest and mow with agricultural machines that do not have built-in devices for driving away or scaring game [12].

Research conducted in the Czech Republic indicates that the problem of destroying the nests of ground-nesting birds can be alleviated by marking the nests with long bamboo poles whose tip is marked in red or orange. The experiment was performed on 52 pairs of bird nests that nest on the ground - one marked and one unmarked (reference), lasted three years and showed positive effects of protection against the effects of agricultural mechanization [13].

Conclusion

The results of research into the impact of agricultural mechanization on animals unequivocally indicate that this impact is significant. Special attention should be paid to the negative consequences and the way of their prevention and elimination. In eliminating those consequences, the application of new technologies based on the use of drones equipped with thermal imaging cameras plays a significant role. The positive effects are mainly related to the feeding of domestic animals on large farms, the use of robotic systems for milking cows, as well as the important role in the prevention and control of zoonoses.

References

[1] E. Aguilera, G.I. Guzmán, M. González de Molina, D. Soto, & J, Infante-Amate. From animals to machines. the impact of mechanization on the carbon footprint of traction in Spanish agriculture: 1900–2014. Journal of Cleaner Production, 221, (2019) 295–305. https://doi.org/10.1016/j.jclepro.2019.02.247

[2] H. Binswanger, Agricultural Mechanization. The World Bank Research Observer, 1(1), (1986) 27–56. https://doi.org/10.1093/wbro/1.1.27

[3] P. Pingali, Chapter 54 agricultural mechanization: Adoption Patterns and Economic Impact. Handbook of Agricultural Economics, (2007) 2779–2805. https://doi.org/10.1016/s1574-0072(06)03054-4

[4] Wilson, R. T. (2003). The environmental ecology of oxen used for draught power. Agriculture, Ecosystems & Environment, 97(1-3), (2003) 21–37. https://doi.org/10.1016/s0167-8809(03)00118-x
[5] UN.ESCAP "Mechanization solutions for improved livestock management and prevention and control of zoonotic diseases". Institutional Repository - ESCAP. ESCAP (2020) Web. 14 oct 2022 https://hdl.handle.net/20.500.12870/4467
[6] C.H. Jaynes Modern farm vehicles heavier than dinosaurs can damage soil for decades, study finds. EcoWatch. (2022, May 18). Retrieved October 15, 2022, from https://www.ecowatch.com/heavy-farm-vehicles-soil-damage.html
[7] M. Beuković & Z. Popović, Lovstvo, Poljoprivredni fakultet Novi Sad (2014).
[8] N. Irić, "Stradavanje divljači od poljoprivredne mehanizacije." Završni rad, Veleučilište u Karlovcu, (2015). https://urn.nsk.hr/urn:nbn:hr:128:534067
[9] R. Koprivica, B. Veljković, N. Stanimirović, & G. Topisirović, Performance characteristics of the John Deere 5820 harvester used for preparing maize silage for dairy cattle on family farms. Poljoprivredna tehnika (2009). Retrieved October 15, 2022, from https://scindeks.ceon.rs/article.aspx?artid=0554-55870903023K.
[10] Redakcija, Robotizovana muža - prednosti Robota U stočarstvu. Agro saveti. (2021, March 26). Retrieved October 16, 2022, from https://www.agrosaveti.rs/stocarstvo/govedarstvo/robotizovana-muza-prednosti-robota-u-stocarstvu/.
[11] M.C. Celić, Nitko ne želi Pokositi Mladunčad divljači - što poduzeti da se to ne dogodi? Agroklub.com. (2021, May 13). Retrieved October 16, 2022, from https://www.agroklub.com/ratarstvo/nitko-ne-zeli-pokositi-mladuncad-divljaci-sto-poduzeti-da-se-to-ne-dogodi/68235.
[12] Zakon o divljači i lovstvu, "Sl. glasnik RS", br. 18/2010 i 95/2018 – dr.zakon. Available at https://www.paragraf.rs/propisi/zakon_o_divljaci_i_lovstvu.html.
[13] V. Zámečník, V. Kubelka, & M. Šálek, Visible marking of wader nests to avoid damage by farmers does not increase nest predation. Bird Conservation International, 28(2), (2018), 293-301. https://doi.org/10.1017/S0959270916000617.

CHEMOMETRIC COMPARISON OF THE RETENTION BEHAVIOR OF TRIAZINE DERIVATIVES IN RP-UHPLC SYSTEM WITH C18 AND PHENYL COLUMNS AND AQUEOUS MOBILE PHASES WITH METHANOL AND ACETONITRILE AS MODIFIERS

Benjamin Salaković[1], Strahinja Kovačević[1], Milica Karadžić Banjac[1], Jasmina Anojčić[2], Lidija Jevrić[1], Sanja Podunavac-Kuzmanović[1]

[1]University of Novi Sad, Faculty of Technology Novi Sad, Department of Applied and Engineering Chemistry, Bulevar cara Lazara 1, 21000 Novi Sad, Serbia
[2]University of Novi Sad, Faculty of Sciences, Department of Chemistry, Biochemistry and Environmental Protection, Trg Dositeja Obradovića 3, 21000 Novi Sad, Serbia
e-mail: strahko@uns.ac.rs

Abstract

Hierarchical cluster analysis (HCA), as a chemometric pattern recognition method, was applied on chromatographic data of triazine derivatives. The triazine derivatives (8 compounds) with cyclic and acyclic substituents were analyzed applying reversed-phase ultra high performance liquid chromatography (RP-UHPLC). The chromatographic analysis was carried out on C18 and phenyl columns with binary and ternary mobile phases (methanol/water, acetonitrile/water and methanol/acetonitrile/water) with variations in fractions of the modifiers (methanol and acetonitrile) in the mobile phase [1-3]. The retention behavior was described by log$k$, logk_0, C_0 and S parameters. Prior to HCA, the retention data were normalized by *min-max* normalization method. The HCA was carried out by using Python program based on Euclidean distances and Ward's algorithm. Based on the obtained dendrogram, it can be noticed that there is a clear separation of the triazine derivatives based on the presence of acyclic and cyclic substituents in their structure. This indicates statistically significant retention behavior of these two groups of triazine derivatives in the applied chromatographic systems.

Acknowledgements

The present research is financed in the framework of the project of Provincial Secretariat for Higher Education and Scientific Research of AP Vojvodina (Project: Molecular engineering and chemometric tools: Towards safer and greener future, No. 142-451-2563/2021-01/01).

References

[1] B. Salaković, S. Kovačević, M. Karadžić Banjac, J. Anojčić, L. Jevrić, S. Podunavac-Kuzmanović, S. Gadžurić, D. Antonović, VII International scientific-professional symposium "Environmental resources, sustainable development and food production" – OPORPH 2021, Book of abstracts, Tuzla, (2021) 21.
[2] B. Salaković, S. Kovačević, M. Karadžić Banjac, J. Anojčić, L. Jevrić, S. Podunavac-Kuzmanović, S. Gadžurić, D. Antonović, 27th International Symposium on Analytical and Environmental Problems, Szeged, Proceedings (2021) 297.
[3] B. Salaković, S. Kovačević, M. Karadžić Banjac, J. Anojčić, L. Jevrić, S. Podunavac-Kuzmanović, S. Gadžurić, D. Antonović, PHYSICAL CHEMISTRY 2021: 15th International Conference on Fundamental and Applied Aspects of Physical Chemistry, Belgrade, Proceedings (2021) 36-39.

FUTURE QUANTITIES OF SLUDGE FROM WASTEWATER TREATMENT PLANTS ON THE TERRITORY OF AP VOJVODINA

Srđan Kovačević[1], Srđan Kolaković[2], Nemanja Stanisavljević[1], Nikolina Tošić[1], Marko Muhadinović[3]

[1]Department of Environmental Engineering and Occupational Health and Safety, Faculty of Technical Sciences, University of Novi Sad, Trg Dositeja Obradovića 6, 21000 Novi Sad, Republic of Serbia, e – mail: srdjankovacevic@uns.ac.rs
[2]Department of of Hydrotechnics and Geodesy, Faculty of Technical Sciences, University of Novi Sad, Trg Dositeja Obradovića 6, 21000 Novi Sad, Republic of Serbia
[3]Lafarge Beocin Cement Plant, Trg Beočinske fabrike cementa 1, 21300 Beočin, Republic of Serbia

Abstract
In the framework of the research, an assessment of the future amount of waste sludge that would be generated after the construction of the planned 200 waste water treatment plants (WWTPs) that should be built on the territory of Autonomous Province of Vojvodina in the Republic of Serbia was carried out. It is estimated that the annual production of waste sludge will be slightly more than 81 thousand tons (dry sludge) per year. The methods of sustainable use (circular economy of sludge) and the method of safe disposal of sludge resulting from wastewater treatment were also analyzed. Starting from the possible use in Anaerobic Digestion processes for recharging biogas, the residual sludge from Anaerobic Digestion is excellent for use in agriculture. Well-watered sludge can also be used in the cement production industry, or if the sludge is burned (to reduce the final amount of waste), the ash can be used in the construction industry for the production of bricks or concrete/mortar, and finally sludge has potential for possible use for recharging biofuel, bio-plastic etc. Finally, there is a real potential for the use of waste sludge in AP Vojvodina.

Introduction
Due to Serbia's need to reach the EU water treatment and protection standard and Water framework Directive goals, the construction of about 200 WWTPs on the territory of Autonomous Province – AP Vojvodina is planned. Wastewater contains a large number of different compounds, such as solid matter (350-1200 mg/l), dissolved matter (HPK 250-1000 mg/l), microorganisms, nutrients, heavy metals and micro-pollutants [1]. As a result of wastewater treatment, on the one hand, water that is safe for discharge to the water recipient is obtained, and on the other hand, waste sludge remains, which represents a mixture of water (in different ratios of 20-95%), living and dead microorganisms, organic matter , organic and inorganic chemical compounds [2]. This recharged sludge must be transferred so that it can be disposed of safely or it can be used for recharging energy, biofuel, bioplastics, as a fertilizer in agriculture, etc.
Waste sludge created at WWTP can be divided according to the type of technological process in which it was created into primary, secondary (or biological) and chemical. Raw sludge is sludge that has not yet undergone biological or chemical treatment to remove or reduce the concentration of solid and organic matter or pathogens. When sludge treatment is carried out, the so-called treated sludge (eng. biosolid) which can be classified by treatment, such as: (I) Aerobically digested; (II) Anaerobic digestion AD); (III) Alkaline stabilized; (IV) Composted; (V) Thermally dried.

Amount of sludge produced

Determining the amount of sludge that will be generated at the WWTP is very important for the design of the system for the reception, treatment and disposal of sludge and for the treatment of waste water [3].

The best approach for estimating the amount of sludge generated is to base it on data from similar plants (size, technological process, wastewater characteristics) and the expected amount of wastewater for treatment. The specific weight of the sludge can also be calculated using the following formula (formula 1 – wehere SS is: suspended solids) [4]:

$$Specific\ weight\ of\ sludge\ = \frac{1}{\left(\frac{\%\ SS\ \ in\ sludge}{Sludge\ density} + \frac{\%\ sludge\ water\ content}{1.0}\right)} \quad (1)$$

Incorporation of solid materials is also known as solids capture. It is usually expressed in percentages to show the effectiveness of incorporation of solid materials in the body, which will then be treated in the following stages of the transformation. Solid matter loading [kgSS/day] can be represented by expressions 2 and 3 [4]:

$$Effluent\ SS\ load\ in\ sludge\ = Solids\ capture\ \times\ Influent\ SS\ load\ in\ sludge \quad (2)$$

$$SS\ load\ in\ drained\ liquid\ = (1\ -\ Solids\ capture)\ \times\ Influent\ SS\ load\ in\ sludge \quad (3)$$

Table 1 - Characteristics and quantities of mud produced by different processes [4]

Technological process in WWTPs	Karakteristike proizvedenog mulja iz otpadnih voda		
	SS content (%)	Sludge mass (gDS/ES·day)	Sludge Volume (L/PE·day)
Activated Sludge			
• Primary Sludge	2 – 6	35 – 45	0.6 – 2.2
• Secondary Sludge	0.6 – 1	25 – 35	2.5 – 6.0
• Total	**1 – 2**	**60 – 80**	**3.1 – 8.2**
Activated sludge with extended aeration	0.8 – 1.2	40 – 45	3.3 – 5.6
Aerated lagoon	6 – 10	8 – 13	0.08 – 0.22

Production of primary sludge

The amount of sludge generated during the primary treatment depends primarily on the efficiency of the removal of suspended solids (SS) in the primary settling tanks. The typical efficiency in removing od SS in primary flocculation machines is 60 to 65%. the trace of SM removal can be related to the time of hydraulic retention or the surface overflow of the primary clarifier (engl. primary clarifier).

Production of activated sludge

In the activated sludge process, important variables in the quantification of the produced sludge are: the amount of removed substrate (COD or BOD), the mass of microorganisms in the system and non-biodegradable inert SS. The calculation of the net growth of biomass and the amount of waste activated sludge (WAS) is carried out using expressions 4 and 5 [5]

$$P_x = Y(S_0 - S) - k_d X \quad (4)$$

$$WAS = P_x + I_0 - E_t \quad (5)$$

P_x -net growth of biomass expressed as volatile solid substances (VSS, kg/d); Y - gross yield coefficient (kg/kg); S_0 - Influent substrate (COD or BOD kg/d) ;S - Effluent substrate (COD or BOD kg/d);k_d- Coefficient of endogenous decomposition (d-1);X-Biomass at the aeration pool (MLVSS, kg).
Solids Retention Time (SRT), also known as sludge age, is a very important parameter in the process of biological purification with activated sludge. SRT represents the average retention time of sludge in the system and is represented by taxes.

Results and discussion

Quantity of sludge rechargeed from WWTPs in AP Vojvodina

Management of sludge produced at WWTPs represents one of the most difficult problems to be solved. Sludge produced at WWTP represents only a few percent of the volume of processed waste water (after dewatering and condensation), but its treatment and disposal make up to 50% of total operational costs. To calculate the (theoretical) amount of sludge that will be produced as a result of wastewater treatment, we will use the data from table 1.

Table 1 – WWTPs capasity in EP – Population equivalent by regions in AP Vojvodina [6]

Region	Total capacity [EP]
West Bačka	388.200
North Bačka	280.000
North Banat	237.620
South Bačka	879.500
Middle Banats	214.300
South Banatska	394.000
Srem	403.900
Total	**2.797.520**

Table 2 – The amount of sludge produced from WWTPs in AP Vojvodina by regions

Oblast	**Total capacity [ES]**	**Sludge production i WWTPs [tons dry sludge]**	
		daily	**annually**
South Bačka	879.500	70	25.550
South Banat	394.000	32	11.680
North Bačka	280.000	22	8.030
North Banat	237.620	19	6.935
Middle Banat	214.300	17	6.205
Srem	403.900	32	11.680
West Bačka	388.200	31	11.315
Total	**2.797.520**	**223**	**81.395**

The value of waste sludge in the context of the circular economy

Increasing the amount of sludge from wastewater treatment is a global problem in the context of population growth and adequate sanitary protection. Although sludge is considered waste, it can be used as a source of energy or resource, thus replacing an equivalent amount of material and/or energy that should otherwise be provided from non-renewable sources. The treatment and disposal of sludge is very important for the protection of the environment, because of possible organic pollutants, heavy (and toxic) metals and pathogens that can linger in the sludge, which can cause health problems.

The circular economy represents the antithesis of the previous linear model of the economy, which implies the uncontrolled exploitation of natural resources and the flow of materials from the factory through the user to the landfill.

According to the Ellen MacArthur Foundation (EMF), the circular economy is: reconstructive and regenerative by design and aims to make products, components and materials maximally useful and valuable at every moment [7]. Because of the legislation that limits the disposal of sludge at the landfills, as a method of sludge removal, many researchers have tried to find ecologically sustainable ways to reuse sludge. The European Commission considers that "as waste becomes a resource that returns to the economy as raw material, then much greater priority must be given to reuse and recycling" [8]. The reuse of sludge as a raw material in various industries represents an excellent way of managing waste, having in mind the concept of circular economy. Taking into account the fact that the organic components of the sludge are a significant resource in terms of energy and nutrients that are waiting to be used, a study carried out in 2015 by the International Solid Waste Association (ISWA) [9] shows that in the context of the circular economy, the benefit of energy and fuel recharged from waste is that they can replace other energy resources and limit the associated CO_2 emissions.

Nutrients reuse

Considerable amounts of nutrients (approximately 0.5–0.7% phosphorus and 2.4–5.0% nitrogen) are found in sludge, in the form of proteinaceous materials that can be used for fertilizer production. The return and recycling of phosphorus is considered a possible pilot, i.e. case where it can be "proven that circular principles function in practice" [7]. Crystallization is a process that is used to recover phosphorus from WWTP in the form of struvite (NH_4MgPO_4). In the research [10], referring to municipal waste water, TSS from 26-30 kg/EP/year. and tangential fraction from the appropriate fermentation of celluloid mud, it is estimated that 0.07 – 0.15 kg/EU/year can be produced. struvita, which corresponds to income from 0.05 – 0.11 €/EP/year.

Construction material

Complexes of organic carbon and inorganic composites from mud represent the source of valuable materials that can be transformed into products such as artificial lightweight aggregates, clay, bricks and glass by means of thermal processing. For the production of bricks and cement, mud can be used directly without burning. Supplying sludge in its raw form to cement production can be an alternative to existing methods, eliminating some expensive and energy-intensive phases of sludge treatment/disposal. Even more important is that environmentally harmful waste can be turned into a safe and stable product.

Biogas

The primary source of energy at the WWTP is biogas produced by AD reactors, with a content of methane (50–70%) and carbon dioxide (30–50%), as well as some trace nitrogen, hydrogen, hydrogen sulfide and water vapor. AD is one of the most used technologies for the production of biogas at WWTPs. Taking into account that biogas can be used to recharge electricity and heat energy, water vapor and other purposes, its production and maximum utilization are of essential importance.

Conclusion

When it comes to wastewater treatment in AP Vojvodina, the situation is very bad. About 20% of total wastewater (municipal + industrial) is treated, and waste sludge is deposited in landfills. Since there is no legal regulation related to the treatment and disposal of sludge, there is no way to use it efficiently and safely, especially in agriculture.

Because of the EU accession tasks, Serbia must make great efforts in water management, and waste water treatment plays perhaps the most significant role.

As part of the effort to improve the current situation, the study "Investigation and development of the AP Vojvodina waste water collection and treatment model" [6] was conducted, which considered the settlements behind which the WWTP will be built, as well as the required size, treatment technology, etc. The construction of 200 WWTPs for the territory of Vojvodina is planned. As shown in table 2, the planned WWTP should be sufficient for the treatment of 2.8 million PE, which is considered sufficient considering the growth of population and industry in the next 30 or so years. Based on these parameters and the data from table 3, it is estimated that the annual production of waste sludge will be slightly more than 81 thousand tons (dry sludge) per year.

When it comes to the EU, data on the use of waste sludge and the technologies used vary widely. It is estimated that in 2008, more than 10 million tons of dry sludge was produced in 26 EU countries, of which 36% was used in agriculture. However, 5 out of 26 countries (Germany, England, France, Italy and Spain) contributed as much as 75% of the total amount of sludge production [11].

It can be concluded that there is a real potential for the use of waste sludge in AP Vojvodina. Starting from the possible use in AD processes for recharging biogas, the residual sludge from AD is excellent for use in agriculture. Well-watered sludge can also be used in the cement production industry, or if the sludge is burned (to reduce the final amount of waste), the ash can be used in the construction industry for the production of bricks or concrete/mortar, and finally sludge has potential for possible use for recharging biofuel, bio-plastic etc.

Of course, not all applications are equally economically profitable in the case of the Republic of Serbia (even regionally), so a detailed LCA analysis is necessary to select the most profitable use, and this is beyond the scope of this advice.

References

[1] M. Von Sperling, Biological Wastewater Treatment Vol. 1: Wastewater Characteristics, Treatment and Disposal, vol. 1. IWA Publishing, 2007.

[2] S. R. Smith, (2009) “Management, Use, and Disposal of Sewage Sludge,” Waste Manag. Minimization, no. 2, 2009.

[3] Metcalf & Eddy, Wastewater Engineering: Treatment and Resource Recovery, 5th Editio. McGraw-Hill Education, 2014.

[4] C.V. Andreoli, M. Von Sperling, F. Fernandes, M. Ronteltap (2007) Biological Wastewater Treatment Vol. 6: Sludge Treatment and Disposal. IWA Publishing.

[5] I. S. Turovskiĭ and P. K. Mathai (2006) Wastewater sludge processing. Wiley-Interscience,

[6] Kolaković et al., (2013) “Research and development of a waste water collection and treatment model in support of the spatial planning documents of the settlement and AP Vojvodina”.

[7] Ellen Macarthur Foundation; McKinsey & Company (2015), “Growth within: a circular economy vision for a competitive europe,”.

[8] European Commission, (2012) “Communication from the Commission to the European Parliament, the Council, the European Economic and Social Committee and the Committee of the Regions. Roadmap to a Resource Efficient Europe,”

[9] “ISWA: Task Force Resource Management.” https://www.iswa.org/iswa/iswa-groups/task-forces/task-force-resource-management/

[10] D. Crutchik, N. Frison, A. L. Eusebi, and F. Fatone (2018) “Biorefinery of cellulosic primary sludge towards targeted Short Chain Fatty Acids, phosphorus and methane recovery,” Water Res., vol. 136, pp. 112–119, Jun. 2018, doi: 10.1016/j.watres.2018.02.047.

[11] Eurostat, “Sewage sludge production and disposal,” 24-02-2020, (2020) https://appsso.eurostat.ec.europa.eu/nui/show.do?dataset=env_ww_spd&lang=en

ROSEHIP (*ROSA CANINA*) AS A MEDICINAL PLANT IN FRUIT GROWING

Kurjakov Aleksandar[2], Blagojević Milan[1], Rašković Vera[1], Stošić Nemanja[1], Jelena Robinić[1], Stefan Marković,[1] Vlajić Sobodan[3]

[1] Academy of Applied Studies Šabac. Unite for Agricultural Business Studies and Tourism, Republic of Serbia
[2]Van Iperen, Novi Sad, Serbia
[3]Institute of Field and Vegetable Crops, Novi Sad, Serbia
e-mail: markovicstefaan@gmail.com

Abstract

Rosehip (*Rosa canina)* is a modest plant in terms of the requirements and conditions of growth and cultivation, so it has a very wide distribution area and belongs to the Rosaceae family. However, rose hips are a real treasure trove of vitamin C, where certain selections can contain up to 5 g of vitamin C per 100 g of fruit. Rosehip is extremely rich in K, carotenoids lycopene and B carotene, invert sugar and sucrose, pectins and tannins, and the oil and phospholipids found in rosehip oil. It is mostly collected from natural populations, and there are very few plantations under sipura, although there are good conditions for it. Many rosehip clones have been selected in the world, both from the Japanese rose (*Rosa rugosa*) and from the dog rose (*Rosa canina*). During 2022, the level of vitamin C was measured on the genotypes at the Sombor locality, and the variations were from 237.4 to 1752 g of vitamin C. The clones are large-fruited, very robust, with few or no spines, especially on the part of the shoot where the fruits are placed, so harvesting is much easier. Several such clones originating from the Czech Republic are propagated and grown in Serbia on rather modest areas. The reason for this is the lack of information on the part of producers, the lack of planting material and the lack of interest from buyers. In the last few years, however, there has been a growing interest in rose hips as organic food. Rosehip can be grown as a subculture with walnut or as an intercrop with apricot or peach. Harvesting of rose hips for processing is done at full technological maturity, i.e. when the fruit is completely red. Rosehip ripens at the end of August and the beginning of September. Harvesting is done by hand in auxiliary vessels, and then it is delivered to shallow open vats in which it is delivered to the market. Exceptionally, rose hips can be packed in red plastic bags with a volume of 6-10 kilograms. Considering that one well-kept bush can produce 5-6 kilograms or more, that is, the yield per hectare can be around 10 tons or more. The exploitation period of šipurka is 20-25 years.

APPLICATION AND DEVELOPMENT OF A METHOD FOR ESTIMATING GEOGENIC RADON POTENTIAL

Robert Lakatoš[1], Sofija Forkapić[2], Ljiljana Gulan[3], Selena Samardžić[1], Dušica Spasić[3], Jelena Živković-Radovanović[3], Jan Hansman[2]

[1]Faculty of Technical Sciences, University of Novi Sad, Trg Dositeja Obradovića 6, Novi Sad, Serbia
[2]Faculty of Sciences, University of Novi Sad, Department of Physics, Trg Dositeja Obradovića 4, Novi Sad, Serbia
[3]Faculty of Sciences and Mathematics, University of Priština in Kosovska Mitrovica, Lole Ribara 29, Kosovska Mitrovica, Serbia
e-mail: laki@uns.ac.rs

Abstract
The process of radon migration from the Earth's crust is a complex process and depends on several parameters, such as: soil permeability, radium and uranium concentrations in soil, presence of cracks, variation of temperature and pressure, and other environmental parameters. Radon-priority areas are common defined in two ways, the first is by direct measurement of the radon indoor concentrations, and the other by indirect testing of radon in the soil and geological parameters, all to find a dominant transport of radon to the interior of buildings. In this study a new method for estimation geogenic radon potential was developed. Based on the percentage weight of fine fraction in soil samples and measured radon concentrations in soil, the geogenic radon potential was estimated. The proposed method was applied in two distinguished regions of Serbia with different geological substrate and the obtained results were discussed and compared in this study. Soil gas radon concentrations vary between 5 and 81 kBq/m^3 indicating variability in radium and uranium content and soil granulation related to different parent soil lithologies.

Introduction
Radon maps that aim to labels radon-prone areas in Europe are most often defined through radon in soil measurements and geological parameters [1, 2, 3]. Geogenic radon potential GRP could be estimated using the soil granulometric composition which affects soil permeability for radon and the presence of radon in the soil. The methodology of GRP determination proposed in [4] which is based on radon indexes according to the weight percentage of fine fraction in soil (particles smaller than 65 μm) and radon in soil gas concentrations (Table 1) was used. Soils with the weight percentage of the fine fraction below 15% are classified as high permeable, in the range 15-65% as medium permeable, and in the case of the fine fraction above 65% as low permeable.

Table 1. Assessment of radon index (risk) [4]

Radon index classification	Soil gas radon concentration C [kBq/m^3]		
Low	C<30	C<20	C<10
Medium	30≤C<100	20≤C<70	10≤C<30
High	C≥100	C≥70	C≥30
	Low permeability	Medium permeability	High permeability

A method that includes soil permeability estimates and radon in soil concentration measurements was used to assess radon potential for the first time in our region, mainly in Vojvodina region - the Northern Province of Serbia. Vojvodina region (Northern Province of Serbia) is a distinctly flattened lowland with altitudes of 68 to 120 m that belongs to the southern parts of the Pannonian Basin. It was mostly formed at the beginning of the Miocene by deposition of marine sediments: conglomerates, sandstones, marls, and clays. During the Pliocene, the Pannonian Sea has been transformed into the Pannonian Lake, or a system of lakes that are more like ponds and swamps. At this stage, in Vojvodina part of the Pannonian Basin deposited a large amount of sediment (paludal layers-sand, sandy siltstones, siltstones, and clay) [5]. And finally, in the Pleistocene (Quaternary era), the aeolian process during the inter-glacial formed light sediments loess - the most important parent substrate in Vojvodina, on which the agricultural land was created [6].

To examine the effect of lithological types to GRP, study was continued on three locations (Sokolica, Grabovac and Rudare) near the town Kosovska Mitrovica on the south which belongs to Vardar's zone with volcanic rocks in the geological substrate. This is a hilly terrain with an elevation from 520 to 720 m a.s.l. close located to Trepča, one of the largest industrial and mining complexes of Europe, included 40 mines, several flotation tailings, smelters and few factories. The local geology is characterized by numerous rocks like schists, sandstones, phyllites and quartzites formed in the Paleozoic era and magmatic rocks from Triassic (diabase, basalts and serpentinites). Quaternary fluvial and alluvial deposits overlap the terrain along the River Ibar valley [7]. However, vulcanite from Miocene (dacites, andesites and latites) dominate in the study area with sedimentary rocks of the Jurassic age such as marls, sandstones, shales and argillites. Hence, in the geotectonic and seismic terms examined area is characterized by different vertical movements forming a network of seismogenic faults that classified it as a moderate seismic area [8, 9].

Experimental

On 17 locations covering several geological units, the soil gas radon concentrations were accompanied by gamma spectrometry analysis of soil, indoor radon measurements (active and passive testing), and particle size distribution of soil samples. Indoor radon concentrations in selected houses were determined by several methods: passive by charcoal canisters or CR39 track detectors or active with the RAD7 (Durridge Company Inc.) radon monitor. Radon in soil concentrations were measured by RAD7 active device using sniff mode and grab protocol. The stainless soil gas probe was inserted to the depth of 80 cm from which 3.5 l of soil gas was extracted during the pumping (the airflow rate was about 0.7 l/min). Soil samples were taken from the given location, as well as stone, which was probably used in the construction of the house for gamma spectrometric analysis of radionuclide content. These samples were dried to constant mass, crushed, sieved and packed in plastic boxes of cylindrical geometry which were hermetically sealed and left for 40 days to establish a secular radioactive equilibrium. Gamma spectrometric measurements were performed with HPGe detector GMX type, with a resolution of 1.9 keV and a nominal efficiency of 32%. The passive protection around the detector is made of 12 cm thick lead. Gamma spectra were collected and analyzed using Canberra Genie 2000 software. Gamma lines of first daughter ^{234}Th were used to determine the activity concentration of uranium ^{238}U. A particle size distribution analysis was conducted using a Malvern Mastersizer 2000 Particle Size Analyzer capable of analyzing particles between 0.02 μm and 2000 μm. Based on particle size analysis the following fractions were determined: coarse sand (500-2000 μm), medium sand (250-500 μm), fine sand (62.5-250 μm), silt (3.9-62.5 μm), and clay (<3.9 μm).

Results and discussion

Based on the obtained values of the percentage weight of fine fraction in soil samples and measured radon concentrations in soil, the geogenic radon potential was estimated according to the criteria given in Table 1, and the results for the tested sites are shown in Table 2. GRP estimations are compared to maximal indoor radon concentrations measured in the neighboring houses and activity concentrations of radium, thorium and uranium detected in soil.

Table 2. Maximal indoor radon concentrations and radon in soil concentrations with radium, thorium and uranium concentrations in soil samples collected from the surrounding areas of houses with a percentage of fine fractions and GRP estimations

Location	^{222}Rn indoor [Bq/m^3]	^{226}Ra [Bq/kg]	^{232}Th [Bq/kg]	^{238}U [Bq/kg]	^{222}Rn in soil [kBq/m^3]	fine fraction (<65 μm) %	GRP
Sremska Mitrovica1	135(49)	29.8(1.4)	44(3)	< 40	32.2(2.8)	41.93	Medium
Sremska Mitrovica 2	380(6)	33(5)	47.2(2.9)	31(12)	25.1(2.5)	45.61	Medium
Sremska Mitrovica 3	133(49)	39.4(1.9)	46(10)	< 70	35(3)	45.99	Medium
Bački Petrovac	334(11)	37(6)	53(3)	25(11)	46(3)	59.49	Medium
Kulpin	144(6)	30.0(2.5)	41.3(2.1)	24(8)	12.8(1.7)	45.35	Low
Petrovaradin	173(10)	28.8(1.9)	35(6)	34(7)	10.5(1.7)	42.06	Low
Šajkaš	26(4)	33(3)	34(6)	51(13)	5.0(1.2)	51.14	Low
Beška	79(6)	24.2(1.4)	34(8)	26(21)	9.0(1.5)	40.28	Low
Novi Sad 1	110(7)	23.0(2.2)	28.8(2.6)	15(8)	21.7(2.3)	29.48	Medium
Novi Sad 2	90(6)	23.8(1.8)	24.8(2.1	< 12	5.9(1.2)	42.81	Low
Kikinda	54(6)	17.6(1.4)	27.4(2.0)	< 16	8.8(1.5)	35.27	Low
Novi Bečej	238(63)	26.3(1.7)	31.5(2.0)	37(5)	8.8(1.5)	38.44	Low
Čonoplja	262(9)	33.8(2.0)	32(10)	28(9)	12.6(1.7)	66.25	Medium
Sombor	384(78)	38(4)	45(10)	34(8)	1.1(0.6)	64.62	Low
Sokolica	362(78)	61.5(1.7)	88(3)	155(8)	81(5)	26.68	High
Grabovac	926(199)	67.9(0.9)	83(3)	134(7)	28.7(2.7)	28.78	Medium
Rudare	2843(217)	50.3(1.0)	79.4(2.8)	106(6)	7.5(1.3)	32.37	Low

The activity concentrations of natural radionuclides in three soil samples from Kosovo and Metohija are above the usual values for agricultural land in Vojvodina, for which there is a rich system of measurements [10]. Also, the particle size distributions for these three soil samples are shifted towards a larger fraction (Figures 1) and based on that higher soil permeability and higher GRP could be expected. However, on Grabovac and Rudare locations moderate and low radon concentrations in soil were detected (28.7±2.7 kBq /m^3 and 7.5±1.3 kBq/m^3, respectively). which implies the moderate and low radon risk index. Large variations in indoor radon concentration in the house in Rudare can be explained by the existence of a deep fault zone and a seismotectonic zone in the vicinity of Kosovska Mitrovica that allows the transport of radon through cracks during the mining or other seismic activities. Unlike the soil in Kosovo and Metohija, the land of Vojvodina has granulation shifted to a finer fraction and thus the assessment of the radon potential to moderate and low.

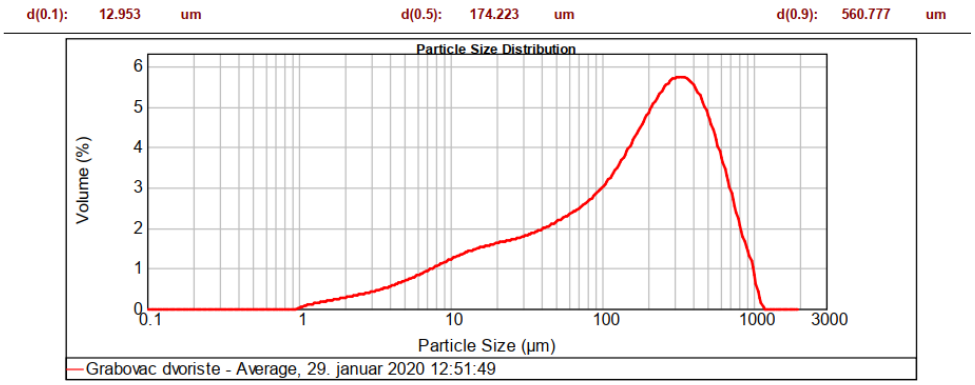

Figure 1. Particle size distribution of soil sample from Grabovac near Kosovska Mitrovica

Conclusion

The estimated geogenic radon potential of the sites shows the previously stated claims that the indoor radon concentration is not closely related to the estimation of GRP. According to obtained measurements and soil type comparison it was point out that in soils originated from the oldest (volcanic) rocks the particle size distributions are removed towards a larger fraction. unlike to youngest lithological types of soils (alluvium and loess) which particle size distributions are shifted to the fine fraction. The particle size distribution is one more factor which can be used in radon potential estimations. The need for further radon investigations in the mining area of Rudare is emphasized according to the obtained high radon levels in houses.

Acknowledgements

The authors acknowledge financial support of the Ministry of Education. Science and Technological Development of the Republic of Serbia (Grant No. 451-03-68/2020-14/ 200125; Grant No. 451-03-68/2020-14/200156: "Innovative scientific and artistic research from the FTS (activity) domain" and Grant No. 451-03-9/2021-14/200123).

References

[1] G.Cinelli. L.Tositti. B.Capaccioni. E. Brattich and D.Mostacci. 2014. Soil gas radon assessment and development of a radon risk map in Bolsena. Central Italy. Environ Geochem Health DOI 10.1007/s10653-014-9649-9

[2] Miles. J.C.H.. Appleton. J.D.. 2005. Mapping variation in radon potential both between and within geological units. J. Radiol. Prot. https://doi.org/10.1088/0952-4746/25/3/003

[3] Kemski. J.. Siehl. A.. Stegemann. R.. Valdivia-Manchego. M.. 2001. Mapping the geogenic radon potential in Germany. in: Science of the Total Environment. https://doi.org/10.1016/S0048-9697(01)00696-9

[4] I. Barnet. P. Pacherova. M.N.. 2008. Radon in geological environment—Czech experience Czech Geological Survey Special Papers. No. 19. Prague.

[5] V. Hadžić. P Sekulić. J. Vasin. Ljiljana Nešić: GEOLOGICAL BASIS OF THE LAND COVER OF VOJVODINA. EKONOMIKA POLJOPRIVREDE 4/2005. UDK: 631.434:550.8(497.113)

[6] Košćal. M.. Menković. Lj. Knežević. M.. Mijatović. M.. 2005. Geomorphological Map of Vojvodina with Interpreter. Geozavod - Gemini Belgrade. Republic of Serbia - AP Vojvodina. Executive Council of AP Vojvodina Provincial Secretariat for Energy and Mineral Resources. Novi Sad.

[7] Geological Atlas of Serbia 1:2000000. 2002. The Serbian ministry of natural resources and environmental protection. Barex. Belgrade.

[8] Dimitrijević. M.D.. 1997. Geology of Yugoslavia. Geol. Inst. GEMINI. Belgrade

[9] Giardini. D.. Woessner. J.. Danciu. L.. Crowley. H.. Cotton. F.. Grünthal. G.. Pinho. R.. Valensise. L. and the SHARE consortium. 2013. SHAREEuropean Seismic Hazard Map for Peak Ground Acceleration. 10% Exceedance Probabilities in 50 years. Swiss Seismological Service. ETH Zurich. https://doi.org/10.2777/30345

[10] Bikit I. Slivka J. Conkic L. Krmar M. Veskovic M. Zikic-Todorovic N. Varga E. Curcic S. Mrdja D: Radioactivity of the soil in Vojvodina (Northern Province of Serbia and Montenegro). Journal of Environmental Radioactivity. 2004. Vol. 78. No. 1. str. 11- 19.

APPLICATION OF AN INDUCED FLUOROMETRY-BASED METHOD IN ALGAL GROWTH INHIBITION TESTS

Diána Lázár[1], Szandra Klátyik[1], Eszter Takács[1], Attila Barócsi[2], László Kocsányi[2], Sándor Lenk[2], László Domján[3], Gábor Szarvas[3], Edina Lengyel[4] és András Székács[1]

[1]Agro-Environmental Research Centre, Institute of Environmental Sciences, Hungarian University of Agriculture and Life Sciences, Herman O. út 15, H-1022 Budapest, Hungary
[2]Department of Atomic Physics, Budapest University of Technology and Economics, Műegyetem rkp. 3, H-1111 Budapest, Hungary
[3]Optimal Optik Ltd., Dayka Gábor u. 6/B, H-1118 Budapest, Hungary
[4]Department of Limnology, University of Pannonia, H-8200 Veszprém, Egyetem u. 10, Hungary
e-mail: lazar.diana@uni-mate.hu

Abstract

Aquatic ecosystems are strongly exposed to various micropollutants from agricultural origin. The harmful effect can be expressed directly on aquatic organisms and indirectly through the food chain. The use of ecotoxicity assays mainly in aquatic environments, and corresponding water quality assessment are undoubtedly important. Project Aquafluosense was designed to develop instrument prototypes of a fluorescence-based setup for *in situ* measurement of algal biomass and for application of flurescence in ecotoxicity assays. Fluorescence-based determination of algal density was validated by conventional methods and signals obtained by the fluorometer correlated well with the conventional methods for algal density determination. The applicability of the fluorometer developed was demonstrated in ecotoxicity assays using the herbicide active ingredient isoxaflutole in neat and formulated forms.

Introduction

The composition and quantity of the algal biomass are essential indicators of quality and ecological status of natural water bodies and aquatic ecosystems. Micropollutants of agricultural origin, including pesticide active ingredients, co-formulants, mycotoxins and fertilizers, can enter the surface water system by leaching and runoff, and can directly and indirectly trigger adverse effect on aquatic organisms and human health via contamination of the drinking water base [1].

Algal biomass, as an indicator of water quality and ecotoxicological effects, can be measured by several techniques. The most commonly applied methods include the determination of algal cell numbers by microscopy and optical density (OD) by spectrohotometer, measurement of dry mass and the main photosynthetic pigment content of algal cells [2]. The primary source of endogenous fluorescence in algae is the induced fluorescence signal by chlorophylls responsible for photosynthesis [3]. Thus, efficiency of photosynthesis can also be characterized by fluorescence induction kinetics describing changes in the photosynthetic process and the physiological state of algal cultures [4]. Monoculture of various microalgal species (e.g. *Raphidochelis subcapitata*) are often used as test organisms in ecotoxicity assays to determine side effects of agricultural pollutants.

Isoxaflutole (5-cyclopropyl isoxazol-4-yl-2-mesyl-4-trifluoromethylphenyl ketone) is an active ingredient in several commercially available herbicidal formulations for preemergence control of weeds. The mode of action of isoxaflutole is to inhibit the enzyme 4-hydroxyphenylpyruvate dioxygenase. As a pigment inhibitor, it blocks the biosynthesis of carotenoid pigments, which protect chlorophyll from decomposition by sunlight. Thus, chlorophyll pigments are photo-oxidized, chloroplasts break down, and as a result the entire plant necrotizes and eventually dies

[5,6]. Isoxaflutole was first registered for use on corn in 1999, and it was also registered in 2020 for use on genetically modified (GM), herbicide-resistant soybean. The US Environmental Prottection Agency is presently considering an application to register isoxaflutole use on herbicide-resistant GM cotton [5,7]. With introduction of GM crops in agricultural practices, the application rate and the amount of the corresponding active ingredient increases, as the word-wide application of glyphosate on glyphosate-resistant GM crops showed [8]. Due to its increasing use, isoxaflutole has been detected, as emerging pollutants, in surface waters together with its metabolites of diketonitrile and benzoic acid [9], and it has been classified as a persistent water pollutant substance [5].

The aim of this study was to determine the ecotoxic effect of isoxaflutole herbicide active ingredient by the conventionally applied guideline for growth inhibition and by using the newly developed instrument for investigating the biomass and the efficacy of the PSII photocemical system of microalgae. The instruments were developed in the frame of project Aquafluosense (NVKP_16-1-2016-0049). The project strategy applied induced fluorescence as a signal to be detected, and utilize it for a range of purposes in water quality analysis [10,11]. One of the purposes is ecotoxicity assessment of plant protection products (PPPs). PPPs contain, in addition to their active ingredients, various additives, co-formulants, which are considered to be inert from the point of view of the main biological effect of the PPP. Nonetheless, numerous studies have confirmed higher toxicity of PPP formulations than of the active ingredients themselves, suggesting additive or synergistic effects between the active ingredients and the additives in different formulations [12]. In the present work we report the use of our novel fluorometer prototype detecting algal density in water for the assessment of algal toxicity of agrochemicals.

Experimental

The model green alga species, *R. subcapitata*, Korshikov (NIVA-CHL1) was obtained from public collections. Monocultures of test species were maintained and diluted in Z8 medium [13]. Ecotoxic effects of isoxaflutole (Figure 1) and its formulated PPPs (Merlin Flexx and Merlin 750 WG) were determined by the OECD 201 guideline [14] and by the newly developed fluorescence-based instrument. The active ingredient content for Merlin Flexx and Merlin 750 WG are 20.3% and 75%, respectively. Beside the active ingredient, both PPPs contain co-formulant agents at different concentrations (Table 1).

Table 1. Co-formulant agents in isoxaflutole-based plant protection products (Merlin Flexx and Merlin 75 WG) investigated in this study.

Plant protection product			
Merlin Flexx		**Merlin WG**	
co-formulant	**concentration (%)**	**co-formulant**	**concentration (%)**
cyprosulfamide	20.3	kaolin	5 – 15
benzisothiazol-3(2H)-one	0.005 – 0.05	other ingredients (non-hazardous) to 100%	10 – 20
alkyl polyglycoside	1 - 5		

The response of the guideline applied is the reduction of growth in a series of algal cultures exposed to different concentrations of test substances. Growth and growth inhibition are quantified from measurements of the algal biomass with determination of optical density and chlorophyll-a-content by spectrophotometer (UV/VIS Camspec single beam M330, Camspec,

Crawley, United Kingdom). For the quantification of chlorophyll content the Felföldy-formula was applied [15].

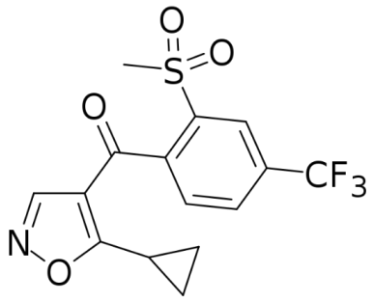

Figure 1. Chemical structure of the herbicide active ingredient, isoxaflutole.

For the determination of adverse effect of test substances on PSII photochemical system and vitality index, the newly developed, fluorescence-based instrument, FluoroMeter Module (FMM) was applied. The FMM [16] was also equipped with an instrument capable of accommodating standard size 96-well microplates (Figure 1b). The FMM instrument allows the recording of conventional Kautsky induction kinetic curves, which were simultaneously detected at two maxima of Chl-a fluorescence. The instrument was equipped with laser diode (10 mW) as excitation source providing excitation wavelength of 635 nm. Detection was performed at 690 nm ($\Delta\lambda = 10$) and 735 nm ($\Delta\lambda = 10$). For the instrument, a 96-well microplate holder was developed that allows parallel determination of samples. The photochemical efficiency of the algae photosynthetic system PSII (Fv/Fp, where Fv refers to the variable fluorescence, while Fp refers to the peak of the fluorescence) and changes in the fluorescence decrease ratio (Rfd= Fq/Fs, where Fs is the observed steady-state fluorescence and Fq is the fluorescence quenching capacity calculated as Fp-Fs) characterized the photosynthetic activity and vitality index, respectively [17].
Validation of fluorescence-based method was performed by comparison with other methods and correlation coefficients (R^2 value) were determined. A three-fold dilution series of six concentrations of green *R. subcapitata* were used for quantitative measurements. OD, chlorophyll content and cell concentration with Bürker chamber were measured for each concentration, together with the determination of the fluorescence signal intensities using the FMM. ODs were measured at 750 nm with a CAM-Spec.M33 UV–visible spectrophotometer. Chlorophyll was extracted and measured following the method of Wetzel et al. [18]. Samples were placed in a Bürker chamber and cell numbers were counted using a Nikon Labophot 2 microscope at 20x and 40x magnifications.

Results and discussion

Ecotoxicity assays were performed to determine the effects of isoxaflutole and its formulated products on the growth of *R. subcapitata* by measurement of OD and chlorophyll-a content in the algal growth medium. The same trend in toxicity was determined for both parameters that are recommended by the OECD 201 guideline. Isoxaflutole was determined as the most toxic component (EC_{50}OD = 0.034 mg/L). Co-formulants in Merlin Flexx (cyprosulfamide and 1,2-benzisothiazol-3(2H)-one) decreased the toxic effect of the active ingredient by nearly over 200-fold (EC_{50}OD = 33.7 mg/L), as the isoxaflutole-equivalent EC_{50} value was 6.84 mg/L. An EC_{50}OD value of 0.20 mg/L was determined for 1,2-benzisothiazol-3(2H)-one, while cyprosulfamide, used as a herbicide safener for isoxaflutole, did not exert algal toxicity below its OECD limit test value (100 mg/L). For Merlin 750 WG an EC_{50}OD of 0.64 mg/L was

determined indicating a somewhat weaker (one order of magnitude) decreasing effect on the toxicity of isoxaflutole by the additives (e.g. kaolin) present.
Determination of two photochemical parameters (Fv/Fp - photochemical efficiency of PSII photochemical system and Rfd – vitality index) were determined by the newly developed fluorescence-based instrument. Both parameters characterize the functioning of the PSII photochemical system in green plants. The Fv/Fp parameter was not found to be good in ecotoxicity studies. However, EC_{50} values of the Rfd parameter EC_{50} were determined to be 0.015 mg/L, 27 mg/L and 0.6 mg/L for isoxaflutole, Merlin Flexx and Merlin 750 WG.
For validation, results showed strong correlation among different methods applied for determination of algal biomass. The correlation of results obtained with FMM correlated with OD determination, Bürker-chamber cell counting and Chlorophyll-a-content by ethanol at the R^2 values of 0.98, 0.98 and 0.99, respectively.

Conclusion

Project Aquafluosense provided a fluorescence-based instrument appropriate for ecotoxicological assays on algae test species. Fluorescence-based determination of algal density and application of Rfd (vitality index) as endpoint in ecotoxicity assay was validated by conventional methods (Bürker chamber cell counting, optical density measurement, chlorophyll extraction with ethanol), and signals obtained by the fluorometer correlated well with the conventional methods for algal density. Isoxaflutole herbicide active ingredient and its formulated PPPs (Merlin Flexx and Merlin 75 WG) exerted harmful effect on algal growth. The most toxic effect was determined for neat isoxaflutole (EC_{50}OD=0.034 mg/L). Co-formulants in formulated products increased the effect of the active ingredient, however there occurred a significant difference between the products. The difference in amount and type of co-formulants resulted in difference in ecotoxic effect.

Acknowledgements

This research was supported by project Aquafluosense, NVKP_16-1-2016 0049 funded by the National Research, Development ND Innovation Fund of Hungary within the National Competitiveness and Excellence Program.

References

[1] R. Verro, A. Finizio, S. Otto, M. Vighi, Environ. Sci. Technol. 43 (2009) 530–537.
[2] C. Butterwick, S.I. Heaney, J.F. Talling, Br. Phycol. J. 17 (1982) 69–79.
[3] D.J. Suggett, P. Ondrej, M.A. Borowitzka (Eds.) Chlorophyll a fluorescence in aquatic sciences: methods and applications. Vol. 4. Dordrecht: Springer, 2010; pp. 293-309.
[4] S. Lenk, P. Gádoros, L. Kocsányi, A Barócsi, Eur. J. Phys. 37 (2016) 064003.
[5] United States Environmental Protection Agency. Pesticides – Fact Sheet for Isoxaflutole. 1998.
[6] K.E. Pallett, J.P. Little, M. Sheekey, P. Veerasekaran, Pestic. Biochem. Physiol. 62 (1998) 113-124.
[7] United States Environmental Protection Agency. Final Registration of Isoxaflutole on Isoxaflutole-Resistant Soybeans, 2020.
[8] A. Székács, B. Darvas, In: M.N.A.E.-G. Hasaneenm (Ed.), InTech, Rijeka, Croatia, 2012, 247–284.
[9] M.T. Meyer, E.A. Scribner, S.J. Kalkhoff, Environ. Sci. Technol. 41 (2007) 6933-6939.
[10] Aquafluosense. Development of a Modular, Direct and Immunofluorimetry as Well as Plasma Spectroscopy Based Detector and Instrument Family for In Situ, Complex Water

Quality Monitoring, and Application Studies. Available online: http://aquafluosense.hu (accessed on 28 October 2022).
[11] D. Csősz, S. Lenk, A. Barócsi, T.L. Csőke, Sz. Klátyik, D. Lázár, M. Berki, N. Adányi, A. Csákányi, L. Domján, G. Szarvas, A. Nabok, M. Mörtl, A. Székács, Proceed. Optic. Sens. Sens. Cong., San Jose, CA, USA, 25–27 June 2019; OSA: Washington, DC, USA, 2019.
[12] Sz. Klátyik, P. Bohus, B. Darvas, A. Székács, Front. Vet. Sci. 4 (2017) 146.
[13] Z8 Medium. https://www-cyanosite.bio.purdue.edu/media/table/Z8.html (accessed 2022-10-28).
[14] OECD (Organisation for Economic Cooperation and Development) Freshwater Alga and Cyanobacteria, Growth Inhibition Test (201). OECD guidelines for the testing of chemicals, section 2011, 2 (10.1787).
[15] L. Felföldy, Vízügyi Hidrobiológia 16. 1987. Budapest: VGI. 258 pp.
[16] A. Barócsi, S. Lenk, L. Kocsányi, C. Buschmann, Photosynthetica 47 (2009) 104–111.
[17] W.J. Vredenberg, Photosynthetica 56 (2018) 139-149.
[18] R.G. Wetzel, G.E. Likens, Limnological Analyses; Springer Science & Business Media, 2013.

INTEGRATED SYSTEM FOR OBTAINING COMBUSTIBLE GASES

Corina Macarie, Ionel Balcu, Doru Buzatu, Paula Sfirloaga

National Institute for Research and Development in Electrochemistry and Condensed Matter, 144 Dr. A. PaunescuPodeanu, 300569, Timisoara, Romania, Tel.: +40 256 222119
e-mail address:mac_cora@yahoo.com

Abstract

This paper starts from the idea of transforming CO_2 from various sources into methane through the reaction with hydrogen obtained through the electrolysis of water in which energy from renewable sources such as wind or solar energy is used.

The paper develops an ecological application of the use of methanizers, namely the reduction of carbon dioxide from flue gases. Flue gases with a CO_2 content, depending on the nature of the fuel, will be introduced into a methanizer, as through the combination of CO_2 with H_2, it will lead to the formation of CH_4. The new composition of the combustion gases, with CH_4 instead of CO_2, is even more polluting for the environment, but in certain situations their combustion can be used, producing useful energy, the overall yield resulting from two combustion processes in series.

Experimental study of the methanation process at the laboratory level can be done with a facility that aims to determine the optimal operation and find suitable conditions for the carbon dioxide methanation catalysts. The Methanation Test Facility was designed and commissioned to investigate the catalytic methanation of carbon dioxide and hydrogen.

The paper presents a work flow, with the notification of the total energy efficiency and the assessment of the final CO_2 pollution, which is much less compared to the classic case of the direct evacuation of combustion gases into the atmosphere.

Acknowledgements

This work was supported by a grand of the Romanian Ministry of Research and Innovation CCCDI-UEFISCDI, project number PN-III-P2-2.1-PED-2019-2350, 322 PED "Carbon dioxide methanizer design for sustainable low carbon energy systems development"

References

[1] Bailera, M., Lisbona, P., Romeo, L.M., Espatolero, S. Power to Gas projects review: Lab, pilot and demo plants for storing renewable energy and CO2. Renew. Sustain. Energy Rev. 2017, 69, 292–312.
[2] Martin, M.R., Fornero, J.J., Stark, R., Mets, L., Angenent, L.T. A Single-Culture Bioprocess of Methanothermobacter thermautotrophicus to upgrade Digester Biogas by CO2-to-CH4 Conversion with H2. Archaea 2013, 2013, 157529.
[3] Enzmann, F., Mayer, F., Rother, M., Holtmann, D. Methanogens: Biochemical background and biotechnological applications: Mini-Review. AMB Express 2018.

YIELDS OF THE CHARDONEY VARIETY IN THE VINEYARDS OF VOJVODINA DURING 2022

Stefan Marković, Blagojević Milan, Rašković Vera, Stošić Nemanja, Robinić Jelena

Academy of Applied Studies Šabac. Unite for Agricultural Business Studies and Tourism, Republic of Serbia
e-mail: markovicstefaan@gmail.com

Abstract

In recent years, vineyards with this variety have been growing more intensively in Vojvodina. The variety belongs to the mid-late era of ripening, the yield of grapes varies and ranges from 6000 to 10000 kg/ha. This white wine variety suit moderately fertile, loose, calcareous and warm soils. It has a good affinity with the rootstocks Kobber 5BB, Teleki 8B, SO4. The sugar content ranges from 20 to 24%, and the total acid content from 6 to 8 g/l. The content of sugar (%) and acid (g/l) was determined using an Excel Schwolder, and by titration with NaOH with the help of bromothymol blue. Research was carried out during 2022 in the locations of Banoštor, Subotica and Vršac, which belong to the Fruška Gora, Subotica-Horgoško and Vršac vineyards. At the Banoštor location, in a 12-year-old vineyard planted on the type of soil of arable land, a yield of 8.1 t/ha was measured, where we determined the content of total acids at 6.2 g/l and the content of total sugars at 20.7%. At the location of Subotica, in a 22-year-old vineyard, which was planted on a sandy soil type, a yield of 8.8 t/ha was measured, where we determined the content of total acids 6.5 g/l and the content of total sugars 23.4%. At the Vršac location, in a 20-year-old vineyard planted on sandy loam soil, a yield of 8.4 t/ha was measured, where we determined the content of total acids at 6.8 g/l and the content of total sugars at 22.2%. The poor distribution of rainfall for viticulture indicates that younger vineyards achieved lower or similar yields, of lower quality compared to older plantations that were planted on more permeable and poor soil types.

PREVENTION OF OCCURANCE OF SELECTED MYCOTOXINS IN FEED WAREHOUSE FOR MILKING COWS

Nada Marković[1], Srđan Kovačević[2]

[1]*Administration for inspection affairs of Montenegro, inspector for hydrocarbons, Razvršje,130Oktobarske Revolucije, Podgorica*
[2]*Department of Environmental Engineering and Occupational Health and Safety, Faculty of Technical Sciences, University of Novi Sad, Trg Dositeja Obradovića 6, 21000 Novi Sad, Republic of Serbia*
e-mail: nadamarkovic71@t-com.me

Abstract
The aim of this work was to examine the presence of Fusarium toxins in feed for milking cows in summer and winter. Food samples for milking cows were sampled from a cow farm in the vicinity of Nikšić, Montenegro, in winter and summer. The determined concentrations of the examined mycotoxins in the food samples for feeding milking cows were lower than the maximum allowed concentrations prescribed by the Regular Acts of Montenegro. The obtained results indicate that there was no significant difference in the concentrations of the tested mycotoxins in the food for feeding milking cows during the summer and winter periods, which suggests that with good production and storage practices, food can be protected from mycotoxicological contamination, and cow's milk and meat.

Introduction
Mycotoxins are toxic, secondary metabolites of toxin-producing species of mold [1]. So far, several hundred mycotoxins have been discovered, which are produced mainly by molds from the genera Aspergillus, Penicillium, Fusarium and Alternaria [2]. Available scientific literature indicates that during recent years the occurrence of climate changes has been recorded, which has shown a great impact on the appearance of mycotoxins[4]. .
Fusarium toxins represent the most dominant group of mycotoxins, the most important representatives of this group in our country are Deoxynivalenol (DON) and Zearalenone (ZEA) [3].
Mycotoxins in humans and animals can cause alimentary diseases accompanied by mutagenic, carcinogenic, teratogenic, estrogenic, dermatoxic, immunosuppressive and neurological effects, and can also lead to death [3]. The presence of mycotoxins in food can cause great economic losses [3].
When it comes to animal feed, a special problem is storage, because during inadequate storage, the development of toxic mold species and the production of mycotoxins can occur[5]. In Republic of Montenegro, there is a lack of tests of this type, so the aim of this work was to examine the presence of Fusarium toxins in food for milking cows in both summer and winter.

Experimental
The determination of the DON content in feed for milking cows was performed on a liquid chromatograph with a Shimadzu RF 10 Axl fluorescent detector, analytical column Kinetex EVO C 18 150X 4.6 MM was used for chromatographic separation. A liquid chromatograph with a Quatro Micro API mass spectrometer was used for ZEA analysis. For the preparation of samples for ZEA and DON analysis, sample purification was used on an SPE column (C18 and aluminum oxide in a 3:1 ratio). Which was prepared by filling a polypropylene syringe with a capacity of 6 ml with 0.2 g of silica gel C18 and 0.6 g of neutral aluminum oxide.

Deionized water was used to prepare all solutions.
15 food samples were sampled in the winter and in the summer period in 2019. The following food for milking cows was tested: universal mixture for feeding animals, wheat feed flour, corn mixed feed flour, corn noodles, corn grits, mercantile corn.

Results and discussion

The presence of DON was determined in nine samples, corn feed and wheat cattle meal were contaminated, as well as a mixture for feeding milking cows, the DON concentrations obtained were in the range of 0.2 to 1.8 mg/kg, but according to current legal regulations, no sample was contaminated with this toxin more than MDK. In the winter period, the DON content obtained indicated the same high percentage of positive samples, namely 60%, DON concentrations ranged from 0.2 to 5,3 mg/kg, but no sample exceeded the permitted concentration.

Table number 1. Result of testing the concentration of DON in feed the summer

Number sample	Sample type	Content DON (mg/kg)
1	universal mixture for feeding animals	0,3- 0,07
2	wheat feed flour	1,0-0,21
3	corn mixed feed flour	1,5-0.26
4	corn noodles	0.2-0,003
5	corn grits	1,8-0,33
6	mercantile corn	0,7-0,14

Table number 2. Result of testing the concentration of DON in feed the winter

Number sample	Sample type	Content DON (mg/kg)
1	universal mixture for feeding animals	0,3- 0,04
2	wheat feed flour	1,0-0,21
3	corn mixed feed flour	1,5-0.26
4	corn noodles	5,3-0,42
5	corn grits	1,8-0,35
6	mercantile corn	0,2-0,03

The presence of ZEA was determined in corn and corn-based products, the concentrations of this toxin were in the range of 0.02 to 0.3 mg/kg, in the summer period, while the concentrations during the winter were from 0.02 to 0.11 mg/kg, the maximum concentration of ZEA allowed by the Rulebook of Montenegro is 2 mg/kg in cereals except corn, while in corn and corn products the MDK is 3 mg/kg.

Table number 3. Result of testing the concentration of ZEA in feed the summer

Number sample	Sample type	Content ZEA (mg/kg)
1	universal mixture for feeding animals	0,070- 0,015
2	wheat feed flour	0,280-0,028
3	corn mixed feed flour	0.300-0.060
4	corn noodles	0.02-0,004
5	corn grits	0,030-0,005
6	mercantile corn	0,020-0,004

Table number 4. Result of testing the concentration of ZEA in feed during the winter

Number sample	Sample type	Content ZEA (mg/kg)
1	universal mixture for feeding animals	0,02- 0,003
2	wheat feed flour	0,06-0,011
3	corn mixed feed flour	0.03-0.005
4	corn noodles	0.02-0,004
5	corn grits	0,02-0,003
6	mercantile corn	0,11-0,024

Conclusion

The obtained results show that there was no great difference in mycotoxin concentrations in winter and summer, also these results show that good production and storage practices can protect animal feed from mycotoxins. The employees of the farm from which the food samples were taken paid special attention to the storage of animal feed, well-dried grains were stored, the warehouse was frequently ventilated, as well as temperature control.

Records were also kept on the order of food consumption, after the consumption of one batch of food, the warehouse was disinfected, and special attention was paid to the education of the staff employed on the farm on how to store and store food for milking cows.

Acknowledgements

For the preparation of this paper, I owe special thanks to the Center for Ecotoxicological Testing in Podgorica, where animal feed tests for the mentioned toxins were performed.

References

[1] J. D. Miller J.D. Factros affecting the occurrence of fumonisims in corn. Abstract of papers (p.21) International Conference on the toxicology of Fumonisin, June 28-30, (1999).

[2] M. Peraica, B. Radić, A. Lucić, M. Pavlović, Toxic effects of mycotoksins in humans. Bulletin of the World Health Organization, 77 (9), (1999) 754 -766.

[3] J.He, T. Zhhou, C. Young, J. Boind, M. Scott, Chemical and biological transformations for detoxification of trichothecene mycotoxins in human and animal food chains:a review.Technologu Foof Control. (2010) 21,67-76.

[4] S. Iqbal, M. Asi, S. Jinap .,Variation of aflatoxin M1 contamination in milk and milk product s collected during winter and summer seasons. Food Control. (2013)

[5] R. A. Shelby, D.G. White, E.M. Bauske Differential fumonisin production in maize hybrids. Plant Dis. 78, (1994) 582 - 584.

THE EFFECT OF ENCAPSULATED AMOUNT OF CAFFEINE ON THE MECHANISM OF ITS RELEASE FROM HYDROGELS BASED ON POLY(METHACRYLIC ACID) AND CASEIN

Maja D. Markovic*[1], Vesna V. Panic[1], Rada V. Pjanovic[2]

[1]University of Belgrade, Innovation Center of Faculty of Technology and Metallurgy, Karnegijeva 4, 11000 Belgrade, Serbia;
[2]University of Belgrade, Faculty of Technology and Metallurgy, Karnegijeva 4, 11000 Belgrade, Serbia
**e-mail: mmarkovic@tmf.bg.ac.rs*

Abstract

Researchers are making everyday efforts to develop new drugs or improve present ones in order to enhance therapies of various diseases, especially serious ones like cancer. Drug delivery systems (DDS) are one of the solutions for safer and more efficient therapy. Hydrogels based on poly(methacrylic acid) (PMAA) are extensively investigated as DDS due to their non-toxicity, biocompatibility and pH sensitivity. Many chemotherapeutics are poorly water-soluble, so it is quite challenging to encapsulate them into highly hydrophilic PMAA. In our previous study we overcome this limitation by modifying PMAA with amphiphilic casein and demonstrated that poorly water-soluble model drug – caffeine can be successfully encapsulated and released in control manner from these samples (H hydrogels). In present study we go step forward and investigated how the change in the amount of encapsulated caffeine affect the mechanism of caffeine release from the H hydrogels in medium with pH of 6.8 (which simulates the environment in human intestines). Commonly used models for the analysis of kinetics of drug release from hydrogels: Ritger-Peppas, Higuchi and Kopcha model are employed for the analysis of the mechanism of caffeine release. Presented results indicate that it is possible to adjust the manner and mechanism of drug release by changing the amount of encapsulated drug, due to which the H hydrogels can adapt to the unique requirements of the therapy.

Introduction

Everyday struggle of humanity with various problems such as global warming and huge number of diseases urge researches to develop new innovative solutions, which are safe and effective and in the accordance with the principles of green chemistry. One of the promising tools for the therapies of various diseases are drug delivery systems. These systems are able to deliver drug to the site of action in human body and release it in control manner. Drug bioavailability can be improved, side effects reduced, the number of therapeutic doses can be decreased and therefore, overall therapy would be enhanced. Hydrogels are polymer materials which are recognized as promising systems for drug delivery due to the large number of their tremendous properties [1, 2]. Their 3D network can absorb and retain large amount of water and/or other physiological fluids due to which they have soft structure similar to the living tissue. One interesting group of hydrogels are those based on poly(methacrylic acid) (PMAA) [3]. PMAA hydrogels are non-toxic, biocompatible, highly hydrophilic and pH sensitive because of which they are extensively investigated for drug delivery. Namely, PMAA hydrogels are able to swell in the environments with pH higher than pKa of PMAA and therefore release encapsulated drug in the process [4]. In order to overcome their poor mechanical properties and enable encapsulation of poorly water-soluble drugs (like large number of chemotherapeutics) in our previous research we modified PMAA with amphiphilic casein (H hydrogels) [5]. It was investigated how the change of various synthesis parameters (such as crosslinker amount,

neutralization degree, pH of external medium, the amount of encapsulated active substance etc.) affect the release rate of poorly water-soluble model drug caffeine [4]. The obtained results showed that encapsulation and controlled release of poorly water-soluble active substance was successful and its release rate can be fine-tuned only by changing one of the synthesis parameters [6]. In present study we further deepened our research and employed several models (Ritger-Peppas [7], Higuchi [8] and Kopcha model [9]) to analyze how the change of encapsulated amount of caffeine affected the mechanism of its release from the H hydrogels in phosphate buffer with pH of 6.8 at 37 ºC (PB 6.8).

Experimental

The H hydrogels were synthetized by free-radical polymerization in aqueous solution and all samples had 4 mL of MAA, 4 g of casein, 0.4 mol% of crosslinker - methylenebisacrylamide (MBA) (with respect to the amount of methacrylic acid) and 0.9 ml of 1 wt% aqueous solution of initiator (2,2'-azobis-[2-(2-imidazolin-2-yl)propane] dihydrochloride). 1.859 g of NaOH was added to the reaction mixture of the samples with total neutralization degree of methacrylic acid. 1 g or 2 g of caffeine was encapsulated in both groups of the samples: with non-neutralized and neutralized MAA. The synthesis, the list of used chemicals and the feed composition are presented in our previous research [6]. The prepared samples were denoted as H/xN-y, where xN represented the neutralization degree of MAA (0N – 0% of neutralization degree of MAA or 100N – 100% of neutralization degree of MAA) and y showed the mass of encapsulated caffeine 1 g or 2 g.

In order to better understand the mechanism of caffeine release from the H hydrogels and how the change of caffeine amount affects it, the caffeine release profiles were analysed with three models - Ritger-Peppas (Eq. (1)), Higuchi (Eq. (2)) and Kopcha model (Eq. (3)):

$$\frac{M_t}{M_\infty} = kt^n \quad (1)$$

$$\frac{M_t}{M_\infty} = k_H\sqrt{t} \quad (2)$$

$$\frac{M_t}{M_\infty} = k_1 t^{0.5} + k_2 t^1 \quad (3).$$

In all equations the $\frac{M_t}{M_\infty}$ represents the fractional release of active substance and t is the time of the process of active substance release (min). In Eq. (1) the parameter k shows the speed of active substance release (min^{-1}) and parameter n represents the type of the mechanism of active substance release (diffusion and/or relaxation of polymer's chains). In Eq. (2) the k_H parameter represents the speed of active substance diffusion from the carrier (min^{-1}). In Eq. (3) the k_1 parameter shows the speed of active substance release governed by diffusion (min^{-1}), whereas the k_2 parameter represent the speed of active substance release governed by relaxation of polymer's chains (min^{-1}).

The equations Eq. (1) and Eq. (2) were used in following forms: $\ln(\frac{M_t}{M_\infty}) = \ln(kt^n)$ and $\frac{M_t}{M_\infty} = k_H t^{0,5}$, respectively. The form of Eq. (3) was added into the OriginPro 8.5 program and then it was applied on the caffeine release data ($\frac{M_t}{M_\infty} - t$). The symbol adopted for the "fields of applicability" of applied models was Δα (%).

Results and discussion

The curves of caffeine release in PB were fitted to Ritger-Peppas (R-P), Higuchi and Kopcha model and are presented in Fig. 1., Fig. 2. and Fig. 3., respectively. Determined values of kinetics parameters of chosen models and their fields of applicability are presented in Table 1. The kinetics of caffeine release from H/0N-1 and H/100N-1 were analyzed in our previous

research [4], and only the obtained values of kinetics parameter are presented in Table 1. in order to facilitate the analysis of the results obtained in present study.

R-P model showed that diffusion governed caffeine release from the H/0N-1 sample (n<0.5), whereas polymer chains relaxation was the main mechanism of caffeine release from the H/100N-1 sample (n>1). Both mechanisms (diffusion and relaxation of polymer chains) were involved into the process of caffeine release from the H/0N-2 and H/100N-2 samples. The values of R^2 were between 0.954-0.999 which means that fitting of the R-P model to the data of caffeine release from the H samples was good. The field of applicability of R-P model was relatively high (the values of Δα were between 50.7 % and 85.7 %) taking into account that this model can be applied to the first 60% of the drug release data. Both models R-P and Kopcha model predicted that caffeine was released by diffusion from H/0N-1 and that relaxation of polymer chains was the main mechanism of caffeine release from the H/100N-1 sample.

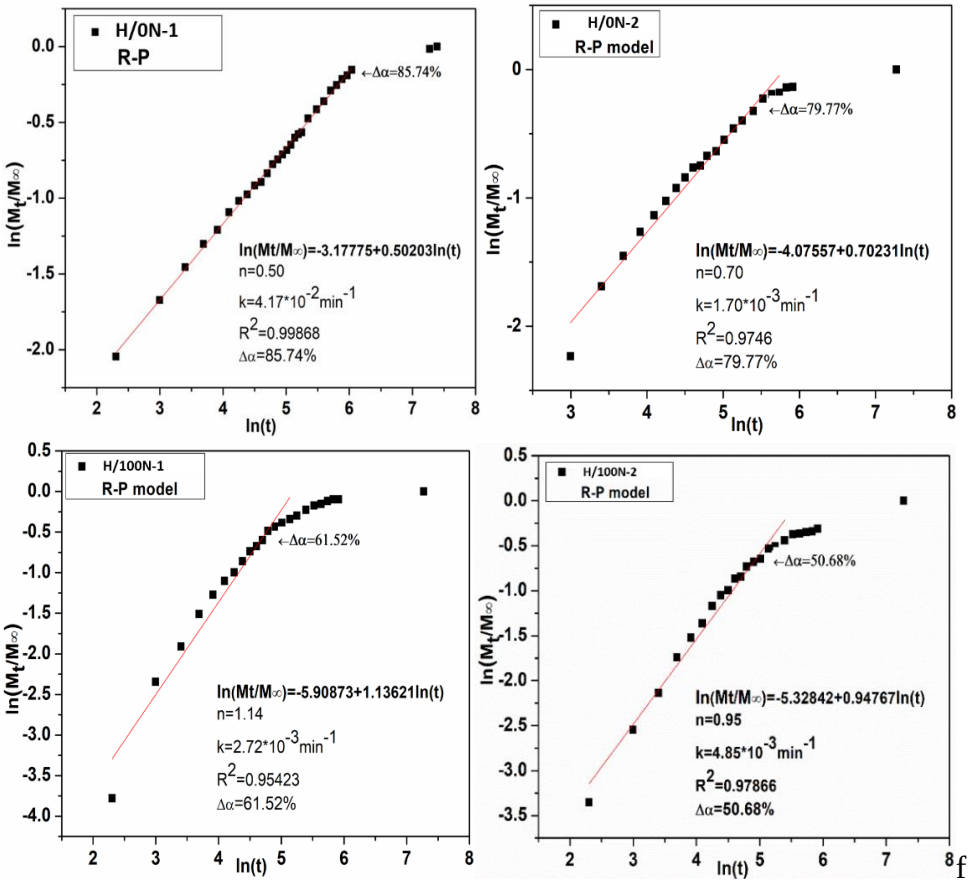

Figure 1. Fitting of the profiles of caffeine release from the H carriers in PB 6.8 with R-P model

It was possible to apply Higuchi model only to the curves of caffeine release from the H/0N-1 sample (R^2~0.999 and Δα was 85.7%). Obtained value of Higuchi parameter k_H was similar to the value of the R-P parameter k and Kopcha parameter k_1, which means that predictions of these three models that caffeine was released by diffusion from the H/0N-1 sample, were good.

The best fitting to the caffeine release data showed Kopcha model (the values of R^2 were between 0.975-0.998). The field of applicability of Kopcha model was between 50.7 % and 56.8%.

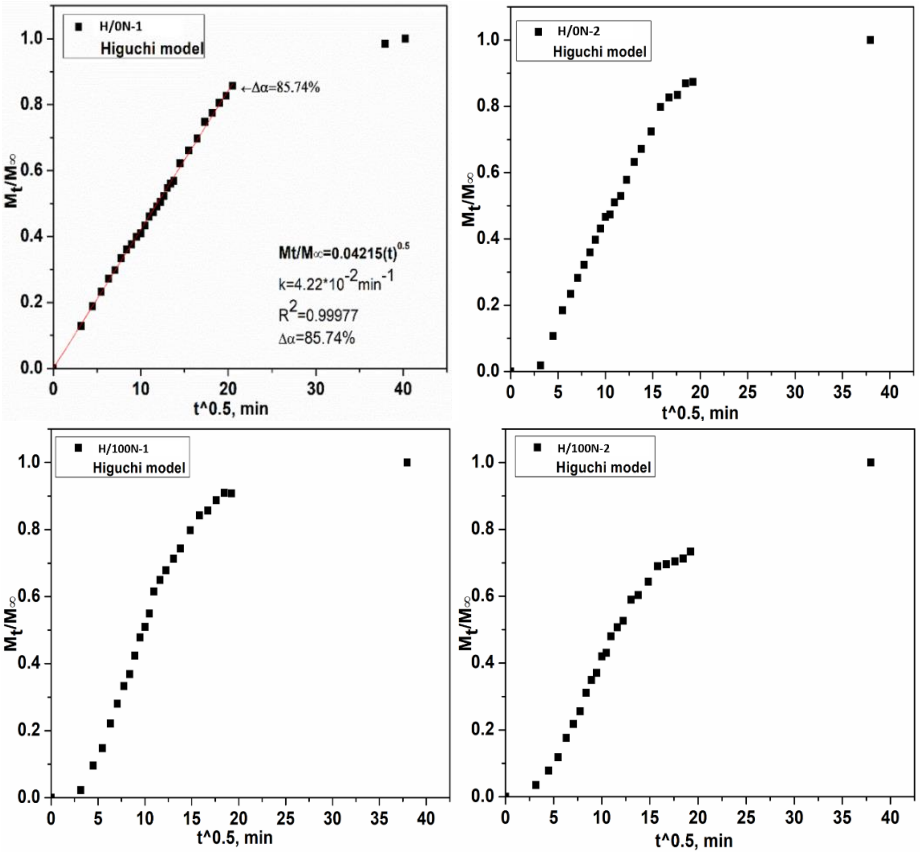

Figure 2. Fitting of the profiles of caffeine release from the H carriers in PB 6.8 with Higuchi model

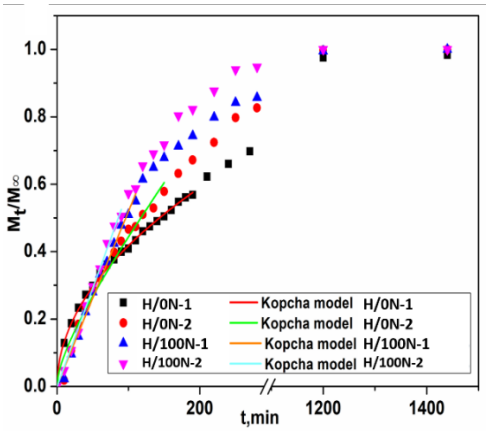

Figure 3. Fitting of the profiles of caffeine release from the H carriers in PB 6.8 with Kopcha model

Table 1. Obtained kinetics parameters of chosen models for each H carrier

Model	Sample	H/0N-1	H/0N-2	H/100N-1	H/100N-2
R-P	n	0.50	0.70	1.14	0.95
	$k*10^2$ (min^{-1})	4.17	1.70	0.272	0.485
	Δα(%)	85.7	79.8	61.5	50.7
	R^2	0.999	0.975	0.954	0.979
Higuchi	k_H*10^2	4.22	-	-	-
	Δα(%)	85.7	-	-	-
	R^2	0.999	-	-	-
Kopcha	k_1*10^2	4.18	2.27	0	5.80
	k_2*10^3	0	2.87	5.81	3.46
	Δα	56.8	60.6	56.1	50.7
	R^2	0.998	0.975	0.993	0.991

Conclusion

In our previous research we demonstrated that only by changing the amount of encapsulated caffeine it is possible to fine tune the manner of the H hydrogels swelling and caffeine release. In order to determine the type of mechanism of caffeine release from these hydrogels in PB 6.8, in present study we employed several models Ritger-Peppas, Higuchi and Kopcha. It was demonstrated that the Kopcha model showed the best fitting to the caffeine release curves and both mechanism (diffusion and relaxation of polymer's chains) governed the caffeine release from the H hydrogels.

Acknowledgements

This work was supported by the Ministry of Education, Science and Technological Development of the Republic of Serbia (Contract No. 451-03-68/2022-14/200287).

References

[1] M.D. Markovic, V.V. Panic, S.I. Savic, V.D. Ugrinovic, R.V. Pjanovic, M.M. Spasojevic, P.M. Spasojevic, Biobased thermo/pH sensitive poly(N-isopropylacrylamide-co-crotonic acid) hydrogels for targeted drug delivery, Microporous Mesoporous Mater. 335 (2022) 111817.

[2] M.D. Marković, J.D. Tadić, S.I. Savić, I.Z. Matić, T.P. Stanojković, D.Ž. Mijin, V.V. Panić, Soft 3D hybrid network for delivery and controlled release of poorly soluble dihydropyrimidinone compound: An insight into the novel system for potential application in leukemia treatment, Journal of Biomedical Materials Research Part A 110(9) (2022) 1564-1578.

[3] M.D. Markovic, S.I. Seslija, V.D. Ugrinovic, M. Kunaver, V.V. Panic, R.V. Pjanovic, P.M. Spasojevic, Green pH- and magnetic-responsive hybrid hydrogels based on poly(methacrylic acid) and Eucalyptus wood nanocellulose for controlled release of ibuprofen, Cellulose 28(17) (2021) 11109-11132.

[4] M.D. Markovic, V.V. Panic, S.I. Seslija, P.M. Spasojevic, V.D. Ugrinovic, N.M. Boskovic-Vragolovic, R.V. Pjanovic, Modification of hydrophilic polymer network to design a carrier for a poorly water-soluble substance, Polymer Engineering & Science 60(10) (2020) 2496-2510.

[5] M.D. Markovic, V.V. Panic, S.I. Seslija, A.D. Milivojevic, P.M. Spasojevic, N.M. Boskovic-Vragolovic, R.V. Pjanovic, Novel strategy for encapsulation and targeted delivery of

poorly water-soluble active substances, Polymer Engineering & Science 60(8) (2020) 2008-2022.
[6] Maja Markovic, Doctoral dissertation- RELEASE KINETICS OF A POORLY WATER-SOLUBLE SUBSTANCE FROM CARRIERS BASED ON POLY(METHACRYLIC ACID), CASEIN AND LIPOSOMES, Belgrade, 2020.
[7] P.L. Ritger, N.A. Peppas, A simple equation for description of solute release II. Fickian and anomalous release from swellable devices, J. Controlled Release 5(1) (1987) 37-42.
[8] T. Higuchi, Rate of release of medicaments from ointment bases containing drugs in suspension, J. Pharm. Sci. 50 (1961) 874-5.
[9] M. Kopcha, N.G. Lordi, K.J. Tojo, Evaluation of release from selected thermosoftening vehicles, The Journal of pharmacy and pharmacology 43(6) (1991) 382-387.

MORPHOMETRICAL ANALYSIS OF RAT AORTA AFTER SUBACUTE DIBUTYL PHTALATE EXPOSURE

Jelena Marković Filipović, Jelena Karan, Ivana Ivelja, Nebojša Andrić,

Department od biology and ecology, Faculty of Sciences, University of Novi Sad, Novi Sad, Serbia
e-mail: jelena.markovic@dbe.uns.ac.rs

Abstract

Dibutyl phthalate (DBP) is an environmental toxic substance. It is a plasticizer present in many industrial and cosmetic products. During processes of production and use, DBP enters the environment, and it is found in atmosphere, soil and water. Bearing in mind that toxic DPB is widespread in the environment, and that human population in exposed to it in everyday life, the aim of our study was to examine whether DBP treatment affects microstructure of aorta. Female Wistare rats, 40 days old at the beginning of the experiment were exposed to DBP added to the diet in concentrations: 0, 100, 500, 5000 mg DBP/kg diet, that correspond to 8.58, 41.34 and 447.33 mg/kg BW/day. Formalin-fixed paraffin-embedded tissue of aorta was cut into 5 μm thin sections and stained with hematoxylin and eosin (HE) staining method. Morphometric evaluation of aortic sections was performed with Motic Images Plus morphometric software. The aortic wall thickness, cross-sectional area (CSA) and lumen diameter was determined. Lumen diameter and CSA showed dose-dependent increment in all DBP-treated groups compared to the control. However, statistical analysis revealed that only CSA in the group treated with highest DBP dose (5000 mg DBP/kg diet) was significantly different. There was no significant difference in wall thickness between control and DBP-treated rats. Obtained results indicate that high dose of DBP, by increasing aortic cross-sectional area, exerts a potentially adverse effect on the aorta.

METAL CONTENT IN THE SURFACE SOILS OF INDUSTRIAL AREAS IN NOVI SAD

Aleksandra Mihailović[1], Jordana Ninkov[2], Jovica Vasin[2], Selena Samardžić[1], Robert Lakatoš[1], Nebojša M. Ralević[1], Savka Adamović[1]

[1]Faculty of Technical Sciences, University of Novi Sad, Novi Sad, Serbia
[2]Institute of Field and Vegetable Crops, Novi Sad, Serbia
e-mail: zandra@uns.ac.rs

Abstract
The scope of this study was to investigate the heavy metal content in the industrial soils of Novi Sad, Serbia. A total of twenty topsoil samples (0–10 cm depth) were collected. The chemical properties of soil as well as the particle size distribution of soil (<2 mm fraction) were determined. Pseudo-total concentrations of cadmium, copper, lead, and zinc were measured using the ICP-OES device. Total mercury content in the samples was analysed using a Direct Mercury Analyzer (DMA) 80 Milestone. The results showed that the conc- entrations of Cu and Zn were found to be elevated at two locations. The concentration of Cd was very high at the same locations. Results revealed that no elevated values were detected for Pb at any location; all values were at the level of those in natural, unpolluted soils.

KEY WORDS: pollution, heavy metals, industrial soils

Introduction
Soil pollution by heavy metals is a widespread problem, posing a significant risk to human health or the environment. Rapid industrial growth and urbanisation of society have, in addition to numerous advantages, also resulted in the intensification of pollution of the environment. When compared to rural areas, urban areas have a higher population density, which results in more intense traffic, and are located closer to industrial plants and other sources of anthropogenic pollution [1]. As a result, the soil in urban areas is more susceptible to the negative effects of these factors. Industrial activities have great effects on heavy metal pollution, ecological risks, and health risks [2]. Heavy metals that have contaminated the soil are responsible for the disruption of natural geochemical cycles. Due to the fact that they are not biodegradable and have complex activity in the soil as well as long biological half-lives of elimination from the body, heavy metals are classified as dangerous pollutants. The aim of the study was to determine the concentration of Cd, Cu, Pb, Zn, and Hg in soil near industrial plants in Novi Sad, Serbia.
Of the five examined metals, copper and zinc are essential for organisms. However, if they are found in the soil in high concentrations, they can be toxic. The remaining three metals, cadmium, lead, and mercury, do not have a natural metabolic role in living organisms, but even in small concentrations they can have negative metabolic effects. Therefore, we can call these metals potentially toxic elements (PTE)[3]. In recent decades, there has been a general trend toward an increase in environmental pollution caused by cadmium (Cd). This is a result of its increased use in industry as well as the use of phosphorus fertilisers [4]. Cadmium is quite mobile in soil and therefore more available to plants than other toxic metals including Pb and Cu. Cadmium is an element of high toxicity, several times greater than arsenic.
All three naturally occurring forms of mercury (Hg) (methyl mercury (MeHg), Hg^0 and Hg^{2+}) have a negative impact on the environment and represent a global risk to human health. The main anthropogenic sources of mercury are ore processing and cement production, especially

coal and oil burning and gold production. Because atmospheric deposition is the primary source of mercury soil pollution that has a cumulative effect, it is of the utmost importance to know the background concentrations of mercury in the soil and to establish soil quality monitoring. Because of the high sensitivity of the equipment used for direct mercury determination in this study, the total mercury content (THg) was able to be determined for all of the soil samples. Mercury is a neurotoxin, making it a particularly hazardous substance for living things to be exposed to.

Copper (Cu) is found in the soil associated with organic matter, iron and manganese oxides, soil silicates, clay and other minerals. A characteristic feature of copper is that it is most often specifically adsorbed or "fixed" in the soil and has very low mobility [5]. Copper found in high concentrations in the uppermost layers of the soil is evidence that it was introduced by human activity (metal smelters, application of mineral fertilizers, waste sludge, fungicides and bactericides, organic fertilizers, etc.).

Lead (Pb) is one of the most common pollutants in urban areas. In addition to pollution due to the long-term use of leaded gasoline in the past decades, significant anthropogenic sources of lead are also lead mines and smelters, coal burning, various industrial processes (production of lead batteries), production of some types of rubber and plastic, and others [6].

Zinc (Zn) is an essential trace element for plant and animal organisms as it is a participant in numerous enzymatic reactions. Conversely, excess zinc in the soil is phytotoxic [7]. The content of Zn in the soil is determined by a number of factors, one of which is certainly the parent substrate from which the soil was formed. As a rule, soils with a fine-grained mechanical composition contain more zinc than coarse-grained soils.

The criteria presented in 2005 based on the average values of a large number of data for the concentration of potentially toxic elements in the soils of the Mediterranean, Central Europe, and Eurasia are shown in Table 1. In the Republic of Serbia, the criteria for non-agricultural land are in force according to the Regulation on the programme of systematic monitoring of soil quality, indicators for assessing the risk of soil degradation and the methodology for developing remediation programmes [8]. This regulation defines the limit values (GV) and remediation values (RV) of certain dangerous and harmful substances on non-agricultural land (Table 3).

Table 1. The content of metals in the soils of Europe (The European Soil Databasee, version V2.0, EUR 19945 EN) [9]

Element mg/kg	Background - Natural Values	Slightly Higher Values	Contamination	High Contamination
Cu	< 36	36 – 100	100 – 500	> 500
Zn	< 140	140 – 500	500 – 3000	> 3000
Cd	< 0,8	0,8 – 5,0	5 – 20	> 20
Pb	< 85	85 – 150	150 – 600	> 600

Experimental

All laboratory analyses were performed at the Laboratory for Soil and Agroecology of the Institute of Field and Vegetable Crops, Novi Sad, accredited according to the standard ISO/IEC 17025 (2005). The surface soil samples from 10 cm depth were collected in industrial zones of the city of Novi Sad, according to the methodology of the reference sample (circle method). One sample represents the average value of several individual soil samples, which were taken in concentric circles around one central point. The soil samples were air-dried at room temperature and milled to a particle size of < 2 mm. Particle size distribution was determined by the internationally recognised pipette method. The size fractions were defined as follows:

coarse sand (2 - 0.2 mm), fine sand (0.2 - 0.02 mm), silt (0.02 - 0.002 mm) and clay (< 0.002 mm). Chemical properties were obtained following standard procedures. The pH value in a 1:5 (V/V) suspension of soil in 1 mol/L KCl was determined using a glass electrode according to ISO 10390 (2010). The free $CaCO_3$ content was determined according to ISO 10693 (1995) by the volumetric method. Oxidation using the sulphochromic oxidation method specified in ISO 14235 was used to determine the amount of organic matter present.

The samples were analysed for pseudo-total contents of Cd, Cu, Pb, and Zn after digesting the soil in concentrated HNO_3 and H_2O_2 (5 HNO_3:1 H_2O_2, and a 1:12 solid:solution ratio) by stepwise heating up to 180 °C using a Milestone Vario EL III for 55 min. The concentration of metals was determined by ICP-OES (Vista Pro-Axial, Varian) in accordance with US EPA method 200.7:2001. The samples were analysed for total mercury content using the Direct Mercury Analyzer DMA 80 Milestone, which combines techniques of thermal decomposition, catalytic conversion, amalgamation, and atomic absorption spectrophotometry ($\lambda = 253.65$ nm) in solid soil samples. The detection limits for the metals studied were: 1.5 mg/kg (Cd), 5 mg/kg (Cu), 5 mg/kg (Pb), 5 mg/kg (Zn), and 0.0033 mg/kg for total Hg content.

Results and discussion

Table 2 shows the results of grain size analysis and basic chemical properties of the soil in industrial zones of the city of Novi Sad. The largest part of the examined soil samples corresponds to the mechanical composition of fine sand, 43.5%, while 13.7% of the examined soils have a clayey mechanical composition. The organic matter (OM) content in the soils varies from 0.22% to 4.70%, and the pH in KCl ranges from 7.07 to 8.46. The pH value and OM content have a significant influence on the accessibility of harmful and dangerous substances in the soil. The content of free $CaCO_3$ in the soil of the investigated localities is in a relatively wide range of classes, from weakly carbonated to highly carbonated soil.

Table 2. Physical and chemical properties of the soil in industrial zones of the city of Novi Sad, (n=20)

	Coarse sand %	Fine sand %	Silt %	Clay %	pH- KCl	$CaCO_3$ %	OM %
Mean	22.18	43.50	20.64	13.69	7.60	10.21	2.33
Median	13.95	40.39	17.70	13.02	7.59	9.97	2.47
Min	1.90	25.34	1.80	1.48	7.07	0.59	0.22
Max	71.10	68.68	35.80	27.20	8.46	28.85	4.70
SD	21.79	12.79	10.01	8.79	0.38	6.95	1.02

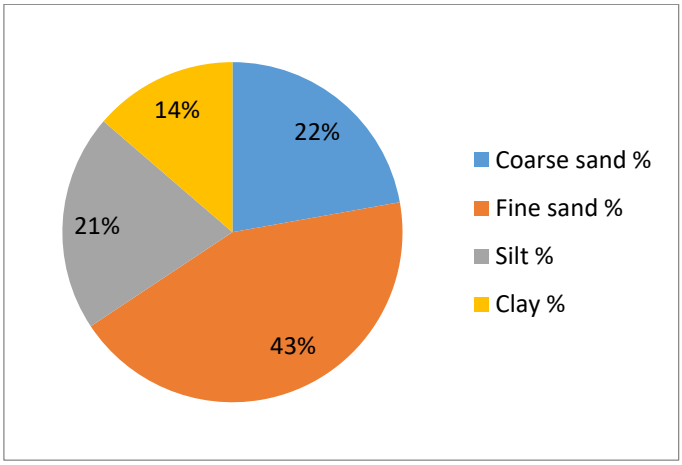

Figure 2. Particle size distribution in the soil of industrial zones in the city of Novi Sad

Statistical descriptions of metal concentrations (mg/kg) in the industrial soils of Novi Sad are shown in Table 3. Cadmium was detected at two locations in this research. Elevated concentrations of cadmium content were found in these samples, with concentrations of 4.54 mg/kg and 17.6 mg/kg, respectively. According to the criteria listed in Table 1, the soil from this locality belongs to contaminated soils.

Table 3. Metal concentrations (mg/kg) in industrial soils of Novi Sad (n = 20)

	Cu	Pb	Zn	Hg
Number of samples	20	20	20	20
Mean	59.12	19.41	111.26	0.086
Median	**29.20**	**14.65**	**75.35**	**0.052**
Min	5.50	3.20	24.80	0.009
Max	368.60	51.00	413.70	0.664
SD	88.62	12.22	102.60	0.141
Limited value	**36.00**	**85.00**	**140.00**	**0.30**
Remediation value	**190.00**	**530.00**	**720.00**	**10.00**

The obtained values of total mercury content (THg) vary in a wide range from 0.009 to 0.664 mg/kg, which is comparable to the Hg concentrations (0.01-1 mg/kg) of unpolluted soils. One sample exceeded the prescribed limit value for mercury concentration of 0.3 mg/kg. The prescribed limit value for copper, which is 36 mg/kg, is exceeded by the values of copper content in soil samples from five locations. Soil from two locations belongs to soils with slightly elevated values (44.0 and 43.6 mg/kg), and at three locations belongs to contaminated soils with concentrations of 368.6 mg/kg, 221.2 mg/kg, and 144 mg/kg, based on the criteria given in Table 1. It was found that samples with high levels of copper also had high levels of cadmium.
In all investigated locations, the lead content was at the level of background concentrations in the soil (Table 2), with the highest measured concentration being 51.0 mg/kg. In previous research [10], significantly elevated values (about 300 mg/kg) of total lead were detected in the vicinity of the traffic crossroads of Novi Sad as a result of the long-term use of leaded gasoline.
As already stated, four of the soil samples in this research exceed the prescribed limit value for zinc (140 mg/kg). These concentrations are slightly higher in comparison to soils in Europe (Table 1). The two samples represent soils that are already contaminated with high levels of cadmium and copper, as previously described. In these two samples, the concentrations of zinc were 368.6 and 413.7 mg/kg, respectively.

Conclusion

Based on the investigations carried out in 20 locations within the industrial zones of the city of Novi Sad, the following conclusions were made:

- The largest part of the examined soil samples (about 43%) has a mechanical composition of fine sand and the smallest part (14%) of clay.
- The largest parts of the investigated soils are weakly to moderately fortified with organic matter. The samples that were tested had a lot of $CaCO_3$, and most of them belonged to the slightly alkaline soil class based on their pH values.
- According to the content of investigated metals in relation to the criteria from the Regulation for non-agricultural soil, Cd exceeds the threshold value in two locations, Cu in five locations, Zn in four tested samples, and Hg in one location. At one of the investigated sites, the cadmium

concentration is higher than the remediation value, while copper concentrations are higher at two of the sites.
- In this research, extremely high concentrations of cadmium and high concentrations of copper and zinc were detected at two locations. These two relatively small areas under the lawn have a higher proportion of sand and are porous, hence the leaching of cadmium through the soil profile over a longer period of time can potentially pollute a larger area. This can take place over a longer period of time.
- The removal and proper disposal of contaminated soil in this area should be the focus of additional research on these locations, and it should be done with the goal of finding a long-term solution to the problem.

Acknowledgements
This research has been supported by the Ministry of Education, Science and Technological Development through the project no. 451-03-68/2020-14/200156: "Innovative scientific and artistic research from the FTS (activity) domain".

References
[17] G. Shi, Z. Chen, S. Xu, J. Zhang, L. Wang, C. Bi, J. Teng, Potentially toxic metal contamination of urban soils and roadside dust in Shanghai, China, Environmental Pollution 156 (2008) 251-260.
[18] Z. Long, Y. Huang, W. Zhang, Z. Shi, D. Yu, Y Chen, C. Liu, R. Wang, Effect of different industrial activities on soil heavy metal pollution, ecological risk, and health risk. Environ Monit Assess. 193(1) (2021).
[19] J. Briffa, E. Sinagra, R. Blundell, Heavy metal pollution in the environment and their toxicological effects on humans, Heliyon, 6(9) 2020.
[20] A. Kabata- Pendias, H. Pendias, Trace elements in soils and plants, 3rd ed., CRC Press, USA. 2001
[21] K.T. Semple, K.J. Doick,K.C. Jones, P. Burauel, A. Craven, H. Harms, Defining bioavailability and bioaccessibility of contaminated soil and sediment is complicated. Environ Sci Technol, 38(12) (2004) 228A-231A.
[22] B.E. Davies, Lead, in: Alloway, B.J. (Ed.), Heavy Metals in Soils. Blackie and Son Ltd., 1995
[23] A. Vanek,L. Boruvka, O. Drabek, M. Mihaljevič,M. Komarek, Mobility of lead, zinc and cadmium in alluvial soils heavily polluted by smelting industry, Plant Soil and Environment 51(7) (2005) 316-321.
[24] "Official Gazette of RS", no. 88/2010 of November 23, 2010
[25] B. Houskova, L. Montanarella, Parent material as a source of natural background values in soils. European Commission-Joint Research Centre, 2005
[10] A. Mihailović, Lj. Budinski-Petković, S. Popov, J. Ninkov, J. Vasin, N.M. Ralević, M. Vučinić Vasić, Spatial distribution of metals in urban soil of Novi Sad, Serbia: GIS based approach, Journal of Geochemical Exploration, 150 (2015) 104-114.

A FIBROCYTE MODEL FOR MONITORING ENVIRONMENTAL CHEMICALS

Krisztián Sepp[1] and Miklós Imre Mózes[1,2,3], Marianna Radács[2], Péter Hausinger[3], Márta Gálfi[2], Zsolt Molnár[2]

[1]Endocrine Unit of First Department of Internal Medicine, University of Szeged, Szeged H-6725, Hungary
[2]Institute of Applied Health Sciences and Environmental Education, Juhász Gyula Faculty of Education, University of Szeged, Szeged H-6725, Hungary
[3]Invasive Cardiology Department, Second Department of Internal Medicine and Cardiology, Faculty of Medicine, University of Szeged, Szeged, Szeged H-6725, Hungary
e-mail: mikeleoden@gmail.com

Abstract
Human activity affects all elements of the Earth's environment and the system of relationships between them. Chlorobenzenes created during chemicalization are capable of modulating the adaptation potential of biological organisms and because of their high frequency of occurrence in the food chain, they can be used as expositors in environmental exposure models. It is necessary to develop a biological model system suitable for the investigation of environmental pollutant chemical agents, which indicates changes quickly and easily.

Introduction
Human society is the highest known complexity in terms of earthly conditions, in which the actors are able to transform the environment according to the needs of their existence through their cooperation. As a result, human activity affects all elements of the Earth's environment and the system of relationships between them [1]. Human activity (e.g. chemicalization) and its consequences - which initially served short-term needs of the society effectively, however, highly chemically stable, substances as xenobiotics synthesized during chemicalization, have already changed the accommodation patterns of biological organisms, which is why such models are necessary with which even discrete changes can be easily tracked. The chemicals burdening the environment are chlorobenzenes (ClBs) with massive chemical stability, which are deposited in the lipophilic phases of living organisms (e.g. brain and endocrine tissues) [2]. They induce a dose-dependent toxic effect in the cells of the affected tissues. Due to their high frequency of occurrence in the food chain [3], these agents can be used as expositors in environmental exposure models.
Fibrocytes are mesenchymal progenitor cells that originate from bone marrow cells, and it can also be known that they carry the mixed morphological and molecular characteristics of hematopoietic stem cells, monocytes and fibroblasts [4, 5]. They are probably precursor intermediate cells of the monocyte differentiation lineage. They show characteristics related to the mesenchymal stromal cells found in the bone marrow, they are multipotent progenitor cells that can produce different mature cell types during their differentiation [6]. *In vitro* experiments have proven that peripheral blood mononuclear cells or CD14+ monocytes are able to transform into fibrocytes during their differentiation. There are many factors that promote or inhibit fibrocyte differentiation, including cytokines, growth factors, immunoglobulins, and environmental artificial chemicals. Fibrocytes also play a key role in wound healing and tissue repair processes. They are unique cells that mediate the proinflammatory properties of macrophages and the tissue-remodelling properties of fibroblasts, so their model study can be very interesting in relation to environmental factors [5, 7].

Aim

The aim of this study was to monitor the effects of different doses of chlorobenzenes (ClB) treatments on the changes in the proliferative activity (e.g. protein production) fibrocytes, in order to develop a biological model system suitable for testing artificial homeostatic disruptor agents.

Methods

***In vivo* protocol**

Male Wistar rats (Charles River, Isaszeg, Hungary, medically certified) from different litters (weighing 120-250 g, aged 4-6 weeks at the beginning of the research) were used for cell culture model systems. The animal care and research protocols were in full accordance with the guidelines of University of Szeged, Hungary. During the research period, rats were kept under controlled relative air humidity of 55-65% and 22±2°C ambient temperature. Experimental animals lived under automated diurnal conditions (12 h dark and 12 h light system) in groups of 10 animals for the end of the research period. Standard pellet food (CRLT/N, Charles River, Magyarország) and tap water were available *ad libitum.* Male Wistar rats were treated with combined ClB (1:1 mixture of 1,2,4- trichlorobenzene /CAS number: CAS Number: 2199-72-6, Sigma Aldrich, USA, St. Louis) and hexachlorobenzene / CAS number: 93952-14-8, Sigma Aldrich, USA, St. Louis), in 1 mL of 0.015% ethanol in distilled water was administered daily) in a dose of 0.1, 1.0 and 10.0 µg/b.w. kg via a gastric tube. The rats were exposed to ClB for 30 (n=10), 60 (n=10) and 90 (n=10) days. Control groups were set up: stress control (n=5, gastrostomy tube insertion group), absolute control (AC) (n=5, untreated group), positive control group (n=5, receives ClB solvent, 0.015% ethanol solution via gastric tube) and negative control group (n=5, receives water via gastric tube). At the endpoints of the experiment (30, 60 and 90 days), after pentobarbital anaesthesia (4.5 mg/b.w. kg, Nembutal, Abbott, USA) the animals were used for study.

***In vitro* protocol**

After anesthesia with pentobarbital (4.5 mg/kg, Nembutal, Abott, USA), from the treated and untreated experimental animals skin sample was taken.

For fibrocyte cell cultures (FC), subcutaneous connective tissue samples were enzymatically treated (trypsin: 0.2 % /Sigma Aldrich, USA, St. Louis/ for 30 minutes; collagenase /Sigma Aldrich, USA, St. Louis/: 30 µg/ml for 40 minutes; dispase /Sigma Aldrich, USA, St. Louis/: 50 µg/ml for 40 minutes, phosphate buffer /PBS-A/; temperature: 37°C/ was used to prepare the solutions) and dissociated mechanically digested (using a nylon-blutex filter with a pore diameter of 83 and 48 µm), then placed in a 6-well plate, which was filled with 50 µl with MEM-α medium supplemented with 10% FCS, 1.0 µg/mL Penicillin+Streptomycin (Sigma Aldrich, USA, St. Louis) and 1% ITS-G supplement solution (Thermo Fisher Scientific inc. Rockford, USA: bovine insulin, transferrin and sodium selenite). The plates containing fibrocytes were incubated at 37°C (5% CO_2) and the culture medium was changed every 2-3 days (sterile PBS+1.0 µg/mL Penicillin+Streptomycin /Sigma Aldrich, USA, St. Louis/) [8].

The induction of cell proliferation was performed on separate reference systems treated with 1 mg/mL benz[c]-acridine (BcA) (Sigma Aldrich, USA, St. Louis) for 168 h, because we can compare the quantitative and qualitative appearance of the tumor clones induced by it with effect of chlorobenzene. *In vivo* ClB pretreated FC were treated with acute exposure of ClB (0.1; 1.0; 10.0 µg/mL) for 168 h. The results obtained were compared with BcA. The protein content of the samples was determined using a modified Lowry method [9] and Pierce BCA Protein Assay Kit (Thermo Fisher Scientific Inc., Rockford, USA).

Statistical analysis

To compare the means of different treatment doses (0.1, 1.0, 10.0 µg/b.w. kg) to the controls during 30, 60 and 90 days long treatments (n=5 in each group of time and dose) two-way ANOVA was run. Dose and time were used as the two factors for analysis.

Results and discussion

According to environmental aspects, if a process originating from an impact factor causes a change in the studied environmental factor or its state (e.g. cell activity, proliferative activity), in this case alteration in protein production may be triggered as direct effect. The results are presented to the absolute control group.

Number of tumor clones as a result of ClB treatments

	Fibrocyte
AC	0
BcA	47.3±4.2*

Table 1 The number of tumor clones in response to the reference absolute control (AC) and benz[c]-acridine (BcA) treatment (number of cells±S.E.M., *:p<0.001)

From the data in Table 1, it is clear that BcA significantly induced tumor clones in the model system.

Fibrocyte tumor clones after treatment			
ClB treatment	**30 days**	**60 days**	**90 days**
ClB 10.0 µg/bw. kg	0	1.32±0.02*	1.71±0.04*
ClB 1.0 µg/bw. kg	0	0	1.1±0.01*
ClB 0.1 µg/bw.kg	0	0	0.32±0.01*

Table 2 The number of tumor clones in fibrocyte (FC) cell populations as a result of each ClB treatment (number of cells±S.E.M., *:p<0.001)

When examining the results of protein production, it can be established that a significant increase (p<0.001) in protein production was observed already at 0.1 µg/bw. as a result of ClB treatments. The model is functional, because the results correlate with the increase of the numbers of tumor clones induced by benz(c)-acridine and also with increased protein production (FC: 28.11 ±2.99 mg protein/plate), compared to the AC groups (FC: 3.56±0.26 mg protein/plate).

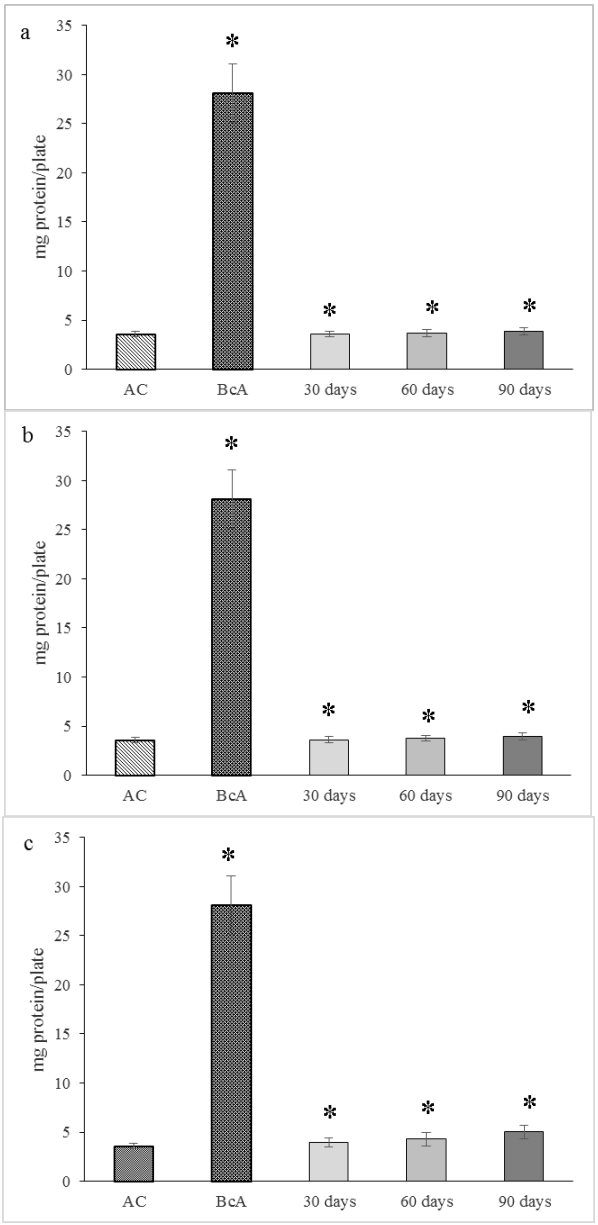

Figure 1 The effect of different ClB exposures on protein production in FC cell cultures (a: 0.1 µg/bw. kg, b: 1.0 µg/bw. kg, c: 10.0 µg/bw. kg doses, *:p<0.001, n= 5/group)

In the case of FC, compared to the AC group, ClB treatments significantly increased protein production in all experimental endpoints. The highest protein production was observed after 90 days of treatment for all three treatment doses (0.1 µg/bw. kg dose: 3.85±0.38 mg protein/plate, 1.0 µg/bw. kg dose: 3.96±0.38 mg protein/plate, 10.0 µg/bw kg dose: 5.01±0.69 mg protein/plate).

ClB can be classified as xenobiotics, which can generate changes in many physiological processes. Living systems are affected by complex environmental exposures *in vivo*, however, if these exposures are very low (subtoxic concentrations), they can exert their effects in a latent manner for a long time. As a result, it is necessary to develop a model that is suitable for evaluating and detecting the effects of subtoxic *in vivo* exposures in a complex manner.

The peripheral system elements, such as mesenchymal-derived fibrocytes could be suitable for examining the effects of ClBs. Such molecules (ClBs) are able to generate changes in the central axis [10] and in the peripheral elements [11].
Therefore we should call these agents (e.g. ClB-s) homeostatic disruptor compounds. The ClB-mix exposures resulted in a dose-dependent increase in cell proliferation.

Conclusion

According to our morphological observations, ClB treatments induced tumor clone formation in the first generations of primary cell cultures in a time- and dose-dependent manner. As a result of treatment with a higher dose of ClBs, tumor clone formation generated in FC cell cultures were detected after only 60 days. The fibrocyte cell cultures responded with a more sensitive reaction to the chemical agents included in the experiment. This means that the ClBs included in the model study exert an effect of both initiation and promotion. Thus, it can be established that ClBs exert a general effect on these model cells.

Acknowledgements

This study was supported by EFOP-3.6.1-16-2016-00008, EFOP-3.4.3-16-2016-00014, TÁMOP-4.2.4.A/2-11/1-2012-0001 and Juhász Gyula Faculty of Education's "Scientific and Artistic Activity Support Grant".

References

[1] Loeb J. Balancing human and natural worlds. Vet Rec. (2020) 187(10):375.
[2] Charisiadis P., Andrianou X. D, van der Meer T. P., den Dunnen W. F. A., Swaab D. F., Wolffenbuttel B. H. R., Makris K. C., van Vliet-Ostaptchouk J. V. Possible Obesogenic Effects of Bisphenols Accumulation in the Human Brain. Sci Rep. (2018) 8(1):8186.
[3] Mrema E.J., Rubino F.M., Brambilla G., Moretto A., Tsatsakis A.M., Colosio C. Persistent organochlorinated pesticides and mechanisms of their toxicity. Toxicology, (2013) 307:74-88.
[4] Krenning G., Zeisberg E.M., Kalluri R. The origin of fibroblasts and mechanism of cardiac fibrosis. J Cell Physiol. (2010) 631-7.
[5] de Oliveira R.C., Wilson S.E. Fibrocytes, Wound Healing, and Corneal Fibrosis. Invest Ophthalmol Vis Sci. (2020) 61(2):28.
[6] Pittenger M.F., Mackay A.M., Beck S.C., Jaiswal R.K., Douglas R., Mosca J.D., Moorman M.A., Simonetti D.W., Craig S., Marshak D.R. Multilineage potential of adult human mesenchymal stem cells. Science, (1999) 284(5411):143-7.
[7] Bellini A., Mattoli S. The role of the fibrocyte, a bone marrow-derived mesenchymal progenitor, in reactive and reparative fibroses. Lab Invest. (2007) 87(9):858-70.
[8] Osborn A., Caruana D., Furness D.N., Evans M.G. Electrical and Immunohistochemical Properties of Cochlear Fibrocytes in 3D Cell Culture and in the Excised Spiral Ligament of Mice. J Assoc Res Otolaryngol. (2022) (2):183-193.
[9] Lowry O.H., Rosebrough N.J., Farr A.L., Randall R.J. Protein measurement with the Folin phenol reagent. The Journal of Biological Chemistry, (1955) 193 265–275.
[10] Nagyeri G., Valkusz Z., Radacs M., Ocsko T., Hausinger P., Laszlo M., Laszlo FA., Juhasz A., Julesz J., Galfi M. Behavioral and endocrine effects of chronic exposure to low doses of chlorobenzenes in Wistar rats. Neurotoxicol Teratol. (2012) 34:9-19
[11] Wei Y., Zhu J. Para-dichlorobenzene exposure is associated with thyroid dysfunction in US adolescents. J Pediatr. (2016) 177:238-243.

SMOKING HABITS, CADMIUM EXPOSURE AND VULNERABILITY TO CHEMICALS OF LUNG ADENOCARCINOMA MALE PATIENTS IN VOJVODINA

Maja Milanović[1], Nataša Milošević[1], Danica Sazdanić Velikić[1,2], Jovana Drljača[1], Sanja Bijelović[1,3], Jan Sudji[1,4], Mirjana Ševo[2], Danijela Lukić[3], Nataša Milić[1]

[1]University of Novi Sad, Faculty of Medicine, Novi Sad, Serbia
[2]Institute for pulmonary diseases of Vojvodina, Clinic for pulmonary oncology, Sremska Kamenica, Serbia
[3]Institute of Public Health of Vojvodina, Novi Sad, Serbia
[4]Institute of Occupational Health Novi Sad, Novi Sad, Serbia
email: maja.milanovic@mf.uns.ac.rs

Introduction

The American Cancer Society estimates that each year, more people die of lung cancer than of colon, breast, and prostate cancers combined. It is evaluated that 87% lung cancers are non-small cell cases, out of which 52% are adenocarcinoma. During their lifetime, 1 in 15 men will be affected by lung cancer and the risk for the smokers is higher.

Experimental

In this research 28 male patients (39-77 years old) with inoperable IIIB and IV stadium of adenocarcinoma, diagnosed in the Institute for Pulmonary Diseases of Vojvodina, Serbia were enrolled. The patients were asked to fulfil questionnaire regarding their exposure to chemicals during lifetime and their smoking habits. The presence of cadmium (Cd) was determined by ICP-MS in their morning urine samples.

Results and discussion

More than one third of the included patients, 35.71% (10/28) had been exposed to various chemicals during their education or in their free time, while 32.14% (9/28) have been exposed to chemicals professionally. The list of chemicals includes ammonia, mineral acids, pesticides, petroleum products, paints, varnishes, glues and organic solvents. Only 2 of them have not been smoking during their lifetime, while 92.86% (26/28) reported that have been or had been heavy cigarette smokers who had started to smoke on average at the age of 19.6 years. As ex-smokers were registered 57.14% (16/28) patients who had been smoking on average for 38 years 25.83 cigarettes a day. Active smokers who were included in this study 35.71% (10/28), smoke on average 29.17 cigarettes daily. Cd was detected in 53.57% (15/28) of total urine samples, 62.50% (10/16) of ex-smokers versus 40.00% (4/10) active smokers.

Conclusion

In this study for the first time, the exposure to chemicals and smoking habits among lung adenocarcinoma male patients in Western Balkan Region are reported.

Acknowledgement

This work was supported by the Provincial Secretariat for Higher Education and Scientific Research, AP Vojvodina, Republic of Serbia [grant number 142-451-2675/2021-01].

APPLICATION OF MODERN MECHANISM ON POULTRY FARMS AND ITS IMPACT ON THE ENVIRONMENT

Milena Milojević, Suzana Knežević, Goran Stanišić

Academy of Vocational Studies Šabac, Unit of Agricultural and Business Studies and Tourism, Vojvode Putnika 56, 15000 Šabac, Srbija
e-mail: milena.n.milojevic23@gmail.com

Abstract
The modern way of raising poultry is significantly different from poultry farming as it used to be. The development of poultry production and increased profitability was contributed, first of all, by the development of science, which found a number of solutions for the rapid increase in the number of poultry and its productivity. The development and application of mechanization and automation contributed to the industrial character of production. Modern poultry farms are equipped with machinery that, in addition to the welfare of poultry farming, contributes to increasing labor productivity, saving labor and improving the general state of the environment on farms. When designing new and expanding existing poultry farms, guidelines for the application of clean technologies are increasingly being used, which aim to reduce negative impacts on the environment. The equipment is characterized by a high degree of automation, and there is an increasing application of information technologies in poultry farming. A big problem on traditional poultry farms is low energy efficiency and increased energy consumption, which can be overcome by using smart control systems, which is also an advantage from an environmental point of view.

Introduction
Agriculture plays an important role in the economy of many countries. Research indicates that there is a correlation between agricultural growth and economic prosperity. In this context, investment in new technologies in the field of agricultural mechanization is significant in the field of poultry farming. The emphasis is on the use of information technologies in poultry farming, which would include: 3D printers, drones, sensors for individual monitoring, artificial intelligence, virtual reality, robots, Internet of Things (IoT) [1].
Poultry farming is the process of raising domestic birds such as chickens, ducks, turkeys and geese for the purpose of obtaining meat or eggs for food. In the past, poultry farming, starting with eggs for planting, and ending with the final products - meat and eggs for consumption, took place as a single process and in different farming systems [2, 3, 4]. Conventional poultry farming on farms, due to inefficient methods and equipment, can lead to financial losses [5]. When using new technologies on poultry farms, it is necessary to control all environmental parameters that affect the growth of chickens, such as temperature, humidity, ammonia [6].
Some of the leading manufacturers of mechanization and equipment in the poultry industry, such as Big Dutchman AG, have developed automated systems of high technical performance.

Experimental
In the paper, two cases of application of new technologies were observed - a farm with modern automated equipment and a SMART poultry farm.

1. Modern automated equipment on poultry farms
Machines and equipment on modern poultry farms include feeders, waterers, ventilation and heating systems, lighting, equipment and fertilizing machines. The equipment is automated,

with minimal use of human labor. The paper analyzes the equipment manufactured by Big Dutchman AG.
An example of an automated feeding system is shown in Figure 1. It is the AUGERMATIC system - tubular floor conveyor.

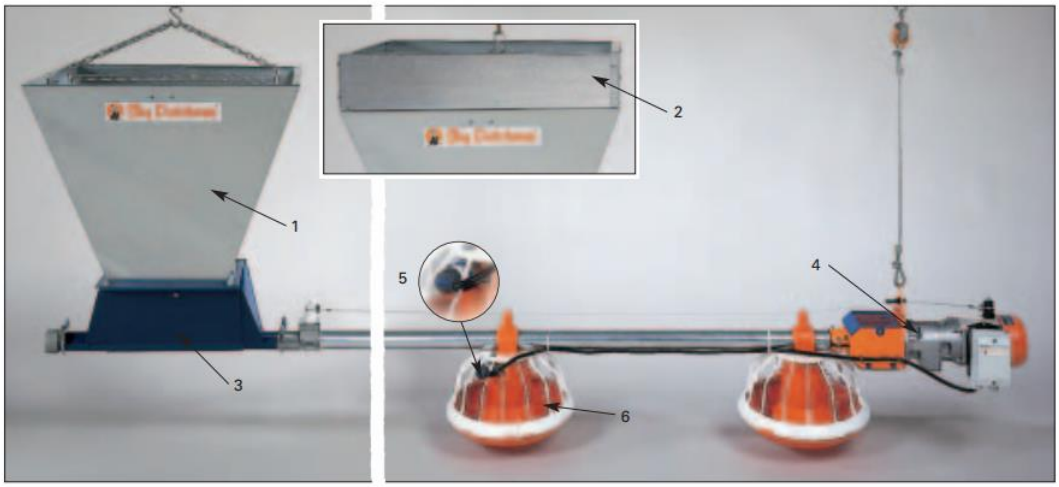

Figure 1. Feeding system AUGERMATIC [7]

Its innovation is reflected in the fact that the upper part of the feeding basket (1) with or without extension (2) is easily separated from the lower part of the food basket (3). In this way, the entire system can be lifted up to the ceiling every time. This makes it possible to reach the maximum height under the feeder during fertilizing. A strong drive unit (4) and a strong spiral allow a transport length of up to 150 m. At the same time all the feeders are filled with food, the sensor (5) and the control feeder (6) automatically turn off the unit.
The choice of a poultry watering system depends on the type of poultry, the area of use, the conditions in the rearing area and the special requirements of the user. One of the solutions are nipple-drinkers, as a reliable and hygienic solution for supplying drinking water (picture 2).

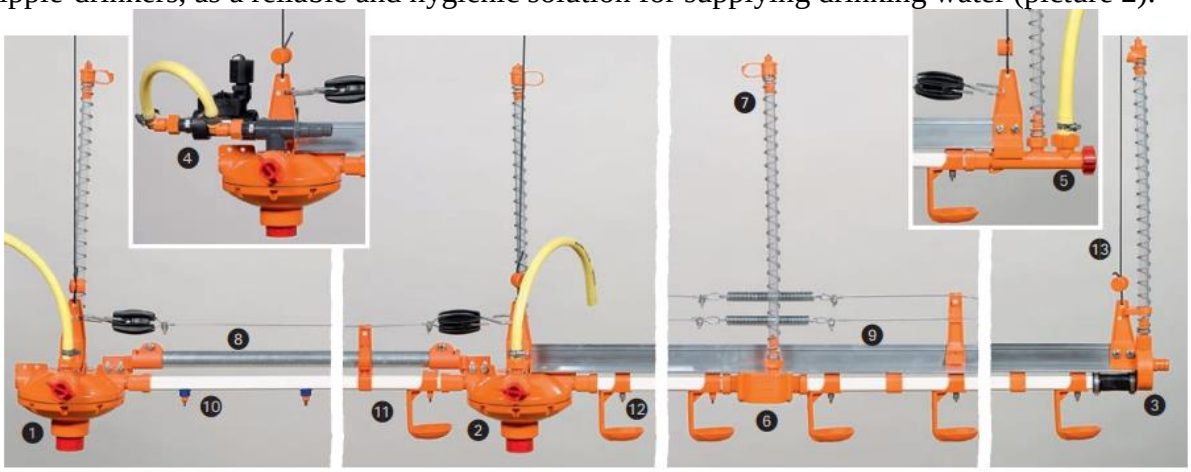

Picture 2. Nipple of the drinking bottle [8]

Van - the ventilation system is an intelligent climate regulation system on the farm. Two different ventilation systems (side and tunnel ventilation) are combined in one facility to ensure stable climate management and optimal ambient conditions for poultry. The application of this solution is recommended in regions where the climate is characterized by large temperature fluctuations (Figure 3).

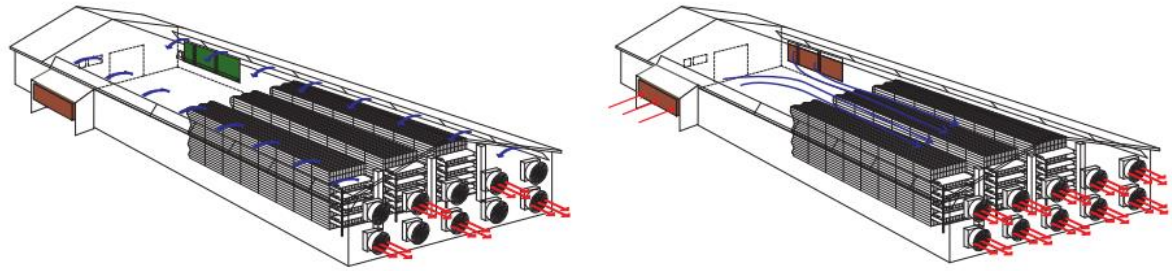

(a) (b)

Figure 3. Combi ventilation system (a-ventilation in side mode, b- ventilation in tunnel mode) [9]

For heating on poultry farms, it is possible to apply different heating systems that can be gas, oil or hot water. The choice depends on the size of the farm and the climate of the area where the farm is located. The goal is to achieve maximum energy efficiency. Big Dutchman offers: JetMaster heaters, devices with flue gas exhaust, gas heaters, recirculation fans for improved hot air distribution, hot water convection heaters, finned tube heaters and infrared heaters [10].

LED lighting is taking precedence on modern farms. There are different types of LED lighting such as: flexible tube lamps (FlexLED, FlexLED HO, FlexLED eco), professional LED ceiling lamps (ZeusLED).

(a) (b)

Figure 4. Use of LED lighting (a- FlexLED, b-ZeusLED) [11]

Such heating and lighting solutions on farms are more favorable from an ecological point of view and in accordance with the principles of sustainable development

1. SMART poultry farm

A smart poultry farm is characterized by features such as automated feed and water supply, egg collection and maintenance of precise poultry environmental parameters. The techniques used are data storage via IoT, GSM - Global System for Mobile Communication, the use of applications on mobile phones that enable the protection of the farm in real time by notifying the farmer via SMS about any alarming situation [12, 13, 14].

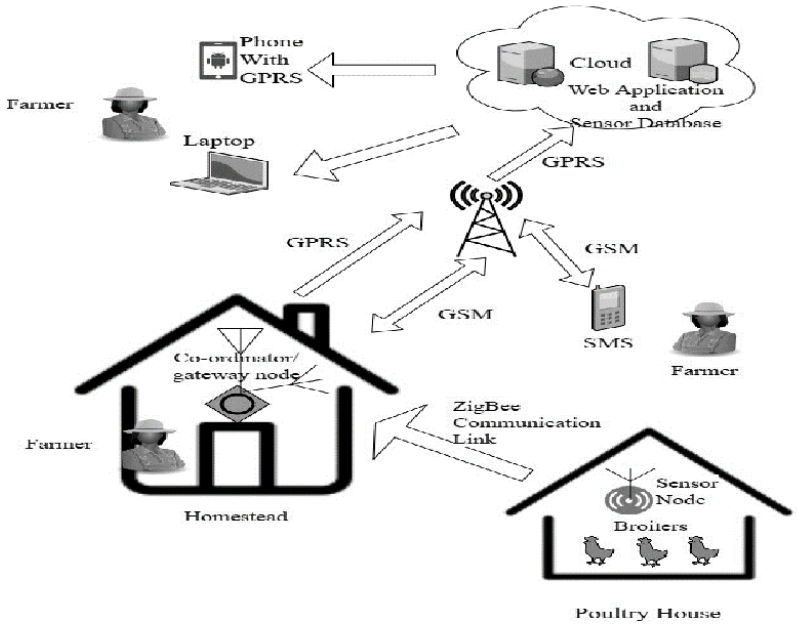

Figure 5. An example of a SMART poultry farm [11]

Results and discussion

Modern poultry farms are characterized by the use of modern mechanization and equipment, which enables higher productivity, better conditions for poultry and easier work for farmers. Processes are automated with the increasing implementation of information technologies. Energy and ecological heating and lighting systems are used. In the world, SMART poultry farms with the implementation of IoT, artificial intelligence systems, drones and robots are extensively used in the segments where it is applicable. Apart from procuring the appropriate software and hardware components, farmers must be trained in the proper use of the applications.

Conclusion

The progress of science, technical inventions and information technologies affects changes in all segments of modern agriculture, including mechanization on poultry farms. These changes bring greater productivity and economic profit, but attention should also be paid to better environmental protection in order to reach the fundamental goals of sustainable development. This paper presents only some innovative and environmentally justified solutions related to the application of modern mechanization - new technologies on poultry farms.

References

[1] A. Kekić, (2018, March 5). *Nove Tehnologije U živinarstvu*. Agroklub.rs. Retrieved October 17, 2022, from https://www.agroklub.rs/stocarstvo/nove-tehnologije-u-zivinarstvu/40609/.

[2] V. Petrović. Živinarstvo, Naučna knjiga (1991). Beograd.

[3] D. Živković, D. Drudarski, S. Mitrović, S. Todorović. Uticaj načina gajenja na ispoljavanje proizvodnih osobina 18-to nedeljnih kokica Isabrown hibrida kokoši. *Zbornik radova "Živinarski dani"* (1991). 78-74, Ohrid.

[4] B. Supić, N. Milošević, T. Čobić. Živinarstvo. Univerzitet u Novom Sadu, Poljoprivredni fakultet (2000). Novi Sad.

[5] M. R. Ahmadi, N. A. Hussien, G. F. Smaisim, & N. M. Falai, A Survey of Smart Control System for Poultry Farm Techniques. In *Proc of the International Conference on Distributed Computing and High Performance Computing (DCHPC2018)* (2019) (pp. 25-27).
[6] E. Hitimana, G. Bajpai, R. Musabe, & L. Sibomana, Remote monitoring and control of poultry farm using IoT techniques. *International Journal of Latest Technology in Engineering, Management & Applied Science*, *7*(5), (2018) 87-90.
[7] Big Dutchman. (n.d.). Retrieved October 20, 2022, from http://bigdutchman.rs/wp-content/uploads/augermatic.jpg.
[8] Big Dutchman. (n.d.). Retrieved October 20, 2022, from http://bigdutchman.rs/wp-content/uploads/8.sistemi-pojenja2.pdf.
[9] Big Dutchman. (n.d.). Retrieved October 20, 2022, from http://bigdutchman.rs/wp-content/uploads/2.CombiTunnel-Ventilation-sr.pdf.
[10] Big Dutchman. (n.d.). Retrieved October 20, 2022, from http://bigdutchman.rs/wp-content/uploads/Heizsysteme-Gefl%C3%BCgel_ser.pdf.
[11] Big Dutchman. (n.d.). Retrieved October 20, 2022, from http://bigdutchman.rs/wp-content/uploads/18-2520-18-2520-LED-Beleuchtung-sr.pdf.
[12] M.M. Islam, S. Sourov Tonmoy, S. Quayum, A.R. Sarker, S. Umme Hani, & M.A. MannanSmart Poultry Farm Incorporating GSM and IoT. 2019 International Conference on Robotics,Electrical and Signal Processing Techniques (ICREST), (2019). 277-280.
[13] S. Arunkumar, and N. Mohanasundaram. Smart poultry farming. *International Journal of Innovative Technology and Exploring Engineering* 8.2 (2018): 289-291.
[14] H. Phiri, D, Kunda, & J. Phiri. An IoT Smart Broiler Farming Model for Low Income Farmers. *International Journal of Recent Contributions from Engineering, Science & IT (iJES), 6*(3), (2018). pp. 95–110. https://doi.org/10.3991/ijes.v6i3.928

SMOKING HABITS AND CADMIUM AS BIOMARKER AMONG LUNG CANCER FEMALE PATIENTS IN VOJVODINA

Nataša Milošević[1], Maja Milanović[1], Sanja Bijelović[1,2], Danica Sazdanić Velikić[1,3], Jovana Drljača[1], Nataša Milić[1], Jan Sudji[1,4], Mirka Lukić Sarkanović[1,5], Ljilja Torović[1,2], Milorad Španović[1,4]

[1]University of Novi Sad, Faculty of Medicine, Novi Sad, Serbia
[2]Institute of Public Health of Vojvodina, Novi Sad, Serbia
[3]Institute for pulmonary diseases of Vojvodina, Clinic for pulmonary oncology, Sremska Kamenica, Serbia
[4]Institute of Occupational Health of Novi Sad, Novi Sad
[5]University Clinical Center of Vojvodina, Clinic for anesthesiology, intensive therapy and pain therapy, Novi Sad, Serbia
e-mail: natasa.milosevic@mf.uns.ac.rs

Introduction

Lung cancer is the second most common cancer (after breast cancer) in women and by far the leading cause of cancer death. According to the American Cancer Society there is chance of 1 in 17 women to be affected by lung cancer in their lifetime, with higher risk for the smokers.

Experimental

In this study 21 women (44-83 years old) with inoperable IIIB and IV stadium of lung carcinoma, diagnosed in the Institute for Pulmonary Diseases of Vojvodina, Serbia were enrolled. All the women were asked to fulfil a questionnaire regarding their smoking habits. Their morning urine samples were collected and analysed by ICP-MS for the presence of cadmium (Cd) in the urine samples.

Results and discussion

More than half of the patients, 52.38% (11/21) enrolled in this study were diagnosed with adenocarcinoma, 23.81% (5/21) had squamous lung carcinoma while 14.28% (3/21) were discovered to have neuroendocrine lung carcinoma and 9.52% (2/21) were identified with small cell lung carcinoma. All of them were or still are heavy smokers who had or have been smoking cigarettes actively on daily basis. They had started to smoke on average at the age of 20 years (the youngest at the age of 12), and have been smoking for almost 41 year on average (15-56 years of smoking experience). Out of nine who have reported that had stopped smoking, only three had quitted smoking for 1 year or longer. Most of them 85.71% (18/21) origin from a family with smokers. On average, they had or have been smoking approximately a pack of cigarettes (18.8 cigarettes a day). In this study Cd was detected in 80.95% (17/21) of samples. All women with neuroendocrine lung carcinoma and small cell lung carcinoma had Cd in their morning urine samples.

Conclusion

To the best of authors knowledge such study has not been performed in Western Balkan Region. The obtained results confirmed that Cd is omnipresent in urine of women with lung cancer and that exposure to Cd is associated with smoking.

Acknowledgement
This work was supported by the Provincial Secretariat for Higher Education and Scientific Research, AP Vojvodina, Republic of Serbia [grant number 142-451-2675/2021-01].

UTILIZATION OF SOY HULL FOR PRODUCTION OF PECTIC FIBER

Maja Milošević[1], Milica Perović[1], Zorica Knežević Jugović[2], Mirjana Antov[1]

[1]Department of Applied and Engineering Chemistry, Faculty of Technology, University of Novi Sad, Blvd. Cara Lazara 1, Novi Sad, Serbia
[2]Department of Biochemical Engineering and Biotechnology, University of Belgrade, Karnegijeva 4, Belgrade, Serbia
e-mail: maja.milosevic@uns.ac.rs

Abstract
Soy hull, a by-product of soybean processing, was investigated as a source of pectic fiber. Pectic fiber was obtained with yield of 5.72 g/100 g_{DW}. Soy hull pectic fiber demonstrated good solubility (83.49%) and high molecular weight with Mw of dominant fraction 3192.6 kDa. These favorable characteristics could indicate a great potential for application in food industry.

Introduction
Pectins are a group of complex structural heteropolysaccharides with α-(1–4)-D-galacturonic acid as the main chain [1]. Pectin is widely used in food industry as stabilizing, thickening and gelling agent, and it keeps gaining more interest in applications such as functional foods, prebiotics, edible packaging, active substance carrier, etc. [2]. Commercial pectin is commonly extracted from citrus peels, apple pomace and sugar beet [3] but as the demand for pectin continually grows, it is necessary to identify and utilize new pectin sources [4]. Soy hull is a by-product of the soybean industry and it's available in large quantities. This raw material could be an alternative source of pectin rich fiber. Furthermore, soy hull can be easily transported and stored, simplifying its handling while avoiding deterioration of the material [1]. The objective of this research was to evaluate soy hull as a potential source of pectin rich fiber. The solubility of obtained fiber was determined as well as its molecular weight.

Experimental
Soy hull was a kind gift from Sojaprotein, Bečej (Serbia). Pectic fiber was extracted in conventional hot-acid extraction, precipitated with ethanol and freeze-dried [3]. Solubility of extracted pectin fiber was determined according to Bouaziz et al. [5]. Molecular weight was determined by HPSEC on Waters HPLC system (1515 isocratic pump and 2414 RI detector) and a PL Aquagel-OH mixed M column (Agilent Technologies) according to Milošević et al. [6].

Results and discussion
Pectic fiber was extracted from soy hull and its yield is given in Table 1. The obtained yield was 5.72 g from 100 g of soy hull dry weight.

Soy hull pectic fiber showed good solubility in water; 83.49% of pectin was dissolved as presented in Table 1.

Table 1. Soy pectic fiber extraction yield and solubility

Pectic fiber yield (g/100 g_{DW})	Solubility (%)
7.72 ± 0.07	83.49 ± 1.97

Figure 1 shows HPSEC profile of soy hull pectic fiber and in Table 2, molecular weights, surface areas and polydispersity indices of different molecular weight fractions of soy hull pectic fiber are given. Soy hull pectic fiber had two distinct peaks (fractions 2 and 3) as well as one smaller peak (fraction 1) corresponding to high molecular weight aggregates. Molecular weight of the dominant fraction was 3192.6 kDa.

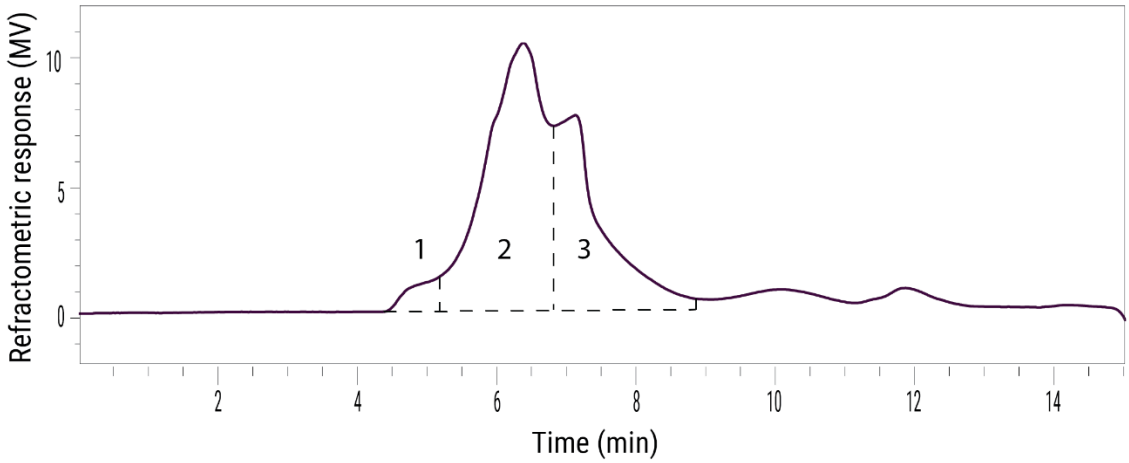

Figure 1. HPSEC profile of soy hull pecic fiber

Table 2. Molecular weights, fraction surface areas and polydispersity indices of soy hull pectic fiber

Fraction	Fraction area (%)	M_p (kDa)	M_w (kDa)	M_n (kDa)	PDI
1	3.5	12885.2	-	-	-
2	61.5	2029.7	3192.6	2266.6	1.4
3	35.0	665.6	543.6	32.6	1.7

M_p - molecular weight of the highest peak; M_w – weight average molecular weight; M_n – number average molecular weight; PDI = M_w/M_n – polydispersity index.

Conclusion

Highly valuable pectic fiber was obtained from soy hull, a by-product of soybean industry. This fiber has exhibited good solubility and high molecular weight. Therefore, pectic fiber from soy hull with these favorable characteristics could be suitable for application in different food products.

Acknowledgements

This research was part of EUREKA project (Grant No E!13082) funded by Ministry of Education, Science and Technological Development, Republic of Serbia.

References

[1] U. Kalapathy, A. Proctor, Food Chem. 73 (2007) 393.
[2] M. Marić, A. Ninčević Grassino, Z. Zhu, F. J. Barba, M. Brnčić, S. Rimac Brnčić, Trends Food Sci. Technol. 76 (2018) 28.
[3] M. Monsoor, A. Proctor, JAOCS 78 (2001) 709.
[4] S. Baississe, D. Fahloul,, Chem. Pap. 72 (2018) 2647.
[5] F. Bouaziz, M. Koubaa, K. Ben Jeddou, F. Kallel, C. Boisset Helbert, A. Khelfa, R. Ellouz Ghorbel, S. Ellouz Chaabouni, Int. J. Biol. Macromol. 93 (2016) 359.
[6] M. Milošević, M. Antov, Food Hydrocolloids 123 (2022) 107201

WASTE POLLUTION PROBLEM ORIGINATING FROM AGRICULTURAL PRODUCTION

Zorica Mirosavljević [1], Vladimir Knežević [2], Bojana Zoraja [1], Višnja Mihajlović [3]

[1]University of Novi Sad, Faculty of Technical Sciences, Novi Sad, Serbia
[2]RKS kompoziti d.o.o., Čelarevo, Serbia
[3]University of Novi Sad, Technical faculty "Mihajlo Pupin", Zrenjanin, Serbia
e-mail: zoricamirosavljevic@uns.ac.rs

Abstract
Waste pollution from agricultural production increasingly large proportions every year. Wild dumps are most often on public areas and in watercourses, and the dominant type of waste is that which originates from agriculture. The paper will determine the most common types of waste originating from agriculture, the problems of their disposal and potential solutions for their disposal.

Introduction
Waste pollution from agricultural production is getting bigger and bigger every year. Wild landfills are most often on public lands and in watercourses, and the dominant type of waste is that left by farmers. The soil is filled with chemicals, and a large number of compounds remain unchanged and reach the human body through food, where they show different effects. Some of the chemicals are extremely toxic, and a large number have been proven to accumulate in the human body and can cause various negative consequences [1], [2], [3].
Today, the use of agricultural land can hardly be imagined without the use of pesticides, herbicides and fungicides. The use of plastics in agriculture represents about 2 % of the over 265 million tons of plastics produced per annum worldwide. This use is globally growing due to an ever more diffusion of intensive and semiintensive agricultural practices [1], [3], [4], [5]. There are almost no alternatives to replacing pesticides in widespread practice and it should be expected that they will be used in the future. Pesticides that are used today are usually of low persistence and their decomposition takes place relatively quickly in the soil. But the mass of their application, with excessive doses, often cause drastic changes in the quality and fertility of the soil.
Also, the irrigation system is a very important item when planning and planting any fruit or any other crop. An irrigation system often requires a lot of money, so people in order to save money resort to seemingly cheaper variants of drip irrigation such as irrigation tapes or hoses with internal drippers. Although these variants are initially cheaper, many manufacturers have convinced themselves over the years that it is better to allocate more money at the beginning for hoses that will last for several years, than to buy cheaper and then buy again every year. Besides being much more cost-effective in the long run, another reason why it's better and smarter to use hoses that can last for years is that in this way we will produce less waste. This abstract aims to highlight the importance of agricultural waste management problems in Serbia with recommendations for solving them.

Experimental
The cadastre of wild landfills, which served as a guide for identifying the aforementioned problem, showed that they are most often on public areas and in watercourses, and the dominant type of waste is that which originates from agriculture [6].
All agricultural waste can be divided into two types:

1. Hazardous waste: packaging from plant protection products and mineral fertilizers, pharmaceutical waste from animal protection products, waste oils and cooling agents from machinery and waste batteries;
2. Non-hazardous waste: plastic films, watering hoses for greenhouse fittings, protective nets, tires from machinery, harvest residues, biodegradable material.

By reviewing the relevant available literature, the results show that the biggest problem is primarily harvest residues, different types of packaging, worn watering hoses, drip systems, and of course foils. Over time, that waste did not decrease, but on the contrary - it increased and took an ever-increasing share of the total waste. Although years ago both the local self-government and the republic allocated funds for the removal of illegal landfills, unfortunately, they always returned to their old place. It can be seen that most of the emphasis is on plastic originating from agricultural waste.

The established subjects of waste management in Serbia are:

1. Republic of Serbia, local self-government;
2. Environmental Protection Agency, professional organizations;
3. Citizens' associations;
4. Manufacturers and sellers of polluting products;
5. Waste owners;
6. Waste operators.

Operators do not have a developed waste collection network. The local self-government does not have an adequate network of operators for this type of waste. Agricultural pharmacies are generally aware of the problems and are ready to cooperate.

The local self-government has complete competence in the management of non-hazardous waste. There are a large number of small farms and they treat agricultural waste as if it were household waste. They have and use the possibility to leave all the waste on their field or in the yard and do not bear any economic costs, but occupy their plots, which is also not good.

As an example of a good practice of agricultural waste recyclin on the territory of Serbia is a company RKS Kompoziti that deal with recycling industrial polymer waste (PP, PE, PVC). Their mission is to give plastic waste second chance and to provide post-consuming life to it. Company goal is to provide simple, quick and economical recycling of industrial plastic waste. Recycling process in this company is divided in several stages: separation, washing, mixing, grinding, agglomeration and regranulation. They obtain products with controlled physical, chemical and mechanical properties. Regranulated product properties can be adjusted according to client’s specification and for such products with constant quality. They also, have manufacturing production lines where they use their regranulation products such as PP tape and PP twine. Production capacity in this factory is more than 20 tons per day. Plastic waste used in manufacturing and recycling processes is provided from domestic industry and from foreign suppliers, with whom they have long-term contracts. Their products are available for domestic and foreign markets [7]. An example of collection, scalding and primary shredding of agricultural waste in RKS komoziti is shown in Figure 1.

Figure 1. Collection, scalding and primary shredding of agricultural waste in RKS kompoziti [7]

By interviewing the director of this company, it was determined that the agricultural waste collection network, especially the drip irrigation system in Vojvodina, is a big problem. The company has a contract with some local companies that produce agricultural waste and successfully solve this problem by recycling waste in their plants and making granulate for new use.

The most dangerous solution for agricultural producers is to set fire to production waste, thereby directly endangering their health and the health of people in the area, because plastic materials come from oil derivatives and they are very toxic. When burning plastic, highly toxic substances are released into the air.

The result of pollution is environmental disturbance of local flora and fauna that we do not have to notice immediately, but the effect can last for a very long time, even years in the case of some substances. Proper sorting, collection and reuse (recycling) reduces the amount of waste and saves raw materials and energy.

By noting the present problem and its consequences to the environment in Serbia, which concern the underdeveloped management system for agricultural waste, the paper will further present recommendations for its potential solution based on the example given in the paper [8].

Results and discussion

Considering that operators in Serbia do not have a developed network for agriculture waste collection, as well as the local self-government that does not have an adequate network of operators for this type of waste, it is recommended to implement the following actions:

1. **Research initiatives for the management of agricultural waste:**

Through research initiatives for the management of agricultural waste it is necessary to determine ways for developing the collection, sampling, and labeling procedures and the methodologies to valorize agricultural waste streams by facilitating their route towards the best waste management alternative.

2. **Determine the best practices in the field of agricultural waste mapping:**

One of the most significant agricultural waste management parameters is the analysis and planning of the collection and disposal of the waste through the implementation of detailed mapping and quantitative characterization of agricultural waste generation (Picuno et al., 2012).

3. **Analyze aspects of mechanical recycling of agricultural waste, with an emphasis on plastic agriculture waste, as well as the infrastructure employed:**

Mechanical recycling is the process of utilizing plastic waste to produce new plastic products [9]. This process's main typical requirements include homogeneity, relatively high purity, and time constancy in the production of the waste flow [10]. [3] established recycling specifications for the agriculture plastic waste. The mechanical recycling process for plastic waste is schematically presented in Figure 2.

Figure 2. Stages of mechanical recycling process for plastic waste [8]

By implementing the previous three steps, it is necessary to define the following:

1. **Define agricultural waste supply chain:**

For the definition of the agricultural waste supply chain, the agricultural waste generation sources must be mapped.

2. **Define design of agricultural waste collection system:**

The choice of the collection system's design carries great significance since the transportation of the waste from the generation sites dramatically affects the overall energy, environmental, and ultimately the financial costs of the process [11]. This analysis's main objective was to conclude to the most energy-efficient and environmental-friendly scenario, with relation to the transportation of the agricultural waste from the location of the sources to the recycling facilities.

Conclusion

Regardless of the existing legislation in the field of handling waste materials, as well as appeals related to proper disposal and the possibility of recycling many waste materials, the proper disposal of agricultural waste in Serbia has not taken root. The solution can be to stimulate local operators in order to expand the network and reward those who hand over such waste. An adequate reward and an adequate punishment can lead to the goal the fastest.

References

[1] I. Blanco, R. V. Loisi, C. Sica, E. Schettini, G. Vox, Resources, Conser. & Recyc., 137 (2018) 229.

[2] C. Sica, R.V. Loisi, I. Blanco, E. Schettini, G. Scarascia Mugnozza, G. Vox, Proceedings of the 43rd International Symposium - Actual Tasks on Agricultural Engineering. Sveučilište u zagrebu, Agronomski fakultet, zavod za mehanizaciju poljoprivrede, Opatija, Croatia, (2015), 745–754, ISSN 1848-4425.

[3] D. Briassoulis, E. Babou, M. Hiskakis, G. Scarascia, P. Picuno, D. Guarde, C. Dejean, Waste Manage. Res. 31 (12) (2013), 1262–1278.
[4] Jr. Hemphill, D. Delbert, HortTechnology 3 (1993). 70–73.
[5] P. Picuno, Polym.-Plast. Technol. Eng. 53 (10) (2014), pp. 1000–1011.
[6] Serbian Environmental Protection Agency: http://www.sepa.gov.rs/index.php?menu=9&id=6003&akcija=showAll#a1
[7] Company RKS Kompoziti: http://rkskompoziti.rs/
[8] P. Z. Morsink-Georgali, N. Afxentiou, A. Kylili, P. A. Fokaides, Cleaner Engineering and Technology, 5 (2021), 100326
[9] T. Meng, A. M. Klepacka, W. J. Florkowski, K. Braman, Waste Manag. 48 (2016)
[10] G. Scarascia-Mugnozza, P. Picuno, C. Sica, Proceedings of World Congress Agricultural Engineering for a Better World. Bonn, Germany (2006)
[11] E. A. Christoforou, P. A. Fokaides, Int. J. Green Energy 12 (2015)

LEGISLATIVE FRAMEWORK REGARDING WASTEWATER TREATMENT IN THE REPUBLIC OF SERBIA AND FLOW AND TRANSPORT MODELLING IN THE DETERMINATION ON EFFLUENT QUALITY OF WASTEWATER TREATMENT PLANT OF BELGRADE CENTRAL SEWERAGE SYSTEM

David Mitrinović[1], Lazar Ignjatović[1], Natalija Pavlović[1], Srđan Kovačević[2], Miodrag Popović[1]

[1] Jaroslav Černi Water Institute, 80 Jaroslava Černog St., 11226 Belgrade, Republic of Serbia
[2] University of Novi Sad, Faculty of Technical Sciences, Department Of Environmental Engineering, 6 Dositeja Obradovića Sq., 21102 Novi Sad, Republic of Serbia
e-mail: david.mitrinovic@jcerni.rs

Abstract
The largest sewerage system in Belgrade is Belgrade Central Sewerage System, which covers the area of about 85% of the sewerage network, with about 1,250,000 inhabitants connected to the sewage infrastructure. The interaction of emission limit values, environmental quality standards, wastewater, effluent and recipient characteristic flows and qualities from the standpoint of environmental impact in the unfavorable environmental conditions was modelled to define the level of wastewater treatment at future Belgrade Central Sewerage System wastewater treatment plant.

Introduction
The largest sewerage system in Belgrade is Belgrade Central Sewerage System (BCSS), which covers the area of about 85% of the sewerage network, with about 1,250,000 inhabitants connected to the sewage infrastructure [1].

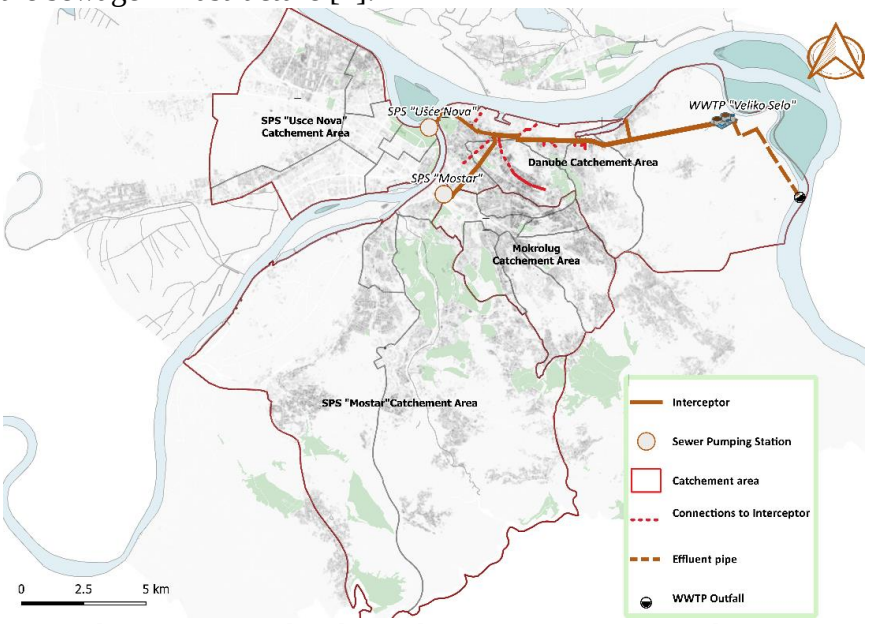

Figure 1. BCSS catchment area with sub-catchments, Interceptor and WWTP Veliko Selo [2]

All wastewater is discharged without treatment into the Sava and Danube Rivers. The level of wastewater treatment that should be reached at future BCSS WWTP was determined based on legislation requirements and the results of numerical modelling of MZ downstream of the effluent discharge point.

Legislation of the Republic of Serbia and the EU Water Framework Directive rely on the so-called combined approach in determining emission limit values (ELV) and environmental quality standards (EQS). Effluent discharge must comply with the more stringent of these two criteria. In this situation, a mixing zone is introduced in the water sector legislation to allow for local relaxation in achieving water quality standards near the point of discharge.
The size of the mixing zone (MZ) should be small enough not to interfere with the use and use of water and appropriate ecosystem uses (recreation, water supply, and fish habitats). Mixing zones are environmentally acceptable because the concentrations and effects of most pollutants decline rapidly after discharge, due to dilution in the MZ. MZs are a widely accepted technical concept introduced into the water legislative framework to ensure flexibility in meeting water quality standards. Within the MZ, the water quality limits may be exceeded, but at its edge, the concentrations of pollutants must meet the standards.

Method

The Law on Waters ("Official Gazette of the RS", No. 30/2010, 93/2012, 101/2016, 95/2018 and 95/2018 – anth. law) stipulates that wastewater, prior to its discharge into the recipient, must be treated to a level that corresponds to emission limit values of pollutants in waters, defined within the Regulation on Emission Limit Values of Pollutants in Waters and Deadlines for their Achievement ("Off. Gazette of the RS", No. 67/2011, 48/2012 and 01/2016)), or to a level that won't jeopardize EQS of the recipient, defined within the Regulation on Limit Values of Pollutants in Surface and Ground Waters and Sediment and Deadlines for their Achievement ("Official Gazette of RS", No. 50/2012), whichever is more stringent. The concept of the mixing zone was introduced for the first time in the Regulation on limit values for priority and priority hazardous polluting substances in surface waters and deadlines for their achievement ("Official Gazette of RS", No. 24/2014). Article 2 (paragraph 4) defines the mixing zone as a part of the recipient in the immediate vicinity of the location where certain priority substances are disposed of from point sources; in the mixing zone, initial mixing with ambient water takes place, and the concentration of priority substances may exceed the EQS level. Article 6 stipulates that the EQS is allowed to be exceeded within the mixing zone, if not affecting the compliance of the rest of the water body with the standards and defined limit values. A mixing zone should be established for a specific emission point/discharge location, and the spread of the mixing zone should be proportional to the concentration of priority substances included in the water permits issued in relation to the regulations on integral prevention and control of environmental pollution and the Water Law. The border of the mixing zone is defined at a distance from the source of pollution where 95% mixing is achieved.

Although the concept of the MZ is defined and adopted, there is yet no regulation at the national level to clearly define its dimensions. It should provide following basic information:

- Specifications of numerically expressed dimensions of the mixing zone in accordance with the type of watercourse and its biological characteristics,
- The width of the mixing zone (WMZ), should be limited to a part of the recipient's cross-section width (CSW), e.g. WMZ = n_tCSW, in order to allow unimpeded passage of river fauna (fish) through the greater part of the cross-section, and/or the mixing zone is limited in the longitudinal direction, e.g. LMZ = n_lCSW, to limit the level of pollution along large sections of the river bank. Factors n_t and n_l, which usually take values from 0.1 to 0.5 for n_t and from 1 to 5 for n_l,
- The specification of the dimensions of the mixing zone can be ad-hoc: after previous environmental assessments and forecasts, the wastewater emitter can request certain dimensions of the mixing zone with guarantees of compliance with the principle of

integral water protection. Based on an impartial assessment, the authorities can accept such a request, or put forth additional requirements and restrictions.

The basic concept of development of BCSS is the construction of Interceptor central collector and a wastewater treatment plant at the Veliko Selo site (WWTP "Veliko Selo") – Figure 1 [1]. The recipient of future WWTP effluent is the Danube River.

Based on previous experiences for wide riverbeds with a large B/H ratio (about 125 at the WWTP "Veliko selo" site), the use of planar hydrodynamic models in the horizontal plane, based on hydrodynamic equations and transport equations averaged over depth, is justified. The mixing of untreated wastewater or effluent and river water, i.e. impact of the untreated wastewater on the Danube and Sava rivers, and of effluent on the Danube River quality indicators was simulated by the RMA2/RMA4 models tandem. The RMA2 model is a hydrodynamic model based on flat flow equations in the shallow domain (depth-averaged Navier-Stokes equations). It solves the Reynolds form of the Navier-Stokes turbulent flow equations on a finite element mesh. Friction is calculated according to Manning's or Shezi's formula, and turbulence is described by turbulent viscosity coefficients. Steady and unsteady flows can be analyzed with the model. The model assumes a hydrostatic distribution of pressures in the vertical direction and as such is suitable for simulating mixing in zones at a greater and intermediate distance from the initial dilution zone. The RMA4 model is a transport model, which calculates transport equations based on the flow solution.

Three models were used, one for the simulation of flow and transport in the Sava River and Danube upstream from the confluence, comprising all the wastewater outlets, second for the Danube downstream of the confluence along the urban area also comprising all the wastewater outlets, and the third is the model of the Danube River downstream from Belgrade for the simulation of the influence of WWTP effluent discharge. The downstream boundary conditions are a fixed water levels at 5 percentile river stage (H_{95}=69.92 m a.s.l., H_{95}=69.86 m a.s.l. and H_{95}=69.80 m a.s.l. respectively) at the most downstream arrays of models' nodes. Danube river flow downstream of confluence was set as 5 percentile flow (Q_{95}=2,149 m_3/s). Wastewater flow at each outlet was set equal to the average discharge, and the effluent flow at the WWTP discharge was set as the sum of all outlet discharges. The representative quality parameter was BOD_5, concentration was set to the average value at the wastewater outlet, ELV for the effluent discharge (Table 1), and average values for the river inflow in the model.

Table 1. The upper limit values of the key parameters of quality of WWTP effluent as stipulated in the legislation

Parameters	Unit	Limit value	Lowest % of reduction
COD	mg/l	125	75
BOD_5	mg/l	25	70-90
SS	mg/l	35	90
Ntot	mg/l	10	80
Ptot	mg/l	1	80

Results and discussion

The level of wastewater treatment that should be reached at WWTP "Veliko Selo" (Figure 1) was determined on the basis of legislation requirements and the results of applied RMA2/RMA4 models for simulation of the effects of current untreated wastewater MZ downstream of the effluent discharge point.

The influence of wastewater treatment on the natural recipients is twofold – the raw wastewater discharge at all outlet points is discontinued, and effluent discharge downstream from Belgrade is introduced. The marked positive effects of the cessation of the detrimental influence of raw

wastewater discharge can be easily inferred from the Figures 2 and 3, and the simultaneous very limited negative effects of the WWTP effluent discharge are illustrated by Figure 4. Having in mind synergy of the listed effects, it is clear that the discharge of effluent of stipulated quality (Table 1) would not jeopardize quality indicators of the recipient even for the Danube low waters, but rather improve them. Therefore, conditions both from Regulation on Emission Limit Values and Regulation on Limit Values of Pollutants are met when effluent quality complies with the ELV from the Regulation on Emission Limit Values of Pollutants in Waters and Deadlines for their Achievement (as presented in Table 1).

Figure 2. Wastewater discharges from BCSS (current state) into the Sava and Danube Rivers upstream from the confluence (average wastewater flow, low waters, dry period), BOD_5 [1]

Figure 3. Wastewater discharges from BCSS (current state) into the Danube River downstream from the confluence (average wastewater flow, low waters, dry period), BOD_5

The elimination of the negative impact of wastewater outlets on Sava River, that are clearly observed on the Figure 2, is perhaps the most significant positive effect of the Interceptor and WWTP on the environment as the Sava River is, due to the much lower discharge, markedly more sensitive than the Danube River.

Figure 4. Effluent discharges from WWTP "Veliko Selo" (future state) into the Danube River downstream from the city area (average wastewater flow, low waters, dry period), BOD_5

The very small dimensions of the MZ of effluent discharge point compared to the width of the Danube River, as well as fast downstream decrease of BOD_5 concentration to the ESV limit of 5 mgO_2/l allow for the circumvention of deficiencies in the legislation regarding the MZs.

Conclusion

The lack of legislative clarity regarding the MZs proves not to be a source of problems in determining the necessary effluent quality for WWTP "Veliko Selo" due to the small dimensions of the MZ of effluent discharge compared to the width of the Danube River, and a huge positive impact of the cessation of untreated wastewater discharge on the recipient's environmental quality upstream the WWTP. Nevertheless, this legislative deficiency poses a significant problem for the large settlements or other wastewater emitters on small watercourses, especially if there is no previous wastewater discharge already negatively influencing the recipient, and this issue must be addressed as soon as possible.

References

[1] D. Mitrinović, N. Pavlović, Ž. Sretenović, F. Fenoglio, B. Samanos, M. Popović, Baseline and options for design of wastewater treatment plants as a part of large sewerage infrastructure: Case Study Veliko Selo (Belgrade Sewerage System), Proceedings of the Contemporary water management: challenges and research directions – International Scientific Conference in the Honor of 75 Years of the Jaroslav Černi Water Institute, Belgrade, Serbia (October 19-20, 2022), pp. 377-396

[2] Jaroslav Černi Water Institute, Project for the treatment and disposal of urban wastewater from the central area in Belgrade – Study on Wastewater Quantities and Quality. Belgrade, Republic of Serbia, 2020

INFLUENCE OF NUCLEATION CENTERS UPON SOLVOTHERMAL GROWTH OF SILVER NANO/MICROCRYSTALS

Radu Banica, Daniel Ursu, Cristina Mosoarca, Mihai-Cosmin Pascariu, Alexandra I. Bucur, Calin Ladasiu

National Institute of R&D for Electrochemistry and Condensed Matter, 144 Dr. Aurel Păunescu-Podeanu, RO-300569 Timisoara, Romania, Phone: +40 256 222119
e-mail: m.crristina@gmail.com

Abstract
Silver nano/microcrystals were obtained at medium pressure in a microwave field by using the solvothermal synthesis. In order to evaluate the nucleation centers' influence upon the formed crystals' morphology, investigations were conducted using scaffolds to stimulate their heterogeneous nucleation. Therefore, besides the silver and chloride nanocrystals used as nucleation centers, SiOx type spheres were used. The results indicate that the presence of the heterogeneous nucleation centers on the SiOx scaffolds plays a crucial role in the silver nano/microcrystals morphology.

Introduction
At present, metallic nanoparticles are widely applied in various domains, ranging from smart electronics, such as conductive films, to environmental remediation and biomedicine [1]. A range of innovative silver-based materials have been introduced in biomedical and pharmacotherapy applications. Kang et al. reported a functionalized β-cyclodextrin-immobilized silver structure as a drug carrier [2,3]. In this study, the influence of nucleation centers on the scaffold surface upon the shape of the silver nano/microcrystals was investigated.

Results and discussion
The samples, namely silver nanowires (S1AN) and silver nano/microcrystals with SiOx scaffolds (S1BSAN), were prepared by solvothermal synthesis in a microwave field. In order to perform their analysis, the samples were isolated by centrifugation and multiple stages of ethanol cleaning, after which they were air dried.
Next, the samples were characterized by scanning electron microscopy (Inspect S – FEI Company), energy dispersive X-ray spectroscopy and ultraviolet–visible spectroscopy (Jasco UV-VIS V 530 – ABL&E-JASCO).
In figure 1a Ag nanowires next to Ag particles are visible, while the figure 2b shows that silver nanowires were not detected on the SiOx type spheres, although other shapes of Ag nanoparticles are present. In figure 1c the scaffold spheres are visible at low magnification.

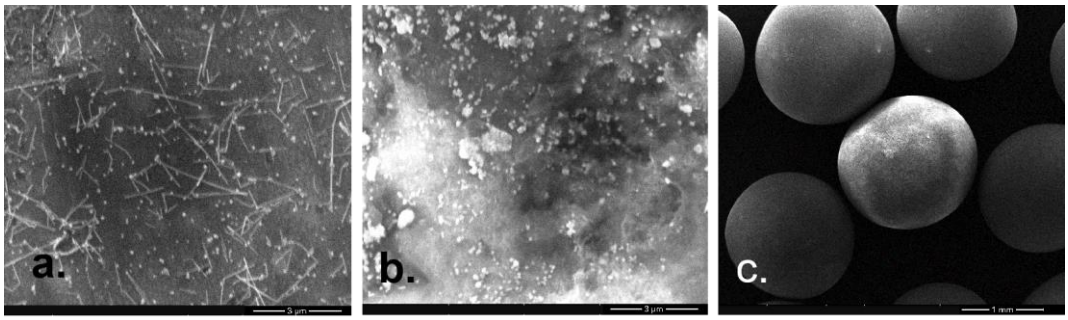

Figure 1. SEM images of a) S1AN, b) S1BSAN, c) S1BSAN samples.

The UV-VIS spectrum from Figure 2 exhibits one relatively sharp surface plasmon resonance peak at 382 nm and another peak at 352 nm that belong to the transversal SPR modes of Ag nanowires.

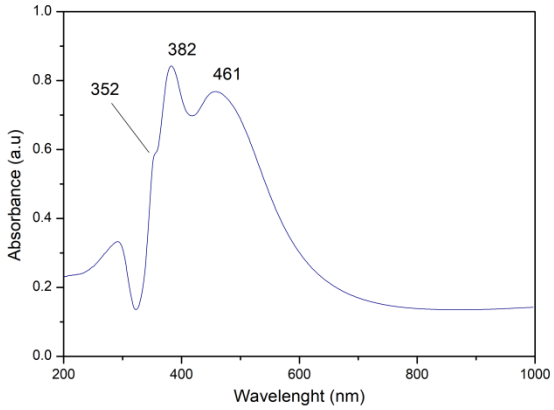

Figure 2. UV-VIS spectrum of S1AN

The 382, 352 and 421 nm SPR peaks suggests that the sample, as seen in the previous SEM images, contain both Ag nanowires and Ag nanoparticles.

Conclusion

It was observed that the presence of the heterogeneous nucleation centers, which compete the AgCl nanocrystals in the nucleation process, determines the entire modification of the morphology for the nano/microcrystals which were previously formed. This fact has a great potential for practical application, e.g. in choosing the type of reactor used for the synthesis process of the silver nano/microcrystals.

Acknowledgements

This work was supported by a grant of the Romanian Ministry of Education and Research, CNCS - UEFISCDI, project number PN-III-P2-2.1-PED-2021-2541 within PNCDI III.

References

[1] K.L. Stinson-Bagby, J. Owens, A. Rouffa, M.J. Bortner, E.J. Foster, ACS Appl. Nano Mater. 2 (2019) 2317–2324.
[2] B.H. Jun, Int J Mol Sci. 20 (2019) 2609.
[3] E.J. Kang, Y.M. Baek, E. Hahm, S.H. Lee, X.H. Pham, M.S. Noh., D.E. Kim, B.H. Jun Int. J. Mol. Sci. 20 (2019) 315.

CORRELATION BETWEEN ANTIOXIDANT CAPACITY AND TOTAL POLYPHENOL CONTENT IN FRUIT JUICE CONCENTRATES

Anna Maria Nagy[1], Eva Stefanovits-Bányai[2]

[1]Holi-Medic Ltd., H-1117 Budapest, 44 Fehérvári street, Hungary
[2]Hungarian University of Agriculture and Life Sciences Institute of Food Science and Technology Department of Foodchemistry and Analytical Chemistry
H-1118 Budapest, Villányi Street 29-43, Hungary,
e-mail: holimedic@gmail.com

Abstract
In our current research, the total polyphenol content and antioxidant capacity of 6 types of 65% fruit juice concentrates (pomegranate, red grapes, oranges, lemons, apples, pineapples) were investigated and compared with TEAC and FRAP methods.
For each juice concentrate, a significant relationship was found between the total polyphenol content and the antioxidant capacity: the most outstanding values were measured for pomegranates, followed by red grapes, followed by oranges and lemons. At the same time, the TPC and FRAP values of apple and pineapple were significantly lower compared to the other 4 types of juice concentrates.

Introduction
In recent decades, numerous publications have proved the paramount importance of the balance between harmful free radicals and antioxidants that protect our bodies in preserving our health [1,2].
Among our diets, the best sources of antioxidants are fruits [3], so their regular consumption plays a significant role in maintaining our body's oxido-reduction homeostasis [4,5]. At the same time, the nutritional values of some fruits (vitamins and minerals, trace elements, flavonoids, polyphenols, etc.) differ significantly, so it is extremely important to choose the right fruit and consume it regularly in the right daily dose [6].
In the temperate zone, seasonal fresh fruits do not produce during the winter period, so most people prefer to consume southern fruits (lemons, orange pomegranates, grapes, pineapples) that are commercially available in winter, in addition to winter-resistant apple varieties that are abundant in summer and autumn in the temperate zone [7].
In our study, we sought to answer which of these foods can contribute most to our health by consuming them from a nutritional scientific point of view.

Experimental
Materials
We tested fruit ***juice concentrates*** with a ***dry matter content of 65%*** in accordance with food safety rules, strictly controlled, produced under the HACCP quality system, stored and distributed in an aseptic manner (Produced by Intercooperation Ltd.).
In our experiment, we used the juice concentrates of domestic and subtropical fruits, which are widely available in the domestic trade: pomegranates, red grapes, oranges, lemons, apples, and pineapples.

Analytical methods
For analytical measurements, the 65% juice concentrates were tested and prepared independently, diluted with distilled water when necessary.

Determination of total phenolic contents (TPC) by Folin-Ciocalteu method: The Folin-Ciocalteu spectrophotometric method by Singleton and Rossi [8], at 760 nm is an electron transfer based on assay and shows the reducing capacity, which is expressed as phenolic content. Gallic acid (GA) was used to prepare the standard curve. The results were expressed as µMGA/g of dry matter (DM).

Determination of antioxidant capacities by TEAC (Trolox-equivalent antioxidant capacity) method: The total antioxidant capacity was measured with Trolox-equivalent antioxidant capacity (TEAC) method described by Miller et al. (1993) [9]. The method is based on ABTS+ free radical scavenging by antioxidants measured with a spectrophotometer. For the calibration Trolox (the hydrophilic analogue of vitamin E) was used.

Determination of antioxidant capacities by FRAP (Ferric Reducing Antioxidant Power) method: Measurement of ferric reducing antioxidant power of the peel extracts was carried out based on Benzie and Strain's procedure [10.], at 593 nm. Ascorbic acid (AA) was used as a standard to prepare the calibration solutions. Results were expressed as µMAA/g DM.

Results and discussion

I.) Results of total phenolic contents (TPC) by Folin-Ciocalteu method

In the course of examining the total polyphenolic content of the 6 types of juice concentrate, it was found that the total polyphenol content of pomegranate juice is outstandingly the highest. Compared to the other juices tested, the following differences occur (in order): 2.1 – 2.1 – 3.0 – 7.0 – 13.6 times the TPC values measured in the red grape – orange – lemon – apple - pineapple samples. (Fig. 1.).

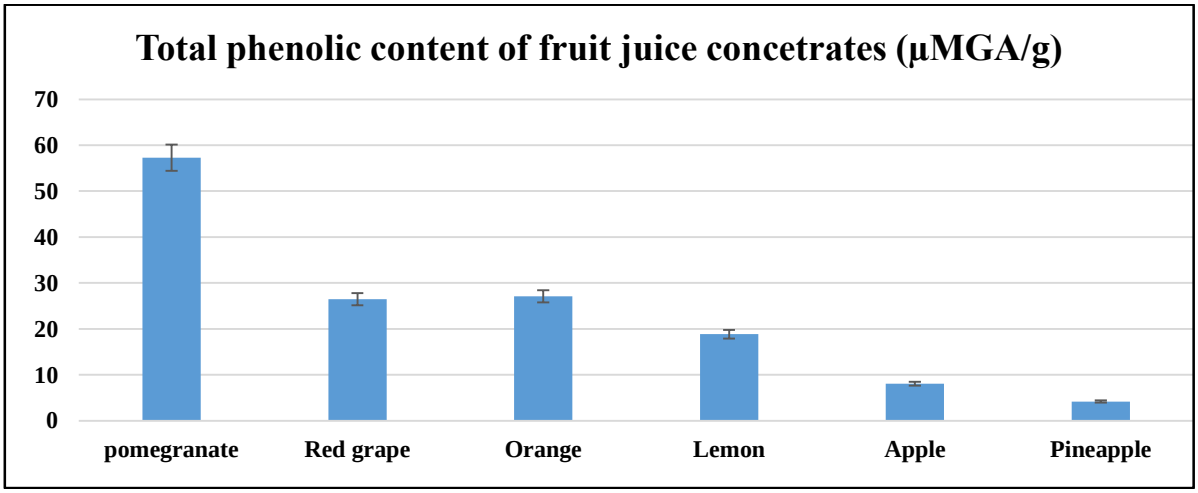

Figure 1. Total phenolic content of different fruit juice concentrates (µMGA/g)

II.) Antioxidant capacity measurement results using TEAC and FRAP methods

Antioxidant capacity can be defined as the combined effect of all antioxidant compounds in the examined sample. More than a hundred methods have been developed in recent decades to measure antioxidant capacity [8], but every examination method has its advantages and disadvantages. Neither method is suitable for accurately modelling the biochemical processes taking place in the body on its own, so it is of paramount importance to formulate a conclusion about the sample based on the combined results of several test methods.

In our current research, we also investigated the antioxidant capacity of 6 types of 65% juice concentrates using the TEAC method based on free radical capture capacity and the FRAP method based on iron-reducing ability (Fig. 2). Our results can be summarized as follows:

Due to the methodological difference between the 2 types of measurement in the 6 types of juice concentrate, the values of the antioxidant capacity measured in the same juice differ significantly (Fig. 2).

When comparing the six types of juice, we measured the highest free radical capture capacity (TEAC) in pomegranate juice and the smallest in apple juice. The antioxidant capacity of pomegranate juice is several times higher than that of the other samples, in order the following: 7.8 – 11.1 – 15.3 – 18.1 – 25.0- 15.3 times the red grape juice – orange juice – lemon juice – apple juice – pineapple juice TEAC values measured in the samples. The total polyphenol content of pineapple is about half that of apples (Fig. 1.), however, its antioxidant capacity, measured by the TEAC method, is almost twice that of apples (Fig.2.). This difference points to the fact that pineapple also contains significant amounts of other free radical capturing antioxidant compounds with non-phenolic components.

Using the FRAP method (Fig. 2.), pomegranate juice also measured the most outstanding antioxidant capacity, several times higher than in other fruit juices: red grape juice – orange juice – lemon juice – apple juice – pineapple juice compared to samples, pomegranate juice showed an antioxidant capacity of 2.9 – 3.3 – 4.1 – 17.6 – 45.5 times higher, which closely correlates with the total polyphenol content measured in these samples.

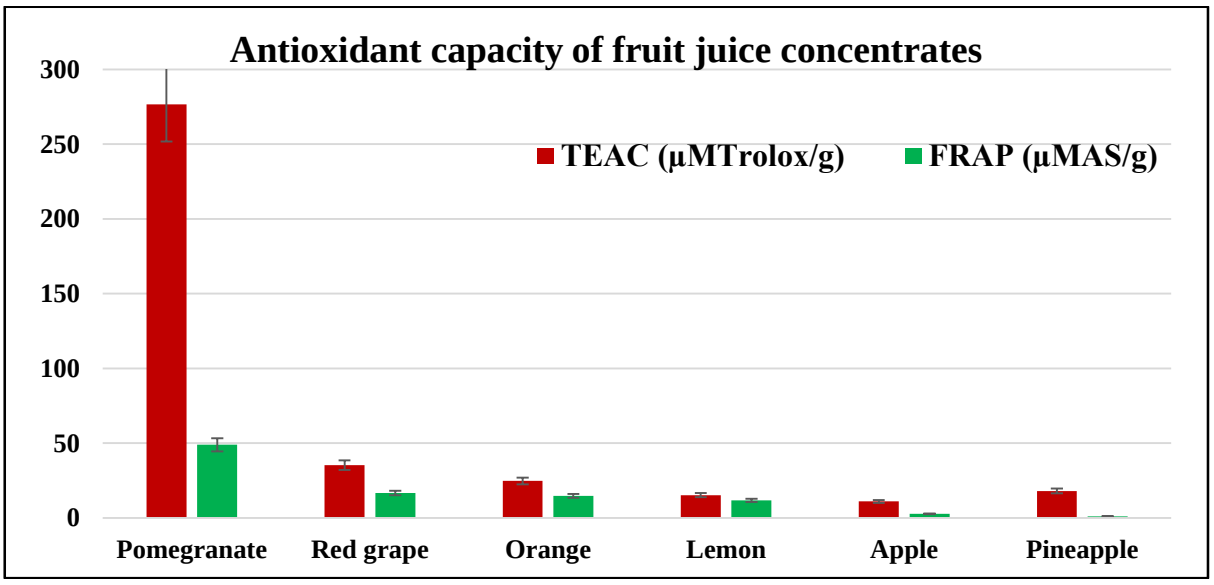

Figure 2. Antioxidant capacity of fruit juice concentrates measured by TEAC (µMTrolox/g) and FRAP (µAA/g) method

The highest correlation (R^2 = 0.9753) was observed between the polyphenol content and the antioxidant capacity measured by the FRAP method.

III.) Discussion

In the course of our study, it can be concluded that the antioxidant capacity values measured by both the TEAC and FRAP methods show a good relationship with the total polyphenol content measured in the 6 types of juice concentrates.
The multifaceted anti-inflammatory and health-protecting effects of plant phenolic components have been confirmed by numerous publications in recent decades [11]. Therefore, the total polyphenol content measured in each fruit juice and the correlated antioxidant capacity values can serve as a guide for which types of southern fruits to prefer to consume during the winter months in order to protect our health.

The analysis of the 6 types of juice concentrates examined by us showed that among the southern fruits, the total polyphenol content of pomegranate is outstanding, and with it the antioxidant capacity measured by both methods, followed by red grapes, then orange and lemon. The antioxidant capacity of pineapples measured by the TEAC method was similar to that of citrus fruits, however, the values of its phenolic components and the antioxidant capacity measured by the FRAP method were significantly lower compared to the juice concentrates listed above.

We measured the lowest antioxidant capacity values in apple juice using both methods (TEAC, FRAP), so their direct role in inflammatory processes does not seem significant. At the same time, it is important to point out that numerous publications have demonstrated the significant soluble fiber (pectin) content of apples, through which it can make a significant contribution to the normal functioning of the entire digestive system and thus the immune system [12].
Among the nutritional values of pineapple, bromelain, the major sulfhydryl proteolytic enzyme, which is not only involved in supporting the digestive system, but also has multiple activities in many areas of medicine, for example "cardiovascular diseases, blood coagulation and fibrinolysis disorders, infectious diseases, inflammation-associated diseases, and many types of cancer" in which possible application should also be highlighted [13].

Conclusion

In our current research, we examined the total polyphenol content and antioxidant capacity of 6 types of juice concentrate, using the TEAC method based on free radical capture capacity and the FRAP method based on iron reduction ability.
Our examinations have shown for all juice concentrates that there is a strong correlation between the total polyphenol content of fruit juices and their antioxidant capacity. Our results can serve as a guide for what type of fruit we should prefer to consume in order to maintain our health.

Acknowledgements

The authors acknowledge the Hungarian University of Agriculture and Life Sciences University's Doctoral School of Food Science for the support in this study.

References

[1] Kehrer, J.P., Smith, C.V. (1994): Free radicals in biology: sources, reactivities and roles in the ethiology of human diseases. In: Frei, B. (ed.) Natural antioxidants in human health and disease, Academic Press, pp. 25-62.
[2] Fraga, C.G., Oteiza, P.I., Litterio, M.C. et al.: Phytochemicals as antioxidanst: chemistry and health effects. Acta Hort. (ISHS), 2012, 939, 63-67.

[3] Hegedűs, A., Papp, N., Pfeiffer, P., Stefanovits-Bányai, É. et al.: A Magyarországon termesztett gyümölcsök antioxidáns kapacitásának összehasonlító elemzése. In: Természetes antioxidáns forrásunk: a gyümölcs. (Szerk.: Hegedűs, A., Stefanovits-Bányai, É.). Kertészettudományi Intézet, AGTC, Debreceni Egyetemi Kiadó. 2012. pp.131-157.
[4] Halliwell, B.: Free radicals, antioxidants and human disease: curiosity, cause or consequence? Lancet, 1994, 344, 721-724.
[5] Martin, C., Zhang, Y., Tonelli, C. et al.: Plants, diet and health. Annu. Rev. Plant Biol., 2013, 64, 19-46.
[6] Hegedűs, A., Papp, N., Abrankó L. et al.: Gyümölcsök szerepe a korszerű táplálkozásban. In: Természetes eredetű hatóanyagok a modern orvoslásban (Szerk.: Blázovics, A., Mézes, M.). Szent István Egyetemi Kiadó, Gödöllő, 2013. pp. 96-101.
[7] WHO Europe:Food and health in Europe: a new basis for action. World Health Organization Regional Publications, European Series No. 96., 2004.
[8] V.L. Singleton, J. A. Rossi, Am. J.Enol. Viticult. 16 (3) (1965) 144-158.
[9] N.J. Miller, C. Rice-Evans, M.J. Davies, V. Gopinathan, A. Milner, Clinic.Sci. 84 (1993) 407-412.
[10] I.F.F. Benzie, J.J. Strain, Anal.Biochem. 239 (1) (1996) 70-76.
[11] Wang, W., Goodman, M.T.: Antioxidant property of dietary phenolic agents in a human LDL-oxidation ex vivo model: Interaction of protein binding activity. Nutr.Res. 1999, 19, 191-202.
[12] Moslemi M. Reviewing the recent advances in application of pectin for technical and health promotion purposes: From laboratory to market. Carbohydr Polym. 2021 Feb 15;254:117324. doi: 10.1016/j.carbpol.2020.117324. Epub 2020 Nov 15. PMID: 33357885.
[13] Hikisz P, Bernasinska-Slomczewska J. Beneficial Properties of Bromelain. Nutrients. 2021 Nov 29;13(12):4313. doi: 10.3390/nu13124313. PMID: 34959865; PMCID: PMC8709142.

HPLC-ESI-TOF-MS CHEMICAL CHARACTERIZATION OF COMFREY ROOT EXTRACT OBTAINED BY SUBCRITICAL WATER EXTRACTION

Nataša Nastić[1], Antonio Segura-Carretero[2,3], Isabel Borrás-Linares[3], Jesús Lozano-Sánchez[3], Kristian Pastor[1], Jaroslava Švarc-Gajić[1]

[1]Faculty of Technology, University of Novi Sad, Bulevar cara Lazara 1, Novi Sad, Serbia.
[2]Department of Analytical Chemistry, Faculty of Science, Avda. Fuentenueva s/n, Granada, Spain.
[3]Functional Food Research and Development Centre, Avda. del Conocimiento s/n, Granada, Spain.
e-mail: natasa.nastic@uns.ac.rs

Abstract

In this work, a study on phytochemical profiles of comfrey (*Symphytum officinale* L.) root extract obtained by subcritical water extraction (SWE) has been carried out. Chemical composition was assessed by high-performance liquid chromatography coupled with electrospray time-of-flight mass spectrometry (HPLC-ESI-TOF-MS) identifying 22 compounds including organic acids, phenolic acids, flavonoids and fatty acids. Great number of phenolic acids and flavonoids were found in the extract obtained by SWE, with citric acid, caffeic acid and derivative, salvianolic acid B, hydroxybenzoic acid, syringetin-3-*O*-glucoside and quercetin 3-*O*-malonylglucoside as the most abundant compounds. Moreover, quercitin-3-malonylglucoside isomers, hydroxybenzoic acid glucoside, cirismaritin isomers, *p*-coumaric acid, hydroxycoumarin and methylcoumarin, among others, were identified for the first time in *S. officinale* root. Overall, the results indicate the potential of SWE for the production of high-quality plant extracts from *S. officinale* root.

Introduction

The global herbal medicine market grows continuously due to lifestyle change and scientific evidence of the beneficial health effects of herbs. Although traditional medicine represents the primary health care for around 80% of the total world population, mainly in the developing countries, the high potential of biologically active plant species remains largely unexplored [1]. In traditional medicine comfrey (*Symphytum officinale* L.) roots are used for the external treatment of joint disorders and musculoskeletal injuries of all kinds [2,3], while its internal use as infusions is very important in the treatment of gastro-intestinal and respiratory tract diseases [4]. The therapeutic properties of *S. officinale* are based on its anti-inflammatory and analgesic effects as well as its activity in stimulating granulation and tissue regeneration. *S. officinale* leaves and roots as the most used parts of this plant, contain allantoin, carotene, hydroxycinnamic acid derivatives, essential oils, vitamin B12 and zinc, which may be responsible for its healing properties.

For numerous plants, there is firm scientific evidence supporting their bioactivities, however traditional methods of preparation often do not use their full potential. In last decades, subcritical water extraction (SWE) attracts lots of attention due to its environmentally friendly character, low price, competitive solvating properties and exceptional selectivity. This technique relying on heated and pressurized water improve extraction efficiency, among others, due to lower viscosity of the solvent and consequently better penetration into the pores of solid particles. SWE is advanced extraction technique that reduces or eliminates the use of organic solvents, being suitable to produce safe pharmacologically active plant extracts and formulations. Therefore, the objective of this study was to carry out SWE for recovery of

bioactive compounds from *S. officinale* root and to perform their characterization by high-performance liquid chromatography coupled with electrospray time-of-flight mass spectrometry (HPLC-ESI-TOF-MS).

Experimental

The commercial samples of dry *S. officinale* roots were purchased from local healthy food retail store in Novi Sad, Serbia. The roots were finely grounded and kept at room temperature and darkness until use.

SWE was performed in a house-made subcritical water extractor. Extraction procedure and apparatus were described previously [5]. Total capacity of high-pressure stainless-steel vessel was 1.7l. Pres- surization of the vessel was performed with nitrogen to prevent possible oxidation. Sample to distilled water ratio was 1:10. Extraction temperature (130°C) and extraction pressure (60 bar) were investigated as independent variables, while all other parameters were held constant (agitation rate of 2 Hz and extraction time of 20 min). After extraction, the vessel was cooled and depressurized. Obtained extract was filtrated and stored in a dark place at 4 °C until analysis.

Chemical profile of bioactive compounds from *S. officinale* root extract was defined using an Agilent 1200-HPLC system (Agilent Technologies, Palo Alto, CA, USA) of the Series Rapid Resolution coupled to an electro-spray time-of-flight mass spectrometer (HPLC-ESI-TOF-MS), previously described by García-Salas et al. [6] with some modifications.

Results and discussion

S. officinale root extract obtained SWE was analyzed by HPLC-ESI-TOF-MS (Figure 1). The identification of the compounds was based on MS spectra interpretation and considering data previously reported in the literature.

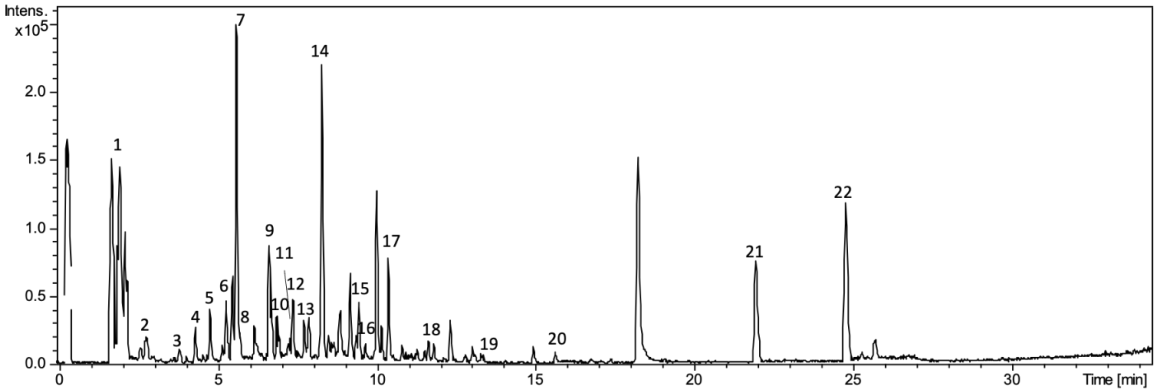

Figure 1. Base peak chromatogram of SWE *S. officinale* root extract obtained by HPLC-ESI-TOF-MS.

Table 1 lists the main peaks detected according to increasing retention time together with experimental and calculated *m/z*, and molecular formula. A total of 22 compounds were tentatively identified in *S. officinale* root belonging to various metabolite families that included anthraquinones, organic, phenolic and fatty acids, and their derivatives. Some of these compounds have been previously reported in *S. officinale* root, however, the TOF-MS enabled identification of 13 phytochemicals that have never been reported in this sample matrix.

Table 1. Proposed compounds tentatively identified in *S. officinale* root extract obtained by SWE using HPLC-ESI-TOF-MS. Numbers designing compounds correspond to peaks as depicted in Figure 1.

Peak	Retention time (min)	*m/z* experimental	*m/z* calculated	$(M-H)^-$	Proposed compound
1	1.98	377.0876	377.0878	$C_{18}H_{17}O_9$	caffeic acid derivative
2	2.33	191.0195	191.0197	$C_6H_7O_7$	citric acid
3	3.85	549.0876	549.0866	$C_{24}H_{21}O_{15}$	quercitin-3-malonylglucoside isomer 1*
4	4.33	549.0875	549.0866	$C_{24}H_{21}O_{15}$	quercitin-3-malonylglucoside isomer 2*
5	4.79	137.0245	137.0244	$C_7H_5O_3$	hydroxybenzoic acid isomer 1
6	5.15	151.0406	151.0401	$C_8H_7O_3$	hydroxyphenylacetic acid*
7	5.6	179.0358	179.035	$C_9H_7O_4$	caffeic acid
8	5.72	313.9725	313.0718	$C_{17}H_{13}O_6$	cirsimaritin isomer 1*
9	6.64	163.0411	163.0401	$C_8H_7O_3$	*p*-coumaric acid*
10	6.88	313.0735	313.0718	$C_{17}H_{13}O_6$	cirsimaritin isomer 2*
11	7.24	271.0971	271.0976	$C_{16}H_{15}O_4$	dihydroxy-dimethoxy-dihydrophenanthrene*
12	7.38	137.0245	137.0244	$C_7H_5O_3$	hydroxybenzoic acid isomer 2
13	7.73	219.0665	219.0663	$C_{12}H_{11}O_4$	dimethoxy-methylcoumarin*
14	8.30	507.1144	507.1144	$C_{23}H_{23}O_{13}$	syringetin-3-*O*-glucoside*
15	9.47	717.1445	717.1461	$C_{36}H_{29}O_{16}$	salvianolic acid B
16	9.65	311.0561	311.0561	$C_{17}H_{11}O_6$	acetyl-monomethyl-trihydroxy anthraquinone
17	10.15	161.0247	161.0244	$C_9H_5O_3$	hydroxycoumarin*
18	11.64	159.046	149.0452	$C_{10}H_7O_2$	methylcoumarin*
19	13.33	137.0241	137.0244	$C_7H_5O_3$	hydroxybenzoic acid isomer 3
20	15.59	329.2344	329.2333	$C_{18}H_{33}O_5$	trihydroxy-octadecenoic acid
21	21.88	221.1542	221.1547	$C_{14}H_{21}O_2$	di-tert-butyl-o-hydroquinone*
22	24.67	205.1596	205.1598	$C_{14}H_{21}O$	di-tert-butyl-phenol*

* Compound identified in *S. officinale* root for the first time.

Conclusion

HPLC-ESI-TOF-MS analysis was used to analyze the chemical profile of *S. officinale* root extract obtained by SWE. In analyzed extract, 22 comfrey metabolites were separated and identified, including 13 newly discovered compounds. Moreover, the most abundant compounds detected by HPLC-ESI-TOF-MS were citric acid, caffeic acid and derivative, salvianolic acid B, hydroxybenzoic acid, syringetin-3-*O*-glucoside and quercetin 3-*O*-malonylglucoside. According to the results, subcritical water as a cost-effective and green solvent has a great potential in exploitation of natural sources of bioactive compounds and production of functional and pharmacologically-active fractions. The present study also highlights the potential application of *S. officinale* root extract as constituents of new added-value formulations.

Acknowledgements

This work was supported by the Serbian Ministry of Education, Science and Technological Development (451-03-68/2022-14/200134).

References

[1] P. Mehta, R. Shah, S. Lohidasan, K.R. Mahadik, J. Tradit. Complement. Med. 5 (2015) 207-227.
[2] M. Kucera, J. Kalal, Z. Polesna, Adv. Ther., 17 (2000) 204–210.
[3] R. Koll, M. Buhr, R. Dieter, H. Pabst, H.-G. Predel, O. Petrowicz, B. Giannetti, S. Klingenburg, C. Staiger, Phytomedicine 11 (2004) 470-477.
[4] E. Roder, Pharmazie, 50 (1995) 83-98.
[5] P. García-Salas, A.M. Gómez-Caravaca, D. Arráez-Román, A. Segura-Carretero, E. Guerra-Hernández, B. García-Villanova, A. Fernández-Gutiérrez, Food Chem. 141 (2013) 869-878.
[6] J. Švarc-Gajić, A. Cvetanović, A. Segura-Carretero, I.B. Linares, P. Mašković, J. Supercrit. Fluids 123 (2017) 92–100.

DETAILED CYTOTOXICITY ASSESSMENT OF THE FORMULATED HERBICIDE ROUNDUP CLASSIC AND ITS CONSTITUENTS

Marianna Oláh[1], Enikő Farkas[2], Inna Székács[2], Robert Horvath[2], Szandra Klátyik[1], András Székács[1]

[1]Agro-Environmental Research Centre, Institute of Environmental Sciences, Hungarian University of Agriculture and Life Sciences, H-1022 Budapest, Herman O. út 15, Hungary
[2] Nanobiosensorics Laboratory, Institute of Technical Physics and Materials Science, Centre for Energy Research, H-1121 Budapest, Konkoly-Thege Miklós út 29-33, Hungary
e-mail: olah.marianna@uni-mate.hu

Abstract

Cytotoxicity of the globally market-leading herbicide ROUNDUP CLASSIC formulation and its components such as the active ingredient glyphosate and the formulating agent POEA (a mixture of polyethoxylated tallow amines) were investigated on the murine neuroectodermal stem cell-like (NE-4C) and osteoblastic (MC3T3-E1) cell lines. The cytotoxic and genotoxic effects on cell viability and cell cycles were evaluated based on the results of flow cytometry, enzymatic-assays, and alkaline single cell gel electrophoresis (Comet) assays, furthermore, the effects on cell morphology and dynamic mass redistribution of cellular contents were assessed with the use of the label-free Epic BenchTop optical biosensor on MC3T3-E1 cells adhered on the surface of the biosensor. Differences in the sensitivity of the investigated cell lines were detected, while the MC3T3-E1 cell line indicated less sensitivity to the effects of the treatments. Furthermore, differences were also observed in the sensitivity of the performed assays. The order of the inhibitory potency of the investigated compounds was as follows: glyphosate IPA salt << ROUNDUP CLASSIC < POEA. The applied Epic technique provides an effective tool for the real-time detection of cytotoxicity.

Introduction

Recently, the intensive use of various plant protection products and the consequent human exposure has been associated with several toxic effects including carcinogenicity, therefore the identification of potential hazards and the estimation of the exposures gained outstanding importance during the risk assessment of pesticides [1–3]. Due to the continuous high application rate of glyphosate, the world market-leading herbicide active ingredient exerts substantial environmental impacts as a ubiquitous surface water contaminant [4–6] and can cause unintended exposure to non-target organisms and humans due to the presence of its residues in the different environmental matrices, food and feeds [7–9]. The side-effect including genotoxic and endocrine-disrupting effects of glyphosate and its formulations have been demonstrated by several studies [10,11], thus strong criticism was expressed when the scheduled EU registration revision of glyphosate (and ROUNDUP) was postponed several times, although there is no uniform opinion regarding to the effects of glyphosate on human health. The US Environmental Protection Agency and the European Food Safety Authority classified glyphosate as a "probably not carcinogenic to humans" compound, while the International Agency for Research on Cancer has identified glyphosate as a "probably carcinogenic to humans" (2A) [7]. The present study aimed to assess the cytotoxic effects including the effects on cell viability, genotoxicity, apoptosis, and cell cycle of glyphosate IPA salt, its formulation (ROUNDUP CLASSIC), and the formulating agent POEA by several methods such as MTT assay, flow cytometry, alkaline Comet assay on the murine neuroectodermal stem cell-like (NE-4C) and osteoblastic (MC3T3-E1) cell lines. Furthermore, the effects of the investigated compounds

on the whole-cell responses of MC3T3-E1 cells were determined with the use of the optical biosensor Epic BT, and the comparison of the sensitivity of the cell lines and the different methods was also performed based on the results of the measurements.

Experimental

The assessment of the cytotoxic effects of ROUNDUP CLASSIC, and its components were performed on two murine neuroectodermal stem cell-like (NE-4C) and osteoblastic (MC3T3-E1) cell lines based on different 96-well microplate-based methods. Cell viability was tested by MTT (3-(4,5-dimethylthiazol-2-yl)-2,5-diphenyl tetrazolium bromide) assay and by flow cytometry. The determination by flow cytometry was performed with the use of the Muse Cell Analyzer (Merck Millipore, Budapest, Hungary), which is a microcapillary cytometry instrument equipped with a fluorescence detector for single-cell analysis and used with different assay kits specific for given cell characteristics, including viability, DNA damage, apoptosis, as well as cell signalling. DNA damages were also detected by the alkaline Comet assays using single-cell gel electrophoresis suitable for the indication of DNA damages in the cells (e.g., damaged fragments from the nucleus). Effects of apoptosis were determined by flow cytometry with the use of two kits suitable for the measurement of annexin levels and caspase activity, while cell cycle analysis was conducted by flow cytometry after staining with propidium iodide [12]. The assessment of the effects on the whole-cell responses of MC3T3-E1 cells was performed with the use of the optical biosensor Epic BT and in 384-well Epic cell assay microplates. The bottom of each well of the microplate contained a 2×2mm RWG sensor, and MC3T3-E1 cells adhered on the surface of the biosensor in serum-containing and serum-free assay media. Responses of the biosensor were recorded for 1 h in real-time with a very high resolution. After the biosensor analysis, actin filaments in the cytoskeleton, focal contacts, as well as the nucleus of the cells were visualized by staining and microscopy, and the 3D structures of cells were assessed by digital holographic microscopy (HoloMonitor M4) [13]. The reported ROUNDUP CLASSIC concentrations are specified to actual dilutions (expressed as mass-per-volume %) of the formulation, while the concentrations of glyphosate and POEA are specified as ROUNDUP CLASSIC equivalent concentrations (mass-per-volume % concentrations of the diluted formulation containing the corresponding concentrations of the given components). Based on the measurements the sensitivity of the cell lines and the different methods was compared.

Results and discussion

Based on the results of the cell viability tests, MTT assays indicated, that all of the investigated compounds affected the viability of the cells. The exposure to ROUNDUP CLASSIC significantly decreased the viability of NE-4C cells. The calculated 24 h IC_{50} values on NE-4C cells were found to be 0.652 ± 0.006%, 0.00995 ± 0.00010%, and 0.00315 ± 0.00007% for glyphosate IPA salt, ROUNDUP CLASSIC, and POEA, respectively. The cytotoxicity of POEA was 200-fold higher for POEA compared to the active ingredient in NE-4C cells. According to the results of flow cytometry, high cytotoxicity was also detected for the formulation and POEA compared to glyphosate IPA salt. The calculated 24 h IC_{50} values were in accordance with the result of the MTT assays on NE-4C cells. Glyphosate IPA salt resulted in substantially lower inhibition of cell viability on MC3T3-E1 cells, compared to the cytotoxic effects of the formulation and POEA. The tendency showed by the 24 h IC_{50} values calculated for NE-4C cells agreed with the trend of the calculated values for MC3T3-E1 cells (24 h IC_{50} = 1.2495± 0.0024%, 0.0187 ± 0.0007%, 0.00936 ± 0.00085% for glyphosate IPA salt, ROUNDUP CLASSIC, and POEA, respectively after the 24-h exposure. Based on the cell viability measurement on NE-4C cells, the sensitivity was higher by the flow cytometric measurement, than in MTT assays, and the

performed testing methods indicated acute physiological effects on both cell lines. Compared to MC3T3-E1, NE-4C cells indicated 1.1–2-fold higher sensitivity to all tested compounds in both viability tests. The effects indicated the explicit cytotoxicity of POEA in good accordance with the scientific literature.

During the evaluation of DNA damages, visualization of the fragmented DNA was performed by Comet assay based on electrophoretic separation, while specific staining of breaks in the double-stranded DNA damages were assessed by flow cytometry. The result of Comet assays indicated 2910-fold and 2247-fold higher levels of DNA migration for POEA, compared to glyphosate IPA salt, and ROUNDUP CLASSIC, respectively. The calculated lowest genotoxic dose (LGD) values were the following: 0.0259%, 0.00002%, and 0.0000089% for the active ingredient, ROUNDUP CLASSIC, and POEA, respectively. Based on the results, MC3T3-E1 cells were less sensitive to DNA damaging effects, than NE-4C cells, and the 24 h LGD values for POEA, ROUNDUP CLASSIC, and POEA were 271-, 120- and 3.2-fold higher for MC3T3-E1 than for NE-4C cells, respectively. Flow cytometric assays for DNS damage (double-stranded breaks) indicated 127- and 3.9-fold higher DNA migration was detected for POEA compared to glyphosate IPA salt and the formulation, respectively, after the 24-h exposure, and the detected LGD values were 0.0376%, 0.00117% and 0.000295% for the active ingredient, ROUNDUP CLASSIC, and POEA. DNA damage was observed also in the negative control in the absence of p53 tumor suppressor protein in the NE-4C cell line. The Comet assay was found to be more sensitive, than flow cytometry for NE-4C cells. The trend of the LGD values on the MC3T3-E1 cell line was similar to the values calculated for NE-4C cells. Compared to the effects of glyphosate IPA salt and the formulation, 401-fold and 8.4-fold higher DNA-damage levels were demonstrated for POEA, respectively. Our results indicated a higher frequency of single-stranded DNA breaks than double-stranded breaks.

The results of the assays for apoptosis evaluated by flow cytometry based on both annexin levels and caspase activity demonstrated the effects on the important regulatory pathway of cell growth and proliferation. Based on the determined annexin levels, the calculated 24 h IC_{50} values for the ratio of total apoptotic cells were 0.246 ± 0.0134%, 0.00238 ± 0.00003%, and 0.00092 ± 0.00005% for glyphosate IPA salt, ROUNDUP CLASSIC, and POEA, respectively on NE-4C cells. A 2.6- fold and a 273-fold higher rate of apoptotic cells was observed for POEA compared to ROUNDUP CLASSIC and the active ingredient, respectively. After the 24-h exposure, the results of the caspase activity measurements, the determined 24-h IC_{50} values for the ratio of apoptotic and dead cells were 0.568 ± 0.043%, 0.00748 ± 0.00012% and 0.00099 ± 0.00002% for glyphosate IPA salt, ROUNDUP CLASSIC, and POEA, respectively, and the highest level of apoptotic and dead cells was observed also for POEA, while 573-fold and 7.5-fold higher level was determined for the formulating agents than for glyphosate IPA salt and ROUNDUP CLASSIC, respectively. The tendency of the calculated 24 h IC_{50} values on the MC3T3-E1 cell line corresponded to the trend of values determined for NE-4C cells and the highest level of apoptotic cells was detected also for POEA. After the 24-h treatment, the ratio of the dead cells increased, while the number of viable cells decreased in a dose-dependent manner. Based on the results, the formulating agents induced apoptosis at a lower concentration compared to ROUNDUP CLASSIC. The results of the applied methods indicated the lower genotoxicity of the active ingredient compared to the formulation and POEA. The observed difference between the two methods for the evaluation of apoptosis, while the determination based on the annexin levels evaluates the level of all apoptotic cells separately along with the dead cells, but the combined level of only the caspase-activated apoptotic cells and the dead cells indicated together by caspase activity assay.

Based on the cell cycle analysis performed by flow cytometry, in the negative control, the majority of NE-4C cells (~46%) were in the growth (G_0/G_1) phase after 24-h exposure, while a

decrease was observed for the investigated compounds. The decrease showed a monotonous dose-dependence for the formulation and POEA at the range of 0.0007–0.0026 ROUNDUP CLASSIC equivalent concentration, while the highest effect of glyphosate IPA salt was observed at the lowest tested concentration and gradually reaches the level of control at higher concentrations. The beginning of DNA replication (S phase) was not affected by glyphosate IPA salt based on the ratio of the cells, but decreased cell ratio was observed for ROUNDUP CLASSIC and POEA treatments. In contrast, in the cell division (G_2/M) phase the cell ratio increased after the treatments, but the highest increase was observed for the active ingredient at the lowest concentration, and a gradually decreased was detected at higher concentrations. Glyphosate IPA salt increased the ratio of NE-4C cells with the increase of the concentration, but the growth of the cell stopped in the G_0/G_1 phase due to the not optimal conditions, and only a small part of the cells get through the checkpoint control to the S phase and then to the G_2/M phase, thus cell ratio is lower in these phases compared to the control. In the negative control, a higher cell ratio (~80%) was detected in the G_0/G_1 phase for MC3T3-E1, than for NE-4C cells. The high relative ratio of cells in the resting (G_0) and first gap (G_1) phase is unique to MC3T3-E1 cells [14], but the cell ratio in G_0/G_1 phase decreased in ROUNDUP CLASSIC- and POEA-treated cells. The ratio of cells in the S phase was also not affected by the treatments, while the ratio of the cells increased in the G_2/M after exposure [12].

The effects of glyphosate IPA salt, ROUNDUP CLASSIC, and POEA were assessed on MC3T3-E1 cells with the use of the optical biosensor Epic BT, where the magnitude of the signal well correlated with the concentration of the investigated compounds. The lowest signals were observed for ROUNDUP CLASSIC and POEA at the highest concentrations. Glyphosate exposure (equivalent to 0.1% ROUNDUP CLASSIC) in a serum-containing medium resulted in late phase response on the cells, possibly due to cell cytoskeletal reactions (the effect was not significant under serum-free conditions). Dose-dependent responses of MC3T3-E1 cells were detected after the exposure of the investigated compound in serum-containing and serum-free media as well. Significant differences were not detected in the calculated IC_{50} values for the formulation and POEA in both assay media, while the IC_{50} values for glyphosate IPA salt were lower in the serum-containing medium. The results indicated the possible cytotoxic effect of ROUNDUP CLASSIC may attribute to the presence of POEA and possibly affected by the active ingredient. According to the visual assessments, elongated cell shape was detected in glyphosate-exposed cells compared to the control group, and reduced distribution of F-actin was observed in the treated groups. The results indicated the possible effects of glyphosate on the morphology of the cytoskeleton and cell adhesion. Based on the visualization, POEA exposure resulted in cytoskeletal collapse, cellular plasma membrane permeabilization, and cell death indicating higher toxicity compared to the effects of the active ingredient and ROUNDUP CLASSIC, furthermore necrosis of the cells was also observed as a result of POEA treatment. The detected effect on morphological changes in MC3T3-E1 cells of ROUNDUP CLASSIC was similar to the effects of POEA, suggesting that, the effect of the formulating agent prevails in the formulation. HoloMonitor technique demonstrated the inhibition of the proliferation in cells exposed to 0.02% ROUNDUP CLASSIC, and the cells became rounded, furthermore, the average optical thickness of the cells increased over time indicating induced apoptosis. POEA treatment (equivalent to 0.02 % ROUNDUP CLASSIC) resulted in a massive reduction of cell area after 5 min, and caused necrosis after 1 h of exposure. At a lower concentration of glyphosate IPA salt (equivalent of 0.02% Roundup solution) significant morphological changes were not detected compared to the control, but glyphosate caused impairments in the cell mobility and cell growth [13].

Conclusion

The results of the performed cytotoxicity assays, the higher toxicity of the formulation and the formulating agent POEA were demonstrated compared to the individual effects of the active ingredient on both of the investigated murine cell lines, however, significant differences were observed in the sensitivity of the cell lines based on the results of the applied assays. Generally, the order of the cytotoxic potency of the tested compounds was the following: glyphosate IPA salt << ROUNDUP CLASSIC < POEA for both cell lines, but the higher cytogenotoxic effects observed for the formulation can be explained primarily by the presence of POEA. Based on the cell viability, genotoxicity tests the potential inhibitory and adverse effects of glyphosate, ROUNDUP CLASSIC, and POEA were demonstrated, and additional genotoxic risk for the ecosystem and human health was indicated. During the measurements, the applied Epic BT biosensor provides real-time, unique, and accurate information about the cytotoxicity of the different contaminants, with shorter assay time and the possibility of the early detection of the cytotoxic effects.

Acknowledgements

The research was carried out within the project "Mechanism-Related Teratogenic Hormone Modulant and Other Toxicological Effects of Veterinary and Agricultural Surfactants" (OTKA K109865) of the Hungarian Scientific Research Fund. The authors thank to Emilia Madarász (Institute of Experimental Medicine of the Hungarian Academy of Sciences) for her technical support.

References

[1] M.C.R. Alavanja, M.K. Ross, M.R. Bonner, Canc. J. Clin. 63 (2013) 120–142.
[2] L.P. Agostini, R.S. Dettogni, R.S. dos Reis, E. Stur, E.V.W. dos Santos, D.P. Ventorim, F.M. Garcia, R.C. Cardoso, J.B. Graceli, I.D. Louro, Sci. Total Environ. 705 (2020) 135808.
[3] R.C. Gilden, K. Huffling, B. Sattler, J. Obstet. Gynecol. Neonatal. Nurs. 39 (2010) 103–110.
[4] F. Maggi, L.D. Cecilia, F.H.M. Tang, A. McBratney, Sci. Total Environ. 717 (2020) 137167.
[5] M. Mörtl, G. Németh, J. Juracsek, B. Darvas, L. Kamp, F. Rubio, A. Székács, Microchem. J. 107 (2013) 143–151.
[6] A. Székács, M. Mörtl, B. Darvas, J. Chem. 2015 (2015), 717948.
[7] A. Székács, B. Darvas, Front. Environ. Sci. 6 (2018) 1–35.
[8] A.H.C. Van Bruggen, M.M. He, K. Shin, V. Mai, K.C. Jeong, M.R. Finckh, J. G. Morris Jr., Sci. Total Environ. 616–617 (2018) 255–268.
[9] K.R. Solomon, Pest Manag. Sci. 76 (2020) 2878–2885.
[10] J. Rank, A.-G. Jensen, B. Skov, L.H. Pedersen, K. Jensen, Mutat. Res./Genet. Toxicol. 300 (1993) 29–36.
[11] G. Tóth, J. Háhn, J. Radó, A.D. Szalai, B. Kriszt, S. Szoboszlay, Environ. Pollut. 265 (2020) 115027.
[12] M. Oláh, E. Farkas, I. Székács, R. Horvath, A. Székács, Tox. Rep. 9 (2022) 914–926.
[13] E. Farkas, A. Székács, B. Kovács, M. Oláh, R. Horvath, I. Székács, Hazard. Mat. 351 (2018) 80–89.
[14] M. Liu, F. Fan, P. Shi, M. Tu, C. Yu, C. Yu, M. Du, Int. J. Biol. Macromol. 107 (2018) 137–143.

FEASIBILITY STUDY OF USING A PORTABLE, HIGH REPETITION RATE FIBER LASER FOR LASER-INDUCED BREAKDOWN SPECTROSCOPY

Dávid Jenő Palásti[1], Fernando Alexander Casian Plaza[1], Ádám Bélteki[1], Attila Kohut[2], Zsolt Geretovszky[2], Levente Makkos[3], Gábor Galbács[1]

[1]Department of Inorganic and Analytical Chemistry, University of Szeged, H-6720 Szeged, Dóm square 7, Hungary
[2]Department of Optics and Quantum Electronics, University of Szeged, H-6720 Szeged, Dóm square 8, Hungary
[3]TRUMPF Hungary Kft., H-2220 Vecsés, Lincoln street 1.
e-mail: galbx@chem.u-szeged.hu

Abstract
Laser-induced breakdown spectroscopy (LIBS) is a dynamically evolving elemental analytical method, which has a great array of unique and advantageous features such as quickness, multi elemental detection, virtually none destructiveness and requires little to no sample preparation. The quick advancement of LIBS is partly due to the ever improving properties of pulsed laser sources. One laser type which went through a significant improvement in recent years are the fiber lasers. In this current study we investigate the performance characteristics and feasibility of using a fiber laser for the ignition of microplasmas.

Introduction
LIBS measurements require the focusing of high energy pulsed laser light onto the sample surface. Due to the high irradiance the sample in the focal spot first melts, then evaporates, and from the evaporated sample a microplasma is formed. The analytical information is gained from the spectroscopic observation of this short lived light source.

Due to their robust nature, fiber lasers have recently been more and more widely used in the industry for cutting, welding, marking. Industrial fiber lasers usually employ a fused silica optical fiber doped with rare earth metals as an active medium (amplifier) and the end-on pumping is achieved by a fast semiconductor laser. This construction provides very good cooling, thus enabling stable, continuous operation and high energy/power and also allows a change of the pulse profile (waveform) [1].

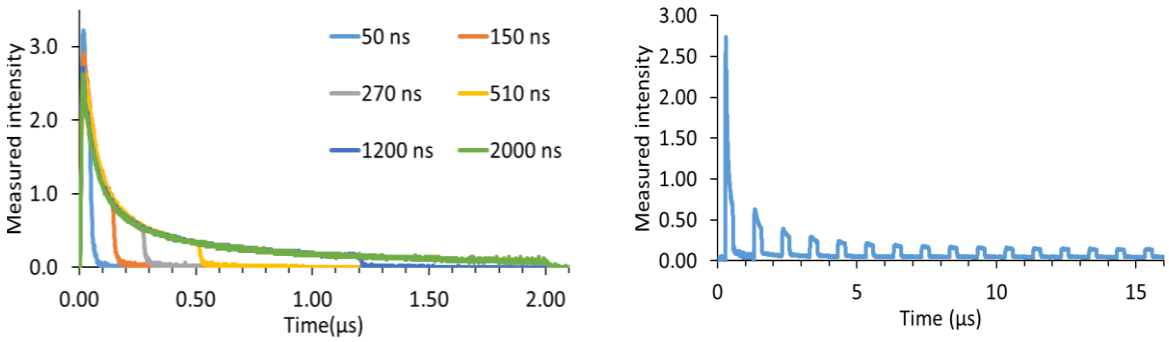

Figure 1. Time resolved intensity profile (on the right) and intensity profile of consecutive laser pulses released from the fiber laser at a high pulse repetition rate (inter-pulse delay is 1 µs)

These sources can provide continuous or pulsed emission, and their pulse repetition frequency (PRF) is much higher (kHz-MHz range) compared to that of typical solid state lasers (usually 1-20 Hz). They are robust, have a long life span (tens of years) and require little

maintenance. Due to the recent developments in this field, the pulse energy of these lasers reaches several mJ, accompanied by ns duration pulses, which brings up the possibility of their use in LIBS [2].

Experimental

During our experiments the laser pulses were provided by a fairly compact (473 mm x 417 mm x 133 mm) TRUMPF Trupulse nano 5020 fiber laser source, which has emission at 1060 nm and has 63 different pre-programmed waveforms. The maximum pulse energy and the length of the waveforms changed between 10 and 2000 ns, 0.35 and 4.95 mJ respectively. The light exiting the fiber laser was collimated into a 10 mm diameter beam and then focused onto the sample surface by a 100 mm focal length lens (Thorlabs, LA4380). Spectra were recorded by either an Avantes FT 2048 CCD spectrometer or an LTB Aryelle 200 Echelle spectrometer with an iCCD detector. The synchronization of the laser source and the spectrometer was achieved by a TTI TG5011 signal generator. Stainless steel and other iron alloys were used as samples.

Crater depths were measured by a Veeco Dektak 8 contact profilometer (Veeco, USA). To measure their depths, the craters were fully mapped, 40 parallel linescans were executed on all of them, then the line with the deepest line was chosen to identify the crater depth. The temporal profile of the waveforms was recorded by the usage of DET10A/M photodetector (Thorlabs, USA).

Results and discussion

As expected, different laser waveforms, even if they have the same energy, have different ablation and laser-induced breakdown spectroscopy properties. Although longer laser pulses have higher ablation rates, but the LIBS signal recorded from them is significantly smaller. It is probably due to the shorter lifetime of the plasma, which suggest that the initial temperature of these plasmas is lower as well.

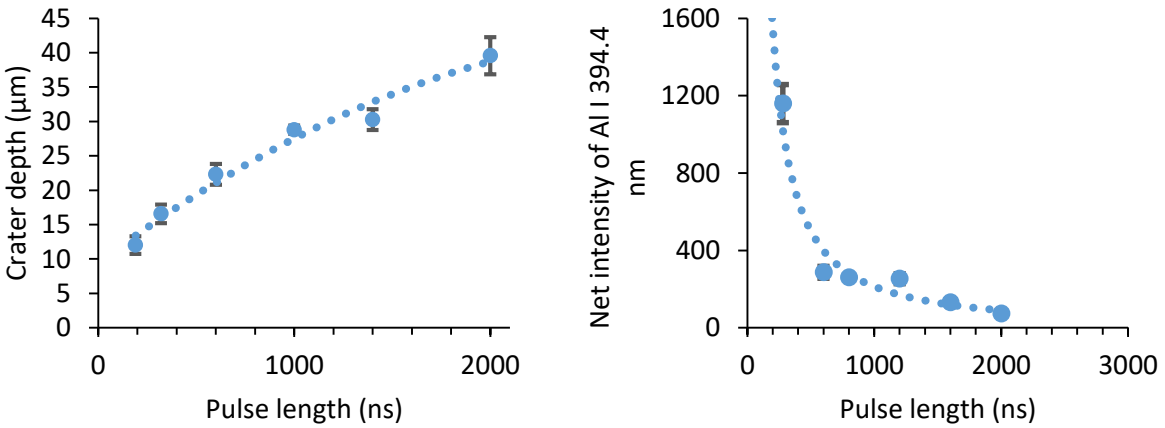

Figure 2. The depths of craters created by laser pulses with the same pulse energy, but different pulse durations (on the left), LIBS signal recorded from microplasmas created by laser pulses with the same pulse energy, but different pulse durations (on the right)

It is known that consecutive laser pulses with small interpulse delays are able to dramatically increase the performance of LIBS [3,4]. These signal enhancing methods are known as double-pulse (DP-LIBS) if only two pulses are used, and multi-pulse LIBS (MP-LIBS), if three or more pulses are used. On the left hand side of the Figure 3. we show the cumulative plasma intensities (t_{int}= 2 ms), and as it can be seen the DP-LIBS is advantageous in the case of elongated (270 ns

long) pulses as well. Although the timing of the second laser pulse is known to have significant effect on the signal enhancement, but seeing the maximum enhancement at an inter pulse delay, when the plasma emission is already over was somewhat surprising. Thus we investigated the pulse energy of the second pulses as well, and found that, the energy of the second laser pulse is quite dependent on the interpulse delay, (right hand side of the Figure 3.). This means that the signal enhancement, what we realized is at least partly due to the increased energy of the second laser pulse.

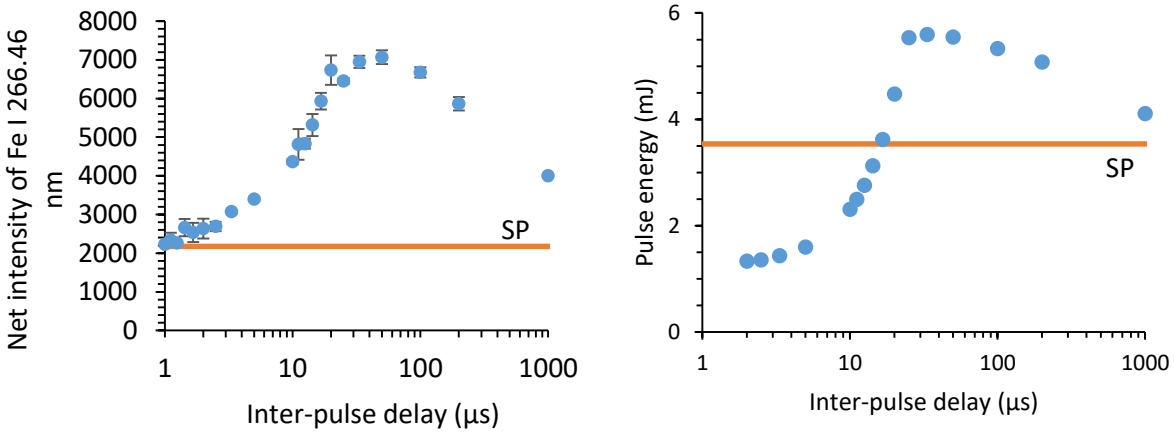

Figure 3. LIBS signal intensities recorded by using 270 ns long consecutive laser pulses of the fiber laser as a function of the inter-pulse delay (on the left), and energy of the second laser pulse in function of the inter-pulse delay time (on the right)

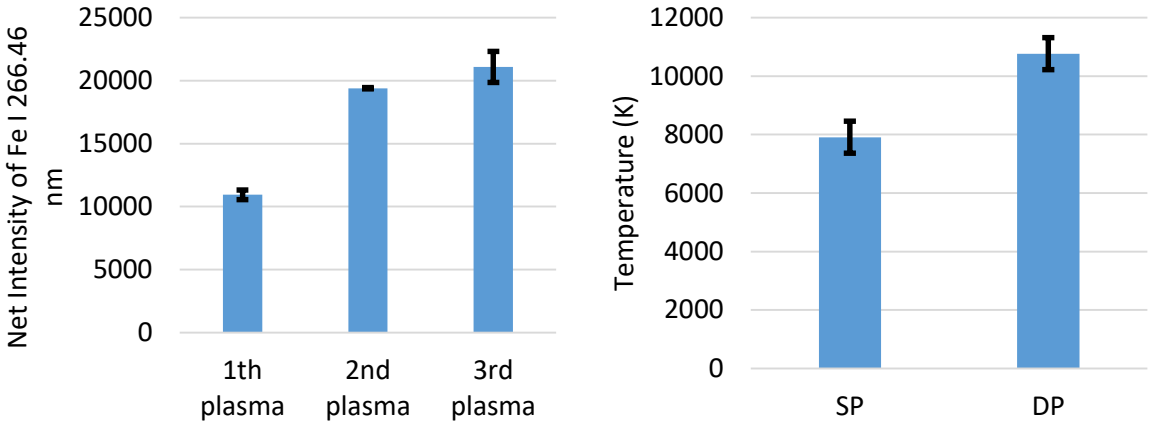

Figure 4. Signal generated by the first second and third laser pulses, when these pulses had roughly the same energy (on the left), Plasma temperatures (using the Boltzmann plot method) of the plasma created by the first and second laser pulses (on the right)

This, however, does not mean that the signal enhancement is only due to the second, higher intensity laser pulse. We investigated the case, when the second and third laser pulses had roughly the same pulse energy, and still a significant increase in the intensity could be realised. In this case the increased signal cannot came from the reheating of the already existing plasma, since it has been already extinguished, but from the sample heating effect of the previous plasma (laser pulse). If not more than a few tens of µs interpulse delay is used, then the sample surface is still warm when the next laser pulse arrives, thus it requires less energy for the ablation, and more is energy can be used to heat the plasma. This way the temperature of the plasmas created by the second and third laser pulses is elevated, as it was observed.

To demonstrate the usefulness of fiber lasers in the elemental analysis, LIBS spectra of stainless steel calibration standards were recorded using both single pulses and double pulses with the optimized waveform and interpulse delay. As it can be seen the DP-LIBS provide much better sensitivity, and the standard deviation of the signal does not grow significantly, hence the limit of detection also improves.

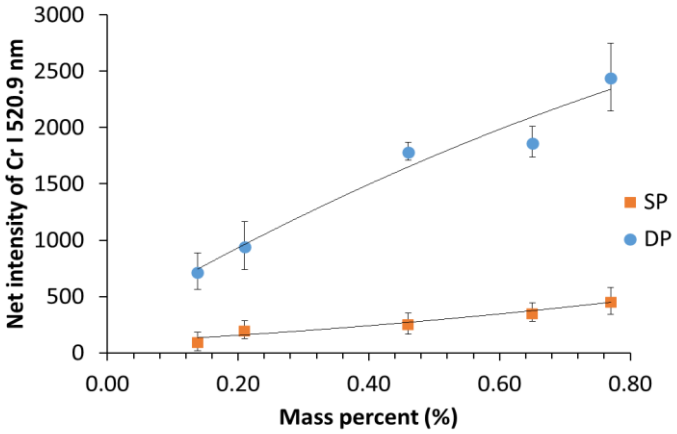

Figure 5. Comparison of calibration curves for cromium in stainless steel in SP and DP mode LIBS

Conclusion

In conclusion we managed to produce good quality LIBS spectra using a conventional fiber laser. The effects of the elongated pulses and high pulse repetition rates were investigated in detail. We also proved that this type of laser source is suitable for quantitative analytical measurements as well.

Acknowledgements

The authors would like to thank the financial aid for the ÚNKP-22-4 - New National Excellence Program of The Ministry for Innovation and Technology from the source of The National Research, Development and Innovation Fund. We are also grateful for the profilometric measurements for Judit Kopniczky and Béla Hopp, researchers of Department of Optics and Quantum Electronics at the University of Szeged.

References

[1] C. Guoqing, W. Zhiyi, *iScience*, 23 (2020) 101101.
[2] M. Baudelett, C.C.C. Willis, L. Shah, M. Richardson, *Optic Express*, 18 (2010) 7905.
[3] G. Galbács, N. Jedlinszki, A. Metzinger, *Microchemical Journal*, 107 (2013) 17-24
[4] X. Fu, G. Li, D. Dong, *Frontiers in Physics*, 8 (2020) 68.

EVALUATION OF BIOMASS GROWTH ON NATURAL SUPPORTS FOR WASTEWATER TREATMENT

Alexandra Ioana Bucur, Mihai-Cosmin Pascariu, Cristina Mosoarca, Corina Orha, Raul Alin Bucur, Radu Banica*

National Institute of R&D for Electrochemistry and Condensed Matter, 144 Dr. Aurel Păunescu-Podeanu, RO-300569 Timisoara, Romania, Phone: +40 721 168275
e-mail: radu.banica@yahoo.com

Abstract

Marine shell exoskeletons are produced yearly in huge amounts, due to both natural causes and human activities. Because of unregulated disposal procedures, such wastes are discarded in open fields or in landfills, which are found all around the world and cause environmental problems in terms of unpleasant odors and area contamination caused by organic matter decomposition. In order to reduce this pollution, scientists look for ways to convert exoskeletons into added-value products with applications in various domains like heterogeneous catalysis, construction, agriculture and environmental protection. Some new niche projects involve water purification, where shells serve as substrate for biofilm growth and provide nutrients for nitrifying bacteria. Such bacteria can decompose the aquatic animal and plant residues, increase the dissolved oxygen, prevent water eutrophication, and prevent the production of odor gas, organic nitrogen, organic sulfide and absorption/decomposition of ammonia nitrogen [1-3].

In this paper we analyze the growth of biomass on marine shell exoskeletons, with applications in wastewater biofiltration. For comparison, commercial charcoal was used as support instead of seashells in a second experiment, because this material is well-known for its applications in water purification. The inoculum was brought from the city's wastewater treatment facility and was recirculated through the bioreactors for three weeks. As a measure of biomass growth, ATP determination was performed using a luminometer and the luciferin-luciferase reagent. Measurements were made at three time intervals, namely 96, 336 and 720 h since the synthetic water began to recirculate in the bioreactors. The ATP data was correlated with the substrates images, acquired using a scanning electron microscope (SEM).

As expected, the analyses revealed an abundant growth of biomass on the charcoal substrate. However, attachment and growth of biomass was also recorded on the seashell substrate, thus being suggested that seashells could be used in wastewater treatment applications, with an almost similar efficiency.

Acknowledgements

This work was supported by a grant of the Romanian Ministry of Education and Research, CNCS - UEFISCDI, project number PN-III-P1-1.1-TE-2019-2116, within PNCDI III.

References

[1] D. Summa, M. Lanzoni, G. Castaldelli, E.A. Fano, E. Tamburini, Resources 11 (2022) 48.
[2] E. Ferraz, J.A.F. Gamelas, J. Coroado, C. Monteiro, F. Rocha, Waste Biomass-Valorization 10 (2018) 2397–2414.
[3] S. Thakur, S. Singh, B. Pal, Fuel Process. Technol. 213 (2020) 106707.

INFLUENCE OF HEAVY METAL IONS ON THE LUMINESCENCE OF ZINC OXIDE-BASED COMPOUNDS

Ioana Perhaiţa[1], Laura Elena Mureşan[1], Codruţa Saroşi[1], Lucian Barbu-Tudoran[2,3], Gheorghe Borodi[2]

[1]"Raluca Ripan" Institute for Research in Chemistry, "Babes-Bolyai" University, Fantanele 30, 400294 Cluj-Napoca,Romania;
[2]Electronic Microscopy Centre, Babes-Bolyai University, Clinicilor 5-7, 400006 Cluj-Napoca, Romania;
[3]National Institute for Research and Development of Isotopic and Molecular Technologies, 65-103 Donath, 400293 Cluj-Napoca, Romania.
e-mail: imperhaita@gmail.com

Abstract
Luminescent zinc hydroxide (ZH) and zinc carbonate (ZHC) compounds were prepared by precipitation with different precipitating agents. The effect of various heavy metal ions on the optical properties of samples was discussed.

Introduction
Environmental pollution, resulting from rapid industrialization has become a source of general serious concern [1]. Heavy metal ions are a major source of water contamination and this has encouraged researchers to develop novel low-cost metal ion sensors to detect their presence. The optical properties of materials can act as indicators of various contaminants presence [2].

Experimental
Various luminescent zinc hydroxy-carbonate compounds were prepared by precipitation using different precipitating agents such as LiOH, NH_3, Na_2CO_3 and $(NH_4)_2CO_3$. Samples were investigated by XRD, FTIR, SEM, BET, UV-Vis and PL.

Results and discussion
The emission intensity and peak position are affected by the concentration of Cu^{2+}. The maximum of emission is centered at 417 nm (ZH) and at 436 nm (ZHC). The quenching effect of the emission is observed above 1 mg/L Cu^{2+} in ZHC and above 11 mg/L Cu^{2+} in case of ZH.

Conclusion
The optical properties of zinc oxide-based compounds are influenced by the interaction with heavy metal ions due to electron transitions which involves donor–acceptor levels and interstitial Zn defects. The results show the potential for use of these materials for identification of heavy metals from wastewaters.

Acknowledgements
This work was supported by a grant of the Romanian National Authority for Scientific Research and Innovation, CNCS/ CCCDI-UEFISCDI, PN-III-P2-2.1-PED-202-2421.

References
[1] M. Yeganeh, A. Azari, H.R. Sobhi, M. Farzadkia, A. Esrafili, M. Gholami, Int. J. Environ. Anal. Chem. (2021) 1-18.
[2] N. Ullah, M. Mansha, I. Khan, A. Qurashi, Trends Analyt. Chem. 100 (2018) 166.

RECOVERY AND FUNCTIONAL PROPERTIES OF RUBISCO PROTEIN FROM CONVENTIONAL AND ENZYMATIC EXTRACTIONS

Milica Perović[1], Maja Milošević[1], Zorica Knežević Jugović[2], Mirjana Antov[1]

[1]Faculty of Technology, University of Novi Sad, Boulevard cara Lazara 1, 21 000 Novi Sad, Serbia
[2] Faculty of Technology and Metallurgy, University of Belgrade, Karnegijeva 4, 11 000 Belgrade, Serbia
e-mail: perovicmilica@uns.ac.rs

Abstract
Protein isolates extracted by conventional and enzymatic protocols from pumpkin leaves were evaluated. Pumpkin leaves represent waste material that can be used for extraction of RuBisCO protein. Results showed that usage of Viscozyme for enzyme-assisted extraction enhanced recovery of protein by 30% compared to conventional extraction protocol. Moreover, protein extracted by enzymatic treatment showed improved solubility and oil holding capacity by 71% and 13%, respectively. Our findings might indicate a possibility of usage of enzyme treatment that would enable production of protein isolate with properties and/or in quantities tailored to their particular application in food systems.

Introduction
Globally, there is a constant search for protein sources that should provide healthier and lower-cost alternatives without compromising product quality and safety. Green leaves, that present waste material, are an alternative source of proteins for human consumption. RuBisCO (ribulose-1,5-bisphosphate carboxylase/oxygenase) is the main protein in green leaves and is the most abundant protein in nature [1]. Moreover, RuBisCO presents a source of protein with good functional and nutritional properties [2].
The basic principle of enzyme-assisted extraction is a disruption of plant cell wall by hydrolyzing its polysaccharides by enzymes in order to enhance the release of intracellular components. Degradation of structural polysaccharides usually is achieved with different carbohydrases [3].

Experimental
Pumpkin leaves were selectively harvested at suitable maturity from the fields where pumpkins were grown (JS&O, d.o.o. Novo Miloševo, Serbia). After harvest, leaves free from decay or damage were washed and stored at -18 °C in the freezer for couple days prior to analysis.
Enzymatic extraction was performed using enzyme preparation Viscozyme (Novozymes) in previously determined dosages. Pumpkin leaves were pressed and suspension containing both solid and liquid streams was enzymatically treated (45 ℃ and pH 5.5 for 1 hour). After extraction, suspension was centrifuged and the contaminant proteins from green protein fraction were removed by thermal denaturation at 55 ℃ for 30 minutes. Subsequently, supernatant from centrifugation was subjected to isoelectric precipitation at pH 4.5. After precipitation, protein curd was collected by centrifugation and freeze dried. Conventional protocol was performed in equal way but without enzymatic treatment.
Oil holding capacity (OHC) of protein isolates was determined according to Tan et al. [4] while solubility was measured by the method described by Perović et al. [5].

Results and discussion

Results showed that protocol with usage of enzyme enabled enhanced recovery of RuBisCO proteins from pumpkin leaves. Improvement of recovery with Viscozyme was approximately 30% compared to conventional extraction process. Additionally, protein extracted with the assistance of enzyme preparation improved solubility and oil holding capacity by 71% and 13%, respectively.

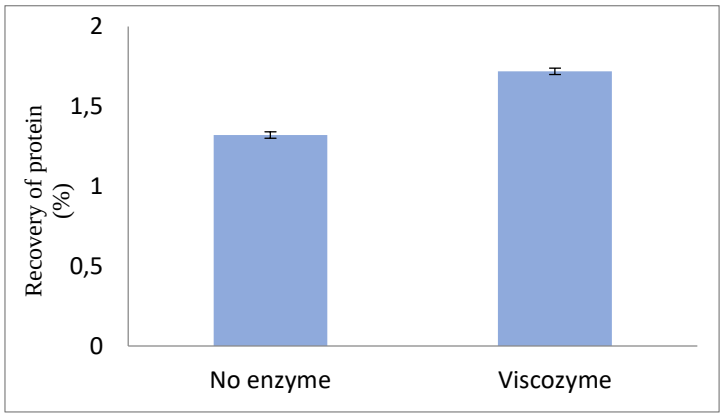

Figure 1. Recovery of RuBisCO protein extracted from pumpkin leaves with and without treatment with enzyme

Table 2. Functional properties of RuBisCO protein extracted from pumpkin leaves with and without treatment with enzyme

	No enzyme	Viscozyme
Solubility (%)	9.40±0.02	16.10±0.07
OHC (g/g)	6.62±0.01	7.49±0.41

Conclusion

Enzymatic treatment of pumpkin leaves with commercional enzyme preparation Viscozyme greatly affected recovery of protein as well as functional properties. Our findings showed that enzymatic extraction enable production of protein isolate in higher amounts and with improved functional properties in comparison to protein isolate from conventional extraction process.

Acknowledgements

The financial support by the Science Fund, Republic of Serbia, Project MultiPromis, Grant No.7751519 is greatly acknowledged.

References

[1] R.J. Ellis, Trends Biochem. Sci. 4 (11) (1979), pp. 241-244.
[2] S. Pérez-Vila, M.A. Fenelon, J.A. O'Mahony, L.G. Gómez-Mascaraque, Food Hydrocolloids. 133 (2022) 107902.
[3] M. Rosset, V.R. Acquaro, A.D.P. Beléia, J. Food Process. Preserv, 38 (3) (2014) pp. 784–790.
[4] E.S. Tan, N. Ying-Yuan, C.Y. Gan, Food Chem. 152 (2014) pp. 447–455
[5] M. Perović, B. Pajin, M. Antov. Food Chem. 374 (2022) 131809

CHEMICAL AND NUTRITIONAL CHARACTERIZATION OF SOYMILK

Georgeta-Sofia Popescu[1*], Florina Radu[1], Ariana-Bianca Velciov[1], Antoanela Cozma[2], Gabriel Bujanca[1], Elisabeth Spataro[3], Mihaela Maria Stanciugelu[4], Nicoleta-Gabriela Hadaruga[1]

[1]Faculti of Food Engineering, University of Life Sciences "King Mihai I" from Timisoara, 300645, 119 Calea Aradului, Romania
[2]Faculti of Agriculture, University of Life Sciences "King Mihai I" from Timisoara, 300645, 119 Calea Aradului, Romania
[3]Faculty of Biology, Babes- Bolyai University, Street Gheorghe Bilaşcu 44, Cluj-Napoca,400015 Romania
[4]Faculty of Sciences, "Lucian Blaga" University of Sibiu, 5-7 Ion Ratiu Street, Sibiu, 550012, Romania
sofiapopescu@yahoo.com, raduflorina@usab.tm.ro, arianavelciov@usab-tm.ro, hadaruganicoleta@usab-tm.ro
**e-mail: sofiapintilie@usab-tm.ro, sofiapopescu@yahoo.com*

Abstract

Soymilk is an alternative to dairy products and it has long been a traditional drink in China, Japan and other parts of Asia. The soybean (*Glycine max*) is the most important bean in the world, providing a wide range of vegetable proteins. Soymilk is a colloidal solution obtained in the form of water extract from swollen and ground soybeans. Soymilk is rich in protein, calcium and has no saturated fat. It is low in calories, being the perfect alternative for people with lactose intolerance. The active ingredients used in the preparation of soymilk are spring water and decorted soybeans. Soymilk is a substitute for cow's milk. This kind of drink is especially used for vegetarian people, people with lactose intolerance, and those who hold religious fasting. The soybean used for soymilk has been purchased from Romanian supermarkets. In our study we used soybeans and homemade soymilk (prepared from us in-house) and two types of soy milk purchased from the Romania supermarket. Homemade vegetable milk was prepared by boiling.

The objective of this study was to evaluate the chemical and physical characteristics of soymilk homemade prepared, and some types of soymilk purchased from Romanian supermarkets. The soymilk has been prepared from analyzed grains and then some chemical and physical characteristics of milk have been assessed.

We investigated moisture and total dry content substance, fat, carbohydrates, and protein content. For soymilk, we established humidity, total solid content, refractive index, total mineral content, and sensory evaluation.

Macronutrients content in soymilk sample are in range from 1.1 (lipids in sample SMC) to 3.7 g/100g (protein in sample SMB), where SMB and SMC are sample of soymilk purchased form supermarket.. The presence of aroma and flavor, darker color, and different viscosity are important attributes in the acceptance of soymilk beverages.

The recipe used by us for the preparation of homemade soy milk needs to be improved in order to improve all the physico-chemical and sensory characteristics.

Keywords: soymilk, sensory evaluation

References

[1] M.M.Terhaag, M.B.Almeida, M.T.Benassi, *Food Sci. Technol, Campinas,* 33 (2013) 387.

[2] H. Kibar, T. Ozturk, *Int. Agrophysics*, 22 (2008) 239-244.
[3] A.V. Torres-Penaranda, C.A. Reitmeier, Journal of Food Science, 66 (2001) 352-356.
[4] K. Liu, Soybeans: chemistry, technology and utilization, New York: Chapman and Hall, 1997
[5] K.D.Setchell, A.Cassidy, J. Nutr., 129 (1999) 758S–767S.
[6] J. Bonifacio da Silva, M.C. Carrao-Panizzi, S.H. Prudêncio, *Pesq. agropec. bras., Brasília,* 44 (2009).777-784.
[7] B. De, A. Shrivastav, T. Das, T. K. Goswami, Appl Food Research, 2022

EFFECT OF DIFFERENT PACKING MATERIALS ON PHYSICOCHEMICAL PROPERTIES OF CARROT AND POTATO

Pradeep Kumar, **Dóra Székely, Mónika Máté**

Department of Fruit and Vegetable Processing Technology, Institute of Food Science and Technology, Hungarian University of Agriculture and Life Sciences, H-1118 Budapest, Villányi út 29-43, Hungary
e-mail: pradiip06@gmail.com

Abstract
Potato (*Solanum tuberosum L.*) and carrot (*Daucus carota* subsp. *sativus* Hoffm.*)* are one of the most popular and most used vegetables around the world. Both the vegetables are thoroughly used in Europe but in these rapidly changing times the present-day consumer want ready to prepare (RTP) or ready to eat (RTE) foods or ingredients. To produce the ready to prepare food its skin must be removed. But this removal of skin reduces the shelf life, sensory characteristics and causes nutrient loss. RTP vegetables can be packed in Polyethylene (PE) packaging but it's one of the most prominent polluter in the world. We used packing material made up of Polylactic Acid (PLA) as our biodegradable packing.
In our experiments, we used three treatments for packing, control (without packing), PE and PLA.
The samples were kept at room temperature for 5 days and we measured weight change, moisture content, color parameters and Total Polyphenol Content (TPC) every day.

Introduction
Potato is the 5th most cultivated agricultural commodity in the world. In the year 2020, 359 MT potato was produced [1]. European countries are second in production of potato, Asia remains the first. The potato tuber is a subterranean swollen stem which evolved to survive from season to season as a dormant storage organ. Starch is the primary form of energy in potato. Thus, potatoes are the major source of energy in the diets of masses across the world. Potatoes contain only about 2% protein on fresh weight basis, but their bioavailability is 90% [2]. They also contain considerable amounts of vitamin B1, B6, B9 and C, calcium, phosphorus, potassium, magnesium, zinc and iron, carotenoids, and tocopherols. Potatoes have better nutrient to price ratio than many other vegetables [1].
Carrot is one of the popular root vegetables grown throughout the world and is the most important source of dietary carotenoids in Western countries. Carrots are multi-nutritional vegetables. It is well known by its high β-carotene content, but its root also contains carotenoids, phenolic compounds, vitamin C, dietary fiber and polyacetylenes [3]. The utilization of carrot and its products is expanding relentlessly due to its recognition as an important source of natural antioxidants having anticancer activity [4]. Total worldwide production of carrot in 2019 was 44.77MT including turnips [1].
Modern consumer is always running out of time and need something which is easier and ready to prepare (RTP). Thus, there is need of RTP of vegetables so that the demand can be satisfied. But conversion into RTP make the vegetables more prone to deterioration, less shelf life and loss of nutrients. Hence, they need to be packed to keep all the characteristics and a significant shelf life.
The PE are mainly produced from fossil fuels and may take thousands of years to biodegrade. Plastics are a menace to the environment and are hurdle in the sustainable development. PLA

can be synthesized from renewable bio-derived monomers, and it is an alternative to conventional petroleum-based polymers [5].
So, we use two types of packing materials simple packing (polyethylene) and biodegradable (polylactic acid) and compared packed vegetables samples with the unpacked ones.

Experimental

Good quality fresh potato and carrot were brought from a supermarket in Budapest. They were peeled using a hand peeler and diced. After dicing they were washed thoroughly in potable running water. Afterwards, the vegetable dices were divided in three different batches. No packing was used for the first batch of vegetable samples it was called Control (C). The other two were packed with polyethylene (PE) and biodegradable polylactic acid (PLA). The measurements were taken daily from all the three batched for a span of 5 days.

Percentage weight loss

Weight loss was determined and expressed as percentage weight loss using the following formulae:
Weight loss (%) = $(W_i-W_f)/W_i * 100$
Where, W_i is the initial weight (g) on day 1 and W_f is the measured weight (g) of each sample on particular day of analysis during storage period.

Moisture content

Moisture content was performed using a moisture content examining machine.

Total Polyphenolic Content

Extraction: 5 g of sample was dissolved in 20 mL of solution containing 80% methanol and 20% distilled water. The mixture was allowed to rest for one hour at room temperature. After the resting period, the mixture was filtered using filter papers and liquid solution was obtained to perform further analysis.
Total Polyphenol Content (TPC) was determined using the method by Singleton and Rossi. The samples were measured at 760 nm and the results were given in mg gallic acid equivalent 100 g^{-1} (mg GAE 100 g^{-1}) [6].

Color values

Color measurements were performed by CIE Lab Color Measuring System with Konica Minolta CR 410 manual digital color meter.

Results and discussion

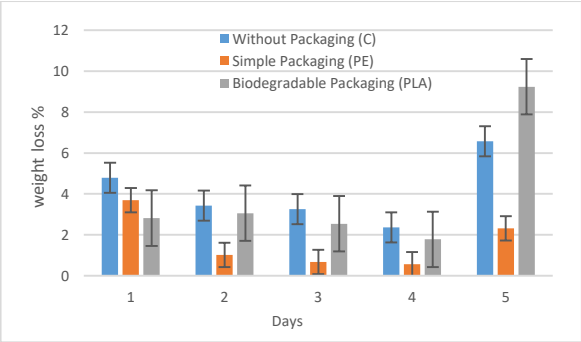

Figure 1a- Rate of weight loss in potato samples

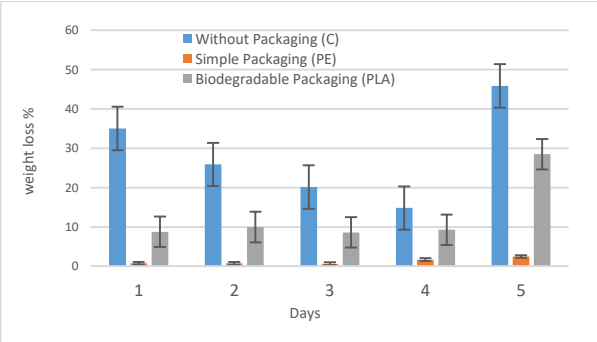

Figure 1b- Rate of weight loss in carrot samples

For weight change PE packing was significantly better than PLA and without packing for potato. In case of carrots, the samples which were kept in PE packing had almost no weight loss. Throughout the storage period the samples kept without packing lost most weight. The least weight loss was seen in the carrot at 0.64% on 3rd day of storage. In their studies [7], [8]

used vaccum drying and PE for packing of potato and carrot. They found similar results and same trend.

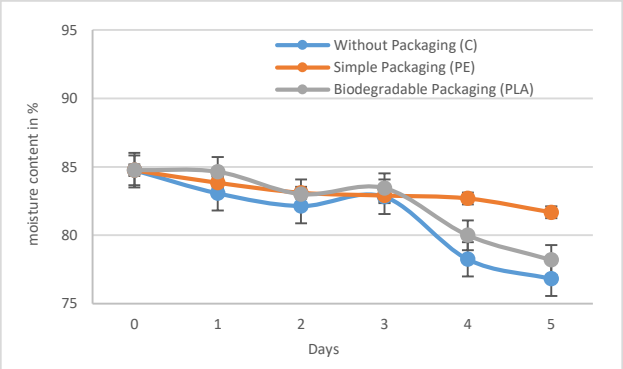

Figure 2a- Change in moisture content of potato samples

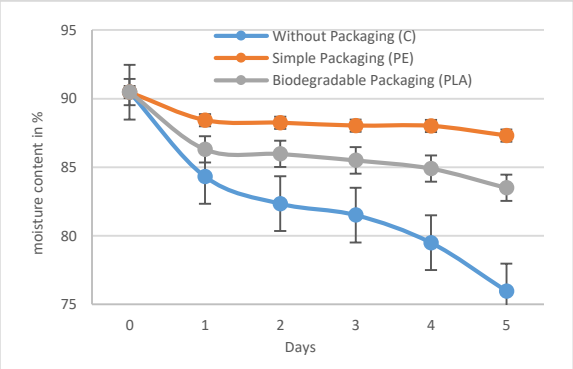

Figure 2b- Change in moisture content of carrot samples

The highest moisture content was seen in the samples with PE packing followed by PLA and then samples without packing. This trend was same in potatoes and carrots and the content of moisture reduced every day. By the end of of storage period samples packaging had around 76% moisture content compared to more than 85 and 90 % on day 1. Our results were in accordance with the experiments of [9].

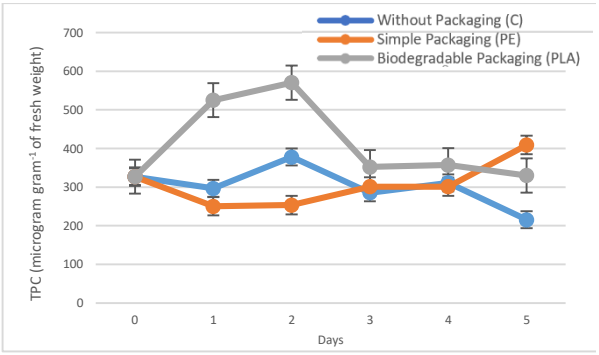

Figure 3a- TPC of Potato samples

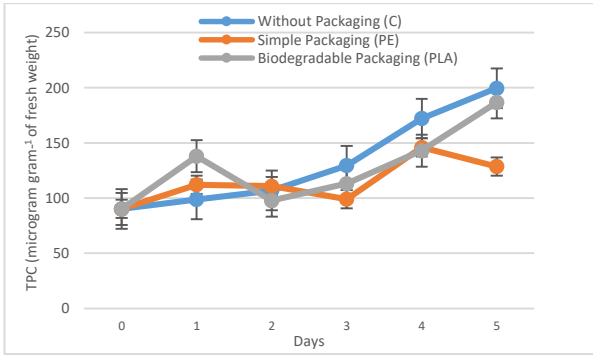

Figure 3b- TPC of Carrot samples

TPC for potato was lowest in PE packed samples while highest in samples without packaging. For carrots initially the TPC was highest in PLA packed samples but by the end of storage period PE packed samples contained most TPC. In all the samples the TPC increased as the storage period increased. Initially the TPC was low for carrot, but it increased with storage time. On the first day it was 90.13 µg g^{-1} FW for carrot and 326.91 µg g^{-1} FW for potato. Opposite trend was seen in the potato samples. Our results also showed that TPC of potato was more than carrot, but these results are in accordance with the literature. Some studies also received similar results in their experiments [10, 11].

There was no significant effect of packing material on color parameters of both the vegetable samples.

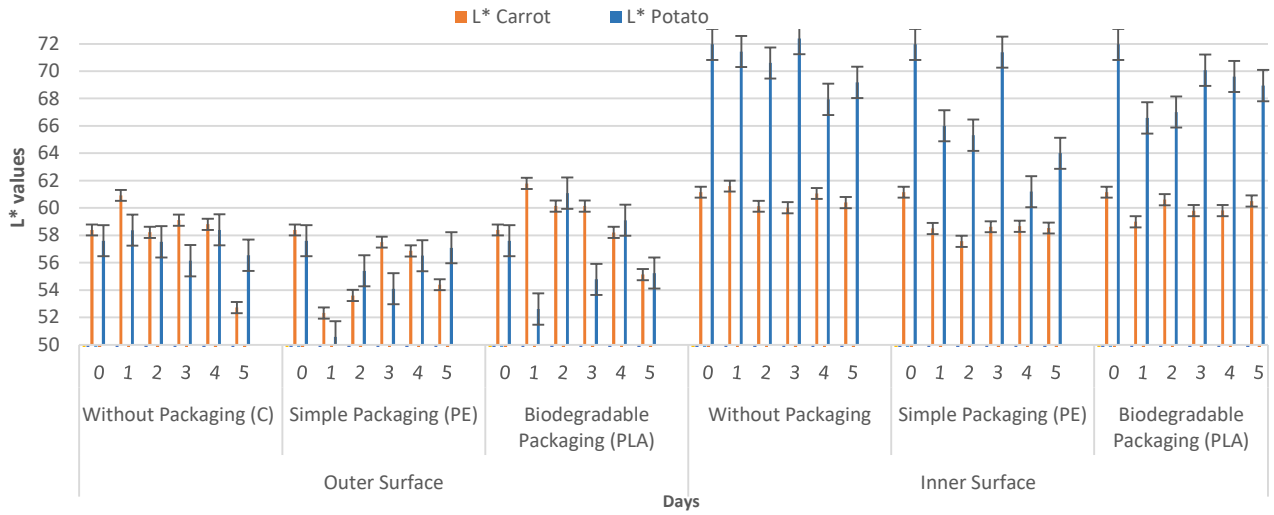

Figure 4a- L* values of potato and carrot samples in different packings

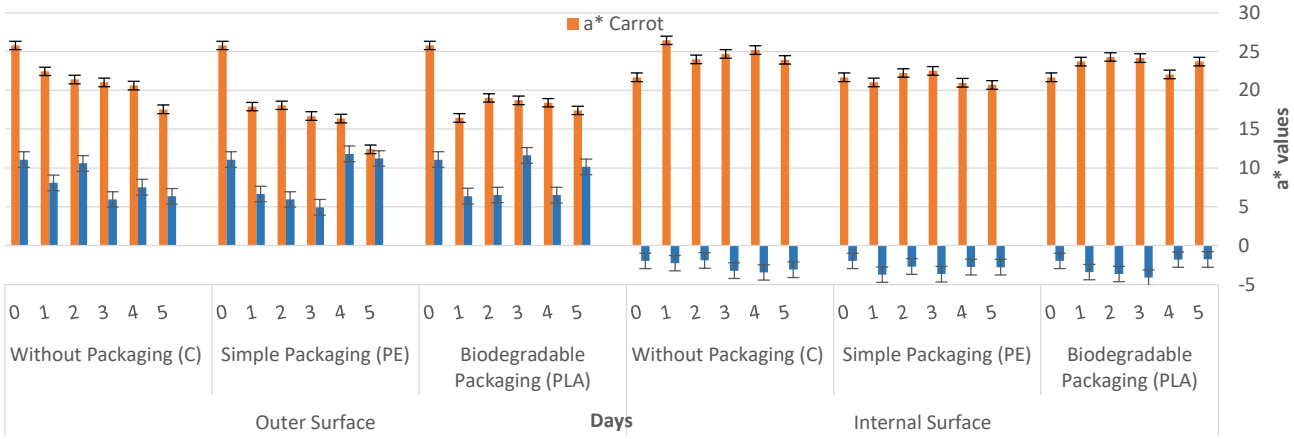

Figure 4b- a* values of potato and carrot samples in different packings

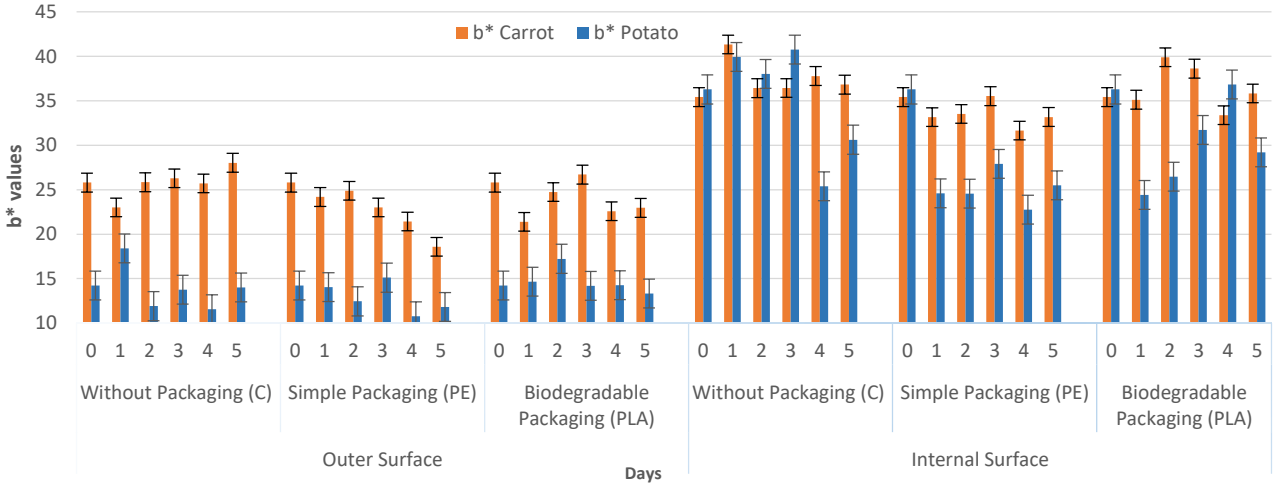

Figure 4c- b* values of potato and carrot samples in different packings

Conclusion

Based on our results we can say that vegetables samples kept in packing performed better than samples without packing in every test. Between the normal (PE) packing and biodegradable (PLA) packing, the PE packing performed better in case of retaining moisture and inhibiting weight loss. The samples kept in PLA packing showed higher TPC values than PE, but this could be due to the more weight loss in PLA packed samples. Eventually PE was found to be a better packing material than PLA in our experiments.

Acknowledgements

The authors acknowledge the Hungarian University of Agriculture and Life Science's Doctoral School of Food Science for the support in this study.

References

[1] FAO STAT. https://www.fao.org/faostat/en/

[2] M. Friedman, "Nutritional Value of Proteins from Different Food Sources. A Review," J Agric Food Chem, vol. 44, no. 1, pp. 6–29, Jan. 1996, doi: 10.1021/jf9400167.

[3] S. KRIVOKAPIC, T. PEJATOVIC, and S. PEROVIC, "CHEMICAL CHARACTERIZATION, NUTRITIONAL BENEFITS AND SOME PROCESSED PRODUCTS FROM CARROT (Daucus carota L.)," The Journal "Agriculture and Forestry," vol. 66, no. 2, Jun. 2020, doi: 10.17707/AgricultForest.66.2.18.

[4] K. D. Sharma, S. Karki, N. S. Thakur, and S. Attri, "Chemical composition, functional properties and processing of carrot—a review," J Food Sci Technol, vol. 49, no. 1, pp. 22–32, Feb. 2012, doi: 10.1007/s13197-011-0310-7.

[5] I. S. M. A. Tawakkal, M. J. Cran, J. Miltz, and S. W. Bigger, "A Review of PolyLactic Acid)-Based Materials for Antimicrobial Packaging," J Food Sci, vol. 79, no. 8, pp. R1477–R1490, Aug. 2014, doi: 10.1111/1750-3841.12534.

[6] Singleton, V. L., Rossi, J. A. "Colorimetry of Total Phenolics with Phosphomolybdic-Phosphotungstic Acid Reagents", American Journal of Enology and Viticulture, 16(3), pp. 144–158, 1965.

[7] N. Aharoni, V. Rodov, E. Fallik, R. Porat, E. Pesis, and S. Lurie, "Controlling humidity improves efficacy of modified atmosphere packaging of fruits and vegetables," Acta Hortic, no. 804, pp. 121–128, Dec. 2008, doi: 10.17660/ActaHortic.2008.804.14.

[8] A. M. C. N. Rocha, E. C. Coulon, and A. M. M. B. Morais, "Effects of vacuum packaging on the physical quality of minimally processed potatoes," Food Service Technology, vol. 3, no. 2, pp. 81–88, Jun. 2003, doi: 10.1046/j.1471-5740.2003.00068.x.

[9] A. Asgar, "Effect of storage temperature and type of packaging on physical and chemical quality of carrot," IOP Conf Ser Earth Environ Sci, vol. 443, no. 1, p. 012002, Feb. 2020, doi: 10.1088/1755-1315/443/1/012002.

[10] S. H. Lee et al., "Antioxidant Contents and Antioxidant Activities of White and Colored Potatoes (Solanum tuberosum L.)," Prev Nutr Food Sci, vol. 21, no. 2, pp. 110–116, Jun. 2016, doi: 10.3746/pnf.2016.21.2.110.

[11] C. Kaur and H. C. Kapoor, "Anti-oxidant activity and total phenolic content of some Asian vegetables," Int J Food Sci Technol, vol. 37, no. 2, pp. 153–161, Feb. 2002, doi: 10.1046/j.1365-2621.2002.00552.x.

SURFACE CHEMISTRY OF "BORON" DOPED CARBON QUANTUM DOTS

Jovana Prekodravac[1], Bojana Vasiljević[1], Vesna Despotović[2], Nataša Zec[3], Biljana Todorović Marković[1]

[1]Vinca Institute of Nuclear Sciences-National Institute of the Republic of Serbia, University of Belgrade, Belgrade, Serbia
[2]University of Novi Sad Faculty of Sciences, Department of Chemistry, Biochemistry and Environmental Protection, Trg Dositeja Obradovića 3, 21000 Novi Sad, Serbia,
[3]Technical College of Applied Sciences in Zrenjanin, Đorđa Stratimirovića 23, 23000 Zrenjanin, Serbia
e-mail: prekodravac@vin.bg.ac.rs

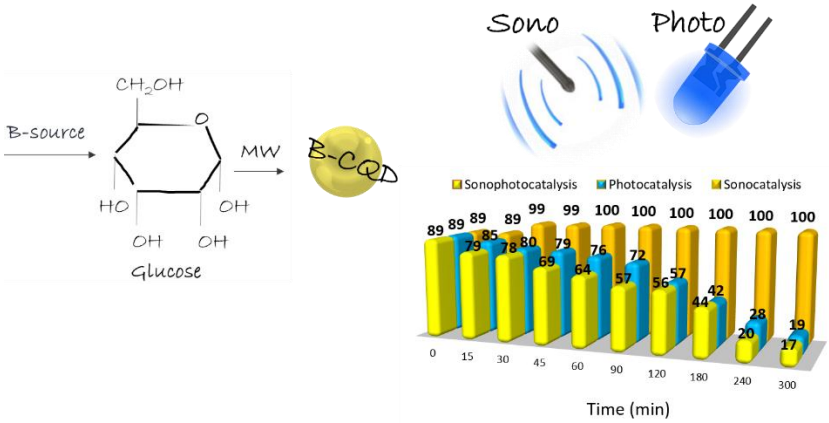

Abstract

Carbon quantum dots (CQDs), are a novel class of carbon nanomaterials that exhibit outstanding physical, chemical, and optical characteristics in addition to strong light absorption. By substituting some of the carbon atoms in CQDs for heteroatoms like N, B, P, and S, it is possible to modify the surface chemistry and electronic properties of the structures, boosting their catalytic activity. Adding B dopant to CQDs changes its surface chemistry and morphology, opening up a wide range of potential uses. The presented study illustrates a quick and environmentally friendly method for producing B-CQDs through microwave-assisted method. According to TEM characterization, the generated B-CQDs had a spherical form, an average diameter of 12 nm, and were negatively charged particles with good water dispersibility and no discernible aggregation. The thorough surface chemistry characterization revealed the presence of B-O and B-C bonds, as well as oxygen-containing surface functional groups in the form of hydroxyl, carbonyl, and carboxyl groups. Additionally, using an RB organic dye as a model molecule, the sonocatalytic, photocatalytic, and synergistic effects of the two processes were investigated.

Introduction

A variety of top-down and bottom-up techniques for CQDs production have been developed over the years [1,2]. While the top-down method indicates the breaking of macromolecules into small-sized CQDs the bottom-up method generally refers to the polymerization and carbonization of simple molecules into CQDs. Because of effective microwave irradiation utilization, the microwave pyrolysis process is one of the bottom-up methodologies that has attracted widespread attention [3,4]. This simple method of producing CQDs rich in oxygen-containing groups allows for faster reactions, reduced energy usage, greater reaction yields, and increased particle size homogeneity while being environmentally friendly. When thinking about

adding dopants to CQDs, the choice of boron as carbon's next-door neighbor in the periodic table of elements with a comparable atomic radius (B: 0.080 nm; C: 0.077 nm) is rather obvious [5]. Adding B dopant to CQD changes its surface chemistry and shape, opening up a wide range of potential usage [6].

The usage of many hazardous organic compounds in the food, cosmetic, and textile industries increases rather fast on a daily level. Therefore, in order to protect the ecosystem, it is vital to treat these compounds since they are the main contributors to water pollution [7]. Due to their capacity to decompose some of the most tenacious water contaminants under the influence of ultrasonic cavitation and light irradiation, the photocatalysis, sonolysis, and sonophotocatalysis processes emerged as the most successful methods in water remediation [8–12].

Here we present a simple and cost effective bottom-up microwave approach for B-CQDs synthesis from glucose as carbon precursor. After detailed characterization of the B-CQDs physical-chemical properties the photo activity of the dots was examined on a model molecule of Rose Bengal organic dye. The synergistic effect of both sono and photo reaction conditions was confirmed after 300 min of system exposure.

Experimental

The glucose water solution (0.1 g ml^{-1}) and boric acid (0.02 g ml^{-1}) were stirred for 30 min on a magnetic stirrer at 600 rpm, followed by heating in a microwave reactor (Anton Paar Monowave 300) for 5 minutes at a fixed temperature (170 °C), to prepare B-CQDs.

Under constant settings of medium pH 7, reaction time 300 min, B-CQD catalyst concentration (0.2 mg ml-1), and RB dye concentration (0.03 mM), tests on sono-, photo-, and sonophotocatalysis were conducted. For the sono testing the tip sonicator with set pulse was applied, while for the photo testing the photoreactor made in our group with six LEDs (6W, 370 nm) was used.

Results and discussion

Exploring the morphology of obtained B-CQDs using TEM, the dots with average particle size diameter between 7.5 to 17.5 nm were observed (Figure 1A). Such a small sized particles showed a good water dispersability without any tendency towards aggregation/agglomeration (Figure 1B). Using UV-vis and PL spectroscopy, the optical characteristics of the B-CQD were investigated (Figure 1C, D). The absorbance at 268 and 356 nm, which corresponds to the existence of π-π^* transitions of aromatic sp^2 domains (C=C) and n- π * transitions of C=O bonds, were detected by UV-vis spectroscopy (Figure C). The PL characteristics of carbon nanoparticles are usually triggered by two factors; one is related to the particle size while the second one is connected to the emission from the defect state or trap state caused by various surface functional groups connected to the carbon core. In the 350-590 nm range, the emission of B-CQDs showed evidence of excitation dependence (Figure 1D). The maximum peak fluorescence emission was observed at 496 nm, after excitation at 390, suggesting the blue-green emission spectrum.

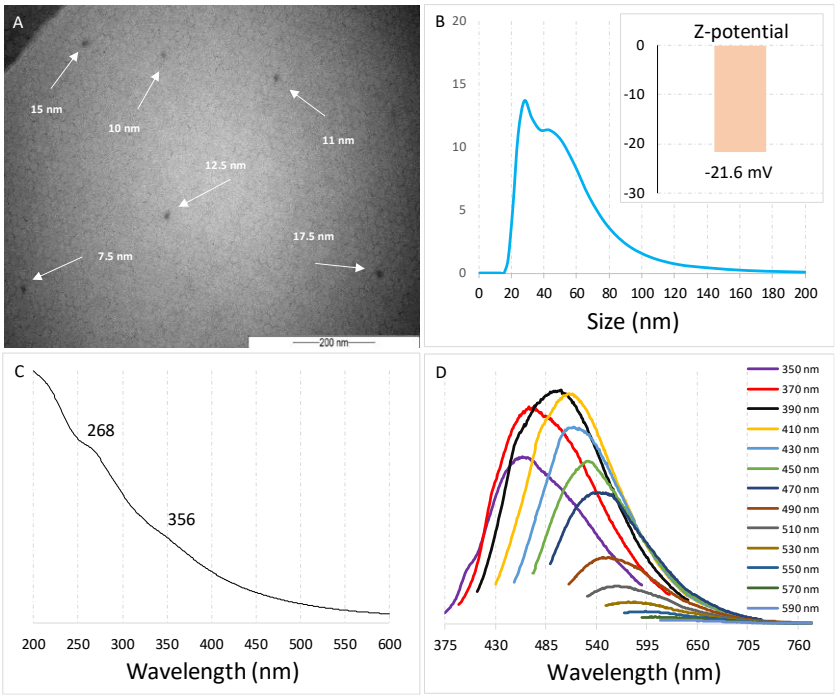

Figure 1. TEM morphology (A), DLS with Z potential measurements (B) and Absorbance/emission spectra (C) for B-CQDs.

According to the FTIR spectroscopy (Figure 2A), examination of the B-CQDs sample indicated the presence of signals at 3200-3400, 2933, 1706, 1612 cm^{-1} attributed to the O-H and C-H groups, and C=O and C=C bonds, respectively. Additional signals at 1393 cm^{-1} and 1026 cm^{-1} correspond to B-O and B-C stretching vibrations.

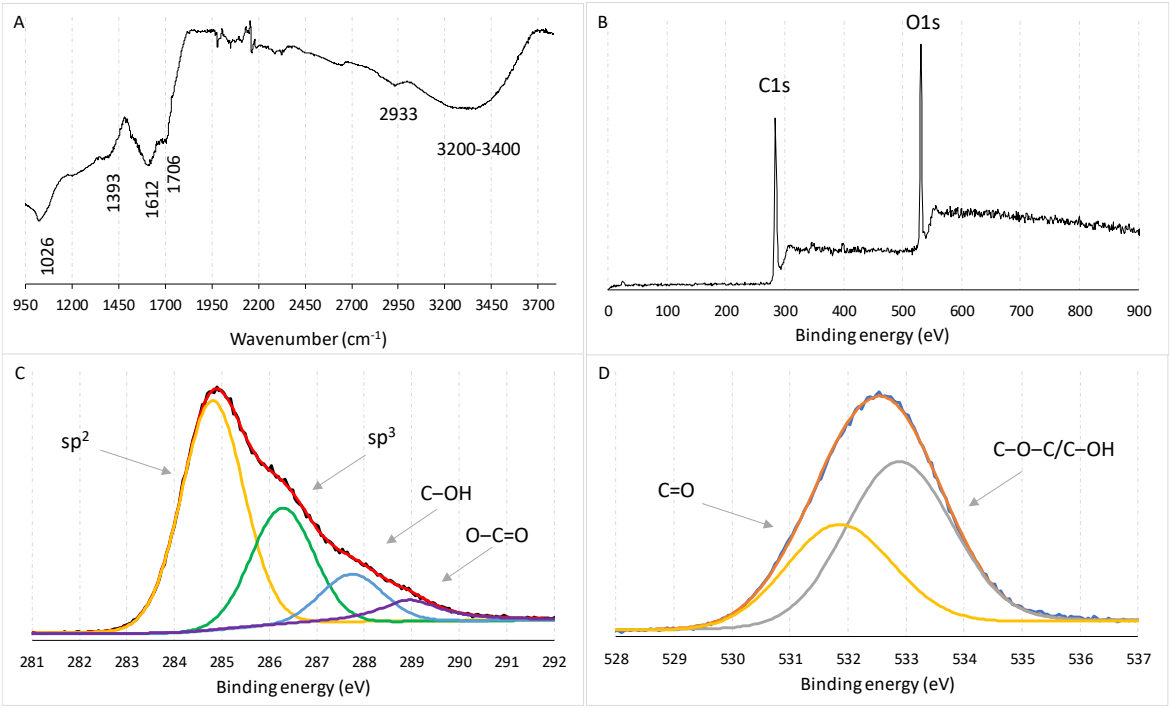

Figure 2. The FTIR results (A), the full scan XPS spectra (B), and the deconvolution of C1s (C) and O1s (D) for the B-CQDs.

Nevertheless, the full scan spectra did not show any existence of B dopant (Figure 2B). Therefore, an additional characterization, using ICP analysis, was performed confirming the presence of B dopant but in a small percentage. The B dopant was present as 0.506 mg per gram of B-CQDs, which was below the detection limit of XPS analysis (0.3 at%).

Under constant conditions of the dye and catalyst concentrations, medium pH, reaction temperature, and time, the synergy of the sono and photo effect on the RB dye removal efficiency was investigated. By keeping the reaction mixture under dark condditions, 11% of the RB dye was absorbed on the catalyst surface. Introduction of the sono effect led to desorption of the dye due to the strong pulse of the ulstrasound tip. On the contrary, the photo treatment resultet in a dye degradation up to 81% after 300 min of irradiation in the presence of B-CQDs as photocatalyst (Figure 3A).

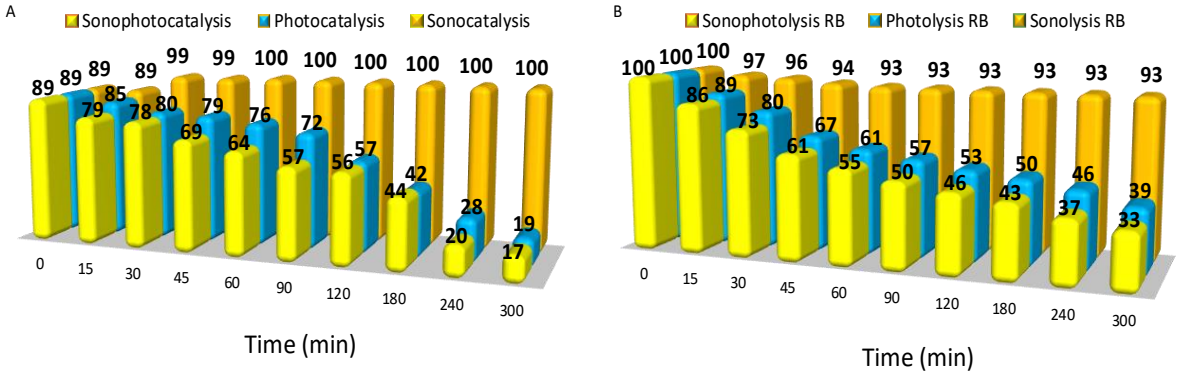

Figure 3. The results of sono, photo and sono-photo experiments: in the presence of a B-CQD catalyst (A) and control experiments without a catalyst (B).

The synergy of the sono-photo effect gave even better results with 17% of residual RB dye after 300 min of treatment (Figure 3A). When comparing obtained results with degradation efficiency in the absence of a B-CQD catalyst (Figure 3B), a much lower degradation percentage was observed in the same time frame. The final result suggested residual RB dye percentage of 93, 39, and 33under sono, photo and sono-photo effect, respectively.

Conclusion

Presented work shows a simple and fast microwave assisted synthesis of B-CQDs under mild reaction conditions such as 170 ºC and 5 min, from glucose water solution and boric acid. Produced B-CQDs with as small percentage of introduced B dopant were spherically shaped dots with average diameter of 12 nm and strong light absorption capacity. Investigating the sono, photo and sono-photo synergy on a RB dye removal efficiency, the B-CQDs acted as a catalyst, improving the degradation percentage after 300 min of the exposure when compared to the control experiments. In comparison to a separate sono and photo method, the results showed that the sonophotocatalytic process had a high synergy index (>1).

Acknowledgements

Presented work was financially supported by the Science Fund of the Republic of Serbia, #7741955, *Are photoactive nanoparticles salvation for global infectional treath?* - PHOTOGUN4MICROBES and by the Ministry of Education, Science and Technological Development of the Republic of Serbia grant number 451-03-68/2022-14/200017.

References

[1] I. Singh, R. Arora, H. Dhiman, R. Pahwa, Turkish J. Pharm. Sci. 15 (2018) 219–230.
[2] X. Wang, Y. Feng, P. Dong, J. Huang, Front. Chem. 7 (2019).

[3] J. Prekodravac, B. Vasiljević, Z. Marković, D. Jovanović, D. Kleut, Z. Špitalský, M. Mičušik, M. Danko, D. Bajuk–Bogdanović, B. Todorović–Marković, Ceram. Int. (2019).
[4] Y. Wang, Q. Zhuang, Y. Ni, Chem. - A Eur. J. 21 (2015) 13004–13011.
[5] Q. Xu, T. Kuang, Y. Liu, L. Cai, X. Peng, T. Sreenivasan Sreeprasad, P. Zhao, Z. Yu, N. Li, J. Mater. Chem. B. 4 (2016) 7204–7219.
[6] A. Pal, K. Ahmad, D. Dutta, A. Chattopadhyay, ChemPhysChem. 20 (2019) 1018–1027.
[7] J. Theerthagiri, R.A. Senthil, D. Thirumalai, J. Madhavan, Handb. Ultrason. Sonochemistry, Springer Singapore, Singapore, 2015: pp. 1–34.
[8] S. Chakma, V.S. Moholkar, Ultrason. Sonochem. 22 (2015) 287–299.
[9] M.F. Khan, S. ul H. Bakhtiar, A. Zada, F. Raziq, H.A. Saleemi, M.S. Khan, P. Muhammad Ismail, A.C. Alguno, R.Y. Capangpangan, A. Ali, S. Hayat, S. Ali, A. Ismail, M. Zahid, Environ. Nanotechnology, Monit. Manag. 18 (2022) 100711.
[10] H.K. Hakki, S. Allahyari, Mater. Chem. Phys. 288 (2022) 126355.
[11] A. Das, P. Ningthoukhongjam, R.G. Nair, Water, Air, Soil Pollut. 233 (2022) 282.
[12] M.F. Khan, G. Cazzato, H.A. Saleemi, R.R. Macadangdang Jr., M.N. Aftab, M. Ismail, H. Khalid, S. Ali, S. ul H. Bakhtiar, A. Ismail, M. Zahid, J. Mol. Struct. 1247 (2022) 131397.

THE INFLUENCE OF LOW AND HIGH TEMPERATURES ON THE GERMINATION OF TOMATO SEEDS (LYCOPERSIEON ESCULENTUM MILL.)

Rašković Vera[1], Blagojević Milan[1], Stošić Nemanja[1], Ljilja Tanasić[1], Vlajić Sobodan[2]

[1]Academy of Applied Studies Šabac. Unite for Agricultural Business Studies and Tourism, Republic of Serbia
[2]Institute of Field and Vegetable Crops, Novi Sad, Serbia
email: blagojevicmilan@ymail.com

Abstract

The production of seedlings and the very process of germinating seeds is certainly significant if it is taken into account that a maximum of about 25,000 plants are planted per ha, i.e. the large number but also the highest germination of the seeds, and later the condition of the seedlings has a great influence on the safety of production. Widespread vegetable crop tomato (Solanum lycopersicum L.) in Serbia with about 20,000 ha. High-temperature stress can be achieved by several mechanisms, and one of those mechanisms is the so-called seed hardening, which improves the germination and adaptability of the seeds. The effect of high temperatures on the development of vegetables that are sensitive to high temperatures affects the morphology, but also the biochemical and physiological content of the tomato plant. According to the researchers, the impact of extreme temperature as well as high temperature variations can damage the intercellular interactions necessary for tomato growth. The study involved the seeds of two tomato varieties; ox heart and apple. for different times of treatment at + 60 °C for 10 min, 20 min, 30 min and 10 hours and at -16 °C the seeds were treated for 3.5 and 10 days. The best results in seed germination were achieved in 20 minutes at 60°C in both varieties. At a temperature of -16 degrees, the best result was achieved with both varieties after 3 days of treatment. The seeds are uniform in size and without damaged seeds. The seeds were placed on two layers of Whatman filter paper in Petri dishes. 10-15 ml of deionized water was added to the Petri dishes. Treatment of seeds with high and low temperatures has a positive effect on the germination of tomato seeds.

THE INFLUENCE OF SOME ABIOTIC FACTORS ON THE DEVELOPMENT OF THE MOST IMPORTANT PHYTOPATHOGENIC FUNGI

Blagojević Milan[1], Rašković Vera[1], Stošić Nemanja[1], Milan Glišić,[1] Vlajić Slobodan[2]

[1] Academy of Applied Studies Šabac. Unite for Agricultural Business Studies and Tourism, Republic of Serbia
[2]Institute of Field and Vegetable Crops, Novi Sad, Serbia
email: blagojevicmilan@ymail.com

Abstract

The intensity of action of each factor that provides plants with favorable conditions for growth and development is designated as optimum for a specific function of the plant. If the intensity of that factor deviates from the optimum, its effect on the plants becomes unfavorable. High temperatures in the course of 2022 have a favorable effect on the intensity of slow-growing, growth and development of phytopathogenic fungi: *Aspergillus spp., Ustilago maydis, Alternaria helianthi, Fusarium oxysporum*. The low temperatures that lasted for a relatively long time until mid-May in 2022 have the greatest favorable effect on the intensity of slow-growing, growth and development of phytopathogenic fungi: *Pythium spp., Fusarium nivale, Pseudocercosporella herpotrichoides, Sclerotinia sclerotiorum, Mycosphaerella fragariae*. Increased moisture intensity has a positive effect on the intensity of slow-growing, the speed of development and the course of diseases of phytopathogenic fungi: *Phytophthora infestans, Sclerophthora macrospora, Pythium spp., Monilia laxa, M. fructigena, Botrytis cinerea, Venturia inequalis*. During the year 2022. due to the reduced intensity of moisture, a significantly lower presence of the aforementioned phytopathogenic fungi was recorded. In the course of 2022, in addition to the influence of low and high temperatures, the lack of air humidity and precipitation has the greatest importance in the weak spread of phytopathogenic fungi. A very reduced level of moisture in combination with low and high temperatures caused greater losses in the yields of cultivated crops during 2022. The yields of cultivated crops during 2022 are very low, so there were absolutely favorable conditions for the development of phytopathogenic fungi and if there had been a high degree of infection, there would not have been yield losses of this magnitude

L.PLANTARUM 299V AS A STARTER PROBIOTIC IN FERMENTED EGG WHITE DRINK

Reem Mourad[1,2], Barbara Csehi[1], Erika Bujna[2]

[1]Department of Livestock Products and Food Preservation Technology, Hungarian University of Agriculture and Life Sciences, 1118, Ménesi út 43-45, Budapest, Hungary.
[2]Department of Bioengineering and Alcoholic Drink Technology, Hungarian University of Agriculture and Life Sciences 1118, Ménesi út 43-45, Budapest, Hungary.
e-mail: Reemmd91@gmail.com

Abstract

Egg white (albumen) is the sticky, colorless part of the egg surrounded by the eggshell. It consists of many functional proteins, especially ovalbumin, ovotransferrin, ovomucoid, ovomucin, and lysozyme. Probiotics are living microorganisms that have a beneficial effect on the human intestine. Recently, supplementing food with probiotics has become an important approach to prevent the adhesion of some harmful bacteria to the intestinal mucosa and reduce the symptoms associated with lactose intolerance and milk protein allergy. Egg white drink is a functional drink that is cholesterol and fat-free, and rich source of protein. In this study egg white drink was fermented by *L.plantarum* 299v as a starter culture using two different carbohydrate sources (fructose and fructooligosaccharides) as samples, and without added sugar were serving as controls.The survivability and pH value of probiotic beverages was investigated during three weeks of cold storage.

After 24 hours of fermentation, the pH decreased to a value of 6.15 and the cell count increased to 8.2 log10 CFU/ml in the control samples.

During 3 weeks of storage, the cell count was higher than 10^8 CFU/ml in all samples with or without added sugar, which is the recommended daily dose of probiotic bacteria. Moreover, the pH decreased to 3.8 when fructose and fructooligosaccharides were added, while the control samples had the highest pH (6.1) during the storage period.

Introduction

L.plantarum 299v is a Gram-positive lactic acid bacteria and a part of phylum Firmicute. Lactobacilli are facultatively heterofermentative microorganism[1] which could be found in plant-based fermented products particularly in sauerkraut, gherkin, and sourdough.It has the ability of adhesion to the intestinal mucosa, it resists to the low pH conditions in the stomach and to the high pH of bile salt in the duodenum [2], in addition to reducing cardiovascular risk [3]. Functional food is a food item that promotes health and human wellness as well as reduces the risk of serious disease [4] [5] particularly cardiovascular complications, osteoporosis, obesity, and cancer [6]. Egg consists of various dietary ingredients which protect against chronic disorder, includinglutein, zeaxanthin, choline, vitamin D, selenium, and vitamin A [7], an extra beneficial nutrient found in eggs is protein. As eggs are one of the rich sources of dietary proteins including all of the important amino acids that have a high numerous biological value [8]. It is used as a standard to compare the other protein from several sources. Egg protein dispensed among the yolk and white (3.6 g in egg white and 2.7 g in egg yolk) in the case of a massive egg with 6.3 g protein in total [9]. Egg whites incorporate ovotransferrin which binds metal ions, ovomucin has antiviral attributes, further it reduces the cholesterol absorption: Lysozyme protects against Gram-positive harmful bacteria [9], and avidin binds to biotin and improves biotin absorption as well as the important role of egg white protein in reducing the visceral fat [10]. Egg white drink (Totu drink) is a functional Hungarian beverage that contains

hen egg white, enzyme, vinegar, salt, and water, it is free of fat and cholesterol, 100 grams of the product contains 0.1 g of carbohydrate, 5.6 g of protein and it provides 23 kcal furthermore, the dry matter reaches a value of 6%.
Our study aims to test the feasibility and the survival of *L.plantarum* 299v in fermented egg white drink as well as the pH value of the final product during 3 weeks of storage under refrigerated conditions using different carbohydrate sources (fructose and fructooligosaccharides) since samples without added sugar were served as a control.

Experimental

- Fermentation : *L. plantarum* 299v has grown in MRS (de Man Rogosa Sharp) broth before 24 hours of the fermentation, then 1% of the liquid starter was added to 100 ml of egg white drink. Different types of carbohydrates solution (fructooligosaccharides, fructose)were added separately to get a 2% sugar concentration in the final products.
- Determination of the pH: By using the pH meter Mettler Toledo InLab expert pro electrode.
- Determination the growth rate: Samples were serially diluted with a saline solution followed by plating the appropriate dilutions (Pour plate method) using MRS agar and incubated for 48-72 hours at 37°C.
- Storage: the studied samples were stored at a refrigerated condition for 3 weeks, as the growth rate and pH value were measured every week.

Results and discussion

After 24 hours of fermentation samples without added sugar had a significantly lowest cell count they reached a value of 8.23 log 10 CFU/mL compared to samples with FOS 9.41 log 10 CFU/mL and samples with fructose 9.28 log 10 CFU/m fig.1. Moreover they were not significantly different from samples in the first and second weeks of refrigerated storage $p>0.05$.
Further, samples with added fructose as a carbon source were not significantly different during the storage period, the cell count ranged (from 9.27-to 9.44) log 10 CFU/mL. Also, the cell count of samples with FOS was not significantly different until the second week of storage then they increased in the third week to 9.73±0.09 log 10 CFU/mL due to sugar metabolizing by *L.plantarum* 299v.
On the other hand, samples with fructose and FOS had no significant difference from each other in the first and second week while samples with FOS were higher in the third week. assamples without added sugar had a significantly lower cell count compared to samples with added sugar during the entire studied period.
It cannot be denied that *L. plantarum* 299v was able to maintain its bioavailability at 4°C for 3 weeks. As some researchers mentioned that the minimum required number of probiotics in fermented food products to have an advantageous health effect on the human body is 10^6 CFU/ml [11] and that was compatible with our results, the cell count was higher than 10^7 CFU/ml during storage time if carbohydrate sources were added or not. Fridge temperature had also been the main role in keeping the survivability of the fermented product, Yoon and co-workers (2006) had the same findings, they evaluate the viability of probiotic cabbage juice during cold storage. The results showed that *L. plantarum* and *L.delbruekii* could maintain their bioavailability at 4 °C for several weeks.

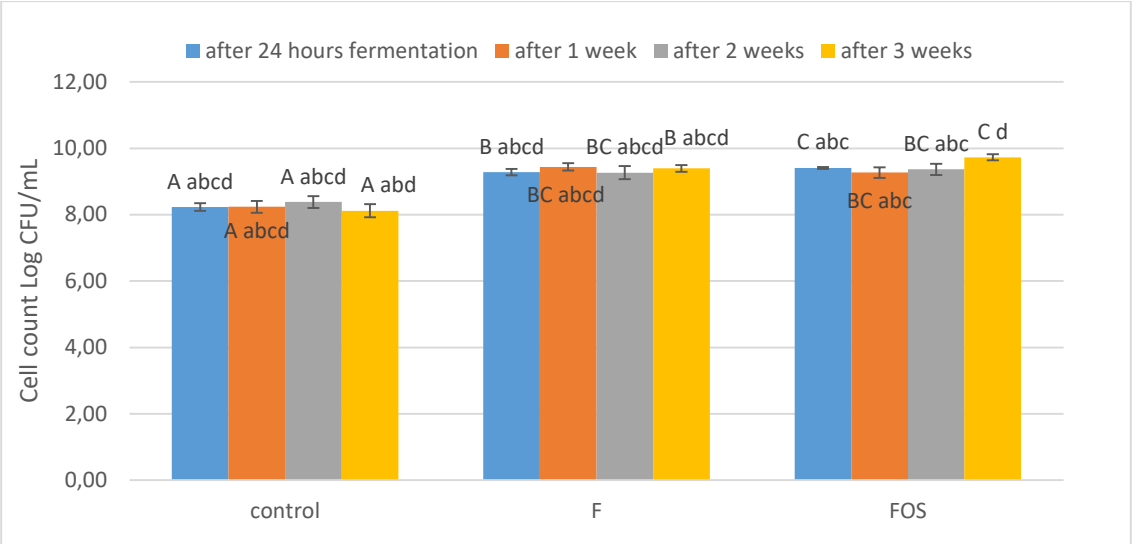

Fig (1): The survivability of *L.plantarum* 299v in fermented egg white drink during cold storage

The bigger case letters express the difference in the cell count when a different sugar type was used in the same storage period, lowercase letters indicate the difference in cell count using the same sugar type in a different storage period. control: samples without added sugar, F: samples with fructose 2%, FOS: samples with fructooligosaccharides 2%.

According to Fig.2. the pH of samples with fructose and FOS were not significantly different from each other during times, while control samples demonstrated the highest pH value compared to the others with added sugar at any period of storage, due to the low cell concentration of *L.plantarum* 299v therefore, the release of lactic acid was less.

On the other hand, the pH values after the first and second week of storage were significantly different from each other. They were both significantly lower and reached a value around pH 5.9 compared to samples after 24 hours of fermentation pH 6.15 and samples in the third week of storage pH 6.08.

The pH value of samples with fructose dropped significantly in the first week of storage, it also decrease in the second week to pH 3.69. The main reason for that may be because of the activity of *L.plantarum* 299v in the egg white drink caused by the consumption of sugar and production of short chain fatty acids and lactic acid [13] which afterward increased and reached a value of pH 3.8 Similar to fructose, the pH value of FOS samples increased significantly in the third week to pH 3.8, that's could be related to the fact that in the case of the lack of the required nutrient in the medium the microorganism starts to consume the organic acids instead thus, moreover due to the constant low pH the cells degrade.

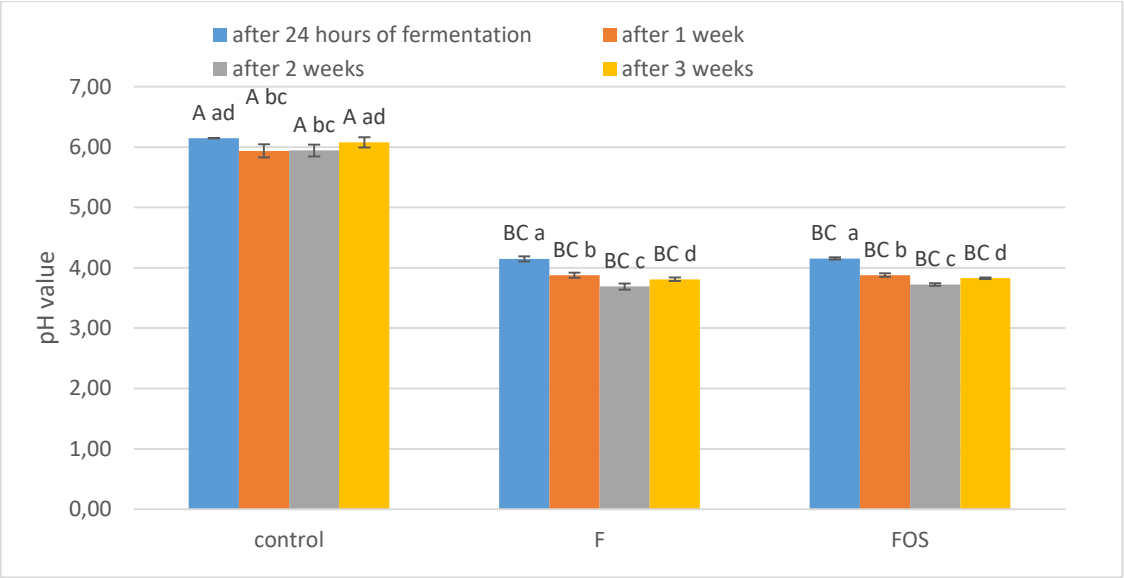

Fig (2): The pH value of fermented egg white drink during cold storage
The bigger case letters express the significant difference ($p < 0.05$) in the pH value when different sugar types were used in the same storage period, the lowercase letters indicate the significant difference ($p < 0.05$) in the pH value using the same sugar type in a different storage period. control: samples without added sugar, F: samples with fructose 2%, FOS: samples with fructooligosaccharides 2%.

Conclusion

Fermented egg white drink is a novel functional drink furthermore a rich source of probiotics and vital protein, while the fermentation extend its shelf life to more than 3 weeks under fridge temperature.

Acknowledgments The Project is supported by Capriovus Ltd.

References

[1] Probi, AB, and LLC JHeimbach. 'Generally Recognized as Safe (GRAS) Determination for the Use of *Lactobacillus plantarum* Strain 299v in Conventional Foods', GRAS Notice (GRN) No. 685, 2016. http://www.fda.gov/Food/IngredientsPackagingLabeling/GRAS/NoticeInventory/default.htm.
[2] Kaźmierczak-Siedlecka, Karolina, Agnieszka Daca, Marcin Folwarski, Jacek Witkowski, Ewa Bryl, and Wojciech Makarewicz. 'The Role of Lactobacillus plantarum 299v in Supporting Treatment of Selected Diseases'. Central-European Journal of Immunology 45 (4 February 2021). https://doi.org/10.5114/ceji.2020.101515.
[3] Naruszewicz, Marek, Marie-Louise Johansson, Danuta Zapolska-Downar, and Hanna Bukowska. 'Effect of Lactobacillus Plantarum 299v on Cardiovascular Disease Risk Factors in Smokers'. The American Journal of Clinical Nutrition 76, no. 6 (1 December 2002): 1249–55. https://doi.org/10.1093/ajcn/76.6.1249.
[4] John, Rinaldo, and Ankit Singla. 'Functional Foods: Components, Health Benefits, Challenges, and Major Projects' 2 (9 June 2021): 61–72. https://doi.org/10.37281/DRCSF/2.1.7.
[5] Siró, István, Emese Kápolna, Beáta Kápolna, and Andrea Lugasi. 'Functional Food. Product Development, Marketing and Consumer Acceptance—A Review'. Appetite 51, no. 3 (1 November 2008): 456–67. https://doi.org/10.1016/j.appet.2008.05.060.

[6] Ghazanfar, Shakira, Ghulam Ali, Rameesha Abid, Arshad Farid, Nahid Batool, Mohammad Okla, Saud Al-Amri, Yasmeen Alwasel, Nosheen Akhtar, and Yasir Hameed. 'An Overview of Functional Food', 2022. https://doi.org/10.5772/intechopen.103978.
[7] Fernandez, Maria Luz. 'Effects of Eggs on Plasma Lipoproteins in Healthy Populations'. Food & Function 1, no. 2 (2 November 2010): 156–60. https://doi.org/10.1039/C0FO00088D.
[8] Kovacs-Nolan, Jennifer, Marshall Phillips, and Yoshinori Mine. 'Advances in the Value of Eggs and Egg Components for Human Health'. Journal of Agricultural and Food Chemistry 53, no. 22 (1 November 2005): 8421–31. https://doi.org/10.1021/jf050964f.
[9] Puglisi, Michael J., and Maria Luz Fernandez. 'The Health Benefits of Egg Protein'. Nutrients 14, no. 14 (January 2022): 2904. https://doi.org/10.3390/nu14142904.
[10] Matsuoka, Ryosuke, and Michihiro Sugano. 'Health Functions of Egg Protein'. Foods (Basel, Switzerland) 11, no. 15 (2 August 2022): 2309. https://doi.org/10.3390/foods11152309.
[11] Martins, E. M. F., Ramos, A. M., Martins, M. L., & Leite Junior, B. R. de C. (2016). Fruit salad as a new vehicle for probiotic bacteria. Food Science and Technology, 36(3), 540–548.
[12] Yoon, Kyung Young, Edward E. Woodams, and Yong D. Hang. (2006): 'Production of Probiotic Cabbage Juice by Lactic Acid Bacteria'. Bioresource Technology 97, no. 12 1427–30. https://doi.org/10.1016/j.biortech.2005.06.018.
[13] Bahrami, Maryam. 'Effect of Lactobacillus Acidophilus on the Physicochemical and Sensory Properties of Aloe Vera', 2019, 6.

PLANT MEDIATED SYNTHESIS METHOD OF COPPER OXIDE NANOPARTICLES

Andrea Rónavári[1], Anita Molnár[1], Judit Papp[1], Zoltán Kónya[1,2]

[1] Department of Applied and Environmental Chemistry, University of Szeged, H-6720, Szeged, Rerrich Béla tér 1, Hungary
[2]MTA, Reaction Kinetics and Surface Chemistry Research Group, H-6720, Szeged, Rerrich Béla tér 1, Hungary
e-mail: ronavari@chem.u-szeged.hu

Abstract
As copper oxide nanoparticles (CuO NP) due to their unique electric, thermal, mechanical, catalytic and magnetic properties, are widely used in various fields such as agricultural, environmental, industrial, and medical. Thus, their large-scale economical production needs to be developed. In the implementation of nanotechnological syntheses, the applications of energy-, time-, and cost-effective synthesis processes by recycling environmentally friendly plant waste material are playing an increasing role. These methods can be easily applied on an industrial scale and are also of great importance in waste recycling. In this regard, the aim of our research was the production of copper oxide nanoparticles using the extracts of several plants (for example green tea, Virginia creeper and coffee arabica). The properties of the obtained particles, such as size and crystal structure, were determined and compared to the chemically synthesized particles. The applicability of different plant extracts during the CuO nanoparticle synthesis were established.

Introduction
Copper oxide nanoparticles utilization has extensively increased in various applications (such as industrial catalyst, gas sensors, electronic materials, biomedicines, environmental remediation) due to their flexible properties, i.e. large surface area to volume ratio [1]. Copper (Cu) is one of eight essential plant micronutrients and is required for many enzymatic activities in plants and for chlorophyll and seed production as well. Due to extensive demand and the widespread utilization of copper-oxide nanoparticles, large-scale and cost-effective nanoparticle syntheses processes are required. However, their large-scale production is hindered by the high costs and the environmentally and legislative issues associated with the conventional production method. Therefore, green methods have emerged, offering sustainable, nature-derived and eco-friendly alternative production ways, thus reducing the ecological footprint of the nanomaterial industry [2].
Among these methods, syntheses using parts of different plants (e.g. leaves, roots, fruits) are noteworthy, as they are simple, cost-, time- and energy-efficient, fast and can even be carried out on an industrial scale [3]. The possible use of plant raw materials in green synthesis definitely makes green synthesis methods competitive with chemical syntheses. Based on environmental aspects, these raw materials should be considered, primarily in connection with waste management and waste recycling.
Related to this, the subject of these work was to synthesize copper-oxide nanoparticles, using different plant materials, mainly from plant waste and to optimize the steps of these syntheses, and then to determine the resulting physical and chemical properties.

Experimental

CuO nanoparticles were produced by a precipitation method [4]. First, the copper salt (copper nitrate ($Cu(NO_3)_2 \times 3H_2O$), copper chloride ($CuCl_2 \times 2H_2O$) or copper sulfate ($CuSO_4$) precursor was dissolved in 100 mL deionized water to form 0.2 M concentration. 25% ammonia solution was slowly dropped under vigorous stirring until pH reached to 12. The resulting black precipitate was washed by deionized water, and was dried at 60 °C for overnight to remove any remaining solvent, then was calcined at 450 °C for 2 h using a tube furnace in air. The obtained sample was ground and kept in room temperature until further use.

A similar process was employed for the green synthesis, except that instead of ammonia solution green tea (GT), Virginia creeper (VC) and coffee arabica (CA) extracts were used. The leaf extracts were prepared by heating the corresponding dry leaves in 100 mL deionized water at 80 °C for 20 minutes, thereafter the extracts were vacuum-filtered, and this filtrate was further used as a reducing agent and also as a stabilizer of the as-synthesized CuO NPs [5]. GT-CuO, VC-CuO and CA-CuO labelled "green" CuO materials were synthesized by adding the corresponding extracts to 0.2 M aqueous copper solution in a 1:1 volume ratio at room temperature and constantly stirring for 24 hours.

The morphological characteristics of the as-synthesized CuO NPs were analyzed by transmission electron microscopy (TEM) using a FEI Tecnai G2 20× microscope at an acceleration voltage of 200 kV. The crystal structure and phase of nanoparticles were verified by X-ray powder diffraction (XRD). The scans were performed with a Rigaku MiniFlex II powder diffractometer using Cu Kα radiation. A scanning rate of 2° min^{-1} in the 10°–80° 2θ range was used.

Results and discussion

In the first experimental part, we investigated the effect of use of different initial copper salts on the properties of the particles. Three different initial salt were used during the syntheses, such as copper chloride, copper nitrate and copper sulfate. XRD measurements were applied to identify the crystal structure and the chemical composition of the synthesized nanoparticles (Figure 1).

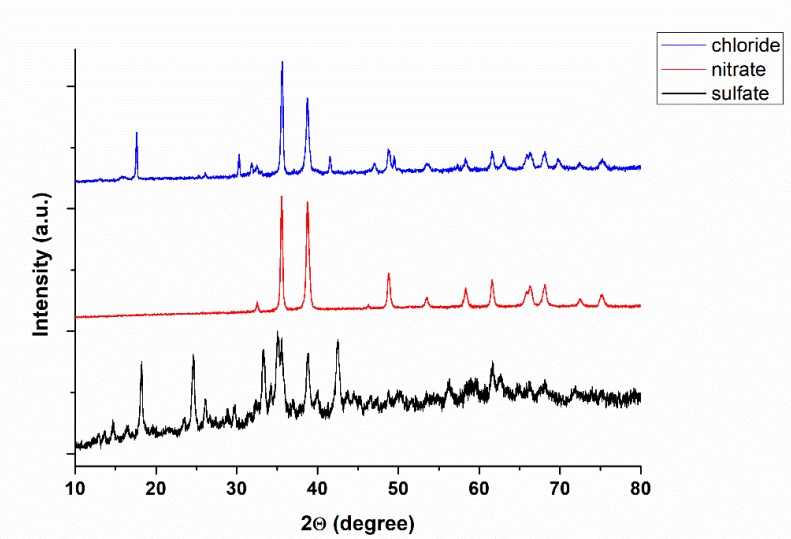

Figure 1. XRD profile of the chemically synthesized CuO nanoparticles. Three different initial salt were used during the synthesis of nanoparticles, such as copper chloride, copper nitrate and copper sulfate.

The characteristic peaks located at 2θ = 32.53°, 35.52°, 38.87°, 48.74°, 61,53° and 68.24° are assigned to (110), (002), (200), (-202), (-113) and (220) plane orientation of monoclinic structure of CuO (JCPDS 892531). As a result, according to these measurements, all copper sources were suitable for the production of CuO NPs. As can be clearly seen in Figure 1, all the obtained samples have the characteristic reflections of CuO NPs, however only the copper nitrate mediated synthesis resulted in pure CuO NPs. According to the TEM measurements, the average size of these particles proved to be around 48.6±9.2 nm. Based on these observations, copper nitrate was used in the plant assisted syntheses and this CuO NP was labelled as "standard".

The effect of the use of different plant extracts during the synthesis of particles was also examined. Green tea, Virginia creeper and coffee arabica extracts were applied during the syntheses. XRD studies were performed to confirm the crystalline structure of the synthesized nanoparticles. The XRD pattern (Figure 2A) of conventional and VC synthesized CuO NPs showed the intense characteristic reflections of monoclinic CuO (JCPDS 892531). However, the GT and CA mediated syntheses were not successful.
Based on these, it is proved that not all plant materials could be involved in the production of CuO particles, only VC-CuO synthesis was suitable.

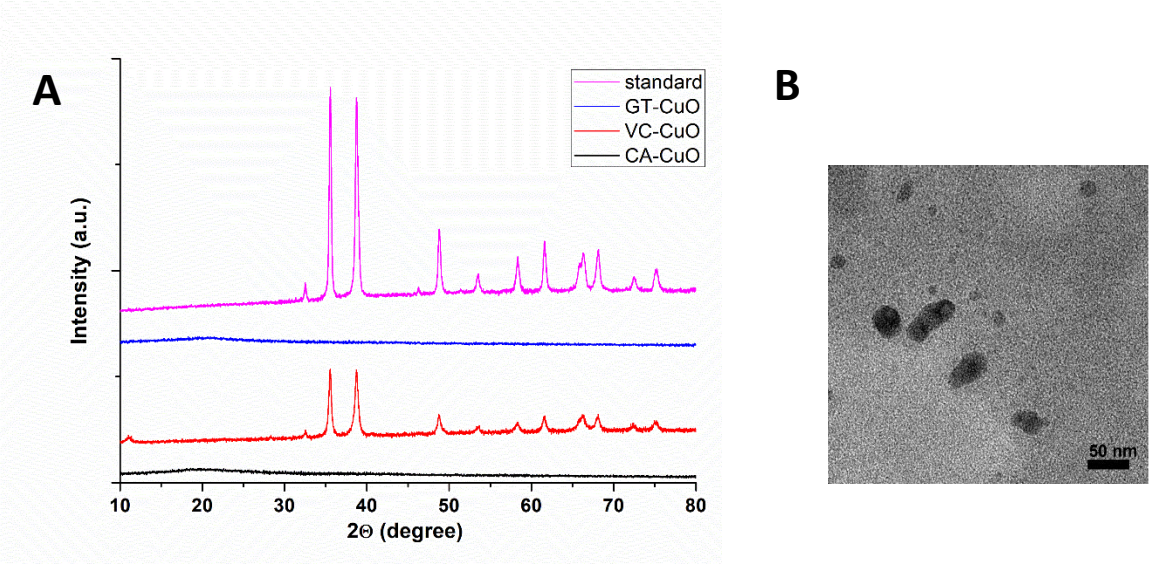

Figure 2. XRD profile of chemically and green synthesized copper oxide nanoparticles (A). Characteristic TEM image of the VC-CuO nanoparticles (B).

According to TEM images, the average size of this VC-CuO sample was around 28±11.2 nm, and polydispersity was observed as in case of the chemical sample. However, these VC-CuO particles were trapped in the matrix of the residual VC extract. Based on what we observed in our previous work [6, 7], this matrix (biomolecular corona) can greatly define the physical, chemical, and biological characteristics of the obtained nanomaterial, therefore further thorough examination should be carried out before their utilization.

Conclusion

We investigated the applicability of green tea, Virginia creeper and coffee arabica extracts during the synthesis procedure of CuO nanoparticles. We successfully carried out the synthesis of CuO nanoparticles with using VC extract. The properties of the obtained nanoparticles were similar to the conventional chemically synthesized nanoparticles. At the same time, we also

drew attention to the fact that the particles produced with VC plant extract contained the remaining plant matrix, which may affect their behavior and activity during their utilization.

Acknowledgements
This work was supported by the János Bolyai Research Scholarship of the Hungarian Academy of Sciences No. BO/00384/21/7 (Andrea Rónavári) and by the grant of the New National Excellence Program of the Ministry for Innovation and Technology No. ÚNKP-22-5-SZTE-583 (Andrea Rónavári).

References
[1] K.L. Medard, H. Hamilton, S.C. van der Moore, J. Chem. Anal. 313 (2007) 163.
S. Naz, A. Gul, M. Zia, IET Nanobiotechnol 14 (2020) 1-13.
[2] M.K. Nazri, N. Sapawe, Mater. Today: Proc. 31 (2020) A38-A41.
[3] S.A. Akintelu, F.A. Folorunso, A.K. Oyebamiji, Heliyon 6 (2020) e04508.
[4] K. Phiwdang, S. Suphankij, W. Mekprasart, W. Pecharapa, W., Energy procedia 34 (2013) 740-745.
[5] G. Kozma, A. Rónavári, Z. Kónya, A. Kukovecz, ACS Sustain. Chem. Eng. 4 (2016) 291-297.
[6] P. Bélteky, A. Rónavári, N. Igaz, B. Szerencsés, I.Y. Tóth, I. Pfeiffer, M.Kiricsi, Z. Kónya, Int J Nanomedicine 14 (2019) 667.
[7] A. Rónavári, D. Kovács, N. Igaz, C. Vágvölgyi, I.M. Boros, Z. Kónya, Z. I.Pfeiffer, M. Kiricsi, Int J Nanomedicine 12 (2017) 871.

DETERMINATION OF ELECTRONIC PROPERTIES OF TRIAZINE DERIVATIVES BY HARTREE-FOCK METHOD AND ESTIMATION OF THEIR INFLUENCE ON RETENTION BEHAVIOR IN RP-UHPLC SYSTEM

Benjamin Salaković[1], Strahinja Kovačević[1], Milica Karadžić Banjac[1], Jasmina Anojčić[2], Lidija Jevrić[1], Sanja Podunavac-Kuzmanović[1]

[1]University of Novi Sad, Faculty of Technology Novi Sad, Department of Applied and Engineering Chemistry, Bulevar cara Lazara 1, 21000 Novi Sad, Serbia
[2]University of Novi Sad, Faculty of Sciences, Department of Chemistry, Biochemistry and Environmental Protection, Trg Dositeja Obradovića 3, 21000 Novi Sad, Serbia
e-mail: benjamin.salakovic@uns.ac.rs

Abstract
In this study, electronic properties of a series of *s*-triazine derivatives with acyclic and cyclic substituents were calculated by using Gaussian 16 software [1]. The Hartree-Fock method and 6-31G basis set were applied. The calculated electronic properties were the energy of Highest Occupied Molecular Orbital (HOMO), the energy of Lowest Unoccupied Molecular Orbital (LUMO) and the energy of optimal structure for each molecule. According to the HOMO energy, the compounds with acyclic and cyclic were clearly separated. Namely, compounds with cyclic substituents had higher values of HOMO energies than the compounds with acyclic substituents. Based on the LUMO energies, the compounds were not separated since the LUMO orbitals are only on the triazine ring and are energetically similar. The electronic properties were correlated with the retention parameters ($\log k_0$, $\log k$, S and C_0) of the studied compounds. The retention parameters were determined by using revered-phase ultra-high performance liquid chromatography (RP-UHPLC) with C_{18} stationary phase and mobile phase as a mixture of methanol and water [2]. The volume fraction of methanol in the mobile phase varied from 50 to 85 (v/v). The outstanding linear correlations between certain retention parameters and electronic properties were obtained, so the retention mechanism in the applied chromatographic system could be explained.

Acknowledgements
The present research is financed in the framework of the project of Provincial Secretariat for Higher Education and Scientific Research of AP Vojvodina (Project: Molecular engineering and chemometric tools: Towards safer and greener future, No. 142-451-2563/2021-01/01).

References
[1] https://gaussian.com
[2] B. Salaković, S. Kovačević, M. Karadžić Banjac, J. Anojčić, L. Jevrić, S. Podunavac-Kuzmanović, S. Gadžurić, D. Antonović, 27th International Symposium on Analytical and Environmental Problems, Proceedings (2021) 297.

SCREENING AND SEQUENCING OF SIALYLATED GLYCOSPHINGOLIPIDS IN HUMAN GLIOBLASTOMA BY ION MOBILITY MASS SPECTROMETRY

Mirela Sarbu[1], David E. Clemmer[2], Željka Vukelić[3], Alina D. Zamfir[1,4]

[1]Department of Condensed Matter, National Institute for Research and Development in Electrochemistry and Condensed Matter, 300224 Timisoara, Romania
[2]Department of Chemistry, The College of Arts & Science, Indiana University, IN 47405-7102, Bloomington, Indiana, USA
[3]Department of Chemistry and Biochemistry, Faculty of Medicine, University of Zagreb, 10000, Croatia
[4]Department of Technical and Natural Sciences, "Aurel Vlaicu" University of Arad, 310130, Arad, Romania
e-mail: mirela.sarbu86@yahoo.co.uk

Abstract
High performance ion mobility separation mass spectrometry (IMS MS) was thoroughly optimized to allow the discovery of glioblastoma multiforme (GBM)-specific structures and the assessment of their roles as tumor markers or possible associated antigens. Ganglioside (GG) separation by IMS according to the charge state, carbohydrate chain length, degree of sialylation and ceramide composition, led to the identification of no less than 160 distinct components [1], which represents 3 folds the number of structures identified before. The detected GGs and asialo-GGs were found characterized by a high heterogeneity in their ceramide and glycan compositions, encompassing up five Neu5Ac residues. The tumor was found dominated in equal and high proportions by GD3 and GT1 forms, with a particular incidence of C24:1 fatty acids in the ceramide.

Introduction
GBM, the most widespread primary brain tumor in adults, accounts for 45.2% of malignant primary brain and central nervous system tumors. With a rapid infiltration rate into the nearby tissue, GBM has drawn a significant attention because of its poor prognosis and the limited treatment options available. In GBM, nearly all tumor cells exhibit aberrant cell-surface glycosylation patterns due to the alteration of their biosynthesis or post-synthesis modification process. Hence, the research nowadays is focused on the determination of the molecular mechanisms related to GBM tumor invasion and the discovery of innovative approaches for invasiveness suppression. Since GGs are tumor-associated antigens, we have introduced here IMS MS for the discovery of GBM-specific structures.

Experimental
GGs were extracted from a brain tumor localized in the frontotemporal cortex of the right hemisphere in a male patient, age 47. Following the surgical removal of the tumor, the histopathological analysis has shown that the tumor is GBM, grade IV. The extracted GGs were dissolved in methanol to the concentration of 5 pmol/mL and infused into a Synapt G2S instrument. The signal was acquired for two minutes in the negative ion mode at 1.5kV ESI voltage and 45 V cone voltage respectively. To enhance the separation, IMS wave velocity was set at 650 m/s and IMS wave height at 40 V. MS/MS was performed by collision-induced dissociation (CID) after mobility separation in the transfer cell, using energies between 40-65eV.

Results and discussion

The 2D data set of GBM GGs revealed the GG separation into mobility families based on their charge state, carbohydrate chain length, and the degree of sialylation. IMS MS offered a reliable separation, given the detection and identification in GBM of 215 ions, corresponding to no less than 160 distinct glycoforms, more than triple the number of GGs previously discriminated in GBM with no separation prior to MS. The inspection of the data has shown that GD3 species predominate in GBM, with 36% of the total number of discovered GGs. Moreover, this study has demonstrated that, in addition to GD3, GT1 species are also associated with GBM. Correlated with previous findings, these results, documenting for the first time such a high expression of GD3 and GT1 species in GBM, have a particular biological significance. The expression of GD3 fraction, actually a minor constituent of adult brain, however, with a crucial role in brain development, is markedly increased in a variety of malignant cancers, being directly connected with tumor cell proliferation, invasion and implicitly with the degree of malignancy. Moreover, in view of our present findings and the earlier connection of GT1 with highly proliferative primary and secondary brain tumors, the elevated incidence of GT1 species found here in GBM support the biomarker role of GT1 as well, along with GD3 glycoforms. The incidence of unsaturated fatty acids residues, such as C24:1 as well as of fatty acids with odd number of carbon atoms, *i.e.* C17, C19 is another characteristic pattern of GGs in glioma tumors. By the occurrence of only one mobility feature and the diagnostic fragment ions, the IMS tandem MS conducted using collision-induced dissociation (CID) disclosed for the first time the presence of GT1c(d18:1/24:1) newly proposed here as a potential GBM marker.

Conclusion

The goal of this study was the application of IMS MS to identify the ganglioside pattern uniquely developed in GBM, the most aggressive brain tumor, with the poorest prognosis among all brain cancers. IMS in combination with highly sensitive (-) nanoESI and tandem MS by CID, provided an exhaustive structural and compositional investigation of GBM gangliosides due to the advantages of the platform. The major outcome of this study is that, by IMS MS and CID MS/MS various novel species could be identified and added to the currently existing panel of glioblastoma tissue-associated structures, since the number of the GGs identified here is three times higher than ever discovered in this tumor type.

Acknowledgements

This work was supported by the Romanian National Authority for Scientific Research, UEFISCDI, through projects PN-III-P4-ID-PCE-2020-0209 granted to A.D.Z. and PN-III-P1-1.1-PD-2019-0226 granted to M.S.

References

[1] M. Sarbu, L. Petrica, D.E. Clemmer, Ž. Vukelić, A.D. Zamfir, J.A.S.M.S. 32, (2021) 1249-1257.

THE INFLUENCE OF TEMPERATURE ON THE PHYSICO-CHEMICAL PROPERTIES OF PEROVSKITE MATERIALS WITH A HEXAGONAL STRUCTURE

Paula Sfirloaga, Maria Poienar, Ionel Balcu, Corina Macarie, Paulina Vlazan

National Institute for Research and Development in Electrochemistry and Condensed Matter, str. Dr. A. Paunescu Podeanu 144, 300569 Timisoara Romania
e-mail: paulasfirloaga@gmail.com

Abstract

The rare-earth manganite, yttrium manganese oxide ($YMnO_3$) is a multiferroic material possessing ferroelectricity and magnetism properties simultaneously, which attracted much research interest from the past two decades. $YMnO_3$ exists in three phases; such as amorphous, hexagonal phase and an orthorhombic phase (Pbnm space group) whose chemical compositions are identical [1]. Hexagonal $YMnO_3$ with P63cm space group is one of the most intensively studied materials [2].

In this paper, a comparative study between perovskites materials obtained through sol-gel method, followed by thermal treatment at different temperature was performed. The obtained materials were studied morpho-structural by X-ray diffraction (XRD), Fourier-transform infrared spectroscopy (FT-IR), specific surface (BET), scanning electron microscopy (SEM) and semi-quantitative analysis (EDX). The physico-chemical properties of perovskites materials obtained through sol-gel method have been analyzed with the aim of studying the relationships between structure and properties in this class of materials the influence of the thermal treatment on the induced properties.

X-ray diffraction analysis revealed the formation at 800 and 1000°C of single-phase compounds with the average crystals size between 27-29 nm, crystallized in the hexagonal structure with P63cm space group. From the morphological analysis of the surface, it can be seen that the particles are spherical and very agglomerated, and the quantitative analysis showed that the obtained materials are pure, only the elements O, Mn, Y being present. Moreover, from the quantification of the elements, it can be observed that the stoichiometry of the ABO_3 compound has been preserved.

Acknowledgements

This work was supported by theExperimental Demonstrative Project 683PED / 2022. The authors thank C. Ianasi for help during the materials characterization.

References

[1] I. Iliescu, M. Boudard, L. Rapenne, O. Chaix-Pluchery, H. Roussel, Appl. Surf. Sci. 306 (2014) 27–32.

[2] O. Nirmala, P. Sreedhara Reddy, V. Diwakar Reddy, Mater. Today: Proc. 23 (2020) 490-494.

A COMPARISON OF CADMIUM CONTENT IN WATER SAMPLES WITH TWO METHODS

Marjana Simonič

University of Maribor, Faculty of Chemistry and Chemical Engineering, 2000 Maribor, Smetanova 17, Slovenia
e-mail: marjana.simonic@um.si

Abstract
Cadmium (Cd) is a natural element found in soils and rocks. It is used in the metal industry, plastics, ceramics, and in the manufacture of batteries. Due to leaching, it could be found in drinking water sources. Cadmium is toxic to humans. Thus, the aim of the research was to determine Cd in real water samples. A comparison was made between the methods of inductively coupled plasma mass spectrometry ICP-MS and graphite furnace atomic absorption spectroscopy (GF-AAS). The measurement uncertainty was determined. We have developed a useful method for trace analysis of Cd in waters in the microgram per litre range.

Introduction

Cd is very toxic to humans. [1]. Occupational or environmental cadmium exposure can lead to a variety of adverse health effects. It attacks kidneys in such a manner that causes the formation of kidney stones or even renal failure. The stone formation could further lead to osteoporosis and skeleton damage.
About 5100 tons of sewage sludge are discharged into the sea every day [2], and this sludge contains toxic metals, such as Cd. Due to Cd pollution, several pathologies are observable in the area surrounding the source of pollution. Various analytical methods such as electrochemical methods and inductively coupled plasma mass spectrometers have been used for the determination of Cd. On the other hand, the application of graphite furnace (also known as electrothermal) atomic absorption spectrometry GFAAS is rather rare [3]. Some interferences are divided into physical, chemical, and spectral. Physical could be eliminated by careful use of standard solutions. Chemical interferences are caused by the volatility of the samples.
A method is proposed for the simultaneous determination of Cd and Pb in medicinal plants by direct mud sampling through GF-AAS [4]. The analytical performance in Thermo-Spray Flame Furnace Atomic Absorption Spectrometry (TS-FFAAS) by using different systems of sample injection was studied [5]. Comparison of the results obtained by the proposed technique with other validated methods showed good agreement.
The main objective of the work reported here was to determine the Cd concentrations in the selected water samples. A comparison was made between the two methods of of inductively coupled plasma mass spectrometry (ICP-MS) and graphite furnace atomic absorption spectroscopy (GF-AAS).

Experimental

Samples
Public pipe water (Maribor, Slovenia) was analyzed as a real water sample (denoted VT, VH, VG, VM). Next sample was rainwater (denoted DD) and bottled water (denoted Z). Samples were quantified in triplicates, and recovery data were calculated.

Calibration curve preparation
Certified reference material CRM12-3-10, SPS-WW1 was used.

Working standard solutions were prepared daily by diluting the stock solution with Milli-Q water in the range from 0.5 ug/L to 3 ug/L in 10 mL glass flasks. The GTAAS method was applied on Varian SpectrAA DUO AA 240Z GTA 120 Spectrometer in comparison with ICP-MS analyses (Figure 1). Graphite tube atomizer was used and programmable heated up to the atomization temperature. The photomultiplier tube served as a detector. The measurements were performed at 228 nm.

Figure 1. GTAAS (left) and ICP-MS

Results and discussion

Water sample analysis

Recoveries in the ranges from 90 % to 115 % for GF-AAS and from 95 to105 % with ICP-MS were confirmed.

Calibration curve

Calibration curve is presented in Figure 2. The correlation coefficient R^2 values were greater than 0.999, and the quality coefficient was 2.14 %. The linearity was confirmed. Reproducibility was confirmed with *RSD* lower than 5 % as can be seen from Table 1. The limit of detection and the limit of quantification were determined at 0.47 µg/L. and 0.49 µg/L, respectively.

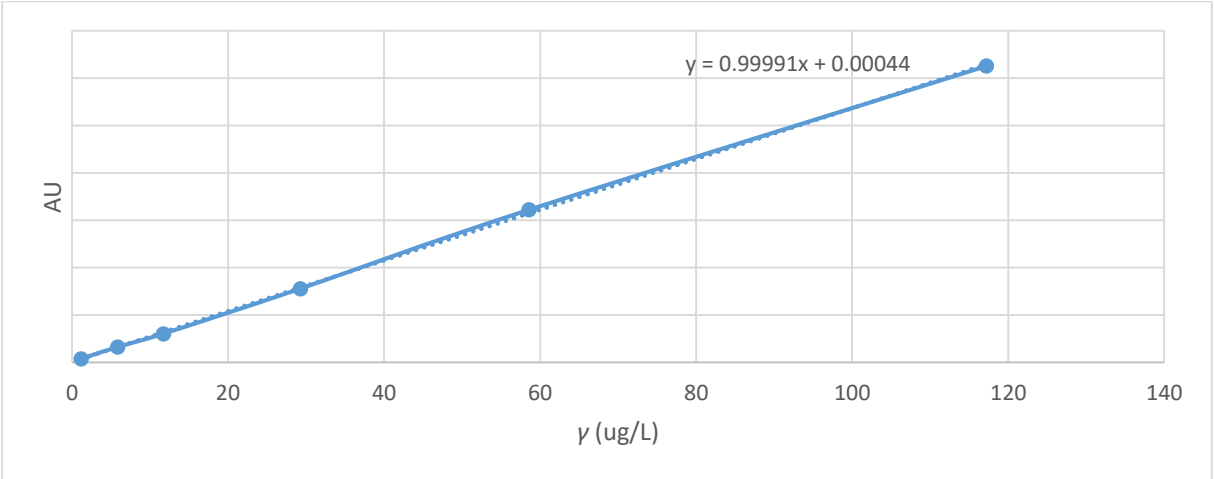

Figure 2. The calibration curve for Cd in the concentration range from 0.5 µg/L to 100 µg/L

The matrix effect was detected by t-tests. It is seen that in column 3 and 4 t exceed *t*(tab), therefore there is a matrix effect with GF-AAS method.

Table 1. Matrix effect study

	Blank	*Blank+drinking water*	*Drinking water*
intercept	0.001	0.061	0.046
slope	1.001	0.847	0.843
t	0.076	9.096	11.328
t(tab)	2.776		

Rh was used as an internal standard in ICP-MS. There was no matrix effect detected. Recoveries in the ranges from 90 % to 115 % for GF-AAS and from 96 to 104 % with ICP-MS were confirmed (Figure 3).
To evaluate reproducibility, 3 replicates were prepared for each concentration, and these were used to measure the recovery of Cd in the solution.

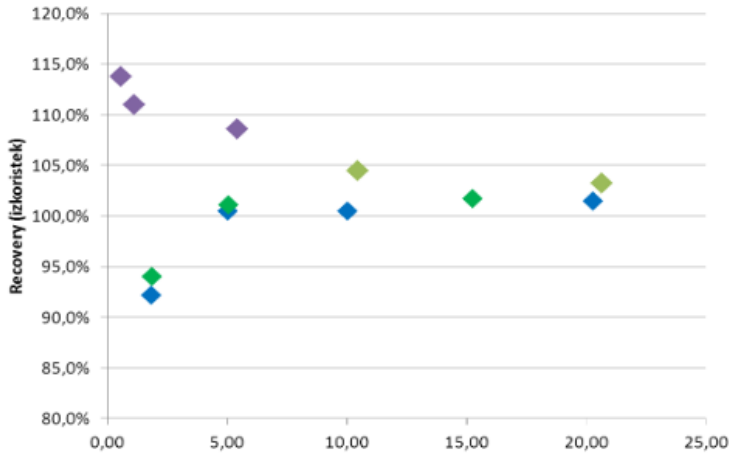

Figure 3. GF-AAS recoveries

RSD pooled was below the reported 5.3 % for Cd [3]. As seen from Table 2, *RSD* values for both methods were lower.

Table 2. *RSD* values for both methods

γ [mg/L]	*RSD* (%) GF-AAS	*RSD* (%) ICP-MS
0.5	1.82	0.82
5	1.35	0.35
10	2.51	0.31
15	1.28	0.28
20	1.23	0.23
RSD pooled	1.95	0.45

Reproducibility
Table 3 represents the reproducibility of the samples. The HORRAT and Grubbs tests were performed for GF-AAS. The outliers were not found.

Table 3. The HORRAT and Grubbs test's results

Sample	*HORRAT Max 2*	*Grubbs Max.1.887*	
		Min	*Max*
DD3	0.05	1.347	1.711
DD4	0.07	0.809	1.736
DD12	0.04	0.935	1.870
DD14	0.12	1.510	1.175
VCC	0.07	1.225	1.471

The obtained values for reproducibility were much lower using ICP-MS.

Conclusions

The aim of this study was to determine the concentration of Cd in water samples using GF-AAS in comparison with ICP-MS. The method conditions were verified by determination of matrix effect, linearity, precision, accuracy, and LOD. The standard addition method was used and based on the slopes with the t-test it was determined that the matrix affects the measurements. The linearity of the method was confirmed with the correlation coefficients greater than 0.999 from 0.5 to 3.0 µg/L. The recoveries ranged from 90 to 115 %, which was satisfactory. The low RSD (≤ 1.9 %) clearly indicates the reproducibility and the successful application of the developed GF-AAS method for the quantitative measurement of Cd in various real water samples.

Acknowledgements

The author would like to thank funder the Slovenian Research Agency and Support of Research and Development Programme P2-0414.

References

[1] B. Pan, Y. Cai, B. Liu, K. Cai, W. Lv, J. Tian, W. Wang, J. Environ. Manage. 302, Part A (2022) 114039.
[2] M. Melila, R. Rajaram, A. Ganeskumar, M. Kpemissi, T. Pakoussi, S. Agbere, J. M. Lazar, G. Lazar, K. Amouzou, B. A. Paray, A. Gulnaz, J. Trace Elem. Med. Biol. 69 (2022) 126890.
[3] S. Murko, R. Milačič, M. Veber, J. Ščančar, J. Serb. Chem. Soc. 75(1) (2010) 113-128.
[4] F. M. Fortunato, A.G. Neto, J. Anchieta, G. P. G. Freschi, At. Spectrosc. 3384 (2012) 138-142.
[5] G. Carrone, E. Morzan, R. Candal, M. Tudino, Microchem. Part A 160 (2021) 105608.

CONNECTION BETWEEN ROAD DENSITY AND LANDSCAPE FRAGMENTATION IN HUNGARY USING KERNEL DENSITY BASED ON GIS METHODS

Seyedehmehrmanzar Sohrab, Péter Szilassi, Boudewijn van Leeuwen

[1]*Department of Geoinformatics, Physical and Environmental Geography, University of Szeged, Egyetem u. 2-6, H-6722 Szeged, Hungary*
e-mail: mehrmanzar_sohrab@geo.u-szeged.hu

Abstract
Humans have recently caused significant landscape fragmentation by developing transportation infrastructure. We used Kernel density estimation (KDE) to analyze the road density distribution in Hungary, and then we assessed landscape fragmentation after imposing the road density onto the land-use map of Hungary, using Mean Patch Area, Patch Density, and Number of Patches as three important landscape metrics. Our analysis shows that roads, as expected, are mainly located in artificial lands (58.15%) and farmland (28.16%) landscapes. PD and NP increased by 69.59% and 69.51%, respectively, at the landscape scale, while AREA MN decreased by 41%. It has been proved by Spearman's rank correlation coefficient analysis which showed that the road density showed a positive correlation with PD and NP and a negative correlation with AREA_MN. This means that the higher the road density, the higher the PD and NP values, and the smaller the patch area. Furthermore, landscape fragmentation is positively related to road density, and as the road system became denser, the landscape became more fragmented. Understanding the effects of road networks on various land uses can aid in the development of sustainable road systems in Hungary.

Introduction
Landscape fragmentation is one of the consequences of increased socioeconomic pressures that many parts of the world are experiencing today [1]. However, little research has been devoted to landscape fragmentation in Hungary. Roads are considered a major environmental problem and one of the main causes of biodiversity loss and landscape fragmentation [2]. The development and presence of roads can reduce landscape permeability, leading to habitat loss, and increasing habitat fragmentation [3]. Road density (i.e., km/km^2) is a useful index of the road network in a landscape and has been linked to several ecological effects of roads [4]. The combination of road density analysis and landscape metrics may aid in predicting road ecological impacts at landscape scale [5]. In this article we first assessed the spatial structure of the road network in Hungary then we analyzed the landscape fragmentation related to the road network at landscape level based on Mean Patch Area (AREA_MN), Patch Density (PD), and Number of Patches (NP) metrics. Finally, we investigated the connection between road density and the landscape metrics in Hungary.

Experimental
We downloaded the road network dataset for Hungary from GEOFABRIK [6], which has data extracts from the Open Street Map project (OSM) which are normally updated every day. We also we downloaded Corine Land Cover 2018 published by Copernicus Land Monitoring Service with 10000 m^2 resolution. In the first step, we reclassified the road network map into 5 main classes: motorway, primary, secondary, links, and residential (figure 1). The road density map was created and visualized in Arc Map 10.6.1 and in ArcGIS Pro was the KDE function was used to calculate the density of features in a neighborhood around those features using a

distance-based filter. The distribution of the Kernel density of the road system is estimated with the KDE function based on a 10,000 m^2 grid size applied to reflect the spatial structure of the road network in the urban area of Hungary. The CORINE land use map was then reclassified into 13 classes by aggregating similar classes together (figure 2).

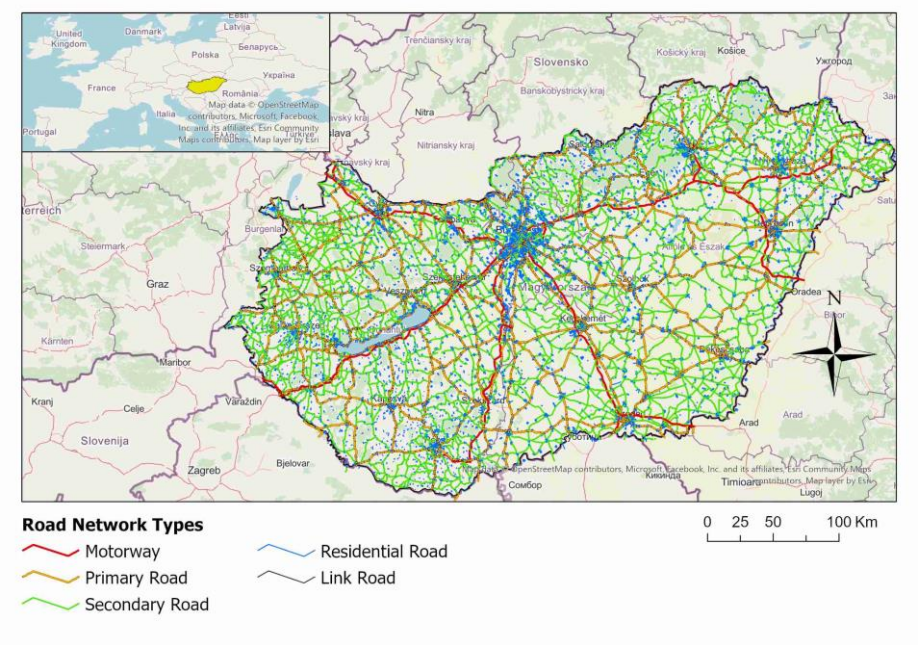

Figure 1. Reclassified road network map of Hungary.

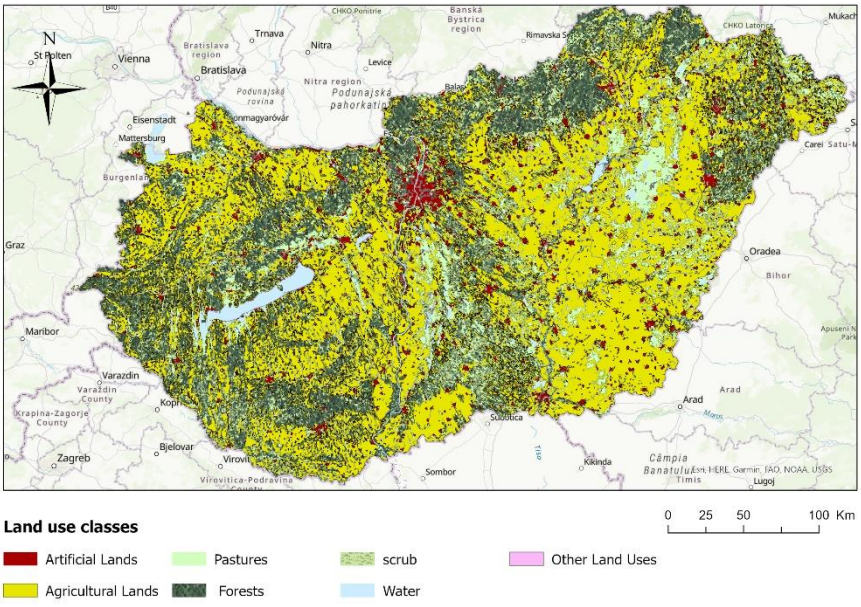

Figure 2. Reclassified CORINE 2018 land use map of Hungary.

In the following step, we calculated three landscape metrics using Fragstats software version 4: PD, AREA MN, and NP before and after superimposing roads within each land use class. The ratio of the three metric changes was used to quantify the degree of landscape fragmentation caused by roads. The metrics were selected because of their ability to describe the state of the landscape fragmentation [8]. The results of the ratio calculation based on the afore mentioned metrics were compared to earlier studies [2], [5], [9]–[11]. In addition, we used Spearman's

rank correlation coefficient in IMB SPSS Statistics software version 28.0.0 to investigate the relationship between road density and landscape metrics. The flowchart of our analysis is shown in figure 3.

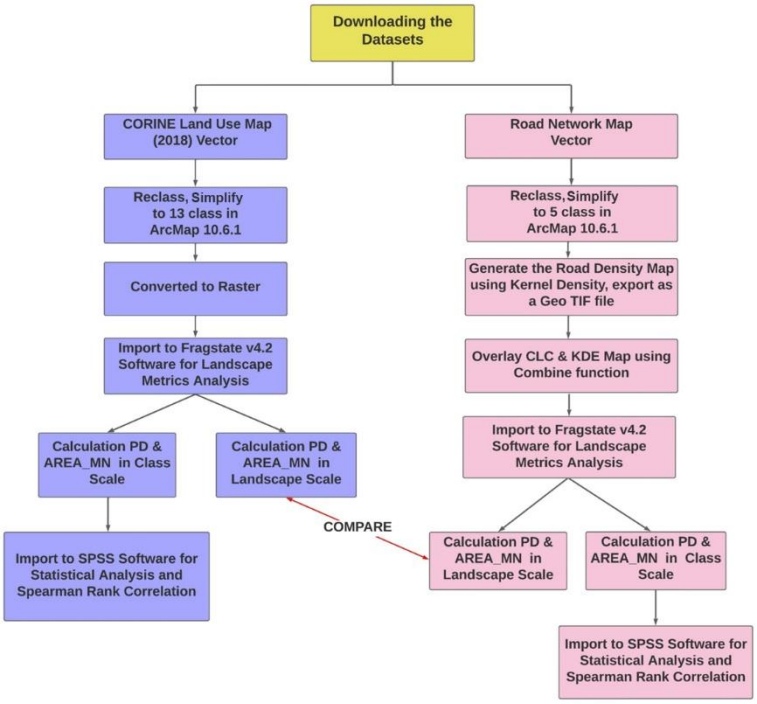

Figure 3. Flowchart of the analyzing process

Results and discussion

According to the KDE map, roads were generally concentrated in areas with a high density of residential roads close to urban areas (Budapest, Debrecen, Miskolc, Pecs, Szeged, Kecskemet, Gyor) (figure 4).

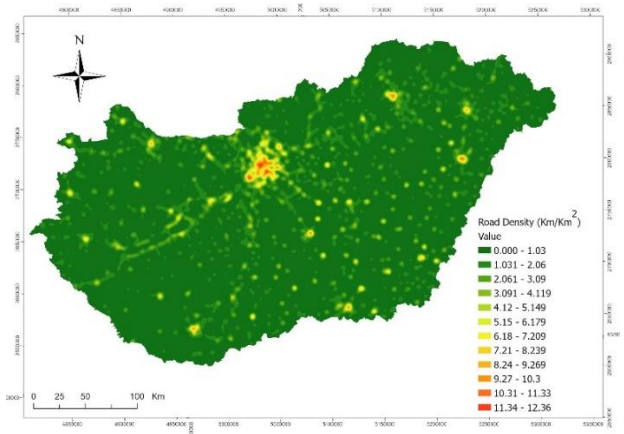

Figure 4. Road density map of Hungary.

According to our land use analysis results based on the CORINE land use map of 2018, agricultural lands cover more than half of Hungary. The outcomes are displayed on figure 5. As expected, our findings show that the majority of roads are distributed in artificial lands, with agricultural land coming in second. As a result, roads tend to cluster in artificial lands. This result is comparable to [5]. Roads are also spread throughout farmlands because farming is impossible without roads (figure 6).

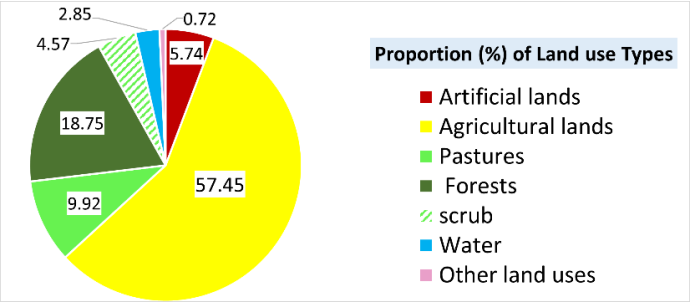

Figure 5. The proportion of main land use types in Hungary based on CORINE landcover 2018.

After imposing the road system onto the land use map, PD and NP increased at the landscape scale while AREA MN decreased (table1). Landscape fragmentation was defined as the process of decreasing AREA MN while increasing PD and NP. As a result, we can conclude that the higher the road density, the higher the PD and NP but the smaller the patch areas. It has also been confirmed by [11].

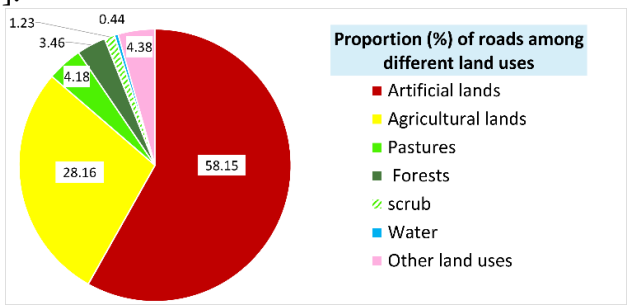

Figure 6. Proportion of roads among different land uses in Hungary. 100% is equal to total length of roads in Hungary.

Furthermore, Spearman's rank correlation coefficient revealed a positive relationship between landscape fragmentation and road density. When the road system became denser, the landscape became more fragmented (table 2). This suggests that road density has a significant positive relationship with landscape fragmentation, which is consistent with previous research [2], [5], [12] However, this is in contrast to a previous study conducted in the United States. [13].

Table 1: Values of landscape metrics before and after imposing roads in landscape scale

Description	**NP**	**PD (NP/Km^2)**	**AREA_MN (ha)**
Before imposing the Road density map	28185	0.3029	330.1483
After imposing the Road density map	47778	0.5137	194.655
Change	19593	0.2108	-135.4933
change%	**69.51**	**69.59**	**-41.04**

Table 2: Results of Spearman's rank correlation coefficient between RD and landscape fragmentation in Hungary. ** Correlation is significant at the 0.01 level (2-tailed).

		NP	PD	AREA_MN
RD_Mean	Correlation Coefficient	**0.549****	**0.547****	**-0.357****
	Number of pairs	80	80	80

Conclusion

The results showed that road kernel densities were generally concentrated in areas with a high density of residential roads close to urban areas. The density of roads varies depending on the type of land cover. More than half of all roads are concentrated in artificial lands, and 90% of all artificial lands are covered by roads. However, fragmentation analysis revealed a strong positive correlation between landscape metrics PD and NP and road density, while we discovered a negative correlation between AREA MN and road density, implying that the higher the road density, the greater the PD and NP but the smaller the patch areas. As a result, we concluded that the landscape becomes more fragmented as the road network becomes denser around urban areas.

References

[1] P. Ileana *et al.*, "Landscape and Urban Planning Landscape fragmentation in Romania ' s Southern Carpathians : Testing a European assessment with local data," vol. 143, pp. 1–8, 2015, doi: 10.1016/j.landurbplan.2015.06.002.

[2] Y. Kaynaklanan, P. Parçalanmasının, and P. Planlama, "Assessment of Road-Induced Landscape Fragmentation and Implications for Landscape Planning : the case of İzmir Province," vol. 9, pp. 699–709, 2019, doi: 10.17714/gumusfenbil.544540.

[3] V. J. Bennett, "Effects of Road Density and Pattern on the Conservation of Species and Biodiversity," *Curr. Landsc. Ecol. Reports*, vol. 2, no. 1, pp. 1–11, 2017, doi: 10.1007/s40823-017-0020-6.

[4] P. Csorba, "Landscape ecological fragmentation," *Stud. Univ. Vasile Goldis Arad, Ser. Stiint. Vietii*, vol. 21, no. 2, pp. 429–436, 2011.

[5] X. Cai, Z. Wu, and J. Cheng, "Using kernel density estimation to assess the spatial pattern of road density and its impact on landscape fragmentation," *Int. J. Geogr. Inf. Sci.*, vol. 27, no. 2, pp. 222–230, 2013, doi: 10.1080/13658816.2012.6639

[6] "Geofabrik," 2022. https://download.geofabrik.de/europe.html.

[7] K. McGarigal and B. J. Marks, "FRAGSTATS: spatial pattern analysis program for quantifying landscape structure," *Gen. Tech. Rep. - US Dep. Agric. For. Serv.*, no. PNW-GTR-351, 1995.

[8] E. Uuemaa, M. Antrop, J. Roosaare, R. Marja, and Ü. Mander, "Landscape metrics and indices: An overview of their use in landscape research," *Living Rev. Landsc. Res.*, vol. 3, no. January 2014, 2009, doi: 10.12942/lrlr-2009-1.

[9] D. Geneletti, "Using spatial indicators and value functions to assess ecosystem fragmentation caused by linear infrastructures," *Int. J. Appl. Earth Obs. Geoinf.*, vol. 5, no. 1, pp. 1–15, 2004, doi: 10.1016/j.jag.2003.08.004.

[10] S. C. Saunders, M. R. Mislivets, J. Chen, and D. T. Cleland, "Effects of roads on landscape structure within nested ecological units of the Northern Great Lakes Region, USA," *Biol. Conserv.*, vol. 103, no. 2, pp. 209–225, 2002, doi: 10.1016/S0006-3207(01)00130-6.

[11] X. Chang, X. Huang, X. Jiang, and R. Xiao, "Impacts of Transportation Networks on the Landscape Patterns — A Case Study of Shanghai," pp. 1–13, 2022.

[12] Y. Miao, T. Dai, X. Yang, and J. Song, "Geography and Sustainability Landscape fragmentation associated with the Qingzang Highway and its influencing factors — A comparison study on road sections and buffers," *Geogr. Sustain.*, vol. 2, no. 1, pp. 59–67, 2021, doi: 10.1016/j.geosus.2021.03.001.

[13] E. G. Irwin, N. E. Bockstael, O. Hg, D. Puga, and T. Ma, "The evolution of urban sprawl : Evidence of spatial heterogeneity and increasing land fragmentation," 2007, doi: 10.1073/pnas.0705527105.

CHEMICAL COMPOSITION AND YIELD OF WHITE MUSTARD AS AFFECTED BY INORGANIC, ORGANIC AND METALLURGICAL SLAG AMENDMENTS IN ACID SOIL

Aleksandra Stanojković-Sebić[1], Radmila Pivić[1], Aleksandar Stanojković[2]

[1]Institute of Soil Science, Teodora Drajzera 7, 11000 Belgrade, Republic of Serbia
[2]Institute for Animal Husbandry, Autoput 16, 11080 Belgrade-Zemun, Republic of Serbia
e-mail: astanojkovic@yahoo.com

Abstract
White mustard (*Sinapis alba* L.), is a quick-growing long-day annual which prefers light well-drained soil with neutral pH, but the plant tolerates moderately acid and alkaline soils ranging from 5.5 to 8.3. Thus, highly acidic soil conditions could stunt its growth and a necessary lime should be applied. The aim of this study was to determine the effect of Ca - containing metallurgical slag usage, sampled from steel factory area, as well as the effects of commercial lime material and fertilizers, on macro and trace elements content in aerial biomass of white mustard, grown on Stagnosol (a soil with high acidity), through greenhouse vegetative experiments, in 2019. The effects of metallurgical slag were compared to those of commercial lime material ($CaCO_3$) in combination without and with standard inorganic NPK and organic (NPK nutrient of animal origin) fertilizers. P was determined by spectrophotometer, K - by flame emission photometry, and N - using elemental CNS analyzer. In the determination of Fe, Zn, Cu and Cd, ICP-AES was used. Used lime materials, along with metallurgical slag, particularly in combination with organic fertilizer, showed positive effects on elemental composition of white mustard and its yield. The high and toxic concentrations of trace elements in herb comparing to untreated soil were not significantly increased and were within the permissible levels in plants in all the variants in spite of their higher content in metallurgical slag. Based on the results obtained in present study, high potential has been estimated in the application of the studied alkaline metallurgical slag, particularly when combined with organic and inorganic fertilizers, to acid soils toward amelioration their fertility without adverse effects.
Keywords: Metallurgical slag, commercial lime material, inorganic and organic fertilizers, *Sinapis alba*, Stagnosol.

Introduction
Acid soils are widespread and limit plant production all over the World. They cover approximately 30-40% of arable soils and more than 70% of potential arable soils [1]. A similar situation exists in the Republic of Serbia, where long-term research showed that there are over 60% of acidic soils, and that their productivity is increasingly becoming a limiting factor in plant production. It is considered that the constant increase in their surface area is the result of intensive production technology, uncontrolled use of inorganic fertilizers, the impact of acid rain, as well as the lack of organic fertilizers usage [2]. Crops vary greatly in their soil affinity and ability to tolerate low pH. White mustard (*Sinapis alba* L.) is an annual plant with a strong root system with numerous root hairs that contribute to drought resistance. It is grown for its young leaves with a sharp smell, which are used raw in salads, but also for its aromatic seeds, from which mustard is obtained by a special technological process. Commonly, wild plants grow in the fields, but they are also cultivated [3]. There are no special plant requirements for the soil if it is properly fertilized. White mustard grows best in light well-drained soil with neutral pH, although it can tolerate moderately acid and alkaline soils ranging from 5.5 to 8.3 [4], reacting very well to limestone. It is not recommended to grow on halomorphic soils, although extremely acidic soil conditions could significantly reduce or impede

its growth and development [5]. Thus, a necessary lime should be applied. The use of traditional commercial alkaline liming materials to acid soils for the amelioration of acidity consequently improving crop production is a common practice [6]. Along with these materials present in Serbia and regarding its alkaline nature, metallurgical slag, sampled from steel factory area, can be of great importance. Although the significant quantities of metallurgical slag are generated as waste material every day from steel industries, its physicochemical property offers a high potential for its utilization in agriculture. As metallurgical slag contains fertilizer components such as CaO, SiO_2 and MgO, its alkaline property remedies soil acidity [7]. In addition to these three components, it also contains components such as FeO, MnO and P_2O_5, so it has been used for a broad range of agricultural purposes. White et al. [8] reported on field trials in Pennsylvania that crop yields of corn, wheat, oats, buckwheat and soybeans with metallurgical slag application were as good or better than an equivalent amount of limestone. Huang et al. [6] stated that converter slag is used to produce siliceous and phosphorus fertilizer, as well as micronutrient fertilizer, in Germany, USA, France and Japan. Some slags may contain elevated levels of trace metals such as Fe, Cd, Cr, Cu, Pb, Mo, Ni and Zn, that occur naturally in soil, and many of them are essential plant nutritive in low concentrations. Although there are varying concentrations of trace elements in metallurgical slags, their bioavailability is very low [7].

The aim of this research was to investigate the effect of Ca-containing metallurgical slag, a by-product from steel factory, on yield and chemical composition (N, P, K, Fe, Zn, Cu, Cd) of the aerial biomass of white mustard, grown on Stagnosol (a soil with high acidity) and performed in semi-controlled greenhouse conditions. The effects of metallurgical slag were compared to those of commercial lime material ($CaCO_3$) in combination without and with standard inorganic NPK and organic (NPK nutrient of animal origin) fertilizers.

Experimental

The research was performed in Institute of Soil Science in greenhouse vegetative experiments using plastic pots, from the first decade of May to the second decade of July, in 2019. Each pot was filled with 3 kg pot^{-1} of homogenized soil - Stagnosol [9], brought from an experimental field of Institute - Varna, near Šabac town. In every plastic pot ten white mustard seeds were sown.

Chemical characteristics of Stagnosol plowed layer, used in present research, were determined in our previous study [2]. Accordingly, the soil is characterized by very acid soil reaction, low content of available P, then, it is well supplied with available K, medium provided with total N, Cu and Zn, and very highly provided with Fe. Content of toxic heavy metal Cd was low and far from the maximum limiting value of 0.8 mg kg^{-1} [10].

In the experiments the comparison of metallurgical slag (MS) effects in relation to the effects of lime material (calcite - $CaCO_3$, containing 60% of carbonate), and in combination with and without inorganic NPK [composite NPK (15:15:15)] and commercial organic (solid NPK 4:3:4 nutrient of animal origin - Nervosol Complex, NC) fertilizers, were studied. The following seven designed variants were carried out in three replications: control (untreated soil) - V1; $CaCO_3$ - V2; NPK inorganic fertilizer + $CaCO_3$ - V3; NC + $CaCO_3$ - V4; MS - V5; NPK inorganic fertilizer + MS - V6; NC fertilizer + MS - V7. Before sewing the mustard, the amount of fertilizers, lime and slag was measured according to the experimental design and mixed with soil (calculated as for 1 ha): NPK fertilizer (15:15:15) = 500 kg ha^{-1}; NC fertilizer = 170 kg ha^{-1}; $CaCO_3$ = 4 t ha^{-1}; MS = 4 t ha^{-1} (same as the amount of $CaCO_3$). Both MS and $CaCO_3$ with granulation of 0.2 mm were used in the experiment.

The samples of metallurgical slag used in present study were taken during spring 2009 from different deposition sites of Steel factory – Smederevo, Serbia (previously US Steel, now Hesteel Serbia), located approximately 60 km South-East from Belgrade. Chemical composition of MS applied (Table 1) was determined in our previous study [2]. Accordingly, this material has very

alkaline reaction, with the content of calcium in oxide forms (CaO) from 33-45%, of which about 50% is easily soluble in 1 M ammonium acetate; content of the total magnesium was mainly in forms of MgO, while nearly all the amount of P is in available forms for plants; contents of the total Fe and Mn are high, but with lower amounts of their soluble forms; Zn is contained in lower amounts, while the content of Cu is a little higher.

Table 1. Chemical composition of MS [2].

Parameter	Mean ± STDV	Parameter	Mean ± STDV
pH in H_2O	12.48±0.04	Total P (%)	0.61±0.10
Total Ca (%)	26.20±3.48	Total Fe (%)	15.34±0.79
Total CaO (%)	36.60±4.83	Available Fe (mg kg $^{-1}$)	3.38±0.96
Total $CaCO_3$ (%)	65.80±8.64	Total Mn (%)	1.80±0.15
Available Ca (%)	17.18±1.98	Available Mn (mg kg $^{-1}$)	3.12±1.04
Total Mg (%)	0.41±0.04	Total Zn (%)	14.60±5.59
Available Mg (%)	0.70±0.02	Total Cu (%)	228.8±15.4

Organic fertilizer used is a solid NPK 4:3:4 nutrient of animal origin, commercially called Nervosol Complex (NC). According to its main chemical composition, it consists of 4% of total N, 4% of organic N, 3% of P (P_2O_5 form), 4% of K (K_2O form), and 30% of organic C [11].
The aerial biomass of white mustard plants was taken shortly before their final phases of growth from each experimental variant and replicate in experimental pots. Biomass was then air-dried and the yield of plants was measured and expressed in g pot^{-1}, after which it was dried for 2 hours at 105^{o}C and weighed again for chemical analyses, using gravimetric method for determination of dry matter content of plant tissue [12]. The content of N was determined on elemental CNS analyzer Vario EL III [13]. The content of P was determined by spectrophotometer with molybdate [14], and the content of K - by flame emission photometry [15]. In the determination of trace elements - Fe, Zn and Cu, as well as the toxic heavy metal Cd, inductively coupled plasma-atomic emission spectrometry (ICP-AES) was used, after microwave oven extraction and moisture content [16].
The effects of V1-V7 experimental variants on the studied chemical parameters and yield of the plants were evaluated using the SPSS analysis of variance, followed by Duncan's Multiple Range Test (DMRT). Significant differences between means were tested by the LSD test at P = 0.05.

Results and discussion

Certain types of soil, acid particularly, require the periodic application of soil conditioners such as commercial liming materials to provide aeration, increase moisture retention, and promote root permeation and growth. In several experiments in European countries it was determined the ability of metallurgical slag to raise the pH of acid soils [7, 17]. The optimum pH range in soil for growth of most crops in soil is between 5.5 and 7.0, within which most plant nutritives are available [18].
Table 2 shows that the macroelements content in white mustard aerial parts statistically significantly differs (*P**) between the variants for P and K at P<0.05, and no significantly differs (NSD) for N. Nevertheless, there is a noticeably tendency of an increase in the content of N, P and K in tested plant material in the variants that included NC fertilizer and NPK inorganic fertilizer, respectively, in combination with MS (V6 and V7), in relation to other variants. In relation to the untreated soil (V1), all studied variants from V2 to V7 showed positive effects both on increase of yield and valuable chemical composition of white mustard. Improved organic and mineral nutrition in combination with MS would explain the promotion of white mustard biomass growth which led to the promotion of its yield. The data on yield of white

mustard were in accordance with chemical ones, meaning that the yield was highly significantly higher (*P****) at P<0.05 in variants V6 and V7 (Table 2).

Table 2. Effect of tested variants on macroelements content in mustard dry biomass and its yield*

Variants	Macroelements			Yield (g pot^{-1})
	N (%)	P (mg kg^{-1})	K (mg kg^{-1})	
V1 - control (untreated soil)	3.28±0.09^{ab}	0.49±0.03^{cd}	2.98±0.51^{c}	4.09±0.10^{b}
V2 - $CaCO_3$	3.35±0.11^{ab}	0.64±0.09^{ab}	3.35±0.37^{abc}	4.15±0.13^{b}
V3 - NPK mineral fertilizer + $CaCO_3$	3.37±0.32^{a}	0.58±0.04^{abcd}	3.72±0.24^{ab}	4.28±0.13^{b}
V4 - NC + $CaCO_3$	3.36±0.35^{a}	0.57±0.08^{bcd}	3.69±0.32^{ab}	5.09±0.12^{b}
V5 - MS	3.34±0.11^{b}	0.51±0.07^{d}	3.02±0.29^{c}	5.09±0.09^{b}
V6 - NPK mineral fertilizer + MS	3.67±0.17^{a}	0.65±0.05^{abc}	3.77±0.41^{ab}	5.57±0.20^{a}
V7 - NC fertilizer + MS	3.69±0.17^{a}	0.66±0.03^{a}	3.90±0.30^{a}	5.62±0.18^{a}
P value	NSD	*	*	***
LSD (0.05)	0.448	0.106	0.558	0.237

*means ± STDEV; LSD - least significant difference; NSD - no significant difference at P=0.05; *, **, *** - statistical significant differences at P<0.05, P<0.01 and P<0.001, respectively; values followed by the same letter in a column are not significantly different at P<0.05.

Table 3. Effect of tested variants on the trace elements content in mustard dry biomass

Variants	Trace elements (means ± STDEV), in mg kg^{-1}			
	Fe	Zn	Cu	Cd
V1 - control (untreated soil)	108.11±2.11^{a}	59.59±2.24^{de}	7.79±0.32^{d}	0.27±0.08^{b}
V2 - $CaCO_3$	118.62±7.48^{a}	71.24±8.93^{c}	8.58±0.64^{c}	0.38±0.09^{ab}
V3 - NPK mineral fertilizer + $CaCO_3$	125.08±25.98^{a}	74.57±3.81^{abc}	9.21±0.55^{abc}	0.36±0.07^{ab}
V4 - NC + $CaCO_3$	108.50±1.56^{a}	47.69±2.03^{e}	9.16±0.34^{abc}	0.34±0.08^{ac}
V5 - MS	117.13±3.66^{a}	78.79±3.13^{a}	9.36±0.27^{a}	0.43±0.05^{a}
V6 - NPK mineral fertilizer + MS	117.33±13.71^{a}	71.94±4.53^{bc}	9.15±0.31^{abc}	0.38±0.07^{ab}
V7 - NC fertilizer + MS	112.64±8.29^{a}	67.45±5.93^{cd}	9.24±0.42^{ab}	0.31±0.06^{ab}
P value	NSD	***	***	NSD
LSD (0.05)	19.103	7.611	0.528	0.142
Reference value				
Normal	50[1]	15[3]	3[3]	<0.1-1[3]
Critical	250[1]	150[2]	15[2]	5[2]
MPL	600[2]	200[2]	20[2]	10[2]

LSD - least significant difference; NSD - no significant difference at P=0.05; *, **, *** - statistical significant differences at P<0.05, P<0.01 and P<0.001, respectively; values followed by the same letter in a column are not significantly different at P<0.05; MPL - maximum permissible levels; literature source: [1][19], [2][20], [3][21].

Table 3 shows that the trace elements content in white mustard aerial parts statistically highly significantly differs (*P****) between different variants at P<0.05 for Zn and Cu, and no significantly differs (NSD) for Fe and Cd. Moreover, there was not found higher accumulation of Fe in plants in the variants where MS was applied in spite of Fe significant content in it. According to the reference values [21], the content of Cd was within the safety limits and permissible levels in all the variants, which is a highly desirable outcome. The present results of the trace elements content confirm the statements of several authors [22, 23]. The nature of tested treatments and their combinations have an impact on trace elements accumulation, their mobility and storing capacity in plant tissues [22]. Some of them may pose a toxicity threat if present at elevated levels as their availability and mobility increases under acidic conditions [23].

Conclusion

All tested treated variants showed positive effects both on increase of yield and chemical composition of white mustard in relation to the control, particularly when $CaCO_3$ and metallurgical slag are combined with inorganic and organic fertilizer. Comparing to control,

trace elements were not significantly increased in spite of their higher content in studied metallurgical slag. Through experiments in greenhouse pot conditions, as well as using various laboratory accredited analysis, application of metallurgical slag has shown some of the potential benefits and made it a favourable potential material for liming the acid soils.

Acknowledgements
Ministry of Education, Science and Technological Development of Republic of Serbia, Contract No. 451-03-68/2022-14/200011

References

[1] H.R. Von Uexkuell, E. Mutert, Plant Soil 171 (1995) 1.
[2] R. Pivić, A. Stanojković, S. Maksimović, D. Stevanović, Fresenius Environ. Bull. 20 (2011) 875.
[3] https://www.agroklub.rs/sortna-lista/uljarice-predivo-bilje/bela-slacica-87/
[4] S. Snapp, K. Date, K. Cichy, K. O'Neil, Extension Bulletin E-2956, Department of Crop and Soil Sciences, Michigan State University, 2006.
[5] https://agrosmart.net/2016/12/22/tehnologija-odgoja-bele-slacice/
[6] Y. Huang, X. Guoping, C. Huigao, W. Junshi, W. Yinfeng, C. Hui, Procedia Environ. Sci. 16 (2012) 791.
[7] National Slag Association, http://www.nationalslag.org/tech/ag_guide909.pdf, 2011.
[8] J.W. White, F.J. Holben, C.D. Jeffries, Mustards-A Brassica Cover Crop for Michigan, Penn State Bulletin AES 341 (1937).
[9] WRB, World Soil Resources Reports, 106, FAO, Rome, Italy, 2014.
[10] OGRS, Regulation on Limit Values of Pollutants, Harmful and Dangerous Substances in Soil. "Sl. glasnik RS", 30/2018 and 64/2019, 2019.
[11] N. Đurić, B. Kresović, Đ. Glamočlija, Systems of Conventional and Organic Production of Field Crops, Grafos Internacional, Pančevo, Serbia, 2015.
[12] R.O. Miller, in: Y. Kalra (Ed.), Handbook of Reference Methods for Plant Analysis, CRC Press, Taylor & Francis Group, Boca Raton, Florida, 1998, pp. 51.
[13] D.W. Nelson, L.E. Sommers, in: D.L. Sparks (Ed.), Methods of Soil Analysis, Part 3, SSSA, Madison, Wisconsin, 1996, pp. 961.
[14] B. Đurđević, in: D. Miklavčić (Ed.), Manual in Plant Nutrition, Faculty of Agriculture, Osijek, Croatia, 2014a, pp. 60.
[15] B. Đurđević in: D. Miklavčić (Ed.), Manual in Plant Nutrition, Faculty of Agriculture, Osijek, Croatia, 2014b, pp. 62.
[16] Y.P. Kalra, Handbook of Reference Methods for Plant Analysis. CRC Press, Taylor & Francis Group, Boca Raton, Florida, 1998.
[17] M. Rodriguez, F.A. Lopez, M. Pinto, N. Balcazar, G. Besga, J. Agron. 86 (1994) 904.
[18] R. Prasad, J.F. Power, Soil Fertility Management for Sustainable Agriculture. CRC Press, Lewis Publishers, Florida, 1997.
[19] E-D. Schulze, E. Beck, K. Müller-Hohenstein, D. Lawlor, K. Lawlor, G. Lawlor, Plant Ecology, Springer-Verlag, Berlin, Heidelberg, Germany, 2005.
[20] R. Kastori, N. Petrović, I. Arsenijević-Maksimović, in: R. Kastori (Ed.), Heavy Metals in the Environment, Institute of Field and Vegetable Crops, Novi Sad, Serbia, 1997, pp. 196.
[21] A. Kloke, D.R. Sauerbeck, H. Vetter, In: J.O. Nriagu (Ed.), Changing Metal Cycles and Human Health, Springer-Verlag, Berlin, Heidelberg, New York, Tokyo, 1984, pp.113.
[22] O. Riesen, U. Feller, J. Plant Nutr. 28 (2005) 421.
[23] L. Pawlowski, Ecol. Eng. 8 (1997) 271.

THE INFLUENCE OF TIP SONICATION ON STRUCTURAL AND MORPHOLOGICAL PROPERTIES OF GRAPHENE

Andjela Stefanović[1,2], Dejan Kepić[1], Milica Budimir[1], Biljana Todorović-Marković[1]

[1]*Vinča Institute of Nuclear Sciences - National Institute of the Republic of Serbia, University of Belgrade, P.O.B. 522, 11001 Belgrade, Serbia*
[2]*Faculty of Chemistry, University of Belgrade, Studentski trg 12-16, 11158 Belgrade, Serbia*
e-mail: andjela.stefanovic@vin.bg.ac.rs

Abstract
Although ultrasound is frequently used to disperse carbon nanomaterials in suitable solvents, the propagation of high-amplitude ultrasonic vibrations from the tip sonicator was found to be aggressive and has the potential to break down graphene sheets. Here, the effects of tip sonication time on structural and morphological properties of two types of graphene (graphene oxide and electrochemically exfoliated graphene) was investigated by UV-vis spectroscopy and Atomic Force Microscopy. It was found that the structural composition of the graphene was not affected by ultrasounds emitted from the tip sonicator even for the prolonged period of sonication (60 min). Microscopy analysis showed an increased portion of smaller graphene sheets in the sonicated samples for both types of graphene as a result of graphene sheet fragmentation caused by tip sonication.

Introduction
Graphene is a material composed of a single-atom layer of sp^2 hybridized carbon atoms arranged in a hexagonal honeycomb structure with a carbon-carbon bond length of 0.142 nm [1]. Graphene is the first true two-dimensional (2D) material to become a cornerstone in materials science research ever since its discovery in 2004 [2]. Due to its exceptional and distinctive qualities, it is frequently referred to as a wonder material for the future [3]. This unique structure endows graphene with various superior electronic, optical, mechanical, thermal, and magnetic properties, and it has fascinating applications including sensors, capacitors, photocatalysts, nanoelectronics, and nanocomposites [1].
However, graphene's limited dispersibility in water and other common solvents presents a significant processing difficulty. This issue can be solved by graphene being covalently modified by strong oxidants to introduce oxygen functional groups and obtain graphene oxide (GO). In the structure of GO, while the borders of the sheets have carboxyl and carbonyl groups coupled to sp^2 hybridized carbon atoms, the base plane of GO has hydroxyl and epoxy groups connected to sp^3 hybridized carbon atoms [4]. Although the final product, is abundant in functional groups that include oxygen, the graphene sp^2 honeycomb structure is severely disturbed, which has a negative impact on the material's performance [3]. Graphene's oxidized form contains hydrophilic functional groups that make it easier to process in solutions and enable its mass production at a minimal cost. When graphene oxide is reduced in a subsequent stage, the structure is only partially repaired and a significant number of structural flaws remain. Despite the advantages, it is important to eliminate the functional groups that include oxygen to restore graphene's original properties, particularly its electrical conductivity [2].
The electrochemical process of exfoliating graphene in liquids is another potential low-cost mass manufacturing strategy for graphene. Highly oriented pyrolytic graphite (HOPG) is synthetic graphite that is extremely pure [5].
The majority of these procedures are based on a modified Hummer's method, which includes oxidizing graphite using strong oxidants. Depending on the frequency and intensity, ultrasound

provides a strong approach to the synthesis of various nanomaterials. Understanding the effect of sonication on the surface and structure of nanosheets is important because the surface and structure of nanosheets are critical to their properties and uses [1]. If graphene can achieve uniform dispersion, its extraordinary characteristics and structural distinctiveness can increase the performance of nanocomposites. As a result, ultrasonic dispersion of graphene (tip or bath sonicator) for nanocomposite processing is commonly employed to produce uniform dispersion. The tip sonicator is found to be more aggressive, generating ten times the power of a bath sonicator while producing high-quality graphene in a fraction of the time. The solvent dispersion under tip sonication includes breaking down large agglomerates by the propagation of high amplitude ultrasonic vibrations at frequencies ranging from 20 kHz to 1 MHz. Various works have chosen various sonication settings in recent years (time, amplitude, and frequency) [6].

In this work, an investigation of tip sonication effects on two types of graphene (GO and electrochemically exfoliated graphene) was presented. Graphene was subjected to sonication for a short (10 min) and a prolonged (60 min) period of time. The objective was to compare the influence of tip sonication treatments on the GO and electrochemically exfoliated graphene characteristics by analyzing their morphology and chemical structure through complementary techniques.

Experimental

GO and electrochemically exfoliated graphene were prepared as described previously [5, 7]. Each graphene sample was dispersed in deionized MilliQ water using an ultrasound bath to obtain a graphene concentration of 1 mg/ml. After that, graphene dispersions were subjected to sonication using a tip sonicator operated at 300 W and 24 kHz working frequency (Hielscher UP400St ultrasonic processors) equipped with an S24d7 sonotrode (radiating surface of 0.38 cm^2). The dispersions were sonicated at two different times (10 and 60 min) with an amplitude of 72%. To prevent sample overheating, sonication was carried out in an ice bath.

The UV-Vis absorption spectra were recorded using LLG-uniSPEC 2 spectrophotometer. Samples were recorded in quartz cuvettes at room temperature. Atomic Force Microscopy (AFM), Quesant (Agoura Hills, CA, USA), was used for the study of surface morphologies of samples. AFM was operating in the tapping mode, in the air, at room temperature. Standard silicon tip (NanoAndMore Gmbh, Wetzlar, Germany) with a constant force of 40 N m-1 was used. Images were obtained at a scan rate of 2 Hz, with 512 x 512 pixels scan resolution over various square areas. The average size of objects in AFM images was determined by Gwyddion software.

Results and discussion

It was speculated that the tip sonication energy and duration might induce structural changes in graphene. To test this statement, we subjected two types of graphene to tip sonication for short (10 min) and prolonged time (60 min). The temperature of the dispersions was kept constant using an ice bath to eliminate the potential effect of overheating on graphene.

GO dispersion in water has a dark brown color, while the dispersion of electrochemically exfoliated graphene is black. We did not notice any color change both for GO and electrochemically exfoliated graphene even after the prolonged sonication time. The dispersions of GO and electrochemically exfoliated graphene sonicated for 10 min possess long-term stability with no visible agglomeration or sedimentation several weeks after the treatment. However, while GO dispersion sonicated for 60 min also shows long-term stability, electrochemically exfoliated graphene sonicated for 60 min is not stable and tends to

agglomerate. To investigate the structural changes in graphene induced by tip sonication, we performed a UV-vis analysis (figure 1).

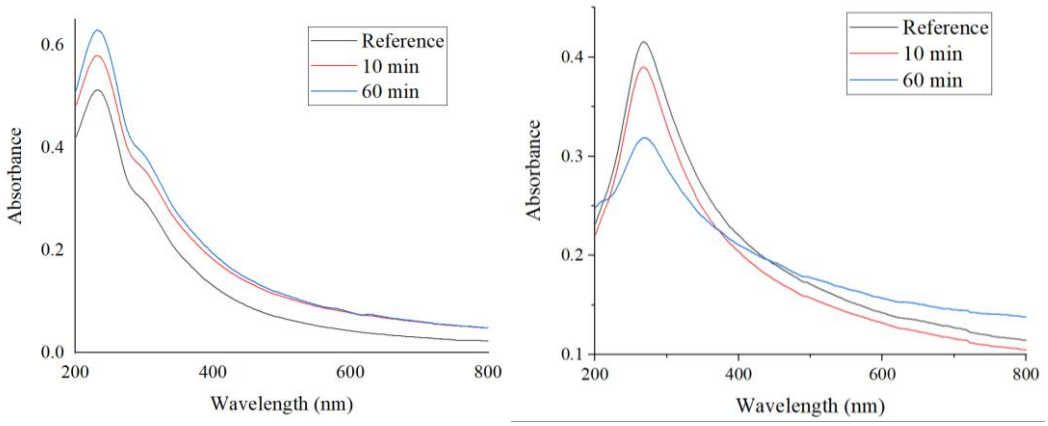

Figure 1. UV-vis spectra of GO (a) electrochemically exfoliated graphene (b) subjected to tip-sonication for 10 and 60 min.

The UV-vis spectrum of GO is characterized by the peak at 230 nm, caused by the π-π* transition of aromatic C=C bonds, and a shoulder at ~300 nm attributed to n-π* transition of C=O bonds. The peak at 230 nm remains its position after the sonication, and the shoulder at ~300 nm can be observed in all the spectra. Exfoliated graphene has only a single broad peak at 270 nm that originates from π-π* transition of aromatic C=C bonds. The peak at 270 nm for electrochemically exfoliated graphene, along with the absence of a 300 nm shoulder peak, suggests that its graphene structure is largely retained [3]. As for GO, the peak at 270 nm in the spectra of electrochemically exfoliated graphene doesn't show any shift. This implies that the sonication of GO and electrochemically exfoliated graphene for selected time intervals didn't induce structural changes in these materials [3].

Morphology analyses of GO and electrochemically exfoliated graphene sonicated using the tip sonicator were conducted by AFM (figures 2-5). In the AFM images, pristine GO is dominated by large sheets with sizes of several micrometers. It was reported previously that electrochemically exfoliated graphene has a broad distribution in the sheet size (2-12 μm) [5]. Both GO and electrochemically exfoliated graphene were present as few-layer graphene (FLG). It is undeniable that tip sonication efficiently dispersed both types of graphene in water. However, as revealed in the AFM results, high-intensity acoustic cavitation caused by tip sonication produces severe fragmentation, defect formation, and further exfoliation of graphene. The fragmentation tends to increase with sonication time which was confirmed by the larger portion of smaller sheet fragments in the images of GO and electrochemically exfoliated graphene sonicated for 60 min.

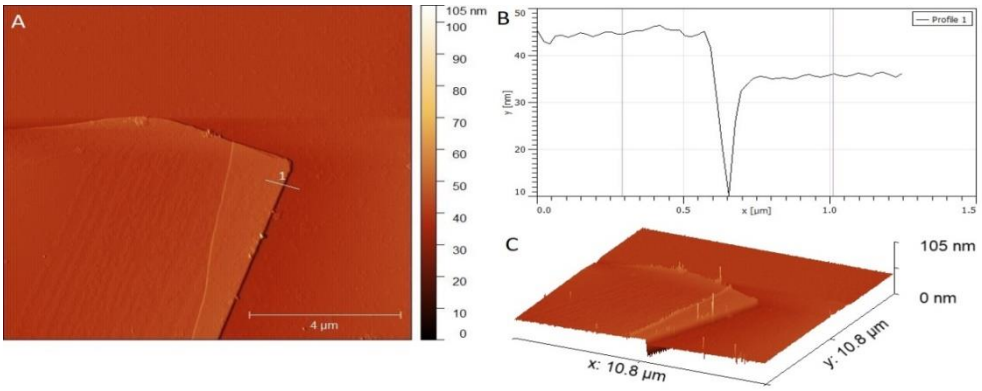

Figure 2. AFM image of GO before sonication (a) the height profile of the scanned surface (b) and 3D representation of the graphene sheet (c).

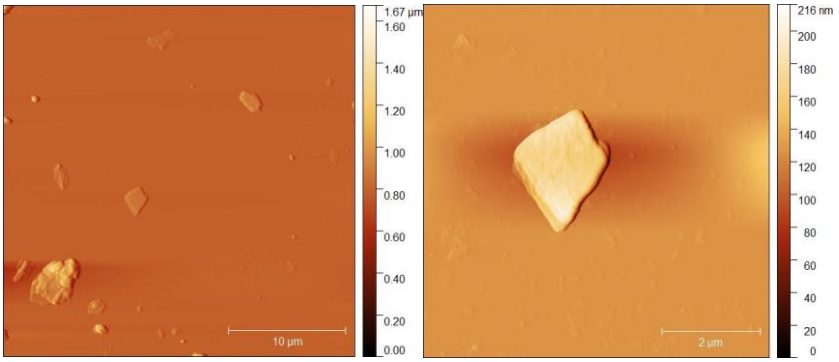

Figure 3. AFM images of GO after 10 min of sonication.

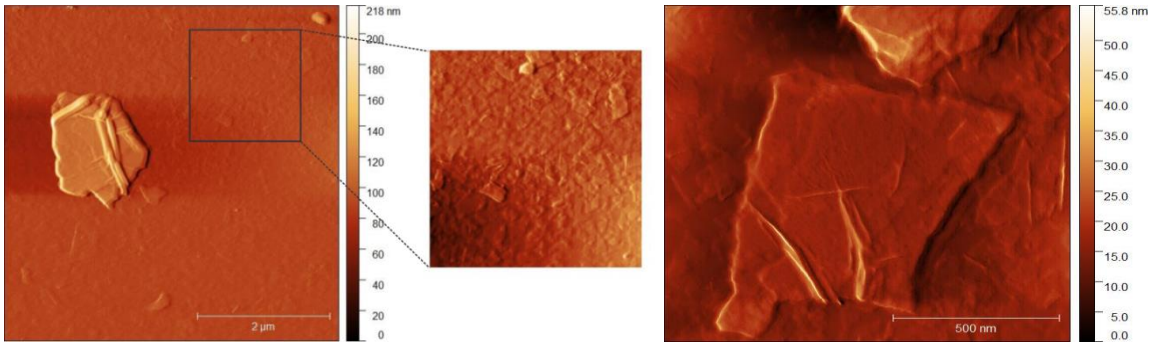

Figure 4. AFM images of GO after 60 min of sonication.

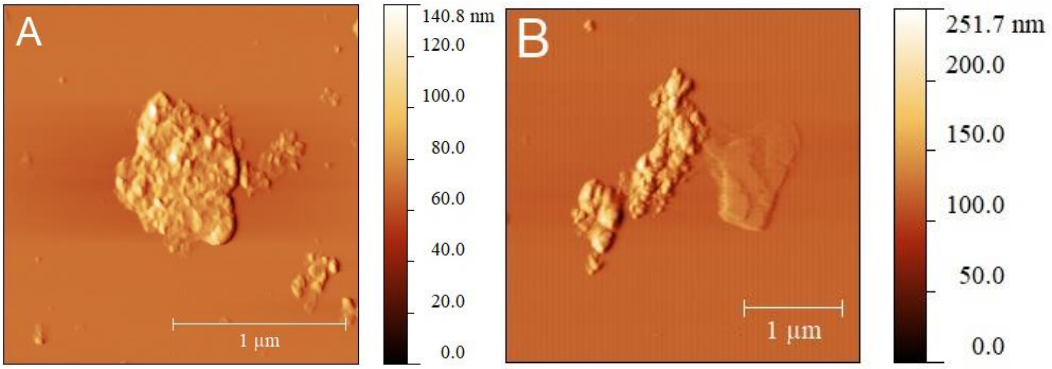

Figure 5. AFM image of electrochemically exfoliated graphene after 10 min (a) and 60 min (b) of sonication.

Conclusion

In this paper, UV-vis spectroscopy and Atomic Force Microscopy were used to explore the effects of tip sonication duration on the structural and morphological features of two forms of graphene (graphene oxide and electrochemically exfoliated graphene). The structural composition of graphene was discovered to be unaffected by ultrasounds generated by the tip sonicator, even after an extended duration of sonication (60 min). As a result of graphene sheet fragmentation produced by tip sonication, microscopy examination revealed an increased share of smaller graphene sheets in the sonicated samples for both forms of graphene.

Acknowledgements

This project has received funding from the European Union's Horizon Europe Coordination and Support Actions programme under grant agreement No 101079151 - GrInShield. The research was also supported by the Science Fund of the Republic of Serbia, #7741955, Are photoactive nanoparticles salvation for global inflectional treath? - PHOTOGUN4MICROBES and by the Ministry of Education, Science and Technological Development of the Republic of Serbia, grant number 451-03-68/2022-14/200017.

References

[1] A. Esmaeili, M.H. Entezari, E.K. Goharshadi, Appl. Surf. Sci. 451 (2018) 112-120.
[2] V. Agarwal, P.B. Zetterlund, Chem. Eng. J. 405 (2021) 127018.
[3] D.P. Kepić, D.N. Kleut, Z.M. Marković, D.V. Bajuk-Bogdanović, V.B. Pavlović, A.J. Krmpot, M.M. Lekić, D.J. Jovanović, B.M. Todorović-Marković, Mater. Charact. 173 (2021) 110944.
[4] D.P. Kepić, A.M. Stefanović, M.D. Budimir, V.B. Pavlović, A. Bonasera, M. Scopelliti, B.M. Todorović-Marković, Radiat. Phys. Chem. 202 (2023) 110545.
[5] Z.M. Marković, M.D. Budimir, D.P. Kepić, I.D. Holclajtner-Antunović, M.T. Marinović-Cincović, M.D. Dramićanin, V.D. Spasojević, D.B. Peruško, Z. Špitalský, M. Mičušik, V.B. Pavlović, B.M. Todorović-Marković, RSC Adv. 6 (2016) 39275-39283.
[6] Z. Baig, O. Mamat, M. Mustapha, A. Mumtaz, K.S. Munir, M. Sarfraz, Ultrason. Sonochem. 45 (2018) 133-149.
[7] D. Kepić, S. Sandoval, Á.P.d. Pino, E. György, L. Cabana, B. Ballesteros, G. Tobias, ChemPhysChem 18 (2017) 935-941.

ENCAPSULATION OF SOME GLUCOSINOLATES FROM CABBAGE AND BROCCOLI HYDROETHANOLIC EXTRACTS IN 2-ISOPROPYL-CYCLODEXTRIN AND γ-CYCLODEXTRIN

Mariana N. Ştefănuţ [1*], Radu Bănică[1], Cristina Moşoarcă[1], Daniel Ursu[1], Adina Căta[1], Ioana M.C. Ienaşcu [1,2]

[1]National Institute of Research and Development for Electrochemistry and Condensed Matter, Dr. A. P. Podeanu 144, 300569 Timişoara, Romania
[2]Department of Pharmaceutical Sciences, Faculty of Pharmacy, "Vasile Goldiş" Western University of Arad, 86 Liviu Rebreanu, 310045 Arad, Romania
e-mail address: mariana.stefanut@gmail.com

Abstract

Plants contain many molecules who can contribute to healing of deseases of human organisms [1,2,3]. This study comprises the obtaining of some extracts from romanian cheap raw materials: cabbage and acclimatized broccoli and encapsulation of these extracts in natural and modified cyclodextrins in order to prevent the loss of their biologycal properties. The obtained complexes were characterized using FT-IR and XRD. The FT-IR spectra of the complexes showed a similar profile to the one of pure cyclodextrin. The decrease of intensity observed for some bands and narrowing of bands proved the formation of hydrogen bonds between the components of extracts and cyclodextrins. The XRD patterns showed an amorphous structure of the obtained complexes. The tools implied in the complexes characterization demonstrated the linkage between the host and guest substances.

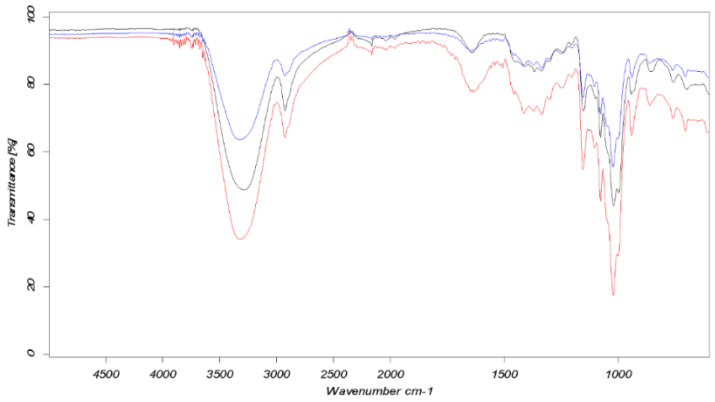

Figure 1. FTIR aspect of encapsulation of two extracts (cabbage and broccoli) in γ-cyclodextrin (black-γCD); (red Complex-γCD-broccoli); (blue- γCD-cabbage)

Acknowledgements

This work is based on research supported by the Romanian Ministry of Research, Innovation and Digitization, project no. PN 19 22 03 01, contract no. 40N/2019 - "Supramolecular inclusion complexes of some natural and synthetic compounds with applications in health" - carried out under the NUCLEU Program.

References

[1] D. Muntean, M.N. Stefanut, A.Cata, V. Buda, C. Danciu, R. Banica, R. Pop, M. Licker, I.M.C. Ienascu, 13 Symmetry (2021), 893.

SUSTAINABLE MANAGEMENT OF FOREST RESIDUE AND WOOD WASTE IN SERBIA

Goran Stojićević[1], Suzana Knežević, Milena Milojević

Academy of Vocational Studies Šabac, Unit of Agricultural and Business Studies and Tourism, Vojvode Putnika 56, 15000 Šabac, Srbija
e-mail: csugoran@gmail.com

Abstract

The exploitation of forest funds in Serbia during 2021, according to data from the Republic Statistical Office, shows that 735,647 m^3 of wood has been cut down, of which 73,601 m^3 is waste. Cut wood is used as industrial and technical wood, but also for firewood. The remains in the cutting of the forest tree include: remnants of bark that has been removed from the enclothes, ends with crust when cutting hulls, thin branches with bark, and stumps with roots. As a result of wood processing, wood waste is created which by size can be classified into three groups - bark, large debris after cutting the enclothal and small remains (sawdust, scraping, wood dust). Forest debris (forest biomass) and wood waste are a significant resource that has not been used enough. In the face of the current global energy crisis and declining reserves of fossil fuels, forest waste and timber waste are becoming increasingly attractive products as demand for wood-based energy is steadily growing and razors, pellets and wood are increasingly being used for firewood. Managing forest waste and wood waste is based on one of the main goals of waste management, which is to reduce the negative impact of waste on human health and the environment in a sustainable way. Rising waste disposal costs and rising environmental awareness are also contributing to the growing importance of waste wood recycling. New methods are being developed for recycling wood waste – it is added in small quantities to the cement or mortar mixture, resulting in stronger and more waterproof material. There is also the use of wood waste in the form of wood flour for obtaining different wood-plastic composite materials. Sustainable management of forest remains and wood waste should be based on the principle of a circular economy whose concept implies that waste does not exist, i.e. it becomes a resource that can be exploited.

Keywords: forest waste, management, Serbia, wood waste

THE ABUNDANCE OF *NEZARA VIRIDULA* AND THE INFLUENCE OF METEOROLOGICAL FACTORS IN 2021 IN THE SOYBEAN CROP IN MAČVA

Stošić Nemanja[1], Blagojević Milan[1], Rašković Vera[1], Arsenović Dušanka[1], Vlajić Slobodan[2], Bajagić Marija[3]

[1]Academy of Applied Studies Šabac. Unite for Agricultural Business Studies and Tourism, Republic of Serbia
[2]Institute of Field and Vegetable Crops, Novi Sad, Serbia
[3]University of Bijeljina, Faculty of Agriculture, Bijeljina, Republika Srpska
email: blagojevicmilan@ymail.com

Abstract

Nezara viridula has 4-5 generations per year, a Mediterranean species, which has expanded significantly thanks to slightly higher temperatures during the winter. After copulation, females lay up to 300 eggs on the underside of a leaf, in groups of 30 to 130. *Nezara viridula* feeds on plant juices from young plant parts and fruits, where the fruits lose their market value. In places where the pods and seeds are punctured, they dry out over time and turn dark. An abundance of 8 to 10 bedbugs in 10 swings with the catcher is considered the threshold of harm. The average number of *Nezara viridula* per 100 m^2 was determined in the Bogatić and Krupanj localities and was 456 individuals and 191 individuals in the Krupanj locality. After removing the crop from the experiment, the yield was determined and the seeds were counted and the percentage damage of soybean seeds was determined. Damaged seeds after exposure to low temperatures were germinated to determine the germination rate compared to undamaged seeds. At the Bogatić site, 9% of the seeds were damaged, and at the Krupanj site, 6% of the seeds were damaged by visual inspection. The germination rate of undamaged soybean seeds at the Bogatić location was 84 seeds, while 77 seeds germinated in the case of damaged seeds. The germination rate of undamaged soybean seeds at Krupanj was 81 seeds, while 73 seeds germinated in damaged seeds. Lower yields of soybeans in both localities are due to low amounts of precipitation in the period of grain filling as well as high temperatures with little atmospheric moisture during flowering of soybeans.

THE INFLUENCE OF THE GRAY OR ASH GRAPE MOTH (*LOBESIA BOTRANA*) ON THE YIELD IN THE SREMSKI KARLOVCI VINEYARD IN 2021

Stošić Nemanja[1], Blagojević Milan[1], Rašković Vera[1], Marković Stefan,[1] Vlajić Slobodan[2], Bajagić Marija[3]

[1]Academy of Applied Studies Šabac. Unite for Agricultural Business Studies and Tourism, Republic of Serbia
[2]Institute of Field and Vegetable Crops, Novi Sad, Serbia
[3]University of Bijeljina, Faculty of Agriculture, Bijeljina, Republika Srpska
email: blagojevicmilan@ymail.com

Abstract

The most important pest on the vine is the grape moth. In some vineyards, it occurs in large populations, which can cause up to 80% of damage. Research on the development of the cluster moth population was monitored on early grape varieties in sremski karlovci during 2021. In the orchard are the table varieties muscat julski, rani kardinal. The flight of the cluster moth was monitored with the help of pheromone traps from 15.4.-1.8.2021 and the trap was inspected every week and the trap was changed every 40 days. Other stages of the cluster moth were examined visually. The vineyard was sprayed for the first time on april 25, 2021. Acaricide active substance phenazaquin. The biggest damage is done by the caterpillar. The caterpillar damages the petiole, flowers and berries of the vine. In addition to the mentioned direct damage, there is a greater danger of indirect damage, due to the decline of the plant's immunity, the appearance of gray mold may occur. Females of the first generation lay eggs on flower buds, petioles, and later on vine flowers. On average, one female can lay a maximum of 120 eggs. During the period of development, the caterpillar can destroy about 50 buds, ie. Newly set fruits. A low population of the ash cluster moth was determined, namely the second generation on june 12 and 20, with a total of 6 butterflies on the trap. One of the reasons for the low population of *L. botrana* is the periodicity of the appearance of this pest. The grape yield of both varieties is negligible.

LITHOCOLLETIS CORYLIFOLIELLA - REPRESENTATION IN THE APPLE ORCHARD DURING 2020-2022 IN MAČVA

Stošić Nemanja[1], Blagojević Milan[1], Rašković Vera[1], Tanasić Ljiljana[1], Bajagić Marija[2], Marković Stefan,[1] Vlajić Slobodan[3]

[1]Academy of Applied Studies Šabac. Unite for Agricultural Business Studies and Tourism, Republic of Serbia
[2]University of Bijeljina, Faculty of Agriculture, Bijeljina, Republika Srpska
[3]Institute of Field and Vegetable Crops, Novi Sad, Serbia
e-mail: nemanjastosic.vpssa@gmail.com

Abstract

Lithocolletis corylifoliella is a miner of "white mines" and is known as a minor apple pest in the territory of Mačva. However, in the event of suitable weather conditions for wintering and development of this insect, and less intensive control with chemical measures, this insect can become a significant pest. The research was conducted in the locality of Mrđenovac (Repubilka Srbija, Mačva). During the growing seasons 2020-2022. the appearance and presence of the white miner *Lithocolletis corylifoliella* in the apple orchard was monitored. The appearance and abundance was monitored using adequate pheromone traps. On the pheromone trap in 2020, the first appearance of imago was recorded on 11.04., while the largest number of imago was determined in 12.08. (5 adults). Also, the appearance and presence were recorded until the imago stopped appearing (23.09.). In 2021, the first appearance of imago was recorded 10 days earlier (01.04.), while the largest number of imago was determined on 15.04. (19 adults). Reporting of imago lasted until 21.09. During 2022, the presence of the first images was recorded 5 days earlier than in 2021 and even 15 days earlier than in 2020 (26.03.). The highest number was recorded on 16.08. (45 adults). The appearance of the image lasted until 09.09. The abilities of an adult caterpillar to easily overwinter in a fallen leaf and the development of a larger number of generations (3-4) are favored by relatively high temperatures during the winter period and throughout the year. This phenomenon is reflected in the earlier appearance of imagos from year to year, but also the sharp jump in the peak number of miner imagos, from 5 to as many as 45 individuals per day in the peak of summer, in a period of only 2 years.

EFFECT OF APPLE POMACE POWDER ADDITION ON RICE FLOUR BASED BISCUITS QUALITY

Beatrix Szabó-Nótin, Csilla Berta Juhász, Ivett Jakab, Mónika Máté

[1]Department of Fruit and Vegetable Processing Technology, [2]Department of Grain and Industrial Plant Processing,
Institute of Food Science and Technology, Hungarian University of Agriculture and Life Sciences
H-1118, Budapest, Villányi street 29-43. Hungary
e-mail: szabo-notin.beatrix@uni-mate.hu

Abstract
Apple pomace is the primary by-product generated during the production of apple juice. This study investigates the effect of apple pomace powder (APP) on baking quality of rise-flour based biscuits. Water activity, moisture content was measured; sensory evaluation, colour investigation, total polyphenol content and texture profile analysis were performed.
By increasing the concentration of apple pomace, the hardness, fracturability, polyphenol content and antioxidant capacity increased, while their brightness, moisture content, water activity and overall popularity decreased. Apple pomace flour addition also increased the sweet taste intensity of cookies suggesting that in bakery products APF evolve a flavor enhancer role. Based on the sensory and compositional attributes, it was concluded that good quality biscuits can be prepared through using 5% and 7.5 % apple pomace powder with rice flour. APP proved to be a promising alternative ingredient in case of biscuits.

Introduction
During processing of apples 25% of the apple mass (eg, skin, stem, seeds, and pulp) being discarded as by-product, what is referred to as apple pomace [1; 2].
Currently, apple pomace has a lot of utilization possibility, as a livestock feed ingredient, for specific nutrient (dietary fiber, polyphenol, etc) extraction for dietary supplements, and as a food ingredient substitute [3]. Apple pomace should be considered for use as a food ingredient for human consumption (pomace in jams and in sauces, confectionery products such as pomace powder for toffees, using pomace powder in bakery products [4, 5, 6]. Dried apple pomace powder (APP) contains high level of the fiber [7]. it can be used in bakery products to enhance dietary fiber and bioactive compounds in the products [8; 9]. This study is aimed to investigate the effect of apple pomace powder on baking quality of rise flour based biscuits.

Experimental
Non enzymatic treated wet apple pomace was obtained from a hungarian juice maker company (Agrana Juice Ltd.). 200g of the pomace were spread in a drying tray with a depth of 0.5 cm, the drying temperature was 80°C and samples were dried in the dryer until reached 4 % moisture content using atmospehric drying equipment (LP 232/1, Hungary). Dried samples were ground into flour using a “PRINCESS” multi chopper and grinder and after it were vacuum packaged. Basic ingredients needed for the preparation of biscuits were all commercially available: rice flour, icing sugar, butter, margarine, vanilla sugar and egg.

Preparation of bakery products

The ingredients were mixed, and after this the biscuits were rounded in shape with diameter of 40 mm and thickness of 6-8 mm and baked in an electric oven at 170 °C for 7 min. The ingredients are shown in Table 1.

Table 1. Ingredients of the biscuits

	RF 0%	RF 5%	RF [illegible]	RF 10%
Rice flour	48.08g	45.67g	44.47g	43.27g
Apple	0 g	2.40g	3.61g	4.81g
Margarine	32.05g	32.05g	32.05g	32.05g
Sugar	16.03g	16.03g	16.03g	16.03g
Egg yolk	2.56g	2.56g	2.56g	2.56g
Vanilla [illegible]	1.28g	1.28g	1.28g	1.28g

Determination of baking loss values

After cooling to room temperature, biscuits were weighed and baking loss (Bl) was determined using the following equation: $Bl = ((w_1-w_2)/w_1)\times 100$, where w_1 is the weight of biscuit prior to baking, w_2 is the weight of biscuit after baking.

Determination of dry material content and water activity

Determination of dry material content of the biscuits was performed by using a MAC-50 rapid moisture analyzer (Radwag Waagen GMBH, Hilden, Germany). To determine the water activity, Novasina, LabMaster-aw equipment was used.

Colour measurements

Colour is a determining factor in the definition of the quality of any food. The colour of the surface of three biscuit samples were also measured with 9 parallels (3 biscuits/3 places) using a Konica Minolta CR400 chromameter. Results were expressed as L*, a*, and b* values. L* is a measure of the brightness from black (0) to white (100), while a* describes the redgreen color (a*> 0 indicates redness, a* < 0 indicates greenness), and b* describes yellow-blue color (b*> 0 indicates yellowness, b* < 0 indicates blueness). To determine the total color difference between two samples using all the three coordinates, the following formula was used: $\Delta E^* = \sqrt{(\Delta L^*)^2 + (\Delta a^*)^2 + (\Delta b^*)^2}$

Texture analyis

Texture analysis of the biscuits was performed using a Stable Micro System TA.XT2 with 2mm Cylinder Probe (P/2). Three biscuit were selected, and the measurement was performed on their center and two side points. The data were recorded, and the analysis of the texture profile was performed by using Texture Expert software. The test parameters were the follows: trigger force: 5g, test speed 0.5 mm s^{-1}, distance reached by the test piece in the sample: 2 mm. Based on the texture profile load (g) in function of time (s), two parameters were chosen as texture indicators: hardness (g) (maximum deformation force during the first mastication cycle), and fracturability (g) [10].

Determination of total polyphenol content

Total phenolics were determined using the Folin–Ciocalteu colorimetric method as described by Singleton and Rossi (1965) [11]. The results were expressed in gallic acid equivalents (GAE, μg ml^{-1} biscuit exract).

Sensory evaluation

During the sensory evaluation, the judges had to score the biscuits on a 100-point scale. The sensory attributes were given different scores. Colour and texture were 20 points, smell 10 points and taste 40 points.

Statistical analysis

For the statistical analysis the mean values were compared by 2-way analysis of variance (ANOVA) when evaluating the sensory attributes of the products ($\alpha = 0.05$). Pair comparison was performed by Tukey HSD post hoc test. The statistical analysis was carried out using SPSS ver.No.23.

Results and discussion

In general, geometry is an important parameter in baking quality of biscuits. Increased volume of baking products is associated with their improved quality [12; 13]. Baking loss refers to the moisture loss during baking: The higher water binding capacity of dough is related to lower baking loss. The baking loss values of the biscuits were the follows: RF 0%: 5.71%; RF 5%: 5.31%; RF 10%: 4.67% and RF10%: 5.42%.

The moisture content of the biscuits were ranged from 5.59-6.52 % RF10 biscuits showed higher a_w values (6.52%), which may result from the water holding capacity of apple pomace [13]. In case of water activity, there was no differences between the values (0,32-0,36). The water activity values of biscuits are below 0.6, what means a microbiological stability, but it can only be stated that these foods are stable with the knowledge of appropriate microbiological tests.

Color is an important parameter in determination of baking quality. During the color measurement, L* and ΔE* values were considered as these properties show the difference between the biscuits the most (Fig. 1). According to the literature the addition of apple pomace decreases the L* value of the samples and increases the color difference [14]. In case of the biscuits, significant differences were observed at 5% significance level. Between RF5 and RL7.5, there is significant difference, but for the other pairings, significant differences are observed, so that RF0 and RF10 biscuits are significantly different from RF5 and RF 7.5, and also from each other ($p<0.000$). Color difference (ΔE*) between control and APP added biscuits was higher, than 6.0, so it indicate huge differences. According to Wenzl-Gerőfy (2014) [15], the critical values are the follows: $\Delta E^* < 1.5$: not perceptible; $1.5 < \Delta E^* < 3.0$: perceptible; $3.0 < \Delta E^* < 6.0$: well perceptible; $6.0 < \Delta E^*$: huge difference.

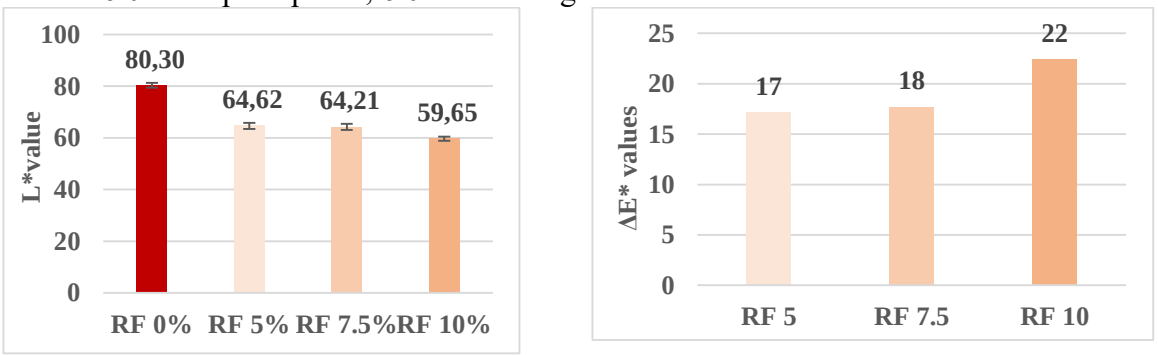

Figure 1. L* and ΔE* values

The decreasing tendency of L* and the color difference between the samples can be caused by the brown color of the pomace and the behavior of polyphenols as substrates, which can lead to enzymatic browning [6]. Melanoids and reaction products formed during the Maillard reaction cause browning in fried products [16; 17].

By the texture measurements, hardness and fracturability were determined (Fig.2.) using the texture profile. Analysis of variance analysis showed that for RL biscuits there is a significant difference between different concentrations. To investigate this further, Tukey's pairwise comparison was performed, which showed the significant difference between each samples. RF 10% samples differ significantly in hardness from each concentration.

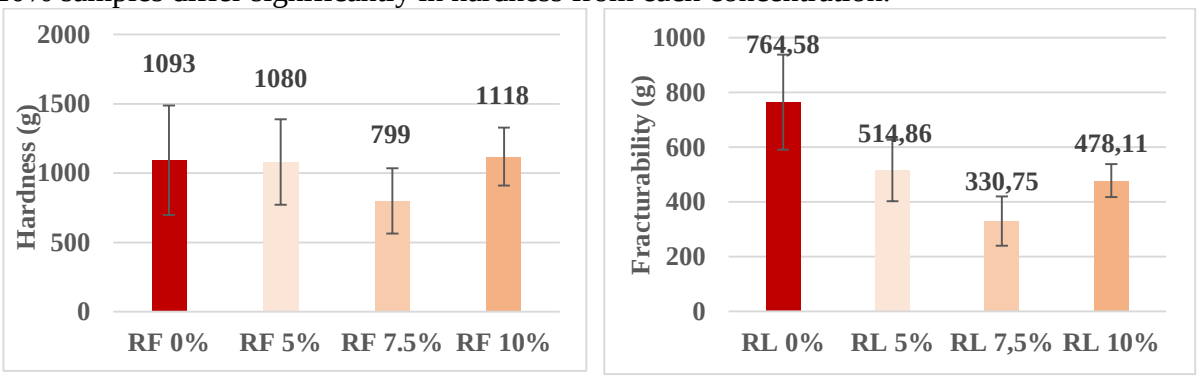

Figure 2. Hardness and fracturability values of the biscuits

As the apple pomace content of the samples decreased, the hardness is increased. Apple pomace has good water holding capacity, so it can soften the texture of the foods in which it is used [13]. Several studies report that the addition of fruit or pomace flour increases the hardness compared to the hardness of reference biscuits [18]. Apple pomace contains fructose, and it may have increased the hardness due to the crystallization of it [13]. The hardness of biscuits depends not only on the apple pomace, but also on the flours used in them (their grain size), the water, the sweetener, and fat, as well as the interactions between the ingredients [19].

Examining the total phenolic content of the samples, there was no significant difference between each sample (p>0000). The polyphenol content of the biscuits increased with increasing apple pomace. In case of the control sample TPC was 14 mg 100 g^{-1}; in case of RF 5 biscuit: 15 mg 100 g^{-1}; RF 7.5: 23 mg 100 g^{-1} and RF 10 biscuit: 24 mg 100 g^{-1} .

Effect of the added apple pomace powder on sensory attributes of biscuits was also investigated. Figure 3. shows the total point numbers of the biscuits in a bar graph. Critics preferred RF5% biscuits the most, but there was no sensory difference in the popularity of RF0% and RF7.5%. These results suggest that these type of biscuits can be fortified with up to 5%-7.5% apple pomace, as there is no sensory difference from biscuit-free biscuits.

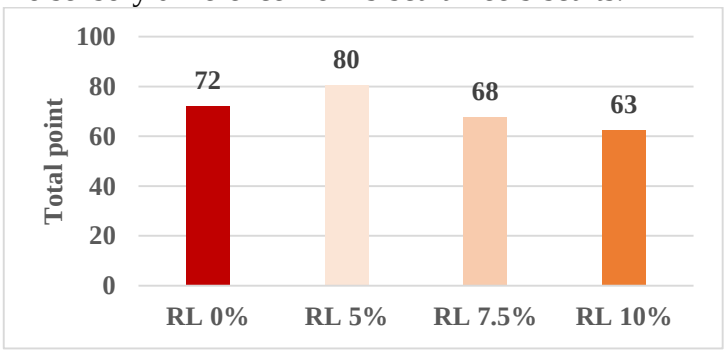

Figure 3. Total points of the sensory attributes

Conclusions

As the apple pomace concentration increased, the hardness and fracturability decreased, while their lightness, moisture content, polyphenol content and overall popularity increased. We can state that in the case of RL5 and RL7.5 biscuits, the biscuits enriched with 5% and 7.5% apple pomace flour proved to be the most suitable by the reviewers. Therefore, apple pomace can be regarded as a nutritional and functional ingredient in bakery products. Future studies are recommended to develop various types of functional baked foods with apple pomace as an ingredient.

References

[1] N. O'Shea, E. K. Arendt, & E. Gallagher (2012) Innov. Food Sci. and Em. Techn., 16, 1–10. DOI: 10.1016/j.ifset.2012.06.002.
[2] H.N.Rabetafika, B. Bchir, C. Blecker, & A. Richel (2014) Trends in Food Sci. and Techn., 40, pp. 99-114. doi: 10.1016/j.tifs.2014.08.004.
[3] E. Gołębiewska, M. Kalinowska & G. Yildiz (2022) 15(5). doi: 10.3390/ma15051788.
[4] H.P.V. Rupasinghe, L. Wang, G.M. Huber, & N.L. Pitts (2008) Food Chem., 107, pp. 1217–1224
[5] A.S. Sivam, D. Sun-Waterhouse, G.I.N. Waterhouse, S., Quek, & C.O., Perera (2011) J. of Food Sci., 76, 97-107
[6] M.L. Sudha, V., Baskaran, & K. Leelavathi, (2007) Food Chem., 104, pp. 686–692
[7] K. Wolfe, X. Wu, & R.H. Liu, (2003) J. of Agr. and Food Chem., 51: 609–614.
8] J. Jung, G. Cavender, & Y. Zhao (2015) J. of Food Sc. and Techn., 52(9):5568–5578. DOI 10.1007/s13197-014-1680-4
[9] M. Bourne, (2002) Food texture and viscosity: concept and measurement. 2nd ed. Academic Press, San Diago California.
[10] V.L., Singleton, & J.A., Rossi, (1965) Am. J. of Enol. and Vitic., 16, pp.144–158.
11] R. C., Hoseney, & D.E., Rogers, (1994) The science of cookie and cracker production, 203–225
[12] B., Pareyt, K., Brijs, & J.A., Delcour (2010) Cer. Chem., 87, pp. 226-230.
[13] H., Chen, G.L., Rubenthaler, H.K., Leung & J.D., Barnowki, (1988) Cer. Chem., 65, pp. 244-247.
[14] M., Alongi, S., Melchior, & M. Anese (2018) Food Sci. and Techn., 100, pp. 300-305.
[15] K., Wenzl-Gerőfy (2014): A CIE L*a*b* színrendszer. 128. ISBN: 978-963-313-202-9
[16] S.I.F.S., Martins, W.M.F. Jongen, & M.A.J.S. Van Boekel, (2001).Tr. in Food Scie. and Techn., 11, pp. 364–373.
[17] H. D. Belitz, W. Grosch, & P. Schieberle, (2009) Food Chem. 4th revised and extended ed. 270–285. Berlin, Germany: Springer-Verlag Berlin and Heidelberg GmbH & Co. KG.
[18] M. Norhidayah, A. Noorlaila, & A. Nur Fatin Izzati, (2014) Int. Food Res. J., 21(6) 2133-2139.
[19] K. Kulp, M. Olewnik, K. Lorenz (1991) Starch, 43 (1991), pp. 53-57

UTILIZATION OF FRUITS POMACE IN MUESLI PRODUCTS

Lilla Szalóki-Dorkó, Hering Melitta, Mónika Máté

Department of Fruit and Vegetable Processing Technology, Institute of Food Science and Technology, Hungarian University of Agriculture and Life Science, H-1118 Budapest, Villányi út 29-43, Hungary
e-mail: Szaloki-Dorko.Lilla@uni-mate.hu

Abstract

Utilization of different fruit by-product was investigated during muesli products development. Sour cherry, cherry and black currant and apple pomace (4 g) was added to the samples besides the other used muesli ingredients such as oat, oil seeds, dried raisin, honey, coconut oil. In this study total polyphenol, total antioxidant (FRAP) content was measured of the mueslis with spectrophotometric methods, furthermore sensory analysis was done to evaluate the consumer acceptance. During our work four muesli products were created using different recipes. Muesli 3 showed the highest total polyphenol (2723.3 mg GAE mg/100 g) and FRAP (10.43 µg/100g) values due to high amount of fruit pomace. The muesli 4 contained the lowest concentration of bioactive compounds. As regard the overall impression of sensory analysis that provides information about the whole acceptance, sample 3 get the highest value (95%). Sample 4 was the next with 85% of overall impression and sample 1 was the third with 73% while the sample 2 was the last in the ranking. Fruit pomace has a great potential due the high bioactive compounds and appropriate sensory properties in aspect from muesli production.

Introduction

The fruit production has increased continuously in the world in the last decade [1]. Along with this large amount of fruit by-products were generated during the fruit processing technologies. The largest proportion of this is the pomace which is rich in bioactive components, dietary fibre, polysaccharides, vitamins etc. and the consumption of it has a health benefit in human nutrition [2; 3; 4]. Therefore, it has become important parts of scientific research and the novel food developments [5].

There are several studies about utilization of fruit pomace. For recovery of bioactive compounds, different solvents-based extraction has been used however other novel techniques including membrane-based methods, ultrasound-assisted and microwave-assisted extractions, high hydrostatic pressure, nanotechnology etc. have higher efficiency against to the conventional method [6; 7]. Fruit pomace can also be utilized for animal feeding, however, due to the low amount of protein it is not present high quality [8]. Furthermore, it can be used as effective functional ingredient for development of fibre in cereal-based products [9].

The aim of this study was to utilize different fruit by-product in muesli product. Muesli samples were created with ca. 5–20% pomace content to replace the fruit furthermore apple pomace was added to increase the fibre content of the samples. However, further objective was to create products with muesli-like sensory properties.

Experimental

Materials

Three differential pomace of fruits were used for muesli product development, namely sour cherry (‘Cigánymeggy’), sweet cherry (‘Szomolyai fekete’) and black currant. These were generated after pressing during the processing technologies. Each pomace contained moisture; therefore, they were condensed together to ca. 40 °Brix before using. To increase the fibre content of the muesli product apple pomace was used, which also a by-product of the apple

processing. The other ingredients of the muesli were the most used components, namely oat, oil seeds (pumpkin seed, sunflower seed), dried raisin, honey, coconut oil.

Methods

Muesli preparation

Four different samples of muesli were prepared under laboratory conditions using similar ingredients to the commercially available fruit muesli bar. The main components were oat, fruit pomace and oil seeds while raisin, honey and coconut oil were used in lower amount. After preparing, muesli samples were baked for 15–20 min at 140°C until solidifying.

Measuring methods

To determine the polyphenol components and antioxidant capacity, extraction was necessary for the analysis of the muesli samples. Samples were homogenize using knife blender and 3 g was weight to a centrifuge tube then 30 mL extraction solvent (60% methanol, 39% distilled water, 1% formic acid) was added. Samples stand for 15 minutes and were centrifuged at 4500 rpm for 5 minutes. The supernatants were used for spectrophotometric measurements and colour measurement.

Total polyphenol content (TPC) was determined according to the method of Singeton and Rossi [10]. The samples were measured at 760 nm and the results were given in mg gallic acid equivalent/100 g (mg GAE/100 g).

Total antioxidant capacity (FRAP) was determined using Benzie and Strain method [11]. The extract of mueslis was measured at 593 nm and the results were expressed in mg ascorbic acid equivalent/100 g (mg AAE/100g).

Sensory analysis was performed using 100 points system to evaluate the muesli samples based on these main properties: taste (max. 30 points), odour (max. 10 points), texture (max. 20 points), colour (max. 20 points) and overall impression (max. 10 points).

T-test was used for analysis of difference between the muesli samples in case of TPC and FRAP. Significant difference was considered when P value was <0.05.

Results and discussion

The final recipe of four different muesli samples can be seen in the Table 1. The difference between the sample 1 and sample 2 is the form of the oil seeds, because oil seeds were grounded in sample 2 to reach smoother texture. The quantity of fruit pomace was 34 g except in case of sample 3, in which 65.2 g was added to create a muesli product with high fruit content.

Table 1. Ingredients of muesli products

Ingredients	Quantity of ingredients (g)			
	Sample 1	Sample 2	Sample 3	Sample 4
Oat	55.0	55.0	32.0	55.0
Pumpkin seed	16.0	16.0	9.2	16.0
Sunflower seed	8.0	8.0	4.6	8.0
Honey	6.0	6.0	5.0	22.0
Coconut oil	11.0	11.0	–	11.0
Dried raisin	–	–	–	12.0
	Fruit pomace			
Sweet cherry	12.0	12.0	20.5	9.0
Sour cherry	12.0	12.0	20.5	9.0
Black currant	6.0	6.0	20.5	–
Apple pomace	4.0	4.0	4.0	4.0

Black currant pomace was missed from sample 4 to avoid the bitter, acrid taste, however it contained dried raisin. In general, all mueslis were sweetened with honey while coconut oil provided the cohesion between the ingredients. In addition, 4 g apple pomace was added to increase the fibre content of the samples. The final muesli products can be seen on the Figure 1.

Figure 1. Muesli product

The polyphenol content of the muesli samples can be seen on the Figure 2. Muesli 3 had the highest values (2723.3 mg GAE mg/100 g) as we expected because this sample contained the highest amount of fruit pomace. The muesli 1 contained by 40% lower value while ca. by 60% lower values were measured in muesli 2 and 4 compared to the sample 3. In case of muesli 2 and 4 similar results were detected however the fruit proportion was the half in muesli 4. This was probably due to the higher amount of honey (22 g). The differences between the TPC values of sample 3 compared to other samples were significantly lower.

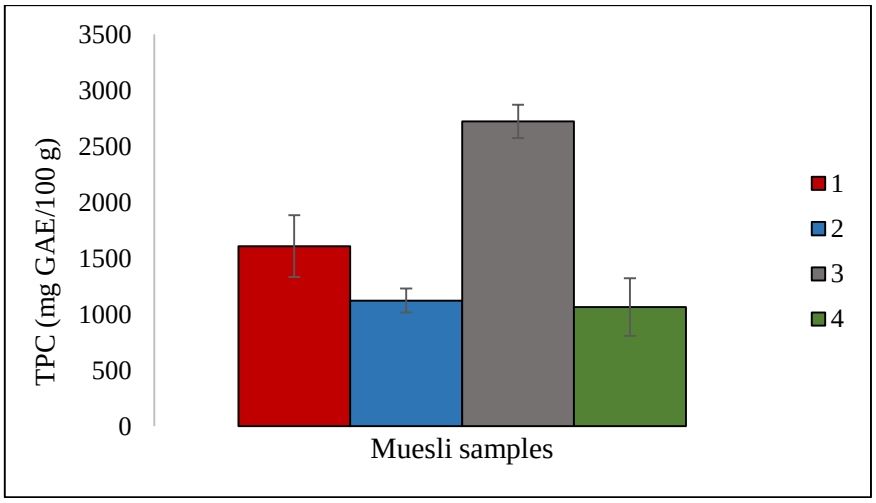

Figure 2. Total polyphenol content (TPC) of four muesli samples

The total antioxidant capacity (FRAP) of the samples showed almost similar tendency as considered in the case of TPC (Figure 3), however the sample 4 had lower value. Muesli 3 showed the highest content (10.45 µg AAA/100 g) which is higher by 50% than the sample 1 and almost higher with 66% than sample 2. The differences between the TPC values of sample 3 compared to other samples were significantly lower. The correlation between the results of TPC and FRAP is 0.9923 value which indicates very strong relationship.

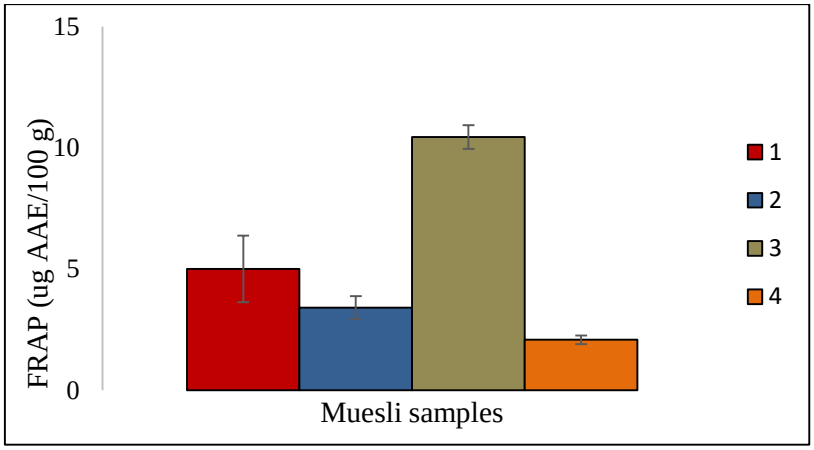

Figure 3. Total antioxidant capacity (FRAP) of four muesli samples

Based on the results of sensory analysis of muesli samples (Figure 3.) can be concluded that the sample which contained higher amount of fruit pomace finished in the first place. This muesli (sample 3) had the highest value in case of taste (90%), overall impression (95%), and odour (75%). The two least liked muesli were samples 1 and 2, however all values were above 60% in both cases. As regard the overall impression that provides information about the whole acceptance, after sample 3, sample 4 was the next with 85% and sample 1 was the third with 73% while the sample 2 was the last in the ranking.

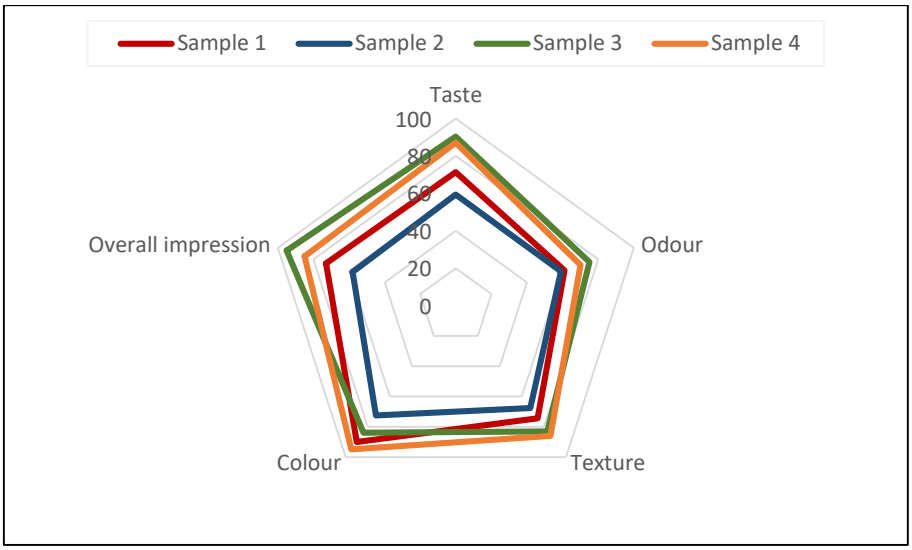

Figure 3. Sensory evaluation of muesli samples

Conclusion

Our study can reveal that the fruit waste generated from the processing industry can be used as an ingredient of muesli product. The sour cherry, cherry and black currant pomace have high content of bioactive compounds, so using as a food component of these waste materials is important way to utilize them. All created muesli samples have very good consumer acceptance and muesli-like properties base on the sensory evaluation.

References

[1] Global production of fresh fruit from 1990 to 2020. https://www.statista.com/statistics/262266/global-production-of-fresh-fruit/ (20 October 2022)
[2] E.-R. Lee, G.-H. Kang, S.-G. Cho, Recent Pat. Biotechnol. 1 (2007) 139–150.
[3] M. Karwacka, K. Rybak, M. Świeca, S. Galus, M. Janowicz, Sustain. 14 (2022) 13012.
[4] Y. Galali, Z.A.Omar, S.M. Sajadi, Food Sci. Nutr. 8 (2020); 8: 3004– 3022.
[5] J. Majerska, A. Michalska, A. Figiel, Trends Food Sci. Technol. 88 (2019**)** 207–219.
[6] C. Sabater, V. Sabater, A. Olano, A. Montilla, N. Corzo, Food Hydrocoll. 98 (2020) 105238
[7] E. Gençdağ, A. Görgüç, F.M. Yılmaz, Food Rev. Int. 34 (2021) 447–468.
[8] D.A Campos, R. Gómez-García, A.A. Vilas-Boas, A.R. Madureira, M.M. Pintado, *Molecules* 25 (2020**)** 320.
[9] A. Quiles, G.M. Campbell, S. Struck, H. Rohm, I. Hernando, Food Rev. Int. 34 (2006) 162–181.
[10] V. Singleton, J. Rossi AJEV 16 (1965) 144–158.
[11] I.F.F. Benzie, J.J. Strain, Anal Biochem. 239 (1996) 70–76.

REDUCING MEMBRANE FOULING WITH 3D PRINTED SPACERS

Nikolett Sz.Gulyás[1], Szabolcs Kertész[2], Cecilia Hodúr[2]

[1]Institute of Environmental Science and Technology, University of Szeged, H-6725 Szeged, Tisza Lajos krt. 103., Hungary
[2]Department of Biosystems Engineering, Faculty of Engineering University of Szeged, H-6725 Szeged, Moszkvai krt. 9., Hungary
e-mail: gulyasn@mk.u-szeged.hu

Abstract

The dairy industry, like most other food industries, produces a large volume of wastewater which contains diluted milk and chemicals (acids, alkalis, detergents). There are many technologies used to treat dairy wastewater, such as biological and physico-chemical methods but they have their disadvantages (high operating costs, high space requirements, operational difficulties). Membrane technologies are promising methods to treat dairy wastewaters. The main disadvantage of membrane filtration in dairy wastewater treatment is membrane fouling, which causes flux decline, decreased membrane life-time, and increased operational cost.
One way to reduce the fouling is to increase the surface shear rate of the membrane. The method for increasing shear rate is to change flow properties (stirring and using 3D printed spacers). 3D printing technology is an emerging and promising technology to create an object through a layer-by-layer fabrication method. 3D printing technology and membrane module design, it could potentially address the membrane fouling problem through the optimization of spacers to increase mass transfer and reduce the concentration polarization at the membrane surface. 3D printing technology could possibly revolutionize the current design of membrane modules and potentially reduce the energy consumption and chemical usage in the wastewater treatment.
Ultrafiltration (*UF*) experiments were performed model dairy wastewater with different transmembrane pressures (0.2, 0.3 and 0.4 MPa) and stirring velocities (200, 300 and 400 rpm). Polyethersulfone (*PES*) UF membranes with molecular weight cut-off (*MWCO*) of 50 kDa and polylactic acid (*PLA*) 3D printed spacer configurations were used. The permeate flux values, resistances and membrane rejection were examined and the effect of spacer was observed.

Acknowledgements

The authors are thankful for the financial support of the János Bolyai Research Scholarship of the Hungarian Academy of Sciences (BO/00576/20/4) and the New National Excellence Program of the Ministry of Human Capacities (UNKP-22-5-SZTE-210)

References

[1] Lee J-Y., Tan, S. W., An J., Chua K. C., Tang Y. C., Fane G. A., Chong H. T. (2016): The potential to enhance mebrane module design with 3D printing technology, Journal of Membrane Science, 499, 480-490
[2] Sarkar, B., Chakrabarti, P. P., Vijaykumar, A., Kale, V. (2006):Wastewater treatment in dairy industries: possibility of reuse, Desalination, 195(1–3), pp. 141–152.
[3] Yanar, N., Kallem, P., Son, M., Park, H., Kang, S., Choi, H., (2020): A New era of water treatment technologies: 3D printing for membranes, Journal of Industrial and Engineering Chemistry, 91, pp. 1-14.

INVESTIGATION OF THE UV/PERSULFATE PROCESS FOR THE ELIMINATION OF TRIMETHOPRIM ANTIBIOTIC – THE EFFECT OF MATRIX AND INORGANIC IONS

Adrienn Szirmai, Luca Farkas, Tünde Alapi

Department of Inorganic and Analytical Chemistry, University of Szeged, H-6720 Szeged, Dóm tér 7, Hungary

Antimicrobial resistance is one of the most emerging health crises due to the release of antibiotics into the environment. The WHO declared in 2019 that antibiotic resistance is among the ten most serious environmental risks. Nevertheless, antibiotic use increased sharply during the COVID-19 pandemic, as more than half of those infected with the coronavirus received antibiotics to prevent bacterial infection. These antibiotics and their biologically active metabolites are present in domestic and hospital wastewater effluents. Various UV-based advanced oxidation methods can be used in the degradation of pharmaceuticals due to the generation of reactive hydroxyl radicals. Besides these processes, sulfate radical ($SO_4^{\bullet-}$) based techniques have become widely investigated in recent years.

This study investigated UV photolysis combined with peroxydisulfate ion (PDS) to eliminate trimethoprim, a widely used and hardly biodegradable antibiotic from aqueous solutions. The low-pressure mercury-vapor lamp emits 254 nm UV light as a light source. The direct UV photolysis is negligible for trimethoprim elimination, and the addition of PDS enhanced the transformation and mineralization rate due to the formation of reactive $SO_4^{\bullet-}$ via direct photolysis.

The effect of inorganic ions, such as Cl^- and HCO_3^-, and biologically treated domestic wastewater as a matrix were also investigated. Biologically treated domestic wastewater diminished the transformation and mineralization efficiency. Using 1.0×10^{-4} M trimethoprim and 1.0×10^{-3} M PDS concentration, the transformation stopped after 3 minutes, and no more than 30% degradation was reached. Using doubled PDS concentration, the negative matrix effect was moderated. Since both Cl^- and HCO_3^- react with $SO_4^{\bullet-}$, their influence was studied separately and together. The degree of inhibition was far below the value expected based on their radical scavenging capacity. The formed secondary radicals, $Cl^\bullet$ and $CO_3^{\bullet-}$, can react with trimethoprim or initiate the formation of other reactive species, such as $^\bullet OH$. The formation of chlorinated products proved the contribution of $Cl^\bullet$ to the transformation. The presence of HCO_3^- diminished the formation of chlorinated products, most likely due to the reaction between $Cl^\bullet$ and HCO_3^- resulting in Cl^- and $CO_3^{\bullet-}$. However, the reactions between inorganic ions and $SO_4^{\bullet-}$ require further investigation due to the complexity of the multi-component solutions containing various reactive species.

Acknowledgment

This work was sponsored by the National Research, Development, and Innovation Office-NKFI Fund OTKA, project number FK132742.

SYNTHESIS AND PHYSICOCHEMICAL EVALUATION OF NEW CHITOSAN-BASED SCAFFOLDS FOR POTENTIAL APPLICATION IN BIOMEDICINE

Martina Žabčić[1], Nataša Nikolić[1], Dušan Mijin[1], Zorica Kačarević Popović[2], Slavica Porobić[2], Julijana Tadić[2,*]

[1]University of Belgrade, Faculty of Technology and Metallurgy, Karnegijeva 4, Belgrade, Serbia
[2]University of Belgrade, Vinča Institute of Nuclear Sciences, National Institute of the Republic of Serbia, Mike Petrovića Alasa 12-14, Belgrade, Serbia
e-mail: julijana.tadic@vin.bg.ac.rs

Abstract
Chitosan is a natural polymer obtained by deacetylation of chitin. Due to its biocompatibility and biodegradability, chitosan-based materials have a wide range of biomedical applications in wound dressings, drug delivery systems, and tissue engineering. Also, studies in the fields of organic and medicinal chemistry show that compounds based on the pyridone core exhibit biological properties including antimicrobial, anticancer, and antioxidant activity, and moreover have the potential as new therapeutics for various diseases from cardiovascular to antitumor therapy. In this study, new biomaterials were synthesized using low and medium molecular weight chitosan polymers and pyridone-based hydrazone. In order to improve stability of the obtained scaffolds, scaffolds' neutralization was carried out using ethanol and sodium hydroxide solutions. The interactions established between chitosan polymer chains and pyridone compound were analyzed by FT-IR spectroscopy. Swelling and degradation tests of the materials were studied in water and PBS, and the influence of different polymer molecular weights on the scaffolds' properties was evaluated. The results indicated that synthetized scaffolds have a high potential for biomedical use.

Introduction
Chitosan is a linear polysaccharide consisted of D-glucosamine and N-acetyl-D-glucosamine units connected by the β-(1-4) glycosidic bond. This polysaccharide shows antibacterial, antifungal, analgesic, and antioxidant activity, hemostatic properties, and excellent biocompatibility [1,2]. All these unique characteristics make chitosan an outstanding candidate for biomedical applications. Development of biomaterials is a very attractive research field aiming to design scaffolds for the regeneration of tissues and organs damaged by disease or injuries [3]. Today, chitosan-based biomaterials have major applications in tissue engineering due to their biocompatibility and therapeutic properties [4]. Pyridone-based arylhydrazones have gained attention in the fields of biomedicine and bioimaging regarding their both biological and optical properties [5-7]. Furthermore, they exhibit antibacterial, antifungal, antioxidant, analgesic, anti-inflammatory, antitubercular and anticancer properties [8]. Taking that into account, in this study, we synthetized new scaffolds using chitosan and pyridone-based arylhydrazones, and evaluated their physicochemical properties important for potential application in biomedical research.

Experimental
Low molecular weight chitosan (50-190 kDa) and medium molecular weight chitosan (190-310 kDa), HIT-LW and HIT-MW, hereinafter, were purchased from Merck, and pyridone-based arylhydrazone was synthetized and characterized in our previous study [9]. In order to prepare

the scaffolds, HIT-LW and HIT-MW were dissolved in the acetic acid (2% v/v) to obtain 2% w/v solutions of HIT-LW and HIT-MW. Prepared chitosan solutions were stirred with heating at 50°C for 3 hours. Previously synthesized pyridone-based compound was dissolved in ethanol (4 mg in 5 ml of EtOH) and added to each HIT-LW and HIT-MW solution. Obtained mixtures were stirred with heating at 50°C for 1 hour. Resulting mixtures HIT-LW-PY and HIT-MW-PY were poured into the Petri dishes and left at -18°C for 24 hours. Frozen mixtures of HIT-LW-PY and HIT-MW-PY were freeze-dried for 48 hours, at a temperature of -50°C and a pressure (~0.1 mbar) to obtain 3D porous scaffolds. Along with the synthesis of new scaffolds, control materials were also synthesized, by freeze-drying HIT-LW and HIT-MW without addition of pyridone. The stabilization of prepared scaffolds was done by using NaOH and EtOH. The materials were immersed in 0.25 M NaOH solution, and in absolute ethanol and 70% ethanol, washed with distilled water, frozen and freeze-dried again. Fourier transform infrared (FT-IR) spectra of the scaffolds were recorded using a Nicolet™ iS™ 10 FT-IR Spectrometer (Thermo Fisher Scientific) with Smart iTR™ Attenuated Total Reflectance (ATR) sampling accessories. The FT-IR spectra were recorded in the 4000-500 cm−1 range with 20 scans per spectrum.

The swelling properties were determined by the conventional gravimetric method [10]. The chitosan-based scaffolds (disc; diameter 20 mm, thickness 0.5 mm) were weighed (W_0) and then immersed in water and weighed in specific time periods (W_s) until constant weight was reached. The equilibrium swelling degree was calculated using equation $SD_{eq} = \frac{W_s - W_0}{W_0}$.

The *in vitro* degradation was tested after incubation of 28 days in PBS at 37˚C [10]. Initial weights of the materials were obtained as W_0. After immersion, the scaffolds were washed in distilled water, frozen and freeze-dried, and then weighted and labeled as W_d. The degradation of the scaffolds (D) was calculated using equation $D(\%) = \frac{W_0 - W_d}{W_0} \cdot 100$.

Results and discussion

The interactions established between scaffolds' components were evaluated by FT-IR spectroscopy. The spectra of the synthetized scaffolds and control samples are shown in Fig. 1. In Fig. 1 A), the spectra of the prepared scaffolds after neutralization in ethanol are presented. The spectra of control scaffolds showed characteristic bands in the regions of 3000–3600 cm^{-1} (–OH and –NH groups of chitosan) and 2800–3000 cm^{-1} (CH groups). The bands at 1652 cm^{-1} and 1563 cm^{-1} were assigned to the amide I and amide II groups. The peak at 1153 cm^{-1} indicated the stretching vibrations of the C–O–C bonds, while the peaks at 1068 cm^{-1} and 1026 cm^{-1} corresponded to the vibrations of the C–O bonds [10]. The spectra of new scaffolds showed the characteristic bands for chitosan polymer including some changes in the intensity of the band in the region of 3000–3600 cm^{-1} indicating hydrogen bonding between chitosan and pyridone-based arylhydrazone. In Fig. 1 B), the spectra of scaffolds stabilized in sodium hydroxide showed same characteristic peaks as the spectra of materials stabilized in ethanol indicating that method of neutralization, i.e., stabilization of the material did not affect the material chemical structure. The hydrogen bonding of chitosan and pyridone-based compound is illustrated in Fig. 2.

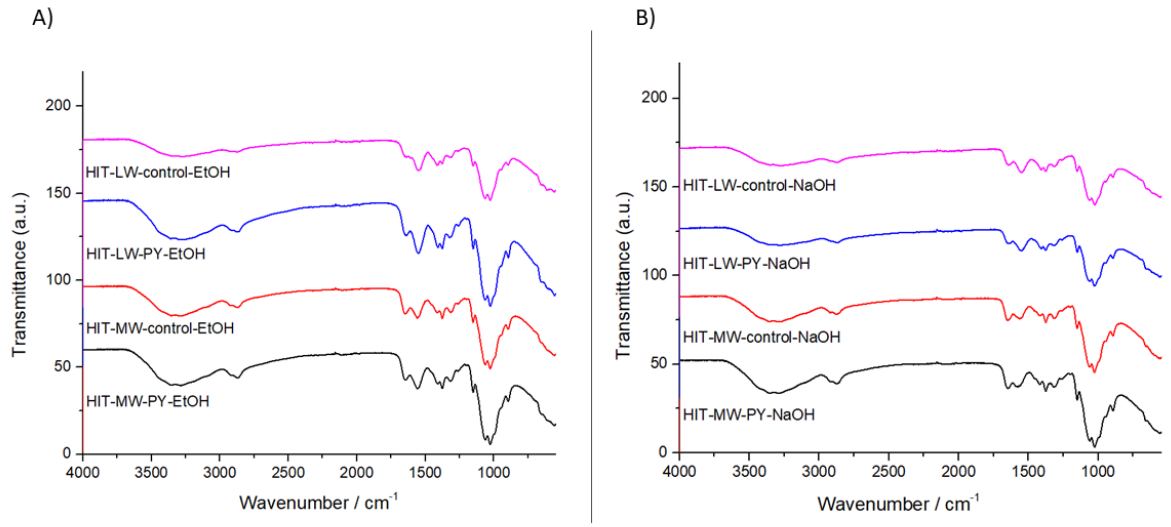

Figure 1. FT-IR spectra of new scaffolds and control samples A) stabilized in EtOH and B) stabilized in NaOH

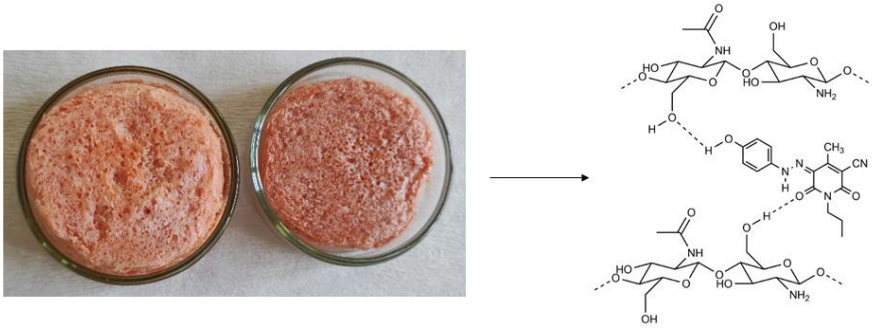

Figure 2. The illustration of synthetized scaffolds and the hydrogen bonding of the chitosan and pyridone-based arylhydrazone

From the standpoint of biomedical application, adequate swelling ability, porosity and degradation are very important factors in scaffold design. The swelling properties of the scaffolds was evaluated in water for 300 minutes, and obtained results are presented in Fig. 3. HIT-LW-PY-EtOH and HIT-MW-PY-EtOH scaffolds swelled very rapidly absorbing a large amount of water, and reaching the equilibrium swelling degree within initial 30 minutes (Fig. 3 A)). The scaffolds HIT-LW-PY-NaOH and HIT-MW-PY-NaOH swelled fast reaching the equilibrium swelling degree, also, within first 30 minutes (Fig. 3 B)). By comparing the HIT-LW-PY-EtOH and HIT-MW-PY-EtOH to the HIT-LW-PY-NaOH and HIT-MW-PY-NaOH, it can be noted that scaffolds stabilized in sodium hydroxide have a lower value of the equilibrium swelling degree (Fig. 3 C)) which may be attributed to their pore size (less porous comparing to the those stabilized in ethanol) obtained after stabilization. Also, the influence of different molecular weights of chitosan polymer on the equilibrium swelling degree was more pronounced in case of the scaffolds obtained by the stabilization in sodium hydroxide. Namely, HIT-MW-PY-NaOH has about a 50% higher value of the equilibrium swelling degree comparing to HIT-LW-PY-NaOH, which can generally be ascribed to the larger and more crosslinked medium molecular weight chitosan chains leading to a greater expansion of the

scaffold's network. However, it is clear that materials treated in ethanol have a higher absorption capacity so the stabilization method affected the scaffolds swelling properties.

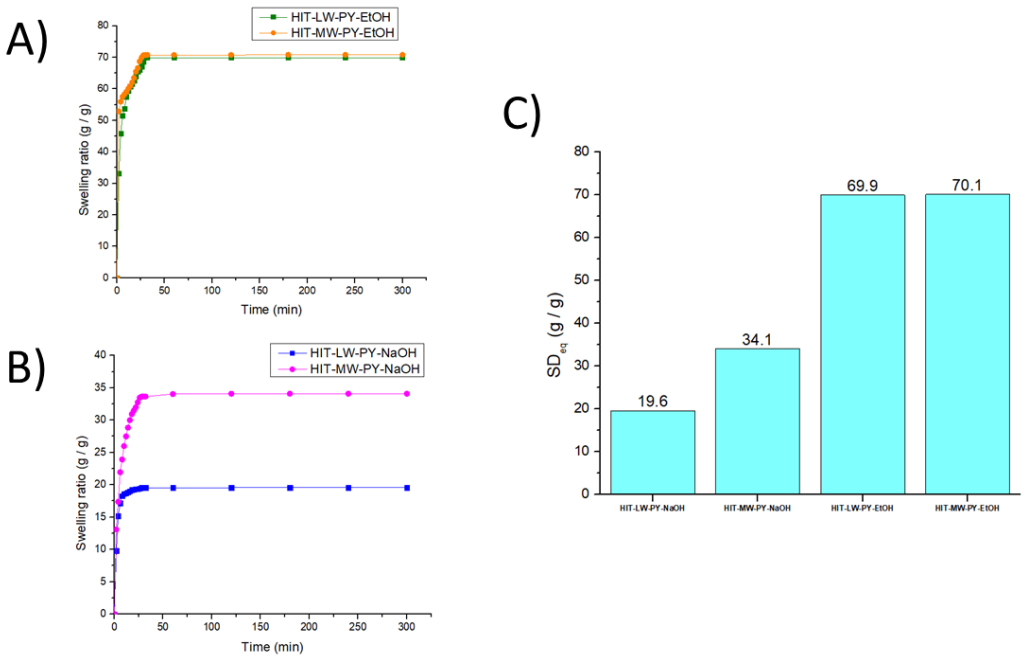

Figure 3. Swelling test in water

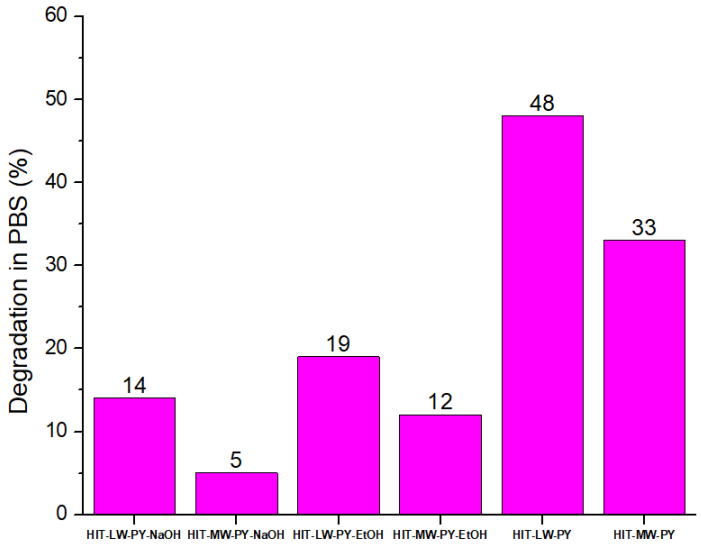

Figure 4. Degradation test in PBS

The degradation properties of the scaffolds were investigated in PBS after 28 days, and obtained results pointed out that molecular mass of chitosan and the method of stabilization affect the degradation degree of synthesized materials (Fig. 4). The scaffolds consisted of the low molecular weight chitosan had a higher degradation degree comparing to the those synthetized of the medium molecular weight chitosan. Also, materials stabilized in sodium hydroxide showed lower degradation in PBS compared to the materials stabilized in ethanol. Contrary, scaffolds that are not stabilized exhibited a significantly higher degradation in PBS indicating the importance of scaffold stabilization for further use.

Conclusion

In this work, new chitosan-pyridone-based scaffolds were synthesized and characterized. The structure of scaffolds and the formation of hydrogen bonds, between chitosan and pyridone derivative, were confirmed and observed by FT-IR spectroscopy. The swelling and degradation

tests in water and PBS highlighted that the scaffolds stabilized in ethanol exhibited adequate physicochemical properties and have the potential for further development and application in biomedical research field.

Acknowledgements
This work was supported by the Ministry of Education, Science and Technological Development of the Republic of Serbia (grant no. 451-03-68/2022-14/200017, 451-03-68/2022-14/200135)

References
[1] F. Croisier, C. Jérôme, European Polymer Journal 49 (2013) 780-792.
[2] F. Luan, L. Wei, J. Zhang, W. Tan, Y. Chen, F. Dong, Q. Li, Z. Guo, Molecules 23 (2018) 516
[3] B. Sultankulov, D. Berillo, K. Sultankulova, T. Tokay, A. Saparov, Biomolecules 9 (2019) 470
[4] A. Madni, R. Kousar, N. Naeema, F. Wahid, Journal of Bioresources and Bioproducts 6 (2021) 11-25
[5] X. Ran, Q. Zhou, J. Zhang, S. Wang, G. Wang, H. Yang, X. Liu, Z. Wang, X. Yu, Organic Chemistry Frontiers 8 (2021) 3631-3638
[6] Y. Ali, S. A. Hamid, U. Rashid, Mini-Reviews in Medicinal Chemistry 18 (2018) 1548-1558
[7] H. Ur R. Shaha, K. Ahmada, H. A. Naseema, S. Parveena, M. Ashfaqa, T. Aziz, S. Shaheena, A. Babras, A. Shahzad, Journal of Molecular Structure 1244 (2021) 131181
[8] J. D. Tadić, J. M. Lađarević, Ž. J. Vitnik, V. D. Vitnik, T. P. Stanojković, I. Z. Matić, D. Ž. Mijin, Dyes and Pigments 187 (2021) 109123
[9] J. Tadić, J. Lađarević, M. Svetozarević, L. Matović, A. Mašulović, D. Mijin, Conference proceedings, ISBN 978-86-85535-08-6, 34, Procesing ’21, Jun 3-4, 2021, Novi Sad, Serbia.
[10] J. Hu, Z. Wang, J. M. Miszuk, M. Zhu, T. I. Lansakara, A. V. Tivanski, J. A. Banas, H. Sun, Carbohydrate Polymers, 271 (2021) 118440.

ENZYME-LINKED FLUORESCENT IMMUNOASSAY FOR MONITORING THE HERBICIDE ACTIVE INGREDIENT GLYPHOSATE IN WATER

Eszter Takács[1], Borbála Gémes[1], Fanni Szendrei[2], Csaba Keszei[2], Attila Barócsi[3], Sándor Lenk[3], László Domján[4], Mária Mörtl[1], Szandra Klátyik[1] András Székács[1]

[1]Agro-Environmental Research Centre, Institute of Environmental Sciences, Hungarian University of Agriculture and Life Sciences, H-1022 Budapest, Herman O. út 15, Hungary
[2]Institute of Isotopes Co. Ltd., H-1121 Budapest, Konkoly-Thege Miklós út 29-33, Hungary
[3]Department of Atomic Physics, Institute of Physics, Budapest University of Technology and Economics, H-1111 Budapest, Műegyetem rkp. 3, Hungary
[4]Optimal Optik Ltd., H-1118 Budapest, Dayka Gábor u. 6/B, Hungary
e-mail: takacs.eszter84@uni-mate.hu

Abstract
Within a modular water quality assessment fluorimeter instrument family, a newly developed enzyme-linked fluorescent immunoassay has been utilized for the quantitative analytical measurement of the herbicide active ingredient glyphosate in surface water. The developed 96-well microplate-based competitive immunoassay with fluorescence detection provides a 2.5-fold lower limit of detection (LOD = 0.09 ng/mL) in the investigated concentration range of glyphosate (0–100 ng/mL) compared to the detection of visual absorbance signals. Additionally, fluorescence detection resulted in a wider dynamic range for glyphosate measurement. Matrix effect was not observed for the undiluted surface water samples, and cross-reaction was not detected between glyphosate and its main metabolite (N-aminomethylphosphonic acid) and structurally similar compounds. The method allows rapid monitoring of glyphosate as a ubiquitous water contaminant of agricultural origin that can affect, due to its global use, both aquatic and terrestrial ecosystems.

Introduction
Various organic micropollutants (e.g., pesticides) have been identified as emerging water pollutants that can exert possible adverse effects on the ecological environments. Due to the intensive use of various plant protection products as still major tools in agrochemical crop protection, continuous monitoring of pesticide residues is required in surface waters [1]. Glyphosate (N-(phosphonomethyl) glycine) is one of the most widely and globally used herbicide active ingredients. Due to the outstandingly high application rate (globally around 800 thousand tons per year, in the European Union 30-9600 tons per year varying among different member states), glyphosate has become a ubiquitous water contaminant [2,3]. The environmental fate of glyphosate in water and in soil is highly affected by various abiotic and biotic factors (e.g., physical and chemical characteristics of the matrix, environmental conditions, pH, composition and stability of the microbial communities capable to facilitate decomposition). The degradation or dissipation of glyphosate can be much slower in the presence of various metal ions (e.g., Al, Mn Fe) in soil due to the substantial complex formation capacity of glyphosate [4]. As a result of its high water solubility, the appearance of glyphosate is a globally observed phenomenon in surface waters [2]. The occurrence of glyphosate as an agrochemical residue was proved in different agricultural products (e.g., soybean, maize, and certain fruits and vegetables), food (e.g., bread, cereal products, honey, olive oil, fruit juices, alcoholic beverages, beer, wine), and biological samples as well (e.g., the urine of livestock and humans) [5,6].

Recently, various quantitative analytical procedures (e.g., spectrophotometric and chromatographic methods) have been developed for the determination of glyphosate [7–10] in different natural samples, but most of these techniques are expensive, time-consuming, and need specialized instrumentation. Within Project Aquafluosense [11], the aim was to develop a new modular induced fluorescence-based instrument family as a water analysis system for *in situ* assessment and monitoring of quality of natural and artificial waters. The aim of the present study was to develop an enzyme-linked fluorescent immunoassay (ELFIA) module prototype within the above-mentioned instrument family for the quantitative detection and monitoring of glyphosate.

Experimental

The immunofluorescence module of the prototype developed within Project Aquafluosense is suitable for the *in situ* quantification of organic micropollutants by the use of immunoanalytical procedures. The development of the instrumentation (e.g., optics, sample holder, and detector electronics) was conducted by consortium partners at the Budapest University of Technology and Economics (Budapest, Hungary) and at Optimal Optik Ltd. (Budapest, Hungary), as described by Gémes *et al.* [12]. During the measurement, the samples were illuminated by an LED light source, and fluorescence emission was detected by a dichroic beam path with silicon photodiodes. The applied competitive ELFIA is based on a phase-heterologous competition and interaction between the immobilized hapten analogue conjugate on the surface of the 96-well microplate and the analyte in the samples. During the immunoassays, the glyphosate analogue haptenic compound prepared by the Institute of Isotopes Co. Ltd. (Budapest, Hungary), and the commercially available N-(phosphonolmethyl)iminodiacetic acid (PMIDA) was reacted with succinic anhydride and conjugated to human serum albumin (HSA). After dialization and lyophilization, the conjugate was used for the production of the coated microplate as the solid phase in this assay. During the analysis 100 µL of standard/control/sample and 40 µL of the derivatization mixture were homogenized, then 100 µL of borate buffer was added, and a 20-minute incubation was applied. The microplates were coated with glyphosate analogue hapten conjugate (0.5 µg/mL), and the unbound conjugate was washed off with washing buffer. After the derivatization, 100 µL chicken polyclonal anti-glyphosate (0.4 µg/mL), as a primary antibody and 20 µL of derivatized standard/control/sample were added to each well, then microplates coated with glyphosate-analogue-HSA conjugate were incubated (at room temperature, 2 h), then the wells were washed with 250 µL of diluted washing buffer, and finally 100 µL of tracer (0.5 µg/mL) goat anti-chicken IgY–HRP, as a secondary antibody was added and incubated (room temperature, 30 min). After washing off the unbound secondary antibodies, 100 µL/well of working solution (1:50:50 v/v mixture of ADHP, peroxide, and enhancer) ensured by QuantaRed Enhanced Chemifluorescent HRP Substrate Kit was added. After a 5-minute incubation, the enzymatic activity was stopped by 10 µL of QuantaRed Stop Solution, and the absorbance of the final product resorufin was detected at 576 nm by a SpectraMax iD3 Multi-Mode Microplate Reader. Fluorescence was measured at 593 nm by the immunofluorescence module developed within Project Aquafluosense [13, 14]. The applicability and the matrix effect were examined in surface water samples of different origins based on a comparison of the calibration curves obtained. Surface water samples were collected from various Hungarian natural and artificial water bodies and their catchment areas (e.g., River Danube, Lake Balaton, Visegrád Trout Lake). The accuracy and specificity of the immunoassay were also tested. Statistical analyses of the standard curves were performed by the comparison of IC_{50} values with the use of the one-way ANOVA method followed by *post hoc* Tukey tests (with a significance level of 0.05).

Results and discussion

A hapten-homologous competitive immunoassay was developed in a heterologous phase format with the use of colorimetric substrates with chromophores for fluorescence and visual detection, and was optimized for the detection of glyphosate in surface water. During the immunoassay on the solid surface of the microplate, a protein conjugate of glyphosate was immobilized to react with the glyphosate-specific antibody resulting in immunocomplex formation, which is competitively inhibited by glyphosate present in the sample. During the measurements, a derivatization step was needed to reach the highest utilization of the antibody avidity and affinity. Based on the calibration curves and LODs determined using both absorbance and fluorescence signals, the two modes of detection were compared (Figure 1). The developed ELFIA for the detection of glyphosate was characterized with LOD values of 0.22 and 0.09 ng/mL, for visual absorbance and fluorescence, respectively. The detection with induced fluorescence resulted in 2.5-fold lower LOD values compared to the visual absorbance, moreover, a wider and steeper dynamic range was provided as well, but the better LOD seems to be as a result of the very low standard deviation (SD) of the maximal signal, rather than the observed accuracy at points of partial inhibition by glyphosate.

Figure 1. Competitive indirect calibration curves of the immunoassay with a detection of absorbance at a wavelength of 576 nm in optical density (OD) units (blue) or fluorescence at a wavelength of 593 nm in relative fluorescence units (RFU) (red) for glyphosate in assay buffer [14].

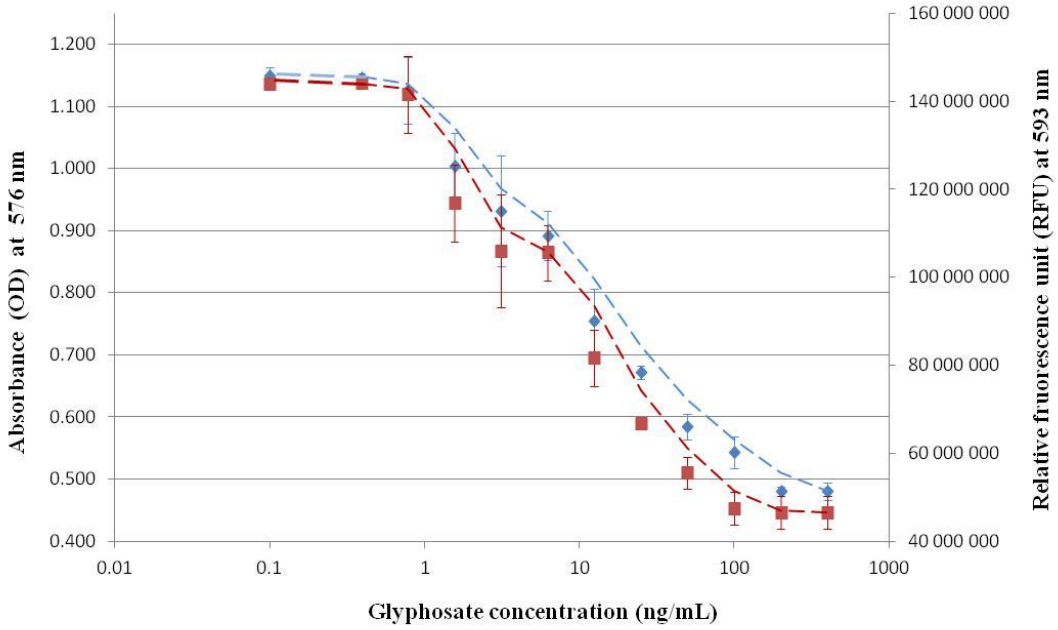

The developed ELFIA method as a part of the modular device system designed by Project Aquafluosense for *in situ* measurements of various parameters characterizing the water quality of natural and artificial water bodies. However, the coating and the blocking steps of the microplate were performed under laboratory conditions before performing the immunoassay. During the coating step, a glyphosate analogue conjugated to HSA was immobilized onto the solid surface of the microplate by passive adsorption, while with the application of the optimal conjugate concentration, the desorption was negligible and did not affect the reliability of the assay. Stabilization of the coated and blocked plates was carried out with the use of 300 µL/well of a 2% aqueous saccharose solution. The duration of the total immunoassay is approximately

3 h (20 min – derivatization, 2 h – incubation with the sample and the first antibody, with washing steps, 30 min – incubation with the second antibody, 2–10 min – signal development) for the measurement of 25 parallel samples in the 96-well microplate format, but the microplates were needed to be the covered during the process to prevent evaporation. Due to the reversibility of HAS adsorption at low pH, the repeated use of the microplates is potentially allowed, however, reuse of the microplates is not common in ELISA/ELFIA protocols.

The results of the determination of the intra-assay and inter-assay SDs indicated that the reproducibility, reliability, and accuracy of the assays is not optimal towards the lower plateau of the typical sigmoid calibration curve, thus the SD of the measurements is higher near the LOD than at the IC_{50} level, which affects the precision of the glyphosate detection. At the lower concentrations, the coefficient of variability (CV) is 25.1 and 15.0 for intra- and inter-assay, respectively, while near the IC_{50} (10.75±9.07 ng/mL), the CV values are 8.7 and 7.7, respectively. Based on the results, structurally similar compounds can affect the results of the measurements only at environmentally not relevant extremely high concentrations, while the detection of glyphosate in soil, surface water, and plant tissue samples can be disturbed by phosphate ions, therefore the inhibition of the glyphosate-specific antibody by phosphate was also needed during the measurements.

During the investigation of the matrix effects in surface water samples, the matrix effect was evaluated by the statistical comparison of IC_{50} values of the calibration curves of ELFIA measurements at the concentration range of 0–100 ng/mL of glyphosate. No matrix effect was observed in the surface water samples (Figure 2), and ELFIA proved to be capable for the accurate detection of glyphosate below the official limit (0.1 ng/mL) of pesticide residues (residues of individual pesticide active ingredients and their metabolites) in drinking water in the European Union [15].

Figure 2. Competitive indirect calibration curves of the immunoassay with a detection of fluorescence at a wavelength of 593 nm in relative fluorescence units (RFU) for glyphosate in assay buffer (blue) and in undiluted surface water samples from River Danube (red) [14]

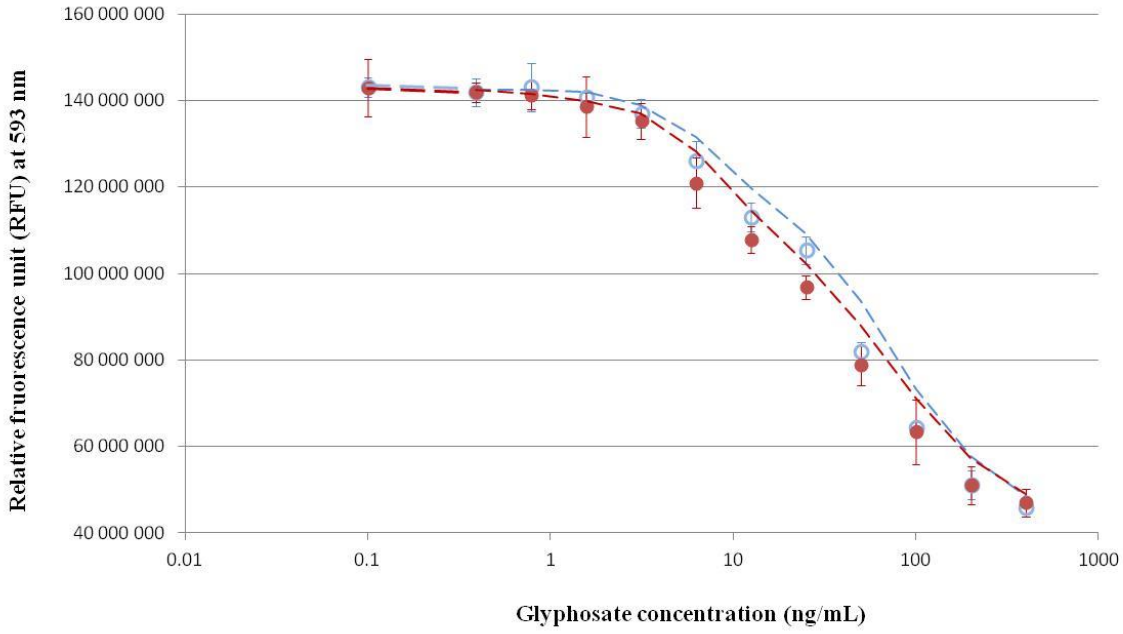

Conclusion

Enhanced sensitivity with a lower LOD was proved for the developed competitive ELFIA method compared to the measurement of the absorbance in the colorimetric assays. The applied glyphosate-specific antibody was not inhibited by AMPA and the other structurally similar compounds in the immunoassay. Fluorescent detection provides a suitable quantitative method for the detection of glyphosate in surface and tap waters below the maximum allowed limit for pesticide active ingredients [15], thus the ELFIA system performed in the immunofluorescence module of the novel, induced fluorimetry-based instrument prototype serves as a more cost-effective, *in situ*, highly sensitive tool of environmental monitoring for glyphosate in surface water.

Acknowledgements

The research was carried out within Project Aquafluosense (NVKP_16-1-2016-0049). The authors thank to László Kocsányi (Budapest University of Technology and Economics) for his expert advice during the development of the instrumentation.

References

[1] A. Székács, M. Mörtl, B. Darvas, J. Chem. 2015 (2015) 717948.
[2] W.A. Battaglin, M.T. Meyer, K.M. Kuivila, J.E. Dietze, JAWRA 50 (2014) 275–290.
[3] A. Székács, B. Darvas, Front. Environ. Sci. 6 (2018) 78.
[4] H. Vereecken, Pest. Manag. Sci. 61 (2005) 1139–1151.
[5] M. Krüger, W. Schrödl, J. Neuhaus, A.A. Shehata, J. Environ. Anal. Toxicol. 3 (2013) 5.
[6] D. Grau, N. Grau, Q. Gascuel, C. Paroissin, C. Stratonovitch, D. Lairon, D.A. Devault, J. Di Cristofaro, Environ. Sci. Pollut. Res. 29 (2022) 32882–32893.
[7] K. Qian, T. Tang, T. Shi, F. Wang, J. Li, Y. Cao, Anal.Chim. Acta 635 (2009) 222–226.
[8] F. Sánchez-Bayo, R.V. Hyne, K.L. Desseile, Anal. Chim. Acta 675 (2010) 125–131.
[9] C.D. Stalikas, C.N. Konidari, J. Chromatogr. A 907 (2001) 1–19.
[10] R. Jan, J. Shah, M. Muhammad, B. Ara, J. Hazard. Mater. 169 (2009) 742–745.
[11] Aquafluosense. Development of a modular, direct and immunofluorimetry as well as plasma spectroscopy based detector and instrument family for in situ, complex water quality monitoring, and application studies. Available online: http://aquafluosense.hu (accessed on 26 October 2022).
[12] B. Gémes, E. Takács, P. Gádoros, A. Barócsi, L. Kocsányi, S. Lenk, A. Csákányi, S. Kautny, L. Domján, G. Szarvas, N. Adányi, A. Nabok, M. Mörtl, A. Székács, Toxins 13 (2021) 182.
[13] Thermo Fisher Scientific Inc. Instructions. QuantaRed™ Enhanced Chemifluorescent HRP Substrate; Thermo Fisher Scientific Inc.: Rockford, USA, 2008; pp. 1–3. Available online: https://assets.thermofisher.com/TFS-Assets%2FLSG%2Fmanuals%2FMAN0011632_QuantaRed_Enhan_ChemiFluores_HRP_Subs_UG.pdf (accessed on 26 October 2022).
[14] E. Takács, B. Gémes, F. Szendrei, C. Keszei, A. Barócsi, S. Lenk, L. Domján, M. Mörtl, A. Székács, Molecules 27 (2022) 6514.
[15] European Parliament and Council, Directive (EU) 2020/2184 of the European Parliament and of the Council of 16 December 2020 on the quality of water intended for human consumption. Off. J. Eur. Union L435 (2020) 1–62.

ELABORATION OF ONE-POT STRATEGIES FOR THE SYNTHESIS OF BODIPY DYES

Zita Tamási, Erzsébet Mernyák

University of Szeged, Department of Organic Chemistry, H-6720 Szeged, Dóm tér 8.

BODIPY (4,4-difluoro-4-bora-3a,4a-diaza-s-indacene) dyes have been discovered in 1968, however they are still widely utilized [1]. Owing to their favorable optical, chemical and biological properties, these dyes might be used in several fields, including bioimaging, optoelectronics and photodynamic therapy. Halogenated BODIPYs appeared as effective photosensitizers, however they display high dark cytotoxicity, owing to the presence of the heavy halogen atoms. Recently, orthogonal BODIPY dimers have come into the focus of attention [2]. The dimeric derivatives might be considered as unique alternatives to halogenated monomers, by exhibiting low dark toxicity and high phototoxicity, even at low concentrations. Nevertheless, the photosensitization mechanism of the dimers is still unclarified. In order to investigate their mechanism of action, there is a great demand for their better accessibility. The current synthetic strategies afford the dimers in very low yields.

Our aim was to elaborate effective methodologies towards the synthesis of BODIPY derivatives. Considering the principles of green chemistry, we planned to simplify the synthetic routes by minimizing the reaction time and the number of the reaction steps.

We worked out a one-pot procedure leading to BODIPY dyes starting from aryl aldehydes or carboxylic acid derivatives. The acylation of the disubstituted pyrrole was achieved in a microwave-assisted reaction, without using an acid catalyst. Functional groups capable of later conjugation were introduced by choosing the appropriate substituted acylating agent or *via* postfunctionalization. The transition metal-catalyzed dimerization of the monomers led to the desired dimers in good overall yield. We believe that optical and biomedical investigation of our newly synthesized BODIPY derivatives might provide valuable information for the design of photosensitizers with improved selectivity.

Acknowledgements
This work was supported by National Research, Development, and Innovation Office-NKFIH through project OTKA SNN 139323.

References
[1] E. Bassan, A. Gualandi, P.G. Cozzi, P. Ceroni, Chem. Sci. 12 (2021) 6607.
[2] N. Epelde-Elezcano, E. Palao, H. Manzano, A. Prieto-Castañeda, A.R. Agarrabeitia, A. Tabero, A. Villanueva, S. de la Moya, I. López-Arbeloa, V. Martínez-Martínez, M.J. Ortiz. Chem. Eur. J. 23 (2017) 4837

WASTEWATER PURIFICATION BY ADSORPTION WITH COMPOSITE MATERIALS

Ljiljana Tanasić[1], Milan Gličić[1], Jelena Tanasić[2], Bojan Damnjanović[3]

[1]*Unite for Agricultural and Business Studies and Tourism, Academy of Applied Studies Šabac, Vojvode Putnika 56, 15000 Šabac, Serbia*
[2]*University of Novi Sad, Faculty of Technology Novi Sad*
[3]*Unit for Medical and Business-Technological Studies, Academy of Applied Studies Šabac, Hajduk Veljkova 10, 15000 Šabac, Serbia*
e-mail: ljiljana3101@gmail.com

Abstract

The dyes to finding in wastewater-containing are very difficult to treat because dyes are recalcitrant molecules and resistant to aerobic digestion. There are more than 100 000 commercially available colors. Many industrial dyes are toxic, mutagenic, teratogenic, and carcinogenic. The synthetic dye cannot be effectively decolorized by traditional methods.

The physical method of adsorption does not lead to the creation of harmful substances and is superior to other methods. Synthetic dyes are considered the most difficult to treat because they contain complex aromatic structures, which make them more stable and harder to biodegrade. Decolorization is the result of adsorption and ion exchange mechanisms and depends on dye/sorbent interactions, sorbent surfaces, particle size, temperature, pH, and contact time. The most important step in wastewater treatment is to provide high-selectivity adsorbents that have a low cost and a long service life. The goal of our work was to prepare effective composite materials based on deacetylated chitin, i.e. poly(D-glucosamine) of medium molecular weight and bio-degradable non-toxic polysaccharide sodium alginate with magnetite nanoparticles for the removal of dyes from aqueous solutions. Composite alginate granules were coated with poly(D-glucosamine) using the layer-by-layer (LbL) application method. During the adsorption process, the dye concentration was monitored using a general spectrophotometric method.

Keywords: wastewater, dyes, adsorption, sodium alginate, magnetite nanoparticles

MONITORING AND STRATEGY TO REDUCE AIR POLLUTION IN CITIES -ŠABAC-

Ljiljana Tanasić[1], Milan Glišić[1], Suzana Knežević[1], Jelena Tanasić[2]

[1]*Unite for Agricultural and Business Studies and Tourism, Academy of Applied Studies Šabac, Vojvode Putnika 56, 15000 Šabac, Serbia*
[22]*University of Novi Sad, Faculty of Technology Novi Sad*
e-mail: ljiljana3101@gmail.com

Abstract
Air pollution in cities is always a topical issue, bearing in mind the fact that a large number of different sources of pollution are concentrated in a relatively small area. The increased dose of air pollution is a consequence of human activities, which negatively affects air quality, that is, it causes air pollution, which directly affects people's health.
The geomorphological characteristics of the Šabac area are very unfavorable from the point of view of air pollution (the city is surrounded by a wide plain, which reduces natural purification processes). The proximity of the Sava River causes increased air humidity, which creates conditions for the transformation of sulfur dioxide into sulfuric acid, which is more toxic than the primary pollutant. The industrial plant is in the immediate vicinity of the city and represents an aggravating factor, due to additional pollution. The vegetation between the industry and the settlement is very sparse, so there is no mitigation effect. The paper presents the results of the presence of pollutants and the reasons for their presence and suggests strategies for reducing pollution.

Keywords: monitoring, pollution, purification, reducing, increased dose.

DOUBLE-LAYER CAPACITANCE CHARACTERIZATION OF PORPHYRIN-MODIFIED GRAPHITE ELECTRODES

Bogdan-Ovidiu Taranu[1], Eugenia Fagadar-Cosma[2]

[1]National Institute for Research and Development in Electrochemistry and Condensed Matter, Dr. A.P. Podeanu street, No. 144, 300569, Timisoara, Romania
[2] Institute of Chemistry "Coriolan Dragulescu", Mihai Viteazu Ave. 24, 300223 Timisoara, Romania
e-mail: b.taranu84@gmail.com

Abstract
Porphyrin-modified graphite electrodes were manufactured and evaluated in terms of their double-layer capacitance. The highest value, of 14.017 mF/cm^2, was obtained for the electrode resulted by drop-casting a layer of 5,10,15,20-tetrakis(4-methoxy-phenyl)-porphyrin from benzonitrile on graphite support. Since a high double-layer capacitance value is characteristic of supercapacitors, out of the investigated samples, this electrode is the most likely to find application in their field.

Introduction
Porphyrins are a class of aromatic compounds that share the basic porphine structure, which is comprised of C, N and H atoms organized as a tetrapyrrolic ring, and is referred to as the porphyrin macrocycle. The structure can be peripherally substituted with different functional moieties and, additionally, almost any metal cation can be bound in its inner core. Changes to the macrocycle lead to porphyrin derivatives that possess various properties, which make them suitable for different applications [1]. For example, in a study reported by Taranu and Fagadar [2], the water splitting electrocatalytic properties of four free-base porphyrin structures were evaluated in alkaline medium after being used to manufacture a series of electrodes *via* their drop-casting on graphite substrates from different organic solvents, in one to three layers. The experimental results allowed the identification of the most electrocatalytically active porphyrin-modified graphite electrodes for the oxygen and hydrogen evolution reactions.

The present work is a continuation of the aforementioned study and focuses on the further electrochemical characterization of these electrodes, in terms of their electric double-layer capacitance - a parameter of importance in the field of supercapacitors. Organic electrode materials, such as porphyrins, are suitable for supercapacitor applications, because their morphology can be tailored and controlled, and they have very fast redox kinetics due to the small HOMO–LUMO gaps, which is consistent with the enhanced electrical conductivity of the material [3].

Experimental
The porphyrins employed in the study are 5-(4-pyridyl)-10,15,20-tris(4-phenoxy-phenyl)-porphyrin (P1), 5,10,15,20-tetrakis(4-methoxy-phenyl)-porphyrin (P2), 5,10,15,20-tetrakis(4-allyloxy-phenyl)-porphyrin (P3) and 5,10,15,20-tetrakis(*p*-tolyl)-porphyrin (P4), and their synthesis was performed using previously published procedures [4-7]. The organic solvents utilized to obtain the porphyrin solutions are N,N-dimethylformamide (DMF), dichloromethane (DCM) and benzonitrile (BN), purchased from Sigma Aldrich and Merck. Potassium chloride from Merck, ethanol from Honeywell and acetone from Chimreactiv (Bucharest) were also used during the study. Aqueous solutions were obtained with double

distilled water. The graphite substrates for electrode manufacturing were rods of spectroscopic graphite, type SW.114 from "Kablo Bratislava", National Corporation "Electrocarbon Topolcany" Factory (Slovakia).

The rods were wrapped in PE tubes, tightly attached to them *via* thermal treatment at 180 °C. The two rod ends were used as follows: one of them was connected to the potentiostat during the experiments, while the surface of the other was modified with the porphyrins by drop-casting them from different solvents and, while the voltammograms were recorded, was immersed into the electrolyte solution. The modification procedure involved: a) the polishing of the substrate surface using silicon carbide paper (800 and 1200 grit sizes) and felt; b) the subsequent washing with double-distilled water, ethanol and acetone; c) the drying at room temperature; d) the application of the porphyrin solution having 0.15 mM concentration on the polished surface (a volume of 10 µL was used to obtain each porphyrin layer) and e) the solvent evaporation stage. Table 1 presents the tags of the manufactured electrodes.

Table 1. The tags given to the porphyrin-modified graphite electrodes

Electrode tag	*Porphyrin*	*Solvent*	*No. of porphyrin layers*
$G_{P1\text{-}DCM\text{-}1}$	P1	DCM	1
$G_{P1\text{-}DMF\text{-}3}$	P1	DMF	3
$G_{P2\text{-}BN\text{-}1}$	P2	BN	1
$G_{P3\text{-}DCM\text{-}1}$	P3	DCM	1
$G_{P3\text{-}BN\text{-}1}$	P3	BN	1
$G_{P4\text{-}BN\text{-}1}$	P4	BN	1

The use of different solvents is justified in light of the ability of porphyrin molecules to self-assemble, resulting in aggregates bearing particular morphologies and properties. One way in which such structures are formed is by drop-casting the porphyrins on solid substrates from solvents having different polarity [8], thus influencing the aggregation mechanism.

The electrochemical setup consisted in a glass cell with three electrodes connected to a potentiostat (Voltalab PGZ 402 from Radiometer Analytical). A Pt plate (S_{geom} = 0.8 cm^2) served as auxiliary electrode, the Ag/AgCl (sat. KCl) electrode was employed as reference and the samples presented in Table 1 were utilized as working electrodes. The electrolyte was 0.1 M KCl aqueous solution. The experiments consisted in the recording of cyclic voltammograms at different scan rate (v) values. The cyclic voltammetry method can be used to determine the electric double-layer capacitance (C_{dl}), namely the capacitance from stored charge in the double-layer region at the interface between the electrode and the electrolyte [9]. First, voltammetry cycles were recorded in a potential range where no faradic currents were present. Second, the capacitive current density (i_{dl}) was calculated using equation (1) and third, the C_{dl} value was obtained as the absolute value of the slope from the i_{dl}-v linear dependence [6, 10].

$$i_{dl} = (i_a + i_c)/2 \qquad (1)$$

Where: i_{dl} [A/cm^2] is the capacitive current density; i_a and i_c [A/cm^2] are the absolute values of the anodic and cathodic current densities at a potential value where only double-layer adsorption and desorption features are present [11].

All potentials are expressed *vs.* the Ag/AgCl (sat. KCl) electrode and all experiments were performed at 23±2 °C.

Results and discussion

Figure 1 presents the plot of the dependence between the capacitive current density and the scan rate for the porphyrin-based graphite electrodes, while Table 2 shows the double-layer capacitance and R^2 values obtained for the same samples.

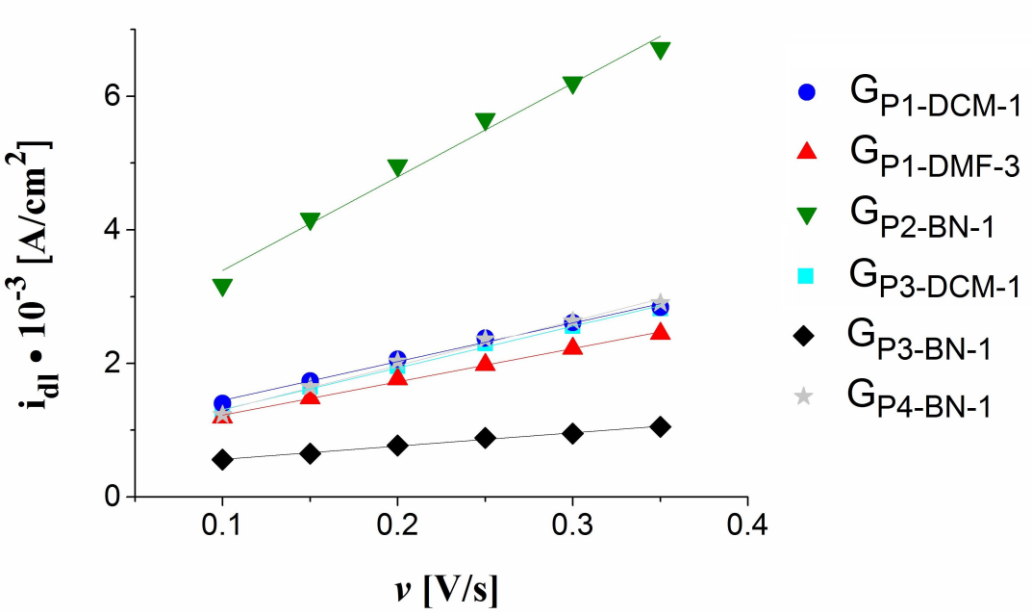

Figure 1. The graphical representation of the dependence between i_{dl} and v for the porphyrin-modified electrodes specified in Table 1, based on data from cyclic voltammograms recorded in 0.1 M KCl electrolyte solution, at v = 0.1, 0.15, 0.2, 0.25, 0.3 and 0.35 V/s.

Table 2. The C_{dl} and R^2 values obtained for the porphyrin-modified electrodes

Electrode tag	C_{dl} [mF/cm^2]	R^2
$G_{P1\text{-}DCM\text{-}1}$	5.798	0.9915
$G_{P1\text{-}DMF\text{-}3}$	4.982	0.9961
$G_{P2\text{-}BN\text{-}1}$	14.017	0.9803
$G_{P3\text{-}DCM\text{-}1}$	6.239	0.9934
$G_{P3\text{-}BN\text{-}1}$	1.983	0.9933
$G_{P4\text{-}BN\text{-}1}$	6.251	0.9927

As can be seen, the highest C_{dl} value, of 14.017 mF/cm^2, was obtained for $G_{P2\text{-}BN\text{-}1}$. The C_{dl} was also expressed in mF by taking into consideration the geometrical surface of the respective electrode (S_{geom} = 0.28 cm^2), and it became ~3.925 mF. Since a high value of this parameter is characteristic of supercapacitors, out of the investigated electrodes the one modified with the P2 porphyrin is the most likely to find application in their domain. It can also be observed that the C_{dl} values for $G_{P3\text{-}DCM\text{-}1}$ and $G_{P3\text{-}BN\text{-}1}$ are quite different, even though only the solvent was changed during their manufacturing. Considering the ability of porphyrin molecules to self-organize into aggregates, this result shows that applying the same porphyrin on graphite substrate from solvents having different polarity can lead to the formation of assemblies with distinct properties.

Conclusion

The porphyrin-modified electrodes that were found in a previous study to possess the best water splitting electrocatalytic properties from a series of such samples have been characterized in the present work in terms of their double-layer capacitance. The highest value was obtained for the $G_{P2\text{-}BN\text{-}1}$ electrode, manufactured by drop-casting one layer of 5,10,15,20-tetrakis(4-methoxy-phenyl)-porphyrin from benzonitrile on graphite substrate.

As a new approach perspective, porphyrins might serve as bipolar organic electrodes by exploiting their capacity of donating or accepting electrons at their inner core. Based on the fact that porphyrins have small HOMO–LUMO gaps, enabling the facile uptake and release of electrons, and thus leading to fast redox reactions, they are suitable for porphyrin-based flexible supercapacitor electrode materials [12].

References

[1] E. Fagadar-Cosma, D. Vlascici, G. Fagadar-Cosma, Porfirinele de la sinteză la aplicații, Eurostampa, Timisoara, Romania, 2008, pp. 10.
[2] B.-O. Taranu, E. Fagadar-Cosma, Processes 10 (2022) 611.
[3] H. Yang, S. Zhang, L. Han, Z. Zhang, Z. Xue, J. Gao, Y. Li, C. Huang, Y. Yi, H. Liu, Y. Li, ACS Appl. Mater. Interfaces 8 (2016) 5366.
[4] E. Fagadar-Cosma, G. Fagadar-Cosma, M. Vasile, C. Enache, Curr. Org. Chem. 16 (2012) 931.
[5] E. Fagadar-Cosma, C. Enache, R. Tudose, I. Armeanu, E. Mosoarca, D. Vlascici, O. Costisor, Rev. Chim. 58 (2007) 451.
[6] B.O. Taranu, E. Fagadar-Cosma, I. Popa, N. Plesu, I. Taranu, Dig. J. Nanomater. Bios. 9 (2014) 667.
[7] E. Fagadar-Cosma, C. Enache, I. Armeanu, D. Dascalu, G. Fagadar-Cosma, M. Vasile, I. Grozescu, Mater. Res. Bull. 44 (2009) 426.
[8] M. Birdeanu, E. Fagadar-Cosma, in: M.V. Putz (Ed.), Quantum Nanosystems: Structure, Properties, and Interactions, Apple Academic Press: Toronto, Canada, 2015, pp. 173.
[9] N.I. Ramli, N.A.B Ismail, F. Abd-Wahab, W.W.A.W. Salim, in: K. Pal (Ed.), Transparent Conducting Films, IntechOpen, London, UK, 2018, pp. 75.
[10] Z. Zhou, W.Q. Zaman, W. Sun, L. Cao, M. Tariq, J. Yang, Chem. Commun. 54 (2018) 4959.
[11] A. Kellenberger, D. Ambros, N. Plesu, Int. J. Electrochem. Sci. 9 (2014) 6821.
[12] J. N'Diaye, M. Elshazly, K. Lian, ACS Appl. Mater. Interfaces, 14 (2022) 28359.

CHARACTERIZATION OF HYDROXYAPATITE COATINGS OBTAINED ON DIFFERENT METAL SUPPORTS USING TWO ELECTRODEPOSITION METHODS

Alexandra Ioana Bucur[1], Paula Ianasi[1], Corina Orha[1], Bogdan-Ovidiu Taranu[1]

[1]National Institute for Research and Development in Electrochemistry and Condensed Matter, Dr. A.P. Podeanu street, No. 144, 300569, Timisoara, Romania
e-mail: b.taranu84@gmail.com

Abstract

The naturally originating or synthesized calcium apatite inorganic mineral known as hydroxyapatite (HA), with the chemical formula $Ca_{10}(PO_4)_6(OH)_2$, is a very promising biomaterial for applications in the orthopedics and dentistry fields, such as bone repair and dental implants [1,2]. However, HA is also a brittle ceramic and because of this it has to be used in combination with metallic or polymeric reinforcing materials [3,4]. Implants obtained by coating HA (as such or doped) on metal substrates benefit from the properties of the ceramic layer that promotes osseointegration [5], prevents metal atom diffusion [4] and has an anticorrosive effect [6], as well as from those of the support that provides fracture, wear and corrosion resistance [3,7]. Various methods are being used for applying the HA coating onto metal substrates [8,9] and the method selection stage from the implant manufacturing process is especially important.

In a previously published paper [3] we described a novel HA electrochemical deposition method, in which one of the two precursors used to synthesize HA (either the phosphate precursor or the calcium one) was present in the electrolysis cell, while the other was added dropwise, simultaneously with the application of the electrochemical potential required to electrocoat the Ti substrate. The current work continues the previous one by comparatively analyzing the HA coatings obtained on different metal supports using the novel electrodeposition method, as well as the standard one [10].

The HA precursors selected for the study were $Ca(NO_3)_2 \times 4H_2O$ and $(NH_4)_2HPO_4$ (equal volumes of 1.75 mM and 1.05 mM solutions, respectively). The metal substrates were polished disks of Ti, Cu, Ni and C55 stainless steel. A potentiostat, a glass cell with heating mantle connected to a thermostat set at 80°C, a Pt plate anode, and a Teflon casing containing each metal disk were used to obtain the HA coated samples. The duration of each experiment was 4 hours, at an applied potential of −1.5 V. Two specimens were obtained for each type of metal substrate - one by using the standard electrodeposition method and the second by employing the novel method. When the novel method was utilized, the added precursor was the Ca precursor. Each of the eight samples was characterized via X-ray powder diffraction (XRD), scanning electron microscopy (SEM) and atomic force microscopy (AFM).

Based on the recorded XRD patterns, for the HA coatings on Cu, Ni, and stainless steel substrates obtained using the standard method only small amounts of electrodeposited crystalline HA were observed. However, larger amounts were formed with the novel method, which indicates that this approach is a more effective way of growing HA crystals on the aforementioned supports. In the case of the Ti substrate, the HA crystallinity was slightly improved when the standard deposition method was employed, but for the sample obtained with the novel method a preferential growth along the c-direction was identified that was more intense than for the specimen resulted using the standard method.

The SEM images recorded on the HA coatings electrodeposited with the novel method revealed a higher degree of uniformity and continuity compared with the coatings applied by

utilizing the standard electrochemical deposition approach. This observation concerns all the types of metal substrates considered in the study.

The conclusions reached based on the SEM data were backed up by the observations made during the AFM characterization of the samples. The 2D and 3D AFM micrographs recorded on the specimens revealed the differences between the coatings obtained using the two deposition methods. In the case of the novel method, the coatings displayed a higher degree of uniformity and continuity than the ones resulted by employing the standard method. A deeper understanding of the differences was made possible by considering the AFM data to calculate the values of several AFM parameters. For example, from among all the specimens, the one obtained on Cu support with the standard deposition method was found to have the highest surface roughness.

References

[1] X. Zhu, A.F. Radovic-Moreno, J. Wu, R. Langer, J. Shi, Nano Today 9 (2014) 478.
[2] S. Boonpok, K. Koonrungsrisomboon, K. Suttiat, P. Yavirach, D. Boonyawan, J. Funct. Biomater. 13 (2022) 99.
[3] A.I. Bucur, E. Linul, B.O. Taranu, Appl. Surf. Sci. 527 (2020) 146820.
[4] L.G. Stefan, M. Abrudeanu, I. Iosub, A.G. Plaiasu, A. Dinu, M. Mihalache, Sci. Bull. Automot. Ser. A (2009) 129.
[5] J. Chamrad, P. Marcián, J. Cizek, Plos One 16 (2021) e0254837.
[6] M. Mirzaee, M. Vaezi, Y. Palizdar, Mater. Sci. Eng. C-Mater. Biol. Appl. 2016, 69, 675–684.
[7] H. Shi, Z. Zhou, W. Li, Y. Fan, Z. Li, J. Wei, Crystals 11 (2021) 149.
[8] S. Awasthi, S.K. Pandey, E. Arunan, C. Srivastava, J. Mater. Chem. B 9 (2021) 228.
[9] A. Ritwik, K.K. Saju, IJIRSET 6 (2017) 103.
[10] D.H. He, P. Wang, P. Liu, X.K. Liu, F.C. Ma, J. Zhao, Surf. Coat. Technol. 301 (2016) 6.

INVESTIGATION OF UV/CHLORINE PROCESSES FOR TRIMETHOPRIM TRANSFORMATION USING LPM (254 nm) AND LED (275 nm) LIGHT SOURCES

Luca Farkas, Teodóra Dragić, Tímea Molnár, Tünde Alapi

Department of Inorganic and Analytical Chemistry, University of Szeged, H-6720 Szeged, Dóm tér 7, Hungary
e-mail: fluca@chem.u-szeged.hu, alapi@chem.u-szeged.hu

Pharmaceuticals are essential in the treatment of many human and animal diseases. Recently, due to their growing consumption and hard biodegradability, the elimination of pharmaceuticals is one of the challenging tasks of water treatment today. Special attention must be paid to removing antibiotics due to the severe ecological and public health consequences of their release into the environment. Nowadays, more than 700,000 deaths happen globally due to infections caused by antibiotic-resistant bacteria strains. Application of advanced oxidation processes as post-treatment is one of the possibilities to remove biologically active trace organic pollutants from treated water.

The low-pressure mercury vapor (LPM) lamp is a widely used light source in water treatment because of the germicidal effect of emitted 254 nm UV light. However, organic pollutants can also be effectively disposed of by adding the appropriate oxidizing agents (O_3, H_2O_2, HOCl, ClO_2, etc.). In recent years interest turned to the application of LED light sources in water treatment due to their several favorable features [1]. In the case of the UV/chlorine process [4], HOCl, a widely used disinfectant, can be an oxidizing agent. HOCl can react directly with organic substances, besides its UV photolysis leads to many different reactive species, including hydroxyl radical, chlorine radical, and others [4]. The formation of reactive species highly depends on the pH as well as the wavelength of the UV radiation.

In this study, the efficacy of the LPM lamp (254 nm) and UV LED (275 nm) were studied and compared for trimethoprim, a widely used antibiotic transformation, using the UV/HOCl process. At 254 nm (LPM lamp), the molar absorbance of the HOCl and OCl^- are the same, while at 275 nm (the wavelength of the maximum of the LED emission spectra), the molar absorptivity of OCl^- is two times higher than that of HOCl. Consequently, pH has a crucial role. Trimethoprim reacts fast with HOCl, while the reactivity towards OCl^- is negligible. At pH 5, the transformation occurs within two minutes without UV irradiation, while at pH 9, there is practically no change. Without the pH setting of the solution, both 254 and 275 nm radiation highly enhanced the transformation rate. One of the drawbacks of the chlorine-based advanced oxidation process is the formation of chlorinated products. The AOX measurements proved that UV/chlorine process generates less chlorinated organic products than the direct reaction of trimethoprim with HOCl.

Acknowledgments

Luca Farkas thanks the support of the ÚNKP-22-3-SZTE-398 New National Excellence Program of the Ministry for Culture and Innovation from the source of the National Research, Development, and innovation fund. This work was sponsored by the National Research, Development, and Innovation Office-NKFI Fund OTKA, project number FK132742.

References

[3] S. M.McKee, E.a Chatzisymeon, Env. Imp. Assessment 97 (2022) 106886
[4] J. De Laat, M.I. Stefan, Chapter 9 – UV/Chlorine process in Advanced Oxidation Processes for Water Treatment: Fundamentals and Applications, IWA Publishing, London, 2017, pp. 383-424

PLANT MEDIATED SYNTHESIS OF ZERO VALENT IRON NANOPARTICLES AND ITS CHARACTERISATION

DraganaTomašević Pilipović[1], Nataša Slijepčević[1], Emilija Svirčev[1], Gábor Kozma[2], Đurđa Kerkez[1], Cora Bartus Pravda[2]

[1]University of Novi Sad, Faculty of Sciences, Department for Chemistry, Biochemistry and Environmental Protection, Trg D. Obradovića 3, 21000 Novi Sad
[2]Department of Applied and Environmental Chemistry, University of Szeged
e-mail: dragana.tomasevic@dh.uns.ac.rs

Abstract
Nanoscale zero valent-iron (nZVI) particles represent an important material for diverse environmental applications because of the exceptional electron-donating properties, which can be exploited for applications such as reduction, catalysis, adsorption, and degradation of a broad range of pollutants. The search for "green" strategies leads to the advancement in the plant-mediated synthesis of ZVI nanoparticles.Within the framework of this work, the possibility of synthesis of nano zerovalent iron (nZVI) was investigated using extracts of oak, mulberry, green tea, pomelo peel, fresh orange peel and orange peel that was previously dried. Also, the subject of the investigation was the characterization of the obtained nanomaterials.

Introduction
Nanoscience and nanotechnology in recent times have purpose to minimize the negative impacts of synthetic procedures and the exploitation of different biomaterials for the synthesis of nanoparticles is considered a valuable approach in green nanotechnology. Biological resources such as plants have been used for the production of energy-efficient, low-cost and nontoxic environmental friendly iron nanoparticles *(Saif et al., 2016)*. One of the most important properties of plants that affects the production of nano zero-valent iron particles (nZVI) is the antioxidant capacity and polyphenols. Polyphenols are the most significant, essential property of plant material in the production of nZVI because antioxidant components can reduce Fe^{3+} ions to zero-valent iron (Fe^0). In order to reduce the costs of the synthesis of nanomaterials, tree leaf extracts can also be used *(Mittal et al., 2013)*. Pomelo citrus peel is characterized by a high content of pectin, essential oils, flavonoids, polysaccharides and other components that can be used in the synthesis of nZVI. Its application reduces the amount of waste caused by its consumption and thereby prevents negative impact on the environment *(Venkateswarlu, 2013)*. The size of the obtained nanoparticles as well as their reactivity depends both on the applied reagents and on the properties of the tea itself *(Chen et al., 2011)* and today, depending on the need, various tea extracts are applied. The aim of this work was to investigate the possibility of synthesizing nano zero valent iron (nZVI) using extracts of oak, mulberry, green tea, pomelo peel, fresh orange peel and orange peel that has been previously dried. Also, the subject of the investigation was the characterization of the obtained nanomaterials. The obtained extracts and nanomaterials were characterized by isoelectric point/point of zero charge (IET), zeta sizer, pH value, total phenol content and antioxidant capacity.

Methods and Materials
Nano zero valent iron was synthesized using extracts of oak and mulberry leaves (OL-nZVI, ML-nZVI), green tea (GT-nZVI), fresh orange peel (FO-nZVI), dry orange peel (DO-nZVI) and pomelo peel (P-nZVI) as a reducing agent. Preparation of Oak and Mulberry extracts were determined by previous testing and analysis *(Machado et al., 2013)*. *Huang et al., 2014*

investigated the optimal time and temperature for the preparation of green tea extract so this method was used in this research. Preparation of pomelo peel (P)/fresh orange peel (FO)/dry orange peel (DO) extracts were performed by *Wei et al., 2016*. Production of nZVI was determined when solution of Fe^{3+} with a molar concentration of 0.1 M was mixed with the prepared extracts in a ratio of 3:1. Characterization of extracts from Oak, Mulberry, commercial Green Tea leaves, Orange and Pomelo Peel was determined by pH, FRAP method and by total content of phenols. pH value of the extracts was measured according to the standard method (ISO 10390:2007), by using SenTix®21 electrode. The antioxidant capacity of the extracts was evaluated by using the "ferric reducing antioxidant power" (FRAP) method *(Pulido et al. 2000)* adapted for microplates. The total content of phenols was determined by using the Folin-Ciocalteu method (ISO, 2005). The pH value of the zero charge point (IET) of nanomaterials was determined by the salt addition method *(Kosmulski, 2009)* and the IET of the samples was calculated from the dependence graph ΔpH (final pH-initial pHi) and initial pH value (pHi). The analysis of particle size distribution was performed on a Malvern Zetasizer Nano ZS device.

Results and discussion

As can be seen from the table 1, the extract with the highest pH value is the oak leaf extract (pH=7.55), while the lowest pH value is the dry orange peel extract (pH=4.08). The total content of phenols in the samples of plant extracts is determined in order to obtain information on whether any plant extract can be applied for the synthesis of this type of nanomaterials (*Weng et al., 2013*). In Figure 1, it can be seen that sample GT has the highest phenolic content (64.5 mg of gallic acid equivalents per gram of dry extract), while the same total phenolic content of 1.9 mg of gallic acid equivalents per gram was detected in samples FO and P. Figure 1 show that the highest antioxidant capacity was obtained for the GT sample (60.3 mg of ascorbic acid equivalents per gram of dry extract), which can be associated with the highest total phenol content in the given sample. The lowest antioxidant capacity was obtained for samples FO and P, which are comparable results to the results of total phenol content in the given samples. In sample FO the antioxidant capacity is 0.9, while in sample P, the antioxidant capacity is 0.2 mg of extracts made from dried plants have been proven to have higher antioxidant capacities ascorbic acid equivalents per gram of dry extract. Because the water evaporates from the plants during drying, which leads to an increase in the concentration of antioxidants in the plants *(Machado et al., 2013)*. This claim was also proven by this test, because the extract of dry orange peel has a higher antioxidant capacity compared to the extract of fresh orange peel.

Characterization of synthesized nanomaterials

The point of zero charge (IET) is defined as the condition at which the surface charge is equal to zero, the surface of metal oxides and other materials. The IET of nanomaterials depends on several factors such as chemical modifications, surface modifications, particle size and particle transformation (*Mwaanga et al., 2014*). When the surface of the material is exposed to the environment in an aqueous solution, the layer of hydroxyl groups breaks down due to the interaction with water molecules.

Table 1. pH values of plant extracts

Extracts	pH
DO	4,08
FO	5,00
P	5,06
OAK	7,55
ML	7,30
GT	5,09

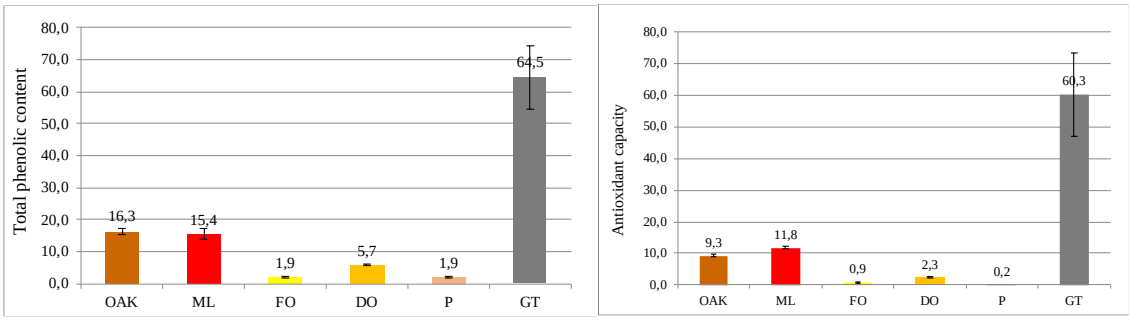

Figure 1. Comparison of the results of the antioxidant capacity of the extracts and total phenol content

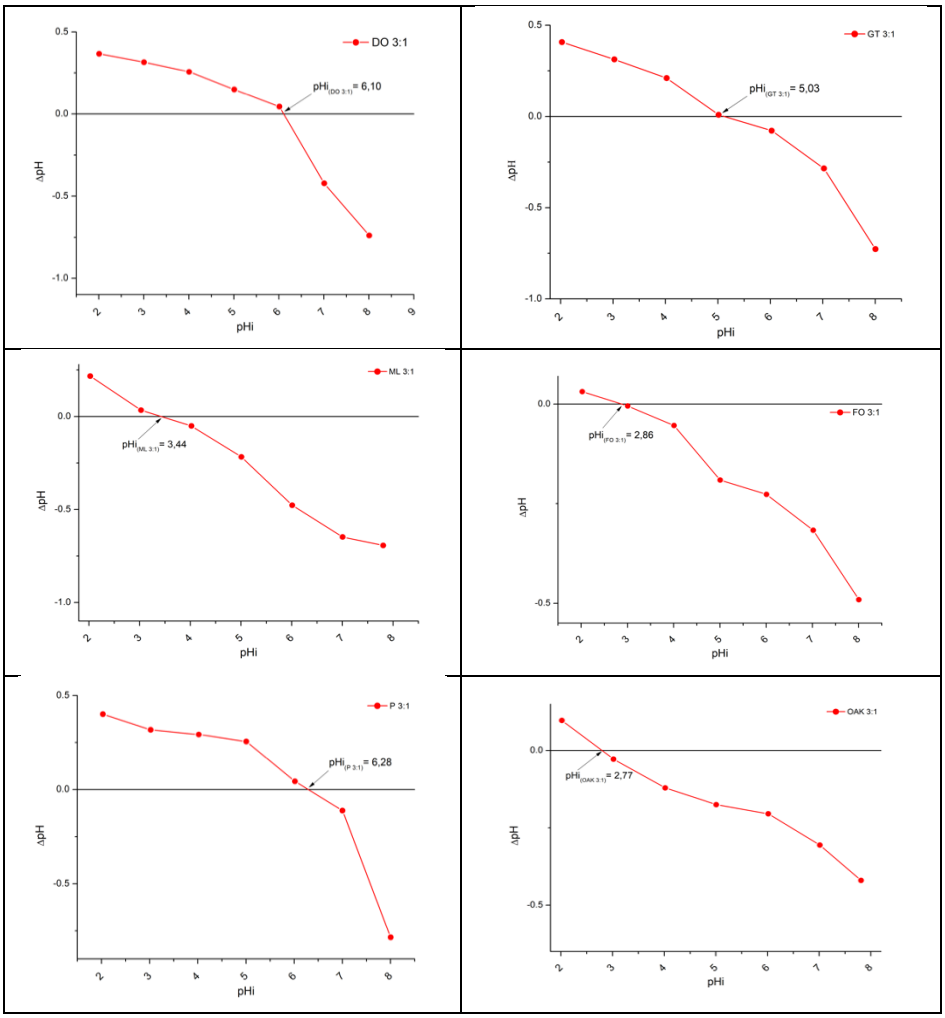

Figure 2. pHi values for synthesized nanomaterials using dry orange peel, fresh orange peel pomelo bark, oak leaf, mulberry leaf, green tea

When the surface hydroxyl groups remain undissociated in aqueous solution, the oxide surface reaches the isoelectric point (pHi) and has zero charge. If the pH is less than pHi the surface will be positively charged and if the pH is greater than pHi the surface will be negatively charged (*McCafferty, 2010*). The values of the pH point of zero charge (pHi/IET) of nanomaterials are presented in Figure 2. Point of zero charge or isoelectric point of nZVI synthesized using dry peel oranges is 6.10, for fresh orange peel is 2.86, for pomelo bark is 6.28, for oak leaf is 2.77, for mulberry leaf is 3.44, for green tea is 5.03.

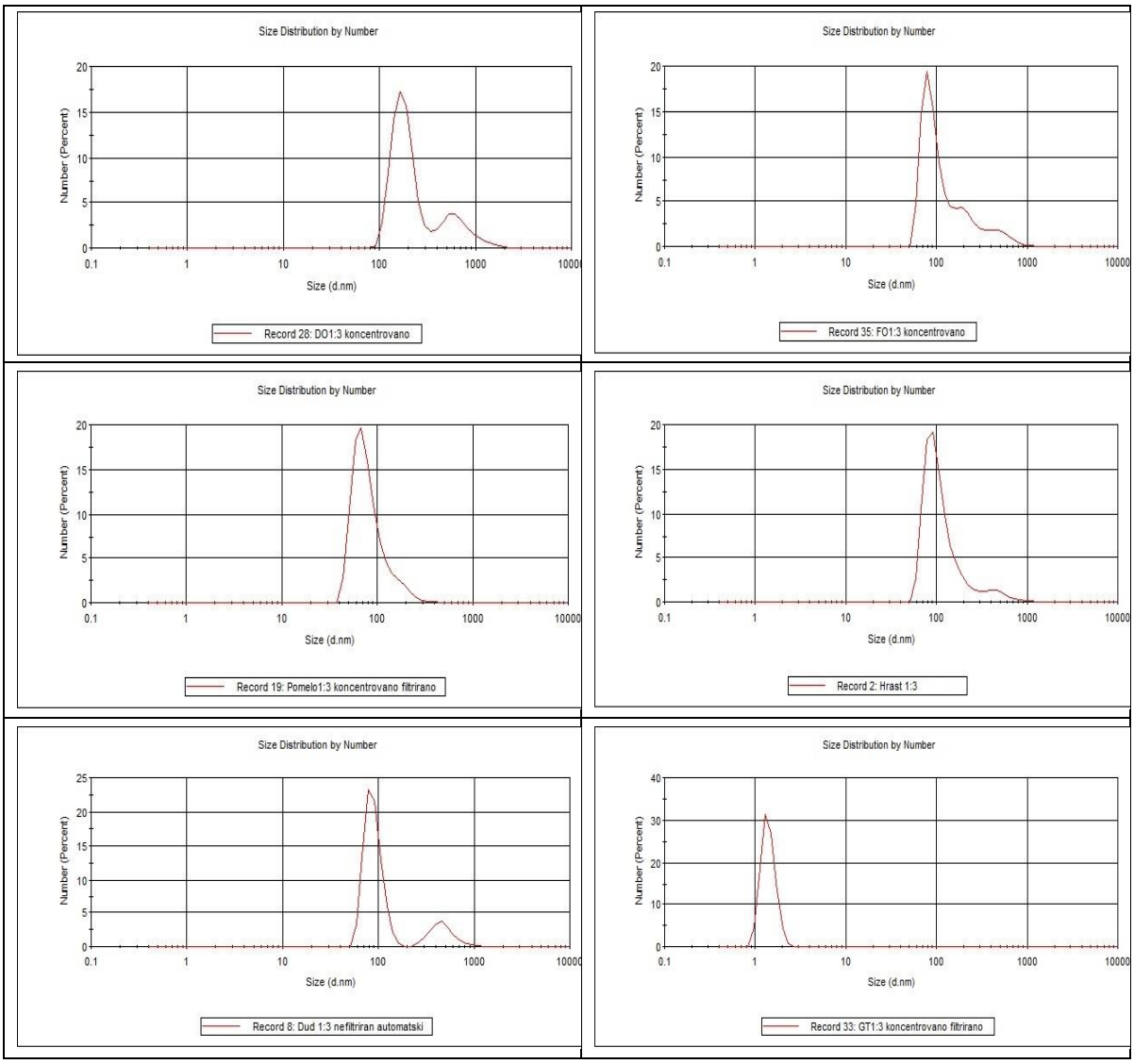

Figure 3. Particle size distribution of nZVI synthesized using plant according to their total number using a zetasizer

Poguberović, 2016 obtained comparable results for the IET sample of green synthesized nZVI from an oak leaf, pHi= 2.4, and for the mulberry leaf obtained a pHi value of 3.80 pH units. The obtained low pHi values of this type of nanomaterial can be explained as a result of the high acidity of the prepared extract of fresh orange peel *(Poguberović, 2016)*. Analysis using a zetasizer was performed in relation to the total number of particles in the sample. The results of the analysis (Figure 3) showed that the size range of nZVI particles in the samples were from **0,7 to 2000** nm, depending on plant using for synthesis. The largest number of particles having smallest diameter of about 2nm are detected for GTnZVI, and the largest number of particles having biggest diameter of about 90 nm are detected for FOnZVI. The other samples have the largest number of particles of around 70nm.

Conclusion

Dry orange peel, fresh orange peel, pomelo peel, oak leaf, mulberry leaf and green tea have been shown to be suitable plants for the synthesis of nano zero valent iron due to their relatively high content of total phenolics which is related to their antioxidant capacity.The most acidic extract was the dry orange peel extract, while the most alkaline extract was the oak leaf extract.

Using the Folin-Ciocalteau method, it was determined that green tea extract has the highest phenol content, while fresh orange peel and pomelo extracts have the lowest phenol content. The results of the FRAP method showed similar trend, where the green tea extract has the highest antioxidant capacity, while the pomelo extract has the lowest antioxidant capacity. The sample with the lowest isoelectric point is the OAK 3:1 sample, while the sample with the highest isoelectric point is the P 3:1 sample. Zetasizer, by analysing the total number of particles, showed that there are particles of different sizes in the samples. The particle size range identified by the zetasizer is from 0.7 to 2000 nm.

Acknowledgements
"Project no. 2019-2.1.11-TÉT-2020-00152 has been implemented with the support provided by the Ministry of Innovation and Technology of Hungary from the National Research, Development and Innovation Fund, and the Ministry of education, Science and technological development of the Republic of Serbia and National Research and Innovation office".

References

[1.] Huang, L., Weng, W., Chen, Z., Megharaj, M., Naidu, R., (2014). Green synthesis of iron nanoparticles by various tea extracts: Comparative study of the reactivity. Spectomichimica Acta Part A: Molecular and Biomolecular Spectroscopy 130, 295-301.
[2.] ISO. International Organization for Standardization, ISO 14502-1 (2005). Determination of substances characteristics of green and black tea-part 1: content of total polyphenols in tea- colorimetric method using Folin- Ciocalteu reagent. p. 14.
[3.] Kosmulski, M., (2009). pH dependent surface charge and point of zero charge.IV. Update and new approach, Journal of Colloid and Interface Science 337, 439-448.
[4.] Machado, S., Pinto, S.L., Grosso, J.P., Nouws, H.P.A., Albergaria, J.T., Delerue- Matos C., (2013). Green production of zero-valent iron nanoparticles using tree leaf extracts. Science of the Total Environment 445-446, 1-8.
[5.] McCafferty, M. (2010). Relationshipbetweentheisoelectric point (pHpzc) and potentialofzerocharge (Epzc) for passive metals. *Electrochemica Acta* 55, 1630-1637.
[6.] Mittal, A.K., Chisti, Y., Banerjee, U.C., (2013), Synthesis of metallic nanoparticles using plant extracts, Biotechnol. Adv. 31, 346–356.
[7.] Mwaanda, P., Carraway, E.R., Schlautman, M.A. (2014). The pH dependence of natural organicmattersorption to nanoparticles and itsabilita to stabilizenanoparticles in aqueoussolutions. *EuropeanScientificJournal*, ISSN: 1857-7881.
[8.] Nadagouda, M.N., Castle, A.B., Murdock, R.C., Hussain, S.M., Varma, R.S., (2010). In vitro biocompatibility of nanoscale zerovalent iron particles (NZVI) synthesized using tea polyphenols. Green Chemistry 12, 114–22.
[9.] Saif, S.; Tahir, A.; Chen, Y. Green Synthesis of Iron Nanoparticles and Their Environmental Applications and Implications. Nanomaterials 2016, 6, 209. https://doi.org/10.3390/nano6110209
[10.] Venkateswarlu, S., Rao, Y.S., Balaji, T., Prathima, B., Jyothi, N.V.V., (2013). Biogenic synthesis of Fe3O4 magnetic nanoparticles using plantain peel extract, 241–244.
[11.] Wei, Y., Fang, Z., Zheng, L., Tan, L., Tsang, E.P., (2016). Green synthesis of Fe nanoparticles using Citrus maxima peels aqueousextracts. School of Chemistry and Environment, South China Normal University, Guangzhou 510006, China.
[12.] Weng, X., Huang, L., Chen, Z., Megharaj, M., Naidu, R., (2013). Synthesisof iron-basednanoparticles by green teaextract and theirdegradationof malachite. *IndustrialCropsandProducts* 51, 342– 347.

A STATISTICAL COMPARATIVE STUDY BETWEEN THE FUNCTIONS OF ALCOHOLS AND THIOLS USING QUANTUM CHEMISTRY METHODS

Marina Alexandra Tudoran*, Zoltan Szabadai

Renewable Energy and Electrochemistry Department, National Institute of R&D for Electrochemistry and Condensed Matter - INCEMC,
144 Aurel Păunescu-Podeanu, RO-300569, Timișoara, Romania
e-mail: alexandra.m.tudoran@gmail.com

Abstract
Using the QSAR method, the present work aims to comparatively study the relationship between solubility (data from literature) and several physical and chemical parameters (computationally calculated) for two classes of analogue compounds, i.e. alcohols and their corresponding thiols. The obtained results show that there are significant differences between the ways in which solubility can be computationally determined for these two classes.

Introduction
Alcohols represent a class of organic compounds in which a hydroxyl group is bonded to a carbon atom sp^3 hybridized. They are quite soluble in water up to 4 carbon atoms, both water solubility and their hydrophilic nature decreasing with increasing the hydrophobic alkyl group [1]. Thiols represents the sulphur analogues of alcohols which contain an SH group instead of the OH group, having two atoms and two lone pairs of electrons surrounding the atoms. Thiols are unable to form intermolecular hydrogen bonds, but they can form strong complexes with heavy metallic cathions [2, 3, 4]. In general terms, solubility represents the solute quantity which can be dissolved in a specific solvent in a given condition, characterizing a unionized substance dissolution in water [5, 6]. When a molecule in gas phase is transferred to aqueous environment, a change in energy occurs, leading to the premise that solubility is an important parameter in modulating molecular properties (e.g. redox potential, pK_a, thermodynamic stability, etc.) [7]. At the same time, water solubility can be explained based on the polarity of molecules, and has an important role in establishing the compound tendency to partition from a phase to another and in determining the distribution and the transport of molecules in environment. There are different ways of expressing the water solubility, either as gram per liter, either as mole per liter (noted with S) and conventionally converted in logarithmic values [5, 6, 8, 9, 10]. As a chemical descriptor, water solubility can be utilized in establishing the bio-concentration in aquatic organisms [10]. Thus it is of a fundamental importance in assessing the risk of molecules and in the process of design and synthesis of agro-chemicals (e.g. pesticides) [6, 10]. Although the experimental approach of determining the solubility returns very precise values, it is inefficient regarding the time and cost when a large data base of molecules is considered. A good alternative is represented by the in silico models, most of them based on the relation established between solubility and the chemical structure of the molecules through quantitative structure-properties relationships (QSPR) or quantitative structure-activity relationships (QSAR). These type of relations are established using simple or multiple linear regression procedure allowing different physical, chemical and structural descriptors to be part in the modelling process [6, 11].
The present study investigates comparatively the relationship between solubility (expressed in two different forms) and several physical and chemical descriptors (hydration energy, surface area and a new computed descriptor, generically named “topo-energy index”) generating the prediction equations for a series of alcohols and their corresponding thiols.

Experimental

The structures of molecules, considered as the working set, were generated by HyperChem 8.0.10 software [12] and pre-optimized using the MM+ force field. Then, the optimized structures were obtained by ab initio method with 6-31G** basis set. The RHF spin pairing was selected with 1e-008 as the accelerated convergence limit for SCF control. The geometry optimization was performed using the "Polak-Ribière (Conjugate gradient)" algorithm with a RMS gradient of 0.01 kcal/(Å mol). The HOMO distribution of the optimized molecular structure was obtained by plotting the 2D contours (carbon – cyan, hydrogen – white, oxygen – red, sulphur – yellow, positive isosurface – green wire mesh, and negative isosurface – violet wire mesh). Using the results obtained from HyperChem the Topo-energy Index was computed as:

$$\text{Topo-Energy Index} = \text{Hydration energy} / \text{Surface area}$$

The relationship between the response variable (solubility) and the explanatory variables (hydration energy, surface area and topo-energy index) was modeled using simple and multiple regression, using IBM SPSS program. For all the data in study the goodness of fit of normal distribution was assessed by applying Kolmogorov-Smirnov One - Sample Test.

Results and discussion

The HOMO orbitals of the optimized structures are presented in Figure 1. The ab initio results for hydration energy, surface area and the computed topo-energy index, and the solubility parameters taken from literatures [13] are given in Table 1. The Kolmogorov-Smirnov test for alcohols and thiols indicates that the *Exact. Sig* (2-tailed) > 0.05 for all of the parameters in study providing no evidence against the null hypothesis of normal distribution.

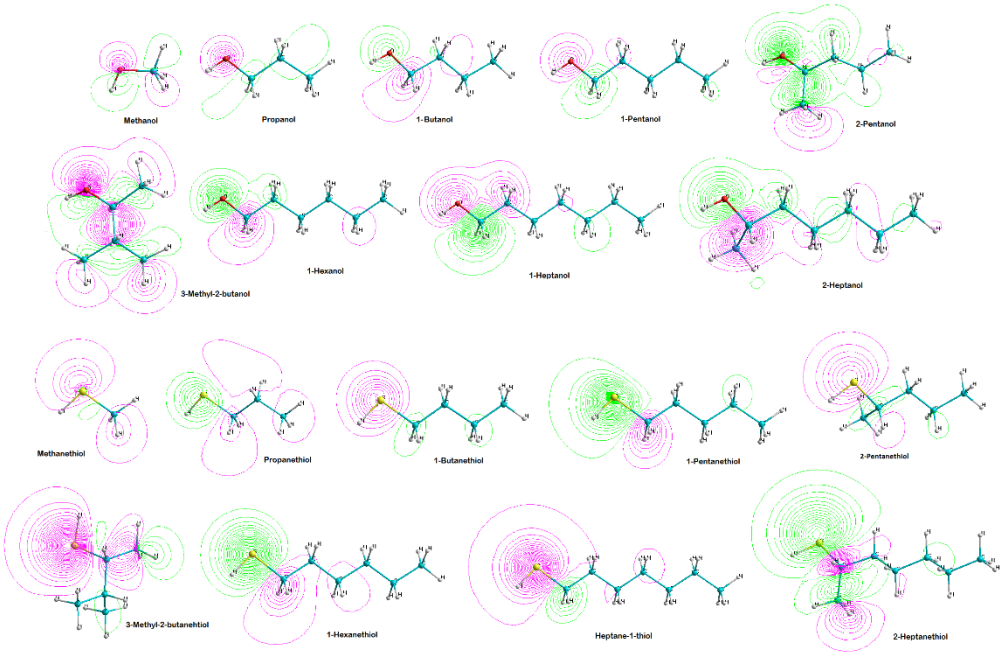

Figure 1. Electronic distribution of HOMO orbitals – alcohols (ball-and-stick model)

To determine whether hydration energy and surface area correlate with log S in case of alcohols, a Pearson test was conducted. There was a significant negative correlation between hydration energy (M = -3.934, SD = 1.611) and log S (M = -0.278, SD = 0.986), r = -0.773, $p < 0.05$, and a strong negative correlation between surface area (M = 271.610, SD = 58.871) and log S, r = -0.970, $p < 0.01$. A multiple regression was carried out to investigate whether hydration energy

and surface area could significantly predict log S. The results of the regression indicated that the model explained 97.3% of the variance and was a significant predictor of log S, $F(1, 6) = 109.347$, $p < 0.01$. Both variables contributed significantly to the model (for hydration energy: B = 0.235, $p < 0.05$, and for surface area: B = -0.022, $p < 0.01$). The final predictive model was:

$$\log S_{alcohol} = 6.604 + (0.235) \times \text{hydration energy} + (-0.022) \times \text{surface area}$$

In order to investigate how well the newly created parameter (i.e. the topo-energy index) predicts the log S value of alcohols, correlation and simple regression were conducted. There was a significant negative correlation between topo-energy index (M = -0.0167, SD = 0.013) and log S, r = -0.773, $p < 0.05$. It was found a significant regression equation (R^2 = 0.598, $F(1, 7) = 10.408$, $p < 0.05$), of the form:

$$\log S_{alcohol} = -1.255 + (-58.374) \times \text{topo-energy index}_{OH}$$

Topo-energy index significantly contributed to the model (B = -58.374, $p < 0.05$).

Table 1. Descriptors of alcohols and thiols

Molecule	**HE (kcal/mol)**	**SA (Å2)**	**TEI**	**logS (mol/L)**	**WS (g/L)**
METHANOL	-7.64	154.88	-0.0493285	1.21	519
PROPANOL	-4.90	221.76	-0.022096	0.81	391
1-BUTANOL	-4.27	250.49	-0.0170466	0.33	158
1-PENTANOL	-3.91	282.26	-0.0138525	-0.37	37.2
2-PENTANOL	-2.91	276.11	-0.0105393	-0.17	59.7
3-METHYL-2-BUTANOL	-2.85	267.03	-0.010673	-0.11	69.2
1-HEXANOL	-3.55	311.84	-0.011384	-1.1	8.22
1-HEPTANOL	-3.18	343.64	-0.00925387	-1.7	2.32
2-HEPTANOL	-2.19	336.48	-0.00650856	-1.4	4.54
METHANETHIOL	-1.41	178.51	-0.00789872	-0.38	20
PROPANETHIOL	-0.12	239.64	-0.000500751	-1.2	4.99
1-BUTANETHIOL	0.32	273.22	0.00117122	-1.5	3.06
1-PENTANETHIOL	0.68	301.84	0.00225285	-2.2	0.62
2-PENTANETHIOL	0.85	292.18	0.00290917	-2.2	0.64
3-METHYL-2-BUTANETHIOL	1	279.20	0.00358166	-2.2	0.61
1-HEXANETHIOL	1.05	334.20	0.00314183	-2.9	0.16
HEPTANE-1-THIOL	1.42	363.25	0.00390915	-3.4	0.056
2-HEPTANETHIOL	1.59	353.08	0.00450323	-3.3	0.061

Following the same procedure, we investigated the relationship between log S and hydration energy and surface area in case of thiols. There was a strong and negative relationship between log S (M = -2.142, SD = 0.995) and hydration energy (M = 0.598, SD = 0.917), r = -0.955, $p < 0.01$, and also between log S and surface area (M = 290.569, SD = 57.884), r = -0.985, $p < 0.01$. The obtained R^2 = 0.973 indicated that 97.3% of the variance in log S is due to the influence of hydration energy and surface area, the effect size being large. The results of ANOVA were significant $F(1, 6) = 106.420$, $p < 0.01$. While surface area contributed significantly to the model (B = -0.014, $p < 0.05$), hydration energy did not (B = -0.187, $p = 0.471$). The obtained equation for the regression line was:

$$\log S_{thiols} = 2.066 + (-0.187) \times \text{hydration energy} + (-0.014) \times \text{surface area}$$

Topo-energy index (M = -0.002, SD = 0.004) calculated for thiols was strong and negative correlated with log S, r = -0.877, $p < 0.01$, according to Pearson correlation analysis. In this case, regression analysis showed that there was 76.9% of the variance explained by the model and the model is significant, $F(1, 7) = 23.253$, $p < 0.05$. The regression equation was:

$$\log S_{thiol} = -1.811 + (-228.154) \times \text{topo-energy index}_{SH}$$

Also in this case, topo-energy index (B = -228.154, $p < 0.05$) makes a significant contribution in predicting log S.

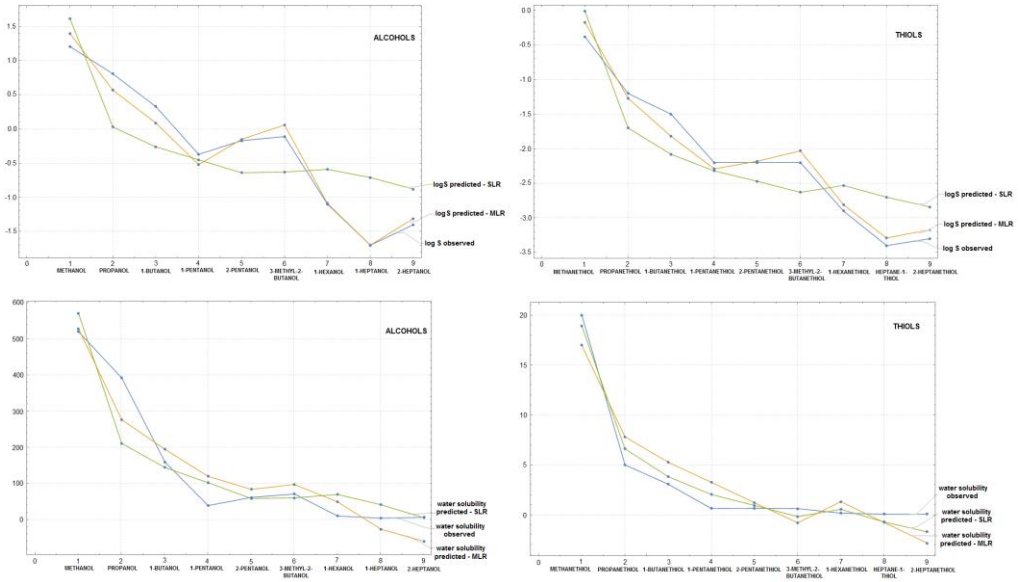

Figure 2. - Observed vs Predicted values of Log S and Water solubility for alcohols and thiols

Comparatively, we wanted to determine the influence of hydration energy, surface area and topo-energy index on water solubility for the same alcohols and thiols. In case of alcohols, Pearson correlation coefficients indicated that there is a strong negative relationship between water solubility (M = 138.798, SD = 188.299) and hydration energy, r = -0.909, $p < 0.01$, and surface area respectively, r = -0.928, $p < 0.01$. According to the results of the linear regression, hydration energy and surface area explained 89.7% of the variance, the model being significant ($F(1, 6) = 26.009$, $p < 0.05$, $R^2 = 0.897$). The hydration energy (B = -47.398, p = .199) and the surface area (B = -1.821, p = .089) have a similar contribution in predicting water solubility. The regression equation was:

$$\text{Water solubility}_{alcohol} = 446.909 + (-47.398) \times \text{hydration energy} + (-1.821) \times \text{surface area}$$

As for the topo-energy index, Pearson correlation coefficient indicated a strong and negative relationship between variables, r = -0.918, $p < 0.01$. It was found a significant regression equation (R^2 = 0.842, $F(1, 7) = 37.301$, $p < 0.01$), with topo-energy index being a significant predictor of the model (B = -13233.415, $p < 0.01$). The obtained equation was:

$$\text{Water solubility}_{alcohol} = -82.762 + (-13233.415) \times \text{topo-energy index}_{OH}$$

In case of thiols, there was a strong and negative correlation between water solubility (M = 3.355, SD = 6.463) and hydration energy, r = -0.927, $p < 0.001$, and surface area respectively, r = -.846, $p < 0.01$. The results of the regression indicated that there was a collective significant effect between predictors and water solubility (R^2 = 0.876, $F(2, 6) = 21.193$, $p < 0.05$). It was found that while hydration energy significantly predicted water solubility (B = -9.343, $p < 0.05$), surface area did not (B = 0.047, p = 0.415). The final predictive model was:

$$\text{Water solubility}_{thiol} = -4.588 + (-9.343) \times \text{hydration energy} + (0.047) \times \text{surface area}$$

In the same way, topo-energy index and water solubility (M = 3.356, SD = 6.463) of thiols were strong and negative correlated, r = -0.983, $p < 0.01$. The results of the regression indicated that the model explained 96.7% of the variance and was significant, $F(1, 7) = 205.550$, $p < 0.001$. The final predictive model was:

$$\text{Water solubility}_{thiol} = 5.770 + (-1663.090) \times \text{topo-energy index}_{SH}$$

It was found that topo-energy index significantly predicted water solubility (B = -1663.09, $p < 0.01$). Figure 2 presents comparatively the observed values and the values obtained using the prediction equations for log S and water solubility for alcohols and thiols.

Conclusion

We used linear regression analysis in order to construct a prediction equation that permits the estimation of log S and water solubility based on the knowledge of the hydration energy, surface area (as coefficients in multiple regression) and a new created topo-energy index (as coefficient in single regression), the dependent variables being significantly correlated with all predictors. In case of log S, we determined that for alcohols molecules, its values can be better predicted using multiple regression, with surface area having a higher contribution in the prediction equation compared to hydration energy. The same direction was maintained also in case of thiols, with the specification that in the prediction equation only the surface area had a significant contribution.

In case of water solubility of alcohols, although R^2 values were very close for both single and multiple regression, we determined that hydration energy and surface area combined are better predictors compared to topo-energy index. However, only surface area is significant in the prediction equation. We obtained a different result in case of water solubility of thiols, in this case topo-energy index being a better and a highly significant predictor.

Acknowledgements

This work was supported by the National Program NUCLEU PN 19 22 "Unpollutant and innovative technologies for health, environment protection and energetic efficiency", Project Code PN 19 22 01 01, Contract No. 40N/2019 "Advanced technologies for materials dedicated to the energy sector".

References

[1] D.R. Bloch, Organic Chemistry Demystified. McGraw-Hill, (2006), pp. 295.
[2] D. Klein, Organic Chemistry, Wiley, (2017), pp. 583.
[3] P.Y. Bruice, Organic Chemistry, Pearson Education, Inc., (2016), pp. 494.
[4] J.G. Smith, Organic Chemistry, McGraw-Hill Education, (2017), pp. 364.
[5] S.D. Sarker, L. Nahar, Chemistry for Pharmacy Students, Wiley, (2007), pp. 1-15.
[6] J. Ali, P. Camilleri, M.B. Brown, A.J. Hutt, S.B. Kirton, J. Chem. Inf. Model., 52 (2012) 420−428.
[7] A. Pomogaeva, D.M. Chipman, J. Chem. Theory Comput., 10 (2014) 211−219
[8] V. Gelmboldt, L. Ognichenko, I. Shyshkin, V. Kuzmin, Struct. Chem., 32 (2021) 309-319.
[9] J. Dai, B. Sun, A. Zhang, K. Lin, L. Wang, Bull. Environ. Contam. Toxicol. 61 (1998) 591-599
[10] H. Birch, A.D. Redman, D.J. Letinski, D.Y. Lyon, P. Mayer, Anal. Chim. Acta, 1086 (2019) 16-28
[11] A.A. Toropov, A.P. Toropova, M. Marzo, E. Benfenati Use of the index of ideality of correlation to improve aquatic solubility model. J. Mol. Graph. Model., 96 (2020) 107525
[12] HyperChem™ Professional, Hypercube, Inc., 1115 NW 4th Street, Gainesville, Florida 32601, USA.
[13] https://hmdb.ca/

NATURAL DEEP EUTECTIC SOLVENTS FOR ENHANCED PIPERINE BIOAVAILABILITY

Denis Uka, Bojana Blagojević, Ružica Ždero Pavlović, Tatjana Jurić, Karolina Mocko Blažek, Teodora Kukrić, Boris M. Popović

[1]*Chemistry & Biochemistry Laboratory, Department of Field and Vegetable Crops, Faculty of Agriculture, University of Novi Sad, 21000 Novi Sad, Trg Dositeja Obradovića 8, Serbia*
e-mail: denis.uka@polj.uns.ac.rs

Abstract

Piperine, bioactive alkaloid from black pepper (*Piper nigrum* L.) and long pepper (*Piper longum* L.) exerts numerous biological activities. The main limitation of its biological potential comes from hydrophobic nature and poor bioavailability. Natural deep eutectic solvents (NADES) are developed as a green alternative to organic solvents due to their physico-chemical properties and biocompatibility. NADESs are formed by at least one hydrogen bond donor (HBD) and one hydrogen bond acceptor (HBA), that when combined at a certain molar ratio present a significant decrease in the melting point becoming liquid at, or near, room temperature. These components are mainly primary metabolites or can be any components that can be found in nature. These systems have shown the greatest potential in the field of green chemistry, since they are abundant, inexpensive, recyclable and attractive for food, cosmetic and pharmaceutical applications.

In our study, five hydrophobic menthol based NADES systems were evaluated for the solubility of piperine, by 2 hours stirring at room temperature. Piperine concentration was measured by HPLC-PDA method on Luna C-18 column, after elution with 70% methanol-water mobile phase. In all tested systems menthol served as HBA and HBDs were limonene, lauric acid, lactic acid, 1,2-propandiol and ibuprofen. Determined piperine solubility values were 23.53±2.31, 45.62±1.99, 129.93±13.39, 44.20±3.87, and 72.05±11.13 mg/ml for these five systems, respectively.

Acknowledgements

This research was financially supported by the Science Fund of the Republic of Serbia, #GRANT No. 7731993, Active Pharmaceutical Ingredient Deep Eutectic Solvents as Novel Therapeutic Agents and Food Supplements – APIDES, and the Provincial Secretariat for Sports and Youth, GRANT No. 116-401-3709/2022-02.

DEVELOPMENT OF NOVEL GAMMA RADIATION DOSIMETER BASED ON METALLOPHTHALOCYANINE

Bojana Vasiljević[1], Ivica Vujičić [1], Tanja Barudžija[1], Maja Krstić[1], Milica Budimir[1], Dušan Mijin[2], Milena Marinović-Cincović[1], Dragana Marinković[1]

University of Belgrade, Vinča Institute of Nuclear Sciences, National Institute of the Republic of Serbia, University of Belgrade, P. O. Box 522, 11001 Belgrade, Serbia
[2]Department of Organic Chemistry, Faculty of Technology and Metallurgy, University of Belgrade, Karnegijeva 4, P. O. Box 3503, 11120, Belgrade, Serbia
e-mail: bojana.vasiljevic@vin.bg.ac.rs

Abstract
In this study, zinc phthalocyanine was evaluated as a possible chemical dosimeter for gamma rays at low-medium dose ranges in solution form and PVA film. The zinc phthalocyanine was successfully synthesized with a high yield under microwave irradiation at 200 °C. The calibration curves of absorbance versus dose of gamma irradiation show excellent linearity over a wider dose range (1 - 25kGy). After being irradiated, the samples' color changed from blue to yellow.

Introduction
Dosimetry is an essential element in the quality control of radiation processing, assuring the correct and uniform supply of radiation doses to a given area. As a result, a variety of dosimetry systems with various dosage sensitivities and dose ranges are utilized for common radiation applications[1]. Such systems present different types of radiochromic solution, gel, and film dosimeters that can be used in low-dose radiotherapy dosimetry due to direct radiation-induced permanent change in the color of dyed materials[2], and high-dose radiation applications such as sterilization, food irradiation, polymers applications, and agriculture[3]. Importantly, the degree of coloration is proportional directly to the amount of absorbed dose[4].
Organic dyes are among the most studied and used chemical dosimeters[5,6]. They have been utilized in solution form or embedded in various polymeric films to measure the distribution of the absorbed dose. These radiochromic thin film dosimeters are often used in radiation processing for routine dose control during gamma and electron-irradiation. The least researched dosimeters among the organic dyes are metallophthalocyanines (MPcs)[7,8], a symmetrical 18π-electron aromatic macrocycle. Their attractive color, together with tremendous chemical and thermal stability, has led us to research more reliable, stable, and less expensive dosimeter systems.
The present work aims to investigate the response of the change in the absorbance versus gamma-irradiation at low-medium dose ranges for zinc phthalocyanine (ZnPc). Microwave-assisted synthesis of ZnPc was successfully performed in a mono-mode microwave reactor at 200 °C. Organic dye has been utilized in the solution or embedded in a polymeric film for dosimetry application.

Experimental
All chemicals: zinc (II) acetate dihydrate, $Zn(CH_3CO_2)_2 \cdot 2H_2O$ (>99%, Sigma-Aldrich), 1,2-dicyanobenzene, $C_6H_4(CN)_2$ (≥98%, Sigma-Aldrich), 2,2,6,6-tetramethylpiperidine, TMP (≥99%, Sigma-Aldrich), polyvinyl alcohol, PVA (95.5-96.5% hydrolyzed, M.W. approx. 85 000-124 000, Sigma-Aldrich), *N*, *N*-dimethylformamide, DMF (>99%, Alfa Aesar), dimethyl sulfoxide, DMSO (>99%, Fisher Chemicals), and methanol (≥ 99%, Sigma Aldrich) were of

the highest purity commercially available and were used without further purification. Mili-Q deionized water (electrical resistivity = 18.2 MΩ cm^{-1}) was used.

Microwave-assisted synthesis of ZnPc ($ZnPc_{MW}$): The starting compounds 1,2-dicyanobenzene (2.5 mmol, 0.327 g) and zinc (II) acetate dihydrate (0.625 mmol, 0.137 g) were dissolved in 1 mL of DMF. The catalyst TMP was added to the reaction mixture under stirring (100 μL). The microwave reaction mixture was irradiated at T = 200 °C ($ZnPc_{MW}$) for 5 min and after cooling to room temperature, the precipitate was filtered off and washed with 3% HCl, water, and methanol, and dried in an oven at T = 60 °C. The resulting deep purple crystals remain after the processing of the reaction mixtures. Yield (68%).
ZnPc/PVA films were prepared by dispersing 4 mL of ZnPc ($1x10^{-4}$M, DMSO) in the 6 mL of 6% PVA/DMSO solution by sonication for 30 min to get a perfectly homogeneous solution. Afterwards, 10 mL of each mixture was poured into Petri dishes for film formation. Good quality and colored films of uniform surface finish were obtained within 8h of drying in a vacuum oven.

Microwave-assisted synthesis was performed in a mono-mode microwave reactor Anton Paar Monowave 300. X-ray diffraction (XRD) measurements were performed by SmartLab® X-ray diffractometer (Rigaku, Japan, www.rigaku.com) using Cu Kα radiation (λ = 1.542 Å). The patterns were collected at room temperature, within a 2θ range of 5–60° in a scan rate of 3°/min with divergent slit of 0.5 mm, operated at 40 kV and 30 mA. The surface morphology of the synthesized compounds was analyzed with atomic force microscopy (Quesant, Ambios Technology, USA) operating in tapping mode in air, at room temperature. Surface morphologies of the deposited samples were studied by Atomic Force Microscope (AFM), Quesant (Agoura Hills, CA, USA), which was operating in the tapping mode, in the air, at room temperature. Standard silicon tip (NanoAndMore Gmbh, Wetzlar, Germany) with the constant force of 40 N m^{-1} was used. Images were obtained at scan rate of 2Hz, with 512 x 512 pixels scan resolution over different square areas. The average size of objects in AFM images and average surface roughness were determined by Gwyddion software (https://www.degruyter.com/document/doi/10.2478/s11534-011-0096-2/html). Attenuated total reflectance Fourier transform infrared (ATR-FTIR) spectroscopic measurements were performed in 400−4000 cm^{-1} range with a spectral resolution of 4 cm^{-1} at room temperature by Thermo Scientific Nicolet iS50 FT-IR spectrometer equipped with built-in all reflective ATR diamond. The ultraviolet-visible (UV/Vis) absorption spectra were recorded on Shimadzu 1800 UV–Vis spectrophotometer equipped with a temperature controller in the range of 200–800 nm. Prepared samples were irradiated by gamma ray flux ^{60}Co nuclide with a photon range of 1.3 MeV (Radiation unit located in Laboratory for radiation chemistry and physics “GAMA” in Vinča Institute of Nuclear Sciences, designed by the Commission Energie Atimique Conservatome from France).

Results and discussion

The phase identity and purity of synthesized $ZnPc_{MW}$ were investigated by XRD. As demonstrated in Figure 1., all of the $ZnPc_{MW}$ sample's reflection peaks could be indexed as β-ZnPc according to the JC-PDS card (No. 39-1882). No traces of any impurity phases were noticed indicating that the products were pure β-ZnPc crystals.

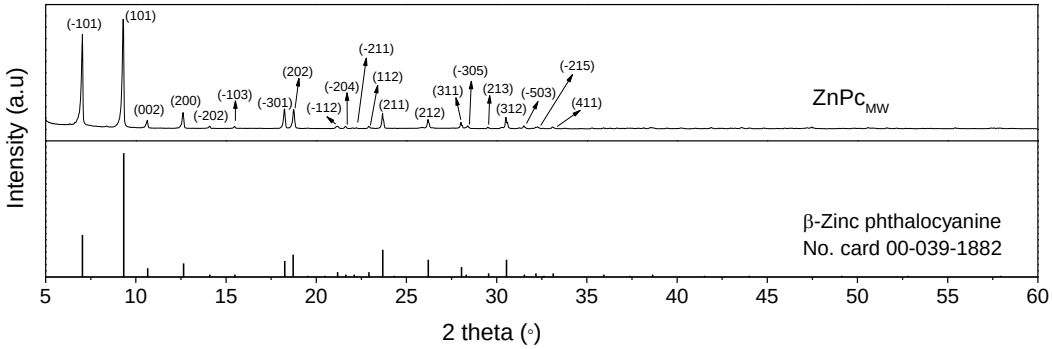

Figure 1. XRD pattern of ZnPc$_{MW}$.

The AFM surface morphologies (Figure 2.) show the flatness properties of the crystal face. The scanned surface in this AFM image is 8x8 μm^2, and in the inset we can see a zoomed surface of 2x2 μm^2. Average RMS surface roughness (calculated from several images covering 8x8 μm^2 surface area) is (124.6 ± 29) nm, the average length of crystals is (4.2 ± 0.8) μm, the average width is (2.4 ± 0.5) μm, and the average height is (0.43 ± 0.02) μm. The stacking structure of a planar ZnPc$_{MW}$ crystal strongly affects its high stability, due to π-π interaction between phthalocyanine moieties.

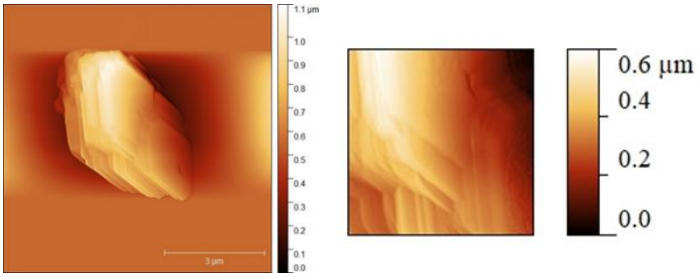

Figure 2. AFM image of ZnPc$_{MW}$ crystals.

The FT-IR spectral measurement is carried out to ascertain the functional group structures for ZnPc. The absence of the characteristic vibrations of C≡ N and the appearance of the absorption peaks at 1480 cm^{-1}, 1452 cm^{-1}, 1330 cm^{-1}, 1162 cm^{-1}, 1115 cm^{-1}, and 886 cm^{-1} assigned to phthalocyanine skeletal vibration indicated that the final products were synthesized successfully. The peaks located at 1407 and 1283 cm^{-1} are assigned to the stretching vibration of the aromatic phenyl ring and C–N= covalent bond, respectively. The absence of metal-free Pcs characteristic absorption peak around 1000 cm^{-1} confirmed the reaction selectivity and purity of the synthesized compound.

Absorption spectra of gamma-irradiated zinc-based phthalocyanines in DMSO under dose at 1, 2, 3, 5, 7, 10, 15, and 25kGy are presented in the Figure 3a. and corresponding photos of the gamma-irradiated solutions are presented in the Figure 3b. There are two broad bands with maxima in the ultra-violet region at a wavelength of 342 nm and in the red region at a wavelength of 667 nm. Each spectrum corresponds to a typical shape for this class of compounds.

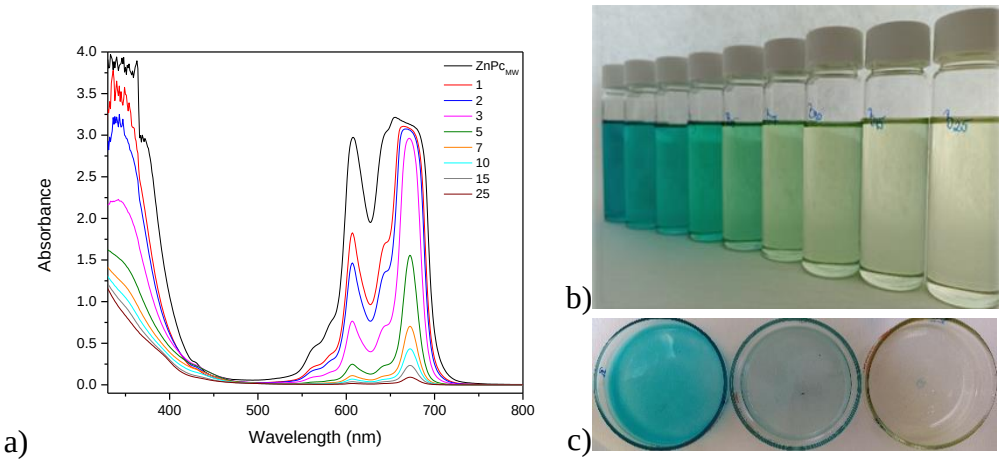

Figure 3. a) Absorption spectra of gamma-irradiated zinc phthalocyanine in DMSO under dose at 1, 2, 3, 5, 7, 10, 15, and 25kGy, and corresponding photos of b) gamma-irradiated zinc phthalocyanines solutions and c) selected ZnPc/PVA films.

The intense color of ZnPc is due mainly to the strong absorbance peak in the red region. Calibration curves of absorbance versus dose of gamma-irradiation demonstrate excellent linearity within the observed doses for all samples, confirming the applicability of the Beer-Lambert law and the absence of significant aggregation effects under gamma rays. The color of solutions is changed from blue to yellow under gamma-irradiation with different doses, which is a consequence of the intensity ratio and wide of the peaks from the second band, at wavelengths of 667 nm and 607 nm. The use of ZnPc/PVA films for dosimetry applications was successfully confirmed, as shown in Figure 3c. Selected solutions of ZnPc incorporated into PVA, irradiated at different doses of gamma irradiation, gave films with colored shades of blue, green, and yellow.

Conclusion

A new chemical dosimeter based on ZnPc has been introduced for gamma-irradiation applications. The compound was successfully synthesized under microwave irradiation. The solutions of organic dye were prepared in DMSO to study the effect of the degree of coloration on the dose response of the ZnPc solution dosimeter. Upon irradiation, the color of the samples changed from blue to yellow. The absorption spectra in the UV-Vis region reveal a gradual decrease of the absorption peak at wavelengths of 667 nm and 607 nm as the adsorbed dose increased up to 25kGy. The application of ZnPc/PVA films for radiation dose applications has been confirmed.

Acknowledgements

The research was funded by the Ministry of Education, Science and Technological Development of the Republic of Serbia (grant number 451-03-68/2022-14/200017).

References

[1] A.L. Melendez-Lopez, A. Paredes-Arriaga, J. Cruz-Castaneda, A. Negron-Mendoza, S. Ramos-Bernal, M. Colin-Garcia, A. Heredia, J. Nucl. Phys. Mat. Sci. rad. A. 6 (2018) 87.
[2] M.M. Eyadeh, K.A. Rabaeh, T.F. Hailat, F.M. Aldweri, Radiat. Meas. 108 (2018) 26.
[3] A. Raouafi, M. Daoudi, K. Jouini, K. Charradi, A.H. hamzaoui, P. Blaise, K. Farah, F. Hosni, Nucl. Instrum. Methods Phys. Res., Sect. B 425 (2018) 4.

[4] F.M. Aldweri, M.H. Abuzayed, M.S. Al-Ajaleen, K.A. Rabaeh, Results Phys. 8 (2018) 1001.
[5] M.A. Rauf, S. Salman Ashraf, J. Hazard. Mater. 166 (2009) 6.
[6] M.F. Barakat, K. El-Salamawy, M. El-Banna, M. Abdel-Hamid, A. Abdel-Rehim Taha, Rad. Phy. Chem. 61 (2001) 129.
[7] H.N. Raval, D.S. Sutar, V.R. Rao, Org. Elect. 14 (2013) 1281.
[8] N. Chaudhary, A. Singh, D.K. Aswal, A.K. Debnath, S. Samanta, S.P. Koiry, S. Sharma, K. Shah, S. Acharya, K.P. Muthe, S.C. Gadkari, Synth. Met. 231 (2017) 143.

ORANGE AND LEMON PEEL POWDERS AS A BIOELEMENT SOURCE

Ariana – Bianca Velciov[1], Adrian Riviș [1], Nicoleta Gabriela Hădărugă [1], Antoanela Cozma [2], Iasmina – Madalina Anghel [3], Gabriel Bujancă [1], Georgeta – Sofia Popescu [1], Maria Rada [4*]

[1]*University of Life Sciences "King Michael I" Timisoara, Faculty of Food Engineering, Food Science Department, Calea Aradului, 300645, Timisoara, Romania*
[2]*University of Life Sciences "King Michael I" Timisoara, Faculty of Agriculture, Department of Soil Sciences, Calea Aradului, 300645, Timisoara, Romania*
[3]*Politehnica University of Timişoara, Materials and Manufacturing Engineering Department, 300222, Timişoara, Romania*
[4]*University of Medicine and Pharmacy "Victor Babes", 2 EftimieMurgu Sq., 300041, Timisoara, Romania*
e-mail: radamariam@gmail.com

Abstract
The purpose of this paper was to evaluate the concentration of some bioelements from citrus peel powder. Peels powder was obtained by drying and grinding citrus peels as a by-product resulting after the preparation of some natural juices. The results obtained by atomic absorption spectrometry of Na, K, Ca, Mg, Fe, Mn, Zn and Cu, shows that the powders taken into the study contain important amounts of essential mineral elements, especially Ca and K (159-182 mg/100g, respectively 211-218 mg/100g) and also appreciable contents of Mg (15.3-23.4 mg/100g), Fe (18.1-34.1 mg/100g), Zn (9.34-11.8 mg/100g), Na (8.75-12.8 mg/100g), Cu (1.27-3.71 mg/100g) and Mn (1.32-2.03 mg/100g).
The concentration of the analyzed mineral bioelements shows, in general, the following decreasing trend: K> Ca> Fe> Mg> Zn> Na> Cu> Mn.

Keywords: *orange peel powder, lemon peel powder, bioelement sources.*

Introduction
The peel of oranges and lemons, resulted as a by-product when obtaining natural juices, still contains important quantities of nutritionally and biologically active compounds, among which are also mineral substances, which could be used as additives to improve the nutritional parameters of many foods: bakery, beverage, chocolate, desserts, ice cream, smoothies, toppings, yoghurts, etc. [1,2,3,4]. These peels may provide a health benefit, beyond the traditional nutrients they contain, as well as prevent diet-related diseases, e.g.: metabolic syndrome, type II diabetes, coronary heart disease, obesity, hypertension, certain types of cancer, gastrointestinal diseases and osteoporosis [5].
Literature data shows that orange and lemon peels are rich in phenolic compounds, vitamins, minerals and dietary fiber with antioxidant properties [2,6,7,8].
The purpose of this study was to obtain powder from orange and lemon peels, as a by-product from the preparation of natural juices in order to evaluate their bioelement contents. Bioelements Na, K, Ca, K, Mg, Fe Mn, Zn and Cu from orange and lemon powders peel prepared under laboratory conditions were analyzed.

Materials and methods

Fruits were acquired in bulk from the fruit local markets in Timisoara. (Romania). Oranges and lemons were washed thoroughly, peeled and the fruit peels were cut into small pieces and oven dried (at 40-50 ^{0}C, until the constant mass).

The bioelements from oranges and lemon peels were carried out according to the method recommended [9]. The determination consists in calcining the powder peels at 550 ^{0}C, followed by solubilizing the ash in HNO_3 0.5 N and measuring the concentrations of mineral elements using the FS Varian 280 Spectrometer.

Results and discussions

The results obtained from the analysis, by of Na, K, Ca, Mg, Fe, Mn, Zn and Cu from orange and lemon peel powders shows that the samples contains important amounts of macro and essential elements (table 1).

Table 1. Mineral composition (mean values) of orange and lemon peel powders

Peel powder	Mineral content, mg/100g							
	Na	K	Ca	Mg	Fe	Mn	Zn	Cu
Orange	12.8± 0.93	218± 9.03	182± 8.06	23.4± 2.53	34.1± 1.83	2.03± 0.52	11.8± 1.03	3.71± 0.43
Lemon	8.75± 0.76	211± 8.65	159± 8.18	15.3± 1.03	18.1± 1.11	1.32± 0.24	9.34± 0.66	1.26± 0.25

The distribution of bioelements analyzed in orange and lemon peel powder is uneven, depending on the fruit from which they come (orange or lemon) and the analyzed bioelement: 12.8 mg/100g Na, 218 mg/100g K, 182 mg/100g Ca, 23.4 mg/ 100g Mg, 34.1 mg/100g Fe, 2.03 mg/100g Mn, 11.8 mg/100g Zn, 3.71 mg/100g Cu - in orange peel powder and 8.75 mg/100g Na, 211mg/100g K, 159 mg/100g Ca, 15.3 mg/100g Mg, 18.1mg/100g Fe, 1.32 mg/100g Mn, 9.34 mg/100g Zn, 1.26 mg/100g Cu - in lemon peel powder.

From all the analyzed elements, potassium and calcium are the best represented. Compared to these, magnesium and iron were determined in much lower concentrations, but much higher levels compared to Na, Zn, Cu and Mn. Comparing the mineral concentrations of the two citrus fruit peel powders, it can be seen that the orange peel powder has a significantly higher content of bioelements.

The obtained results show that the powders from the analyzed fruit peels could be used to improve the mineral content of foods.

Conclusion

Orange and lemon peel powders, obtained under the conditions of this experiment, contain important amounts of essential mineral elements, especially Ca and K, but also appreciable contents of Mg Fe, Zn, Na, Cu and Mn. In general, the concentration of the analyzed mineral bioelements shows the following decreasing trend: K> Ca> Fe> Mg> Zn> Na> Cu> Mn.

Orange peel powder is significantly richer in bioelements, comparable to lemon peel powder.

Orange and lemon peel powders obtained in this experiment can be recommended to be used to improve the mineral content of foods. In addition, due to the increased content of dietary fibers, antioxidants, vitamins, etc. presents a series of benefits regarding the health of the body.

The development of orange and lemon powders, rich in nutritional and biologically active compounds, can be a method of superior valorization of the orange and lemon peels resulting as by-products when obtaining natural juices.

Acknowledgements
The present paper was funded by the Research Project "Research on the use of biologically active substances in order to obtain high-nutrition foods", No 1545/28.02.2019.

References
[1] Dias P.G.I., Sajiwanie J.W.A., Rathnayaka R.M.U.S.K., Chemical composition, orit physicochemical and technological properties of selected fruit peels as a potential food surce, International Journal of Fruit Science, 2020, 20(S2): S240–S251.
[2] Czech A., Zarycka E., Yanovych D., Zasadna Z., Grzegorczyk I., Kłys S., Mineral content of the pulp and peel of various citrus fruit cultivars, Biological Trace Element Research, 2019, 193:555–563 https://doi.org/10.1007/s12011-019-01727-1
[3] Srivastava N., Yadav K.C., Verma P., Kishore K., Rout S., Development of lemon peel powder and its utilization in preparation of biscuit by different baking methods, IJSRD. 2015, 3(08), ISSN (online): 2321-0613
[4] El-Beltagi H.S., Eshak N.S., Mohamed H.I., Bendary E.S.A., Danial A.W., Physical characteristics, mineral content, and antioxidant and antibacterial activities of *Punica granatum* or *Citrus sinensis* peel extracts and their applications to improve cake quality. Plants **2022**, 11, 1740. https://doi.org/10.3390/plants11131740
[5] Belose B.B., Kotecha P.M., Godase S.N. and Chavan U.D., Studies on utilization of orange peel powder in the preparation of cookies, International Journal of Chemical Studies 2021; 9(1): 1600-1602.
[6] Rani V., Sangwan V., Rani V. and Malik P., Orange peel powder: a potent source of fiber and antioxidants for functional biscuits, Int.J.Curr.Microbiol.App.Sci (2020) 9(9): 1319-1325 1319
[7] Feumba Dibanda Romelle, Ashwini Rani P. and Ragu Sai Manohar, Chemical Composition of some selected fruit peels, European Journal of Food Science and Technology, 2016, 4(4): 12-21
[8] Abdelazem R.E., Hefnawy H.T. and El-Shorbagy G.A., Chemical composition and phytochemical screening of *Citrus sinensis* (orange) peels, Zagazig J. Agric. Res.,2021, 48(3).
[9] Abdelwahab A. S. and Abouelyazeed A., Bioactive compounds in some citrus peels as affected by drying processes and quality evaluation of cakes supplemented with citrus peels powder, J. adv. agric., 2018, 23(1): 44-67.

THE EFFECT OF PEROXYDISULFATE ION ON THE PHOTOCATALYTIC EFFICIENCY OF BiOI

Bence Veres[1], Máté Náfrádi[1], Zsolt Pap[2], Tünde Alapi[1]

[1]Department of Inorganic and Analytical Chemistry, University of Szeged, H-6720 Szeged, Dóm tér 7, Hungary
[2]Applied and Environmental Chemistry Department, University of Szeged, H-6720 Szeged, Rerrich Béla tér 1, Hungary
e-mail: veres0629@gmail.com

Heterogeneous photocatalysis is a promising method for eliminating organic substances from water. The efficiency of TiO_2 and ZnO, the most often used and commercially available photocatalysts, is based primarily on the hydroxyl radical ($^{\bullet}OH$) generation and requires UV light. Several photocatalysts have been synthesized during the last decades, which aim to enhance the efficiency of the separation of the photogenerated charges and decrease the energy required for the generation of electron-hole pairs, making to be more cost-effective this process. The operation of photocatalysts, which can be excited by visible light radiation, is mainly based on direct charge transfer. Their efficiency can be enhanced via the application of electron scavengers, especially if the electron scavenger transforms into a more reactive species than $O_2^{\bullet-}$. In this work, the effect of peroxydisulfate ion ($S_2O_8^{2}$, PDS) was studied in the case of BiOI photocatalysts [1]. PDS is an effective electron scavenger, and the formed $SO_4^{\bullet-}$ is a potent oxidizing agent having similar reactivity and potential (E_0 = 1.9 – 2.7 eV) as $^{\bullet}OH$ (E_0 = 2.6 – 3.1 eV) [2]. Thus, applying PDS enhanced efficiency is expected due to the hindered recombination of photogenerated charges and the formation of reactive $SO_4^{\bullet-}$.

The transformation of 1,4-benzoquinone (BQ) and sulfamethoxypyridazine (SMP), and trimethoprim (TRIM) was studied in the presence of PDS in UV (398 nm), and visible light irradiated suspensions. BiOI photocatalyst was proven to be efficient even under visible light irradiation. The PDS addition highly enhanced the transformation rate of both BQ and SPM, while SMP transformation was very slow, and PDS had no positive effect. The reusability test of the photocatalyst showed that the photocatalytic activity did not decrease during three consecutive cycles, and PDS did not cause any structural change in the photocatalyst.

The effect of matrix and matrix components should be investigated for practical reasons. The impact of the biologically treated domestic wastewater as a matrix, and the effect of its main inorganic anions, such as Cl^- and HCO_3^- were studied. The reactions between these ions and $SO_4^{\bullet-}$ produce $Cl^{\bullet-}$, $CO_3^{\bullet-}$ and can affect the transformation rate and way of organic substances. Our results showed that the efficiency of the BiOI photocatalyst had deteriorated significantly, partly because of the organic substances adsorbed on the surface of the BiOI and partly because of the structural changes caused by the HCO_3^-. The harmful effect of HCO_3^- could be partially prevented by lowering the pH.

Acknowledgment
This work was sponsored by the National Research, Development, and Innovation Office-NKFI Fund OTKA, project number FK132742.

References
[1] X. Lv, F. L. Y. Lam, X. Hu, *Front. Catal.*, 2 (2022) 1-24.
[2] N.K.V Leitner, *Sulfate radical ion – based AOPs*, in: Mihaela I. Stefan (Ed.), *Advanced Oxidation Processes for Water Treatment.* (2017) 429–455

EFFECT OF THE CHELATING AGENT ON THE STRUCTURE AND MORPHOLOGY OF THE SYNTHESIZED PEROVSKITE NANOMATERIALS

Paulina Vlazan, Maria Poienar, Daniel Ursu, Anamaria Dabici, Doru Buzatu, Paula Sfirloaga

National Institute for Research and Development in Electrochemistry and Condensed Matter, str. Dr. A. Paunescu Podeanu 144, 300569 Timisoara Romania
e-mail: paulasfirloaga@gmail.com

Abstract

Perovskite with oxides structure are attractive candidates for various applications due to of their structure flexibility and outstanding physical and chemical properties [1]. $YMnO_3$ is one of the most studied materials, with hexagonal structure and space group $P6_3cm$, having a high ferroelectric transition temperature (T_C ~ 900 K) and a low anti-ferromagnetic transition temperature (T_N ~ 70 K) [2,3].

In this work were studied of the $YMnO_3$ nanopowders obtained a sol-gel process using citric acid, urea or ethylenediaminetetraacetic acid (EDTA) as chelating agents. The emphasis was on the effect of the three different chelating agents, on the morpho-structural properties, and on the phase transformations during the heat treatment. The as-prepared samples were characterized by means of techniques such as X-ray powder diffraction (XRD), SEM- EDX and carried out simultaneous differential thermal analysis and thermogravimetric analysis (DTA–TG). Nanocrystalline perovskite yttrium manganese oxide ($YMnO_3$) samples synthesized by sol – gel technique was subsequent heat treatment at 1000 °C for one hour.

The samples were characterized by X-ray diffraction (XRD), scanning electron microscopy (SEM), X-ray energy dispersive spectroscopy (EDS) and ultraviolet-visible (UV–Vis) spectroscopy. The XRD pattern of the prepared samples confirmed the formation of a pure phase of $YMnO_3$ with hexagonal structure and space group: P63cm, according to JCPDS 25-1079. The energy-dispersive X-ray analysis (EDX) results highlight the elemental composition of the samples synthesized.

Acknowledgements

This work was supported by theExperimental Demonstrative Project 683PED / 2022. The authors thank C. Ianasi for help during thematerials characterization.

References

[1] J. Zhao, X. Wang, ACS Omega, 7 (2022) 10483−10491.
[2] N. Kumar, A. Gaur, G.D.Varma, J. Alloys Compd. 509 (2011) 1060 – 1064.
[3] O. Nirmala, P. Sreedhara Reddy, V. Diwakar Reddy, Materials Today: Proceedings 23 (2020) 490–494

CHARACTERIZATION OF HYBRID CHONDROITIN/DERMATAN SULFATE OCTASACCHARIDE DOMAINS IN HUMAN BRAIN BY ION MOBILITY TANDEM MASS SPECTROMETRY

Raluca Ica[1], Mirela Sarbu[1], Roxana Biricioiu[1,2], Ana-Maria Crumpei[1,2], Edie Sharon[3], David E. Clemmer[3], Alina D. Zamfir[1,4]

[1]Department of Condensed Matter, National Institute for Research and Development in Electrochemistry and Condensed Matter, Timisoara, Romania
[2]Department of Physics, West University of Timisoara, Timisoara, Romania
[3]Department of Chemistry, The College of Arts & Science, Indiana University, Bloomington, Indiana, USA
[4]Department of Technical and Natural Sciences, "Aurel Vlaicu" University of Arad, Arad, Romania
e-mail: alina.zamfir@uav.ro

Abstract
We report here on the introduction of a rapid, highly sensitive and reliable approach in a single run, based on ion mobility separation (IMS), high resolution and tandem MS (MS/MS) by collision-induced dissociation (CID) for compositional and structural elucidation of neural chondroitin sulfate (CS) and dermatan sulfate (DS) domains, which implies the determination of the epimerization and the sulfation code of regular and irregular structures. By IMS MS and CID MS/MS, we were able to characterize in details CS/DS octasaccharides from brain obtained after CS/DS chain depolymerization by chondroitin B lyase and to detect sequences that were never found before in the octasaccharide domains of the investigated CS/DS brain fraction.

Introduction
Proteoglycans represent heavily glycosylated proteins, covalently linked to glycosaminoglycans (GAGs), which are sulfated linear polysaccharides. Among GAGs, CS and DS frequently arise as hybrid CS/DS motifs predominantly expressed in mammalian tissue. In brain, CS/DS modulate glial cell maturation, cellular behavior and are implicated in several neurological events. CS/DS are sulfated at either GalNAc and/or IdoA/GlcA in a variety of combinations to yield characteristic patterns and a large structural diversity of domains in human brain, some of which being associated to the diseases of the central nervous system. Therefore, the analysis of CS/DS oligosaccharides in brain and the identification of regularly, over-, and undersulfated alternating motifs became the focus of the research in the field.

Experimental
The CS/DS chain extracted from brain was deploymerized by using chondroitin B lyase, which specifically cleaves the 3GalNAcβ1–4IdoAα1 bond irrespective of the sulfation status of the molecule. Following the size exclusion chromatography, the separated octasaccharide fraction was collected. For the IMS MS analysis, the octamer pool was dissolved in pure methanol to the concentration of 5 pmol/μL and infused into a Synapt G2S mass spectrometer by nanoESI. The signal was acquired in the negative ion mode at 0.9 kV ESI and 30 V cone voltage respectively. IMS wave velocity was set at 650 m/s and IMS wave height at 40 V. Fragmentation analyses for detailed structural investigation was performed by MS/MS using CID at low collision energies within 30-50 eV range.

Results and discussion

The driftscope display (drift time *vs. m/z*) of the total distribution of CS/DS octamer fraction ions has shown that the brain-derived octasaccharide species were separated by IMS MS into mobility families based on the charge state and the sulfation content. Following the digestion with chondroitin B lyase and the IMS MS separation and screening, several distinct unsaturated and saturated GlcA-rich species were detected and identified in the investigated octasaccharide fraction. Apart from the regularly tetrasulfated-[4,5-Δ-IdoAGalNAc(GlcAGalNAc)$_3$] octasaccharide bearing one sulfate group per disaccharide repeat, detected as a tetradeprotonated molecule, a number of unusual species, highly interesting from the structural and biological point of view, were for the first time discovered in brain tissue due to their separation by IMS and the high resolution and mass accuracy provided by the employed MS instrument. These motifs are GlcA-rich chains characterized by either undersulfation such as the monosulfated-[4,5-Δ-IdoAGalNAc(GlcAGalNAc)$_3$] and the trisulfated -[4,5-Δ-IdoAGalNAc(GlcAGalNAc)$_3$] species or oversulfation such as the pentasulfated-[4,5-Δ-IdoAGalNAc(GlcAGalNAc)$_3$], the hexasulfated-[4,5-Δ-IdoAGalNAc(GlcAGalNAc)$_3$] and the octasulfated -[4,5-Δ-IdoAGalNAc(GlcAGalNAc)$_3$] octasaccharides.

In the last stage of research, the rare CS/DS domains, exhibiting the atypical sulfation pattern *i.e.* the under and oversulfated CS/DS chains discriminated by IMS MS were submitted to CID MS/MS, which was carried out after mobility separation in the transfer cell. CID MS/MS data revealed one mobility feature for every isolated ion and a set of product ions, which are of diagnostic value for the determination of the sulfate sites and complete characterization of the sulfation code.

Conclusion

The optimized IMS MS has revealed different species in the CS/DS octasaccharide pool from human brain obtained after chain depolymerization using chondroitin B lyase. Since, to prevent the sample loss, rechromatography was avoided, the octamer fraction contained traces of hexasaccharides, which could be also discriminated by the present approach. Except for the regularly sulfated hexa- and octasaccharide domains, containing one sulfate group per disaccharide repeat, we have discovered five oversulfated structures and one undersulfated motif. Among these, the saturated tetrasulfated- IdoAGalNAc[GlcAGalNAc]$_2$ and pentasulfated- IdoAGalNAc[GlcAGalNAc]$_2$ document the oversulfation of the GAG chain reducing end. CID MS/MS of the $[M\text{-}3H^+]^{3-}$ detected at *m/z* 484.64, corresponding according to mass calculation to the tetrasulfated 4,5-Δ-IdoAGalNAc[GlcAGalNAc]$_2$ generated fragment ions consistent with a hexasaccharide motif having all GalNAc moieties and the first GlcA from the non-reducing end sulfated.

Acknowledgements

This work was supported by the Romanian National Authority for Scientific Research, UEFISCDI, through projects PN-III-P4-ID-PCE-2020-0209 granted to A.D.Z. and PN-III-P1-1.1-PD-2019-0226 granted to M.S.

References

[1] K.L. Medard, H. Hamilton, S.C. van der Moore, J. Chem. Anal. 313 (2007) 163.

[2] B.T. Metan, A. Milne, in: A.C. Thomson, P.T. Bell (Eds.), Introduction to General Chemistry, Chempublishing, Washington, 1994, pp. 547.

EFFECT OF INOCULATION WITH PGPR ON BASIL ANTIOXIDANT ACTIVITY

Ružica Ždero Pavlović[1], Bojana Blagojević[1], Dragana Stamenov[1], Timea Hajnal Jafari[1], Simonida Đurić[1], Boris M. Popović[1]

[1]Faculty of Agriculture, University of Novi Sad, Trg Dositeja Obradovića 8, 21000 Novi Sad, Serbia
e-mail: ruzica.zdero@polj.uns.ac.rs

Abstract
Basil (*Ocimum basilicum* L.) is a widely utilized culinary herb. It is used to flavour foods such as vegetables, meats, fish, etc. In traditional medicine is used for treatment of various disorders such as colds, respiratory diseases, cardiovascular diseases, metabolic and gastrointestinal disorders, etc. The effects of climate changes on agriculture can result in lower yield and nutritional quality of plants. The inoculation of plants with plant growth-promoting rhizobacteria (PGPR) such as *Azotobacter*, *Streptomyces*, and *Bacillus* are well known to lead to improvement in germination, growth, and yield. Also, it was found that PGPR enhance defence capacity of the plant. In this study, the basil seed were inoculated with selected PGPR isolates: Bac3, Azb, and Act. Control seeds were immersed into distilled water. After 6 weeks plant material was collected, and methanol extracts were prepared for antioxidant determinations. The changes in total phenol and flavonoid content, as well as antioxidant activity, were monitored. PGPR applied in the experiment have not cause significant changes in total phenol content. However, treatments with Azb and Act isolates have increased flavonoid content in basil plants. The antioxidant activity of basil plant has been measured as the ability of plant extracts to reduce DPPH radicals. Obtained results show that only treatment with Azb isolates significantly increases the antioxidant activity of basil plants. Results obtained in this study suggested that investigated isolates have different effects on the antioxidant characteristics of the basil plant. Further investigation is still needed to explore the possibility of using these PGPRs as potent bio-fertilizer in basil production.

Keywords: antioxidant activity, basil, inoculation.

Introduction
Basil (*Ocimum basilicum* L.) is a very popular medicinal plant but also is used as a culinary herb. Traditionally, it was used in the treatment of different diseases, like inflammation, bronchitis, tumours, etc. [1]. Results of scientific experiments support these traditional uses of the basil plant. Due to the high content of phenolic acids, flavonoids, and rosmarinic acid in leaf extract, but also aromatic compounds in essential oil basil have a wide spectrum of positive health properties [2]. In medicinal plants, the most investigated is an antioxidant activity because represents the first link between a chemical reaction and biological activity. It is generally accepted that free radicals are responsible for various damages in the body which precede different pathological conditions [3]. The antioxidant activity of phenolic compounds is primarily the result of their ability to be donors of hydrogen atoms and as such remove free radicals with the formation of less reactive phenoxyl radicals (Figure 1). The increased stability of the formed phenoxyl radical is attributed to electron delocalization and the existence of multiple resonance forms.

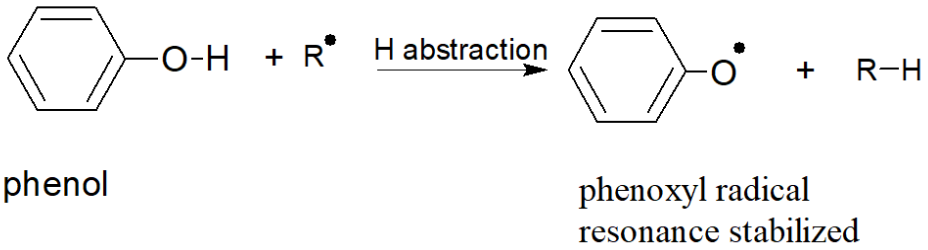

Figure 1. Radical reaction in which phenol as an antioxidant compound quenching an active free radical (**R**•) to **R - H** and itself converted into resonance stabilized phenoxyl radical.

In recent years, biochemical research on secondary biomolecules in plant extracts has received more and more attention due to the tendency to replace synthetic therapeutics with drugs of natural origin [4]. Also, several studies have shown that in response to stress conditions in plants are stimulated synthesis of phenolic compounds, which could enhance antioxidant activity of plant [5, 6].
The purpose of this study was to investigate the effect of PGPR on phenolic content and antioxidant activity of basil plants, in order to test potential of these PGPR isolates to induce accumulation of phenolic compounds in basil.

Experimental

Plant material and extract preparation

In this experiment, the bacterial strains were isolated from natural populations of nettle (*Urtica dioica* L.) rhizosphere soil. From selected PGPR organisms 3 different inoculums were prepared with isolates Bac3, Azb, and Act, and there were used for the inoculation of basil seeds. Plants were grown in controlled conditions for 6 weeks in pots with soil (Figure 2). The dried and powdered plant material was used for biochemical analyses. Methanol extracts were prepared by the method described in Šibul et al. [7] with minor modifications. About 1g of dried plant powder was soaked in 26 ml of methanol (80%) for 90 minutes at room temperature. The mixture was centrifugated at 3500 rpm/min for 10 minutes. The extraction was repeated 4 times with a fresh portion of solvent.

Figure 2. Pots with basil (*Ocimum basilicum* L.) plants at the end of experiment (ø control, and applied PGPR: isolate Azb, isolate Act, and isolate Bac3).

Total Phenolic Content

Total content of phenolics of a methanol extract was determined by the Folin-Ciocalteu procedure and expressed as mg of gallic acid equivalents per g dry weight plant material (mg GAE/g DW) [8]. A volume of 150 µL of distilled water and 50 µl of the corresponding extract were mixed with 1 ml of 0.1 M Folin-Ciocalteu reagent. After 10 minutes, in the mixture was added solution of 7.5% sodium carbonate and the absorbance was measured after 1h at 760 nm.

Total Flavonoid content

For determination of total flavonoid content (TFC) of methanol extracts method described by Chang et al. [9] was used. For analysis, 200 µL of the methanol extract was mixed with 800 µL distilled water, 100 µL of $AlCl_3$ 0.75M solution, and 100 µL 1M Na-acetate solution. After 30 minutes of incubation at room temperature in the dark, the absorbance was measured at 415 nm. The flavonoid content was calculated as a quercetin equivalent from the calibration curve of quercetin standard solutions and expressed as µg quercetin equivalent per g of dry weight plant material (µg QE/g DW).

Antioxidant activity

In order to assess the scavenging activity against DPPH· radical of methanol extracts, the method described by Sánchez-Moreno [10] was followed with minor modifications. The assay mixture contained 2 ml DPPH· solution (30 µmol/l) and 0.2 ml of the methanol extract in different concentrations (0.482 – 3.856 mg/ml). The mixture was shaken vigorously on a Vortex mixer, then incubated for 30 min at 25 °C in the dark, after which the absorbance of the remaining DPPH· was determined at 515 nm. For each sample, three replicates were carried out. Radical Scavenging Capacity (RSC) was calculated by the equation:

$RSC = (A_{control}-A_{sample})/A_{control} \times 100$

where $A_{control}$ is the control and A_{sample} is the sample solution absorbance. The concentration that causes a decrease in the initial absorbance (control) by 50% is defined as IC_{50}. The IC_{50} values for all RSC determinations were determined by polynomial fitting of the inhibition values using software ORIGIN 9.1.

Results and discussion

The TPC values of basil plant samples are given in Figure 3. Control sample had a TPC value of 4.24 mg GAE/g dw. The similar value was obtained for Azb treatment (4.18 mg GAE/g dw). Treatment with Act decreased the TPC value by about 25% (3.20 mg GAE/g dw). Similar TPC values for methanol extract of basil leaves have been reported [11].

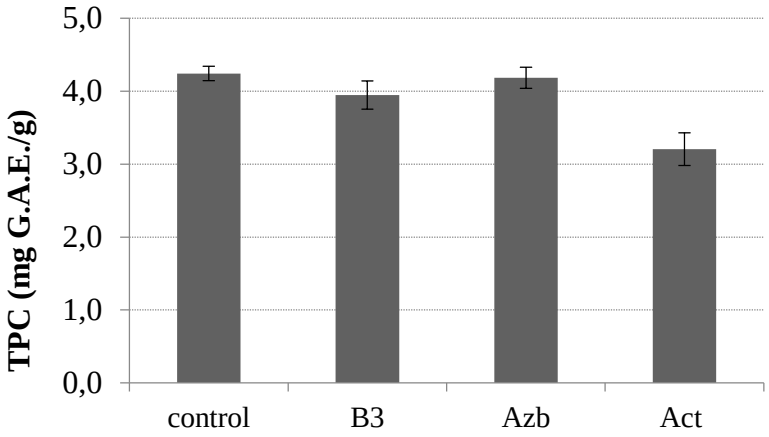

Fıgure 3. Effect of inoculation of PGPR on total phenolic content in basil plants

The TFC values were given in Figure 4. In control plants TFC value was 0.334 µg QE/g dw. The highest TFC value was found in plants inoculated with Azb (0.459 µg QE/g dw). Also, in plants inoculated with Act have been observed increase of TFC compared to control plants. According to the Ghorbanpour et al. [12] accumulation of flavonoids was stimulated by PGPRs inoculation.

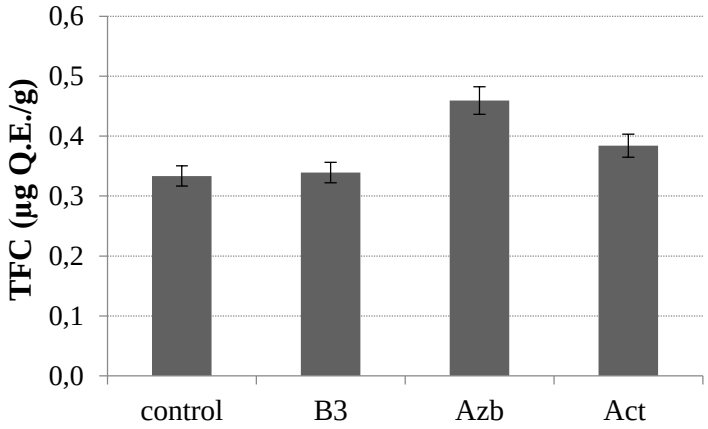

Figure 4. Effect of inoculation of PGPR on total flavonoid content in basil plants

The antioxidant activity of basil plant has been measured as the ability of plant extracts to reduce DPPH radicals (Figure 5) and was expressed as IC_{50} value. This value indicates concentration of extract which is required to achieve 50% scavenging activity. Obtained results show that only treatment with Azb isolates significantly increases the antioxidant activity of basil plants, with IC_{50} value 4.76 mg/ml compared to control (7.14 mg/ml).

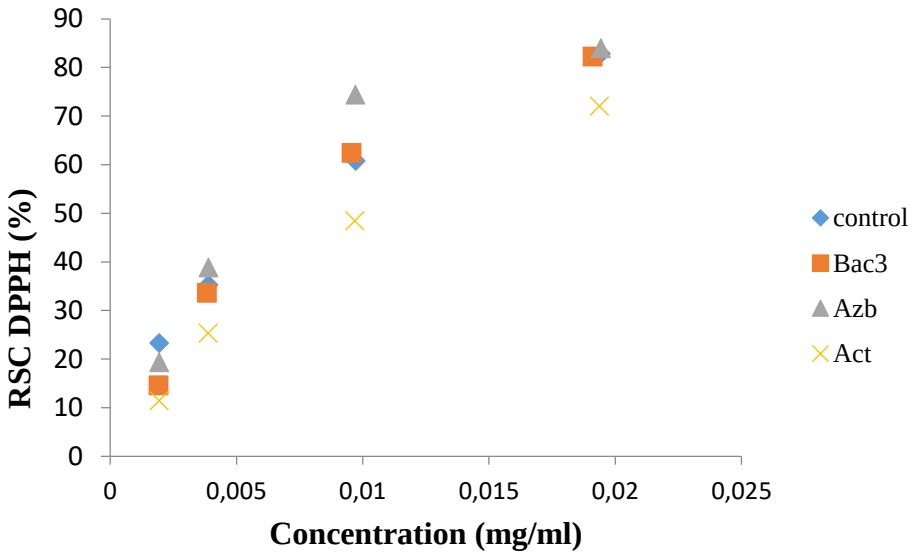

Figure 5. Effect of inoculation of PGPR on antioxidant activity of basil plants

Conclusion

Results obtained in this study suggested that investigated isolates have different effects on the antioxidant characteristics of the basil plant. Further investigation is still needed to explore the possibility of using these PGPRs as potent bio-fertilizer in basil production.

Acknowledgements
This research work was supported by the Ministry of Education, Science and Technological Development of the Republic of Serbia, Serbia (Grant No. 451-03-68/2022-14/200117).

References
[1] S. Filip, Int. J. Clin. Nutr. Diet. 3 (2017) 118.
[2] C. Jayasinghe, N. Gotoh, T. Aoki, S. Wada, J. Agric. Food Chem. 51 (2003) 4442-4449.
[3] B. Halliwel, & J.M.C. Gutteridge (Eds.), Free Radicals in Biology and Medicine, Clarendon Press, Oxford, 1989, pp.416–494.
[4] C.S. Cooper, & P.L. Grover, (Eds), Chemical carcinogenesis and mutagenesis II. Cooper CS and Grover PL Springer-Verlag, Berlin, Heidelberg, 2012, pp. 164-170
[5] R. Ždero Pavlović, B. Blagojević, D. Latković, D. Agić, N. Mićić, D. Štajner, & B.M. Popović, Balt. For. 26 (2020) 420
[6] B. Kiprovski, Đ. Malenčić, S. Đurić, M. Bursać, J. Cvejić, V. Sikora, J. Serb. Chem. Soc. 81 (2016) 1239-1249.
[7] F. Šibul, D. Orčić, E. Svirčev, M.N. Mimica-Dukić, Hem. Ind. 70 (2016) 473-483.
[8] E.A. Ainsworth, & K.M. Gillespie, Nat. protoc. 2 (2007) 875-877.
[9] C.C. Chang, M. H. Yang, H. M. Wen, J. C. Chern, J. Food Drug Anal. 10 (2002).
[10] C. Sánchez-Moreno, J. A. Larrauri, F. Saura-Calixto, J. Sci. Food Agric. 76 (1998) 270-276.
[11] X. Ren, N. Lu, W. Xu, Y. Zhuang, M. Takagaki, Horticulturae 8 (2022) 216.
[12] M. Ghorbanpour, M. Hatami, K. Kariman, P. Abbaszadeh Dahaji, Chem. Biodiver. 13 (2016) 319-330.

$TiO_2/CuMnO_2$ HETEROJUNCTION-BASED SELF-POWERED UV PHOTODETECTORS

Carmen Lazau[1], Mircea Nicolaescu[1,2], Corina Orha[1], Viorel Şerban[2,3], Cornelia Bandas[2]

[1]National Institute for Research and Development in Electrochemistry and Condensed Matter Timisoara, 300569 Timisoara, Romania
[2]Department of Materials and Manufacturing Engineering, Faculty of Mechanical Engineering, University Politehnica of Timisoara, 300222 Timisoara, Romania
[3]Romanian Academy of Technical Sciences, 300223 Timisoara, Romania
e-mail: nicolaescu.mircea13@yahoo.com

Abstract

Self-powered ultraviolet-photodetectors (SPVs) have been very studied lately because they have a great advantage, namely they do not need any external power sources, can operate continuously and independently and do not require high costs to produce them [1]. Over time, it was shown that metal oxide heterojunctions can facilitate photovoltaics for self-powered operation due to their built-in potential which automatically separates generated electron-hole pairs [2]. Therefore, various metal-oxide semiconductor materials (i.e., TiO2, ZnO, CuO, and NiO) have been applied for different types of photovoltaic cells [3], but among them, TiO2 was selected as the most desirable material for photovoltaic devices [4].

In this paper, FTO /n-TiO2 /p-CuMnO2 heterojunction based self-powered UV photodetector was successfully produced in this configuration for the first time. The development process presumes two phases: (a) the TiO2 thin films deposition by the Doctor blade technique (n-type TiO2) on the FTO substrate and, (b) the deposition of CuMnO2 film by spin-coating method (p-type CuMnO2) on the FTO/n-TiO2 structure, respectively. The structural and morphological characteristics of the as-synthesized heterostructures are investigated by techniques such as X-ray diffraction, UV-Vis spectroscopy, scanning electron microscopy, energy dispersive X-ray and atomic force microscopy. The heterojunction characteristics of the TiO2 and CuMnO2 thin films deposited on the FTO substrate are being established by current-time analysis. Measurement of the current time in the dark and UV irradiation were performed to show the sensor response value. The responsivity in the self-powered mode was 2.84 × 107 A W−1 cm2 and in the 1 V bias mode it was 1.82 × 106 A W−1 cm2. Under UV illumination with an intensity of 0.1 mW/cm2 a self-powered current of 14.2 nA was generated. The above results show that of n-TiO2/p-CuMnO2 transparent heterojunction device exhibited a self-powered ultraviolet photodetector with high sensitivity [5].

Acknowledgements

This research was funded by a grant of the Ministry of Research, Innovation and Digitization, CNCS–UEFISCDI, project number PN-III-P1-1.1-TE-2021-0963, within PNCDI III, with contract number TE13/2022 (DD-CyT) and project code PN 19 22 04 01 TINSME, 40 N/2019, and partially by project number PN-III-P2-2.1-PED-2019-4492, contract number 441PED/2020 (3DSAPECYT).

References

[1] Chetri, P.; Dhar, J.C. Mater. Sci. Semicond. Process. 100 (2019), 123–129.
[2] Praveen, S.; Veeralingam, S.; Badhulika, S. Adv. Mater. Interfaces 8 (2021), 2100373.

[3] Krysova, H.; Zlamalova, M.; Tarabkova, H.; Jirkovsky, J.; Frank, O.; Kohout, M.; Kavan, L. Electrochim. Acta, 321 (2019), 134685.
[4] Zhang, D.; Gu, X.; Jing, F.; Gao, F.; Zhou, J.; Ruan, S. J. Alloys Compd. 618 (2015), 551–554.
[5] Lazau, C.; Nicolaescu, M.; Orha, C.; Serban, V.; Bandas, C. Materials, 15 (2022), 15.

ALUMINUM /IRON MIXED OXIDES OBTAINED BY CO-PRECIPITATION METHOD

Mina Ionela Popescu [1,2], Corina Orha[1], Carmen Lazau[1,], Cornelia Bandas[1], Narcis Duteanu[2]

[1]National Institute of Research-Development for Electrochemistry and Condensed Matter Timisoara, A. Paunescu Podeanu Street no 144, Timisoara, Romania
[2]Politehnica University of Timisoara, Romania, P-ta Victoriei no. 2, Timisoara, Romania
e-mail: mina.popescu37@gmail.com

Abstract

In last years, various synthesis methods have been used for production of nanomaterials, composites/nanocomposites. For preparation of catalysts are used different methods such as hydrothermal, sol-gel and co-precipitation. Because Fe_2O_3 -Al_2O_3 mixed oxide system offer many advantages, its important to know if the combination of two transition metal oxides can affect their stoichiometry, surface, catalytic properties and textural structure. The aim of this study is represented by mixed of oxides who was obtained from the synthesis of aluminum nitrate and iron nitrate who was prepared by the co-precipitation method. Then, the characterization studies about the compounds obtained such as hematite, magnetite and the alumina were performed by X-Ray Diffraction (XRD), Scanning Electron Microscopy (SEM), and UV-Vis spectrophotometry.

Introduction

Aluminum oxide is considered an important chemical who was noticed such as good product with different properties like strength product resistance [1], also have a chemical, electrical, optical and thermal properties [2]. Based on oxidation and reduction, co-precipitation on Al with Fe oxides respectively hydroxides induces the dissolution of Fe from the phrases containing Fe and its re-precipitation as Fe-Al [3]. The treatment of two oxides at high temperatures is known to produce new crystalline structures [4]. Iron-substituted alumina, which is a different mixed oxide has been the subject of various investigations into its use in treating industrial effluents, this issue attracting more and more attention today [5].

Experimental

Co-precipitation is a fairly exploited method for obtained iron oxides (nanoparticles) and aluminum oxides. For this study was used aluminum nitrate who was dissolved in ethyelene glycol under the influence of temperature increase, after two hours of stirring the sollutions was ajusted with base. For the second solution was used iron nitrate with distilled water. After washing, the samples were calcined at 800° C (fig.1). The aim of this study was to obtained oxides in different forms such as Fe_3O_4, α-Fe_2O_3 and γ- Fe_2O_3 and Al_2O_3.

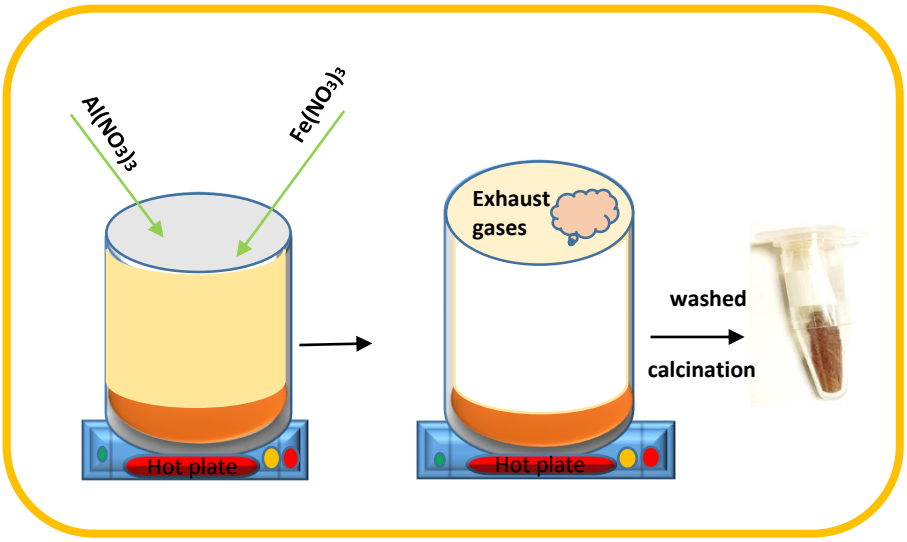

Figure 1. Schematic reprensations of co-precipitaion process

Results and discussion

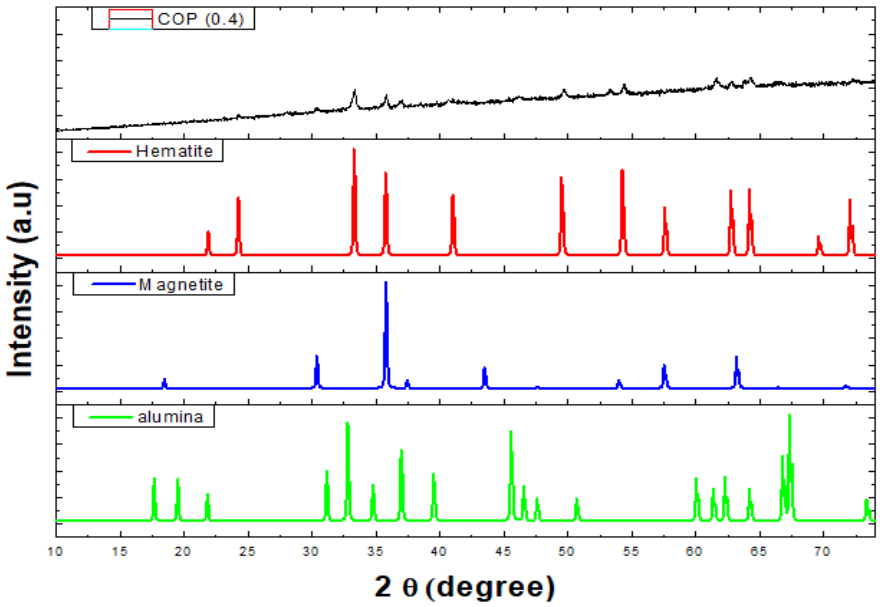

Figure 2. Diffraction peaks in the XRD pattern of red line- hematite (Fe_2O_3); blue line magnetite-Fe_3O_4, green line- aluminum oxide (Al_2O_3);

In this study, from the diffraction spectra results that the iron oxide exists in different phases such as hematite (α-Fe_2O_3), maghemite (γ-Fe_2O_3) and magnetite (Fe_3O_4) with different Fe valence, all of them being known for their low cost and non-toxicity. Diffraction patterns for the sample sintered at 800 °C (by calcination process) were identified as a mixture of Fe_2O_3 and Al_2O_3.

Through the precipitation method, the mix of nitrates led to the obtaining of hematite who representing the largest amount of compound obtained and aluminum oxide with a tetragonal structure resulted.

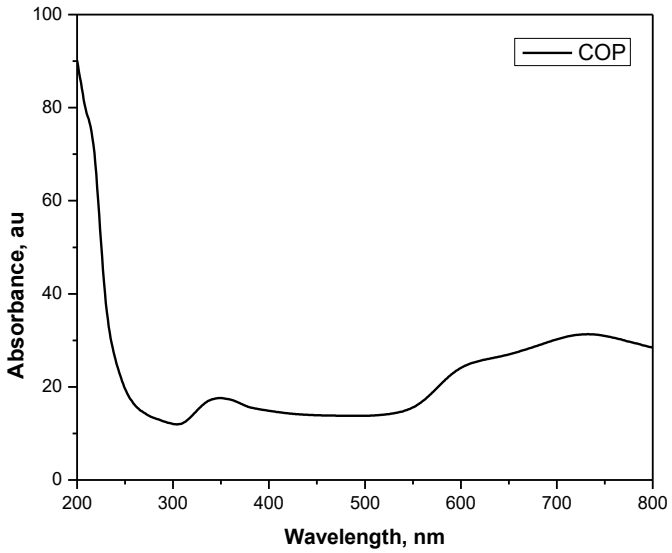

Figure 2. UV-Vis spectrum of mix of aluminium oxide and iron oxide by co-precipitation method

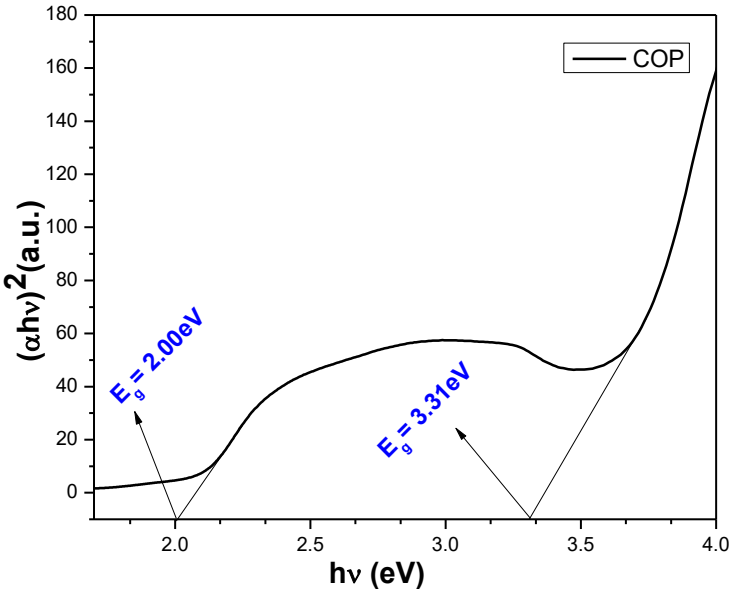

Figure 3. The value of the bandgap

Comparing with the studies of the literature where the value of the band gap is around 2.35 eV for iron oxides [6], [7], we can see that it had a slight decrease (2.0 eV) for iron oxides and (3.1) aluminum oxide [8], using the coprecipitation method (as a synthesis method) which corresponds to studies from the literature.

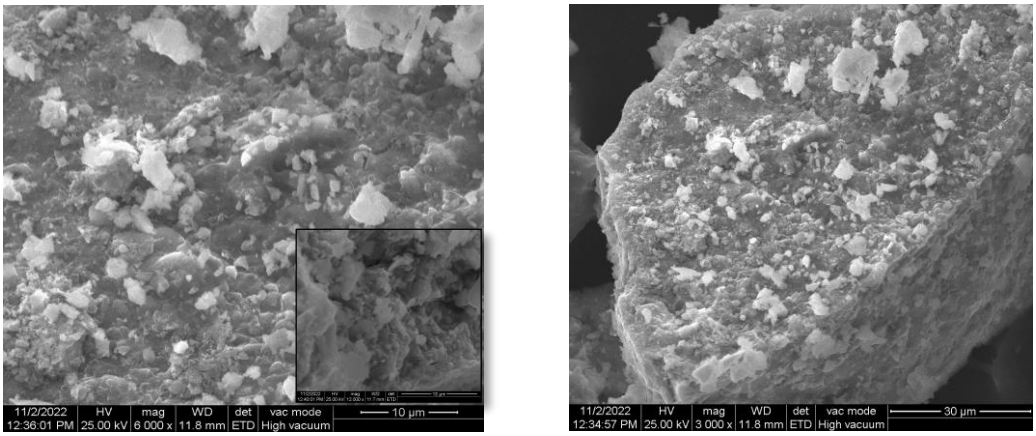

Figure 4. SEM images of the surface of particles sintered at 800 °C

The SEM analysis of the coprecipitation method of aluminum and iron oxides shows that iron oxide exist as clustered and aggretate shape (this prove the presence of hematite) and the surface of aluminum oxide is rough.

Conclusion

This study shows that ions of aluminium metal incorporated into iron oxide nanostructures by co-precipitaion method. The optical band gap, may lead to an enhanced photo catalytic activity.

Acknowledgements

This work was supported by a grant of the Ministry of Research, Innovation and Digitization, CNCS - UEFISCDI, project code project code PN-III-P2-2.1-PED-2019-4492, contract number 441PED/2020 (3DSAPECYT), project number PN-III-P1-1.1-TE-2021-0963, within PNCDI III, with contract number TE13/2022 (DD-CyT); and partially by project code PN19220401 TINSME, 40 N/2019.

References

[1] T.C. Shel, P. Poddar , A.B.M.W. Murad, A.J.M.T. Neger, A.M.S. Choudhury, J. Adv. Chem. Eng. 6 (2016).
[2] M. Pehlivan, S. Simsek, S. Ozbek, B. Ozbek, J. Mater Res Technol. 8 (2019) 1746-1760.
[3] E. Bazilevskaya, D.D. Archibald, M. Aryanpour, J.D. Kubicki, C.E. Martinez, Geochimica et Cosmochimica Acta 75 (2011) 4667- 4683.
[4] A. Muan, C.L. Gee, J. Am. Ceram. Soc., 39 (1956) 207.
[5] I. Jacukowicz-Sobala, D. Ocinski, E. Kokciolek-Balawejder, Waste Manag. Res. (2015) 1-18.
[6] S. Riaz, A. Hussain, Y.J Guo, M Khaleeq-ur-Rehman, S. Naseem, ACEM 16 (2016)
[7] J.A. Joseph, S.B. Nair, K.A John, S. Babu, S. Shaji, V.K. Shinoj, R. R. Philip, J. Appl. Electrochem. 50 (2020) 81-92.
[8] E.O. Filatova, A.S. Konashuk, J. Phys. Chem (2015).

CAPECITABINE REMOVAL FROM WATER USING COMMERCIAL GRANULAR ACTIVATED CARBON

Mina Ionela Popescu [1,2], Aniela Pop [1], Corina Orha [2], AnaMaria Baciu [1], Florica Manea [1]

[1]National Institute of Research-Development for Electrochemistry and Condensed Matter Timisoara, Plautius Andronescu, no. 1, 300224 Timisoara, Romania
[2]Politehnica University of Timisoara, Romania, P-ta Victoriei, no. 2, Timisoara, Romania
e-mail: mina.popescu@student.upt.ro

Abstract

The aim of this study consisted of removal of capecitabine (CCB), a cytostatic that is often used in cancer therapy and its presence in water exhibited negative impact and risk on the human health. Granular activated carbon (GAC) was tested as sorbent in batch system for CCB removal from water, considering its common usage in water/wastewater treatment technology. Influence of operation variables, *e.g*, pH, GAC dose and CCB initial concentrations, was studied to optimize GAC-based sorption for CCB removal.

Introduction

It is known that a large number of pharmaceutical agents are consumed annually wordwide and this has become an increasing source of water pollution [1]. Thus, a main cause of anticancer drugs in the aquatic environment is given by hospital effluents due to forms of pollution, such as the excretion of patients under the chemotherapy procedure [2]. Capecitabine (CCB) has become one of the most well-known anticancer drugs that led to the expansion of the drug list being known as a new compound at patients with different types of cancer[3], and as consequence, its presence in water has been reported.

Granular activated carbon (GAC) – based filtering belongs the mature technology for the water/waste water treatment but its performance for removal emerging pollutants and especial, cytostatics, has not been studied.

In this study, GAC ability to remove CCB from water by adsorption is investigated considering the effect of pH, GAC dose and CCB concentration range.

Experimental

All batch sorption experiments were carried out under stirring conditions (Figure 1). The influence of different parameters were studied in static system, *i.e.*, pH of 3, 5, 7 and 9, GAC dosage of 1, 5, 10 and 20 gL^{-1} and CPB concentrations of 1, 2.5, 5, 10 and 20 $mg \cdot L^{-1}$.

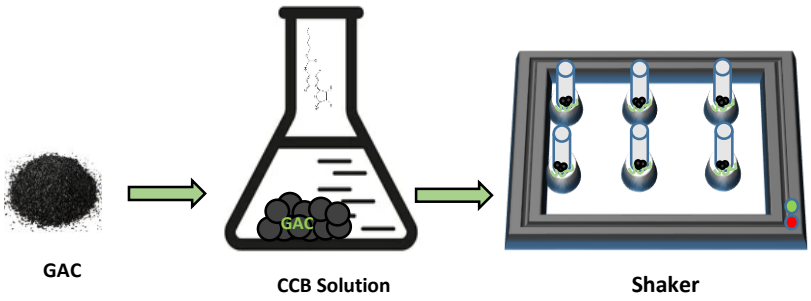

Figure 1. *Schematic representation of batch adsorption*

CCB concentration was assessed in terms of absorbance recorded at A_{240} nm chosen based on UV-Vis spectrum of CCB, presented in Figure 2. Taking into account, the sorption is a separations process that led to same evolution of all UV-Vis peakes, A_{240} was selected to simplity the discussions.
Also, GAC performance was evaluated considering CCB removal degree (η), determined based on equation (1):

$$\eta = \frac{A240,i - A240,f}{A240,i} \cdot 100 \quad (1)$$

where:
A_{240}, i -is the absorbance recorded at the wavelength of 240 nm for initial capecitabine concentration,
A_{240}, f -is the final absorbance recorded at the wavelength of 240 nm for final capecitabine concentration.

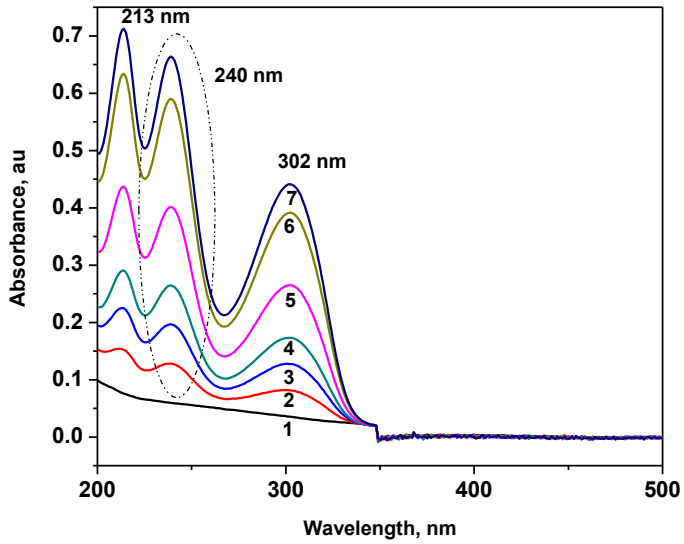

Figure 2. *UV-Vis spectrum of CCB (**1**- based line; **2**-2.5 mg·L^{-1}; **3**-5 mg·L^{-1}; **4**-7.5 mg·L^{-1}; **5**-10 mg·L^{-1}; **6**-12.5 mg·L^{-1}; **7**-15 mg·L^{-1})*

Results and discussion

pH is one of most important variable considered for sorption. Also, CCB is a weak acid that is ionized at pH>7 [4]. Figure 3 presents the results related CCB removal at pH of 3, 5, 7 and 9.

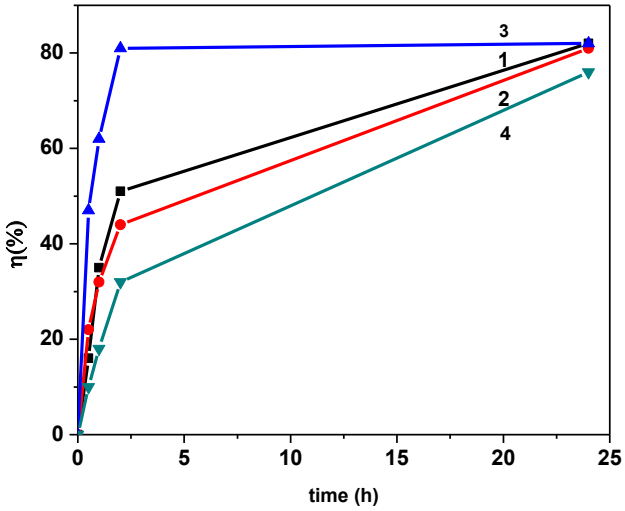

Figure 3. *Time- evolution of CCB removal degree at different pH (**1**-pH3; **2**-pH5; **3**-pH7; **4**-pH9)*

It can be noticed that the worst removal efficiency was achieved at pH=9 and the best one at the neutral pH of 7, for the dose of 5 g·L^{-1}. After 24 h of sorption, the removal efficiency was similarly for all tested pH, which shows that acidic pH necessitates a longer contact time to achieve the equilibrium. Based on above presented results, pH of 7 is recommended as optimum one.

Various GAC doses were tested for neutral of 5 mg·L^{-1} CCB at pH=7 and the results are presented in Figure 4.

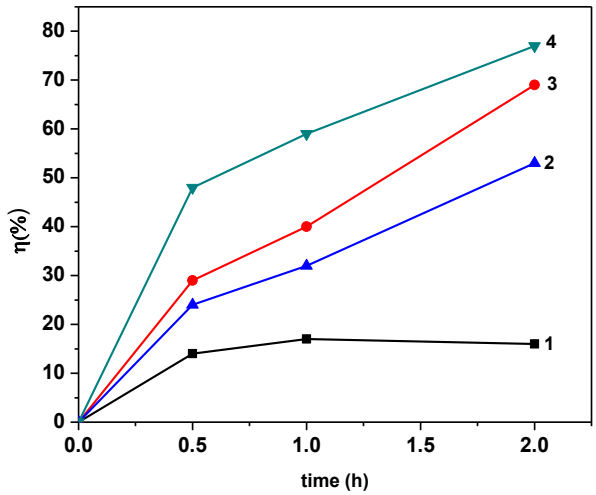

Figure 4. *Time- evolution of CCB removal degree at different GAC doses (**1**- 1 g·L^{-1}; **2**-5 g·L^{-1}; **3**-10 g·L^{-1}; **4**-20 g·L^{-1})*

Increasing GAC dose the CCB removal degree increated, manifested especialy for short time of soprtion. 5 g·L^{-1} CA at pH=7 is tested for removal of CCB with concentrations ranged from 1 mg·L^{-1} to 20 mg·L^{-1}.

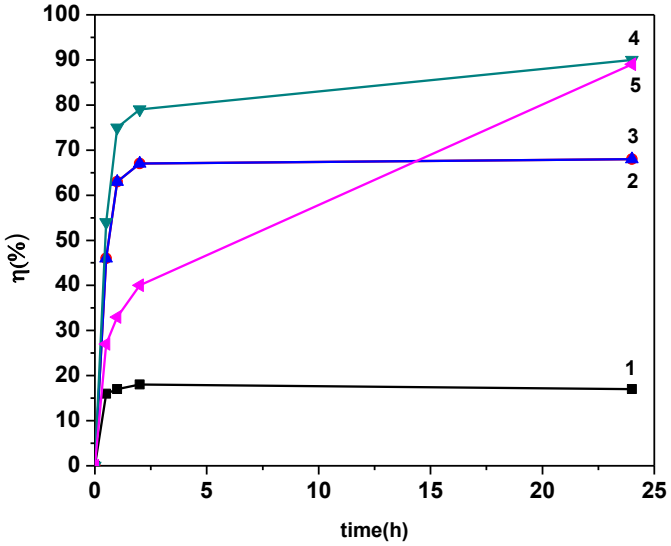

Figure 5. *Time- evolution of CCB removal degree at different initial CCB concentrations (**1**- 1 mg·L^{-1}; **2**- 2.5 mg·L^{-1}; **3**- 5 mg·L^{-1}; **4**-10 mg·L^{-1}; **5**- 20 mg·L^{-1})*

The lowest CCB removal was achieved for the lowest CCB concentration (1 mg·L^{-1}) due to no driving force for sorption process is assured. CCB removal degree increased with initial CCB concentration until 10 mg·L^{-1}, while CCB concentation of 20 mg·L^{-1} was too high considering GAC dose of 5 g·L^{-1}.

For initial CCB concentration ranged from 1 to 10 mg·L^{-1}, the equilibrium was reached after 2 h contact time, while at higher CCB initial concentrations (20 mg·L^{-1}) it is requered 24 h contact time.

Conclusion

This study demonstrated the potential of GAC to remove CCB from water, which support the application of conventional GAC filtering advanced treatment of CCB containing water/wastewater.

Acknowledgements

This work was supported by a grant of the Ministry of Research, Innovation and Digitization, CNCS - UEFISCDI, project code project code PN-III-P2-2.1-PED-2019-4492, contract number 441PED/2020 (3DSAPECYT), project number PN-III-P1-1.1-TE-2021-0963, within PNCDI III, with contract number TE13/2022 (DD-CyT); and partially by project code PN19220401 TINSME, 40 N/2019.

References

[1] J.L. Tambosi, L.Y. Yamanaka, H.J. Jose, J. Quim Nova 33 (2010) 2, 411-420.
[2] R. Guo, F. Zheng, J. Chen, J.RSC Adv, 2015.
[3] N. Negreira, N. Mastroianni, M.L de Alda, D. Barcelo, Talanta 116 (2013), 290 -299.
[4] V. Cheng, M. de Lemos, N. Hunter, N. Badry, J. de Lemos , J. Oncol Pharm Practice (2019), 1-7.

EXPRESSION OF A MEMBRANE TRANSPORTER – SCALE-UP, STABILITY, CONTAMINATION PROFILE, AND CRYSTALLIZATION TRIALS

Gerda Szakonyi[1], Emese Zsuzsanna Galgóczi[1], Lóránt Lakatos[2]

[1]University of Szeged, Faculty of Pharmacy, Institute of Pharmaceutical Analysis, H-6720 Szeged, Somogyi u. 4.,
[2]Lóránt Eötvös Research Network, Biological Research Center, Institute of Plant Biology
e-mail: szakonyi.gerda@szte.hu

Among the methods used to study the structure of membrane proteins, X-ray crystallography can be considered the most frequently used method. However, the crystallization often fails; therefore, a so-called chaperone protein was fused to the target protein to promote crystallization.

During our work, we coupled the fucose transporter of *Haemophilus influenzae* HI0610 with the T4 lysozyme chaperone protein. Gel electrophoresis confirmed that the desired fusion protein was expressed.

BL21(DE3) *E. coli* cells were grown in 2XY, LB, and autoinduction medium to optimize the fusion protein expression. Compared to IPTG-induced samples, the protein produced by autoinduction gave us the most satisfying result. After optimization of the expression conditions, we produced the fusion protein in larger quantities, thus ensuring the production of a sufficient amount of target molecule for crystallization.

The fusion protein was purified further by affinity, size exclusion, and ion exchange chromatography to high prurity.

The purified recombinant protein was then used to determine the secondary structure by circular dichroism. The CD spectrum of the fusion protein mainly showed alpha-helical and parallel beta-sheet secondary structures, which is in agreement with the alpha helical structure of the transporter protein and the beta-sheet N-domain of the T4 lyzozyme. Also, the protein was highly resistant to trypsin treatment, which ensures its stability.

Finally, using the hanging drop technique, we tested more than 300 crystallization conditions resulting in the presence of microcrystals. The observed microcrystals are promising signs for further structural studies; however, additional optimization is necessary.

In the future, we would like to determine the conditions for the transporter's crystallization and understand the protein's structure and stability using other analytical tools.

DYNAMICS OF PHYSICAL AND CHEMICAL PARAMETERS OF THE SAVA RIVER NEAR ŠABAC, SERBIA

Milan Glišić[1], Ljiljana Tanasić[1], Suzana Knežević[1], Jelena Tanasić[2]

[1]Unite for Agricultural and Business Studies and Tourism, Academy of Applied Studies Šabac, Vojvode Putnika 56, 15000 Šabac, Serbia
[2]Faculty of Technology Novi Sad, University of Novi Sad, Bulevar Cara Lazara 1, 21102 Novi Sad, Serbia
e-mail: milan11glisic@gmail.com

Abstract

To understand the quality dynamics of surface water, it is necessary to know the patterns according to which physical and chemical water parameters change in a function of time – daily, seasonally, and annually. For this research, water monitoring data from the Sava River near Šabac during the period from 2015 to 2019 (from June 1st to August 31st during a year and from 7:30 a.m. to 1:15 p.m. during a day) were used. The sampling was carried out at a distance of 20 meters from the coast and a depth of 0.5 m. Determination of physical and chemical parameters (temperature, pH value, electrical conductivity, suspended matter, turbidity, dissolved oxygen, oxygen saturation, ammonium ions, and nitrogen compounds) was performed using standardized methods. To determine the influence of the sampling time (time during the day, day of the year, and year) on the values of physicochemical factors, correlation and regression analyses, as well as the Eta-squared test according to Cohen in the SPSS program, were performed. According to the obtained results, the temperature shows a weak but significant positive correlation with the sampling hour during the day ($r = 0.31$, $p = 0.03$, $\eta^2 = 0.24$), water turbidity shows a weak but statistically significant negative correlation with the sampling date ($r = 0.35$, $p = 0.02$, $\eta^2 = 0.11$), and dissolved oxygen concentration shows a weak but statistically significant negative correlation with the year of sampling ($r = -0.3$, $p = 0.04$, $\eta^2 = 0.44$). The other physicochemical parameters do not show a high correlation with the time, date, and year of sampling, which indicates that for most of the parameters there is no clear trend or pattern of their dynamics when it comes to the periods in which sampling was carried out.

DYNAMICS OF FAECAL INDICATORS IN THE SAVA RIVER NEAR ŠABAC, SERBIA

Milan Glišić[1], Biljana Delić Vujanović[1], Ljiljana Tanasić[1], Bojan Damnjanović[2]

[1]Unite for Agricultural and Business Studies and Tourism, Academy of Applied Studies Šabac, Vojvode Putnika 56, 15000 Šabac, Serbia
[2]Unit for Medical and Business-Technological Studies, Academy of Applied Studies Šabac, Hajduk Veljkova 10, 15000 Šabac, Serbia
e-mail: milan11glisic@gmail.com

Abstract

To determine the surface water quality, we traditionally rely on faecal indicators - organisms that, by their presence, indicate the possible presence of pathogens in the environment. Therefore, it is of great significance to know the patterns of variation in the concentration of faecal indicators in surface waters because it directly indicates how water quality improves or deteriorates during a day, a year, or a multi-year period. For this research, water monitoring data from the Sava River near Šabac during the period from 2015 to 2019 (from June 1st to August 31st during a year and from 7:30 a.m. to 1:15 p.m. during a day) were used. The sampling was carried out at a distance of 20 meters from the coast and a depth of 0.5 m. The groups of faecal bacteria monitored are total coliforms, faecal coliforms, and faecal enterococci. Bacteria detection was performed using a method based on the enzymatic decomposition of different substrates. Enumeration of bacteria is determined based on the number of positive enzymatic reactions, which was translated into the the most probable number of bacteria in 100 ml of water sample (MPN/100 ml). To determine the influence of the sampling time on the abundance of faecal indicators, correlation and regression analyses, as well as the Eta-square test according to Cohen in the SPSS program, were performed.

The abundance of faecal indicators was positively correlated with the sampling time in the period from 7:30 to 1:15 p.m. Nevertheless, this correlation was statistically significant only in the case of total coliforms, although the values of the Eta-squared test indicated a high dependence of all three groups on the sampling time. In the case of all three groups of indicators, the correlation with the sampling date during the year was negative, which indicates that during June, July, and August, there was a slight decrease in their number. However, this correlation was not statistically significant enough. In other words, the abundance of faecal indicators in the Sava River near Šabac does not show a significant dependence on the sampling date during this period. Total and faecal coliforms do not show a significant correlation with the year of sampling, and the value of the Eta-squared test also indicates a low dependence. However, if the average number of total coliforms per sample is monitored each year, it can be observed that it was increasing in the period from 2016 to 2019. Faecal coliforms also had a positive but less pronounced trend. When it comes to faecal enterococci, if the maximum recorded value was excluded from the analysis due to the large deviation, their correlation with the year of sampling was weak but statistically significant. Also, the average annual values were higher and higher from year to year during the entire observed period, which indicates a clear and very pronounced positive trend in their numbers.

For scientific research, it is necessary to plan the sampling in a specific way, depending on whether the subject is diurnal, seasonal, or annual dynamics. Data obtained by the standard monitoring program are not suitable for observing the complete dynamics of faecal indicators.

MODERN ADSORBENTS FOR HEAVY METALS CAPTURED FROM WASTEWATER INTO THE CIRCULAR ECONOMY

Adina-Elena Segneanu[1], Melinda Cepan[2] Claudiu Cepan[2], Maria Mihailescu[2], Marin Catalin[3], Ioan Grozescu[2]

[1] *Institute for Advanced Environmental Research-West University of Timisoara (ICAM-WUT)* Oituz nr. 4, Timișoara, Romania
[2] *Politehnica University of Timisoara, Piața Victoriei 2, 300006 Timișoara, Romania*
[3] *West University of Timisoara, Blvd.V. Parvan 4, 300223, Timisoara, Romania*
e-mail: adina.segneanu@e-uvt.ro

Abstract
Intensive industrialization as a requirement of the development of modern society has harmed the environment with severe repercussions on biodiversity, human health and food security. Special efforts are made to set highly effective methods for environmental remediation in the circular economy.

Introduction
Heavy metal pollution of industrial effluents is one of the main problems recognized at the global level. There are several techniques for decontamination with heavy metals: chemical, electrochemical, membrane separation, ion exchange, reverse osmosis, electrodialysis, and adsorption. The implementation of a method at an industrial level requires several requirements: high performance, ease of operation, and economic efficiency. And many of these methods of removing heavy metals are expensive and, in addition, generate secondary products that require additional steps of decontamination and subsequent storage.
Adsorption is considered the most advantageous method of removing heavy metals in terms of cost and efficiency. Many adsorbents are known: as natural or synthesized. Recent research is focused on testing waste from the food industry or agriculture as adsorbents for various heavy metals removal from wastewater.
The mixed research team composed of researchers from the Western University of Timisoara and the Politehnica University of Timisoara are engaged in research studies aimed at the valorization of some biowaste and industrial waste for the preparation of new engineered adsorbents with high performance for removing heavy metals from wastewater.

Experimental
Regardless of its nature, the waste is subjected to an appropriate heat treatment to avoid altering the adsorption properties, followed by a micronisation stage. Different techniques were used to characterized the new adsorbents: nitrogen adsorption-desorption isotherms, FTIR spectroscopy, XRD spectroscopy, microscopy SEM coupled with EDX.
The heavy metal initial and final concentration were determinate through atomic absorption spectroscopy.

Results and discussion
The results obtained in the characterization of the physico-chemical properties of the new prepared materials showed that a substantial increase in surface area and pore size was achieved.

The effect of different parameters like temperature, pH, contact time, adsorbent dosage, and initial and final concentration on the adsorption rate of the new materials prepared was systematically investigated. The adsorption behavior of the new adsorbents was investigated using adsorption isotherm, kinetic, thermodynamic and desorption studies, and adsorption mechanism.
Studies of the adsorption process have demonstrated an increase in the adsorption performance compared to the adsorption capacity of each waste.
In addition, the feasibility of adsorbents was demonstrated by remediating heavy metal-contaminated soil sludge samples.

Conclusion

The results of our studies have shown that reusing waste can be used to obtain ecological, low-cost and high-performance materials for the sustainable management of wastewater and waste.

References

[1] WHO (World Health Organization), Health through safe drinking water and basic sanitation; http://www.who.int/water_sanitation_health/mdg1/en/index.html (2008).
[2] P. Ghisellini, C. Cialani, S. Ulgiati, A review on circular economy: the expected transition to a balanced interplay of environmental and economic systems. J. Clean Prod. 114, (2016) 11–32;
[3] R.K., Gautam, S.K. Sharma, S. Mahiya, C. Chattopadhyaya Mahesh, Major contaminants in industrial and domestic wastewater a contamination of heavy metals in aquatic media: transport, toxicity and technologies for remediation, Heavy Metals in Water: Presence, Removal and Safety (ed. Sharma S.K.) (The Royal Society of Chemistry, 2015).
[4] Fernández-Reyes B., Ortiz-Martínez K., Lasalde-Ramírez J.A., Hernández-Maldonado A.J., Engineered adsorbents for the removal of contaminants of emerging concern from water. Contaminants of Emerging Concern in Water and Wastewater: (2020) 3–45.
[5] Qasem N.A.A., Mohammed R.H., Lawal D.U., Removal of heavy metal ions from wastewater: a comprehensive and critical review. npj Clean Water 4 (2021) 36.
[6] Segneanu, AE., Marin, C.N., Vlase, G. *et* al, Highly efficient engineered waste eggshell-fly ash for cadmium removal from aqueous solution, Scientific Reports,, 12 (2022) 9676.
[7] Cepan C, Segneanu A-E, Grad O, Mihailescu M, Cepan M, Grozescu I., Assessment of the different type of materials used for removing phosphorus from wastewater, Materials,14(16) (2021) 4371